UNIVERSITAT DE BARCELONA

Molecular mechanisms regulating osteoblast differentiation: miR-322/Tob2 and PI3K/SMAD networks

Beatriz Gámez Molina

Universitat de Barcelona

Doctoral Program in Biomedicine

2015

Molecular mechanisms regulating osteoblast differentiation: miR-322/Tob2 and PI3K/SMAD networks

This thesis has been conducted under the supervision of Dr. Francesc Ventura Pujol in the Department of Ciències Fisiològiques II at the Universitat de Barcelona

Beatriz Gámez Molina

Dr. Francesc Ventura Pujol

Doctoral thesis submitted by Beatriz Gámez Molina to obtain the PhD degree by the Universitat de Barcelona

ACKNOWLEDGMENTS

Recuerdo como si fuera ayer cuando me entrevisté con Francesc Ventura para empezar el proyecto de máster. Para qué engañarnos, todo me sonó a chino ☺, pero me llevé la sensación de que era una persona especial y que allí estaría bien. Y así fue. No creo que pudiera haber tenido un mejor director de tesis (y a la vez compañero de poyata). No sólo porque es una de las personas que más admiro sino porque además es buena persona y hace que el laboratorio sea un sitio confortable y divertido. Sé que vaya donde vaya de postdoc difícilmente lograré algo que se asemeje a lo que él es capaz de crear en el 4171. Francesc, gràcies per formar part del lab com un company més. Per animar-me en els moments estressants i felicitar-me per qualsevol petit èxit desde el primer moment. Espero que hagis gaudit igual que jo de la ciència que hem compartit!

Y como un anexo a Francesc, solito cuando llegué al 4171, me encontré al señor Edgardo. He escrito, borrado y reescrito varias veces ya este párrafo, pero realmente no hay nada que no nos hayamos dicho ya. Que eres una de las personas más inteligentes que conozco, que me enseñaste todo aquello de lo que luego te sentiste tan orgulloso de mí y que, sin esperarlo, me encontré con un amigo de verdad. Horas y horas en el estabulario y alguna que otra borrachera forjaron una amistad entrañable. Y risas, muchas risas. Siento haberme reído de tus desgracias científicas (y no científicas), but you knoooow deep in my heaaart I still love youuuu. ¡Ay Edgardito! Cuánto te he echado de menos desde que te fuiste… pero hasta eso también te lo he dicho a tí muchas veces. Gracias por estar aquí el día de mi tesis y en muchos otros momentos.

Y cuando ya veía la marcha de Eddie cerca, llegó Natalia. Has sido una muy buena compañera y aunque el hueco que dejó Eddie era difícil de rellenar siempre has estado ahí escuchando mis historietas ☺. ¡Juntas con Eddie hicimos que la Gimcana de Bellvitge fuera una realidad! Dale duro al lab ahora que te has quedado un poco solita y te viene la recta final. Y no dudes en

pedirme ayuda si me necesitas (sea de laboratorio o no), aunque te las has apañado muy bien sola desde el principio, estás hecha una crack.

¡Rubén! ¡Eres el próximo en doctorarte en el 4171! Te deseo mucha suerte en lo que te queda de camino y espero que hagas lo que hagas después la vida te depare cosas bonitas. Y lo mismo para ti Jose. Justo ahora arranca todo, pero el proyecto y el interés que le pones harán que te vaya de maravilla. ¡Aaaay Alcira! tu llegada fue una bendición. Gracias por solucionarnos cualquier problema con esa rapidez y eficacia. Y por los millones de puntas y buffers que has hecho. Hubo un antes y un después en el lab. Gracias por todo.

¡BUALAAAA! ¡BUALAAAA! ¡Carol por favor! Te perdono que bebas "claras" pequeñas, pero que no sepas cargar una 384 y me dejes en evidencia delante del jefe no ehhh ☺. Vaya fenómeno estas hecha. Da igual si te vas fuera, o no, o si te vas para el máster y vuelves, o si te vas y yo que sé qué lío tienes. Vas a triunfar en lo que te propongas hacer. Porqué eres responsable, lista, trabajadora y tienes una fuerza para la vida que ya me gustaría a mí. Gracias por alegrarme los días con velas homeopáticas y pastelitos de chocolate y zanahoria. Eres única.

Y de quien iba a hablar en primer lugar después de la gente del lab si no es de las GORDAS. Sin vosotras mi paso por Bellvitge hubiera sido muy, muy distinto. Y con distinto quiero decir menos divertido, menos dulce y por supuesto, menos calórico ☺. ¡Petrushiii! Fuimos las fundadoras del grupo y las creadoras del viaje anual a sitios que acaban en –onia ☺. También hemos tenido tiempo de vivir juntas algún que otro mal momento, gracias por estar siempre ahí y por demostrarme que te importo de verdad. Eres una gran amiga. Thanks. ¡Bettushiiii!!! Tú, concretamente…¿cuándo empezaste a juntarte con nosotras? ☺ Pasamos de hablar durante los ratos de campana a reírnos a carcajadas en la salita del café. Eres divertida, espontánea y única y por eso te haces querer tanto. Y quien diga lo contrario es que no sabe ver que detrás de esa fábrica de gestos y caras locas hay una persona fantástica. ¡Criiiiiiiiisssssss!!! ¡POLICÍA! Has marxat i et trobem taaaant a faltar! Ja t'ho vam dir, el club de les Betrines no és el mateix sense tu. Encara ara es fa raro passar pel teu lab i no veure els rínxols (els de veritat) al girar la vista cap a la teva taula, o no escoltar el teu riure energètic des del 4171. Ha sigut un plaer

compartir el camí amb tu, t'apunto a la llista de grans persones que m'emporto d'aquesta etapa.

Hubo otro grupo de gente entrañable que me hizo las cosas más fáciles al llegar a Bellvitge: Andy, Laura y Miguel. Seguramente en un principio me acogisteis como la nueva compi de vuestro más que amigo, hermano Eddie. Pero con el tiempo me he dado cuenta de que me queréis y aunque estéis lejos, siempre estáis ahí para recordármelo. Gracias por ser sinceros y por contar conmigo. Andy, no sé si eres más inteligente o cariñoso. Gracias por darme tus consejos en lo profesional y lo personal y Laura, tot i que et tinc més llunyana, sé que també puc comptar amb tú. ¡Os iré a visitar pronto! ¡Miguelitoooo! No has podido venir desde China para mi tesis, pero bueno, otra vez será ☺. Gracias por estar ahí siempre interesado en como me van las cosas, eres un encanto.

Del resto de personas de Bellvitge, a todas os recordaré con mucho cariño. Y todas me habéis ayudado en un momento o en otro, sea con un anticuerpo o con una charla agradable en la salita del café.

Per l'apo-imperi d'en Joan Gil ha passat molta gent desde que vaig començar i tots heu sigut sempre molt macos amb mi: Diana, Cami, Alba, Helena, Mariela… Dani, t'haig de dir que em feies molta por al principi….i al final (jajaja es conya) però la veritat es que al final et fas estimar ☺. I tu Anna, ets la perfecció personificada, però sempre et recordaré netejant el plat després de dinar amb la boca oberta, ho sento, va ser molt divertit. Sonia i Jose, un plaer haver-us conegut! Sou el futur del 4175!

La porta del 4165 sempre s'ha obert amb un somriure. Ramón, vas donar-me l'oportunitat de ser professora, algo que mai m'havia plantejat i que avui en dia m'agradaria continuar fent en un futur. Gràcies per confiar en mi quan acabava d'arribar, gràcies a allò en part, he pogut tirar endavant aquesta tesi. I tu, Anna Manzano, me ayudaste mucho cuando aterricé y casi de un día para otro tenía que empezar a dar clase, siempre te estaré agradecida. Siempre estás dispuesta a ayudar, eres un encanto. Ana Rodríguez y Helga, ha sido un placer compartir con vosotras estos últimos años. ¡Os deseo que os vaya muy bien lo que os queda de doctorado!

Junto con Petra, en el 4159/62 también he compartido momentos con Anna Vidal, Elena, Juan y en los últimos tiempos con Pau y Xevi. Espero que todo os vaya muy bien, ha sido muy agradable compartir mis días en Bellvitge con gente como vosotros. Y también con gente como la del lab de Raúl: Tania, Tanit, Sonia, Xavi, Carla, Héctor, Xabi, Alejandro… habéis sido muy majos, ¡sobretodo por perpetuar la gimcana anual del departamento! ¡Pasaréis a la historia como los primeros ganadores! ¡Yuhuuu!

Hay que decir que también he pasado bastante tiempo de mi doctorado en el 4114, principalmente pidiendo anticuerpos ☺. Gracias a Tai y Susana como representantes actuales del 4114. A demás, habéis sido el hogar de entrañables estudiantes brasileños como Leo o Verónica. Gracias por hacer tan bien de anfitriones.

Por el pasillo, más gente me ha sacado una sonrisa de vez en cuando. Com en Josep Maria! Gràcies per preocupar-te sempre de la paperassa. A Joan y Diana, ¡sois tan guapos como majos!. També amb el Xavi de Fármaco hem rigut de tant en tant parlant del desastre monumental que hi ha a la sala de virus ☺. Y hablando de virus, gracias a Fran por la ayuda recibida en mis primeros contactos con los retros.

También quiero agradecer a la gente de Serveis. Sois un gran apoyo científico pero también sois personas encantadoras que hacen la vida más fácil. Esther, Benja, Bea, gracias por todo. También a Eva de la 5ª por ayudarme en todo lo que he necesitado. Qué fácil haces que sea todo. Gracias por tu tiempo perdido entre mis días de histología.

También en el estabulario me he encontrado gente que me ha hecho las cosas fáciles. Todos me habéis ayudado en algún momento, pero quiero hacer una mención especial a Lara, que me ayudó muy, muy al principio y más tarde y durante mis épocas de colonias descontroladas a Bea Gamarra. Que si estos con Doxi, que si aquellos los separas al nacer, que si ¡qué locura!. No sólo me llevaste la sala de maravilla, sino que a demás nos echamos muchas risas allí. Gracias por todo.

Si hay algo que no he mencionado aún y que echaré en falta a partir del momento que deje Bellvitge eso será la salita del café. Allí he tenido la oportunidad de hablar de cosas banales y no tan banales y de reírme a

carcajadas con muchos compañeros pero también con muchos jefes. José Carlos, eres raro, sí, pero eres la leche ☺ y José Luís, ha sido muy agradable conversar contigo, de fútbol o de esos temas raros que salen durante el café. La salita también fue el lugar para coincidir con la gente del 4108: Avelina, Pepita, Fina, Edu. Allí hemos hablado desde de temas carnales a temas paranormales. Casi nunca hemos estado de acuerdo, pero eso es lo divertido, ¿no?. ¡Esther! Gracias por ser mi aliada en muchas conversaciones, ¡menos mal!☺. Pablo, Santi, Biel, Àurea, també vosaltres heu fet que la saleta prengés un caire amable. Gracias a todos por formar esta pequeña familia laboral.

Obviamente, mucha gente me ha acompañado durante la tesis y ya formaban parte de mi vida. Montse, Amalia, Jessi, Mariona, Elenita, Estela… todos os habéis ido preocupando por mí y mis avances y me habéis hecho llegar lo orgullosos que estáis de mí. Os quiero y me gusta que forméis parte de mi vida. Y lo mismo para muchos amigos que no veo muy a menudo pero que siempre se alegran por mis logros. ¡Carmencooots! ¡tu has sido un regalo extra de mi tesis! ¿¿Cómo se puede querer tanto a alguien que se conoce en tan pocos días?? Pregúntenle a Carmen.

Y por supuesto tengo que acabar con el respaldo más importante que he tenido: mi familia. ¡¿Qué decir?! Para mí son los mejores sin duda. Siempre han estado ahí. Cuando he estado loca, riendo, bailando y llorando. ¡Porque mira que he llorado, ehh! Papa, se que en su momento creíste que no era lo mejor dejar un trabajo fijo para irme al paro a intentar hacer ciencia, pero aún así me has ayudado siempre que me ha hecho falta, como siempre en la vida. Gracias por todo. Lo mismo contigo mama. Sé que lo que está por venir te da pena, y aunque no lo creas, a mí más. Y miedo. Pero nunca hemos elegido el camino fácil, sino el que queríamos, ¿verdad? Te quiero. ¡Cristi! Gracias por estar ahí siempre con un "ola ke ase" ☺. Me alegras mucho los días y se que siempre estás ahí si te necesito. Os quiero mucho.

Y por último, GRACIAS Edu. Porque verdaderamente tu has sido el apoyo incondicional de esta tesis y el de mi vida entera desde hace más de 13 años. Tu has confiado siempre en mí, incluso cuando yo no lo he hecho, y te has alegrado de mis objetivos cumplidos casi más que yo. Sé alzar la vista y verme en cualquier lugar del mundo y en cualquier circunstancia laboral en un futuro, pero no sé alzarla y no verme haciendo esas cosas junto a tí. Me encanta la pequeña familia que formamos junto con Garuchi ☺. Te quiero.

PREFACE

Esta tesis se empezó a esbozar hace 5 años, casi sin avisar de que iba a ser una tesis, como parte de un intento por reconducir mi carrera como veterinaria. El cambio fue duro. Pasar de sueros, cirugías y clientes a una poyata, DNA y PCRs. ¡Pero qué bonito ha sido! ¡Qué alegría darme cuenta a tiempo de que la ciencia me divierte y apasiona mucho más que la medicina veterinaria! Y así, poco a poco, a lo tonto, todo ese trabajo y ese jugar a ciencia han desembocado en una tesis que nunca imaginé que se cruzaría en mi camino.

El recorrido no ha sido fácil, pero tampoco difícil. Enseguida me di cuenta de que el trabajo en el laboratorio estaba lleno de sentimientos contrariados. Lo que parecía comenzar con buen pie podía torcerse en cualquier momento y viceversa. Y así, bajo esa premisa, inicié una lista de lo que empecé a denominar pequeñas alegrías y pequeñas tristezas de laboratorio, recolecta a la cual se unieron mis compañeros y que resultó en una hoja llena de anécdotas que cuelga en la nevera del 4171. Y ahora, 5 años después, al releer y recordar todos esos momentos alegres, pero también los tristes, me sorprendo riéndome incluso a carcajadas, lo cual indica, seguramente, que realmente no fueron tan tristes.

Pequeña alegría de laboratorio

Aquello que durante el trabajo en el lab, por un instante, y aunque ajeno a la ciencia, te hace feliz. ☺

ABBREVIATIONS

ABD	Adaptor-Binding Domain
ACVR	Activin A Receptor
AGO	Argonaute
ALK	Activin receptor-Like Kinase
ALP	Alkaline Phosphatase
AP	Activator Protein
ATF	Activating Transcription Factor
BAMBI	BMP and Activin Membrane-Bound Inhibitor homolog
BCR	Breakpoint Cluster Region
BGP	Bone Gla Protein
BM-MSC	Bone Marrow-Mesenchymal Stem Cell
BMD	Bone Mineral Density
BMP	Bone Morphogenetic Protein
BMU	Basic Multicellular Unit
Brg1	Brahma-Related Gene-1
BSP	Bone Sialoprotein
Caf1	CCR4-Associated Factor 1
Cbfa1	Core-Binding Factor α1
CBP	CREB-Binding Protein
CCD	Cleidocranial Dysplasia
CCR4	Carbon Catabolite Repression 4
Cdc42	Cell Division Cycle 42
CREB	cAMP Response Element Binding
Dan	Differential screening-selected gene aberrative in Neuroblastoma
DBD	DNA-Binding Domain
DC-STAMP	Dendritic Cell-Specific Transmembrane Protein
DGCR-8	diGeorge syndrome Critical Region gene
Dlx	Distal-Less homeodomain-containing family
DNA-PK	DNA-dependent Protein Kinase
dsRBD	double strand RNA-Binding Domain
ECM	Extracellular Matrix
eIF	eukaryotic initiation Factors
EMT	Epithelial-Mesenchymal Transition

ERK	Extracellular signal-Regulated Kinase
FGF	Fibroblast Growth Factor
FOP	Fibrodysplasia Ossificans Progressiva
FOXO	Forkhead box protein
GLUT4	Glucose Transporter Type 4
GPCR	G Protein-Coupled Receptor
GSK3	Glycogen Synthase Kinase 3
IBSP	Integrin-Binding Sialoprotein
IGF	Insulin-like Growth Factor
Ins1P	D-myo-inositol-1-phosphate
IRES	Internal Ribosome Entry Sites
IRS	Insulin Receptor Substrate
iSH2	Inter Src-Homology 2
JNK	c-Jun N-terminal Kinase
LIMK	LIM domain Kinase
M-CSF	Macrophage Colony-Stimulating Factor
MAPK	Mitogen-Activated Protein Kinases
MEF	Mouse Embryonic Fibroblast
MH	Mad Homology
MMP	Matrix Metalloproteinase
MSC	Mesenchymal Stem Cell
Msx	Msh homeobox
NES	Nuclear Exportation Signal
NLS	Nuclear Localization Signal
NOT	Negative on TAT-less
NOT1	Negative on TAT-less 1
NPY	Neuropeptide Y
NTX	N-terminal telopeptide of type I collagen
OC	Osteocalcin
ON	Osteonectin
OPG	Osteoprotegerin
OPN	Osteopontin
OSE	Osteoblast Specific cis-acting Element
PABP	Poly(A)-Binding Protein
PACT	Protein Activator of PKR
PAK	p21-activated kinase
PAZ	PIWI-AGO-ZWILLE
PDGF	Platelet-Derived Growth Factor
PDK	Phosphoinositide-Dependent Kinase

PHLDA	PH-Like Domain family A
PHLPP	PH-Domain Leucine-rich repeat-containing Protein Phosphatase
PI	Phosphoinositide
PI3K	Phosphatidylinositol 3-Kinase
PIP_2	Phosphatidylinositol (4,5) P_2
PIP_3	Phosphatidylinositol (3,4,5) P_3
piRNA	piwi-interacting RNA
POC	Primary Ossification Center
PP2A	Protein Phosphatase 2 A
PPM1A	Protein phosphatase Mg^{2+}/Mn^{2+} dependent 1A
PRR	Proline-Rich Region
PS	Primary Spongiosa
PtdIns	Phosphatidylinositol
PTEN	Phosphatase and Tensin homolog deleted on chromosome 10
PTH	Parathyroid Hormone
RANK	Receptor Activator of NFκB
RANKL	Receptor Activator of NFκB Ligand
RBD	Ras-Binding Domain
RISC	RNA-Induced Silencing Complex
Runx	Runt-related transcription factor
SATB	Special AT-rich Binding Protein
SBE	Smad Binding Elements
SCP	Smad C-terminal domain Phosphatase
SH	Src-Homology
Shh	Sonic Hedgehog
SHIP	Src-Homology-containing Phosphatase
SIBLING	Small Integrin-Binding Ligand with N-linked Glycosilation
siRNA	Small Interference RNA
SOC	Secondary Ossification Centre
Sox	Sry-related HMG box
TAK	TGF-β Activated Kinase
TBP	TATA Binding Protein
TFIIB	Transcription Factor II B
TGFβ	Transforming Growth Factor β
TRAF	TNF Receptor-Associated cytoplasmic Factors
TRAP	Tartrate-Resistant Acid Phosphatase
TRB3	Tribbles 3
TRBP	TAR RNA-Binding Protein
TRK	Tyrosine Kinase Receptor

Vps34 Vacuolar Protein Sorting 34

CONTENTS

FIGURES

Introduction

Results

TABLES

Pequeña alegría de laboratorio#1

Que al coger un puñado de *eppendorfs* caigan el número justo que necesitas

INTRODUCTION

1 THE BONE

The skeleton is mainly formed by cartilage and bone and performs several functions. It represents the protection and support of soft organs and tissues of the organism allowing the insertions of muscles and tendons and therefore providing motion to the body. It also houses hematopoiesis and is the main reservoir for calcium and phosphate. More recently, bone has been described as an endocrine organ for its whole-body regulatory functions including its role in glucose homeostasis and in male fertility through the control of osteocalcin levels (Ferron et al., 2012; Karsenty and Oury, 2012; Oury et al., 2011).

The bone tissue is a porous and mineralized structure made up of cells, vessels, and crystals of calcium compounds (hydroxyapatite). Although chemically identical, two different types of bone structures can be distinguished in adult bone: cortical and trabecular (or cancellous). The cortical bone, representing 80% of the skeleton, has a slow turnover rate and a high resistance and constitutes the outer part of the skeletal structures. It is dense and compact and is majorly calcified, providing mechanical strength and protection. On the other side, the trabecular bone is less dense, more elastic and has a higher turnover rate therefore exhibiting a major metabolic function. It is mainly found inside the long bones but also in the inner portions of the pelvis and other flat bones (Hadjidakis and Androulakis, 2006).

1.1 Bone Composition

Bone tissue consists of different cell types coming from a mesenchymal origin and an extracellular matrix (ECM) produced by these cells.

1.1.1 Extracellular matrix

Bone extracellular matrix serves not only as a scaffold for cells but also as a reservoir for growth factors and cytokines, playing a role in tissue architecture and homeostasis.

ECM is considered a dynamic network of molecules secreted by cells that in turn regulate cell behavior by modulating their proliferation and differentiation. The ECM is synthesized primarily by osteoblasts and can be divided in an organic and inorganic fraction.

The inorganic or mineral phase of bone is basically formed by crystals of hydroxyapatite [$Ca_{10}(Po_4)_6(OH)_2$] which are found within the collagen fibers and in the matrix. The first step of mineralization is the formation of hydroxyapatite crystals inside matrix vesicles that bud from the surface membrane of hypertrophic chondrocytes and osteoblasts. Then hydroxyapatite propagates into the extracellular matrix and is deposited between collagen fibrils (Orimo, 2010). This fraction of the ECM represents the main mineral reservoir of the body, containing almost the 99% of calcium and the 88% of phosphates of the organism.

The organic fraction is mainly composed by type I collagen which is a triple-helical molecule containing two identical α1 (I) chains and a structurally similar, but genetically different α2 (I) chain. This structure provides flexibility to the bone. In the non-collagenous fraction of the organic phase we can find a large number of proteins that are classified according to their structural characteristics. Bone sialoprotein (BSP), also called IBSP (integrin-binding sialoprotein), is a SIBLING (small integrin-binding ligand with N-linked glycosilation) glycoprotein that is considered to be the initiator of the mineralization process by means of its affinity for calcium and its involvement in the formation of hydroxyapatite crystals. BSP, as all members of the SIBLING family, contains a RGD domain (Arg-Gly-Asn), the cell attachment consensus sequence that binds to the integrin class of cell surface molecules. Thus, bone cells can bind to RGD sequences thereby promoting bone formation but BSP (together with osteopontin) is known to additionally anchor osteoclasts and so it has a role also in bone resorption. Actually, BSP is expressed by hypertrophic chondrocytes, osteoblasts, osteocytes and osteoclasts (Yingzi Yang, 2013).

Osteopontin (OPN) is also a glycoprotein of the SIBLING family with similar functions to those of BSP and as stated above, is considered to play a significant role in both mineralization and resorption bone.

Other important glycoproteins are osteonectin (ON) and alkaline phosphatase (ALP). ALP is an enzyme primarily bound to the cell surface through a phosphoinositol linkage that is cleaved and therefore it can be found within the mineralized matrix. It is known that ALP hydrolyzes inhibitors of mineral deposition such as pyrophosphates (PPi) providing inorganic phosphate (Pi), which increases local phosphate concentration, and facilitates hydroxyapatite formation therefore promoting mineralization (Orimo, 2010). Balance between the concentration of PPi and Pi is thought to be critical in the

mineralization process and in fact, mice lacking tissue non-specific ALP have impaired mineralization (Anderson et al., 2004).

Osteonectin is a phosphorylated glycoprotein that is transiently produced in non-bone tissues that are rapidly proliferating or remodeling but it is also found constitutively expressed in other tissues. This ubiquitous expression is indicative of a fundamental biological role besides its positive role in bone formation (Boskey et al., 2003). ON is secreted by osteoblasts and has affinity for collagen fibers.

Osteocalcin (OC) also named bone gla protein (BGP, BGLAP) is classified as a Gla-containing protein and is the most abundant protein within the group of non-collagenous proteins. OC is produced specifically by osteoblasts being an important osteoblast marker during differentiation. First approaches to osteocalcin role in bone development were disappointing since *Bglap*-null mice were essentially normal, just presenting a slightly increase in its bone mineral density (BMD) (Ducy et al., 1996). Osteocalcin carries three glutamic acid (Gla) residues that once carboxylated, enhance calcium binding thereby stabilizing hydroxyapatite in the matrix and therefore having a role in the control of mineral deposition and remodeling. OC decarboxylation increases its solubility becoming an endocrine factor able to impact distant organs others than bone. Actually, OC has been described as an osteoblast specific hormone and has been reported to be involved in the regulation of energy and glucose metabolism in mice as well as to affect male fertility through its action on the Leyding cells of the testis (Karsenty and Oury, 2014; Lee et al., 2007; Oury et al., 2013). γ-carboxylation of osteocalcin occurs inside the endoplasmic reticulum of the osteoblast and requires vitamin K as a co-factor. When the ECM is reabsorbed by the action of osteoclasts an acidic environment is produced (pH: 4.5), fact that produces the chemical decarboxylation of the osteocalcin. OC measurements in serum have been proved as a valuable marker of bone turnover since the ratio of carboxilated and undercarboxylated osteocalcin (unOC) can indicate some metabolic disease states.

Obviously, there are additional proteins as fibromodulin (FMOD) or osteoglicin (OGN) as well as other numerous minor components in bone tissue that can affect its properties.

1.1.2 Bone cells

In bone, as well as in cartilage, the ECM resident cells produce local factors, inflammatory mediators, and matrix-degrading enzymes. Different cell types are essential for a normal bone development and function.

Chondrocytes

Chondrocytes (cartilage-forming cells) derive from osteo-chondroprogenitors and are the first skeleton-specific cell type to appear during development. Their role goes beyond allowing bone formation to occur. Indeed, chondrocytes are required for the longitudinal growth of the skeleton and are also needed in joints to allow mobility of various skeletal elements. In osteochondral ossification, once progenitors commit to the chondrocytic fate, they further differentiate into chondrocytes, which proliferate, mature, exit the cell cycle and undergo hypertrophy, forming an avascular cartilaginous template. This process will be more accurately described in section 1.2.2. Chondrocytes secrete matrix elements as type II collagen, aggrecan and other matrix molecules. As development proceeds, hypertrophic chondrocytes express collagen X and direct the mineralization of the surrounding matrix while signaling to adjacent perichondrial cells to direct their differentiation into osteoblasts. Moreover, they also stimulate the invasion of blood vessels (Karaplis, 2008)

Osteoblasts and osteocytes

Osteoblasts are the responsible for the production and secretion of bone matrix elements. Moreover, osteoblasts produce a range of growth factors including insulin-like growth factors (IGFs), platelet-derived growth factor (PDGF), transforming growth factor-beta (TGFβ) and bone morphogenetic proteins (BMPs). They originate from multipotent mesenchymal stem cells (MSCs), which also have the capacity to differentiate into adipocytes, chondrocytes, myoblasts or fibroblasts. Osteoblasts represent around 5 to 10% of the total amount of bone cells and their activity is regulated in an autocrine and paracrine manner by the factors above-mentioned (Karaplis, 2008).

During bone formation, osteoblasts produce matrix components that will further mineralize, leaving some mature osteoblasts entrapped in the new bone matrix (osteoid). These cells are further called osteocytes and represent around 95% of all the bone cells. Compared to osteoblasts, they reduce their activity but still produce matrix proteins. Moreover, they change from the osteoblast cuboidal shape to a dendritic morphology. Osteocytes form numerous long cell processes before matrix calcification, which results in a network of thin canaliculi that permeates the entire bone matrix. They are also responsible for the transduction of mechanical stimuli into chemical signaling cascades. Older osteocytes are located deeper within the calcified bone and are finally phagocytized and digested during osteoclastic bone resorption. Recent studies also involved osteocytes as a main source of RANKL (receptor activator of NFκB ligand) and therefore tightly related to bone resorption (O'Brien et al., 2013; Yingzi Yang, 2013). Different *in vivo* models based on a thymidine-kinase transgene

were used to totally deplete osteoblasts but not osteocytes. These phenotypes revealed no changes in bone resorption markers neither in basal or PTH (parathyroid hormone) stimulated RANKL mRNA levels, despite the lack of bone formation (Corral et al., 1998; Galli et al., 2009). Moreover, additional researches demonstrated that osteoclast formation was greatly reduced in genetically manipulated mice that selectively lack RANKL in osteocytes (Nakashima et al., 2011; Xiong et al., 2011).

Some osteoblasts that are not embedded during matrix mineralization remain on the bone surface, becoming the so-called flat lining cells (or bone-lining cells). The rest will undergo programmed cell death (apoptosis).

Osteoclasts

Unlike osteoblasts and osteocytes, osteoclasts arise from a hematopoietic origin (mononuclear lineage). They are giant multinucleated cells mainly found in contact with a calcified bone surface within a lacuna, result of its own resorptive activity. Osteoclasts resorb bone by acidification and proteolysis of the bone matrix. After adhesion to the ECM, osteoclasts mobilize the hydroxyapatite crystals by digestion of their link to collagen and the residual collagen fibers are digested by either cathepsins or activated collagenases. Thus, they are in charge of the degradation and therefore of the remodeling of the bone tissue. Further information about molecular mechanisms involved in osteoclast differentiation will be addressed in section 2.3.

1.2 Skeletal Morphogenesis

1.2.1 Early skeletal patterning

Cartilage and bone tissues are mesoderm-derived tissues formed by chondrocytes and osteoblasts respectively, during embryogenesis. A common mesenchymal progenitor cell, known as osteochondral progenitor, gives rise to both chondrocytes and osteoblasts.

Two different phases can be distinguished in skeletogenesis. The first phase is the formation of mesenchymal condensations and is also referenced as skeletal patterning. In this step, mesenchymal progenitor cells aggregate at the future skeletal locations and take the shape of the skeletal elements to be. Axial skeletal elements arise thanks to somites (segmented mesodermal structures located on either sides of the neural tube) and its patterning is controlled by a traveling wave of cycling gene expression generated by Notch, Wnt/β-catenin and fibroblast growth factor signaling pathways. Lateral plate mesoderm forms the limb mesenchyme, from which limb appendages are derived. Limb patterning and growth along the proximal-distal,

anterior-posterior and dorsal-ventral axes are controlled by signaling interactions and feedback loops involving FGF, Wnt, Sonic Hedgehog (Shh) and BMPs. However, although mesenchymal cells driving skeletal patterning during embryogenesis mostly proceed from a mesoderm origin, they can also come from other cell lineages. It is the case of the neural crest cells, which come from ectodermic origin and give rise to craniofacial bones after a trans-differentiation process called epithelial-to-mesenchymal transition (EMT). Thus, skeletal patterning is mediated by several major signaling pathways that are also used later in skeletal development to control other processes such as cell fate determination, proliferation or maturation (Yingzi Yang, 2013).

During the second phase of skeletogenesis, the differentiation of the three bone-specific cell types occurs together with a vascular invasion that allows the final bone formation. The cell differentiation process of the three lineages (chondrocytes in cartilage and osteoblast and osteoclasts in bone) occurs thanks to a series of complex and finely tuned mechanisms involving several transcription factors. After the formation of mesenchymal aggregates, osteochondral progenitors in these condensations must form either chondrocytes or osteoblasts. SOX9 and RUNX2 are master transcription factors required for the determination of chondrocyte and osteoblast cell fates and are co-expressed in the osteochondral progenitors. The molecular mechanisms involved in the differentiation of each cell type will be covered later in this thesis (see chapter 2) (Karaplis, 2008; Yingzi Yang, 2013).

1.2.2 Embryonic development

Bone formation can be achieved throughout two different mechanisms, both of them initiated by the above-mentioned condensations of mesenchymal tissue. Thus, bone can develop by endochondral ossification (mesenchymal stem cells differentiate into chondrocytes that form a cartilaginous matrix template that will be progressively replaced by bone matrix) or by intramembranous ossification (direct differentiation of mesenchymal cells into osteoblasts).

Endochondral bone formation

Endochondral bone formation is the main type of ossification by which skeletal elements arise and is the responsible for the formation of the axial and appendicular skeleton. It is also involved in the longitudinal growth of long bones and in fracture healing. The main distinctive trait of endochondral bone formation is that a cartilage mold is formed before the ultimate bone structure (Figure I-1).

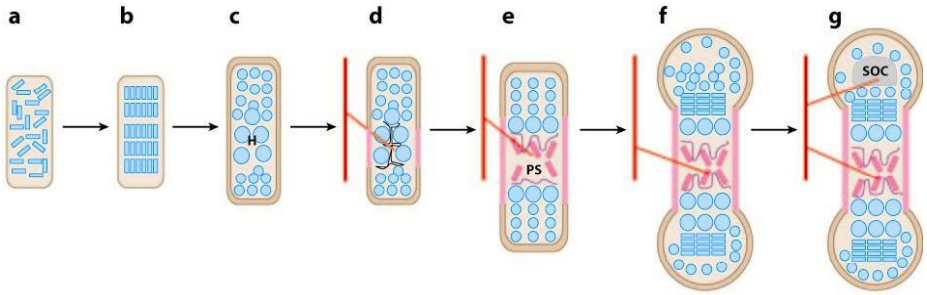

Figure I-1. Schematic representation of endochondral bone formation. (a) Mesenchymal cells (blue) condense in the location of the future skeletal element. **(b)** Cells of condensations differentiate in chondrocytes and start to proliferate. **(c)** Hypertrophic chondrocyte differentiation. **(d)** Perichondrial cells differentiate in osteoblasts, forming bone collar (pink). Hypertrophic chondrocyte apoptosis favors matrix mineralization and blood vessel invasion (red). **(e)** Osteoblasts accompany vascular invasion, forming the primary spongiosa (PS). **(f)** Chondrocytes continue to proliferate, lengthening the bone. Osteoblasts of primary spongiosa form trabecular bone, while at the bone collar osteoblasts form cortical bone. **(g)** The secondary ossification center (SOC) forms through cycles of chondrocyte hypertrophy, vascular invasion, and osteoblast activity. Adapted from (Karsenty et al., 2009).

After early patterning events, mesenchymal condensations are determined. Subsequently, during endochondral ossification and around embryonic day 10.5 in mouse (E10.5), cells from mesenchymal aggregates differentiate into chondrocytes and start to produce an ECM made of type II rather than type I collagen (as it was the case of mesenchymal cells). Furthermore, while chondrocytes start proliferating, cells at the periphery do not differentiate into chondrocytes and keep producing type I collagen creating a structure called perichondrium. Around E13.4 chondrocytes located in the center of the condensations stop proliferating and begin to elongate to form pre-hypertrophic chondrocytes. At some point, pre-hypertrophic chondrocytes exit the cell cycle and become bona fide hypertrophic chondrocytes changing their production of type II for the type X collagen (Figure I-1) (Karsenty et al., 2009; Yingzi Yang, 2013).

While hypertrophic chondrocytes undergo apoptosis, blood vessels invade the hypertrophic cartilage to form a nascent bone marrow cavity. The role of the invading blood vessels is to bring perichondrial cells that will differentiate into mature osteoblasts to the middle of the cartilage mold, forming de so-called primary spongiosa (PS) (Figure I-1). Moreover, blood vessel will also supply the osteoclast-like resorptive cells that will degrade the existing cartilage matrix to produce the marrow cavity. This region is also known as primary ossification center (POC). Cells from perichondrium that achieve the POC ultimately become osteoblasts and produce a bone matrix rich in type I collagen on top of the ECM-rich type X collagen. While osteoblasts within POC will produce the trabecular bone, osteoblasts from perichondrium will generate cortical bone (Karsenty et al., 2009).

Proliferating and hypertrophic chondrocytes become arranged in columns into an avascular structure called the growth plate that is found at each end of the expanding bone. The same sequence of events is present in this growth plate: proliferation, hypertrophy and apoptosis of chondrocytes and the subsequent replacement of the cartilaginous ECM for the bone ECM. These events will produce the longitudinal growth of long bones establishing the secondary ossification center (SOC) (Karsenty et al., 2009).

Intramembranous ossification

Intramembranous ossification is responsible for the formation of the flat bones of the skull, some facial bones and others. It also takes place in the transversal growth of the long bones and in fracture healing.

Unlike endochondral ossification, mesenchymal cells from condensations directly differentiate into osteoblasts, producing and secreting the elements of the ECM that will further surround them becoming osteocytes. Meanwhile, peripheral mesenchymal cells remain as osteoprogenitors in order to give rise to new osteoblasts during bone growth.

1.3 Bone Remodeling

Bone is a highly dynamic tissue and an important site of continuous tissue remodeling during development, homeostasis and repair. Adult bone is continually remodeled throughout life by a physiological process called bone remodeling in which old bone is replaced by new tissue. Moreover, remodeling is also initiated after bone lesion or injury, leading to bone repair or bone regeneration.

The remodeling cycle occurs continuously at discrete sites throughout the skeleton in response to mechanical and metabolic influences. Bone remodeling requires the coupled activities of bone resorption and bone formation directed by osteoclasts and osteoblasts respectively and any imbalance between both processes may lead to metabolic bone diseases, such as osteoporosis. The coordinated actions of osteoblasts and osteoclasts are described as the basic multicellular unit (BMU) in which the amount of bone destroyed by osteoclasts in these units counterpart the amount of bone produced by osteoblasts (Figure I-2). The BMUs in cortical and trabecular bone differ greatly in their structures and in the way in which they remove and replace bone (Hadjidakis and Androulakis, 2006; Sims and Gooi, 2008).

It has been shown that also bone-lining cells exert crucial activities for bone remodeling. After osteoclast activity, bone-lining cells enter the lacuna in order to clean its bottom from bone matrix leftovers (Everts et al., 2002).

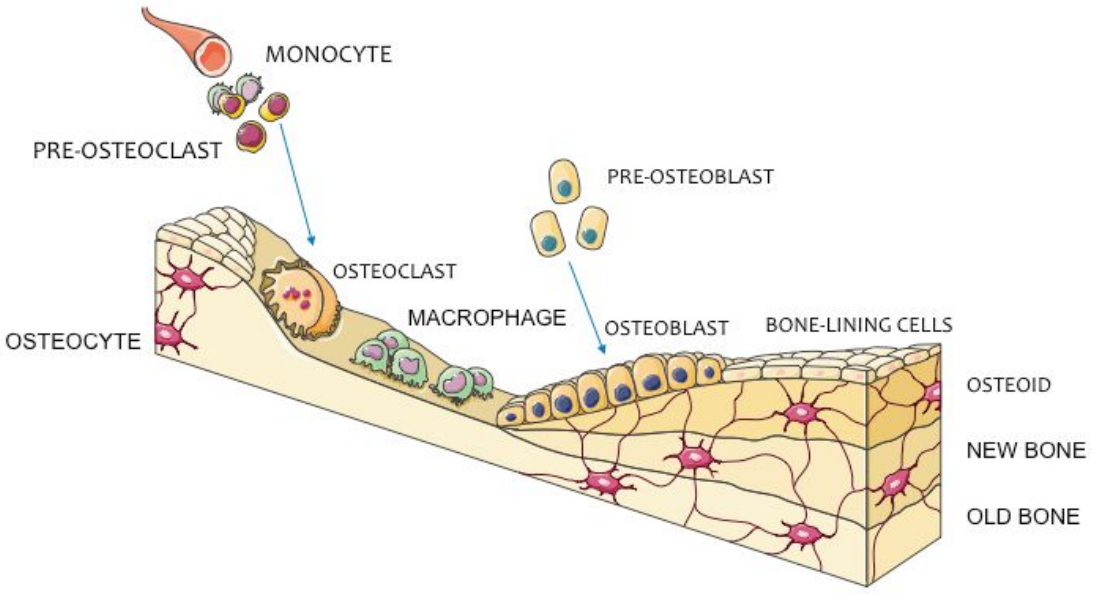

Figure I-2. Basic multicellular unit. Bone remodeling is a lifelong process where mature bone tissue is removed from the skeleton by activated osteoclasts (bone resorption) and is replaced by new bone tissue. Image from Servier Medical Art.

2 TRANSCRIPTIONAL REGULATION OF BONE DEVELOPMENT

Multipotential mesenchymal stem cells are a heterogeneous cell population that can differentiate into osteoblasts, chondroblasts, adipocytes and myoblasts. MSCs were first isolated from bone marrow (bone marrow mesenchymal stem cells, BM-MSCs) although later MSCs from other origins have been described. Differentiation toward these lineages is controlled by a multitude of cytokines, which regulate the expression of cell-lineage specific sets of transcription factors. Among the cytokines involved in osteoblast differentiation are the Hedgehogs, BMPs, IGFs, TGFβ, PTH and Wnts. The signal transduction cascades initiated by some of these cytokines and their effect on osteoblast differentiation will be discussed in further chapters (see chapters 3 & 4).

2.1 Transcriptional Control of Osteoblast Differentiation

Lineage commitment from MSC to osteoblast has been well characterized. As previously mentioned, during embryogenesis bone development occurs either by endochondral or intramembranous ossification. In both mechanisms, osteoblasts and chondrocytes arise from mesenchymal cell condensations and the factors that contribute to the transcriptional control of these differentiation processes have been widely studied (Karsenty, 2008; Nakashima and de Crombrugghe, 2003). *Osterix* (*Osx*), *Runx2*, *Dlx5*, *Msx2* and *Atf4*, among others, have been identified as essential transcription factors for osteoblast differentiation (Karsenty, 2008; Nakashima and de Crombrugghe, 2003).

From a common osteo-chondroprogenitor, the osteoblast differentiation process encompasses different well-characterized stages. The above-mentioned transcription factors (*Osx*, *Runx2*, *Atf4*) are indispensible to induce the progression towards the osteocyte fate, the most mature form of differentiation. Furthermore, each step of osteoblast progression can be clearly recognized by a cohort of molecules differentially expressed (Figure I-3). RUNX2 plays an essential role in the first step of differentiation into pre-osteoblast. Pre-osteoblast specific markers include *alkaline phosphatase (Alpl)* and low levels of *type I collagen (Col1a1)*. Later, they require osterix (OSX) to reach the mature osteoblast stage and to be able to synthesize extracellular matrix proteins. Functional osteoblasts additionally express osteocalcin and bone sialoprotein markers and they are responsible for the future mineralized bone matrix. While the majority of osteoblast population undergoes apoptosis, a small fraction will differentiate into osteocyte after matrix-embedded and will work as important mechano-sensors controlling bone formation (Karsenty, 2008).

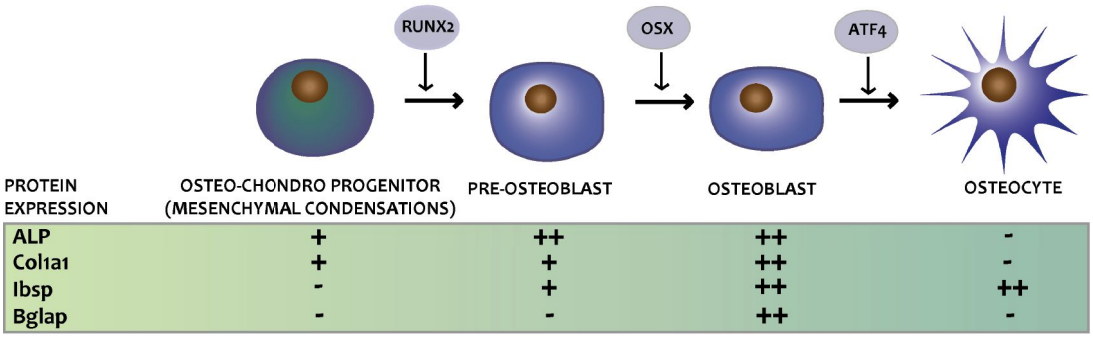

Figure I-3. Osteoblast differentiation regulation by transcription factors. The key osteogenic factors RUNX2 and OSX drive the differentiation of cells from mesenchymal condensations towards osteoblast. In the green box the relative expression of the main proteins present in bone ECM during the different osteoblast differentiation steps.

2.1.1 Runx2

Runx2 (runt-related transcription factor 2)/*Cbfa1* (core-binding factor α1) is the first to be expressed in mesenchymal condensations and from the perspective of molecular biology, it is one of the key transcription factors, together with *Osterix* (Ducy, 2000; Ducy et al., 1999; Karsenty et al., 1999). *Runx2* is expressed as early as E10.5 and is necessary and sufficient to identify cells as osteo-chondroprogenitors, since *Runx2*-null mice are unable to produce mature osteoblasts (Ducy et al., 1997; Komori et al., 1997; Nakashima and de Crombrugghe, 2003). From this stage to chondroblast commitment, *Runx2* levels decrease until almost disappearing at E16.5, whereas in osteoblast differentiation *Runx2* expression remains and induces osteocalcin at around E15.5.

Even so, the levels of *Runx2* during osteoblast differentiation are also fluctuant. While *Runx2* is crucial for the initial steps of osteoblast commitment, studies forcing ectopic overexpression of this transcription factor showed abnormal maturation of the osteoblasts, thereby suggesting that *Runx2* reduction is essential at the latest steps of differentiation (Komori, 2006; Liu et al., 2001).

The Runx family (including *Runx1*, *Runx2* and *Runx3*) is characterized by the presence of a runt domain, a 128-length amino acid domain able to bind to specific consensus DNA sequences 5'-PuACCPuCCA-3' (Ziros et al., 2008). RUNX2 is functionally bound to Cbfβ, establishing a heteromeric complex that works as a transcription factor (Tang et al., 2000). Although Cbfβ is necessary for Runx2 function in bone development, the mice phenotype derived from the lack of *Cbfβ* is milder than the resulting from the *Runx2* loss, suggesting that RUNX2 can somehow regulate bone formation without Cbfβ (Kundu et al., 2002; Nakashima and de Crombrugghe, 2003). Studies suggest that Cbfβ does not bind to DNA itself but enhances the DNA-binding capacity of Runx proteins and increases their half-life by stabilizing them against degradation (Huang et al., 2001; Ziros et al., 2008).

Two different isoforms from *Runx2* gene can be found. The expression of the *Runx2* gene is controlled by two promoters that are separated by exon 1 and a large intron. The proximal (P2) and the distal (P1) promoter generate two major transcripts, namely type I (starting with the sequence MRIPV) and type II (starting with the sequence MASNS) respectively. These promoters give rise to two RUNX2 isoforms with distinct N-terminal length but without any major impact in their activity. Although both isoforms are expressed in chondrocytes and osteoblasts, type II isoform is mainly found in osteoblasts and therefore P1 is considered the bone-specific promoter (Stock and Otto, 2005; Ziros et al., 2008).

In humans, heterozygous insertions, deletions and non-sense mutations leading to translational stop codons in the DNA-binding domain or in the C-terminal trans-activating region of the *Runx2* gene underlie the rare skeletal disorder cleidocranial dysplasia (CCD), characterized by defective development of cranial bones (Lee et al., 1997; Mundlos et al., 1997; Otto et al., 1997).

Runx2 expression is regulated by several signaling pathways, including vitamin D3 (1,25(OH)2D3), Wnt and TGFβ/BMP2, among others. SMAD1 and SMAD3 are proteins involved in the signal transduction of BMPs and TGFβ respectively. Both interact with RUNX2 and are involved in its transcriptional regulation activity (Zhang et al., 2000). Among the negative upstream factors regulating RUNX2 there are *Twist*, *Hoxa2* or *p53*. Moreover, RUNX2 also acts as a transcriptional repressor of itself through binding to the response elements present in its own promoter (Drissi et al., 2000).

RUNX2 regulates the expression of numerous osteoblastic genes such as *SP7/Osterix*, *Alpl (alkaline phosphatase)*, *Col1a1*, *Spp1 (osteopontin)*, *Ibsp (bone sialoprotein)* and *Bglap (osteocalcin)* (Ducy and Karsenty, 1995; Ducy et al., 1997). RUNX2 operates by binding to the osteoblast specific cis-acting element 2 (OSE2), which is found in the regulatory region of all main osteoblast-related genes.

Post-transcriptional modifications also regulate *Runx2* expression mainly by ERK/MAPKs (extracellular singal-regulated kinase/mitogen activated protein kinases) phosphorylations and by the effect of several microRNAs on its 3'UTR.

2.1.2 Osterix

Following expression of *Runx2* in osteoprogenitors, *Osterix* further strengthens the establishment of bone cell phenotype. *Osx/SP7* belongs to the Sp/Kruppel-like family of transcription factors because of its characteristic DNA-binding domain (DBD) consisting of three tandem C2H2-type zinc finger motifs at the C-terminus. These zinc-fingers allow DNA binding to GC rich DNA sequences, a characteristic of the *Sp* family members (Nakashima et al., 2002). *Sp* transcription factors have the ability to recruit the transcription complex TFIID (transcription factor II D), thereby initiating the transcription of genes that do not contain TATA boxes. In fact, osterix does not bind to TATA Binding Protein (TBP) but to TFIID (Hatta et al., 2006). Moreover OSX also recruits a transcriptional co-regulator called Brg-1 (brahma-related gene-1) at its C-terminal region. Osterix sequence also contains a proline-rich region (PRR) close to its N-terminal end.

There are two different isoforms of *Osx*, a long and a short one. The long one is the main isoform and the difference with the short one lies in the 5' extreme, since they use two different alternatively spliced first exons (Gao et al., 2004; Milona et al., 2003).

During embryonic development, *Osterix* expression starts in differentiating chondroblasts, in the surrounding perichondrium and in the mesenchymal condensations of the intramembranous ossification bones.

Osx expression begins at around day E13.5 and promotes the expression of osteoblast markers such as *Alpl*, *Ibsp*, *Col1a1* and *Bglap* and thereby is critical for the switch from pre-osteoblasts to functional osteoblasts and for the expression of the proteins of the ECM (Nakashima et al., 2002; Ortuno et al., 2013).

Osterix is located downstream of *Runx2* since *Osx*-null mutant mice *Runx2* expression is comparable to that of wild-type (Nakashima and de Crombrugghe, 2003). Actually, RUNX2 directly binds to *Osx* promoter since the promoter of the *Osx* gene contains a consensus Runx2-binding sequence (Nakashima et al., 2002; Nishio et al., 2006;

Yoshida et al., 2012). However, BMP regulation of *Osterix* can be either dependent or independent of RUNX2 (Lee et al., 2003; Ulsamer et al., 2008). Furthermore, several studies are focused on a possible Runx2-Osx cooperation. Nishimura et al. demonstrated direct binding of both transcription factors for the regulation of the matrix metalloproteinase 13 (MMP13) activity (Nishimura et al., 2012) and our group has also described cooperation of both proteins in the induction of *Col1a1*, *Fmod* and *Ibsp* mRNAs (Artigas et al., 2014; Ortuno et al., 2013).

Osterix has been shown to be positively regulated by BMP, IGF1 and MAPK signaling pathways in undifferentiated MSCs (Celil and Campbell, 2005; Celil et al., 2005), and can also regulate its own expression by interacting with its own promoter (Yoshida et al., 2012). Other known positive-regulators of osteoblast function as ascorbic acid or vitamin D3 are also regulating *Osterix* expression. The transcriptional activity of Osterix can be also regulated by post-transcriptional modifications such as MAPK phosphorylations (Artigas et al., 2014; Choi et al., 2011; Ortuno et al., 2010) or the activity of several microRNAs.

2.1.3 Dlx5

Dlx5 (distal-less homeodomain-containing family 5) belongs to the homeodomain family and is a BMP-responsive gene activated through a responsive element in its proximal promoter (Miyama et al., 1999). It is part of the Distal-less homeobox factors (Dlx) and acts as a transcription factor for important osteoblastic genes.

DLX5 activates *Runx2* since multiple elements of response have been identified in the *Runx2* promoter (Hassan et al., 2006; Lee et al., 2005). Although *Dlx5* knockout mice have severe developmental defects mainly at craniofacial level, *Runx2* expression is not affected (Acampora et al., 1999). Thus, this and other studies suggest that even though *Dlx5* is able to work as a transcription factor for *Runx2* in osteo-chondroprogenitors, it is not essential for its expression (Liu et al., 2007a; Robledo et al., 2002).

Osteocalcin and alkaline phosphatase are also targets of DLX5 hereby mediating their expression. Moreover, *Dlx5* is related to *Msx2* in terms of cooperation for the expression of some genes as *Osteocalcin*. However direct competition of Dlx5 and Msx2 for the same DNA binding site has been reported, as in the case of *Alpl* (Acampora et al., 1999; Kim et al., 2004; Miyama et al., 1999). MSX2 and DLX5 recognize the same response elements (homeodomain type, ATTA) therefore competing for the binding to other genes as *Runx2* or *Col1a1* (Dodig et al., 1996; Lee et al., 2005).

Our group elucidated that *Dlx5* interacts with the *Osx* promoter, which mediates the induction of *Osx* after BMP-2 stimulation independently of RUNX2 activity. Moreover, *Dlx5* is modified post-transcriptionally by p38 increasing its transactivation activity (Ulsamer et al., 2008).

2.1.4 Others transcription factors: Msx2, ATF4, AP1.

A growing number of transcription factors have been identified during bone formation. *Msx2* is also a homeodomain-containing transcription factor and appear to act mainly as a negative regulator of osteogenesis. It has been above described the direct competition between DLX5 and MSX2 for the same binding site in genes involved in osteoblast differentiation. *Msx2* is expressed in osteoprecursors and then diminishes during progression to osteoblast. However, *Msx2*-null mice present bone developmental defects (Satokata et al., 2000).

ATF4 (activating transcription factor 4) is a member of the CREB (cAMP response element-binding) family and seems to exert an important role by assuring that osteoblasts fulfill their function. *Atf4*-deficient mice display a delayed skeletal development and thereafter develop a severe low-bone-mass phenotype (Yang et al., 2004). Moreover, ATF4 is also involved in the osteoclast differentiation and its important paper in amino acid import into cells favors the synthesis of type I collagen (Karsenty, 2008; Karsenty et al., 2009).

Activator proteins 1 (AP1) are a small family of transcription factors that includes proteins of the Jun and Fos family. *JunB* a member of the Jun family display a positive role in bone formation as validated by its knockout mice (Kenner et al., 2004).

Importantly, although the most important genes have been reviewed in this introduction chapter, several other genes are affecting each of the transcription factors described above and many other genes have been studied in regarding to their impact in bone development.

2.2 Regulation of Chondroblast Differentiation

During chondrocyte commitment from MSCs, RUNX2 transcription factor also develops an important paper due to its inhibitory effect. Additionally, RUNX2 (and RUNX3) are transiently necessary for pre-hypertrophic chondrocytes to further arise hypertrophic (Yoshida et al., 2004)

Sox9 (Sry-related HMG box) is one of the main characters of chondrocyte differentiation and its absence leads to a failure in chondrocyte commitment in *Sox9*$^{-/-}$

MSCs or knock out mice. The lack of *Sox9* in these models produce several alterations although it has been proved that other members of the same family also play important roles (Bi et al., 1999b; Bi et al., 2001; Lefebvre et al., 2001; Mori-Akiyama et al., 2003). *Sox9* is an early chondrogenic marker and is necessary for commitment of osteo-chondroprogenitors and for *Runx2* expression during mesenchymal condensations generation because *Sox9* inactivation at this moment has been proved to revoke this process (Akiyama et al., 2002; Akiyama et al., 2005).

2.3 Regulation of Osteoclast Differentiation

The step from pre-osteoclast mononuclear cells to osteoclasts is dependent on cell-cell fusion, and is controlled by a chronological exposure of specific factors that activate intracellular signaling cascades (Figure I-4). M-CSF (macrophage colony-stimulating factor) and RANKL (receptor activator of NFκB ligand) are the two main cytokines involved in osteoclast differentiation (Manolagas, 2000). M-CSF activates c-Fms receptor, present in early osteoclast precursor, and acts as a survival/proliferation factor by activating other molecules as AKT, microphthalmia transcription factor (MITF) or the anti-apoptotic protein Bcl-2 (B-cell leukemia/lymphoma-associated gene 2). Moreover, M-CSF stimulates the expression of RANK (receptor activator of NFκB).

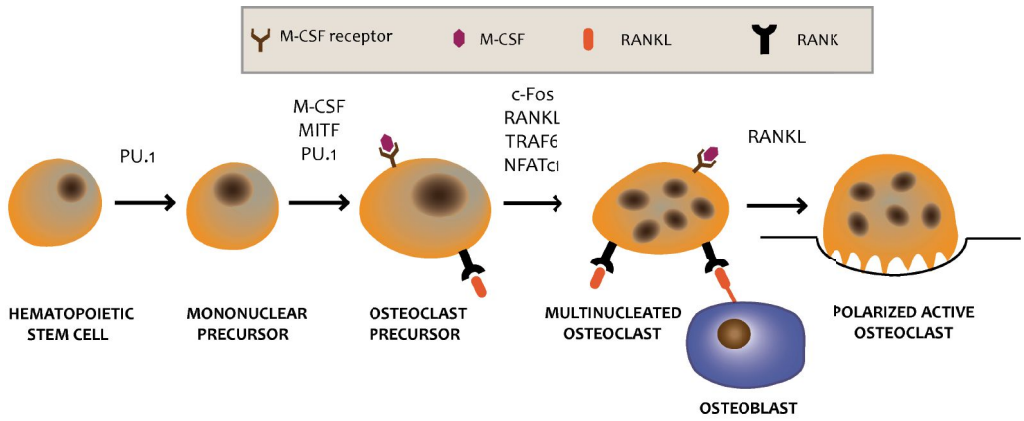

Figure I-4. Osteoclast differentiation and activation. Osteoclast transcription factors are represented in the osteoclastic differentiation step where they act. Osteoblast-osteoclast communication is also represented in final steps of osteoclast differentiation where is necessary for the achievement of a fully activated osteoclast.

Rankl is a member of the TNFα superfamily present in osteoblasts and stromal cells and can be a membrane-anchored molecule but can also be released as a soluble molecule following proteolytic cleavage. The RANK-RANKL signaling system links osteoblast lineage and hematopoietic-derived cells for osteoclast differentiation and

activation. Together with M-CSF, RANK signaling is the main signaling pathway in terms of osteoclast maturation (Tanaka et al., 2005). RANK stimulation leads to the recruitment of TNF receptor-associated cytoplasmic factors (TRAFs), mainly TRAF6, leading to the activation of several pathways, including the nuclear factor and activator of transcription NFATc1. NFATc1 is widely accepted as the key transcription factor in osteoclast differentiation (Gohda et al., 2005; Kobayashi et al., 2001). NFATc1 eventually regulates several osteoclast-specific genes in cooperation with other transcription factors: AP-1, PU.1, Mitf and c-Fos (Crotti et al., 2008; Takayanagi et al., 2002; Tondravi et al., 1997). Their transcriptional targets are osteoclast-specific genes such as tartrate-resistant acid phosphatase (TRAP), cathepsin K, calcitonin receptor or DC-STAMP (dendritic cell-specific transmembrane protein) (Kukita et al., 2004).

RANK signaling can be blocked by OPG (osteoprotegerin), therefore inhibiting osteoclast differentiation due to suppression of RANKL stimuli. OPG is produced by osteoblasts and is also known as tumor necrosis factor receptor superfamily member IIB (TNFRSF11B). OPG is a decoy receptor for RANKL, thereby reducing the differentiation of osteoclasts precursors. Thus, the RANKL/OPG ratio must be accurately balanced in order to control osteoclastogenesis.

Several other proteins are needed for a fully osteoclast activity as integrin β_3 (important for the recognition and attachment to bone matrix), matrix-degrading enzymes as matrix metalloproteinases (MMP) and cathepsin K, which are released through the ruffled border membrane enabling the decalcification and degradation of the bone matrix.

3 BONE MORPHOGENETIC PROTEINS

Bone morphogenetic proteins (BMPs) are the largest subfamily of the TGFβ superfamily and are profoundly involved in skeletogenesis (Miyazono et al., 2010; Shi and Massague, 2003). They were originally identified as factors that induce bone formation when implanted at ectopic sites (Urist, 1965).

BMPs are synthesized as large precursor proteins that are first secreted and then proteolitically cleaved upon dimerization by serine proteases (Cui et al., 1998). The mature forms derive from the C-terminal region and may form homodimers by means of disulfide bonds in order to be functional (Massague, 1990; Scheufler et al., 1999). There are more than 20 members within BMP family that can be further classified in at least four groups according to the similarity of their sequence: BMP-2/4 group, BMP-5/6/7/8 group, growth and differentiation factor-5/-6/-7 (GDF-5/6/7) group and BMP-9/10 group (Massague, 1998; Massague et al., 1994; Wagner et al., 2010).

BMPs function is essential for osteoblast differentiation and bone homeostasis but its expression is also crucial during embryonic development where BMP gradient together with other cytokines orchestrate the skeletal patterning (Gurdon and Bourillot, 2001).

3.1 BMP Receptors

Bone morphogenetic proteins bind to a heterotetrameric complex of transmembrane receptors known as type I and II serine/threonine kinase receptors (Mueller and Nickel, 2012). Both types of receptors contain an N-terminal extracellular binding domain, a single transmembrane region, and an intracellular serine/threonine kinase domain

(Feng and Derynck, 2005; Miyazono et al., 2010; Shi and Massague, 2003). Strong evidence confirms that both type I and II receptors, acting in coordination, are required for complete signal transduction. BMPs can bind to type I in the absence of type II receptors but when both types are present in the membrane of target cells their binding affinity is highly increased (Hinck, 2012). Based on their structures and functions, type I BMP receptors can be divided into the Bmpr1A and Bmpr1B group (also known as Alk3 and Alk6) and the Acvrl1 and Acvr1 group (also known as Alk1 and Alk2) (Hinck, 2012). These groups show slight preferences for binding to specific BMPs. For instance, BMP-2 and -4 bind preferentially Bmpr1A and Bmpr1B whereas BMP-5, -6, and -7 additionally bind to Acvr1 (Liu et al., 1995). It is also well established that BMPs bind to three distinct type II receptors, namely Bmpr2, Acvr2A, and Acvr2B. Combinatorial interactions of different type I and II receptors should allow selectivity and specificity of ligand binding as well as intracellular signaling in target cells (Shi and Massague, 2003).

Type I receptors have a GS sequence (rich in glycine and serine) closed to the kinase domain, thereby hiding its active center. In the absence of ligand, small amounts of pre-existing homo- and hetero-dimer receptor complexes are present at the cell surface (Ehrlich et al., 2012). However, in the presence of BMP ligand dramatically increases oligomerization, and a complex including two receptors of each type is formed. Then, type II receptors phosphorylate type I in the GS sequences leading to their activation and autophosphorylation (Shi and Massague, 2003). Since type II receptors do not present GS sequences and kinase activity does not increase *in vitro* after ligand bound, these receptors are considered to be constitutively actives (Ventura et al., 1994). Thus, upon phosphorylation of GS sequences type I receptor becomes active and results the major intracellular transducer of the BMP pathway.

3.2 Smad Signaling Pathway, the BMP-Canonical Transcriptional Outcome

Smad family proteins were the first identified substrates for type I BMP receptors. Smad proteins are highly conserved and they have been classified in three groups according to their structural and functional properties: R-Smads (receptor-regulated Smads), Co-Smad (common mediator Smad) and I-Smads (inhibitory Smads) (Figure I-5).

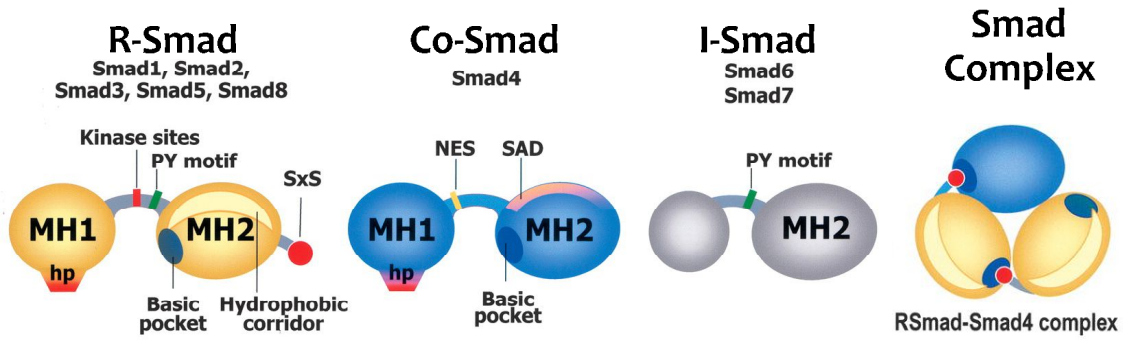

Figure I-5. Smad proteins and their structural elements. Smad proteins consist of two conserved globular domains—the MH1 and MH2 domains—and a variable linker region. In R-Smads and Smad4, the MH1 domain contains a β-hairpin structure for binding to DNA. I-Smads lack MH1 domain. The linker region of R-Smads contains multiple phosphorylation sites for MAPKs, CDKs, and other protein kinases. In R-Smads and I-Smads, the linker region contains a PY motif for recognition by Smurf ubiquitin ligases. The linker region of Smad4 contains an NES (Nuclear export signal). The MH2 domain contains a basic pocket for interaction with activated type I receptors in the case of the R-Smads, and in both the R-Smads and Smad4 for interaction with the pS–x–pS motif (red ball) of R-Smads (in Smad complexes). Schematic hetero-trimeric Smad complex consisting of two R-Smad molecules and one Smad4 (only the MH2 domains are shown). Adapted from (Massague et al., 2005).

R-Smads include Smad 1, 5 and 8 and they are formed by two different domains: an N-terminal domain or MH1 (mad homology domain 1) and a C-terminal domain MH2. A variable region named linker region binds both domains (Figure I-5). The MH2 domain is responsible for interaction with receptors, oligomer formation with other Smads, interaction with various DNA-binding proteins, and transcriptional activation. In basal conditions, R-Smads are auto-inhibited as monomers by the interaction between MH1 and MH2 domains. Once type I receptor (BMPRI) is phosphorylated and activated, phosphorylates R-Smads at the SXS (serine-x-serine) motif of the MH2 domain thereby disrupting the auto-inhibitory contact of Smad monomers and favoring the formation of complexes with other Smads (Feng and Derynck, 2005) (Shi et al., 1997). The activator C-terminal phosphorylation of R-Smads by BMP receptors is determined by the L45 loop present in the type I receptor which is only available in its active conformation (Feng and Derynck, 1997) (Feng and Derynck, 2005). Thus, R-Smad phosphorylation favors the formation of complexes composed by 2 R-Smads and 1 co-Smad (Smad4), interacting through their MH2 domain (Figure I-6).

Smad4 does not present any SXS domain so it cannot be phosphorylated by BMP receptors. However, its structure contains a nuclear import signal (NLS, nuclear localization signal) whose exposition is restricted to the conformation acquired while being part of the active R-Smad complexes. After translocation, they execute distinct transcriptional regulatory functions (Figure I-6) (Feng and Derynck, 2005; Hill, 2009).

Smad4 binds to specific DNA sequences (AGAC) named SBEs (Smad binding elements) and BMP-specific R-Smads bind to GC-rich sequences (GCCCGnCGC motif). For instance, R-Smads physically interact with RUNX2 upon activation of BMP receptors and they cooperatively activate the transcription of target genes, leading to induction of osteoblast differentiation (Zhang et al., 2000). *Osterix* is also induced by BMP in mesenchymal progenitor cells. Among the several BMP target genes, *Id* genes are induced by BMP in various cell types and are one of the most important targets of BMPs (Korchynskyi and ten Dijke, 2002; Miyazono and Miyazawa, 2002). Indeed, *Id1* gene is classified as an early response gene (expressed in mesenchymal cells 2 hours after BMP stimulation).

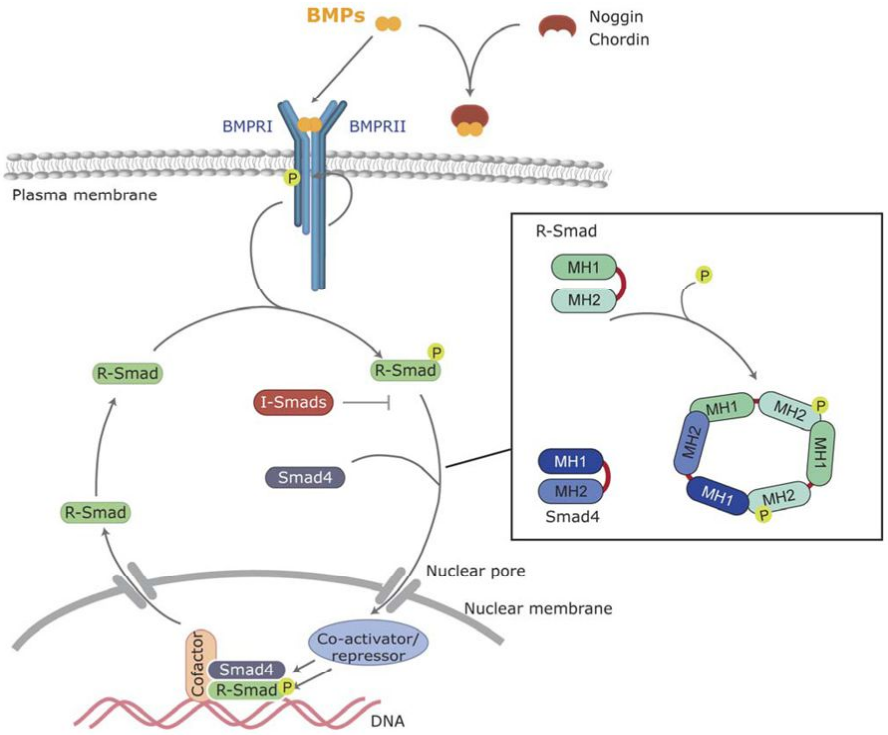

Figure I-6. Canonical BMP signaling. BMPs bind to the BMP receptors type I and II, and then type II receptor phosphorylates and activates the type I BMP receptor. Activated type I receptor phosphorylates R-Smads, which associate with the common Smad (Smad4) and enter the nucleus, where they regulate transcriptional processes. BMP signaling can be inhibited by extracellular antagonists, such as Noggin and Chordin, or intracellularly by I-Smads. From (Gamez et al., 2013).

Once the signaling is over and R-Smads are dephosphorylated by nuclear phosphatases, the dissociation of heterotrimeric complexes occurs. Smad4 is then moved to the cytoplasm thanks to its nuclear exportation peptide (NES, nuclear exportation signal) (Feng and Derynck, 2005; Massague et al., 2005). Thus, phosphatases play a role in regulating BMP signaling and distinct phosphatases have been proposed to catalyze the removal of phosphates from the SXS motifs such as

Small C-terminal domain phosphatases (SCPs) or PPM1A (protein phosphatase Mg^{2+}/Mn^{2+} dependent 1A) (Bruce and Sapkota, 2012).

Therefore, the Smad trimeric structure acts as a transcriptional complex able to drive the expression of multiple genes. Smads are regulating DNA expression by different mechanisms: direct DNA binding, interacting with other transcription factors bound to DNA or associating with chromatin remodelers, transcriptional co-activators or co-repressors (Shi and Massague, 2003).

Intracellular BMP signaling is subjected to a growing number of cross-talk mechanisms in order to integrate a final cell response. Smad6 and 7 are inhibitory Smads (I-Smads) that contain only a MH2 domain that varies greatly in comparison to the R-Smads (Figure I-5). Generally, I-Smads can exert their inhibitory role being part of the co-Smad/R-Smad complexes, modulating the ubiquitination and degradation of R-Smads and co-Smads and inhibiting the phosphorylation of Smads by binding to the receptor complexes (Derynck and Zhang, 2003; Wicks et al., 2006). Degradation of Smads is also regulated by mitogen-activated protein kinase and GSK3 (glycogen synthase kinase 3) phosphorylations, allowing specific interaction with MAP kinase and Wnt signaling cascades (Fuentealba et al., 2007).

3.3 BMP Antagonists

Apart from I-Smads, other molecules are regulating the BMP pathway in different steps of the BMP stimulus. Co-receptors have been shown to modulate ligand binding and downstream signaling events. For instance BAMBI (BMP and activin membrane-bound inhibitor homolog) is a transmembrane protein, structurally related to type I receptors that act as pseudoreceptor. BAMBI forms a stable receptor complex but, since it lacks the intracellular kinase domain, inhibits transduction by titrating available type II receptors (Onichtchouk et al., 1999).

Other molecules work as inhibitors by physically preventing BMPs from binding to their related receptors. Among these extracellular antagonists there is noggin, which can bind to BMP-2 (and also BMP-4 and -7) and prevent its binding to BMP receptors through blocking of the epitopes needed for receptor binding (Figure I-6). Basal levels of noggin in osteoblasts are limited but they increase after BMP-2,-4 and -6 stimulation, as a negative feedback limiting excessive exposure of skeletal cells to BMPs (Gazzerro and Canalis, 2006). Detailed mutational analysis excluded noggin mutations as a cause for fibrodysplasia ossificans progressiva (FOP) as was previously suggested (Xu et al., 2000).

Similarly to noggin, chordin also blocks the binding of BMP-2, -4 and -7 to their receptor (Figure I-6). Chordin and BMP form a complex that becomes a substrate for the zinc metalloprotease BMP-1/tolloid, which cleaves chordin and inactivates its biological activity releasing free BMPs to the extracellular space (Gazzerro and Canalis, 2006). Moreover, the cleavage of chordin by BMP-1 is modulated by twisted gastrulation (TSG), which can associate with the chordin/BMP/BMP-1 complex enhancing chordin proteolysis by BMP-1 and favoring the release of BMPs. Chordin is expressed mainly in undifferentiated chondrocytes where it acts as an inhibitor of cell differentiation but its expression in osteoblast cells is limited. Other members of chordin family are involved in BMP signaling regulation, most of them as BMP antagonists although some of them can also promote BMP effects (Gazzerro and Canalis, 2006).

Twisted gastrulation is required for the proper establishment of the dorso-ventral axis during skeletal patterning. Furthermore, TSG can display both BMP antagonist and agonist function. The agonist function has been explained above, where TSG binds to and enhance chordin/BMP/BMP-1 preformed complex. Antagonist function relies on its capacity to bind directly with BMP-2 or -4 (or with a BMP-chordin preformed complex) enhancing the capacity of inhibition of the complex (Gazzerro and Canalis, 2006).

The Dan (differential screening-selected gene aberrative in Neuroblastoma) family is expressed primarily during embryonic development but two of its members, gremlin and sclerostin, are important regulators of BMP activity in the adult skeleton. Gremlin binds to BMP-2, -4 and -7 with high affinity and although basal levels of gremlin are modest, BMP signaling increases them. Sclerostin, encoded by the SOST gene binds to BMP-2, -4, -5, -6 and -7 with low affinity but its loss increases bone mass as seen in sclerosteosis. The mechanism of action of sclerostin is controversial since it binds to Wnt co-receptors and inhibits Wnt/β-catenin canonical signaling pathway. Moreover, noggin and sclerostin form a complex that attenuates their activity abolishing the antagonistic effect of noggin on BMP signaling.

Generally, the expression of all extracellular BMP antagonists described above is BMP-dependent indicating a potential for local regulation of BMP activity. Additionally, most of them are characterized by the presence of conserved cysteine-rich (CR) domains consistent with cysteine knot structures, functional motifs that determine the folding of the peptide thereby exposing specific hydrophobic residues and facilitating protein-protein interactions.

Other molecules can also interact with BMP signaling through interaction with phosphorylated R-Smad/Smad4 heterodimer in the nucleus, as is the case of p300/CBP or by regulation of the ubiquitin-proteasome proteolytic pathway as in the case of

Smurf (Smad-ubiquitination regulatory factor) E3 ubiquitin ligases (Gazzerro and Canalis, 2006).

3.4 Non-Canonical Signaling from BMP Receptors

In addition to Smads, BMPs activate other intracellular signaling pathways relevant to their cell functions. Non-canonical BMP signaling includes Rho-like small GTPases, phosphatidylinositol 3-kinase/AKT (PI3K/AKT), LIMK1 or various types of MAPKs (ERK, JNK, p38).

3.4.1 MAPKs

MAPKs (mitogen-activated protein kinases) are involved in BMP signaling and in the control of the BMP-transduction signal during osteoblast differentiation. MAPKs have been identified as regulators of bone formation placing them as central transducers in the regulation of bone mass (Figure I-7) (Greenblatt et al., 2013; Rodriguez-Carballo et al., 2014). MAPKs can be classified in ERKs (extracellular signal-regulated kinases), JNKs (c-Jun N-terminal kinases) and p38 MAPKs and generally, while ERKs are activated by growth factors as IGFs and FGFs, JNKs and p38 MAPKs are stimulated by cytokines as TGFβ and BMPs.

MAPK pathways work through phosphorylation cascades including three different levels of kinases: MAP3K (MAPK kinase kinase), MAPKK (MAPK kinase) and MAPK. It was described that that p38 and JNK pathways are stimulated by BMP through TAK1 (TGFβ activated kinase 1) thereby regulating stress-induced apoptosis (Kimura et al., 2000; Shirakabe et al., 1997).

In osteoblasts, p38 MAPKs is activated by MKK3/6 (MAPKK) that in turn is activated by TAK1 (MAP3K) (Greenblatt et al., 2010). BMP-induced p38 MAPK signaling is initiated as in the case of Smads, by receptors BMPRI and BMPRII. In this case, BMP ligand couples to a BMPRI homodimer, thereby recruiting a BMPRII and thus, forming a heterocomplex that will activate the MAP3K TAK1 through the recruitment of TRAF6 to activated receptor complexes (Nohe et al., 2002; Yamashita et al., 2008). Thus, p38 will phosphorylate multiple targets positively regulating osteoblast differentiation. Our group, among others, has described new p38 phosphorylation sites as in the case of DLX5 and OSX (Ortuno et al., 2010; Ortuno et al., 2013; Ulsamer et al., 2008). Moreover, we reported that p38 activity is essential for the cooperation and interaction of RUNX2 and OSX (Artigas et al., 2014).

Our group also characterized the osteoblast-specific *p38alpha* mutant mice. *p38alpha* deletion in osteoprecursors leads to an osteopenic phenotype not only when disrupted in embryogenesis but also during adulthood (Rodriguez-Carballo et al., 2014). Furthermore, p38α mutant mice also presented changes in adipose tissue through a decline of NPY (neuropeptide Y) expression in bone (Rodriguez-Carballo et al., 2015).

Greenblatt et al. revealed that *p38beta* (besides *p38alpha*) and upstream MAPK (*Mkk3* and *Mkk6*) are also essential for a normal bone formation as deletion of any of them profoundly reduce bone mass secondary to defective osteoblast differentiation. TAK1 deletion also leads to impaired osteoblast differentiation. All the above phenotypes were ultimately affecting p38 activity and it was described that the TAK1-MKK3/6-p38 MAPK axis phosphorylates RUNX2 promoting its association with the co-activator CREB-binding protein (CBP) required to regulate osteoblast programs (Greenblatt et al., 2010).

ERK1 and ERK2 are also expressed in osteoblasts and are relevant in bone development as seen in the phenotype of the double *Erk* mutant mice (Matsushita et al., 2009). Several studies have also described essential RUNX2 phosphorylations driven by ERKs (Xiao et al., 2002a; Xiao et al., 2002b; Xiao et al., 2000).

JNK activity is also involved in osteoblast activity. However, the JNK pathway is by far the least understood MAPK pathway in osteoblast. There is no bone-specific JNK-deficient mouse yet but *in vitro* studies suggest that JNK also functions as a positive regulator of osteoblast differentiations (Liu et al., 2005). JNK is a critical regulator of AP-1 activity through phosphorylation of JUN, JUNB or JUND and AP-1 transcription factors are important mediators of osteoblast differentiation. *JunB*-deficient mice present an osteopenic phenotype due to an early block in osteoblast differentiation and defects in osteoblast proliferation (Kenner et al., 2004).

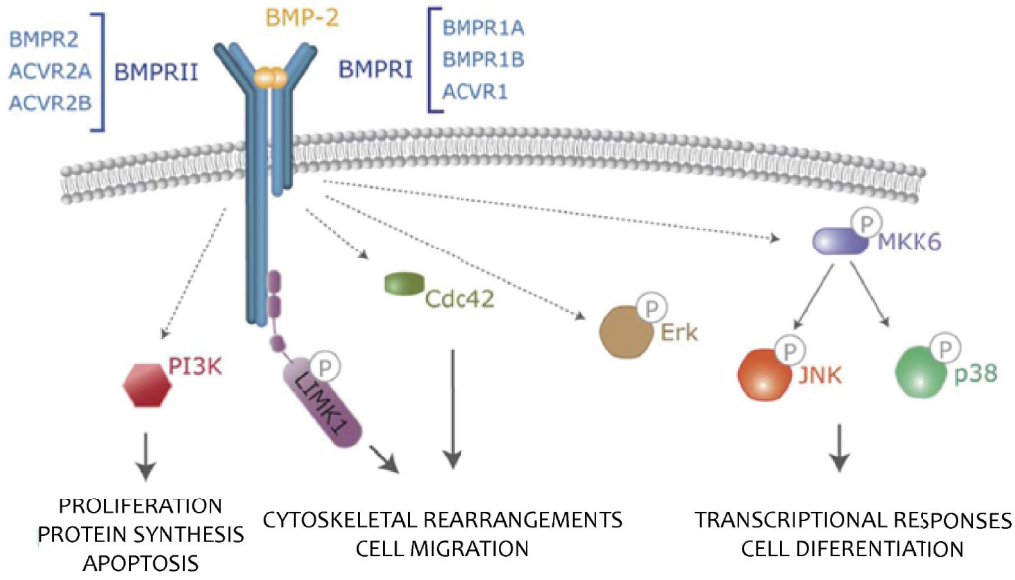

Figure I-7. Non-canonical BMP pathways. Additionally to Smad activation, BMP signaling comprises several non-canonical cascades which include TAK-p38, PI3K, Cdc42 or activation of LIMK. Adapted from (Gamez et al., 2013).

3.4.2 Other Non-Canonical BMP Pathways

Besides MAPK stimulation, there are other BMP-dependent non-canonical pathways. Several studies suggest that BMP-mediated cell migration requires activation of the small GTPase Cdc42 and LIMK activities. LIMK activity depends on LIMK binding to the long cytoplasmic tail of BMPRII receptors. Actually, BMP-BMPR II interaction disrupts BMPRII-LIMK contact therefore promoting its activity in cytoskeleton rearrangement (Foletta et al., 2003; Lee-Hoeflich et al., 2004). Moreover, additional data indicate that activation of LIMK also requires the activation of PAKs (p21-activated kinases) through Cdc42 and PI3K, as well as p38 activities (Gamell et al., 2008; Gamell et al., 2011). Thus, results from our group and others demonstrate that activation of PI3K signaling by BMPs is also essential for the biological function of this family of cytokines (Gamell et al., 2008).

4PI3K PATHWAY

Among the several signaling pathways involved in osteoblast differentiation and bone formation, there is the phosphatidylinositol 3-kinase (PI3K) pathway. PI3K is an important lipid kinase that controls a number of cellular functions including proliferation, survival and motility.

4.1 Phosphatidylinositols

Phosphatidylinositol (PtdIns) consist of a D-myo-inositol-1-phosphate (Ins1P) linked via its phosphate group to diacylglycerol. The inositol head group of PtdIns has five free hydroxyl groups as many as three of which have been found to be phosphorylated in cells, in different combinations. The 2 and 6 positions in these lipids have not been documented to become esterified with phosphate. PtdIns and its phosphorylated derivatives are collectively known as phosphoinositides or PIs (Figure I-8) (Vanhaesebroeck et al., 2001).

PIs reside in membranes and are substrates for kinases, phosphatases and lipases resident in or recruited to these membranes. PtdIns is the most abundant inositol lipid in mammalian cells under basal conditions, present at levels 10 to 20 times higher than those of PtdIns4P and PtdIns(4,5)P_2.

Four species of 3-PI have been identified in eukaryotic cells: PtdIns3P, PtdIns(3,4)P_2, PtdIns(3,5)P_2 and PtdIns(3,4,5)P_3. Phosphoinositide 3-kinases (PI3Ks) can phosphorylate the 3-hydroxyl group of the inositol ring in three different substrates: PtdIns, PtdIns4P and PtdIns(4,5)P_2. However, in cells their preferred substrate appears to be PtdIns(4,5)P_2.

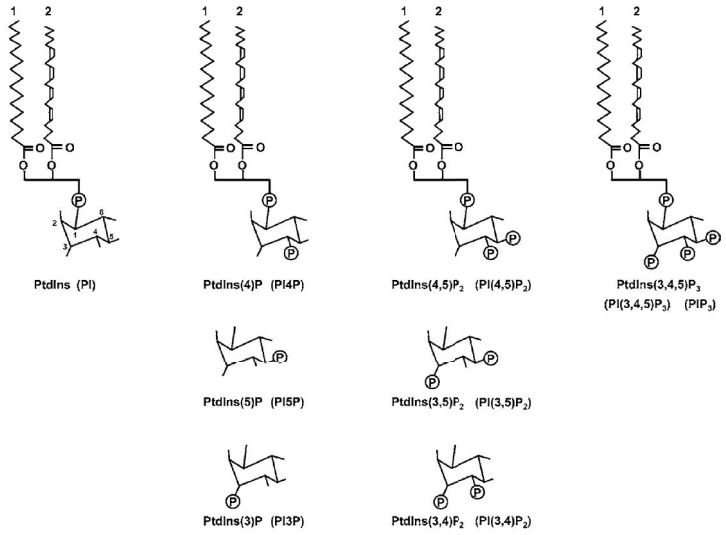

Figure I-8. Schematic structures of phosphoinositides. Eight different phosphoinositides are found in mammalian cells. The relative abundance of fatty acids which are esterified to the glycerol moiety in these lipids is largely unknown. 1: stearoyl, 2: arachidonyl, is depicted on the basis of the very limited information available. Image adapted from (Hawkins et al., 2006).

4.2 PI3-kinase Family

PI3Ks are a family of enzymes that were originally defined on the basis that they could catalyze the phosphorylation of the 3-position of the inositol ring in one or more phosphoinositide substrates. The PI3K family is divided into three classes (I-III) based on their substrate preferences and subunit composition (Figure I-9). The function of the various PI3-kinases has been widely studied at the biochemical and cellular level, generally through the use of PI3K-inhibitory compounds such as wortmannin and LY294992, without definitive knowledge of the specificity of these drugs for their target isoforms.

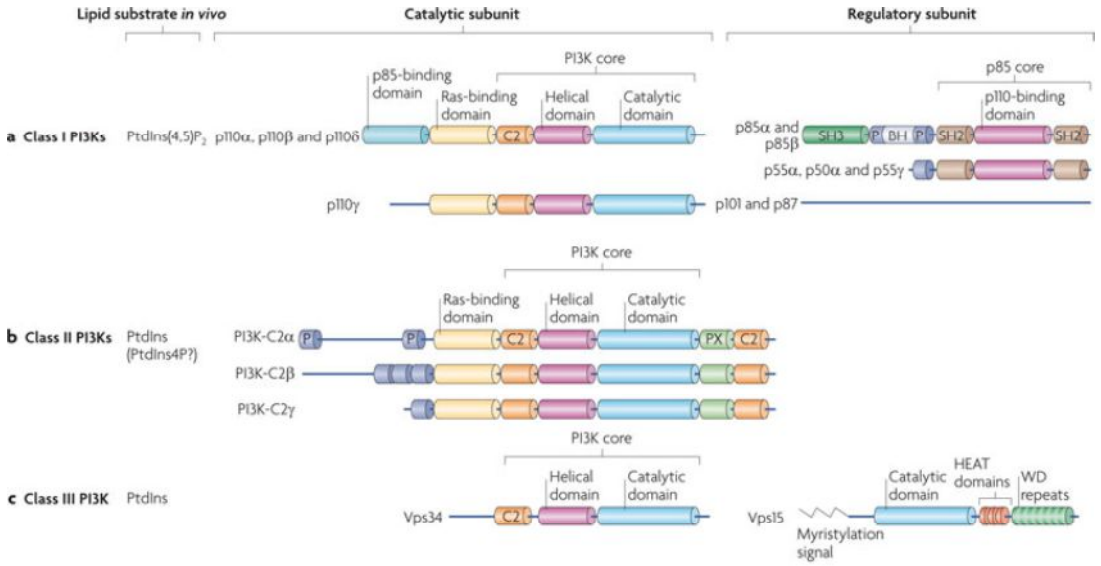

Figure I-9. PI3Ks are divided into three classes based on their structural and biochemical features. Adapted from (Vanhaesebroeck et al., 2010a).

In mammals, class I PI3Ks are present in all cell types. Class I PI3Ks are activated by various cell surface receptors, leading on further subdivision of this class into subfamilies IA and IB based on the classical notion that the IA members are activated upon receptor tyrosine kinase (TRK) stimulation whereas IB are activated by G-protein coupled receptors (GPCRs) (Figure I-10). Class IA and IB PI3Ks can additionally be distinguished according to their regulatory and catalytic subunits. Class IA enzymes are dimers of p110α, p110β or p110δ catalytic subunits and p50-p55/p85 regulatory subunits. The class IB enzymes are dimers of the p110γ catalytic subunit and either p101 or p84 regulatory subunits. Extended information of PI3Ks is presented in the following section (Vanhaesebroeck et al., 2001; Vanhaesebroeck et al., 2012).

In vitro, class II PI3Ks have a lipid substrate specificity that is clearly distinct from that of class I and III. They can use PtdIns, PtdIns4P and PtdIns(4,5)P_2 as substrates, with a strong preference for PtdIns. Mammals have three class II PI3K isoforms: PI3K-C2α, PI3K-C2β and PI3K-C2γ. In contrast to class I PI3Ks, which appear to be mainly cytosolic, class II are predominantly associated with the membrane fraction (Vanhaesebroeck et al., 2001). They lack regulatory subunits but have amino- and carboxy-terminal extensions compared to those of class I and III including an additional C-terminal C2 domain, which could mediate protein-protein interactions. This extra C2 domain is the defining feature of the class II PI3Ks. The roles of class II PI3Ks in mammals are mostly unknown although evidence is suggesting that they are likely to represent an alternative route for phosphorylation of PtdIns to form PtdIns3P in certain contexts of cell-surface receptor activation and/or endocytosis (Katso et al., 2006; Wheeler and Domin, 2006). They also have been implied in the regulation of cell adhesion and in the

reorganization of actin cytoskeleton (Figure I-10) (Domin et al., 2005; Maffucci et al., 2005).

Class III PI3Ks have only one catalytic member, vacuolar protein sorting 34 (Vps34) also known as PI3c3 in mammals, which uses PtdIns as substrate and binds Vps15 (PIK3R4 in mammals) constituting a heterodimer (Figure I-10). Vps34 is conserved from lower eukaryotes to plants and mammals and is an endosomal kinase that can acquire multiple functions through association with distinct multiprotein complexes. Vps34 has a lipid substrate specificity limited to PtdIns, generating PtdIns3P that represents a major regulatory pathway defining and controlling the passage of proteins and membranes trough the endosomal/lysosomal compartments (Lindmo and Stenmark, 2006).

Despite the PI3K classification, all PI3K catalytic subunits share a homologous region that consists of a catalytic core domain formed by a catalytic domain, a helical domain and a C2 domain (Figure I-9).

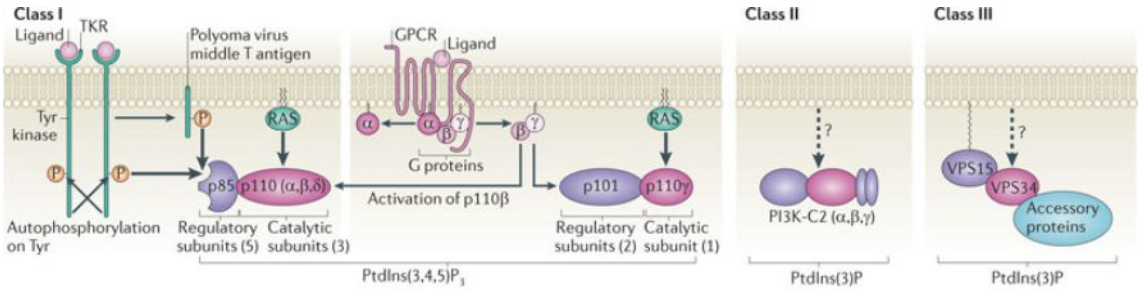

Figure I-10. Classification of PI3Ks and receptors involved in mammalian PI3K signaling. PI3Ks are stimulated through distinct inputs. Class I PI3Ks bind to phosphorylated Tyr (pTyr) in a specific amino acid sequence context, thereby bringing class I PI3Ks into contact with their lipid substrates. The p110γ isoform does not bind to a p85 subunit but binds to the unrelated p101 or p84 regulatory subunits, which link p110γ to Gβγ subunits released from heterotrimeric G proteins downstream of G protein-coupled receptors (GPCRs). Class II PI3Ks (PI3K-C2α, β or γ) do not constitutively associate with regulatory subunits. The class III PI3K is Vps34, which forms a constitutive heterodimer with the myristoylated Vps15 protein. Adapted from (Vanhaesebroeck et al., 2012).

4.3 Phosphatases Involved in the Metabolism of 3-Phosphoinositides

There are several inositol lipid phosphatases able to counteract PI3K signaling. The PI-phosphatases can be classified by means of their structure in three different families: the 3- and 4-phosphatases from the Cx_5R families and the type II 5-phosphatases. While the Cx_5R family members share a consensus sequences (CxxxxxR) in their catalytic

core region, the type II 5-phosphatases have two more extensive motifs in their catalytic core domain.

The termination of PI3K signaling by degradation of PIP_3 ($PtdIns(3,4,5)P_3$) can be mediated by at least two different types of phosphatases. The Src-homology 2 (SH2)-containing phosphatases (SHIP1 and SHIP2) dephosphorylate the 5 position of the inositol ring to produce $PI(3,4)P_2$. Although this dephosphorylation impairs some signaling downstream of PI3K, $PI(3,4)P_2$ can still mediate PI3K-dependent responses and may mediate events independent of those stimulated by $PI(3,4,5)P_3$. While SHIP1 is mostly found in hematopoietic cells, SHIP2 is widely expressed in the rest of cell types.

PTEN (phosphatase and tensin homolog deleted on chromosome 10) is a 3-phosphatase from the Cx_5R family that dephosphorylates the 3 position of $PI(3,4,5)P_3$ (PIP_3) to produce $PI(4,5)P_2$ (PIP_2). PTEN is essential for its role in down-regulating the PI3K target AKT/PKB (Figure I-11). First, *Pten* was identified as the frequently lost tumor suppressor gene in a region of human chromosome 10. Later, PTEN was described as a lipid phosphatase that hydrolyzes the 3-phosphate on the second-messenger molecule PIP_3 to generate PIP_2 (Maehama and Dixon, 1998). The link between the PI3K pathway and PTEN was cemented by the finding that deletion of *Pten* in mouse embryonic fibroblasts (MEFs) activated AKT and elevated intracellular $PI(3,4,5)P_3$ levels (Stambolic et al., 1998). Moreover, although the regulation of PTEN is poorly characterized, it is well known that over-activation of PI3K signaling by inactivation of PTEN is frequent in human tumors (Thorpe et al., 2015; Vanhaesebroeck et al., 2010b).

Thus, steady-state PIP_3 levels are tightly controlled by the combined effects of stringent PI3K regulation and the action of PIP_3 phosphatases as PTEN, SHIP1 and SHIP2 (Cantley and Neel, 1999; Engelman et al., 2006).

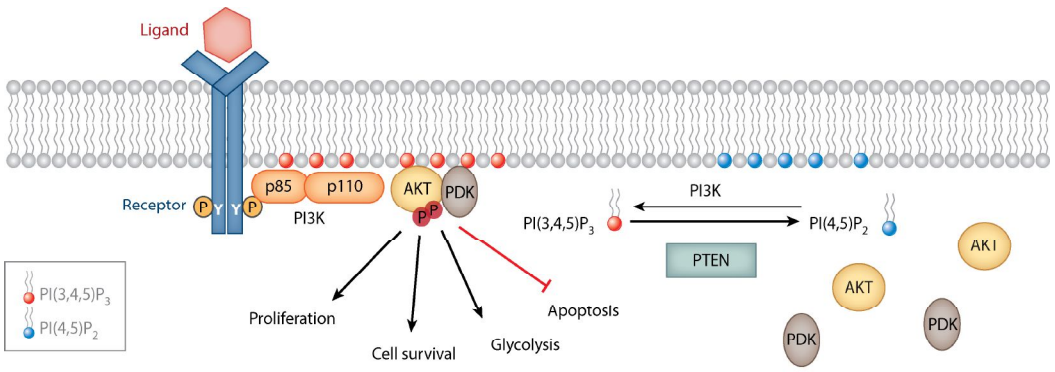

Figure I-11. Schematic overview of PI3K/AKT signaling and PTEN function. PTEN is down-regulating the PI3K signaling through dephosphorylation of PIP_3. Adapted from (Worby and Dixon, 2014).

4.4 Class IA PI3Ks

Class I enzymes are now generally considered to preferentially phosphorylate PtdIns(4,5)P_2 (PIP_2) and hence synthesize PtdIns(3,4,5)P_3 (PIP_3), which represent the messenger molecule for PI3K intracellular signaling.

Class IA PI3K is a dimer consisting of a p85 regulatory subunit and a p110 catalytic subunit. As introduced previously, mammals have three class IA p110 isoforms, p110α, p110β and p110δ and are encoded by three separate genes (*PIK3CA*, *PIK3CB*, and *PIK3CD* respectively). Class IA has five variants of p85 regulatory subunits that are generated by the expression of three different genes (*PIK3R1*, *PIK3R2* and *PIK3R3*) namely p85α, p85β and p55γ. In addition, *PIK3R1* gene gives rise to two shorter isoforms, p55α and p50α, due to alternative transcription start sites. All these splice variants make functional complexes with p110 subunits (Vanhaesebroeck et al., 1997a).

A single type of class IA catalytic/adaptor heterodimer is present in *Drosophila melanogaster* (Dp110/p60) and *C. elegans* (AGE-1/AAP-1) but no class IA PI3K family members have been found in yeast or plants (Vanhaesebroeck et al., 1997a).

4.4.1 Regulatory subunit structure and function

The p85/p55 regulatory subunits bind tyrosine-phosphorylated residues of activated receptors or specific adaptor molecules (Engelman et al., 2006; Vanhaesebroeck et al., 2001). The regulatory subunits contain two SH2 domains that bind with high affinity to phosphorylated Tyr-X-X-Met motifs found in receptors (Figure I-12) (Songyang et al., 1993). This SH2 interaction activates the class IA dimers thereby initiating the PI3K signaling. All isoforms of the PI3K regulatory subunit contain these two SH2 domains, which allow them to bind to several growth factor receptors but also to phosphotyrosines of specific IRS (insulin receptor substrate).

The region between the two SH2 domains is called inter-SH2 (iSH_2) domain and it is the region that binds to the ABD N-terminal domain (ABD, adaptor-binding domain) of p110α, p110β and p110δ (Figure I-12). This domain is also called p85 binding domain (p85 BD) (Holt et al., 1994; Hu and Schlessinger, 1994; Klippel et al., 1993).

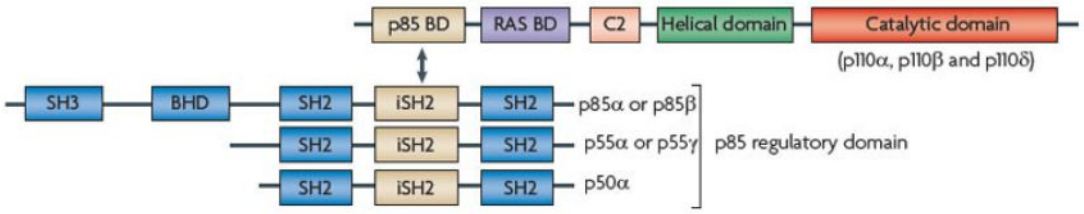

Figure I-12. Class IA phosphoinositide 3-kinases. Class IA PI3Ks are heterodimers consisting of a p110 catalytic subunit and a p85 regulatory subunit. There are three p110 catalytic isoforms: p110α, p110β and p110δ and also three p85 isoforms: p85α (and its splice variants p55α and p50α), p85β and p55γ. Adapted from (Liu et al., 2009).

p85 subunit inhibits p110 and activation of p85-p110 dimers reflects disinhibition of the p110 subunit (Backer, 2010; Yu et al., 1998). However, the activation of p85-p110 dimers does not involve the dissociation of p85 from p110 since p110 is easily degraded as a monomer.

The iSH2 domain of p85 is sufficient to bind p110 but inhibition of p110 by p85 additionally requires the N-terminal SH2 domain linked to the iSH2 domain. The stabilization of the p110 subunit by binding to p85 is not as yet fully understood. It has been suggested that once p85 and p110 are bound by the iSH2-ABD domains, p85 N-terminal SH2 domain (nSH2) adopts a conformation that allows contact with its own iSH2, forming a close contact with residues 571-598 in the iSH2 domain. Truncation of these specific residues of the iSH2 domain seems to abolish inhibition of p110 leading to a constitutively active PI3K. This suggests that the orientation of the nSH2 relative to the iSH2 is critical for p110 inhibition (Shekar et al., 2005).

The longest class I regulator isoform p85 also contains a single N-terminal Src-homology 3 (SH3) domain and two proline-rich domains flanking a BCR homology domain, which is thought to interact with proline rich proteins and small GTPases respectively. The BCR (breakpoint cluster region) homology domain is homologous with a domain of the BCR gene product and it binds to Rac and Cdc42 (cell division cycle 42) and has TAP (GTPase-activating protein) activity towards the Rab GTPases.

4.4.2 p110 catalytic subunit structure

Class IA catalytic subunit, namely p110, is a 110-kDa protein that dimers with the regulatory subunit. As previously specified, class IA PI3K include three different isoforms: p110α, p110β and p110δ. p110α and β are widely distributed in mammalian tissues while p110δ is mainly restricted to leukocytes (Vanhaesebroeck et al., 1997b). Although distribution of p110 isoforms can be different, the overall domain structures of all three isoforms are quite similar. They all contain an N-terminal adaptor binding

domain (ABD, p85BD), followed by a Ras-binding domain (RBD), a C2 domain, a helical domain and the catalytic kinase domain (Figure I-12) (Engelman et al., 2006).

As seen above, SH2 domains of regulatory subunits are necessary for p85/p110 activation and iSH2-ABD contact is the major interaction responsible for the formation of the dimer. Additionally, p110 subunits have a Ras binding domain, allowing the binding of activated Ras and Ras family members. It is unclear which isoforms of Ras interact with the different PI3K family members although some isoform-selective functional interaction between Ras and PI3K family members have been suggested (Rodriguez-Viciana et al., 2004).

It was above-mentioned that monomeric p110α is stabilized by dimerization with p85α (Yu et al., 1998). This stabilization generates a problem for overexpression studies since N-terminally tagged p110 show higher stability (and therefore higher activity than wild type p110) and C-terminal tags may inhibit the activity of p110α (Backer, 2010).

Studies of p110 using engineered mice

As stated above, inhibitors have been used in order to elucidate PI3Ks activities. Researches have also begun to investigate the physiological roles played by the different isoforms of PI3-kinases using mouse genetics to dissect their function and regulation.

Homozygous deletion of *p110α* is embryonically lethal between E9.5 and E10.5 as a result of severe proliferative defects (Bi et al., 1999a). Remarkably, p85 is overexpressed in these embryos, possibly exerting a dominant-negative effect on signaling via *p110β* and *p110δ*. Similarly, mice carrying a kinase-dead knock-in mutation (D933A) in *p110α* die early in embryonic development, but mice heterozygous for this allele are fertile and viable, although smaller than their wild-type siblings (Foukas et al., 2006). To bypass the issue of embryonic lethality of systemic *p110α*-loss-of-function, mice with conditionally targeted *Pik3ca* allele (in embryonic fibroblasts) have been generated. In the same study, ablation of *p110α* in MEFs severely reduced the response to insulin and IGF1, as well as epidermal growth factor (EGF) (Zhao et al., 2006).

Transgenic mice also corroborated class I PI3K implication in cell growth. While mice expressing a cardiac-specific constitutively active *p110α* increase heart and cardiomyocyte size, animals expressing kinase-dead *p110α* reduce their heart dimension (Shioi et al., 2000).

Bi et al. also generated the *p110β* knock-out mice, and similarly, were found to die early in embryonic development while the heterozygous mice were viable (Bi et al., 2002). Later, mice carrying a conditional *Pik3cb* allele were generated. These animals lack *p110β* in liver, but did not seem to have a major effect on signaling downstream of the

insulin receptor in liver itself or in the isolated MEFs (Jia et al., 2008). Nevertheless, these mice lacking *p110β* had signs of impaired insulin metabolism.

4.5 Class I PI3K Signaling Inputs

A wide variety of cell-surface receptors are linked with the stimulation of class I PI3Ks including receptors for the majority of growth factors and many inflammatory stimuli, hormones, neurotransmitters and antigens. A general view of the stimulation of distinct p110 isoforms is represented in Figure I-13. Class IA heterodimers are adapted to receive regulatory inputs from receptors by the activation of protein tyrosine kinases as their proximal signal transducing elements. The protein tyrosine kinase involved can be part of RTK itself as is the case of many growth factor receptors: PDGF, EGF and IGF.

These receptors are able to phosphorylate critical tyrosine residues within the so-called activation motifs, which can be present on the receptors themselves or on receptor-associated proteins, often called adaptors. The activation motifs are (P)Tyr-X-X-Met motifs and p85/p110 dimers are activated when one or both of the p85 SH2 domains bind to these phosphorylated residues (Fantl et al., 1992; Songyang et al., 1993).

Once SH2 domains bind to these specific motifs at RTK, class IA PI3Ks recruit into receptor signaling complexes. However, the mechanisms leading to activation of PI3Ks in signaling complexes are poorly understood.

Growth factor stimulation can also result (through RTK) in the phosphorylation of the adaptor proteins IRS1 (insulin receptor substrate 1) that in turn recruits the PI3K heterodimers and activates the lipid kinase activity. IRS1 represents the major substrate of the IGF1 and insulin receptor and contains multiple tyrosine phosphorylation motifs that serve as docking sites for SH-2 domain containing proteins (Myers et al., 1993).

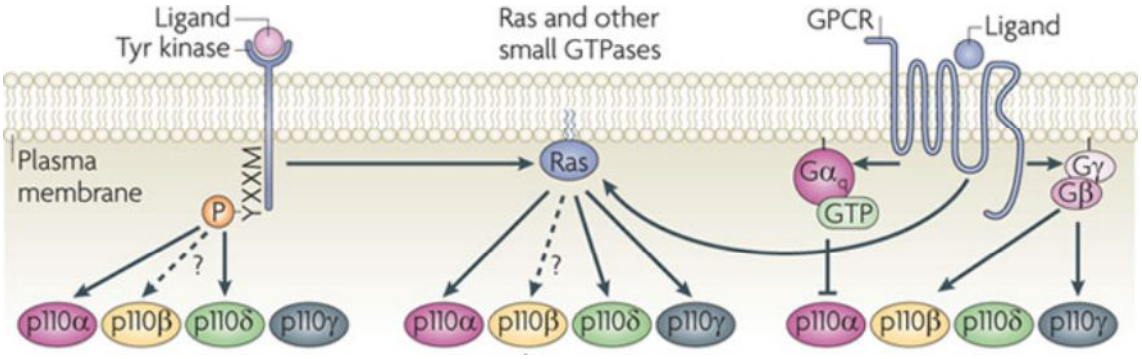

Figure I-13. Upstream signals feeding class I PI3Ks. SH2 domains of the p85 regulatory protein can bind directly phosphoTyr-X-X-Met (YXXM, where X is any amino acid) motifs generated by tyrosine kinases in tyrosine kinase receptors (TKR) and associated proteins, resulting in the activation of the class I poshphoinositide 3-kinases. Tyrosine kinase pathways and G protein-coupled receptors (GPCRs) can also activate Ras, which in turns activates class I PI3Ks. Direct interaction of PI3Ks with Gα or Gβγ subunits, which are downstream of GPCRs, can engage class I PI3Ks. p110α might be inhibited by Gα, whereas p110β and p110γ are activated by Gβγ subunits (right). Adapted from (Vanhaesebroeck et al., 2010a).

Another important element governing the activity of class IA PI3K is the direct association of the GTP-bound form of Ras with the RBD (Ras-binding domain) motif in the p110 subunit. Activation of Ras is a key signaling event downstream of many different receptor types, which occur in parallel with class I PI3K activation. All p110 subunits have an RBD, but the ability of GTP-Ras to interact with p110β is unclear (Kang et al., 2006; Rodriguez-Viciana et al., 2004). While the RBD of p110α and p110δ have been seen to interact with Ras, p110β RBD interacts with other members of Ras superfamily: Rac1 and Cdc42 (Fritsch et al., 2013).

Class IB PI3Ks are activated by G-protein coupled receptors (GPCRs). There is direct binding and activation of these PI3Ks by Gβγ that are liberated by dissociation of the heterotrimeric G-protein although the precise binding site is unknown. Moreover, GTP-Ras is known to bind directly p110γ and evidence indicates that this interaction plays an important role in the activation of PI3K activity downstream GPCRs (Burke and Williams, 2015; Suire et al., 2006).

Although p110 isoforms have homology in their sequences it has been reported that they are regulated differentially, as seen by the p110β lack of sensitivity to Ras. In addition, Gβγ subunits of heterotrimeric G proteins have been described to directly activate class IA p110β subunit but not p110α or p110δ (Kurosu et al., 1997; Maier et al., 1999).

4.6 Downstream Signaling via p85/p110 Pathway

Once class IA PI3K dimers are activated mainly by tyrosine kinase receptors, p110 catalytic subunit (which has been recruited near the plasma membrane) produces the conversion of PIP_2 to PIP_3. PIP_3 acts as the messenger molecule of PI3K pathway recruiting molecules that bind to itself and thus, spreading the signaling downstream.

PIP_2 and PIP_3 bind signaling molecules containing pleckstrin-homology (PH) domain and recruit them to activation sites within the plasma membrane. In most cases, it is still unclear how PIP_3 engagement with the PH domain of an effector protein regulates its activity. Even so, usually this interaction is of sufficient affinity that the target protein undergoes a net change from a predominantly cytosolic to a plasma membrane location. These translocation events are considered to be activators since target proteins are brought into proximity with substrates or binding molecules. PIP_3 effects can also be activators by producing conformational changes thereby increasing their catalytic activity or altering their affinity for binding partners (Vanhaesebroeck et al., 2001).

Among all these effector proteins, the serine/threonine kinase AKT has been most extensively studied as a critical PI3K effector. However, several effectors proteins are sensitive to the increase in the concentration of these lipids, influencing on a very large signaling net. Other PH domain-containing proteins that are activated by PIP_3 include regulators of small GTPases such as guanosine nucleotide exchange factors (GEFs) and GTPase-activating proteins (GAPs) and protein tyrosine kinases of the Tec family. GEFs and GAPs are responsible for the activation and inactivation of small GTPases, required for remodeling the actin cytoskeleton. Tec family members regulate both acute events (changes in cytosolic calcium concentrations) and long-term events (changes in gene expression) (Cantley, 2002; Welch et al., 2002).

4.6.1 AKT activation

AKT, also known as protein kinase B (PKB) is a ubiquitously expressed serine/threonine kinase with an N-terminal PH domain that selectively binds 3-phosphoinositides. There are three AKT isoforms (AKT1/PKBα, AKT2/PKBβ, and AKT3/PKBγ) with extensive homology to protein kinases A, G and C within their kinase domains and, therefore, they are members of the AGC kinase family. The C-terminus of the AKT kinase domain contains a regulatory hydrophobic motif, which is also a hallmark of all AGC kinases (Figure I-14).

Another AGC kinase, PDK1 (phosphoinositide-dependent kinase 1) also contain a PH domain and it is the responsible for the activator phosphorylation of AKT. Although PDK activity seems to be independent from phosphoinositide/PH domain binding, it needs class I PI3K activity in order to be additionally activated and to be able to phosphorylate AKT at its activation loop. This is because PIP_2/PIP_3 binding to the PH domain of AKT is required to make the Thr-308 present in its activation loop available for phosphorylation by PDK (Stephens et al., 1998; Stokoe et al., 1997).

RTK signaling also activates mTOR complex2 (mTORC2) which phosphorylates AKT on the hydrophobic motif Ser-473. DNA dependent protein kinase (DNA-PK) may also mediate Ser-473 phosphorylation in some cases, as under certain conditions of cellular stress. Both Thr-308 and Ser-473 phosphorylations are necessary for a fully activated AKT.

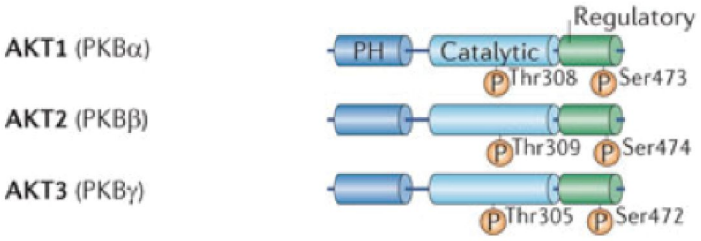

Figure I-14. Schematic picture of the conserved domain structure of AKT1. All AKT proteins consist of an N-terminal PH domain, a catalytic kinase domain and a hydrophobic C-terminal tail (regulatory). The latter is characteristic of AGC kinases. AKT activator phosphorylation sites are indicated. For AKT2 are Thr-309 and Ser-474 and for AKT3 Thr-305 and Ser-472. Adapted from (Song et al., 2012).

Other AKT phosphorylation sites contributing to its activation state are less well characterized. Thr-450 phosphorylation, for example, appears to prime AKT for subsequent phosphorylation by PDK1 after ischemic injury (Shao et al., 2006).

Activated AKT will further become inactivated by the action of phosphatases such as PP2A and PHLPP1/2, which can dephosphorylate Thr-308 and Ser-473 and return AKT to its inactive conformation in the cytosol. PP2A (protein phosphatase 2A) is a member of the B56 family and has been shown to down-regulate AKT activation by decreasing its phosphorylation at the activation loop. PHLPP1 and PHLPP2 (PH-domain leucine-rich repeat-containing protein phosphatase 1 and 2) in return, dephosphorylate the hydrophobic motif residues (Gao et al., 2005).

There are other molecules interfering in AKT activation such as PHLDA3 (PH-like domain family A member 3), a PH-domain only protein that competes for the PIP_3

present in the membrane or TRB3 (Tribbles 3), which directly interacts with AKT and prevents its phosphorylation (Du et al., 2003).

4.6.2 Downstream AKT

In 1996, the minimal recognition motif of AKT was defined as R-X-R-X-X-S/T-B, where X represents any amino acid and B represents bulky hydrophobic residues (Phe,Leu) (Alessi et al., 1996). Over 50 well-validated AKT substrate proteins have been identified so far and some of the most important are summarized in Table I-1.

AKT SUBSTRATES

Substrate protein	Phosphorylation site (s)	Effect of phosphorylation
Glucose homeostasis and metabolism		
AS160	Ser-588 and Thr-642	Stimulates AS160 and GLUT4 trafficking
ATP citrate lyase	Ser-454	Stimulates the enzyme activity
GSK3α	Ser-21	Inhibits GSK3 kinase activity
GSK3β	Ser-9	Inhibits GSK3 kinase activity
NADPH oxidase	Ser-304 and Ser-328	Increases enzymatic activity
PFK-2	Ser-466 and Ser-483	Activates PFK-2
Cell proliferation		
Mdm2	Ser-166 an Ser-186	Prevents Mdm2 degradation
p21	Thr-145	Nuclear exclusion and cell cycle entry
p27	Thr-157	Nuclear exclusion and cell cycle entry
Cell survival		
BAD	Ser-136	Prevents apoptosis induced by BAD
CHK1	Ser-280	Inhibits its function/nuclear exclusion
Caspase-9	Ser-196	Prevents Caspase-9 activation
FoxO1	Thr-24, Ser-256 and Ser-319	Inhibits its transcriptional activity
FoxO3A	Thr-32, Ser-253 and Ser-315	Inhibits its transcriptional activity
FoxO4	Thr-28, Ser-193 and Ser-258	Inhibits its transcriptional activity

AKT SUBSTRATES		
Cell growth and protein translation		
mTORC1-Raptor	Ser-2448	Activates mTORC1 kinase activity
PRAS40	Thr-246	Relieves its inhibitory action on mTORC1
TSC2	Ser-939 and Thr-1462	Relieves its inhibitory action on mTORC1
Cell migration and invasion		
c-Raf	Ser-259	Inactivates Raf-MAPK signaling
b-Raf	Ser-364, Ser-428 and Thr-439	Inactivates Raf-MAPK signaling
EDG-1	Thr-236	Increases endothelial cell migration
Rac-1	Ser-71	Inhibits Rac-1 GTP binding
Neurological function		
CREB	Ser-133	Increases binding with co-activators
GABA(A)R	Ser-410	Increases surface expression at synapses

Table I-1. Key AKT substrates. Detailed list of residues phosphorylated by AKT and their effect. Table adapted from (Vasudevan and Garraway, 2010).

As seen in Table I-1, AKT through its multiple substrates is involved in a wide range of cell processes including proliferation, survival, apoptosis, cell migration and invasion (Burke and Williams, 2015; Vanhaesebroeck et al., 2010a).

AKT is known for its role in glucose metabolism through different mechanisms. The AKT substrate GSK3β is inactivated by AKT phosphorylation and its inactivation leads to increased glycogen accumulation. Moreover AKT is also involved in the regulation of glucose uptake through its effects on GLUT4 (glucose transporter type 4).

GSK3β is also linked to cell proliferation because it phosphorylates cyclin D1. AKT prevents degradation of cycling D1 by phosphorylating and inhibiting GSK3β activity (Muise-Helmericks et al., 1998). AKT also directly inhibits the cell cycle inhibitor p21 and p27 by phosphorylating these proteins near their nuclear localization signal and thereby promoting their cytoplasmic retention. Several other negative regulators of cell cycle are inhibited by AKT (Mayo and Donner, 2001) (Kang et al., 1999).

But besides its effects in promoting cell proliferation, AKT also enhances the survival of cells by blocking the function of pro-apoptotic proteins and processes. AKT phosphorylates BAD, a pro-apoptotic protein, preventing the subsequent caspase

activation and therefore, apoptosis (Datta et al., 1997). Furthermore, AKT also phosphorylates pro-caspase 9 decreasing its protease activity (Cardone et al., 1998). Other pro-apoptotic genes as *Bim* that are transcribed by Foxo proteins are also down-regulated by the effects of AKT.

AKT also exerts its anti-apoptotic effects by the phosphorylation of transcription factors from the Forkhead family. Phosphorylation of FOXOs (forkhead box proteins) occurs in the nucleus and restricts the nuclear entry by promoting their interaction with 14-3-3 and inducing their export from the nucleus (Vasudevan and Garraway, 2010). Thus, AKT blocks FOXO-mediated transcription of target genes that promote apoptosis, cell-cycle arrest and metabolic processes.

Contrary to anti-apoptotic effects, AKT promotes cell growth and protein translation mainly through the TSC-2/mTORC1 pathway. While mTORC2 complex acts as an AKT activator, mTORC1 complex (the rapamycin-sensitive mTOR component) receives stimulatory input downstream of AKT. Phosphorylation of TSC2 by AKT causes the release of the inhibitory effects of the TSC1-TSC2 complex over the small G-protein Rheb. Active Rheb is an activator of mTORC1 and it is well known how mTORC1 promotes cell growth and protein translation through the stimulation of p70 S6K (p70 S6 kinase) and eIF4E proteins (Manning and Cantley, 2007; Vasudevan and Garraway, 2010).

In contrast, in some circumstances AKT activation can be disadvantageous for the cell: strong AKT activation can lead to increased oxidative stress and some pro-apoptotic activity of AKT has been reported (Maddika et al., 2009; Nogueira et al., 2008).

Many other downstream AKT effectors are also involved in the processes described above and in other physiological processes as in angiogenesis, neuronal differentiation and immunity function (Table I-1) (Vasudevan and Garraway, 2010).

4.7 PI3K Inhibitors

Most studies investigating the role of PI3Ks in cell function have been performed in cell cultures although only *in vivo* approaching through animal models can offer an improved physiological view of the impact of PI3K loss.

A key fact for the understanding of PI3K pathway was the discovery in 1993-94 of wortmannin, a metabolite of the fungi *Penicillium funiculosum* with high potent PI3K inhibitory activity (Arcaro and Wymann, 1993; Powis et al., 1994). Contemporarily, Vlahos et al. generated LY294992 (hereafter LY), the first synthetic inhibitor of PI3K (Vlahos et al., 1994). These pharmacological inhibitors were used for the study of PI3K

activity for a long time although they both inhibit all PI3K isoforms, and therefore are called pan-inhibitors.

Wortmannin has more potent inhibitory activity than LY and can also inhibit other PI3K-related enzymes such as mTOR, DNA-PK or MAPKs. Wortmannin interacts with the catalytic subunit p110α and produces covalent modification of a residue involved in the phosphate transfer reaction (Vanhaesebroeck et al., 2001; Wymann et al., 1996). Unlike wortmannin, LY causes reversible inhibition of PI3K and furthermore its half-life is considerably longer (Vanhaesebroeck et al., 2001; Vanhaesebroeck et al., 2012).

Years later, isoform-specific inhibitors started to emerge. In 2003 the first PI3K isoform-selective inhibitor was developed: IC87114. IC87114 specifically inhibits p110δ-containing PI3Ks (Sadhu et al., 2003; Vanhaesebroeck et al., 2012). Later on, other specific inhibitors as TGX-221, PIK-75 or A66 have been identified (Jackson et al., 2005; Jamieson et al., 2011; Zheng et al., 2011).

Currently, specific-PI3K inhibitors are rapidly developing for *in vitro* research but also as potential drugs for clinical trials because of their use as chemotherapy in a wide range of tumors since PI3K and PTEN are very frequently mutated (Rodon et al., 2013).

5 MICRORNAS

Until a few years ago, most of the known non-coding RNAs (ncRNAs) were responsible for generic functions in cells such as rRNAS and tRNAs, involved in mRNA translation, small nuclear (snRNAs), involved in splicing, and small nucleolar RNAs (snoRNAs), involved in the modification of rRNAs. Lee et al. were the first to identify the first microRNA since they discovered that lin-4 gene (controlling the timing for *C. elegans* early larval development) was not coding for a protein but instead a pair of small RNA (Lee et al., 1993). First, it was thought that this type of RNA was exclusive for nematodes but years later, all changed with the discovery of let-7, another gene promoting transition from late-larval to adult in *C. elegans.* Homologs of the let-7 gene were soon identified in the human and fly genomes and in fact, let-7 itself was described in human (Bartel, 2004).

MicroRNAs are short, single-strand, non-coding RNAs approximately 20-25 nucleotides long that have emerged as a novel mechanism capable of post-transcriptionally modifying the expression of mature mRNAs and proteins (Bartel, 2004; Hobert, 2008; Mattick and Makunin, 2006). In addition to microRNAs, there are other major types of small silencing RNAs in animals: siRNAs (small interfering RNAs) and piRNAs (piwi-interacting RNAs), which present different processing enzymes involved in their genesis and have distinctive main functions (Ha and Kim, 2014).

Numerous studies have shown that microRNAs (miRNAs) are important post-transcriptional regulators in virtually all biological processes (Hobert, 2008) and the miRNA field has advanced so rapidly that it has become an integral component of the way we think gene expression is regulated in cartilage and bone development. Cell-specific signaling and transcriptional regulation in skeletal biology are extremely dynamic processes that are highly reliant on dose-dependent responses. As such, they are ideal targets for quantitative regulation by miRNAs. Moreover, the multi-gene regulatory capacity of miRNAs enables them to cooperatively balance the final precursor cell fate.

5.1 miRNA Biogenesis and Function

5.1.1 Transcription

Sequences encoding miRNAs are found around the genome as separate transcriptional units, although some of them are located within introns of coding genes (generally as clustered microRNAs) (Kapinas and Delany, 2011). However, precise locations of miRNA promoters have not yet been mapped for most miRNA genes.

Transcription of miRNAs is mostly mediated by RNA polymerase II activity but can also be carried out by RNA polymerase III (Borchert et al., 2006). Morevore, polymerase II produces the mRNA and some non-coding RNAs, including the small nucleolar RNAs and four of the small nuclear RNAs of the spliceosome. Polymerase III produces mainly some of the shorter non-coding RNAs, including tRNAs and the U6 snRNA (Bartel, 2004).

miRNAs are first transcribed as long primary units called pri-miRNAs, which contain characteristic secondary loop structures (Starega-Roslan et al., 2011). pri-miRNAs are over 1Kb in length and are typically capped and polyadenylated structures where miRNA sequences are embedded. Various miRNAs can be co-transcribed in a single pri-miRNA, possibly inducing additional effects on a single pathway or gene or allowing cross-talk between different pathways (He et al., 2010). The pri-miRNAs' characteristic hairpin helps the microprocessor complex containing the RNAse II endonuclease Drosha and some cofactors, including the double-strand RNA binding-protein DGCR8 (diGeorge syndrome critical region gene), to recognize them from among similar structures present in the nucleus (Han et al., 2006; Seitz and Zamore, 2006).

5.1.2 Processing by Drosha and Dicer

As stated above, Drosha is a nuclear protein belonging to the family of RNase III-type endonucleases that act specifically on double-stranded RNA. Germline deficiency of Drosha causes lethality by embryonic day 7.5 in mice, which reflects the crucial role of miRNAs in development. Drosha has tandem RNase III domains (RIIIDs) and a double strand RNA-binding domain (dsRBD) in its C-terminal end (Figure I-15). Two RIIIDs dimerize intramolecularly to form one processing center. The first RIIID cuts the 3' strand of the stem of pri-miRNA, whereas the second cuts the 5' strand to produce a staggered end with a 2-nucleotide-long 3' overhang (Ha and Kim, 2014). For full activity of the microprocessor complex, the protein DGR8 is needed. While the two dsRBDs of DGCR8 recognize pri-miRNA the conserved C terminus interacts with Drosha. Both DGCR8 and Drosha need their N-terminal region for its nuclear localization in cells.

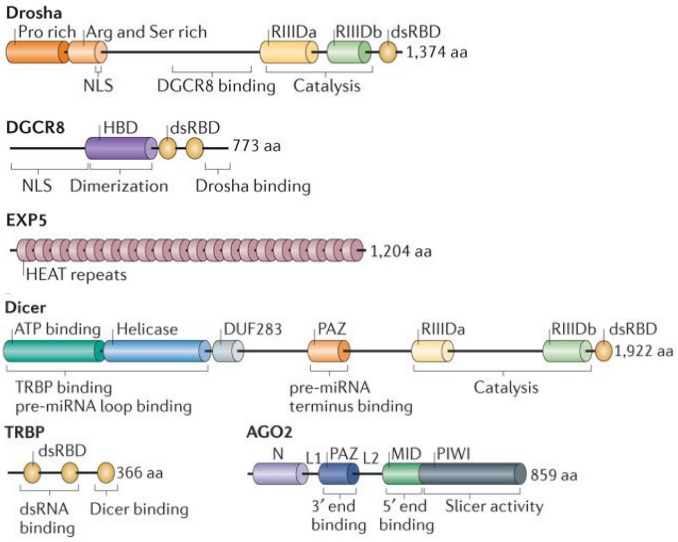

Figure I-15. Schematic structure of molecules involved in miRNA processing. Drosha, DGCR-8, EXP5, Dicer, TRBP and AGO2 proteins are represented. Adapted from (Ha and Kim, 2014).

Drosha cleaves the hairpin at approximately 11 bp away from the "basal" junction between single-stranded RNA and dsRNA, and approximately 22 bp away from the "apical" junction linked to the terminal loop. However, it is unclear how the microprocessor specifically interact with these cleavage sites (Figure I-16). As a result, a 60-80-nucleotide double-strand miRNA precursor (pre-miRNA) is generated. Pre-miRNAs maintain their stem loop configuration and have a two-nucleotide extension at their 3' end.

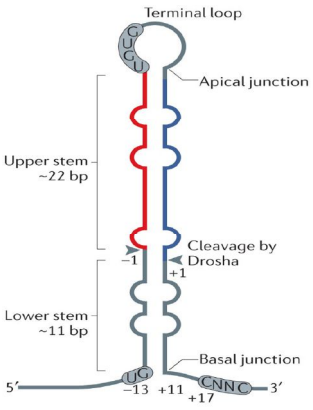

Figure I-16. Pri-miRNA cleavage by the microprocessor complex. Drosha and DGR8 recognize the single-stranded RNA tails. Microprocessor measures 11 bp approximately from the basal junction and around 22 bp from the apical junction and Drosha cleaves the pri-miRNA at these positions. Adapted from (Ha and Kim, 2014).

However, some precursors arising from short introns (mirtrons) are capable of bypassing Drosha cleavage and are exported (as regular pre-miRNA) by exportin 5 to the cytoplasm, where they continue canonical miRNA processing (Lund et al., 2004). The protein exportin 5 (EXP5) forms a transport complex with the GTP-binding nuclear

protein RAN·GTP and a pre-miRNA. After translocation through the nuclear pore complex, GTP is hydrolyzed, resulting in the disassembly of the complex and the release of the pre-miRNA in the cytosol. EXP5 recognizes a dsRNA stem of 14bp in length together with the short 3' overhang.

After Drosha-microprocessor process and pre-miRNA exportation to the cytoplasm, miRNA precursors are cleaved by a second endonuclease (Dicer), resulting in a double strand of about 21-24 nucleotides. Dicer is an RNase III-type endonuclease that similarly to Drosha, forms a C-terminal intramolecular dimer to create a catalytic center. While the N-terminal helicase domain facilitates pre-miRNA recognition, the PAZ (PIWI-AGO-ZWILLE) domain binds to the pre-miRNA (Figure I-15). Dicer binds to pre-miRNA with a preference for a two-nucleotide-long 3' overhang generated by Drosha and cleavage sites are located at a fixed distance from the 3' end of the terminus of dsRNAs (generally 21-25 nucleotides in length).

5.1.3 RISC loading

After Dicer processing, the small RNA duplex is loaded onto an AGO (Argonaute) protein to form an effector complex named RNA-induced silencing complex (RISC). Among the four AGO proteins present in humans (AGO1-4) only Argonaute 2 can cleave perfectly matched target mRNAs (at the center of the mRNA duplex) whereas the rest of AGO proteins can induce translational repression and decay of target mRNAs. While in flies and *C. elegans* there is some preference in the type of AGO protein which load the pre-miRNA (according to the 5' sequence of the RNA duplexes), no sorting system exists in humans. Therefore, all four human AGO proteins incorporate miRNA duplexes (Fabian et al., 2010; Ha and Kim, 2014).

Following miRNA duplex loading to the RISC, the pre-RISC removes one of the strands to generate a mature RISC. The duplex RNA possesses two strands namely the functional guide strand or matured miRNA and the passenger strand. The strand that is recruited into the RISC (functional strand) guides the complex to its target, whereas the other strand (miRNA*) is degraded (Figure I-17).

Which strand will be the guide strand is determined during AGO loading step, mainly on the basis of the relative thermodynamic stability of the two ends of the small RNA duplex. The strand with a higher relatively unstable terminus at the 5' side is typically selected as the guide strand. The first nucleotide is also determinant since AGO proteins select for guide strand those with a U at nucleotide position 1. As seen for other proteins involved in miRNA processing, AGO proteins can also be regulated by numerous modifications (Ha and Kim, 2014).

5.1.4 Target repression or degradation

The 5' end of mature miRNAs contains the seed region (nucleotide positions 2-7 or 2-8), which has the capacity to identify the complementary bases of the 3'-UTR of the target mRNAs and trigger their cleavage and degradation (Guo et al., 2010). Nevertheless, there is usually an imperfect complementarity and the final effect of miRNA activity is a decrease in protein expression due to translational suppression. Interestingly, miRNAs have also been found to target the 5'-UTRs of mRNAs (Lee et al., 2009; Lytle et al., 2007) and to induce target translation (Vasudevan et al., 2007).

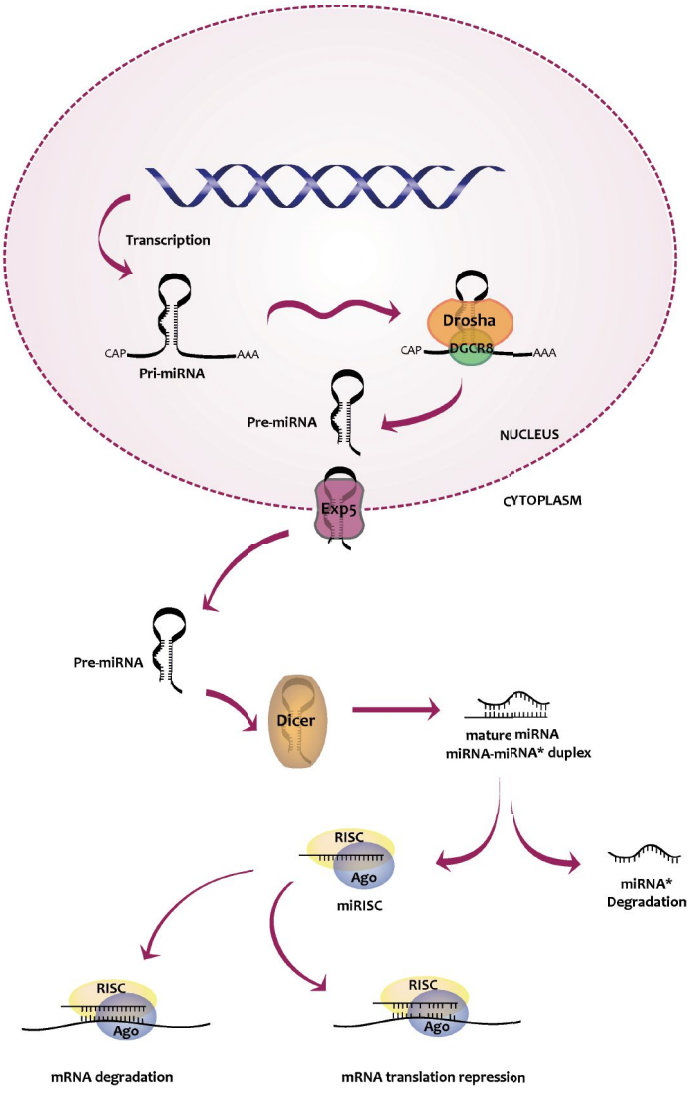

Figure I-17. Biogenesis and function of miRNAs. miRNAs are transcribed as long primary transcripts (pri-miRNAs) in the nucleus and are later recognized by Drosha and its cofactor DGCR8 to generate a pre-miRNA. Pre-miRNAs reach the cytoplasm through exportin 5 and are processed by Dicer into a mature miRNA–miRNA* duplex. RNA-induced silencing complex (RISC) recruits the selected miRNA strand and targets the miRNA–RISC complex to the specific 3'-UTR mRNA, while the miRNA* strand is degraded. Depending on the miRNA–mRNA complementarity, miRNA degrades the target mRNA or inhibits its translation.

5.1.5 mRNA repression

Normally, initiation is the most common target for translational control and all nuclear transcribed eukaryotic mRNAs contain at their 5' end an m^7GpppN group (where N is any nucleotide) termed the 5' cap, which facilitates ribosome recruitment to the mRNA. However, some cellular and viral mRNAs are translated via alternative cap-independent mechanisms involving internal ribosome entry sites (IRESs).

In regular cap-dependent translation, the small ribosomal subunit 40S in a complex together with a number of eukaryotic initiation factors (eIFs) binds the mRNA near the 5' cap and scans the mRNA in a 5'→3' direction until it finds an AUG codon. The eIF4F complex and the poly(A)-binding protein (PABP) bound to the 5' cap and the 3' poly(A) tail respectively and facilitate the recruitment of ribosomes. The recognition of the 5' cap is mediated by at least 10 initiation factors which include the eIF4F complex which in turn is formed by the eIF4A, responsible for unwinding the 5'-UTR, the eIF4E which specifically interacts with the cap, and the eIF4G that binds to both eIF4E and eIF4A and other proteins. Additional proteins present in the initiator complex are, eIF3 which recruit 40S ribosome, and the eIF6, responsible for 60S subunit biogenesis and joining. The PABP, besides binding to the 3' poly(A) tail directly interacts with the eIF4G subunit. Thus, eIF4G subunit binds simultaneously to eIF4E and PABP and therefore brings the two ends of the mRNA in close proximity and thereby promotes the "circularization" of the mRNA. This circularization enhances the rate of translation initiation (Carthew and Sontheimer, 2009; Fabian et al., 2010; Vimalraj and Selvamurugan, 2012).

As mentioned before, in some viral mRNAs, internal ribosome entry sites (IRESs) offer an alternative mechanism of translation initiation (cap-independent) since IRESs provide an internal ribosome-binding site, thus bypassing the requirement for the cap and functioning independently of eIF4E (Fabian et al., 2010).

miRNAs can exert their inhibitory effect by repressing translation initiation or translation elongation process. Experimental data suggest different mechanisms by which miRISC represses mRNA translation initiation. However, there are inconsistences about how miRNAs repress mRNA translation since the models described by experimental work suffer from contradictory evidence. One model proposes that miRISC competes with eIF4E for binding to the mRNA 5' cap structure or that miRISC interferes with eIF4E function. A second model suggests that miRISC stimulates deadenylation of the mRNA tail and therefore translation is repressed because the 5' cap and the PABP-free tail are unable to circularize. The last model proposes that miRISC is able to block the association of the 60S ribosomal subunit with the 40S preinitation complex. Since eIF6 is involved in the biogenesis and

maturation of 60S ribosomal subunits, the recruitment of eIF6 by miRISC may repress translation by preventing the assembly of translationally competent ribosomes at the start codon (Figure I-18) (Carthew and Sontheimer, 2009; Fabian et al., 2010).

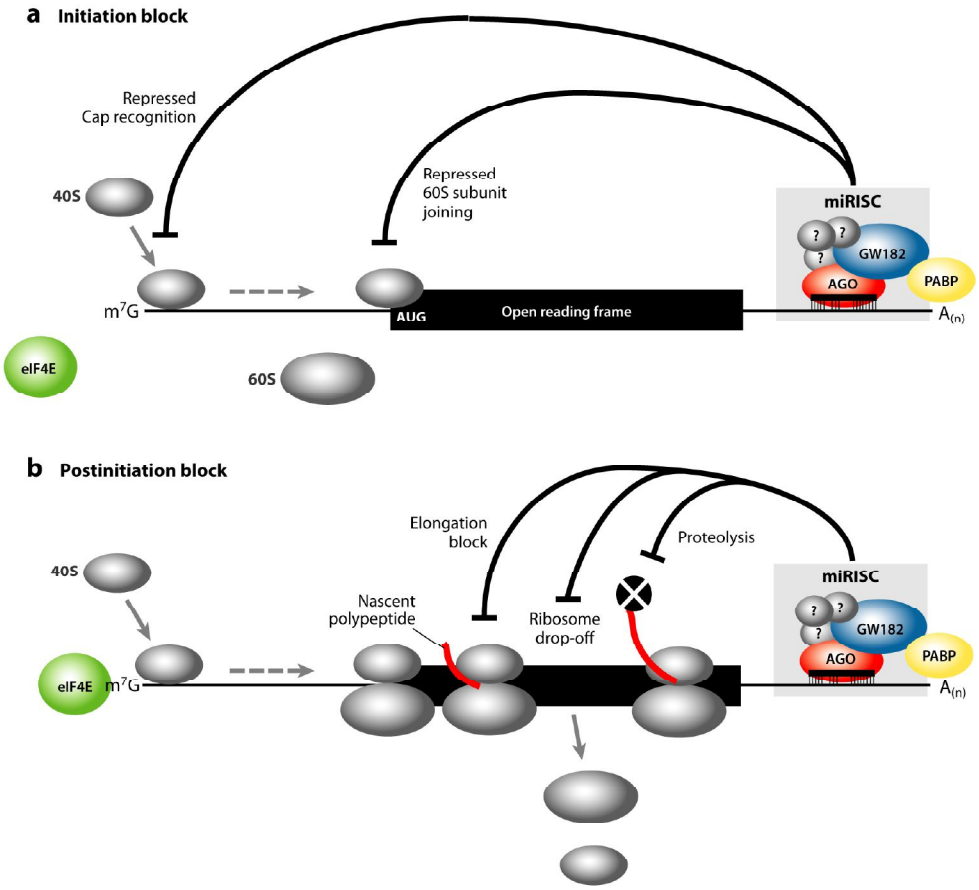

Figure I-18. Proposed mechanisms for miRNA-mediated translational repression. (a) The miRISC can interfere with eIF4F recognition or function and therefore inhibit the circularization of the mRNA thus repressing the translation initiation. Moreover, miRISC can prevent 80S ribosomal complex formation. **(b)** It has been suggested that miRNAs can also inhibit post-initiation processes by inhibiting ribosome elongation, inducing ribosome drop-off or facilitating proteolysis of nascent polypeptides. Adapted from (Fabian et al., 2010).

Repression at post-initiation steps has also been reported although there are not known mechanisms to explain such inhibition. Suggested mechanisms by which miRISC represses mRNA after translation initiation process includes the inhibition of ribosome elongation, induction of ribosome drop-off, or facilitation of proteolysis of nascent polypeptides. However, there is no clear understanding of these proposed mechanisms.

5.1.6 mRNA degradation

Among the AGO proteins, AGO2 is the only that can induce the guide strand-mediated cleavage of target mRNA by the catalytically competent RISC. Slicing competent AGO proteins (AGO2) can cleave one of the strands if the duplex is matched at the center, and removal of the cleaved strand is facilitated by the endonuclease C3PO (component 3 promoter of RISC).

However, miRNA-targeted mRNAs significantly reduce their abundance due to an increase in mRNA degradation that is not explained because of Ago-catalyzed mRNA cleavage but rather because of deadenylation, decapping and exonucleolytic digestion of the mRNA. Moreover, there are studies suggesting that degradation might be an independent mechanism of repression for some targets, not related to previously repressed mRNAs.

The mechanism proposed for miRNA-mediated mRNA destabilization starts with the 3' deadenylation. Both deadenylation and subsequent decapping and decay require AGO and GW182, components of the miRISC. In fact, AGO proteins seems to act as a scaffold to recruit GW182 to the mRNA and in turns, GW182 proteins interact with and recruit the mRNA decay machinery to miRNA-targeted mRNAs. Thus, GW182 recruits the CCR4/NOT1 (carbon catabolite repression 4/negative on TAT-less) complex, which promote the removal of the poly(A) tail. The PABP is also required for miRNA-mediated deadenylation since it is necessary that the C terminus of the GW182 protein directly interacts with the C-terminus of the PABP. Thus, PABP-GW182 interaction interferes with the mRNA circularization in the translation initiation process and with the termination process by blocking PABP binding to the termination factor eRF3 (Fabian et al., 2010).

After deadenylation, proceeds the 5' cap removal, which is produced by decapping enzymes (for example DCP1/DCP2 complex). Ultimately, the mRNA is degraded by exonucleases. Thus, miRISC mediating mRNA degradation requires Argonaute proteins and the processing body (P body) component, which consists of GW182 and the cellular and deadenylation machinery as deadenylases CCR4 and NOT1 and decapping enzymes (Figure I-19).

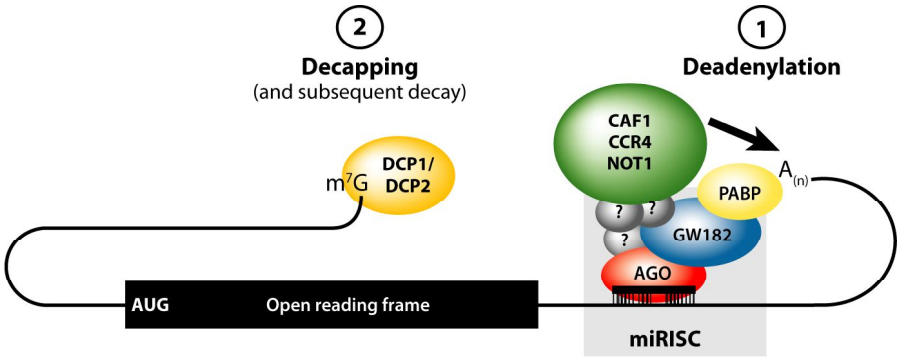

Figure I-19. miRNA-mediated mRNA decay. The scaffold protein GW182 interacts with the AGO protein (also present in the miRISC) and with the PABP protein. Thus, GW182 recruits the CCR4-NOT1 deadenylase complex in order to deadenylate the poly(A) tail. The 5' cap is removed after deadenylation by decapping proteins (DCP1/DCP2 complex in the scheme). Adapted from (Fabian et al., 2010).

5.1.7 Non-canonical miRNA processing pathways

Although the majority of identified miRNAs are produced by the already introduced canonical pathway, there are alternative pathways for miRNA biogenesis that can generate miRNAs. As mentioned previously, it was described that particular microRNAs are able to bypass Drosha-mediated processing step. Introns with the appropriate size can form a hairpin resembling a pre-miRNA and bypassing Drosha cleavage. They are further processed in the cytoplasm by Dicer and are called mirtrons. Thus, mirtrons are microRNAs located in the introns of the mRNA encoding host genes that are processed through a non-canonical pathway (Ruby et al., 2007). However, this bypass and the existence of other non-canonical pathways to achieve miRNA maturation represent the mechanism of biogenesis of only about 1% of conserved miRNAs (Ha and Kim, 2014).

5.1.8 miRNA nomenclature

The nomenclature of miRNAs is not very consistent. The first miRNAs were named after their phenotypes (lin-4, let-7) and then most miRNAs found experimentally received a standard nomenclature where the prefix miR is followed by a dash and a number, the latter indicating the order of its naming (for example miR-125). miR refers to the mature form of the miRNA whereas mir refers to the pre-miRNA. Genes that were found to encode miRNA sisters (with almost identical sequences) are indicated with lowercase lettered suffixes (for example, miR-125a and miR-125b). If a same pre-miRNA generates two nearly identical mature miRNAs but they arise from different loci, a number is added at the end (for example, miR-125b-1 and miR-125b-2). Thus, they are located in different regions of the genome but they both generate almost the same miRNA.

Moreover, each locus produces two mature miRNAs since miRNAs can result from the 5' or 3' strand and therefore they are named with the suffix 5p or 3p (miR-125a-5p or miR-125a-3p) (Ha and Kim, 2014; Moreno-Moya et al., 2014). If the relative expression levels are known, an asterisk after the name indicates that this particular miRNA is found at low levels compared to the miRNA from the opposite arm of the pre-miRNA hairpin (for example, has-miR-30d and has-miR-30d* share a pre-miRNA hairpin but the first one is the most predominant in the cell) (Moreno-Moya et al., 2014).

Furthermore, species can be designated with a three-letter prefix: has for humans (*Homo sapiens*) and mmu for mice (*Mus musculus*).

5.2 Regulation of miRNA Expression

Although several miRNAs have been identified in the last decade, little is known about their transcriptional regulation. Numerous screenings have been performed in order to characterize the miRNA expression scenario during different stages of cell differentiation or processes, but fewer studies have attempted to describe the molecular linkage between the stimuli and their regulatory effect on miRNA expression in full detail. miRNA processing and maturation can be regulated through the interaction of additional proteins with the Drosha complex. Using different models, it has been shown that miRNA expression can be regulated through several mechanisms, including regulation of pre-miRNA nuclear export, Dicer cleavage and regulation of promoter activity by methylation, histone modification or by direct regulation of RNA polymerase II recruitment (Davis-Dusenbery and Hata, 2010).

5.2.1 Transcriptional control of miRNA biogenesis

Experimental data suggest that many characteristics of miRNA gene promoters are similar to those of protein coding genes: the relative frequencies of CpG islands, TATA box, TFIIB (transcription factor II B) recognition, initiator elements and histone modifications. Thus, DNA-binding factors can regulate miRNA transcription as it happens in protein-coding genes. Moreover, as in the case of other genes, transcription of primary miRNA transcripts can be dynamically regulated in response to growth factor stimulation. c-myc, for example, is a transcription factor that regulates almost the 15% of the human genes and it has been reported to also control miRNA expression, as well as p53 (Davis-Dusenbery and Hata, 2010).

The mechanisms of epigenetic control known for protein-coding genes are also present in miRNA genes. Several miRNA loci have been found to be hypermethylated in multiple human cancers and histone modifications have been described in miRNA promoters during development and pathogenesis. For example, in bladder cancer the

expression of miR-127 is reduced due to promoter hypermethylation and in the breast cancer cell line SKBr2, 32 miRNAs are down-regulated following treatment with histone deacetylase (HDAC) inhibitors (Davis-Dusenbery and Hata, 2010).

5.2.2 Control of miRNA processing

Control of miRNA expression can also be achieved by regulating the different steps involved in miRNA maturation. Various post-translational modifications of Drosha and DGCR8 control their expression, nuclear localization and activity. For instance, phosphorylation of Drosha by GSK3β is required for the nuclear localization of Drosha and its acetylation inhibits its degradation and stabilizes it. Moreover, DGCR8 can be phosphorylated by ERK, which increases its stability (Ha and Kim, 2014).

Drosha microprocessor can also be controlled by RNA-binding proteins that selectively interact with Drosha and/or certain pri-miRNAs in order to process specifically some miRNAs, as is the case of p68 and p72 RNA helicases. Other interactions with the microprocessor have been described (Ha and Kim, 2014).

Dicer can interact with dsRBD proteins and be regulated by them. For example, Dicer interacts with TAR RNA-binding protein (TRBP) in humans and can be phosphorylated by the MAPK ERK leading to the preferential up-regulation of growth promoting miRNAs (Ha and Kim, 2014). Dicer can also interact with PACT (protein activator of protein kinase R) although both PACT and TRBP are not essential for Dicer-mediated cleavage. However, they participate in the recruitment of AGO2.

Dicer1 mRNA contains binding sites for let-7 miRNA, which results in a negative feedback loop between Dicer and its product. Thus, Dicer can be regulated by its cofactors and products and further regulate its activity (Ha and Kim, 2014; Hata et al., 2010). Additional interactions have been described regulating every step of miRNA processing

5.3 miRNAs and Skeletal Cell Specification

It is well known that miRNAs play an important role in chondrogenic and osteogenic differentiation during cartilage and bone formation (Hobert, 2008; Kapinas and Delany, 2011). The first *in vivo* approach was performed through conditional ablation of the *Dicer* gene under the control of the *Col2a1* promoter (Kobayashi et al., 2008). Mutant mice displayed severe skeletal growth defects due to a reduction in proliferating chondrocytes, leading to premature death. Evident skeletal phenotypes were similarly seen in mice with *Dicer* deficiency in osteoprogenitor cells (using *Cre* under the 2.3 kb fragment of *Col1a1* promoter). Ablation of *Dicer* in progenitors prevents their differentiation and compromises fetal survival (Gaur et al., 2010). In

addition, Mizoguchi et al. have demonstrated that osteoclast Dicer is also crucial for normal osteoclast resorption and osteoblast activity (Mizoguchi et al., 2010). Osteoclast specific-*Dicer* knock out mice was generated by crossing *Cathepsin K-Cre* mice with *Dicer* flox mice. These mice presented higher bone mass and a decrease in osteoclast surface and number. Additionally, not only osteoclast-related genes but also osteoblast-related ones (*Col1a1*, *Bglap*, *Runx2*) were down-regulated (Mizoguchi et al., 2010). These data suggest that miRNAs are important not only during bone development but also for bone homeostasis throughout life.

Thus, different miRNAs can act as either positive or negative determinants within multiple pathways involved in skeletal development processes. miRNA expression is finely orchestrated, being up- and down-regulated in order to control the differentiation stage of each bone cell, leading to a characteristic temporal miRNA signature in bone development and homeostasis. Nevertheless, despite all the information available about microRNAs and skeletogenesis, few *in vivo* studies have been conducted in order to validate each miRNA and it remains unclear how *in vivo* changes in specific miRNAs compromise normal bone development.

Among the few microRNAs studied *in vivo*, miR-34 family members have been reported as regulators of osteoblast proliferation and/or differentiation (Wei et al., 2012). Wei et al. described for the first time a family of microRNAs that were involved in bone formation. They described that SATB2 is targeted by miR-34s, affecting osteoblast proliferation mainly by means of miR-34b and –c. Thus, miR-34bc$^{Osb-/-}$ mice was generated using *Cre* under the control of the 2.3 kb fragment of *Col1a1* promoter and the resulting adult mice showed increased cortical bone volume, bone mineral density and cortical thickness of long bones (Wei et al., 2012).

SATB2 belongs to the family of special AT-rich binding proteins, members of which are present in the nuclear matrix and can bind to AT-rich sequences, activating the transcription of particular genes (Britanova et al., 2005). *In vivo* studies have shown that SATB2 physically interacts with and enhances the activity of RUNX2 and ATF4 (Conner and Hornick, 2013; Dobreva et al., 2006). Moreover, it increases both *Osteocalcin* transcription by binding to its promoter and *Ibsp* expression by direct attachment to an osteoblast-specific promoter element (Dobreva et al., 2006). Thus, it can be explained why miR-34, by means of SATB2, can regulate *Osteocalcin*, *Ibsp* and possibly other genes (Wei et al., 2012).

A wide range of other osteoblast-related genes are affected by miRNA regulation. miRNAs targeting signaling components of TGF-β, PI3K, BMP, WNT and MAPK pathways have been described. Moreover, specific key osteogenic factors described in section 2.1 such as *Runx2* or *Osterix* are also regulated by microRNAs. *Runx2* mRNA for

example, has a very long 3'-UTR which probably contains multiple regulatory elements (Huang et al., 2010), and it is therefore not surprising that several examples of post-transcriptional *Runx2* mRNA regulation through miRNAs have been described (Gao et al., 2011; Huang et al., 2010; Li et al., 2008).

Pequeña alegría de laboratorio#2

Encontrar de nuevo un *pellet* que creías perdido

OBJECTIVES

OBJECTIVES

Differentiation towards the osteoblast lineage is controlled by a multitude of signal transduction cascades. Several signaling molecules play major roles in controlling skeletal development and although there has been a tremendous progress in the molecular understanding of osteoblast differentiation, there is still a considerable lack of knowledge about the cross-talking network involved in this process.

Thus, the overall aim of this thesis is to describe new aspects of the signaling networks regulating bone biology and the connection with other well-known pathways. Since two clear different objectives were established, the results and discussion sections of this thesis will be also analyzed separately.

1 To study BMP-regulated miRNAs relevant in the mechanism of osteoblastic differentiation and to describe their molecular mechanism of action.

2 To generate and study distinct isoform-specific PI3K osteoblast-specific mutant mice in order to characterize their impact in bone development and homeostasis. To analyze the role of PI3K in the transcriptional regulation of osteoblast differentiation.

Pequeña alegría de laboratorio#3

Que la tensión superficial salve el contenido de un *eppendorf* al caer

RESULTS

1 STUDY OF MIRNAS INVOLVED IN OSTEOBLAST DIFFERENTIATION

1.1 miR-322 Up-regulates Osterix Expression by a SMAD-Independent Mechanism

1.1.1 miRNA expression profile during BMP-2-induced osteoblast differentiation

To identify miRNAs whose expression is altered during osteoblast differentiation, C2C12 cells were treated with BMP-2 (2 nM) in medium without serum for 8 hours. Independent experiments were performed under the same conditions, and an miRNA expression profile was obtained using mirVana miRNA isolation kit and a TLDA array (TaqMan Array Rodent MicroRNA B Card v3) (Figure R-1 A). In agreement with previous results, global analysis indicated that most of the significantly changed miRNAs were down-regulated in response to BMP-2 (Inose et al., 2009; Li et al., 2009a). To verify these results, miR-30a, miR-206, and miR-322 were chosen for further study based on the literature. First we tested the importance of these miRNAs in our model (C2C12 cells) and we found out that the selected miRNAs were expressed at relatively high levels in C2C12 cells (Table R-1). To confirm the array data, kinetic assays of BMP induction in the presence and absence of serum were performed, and the expression of selected miRNAs was detected by qPCR. Time course results were consistent with array data: miR-30a, miR- 206, and miR-322 all steadily decreased after

BMP-2 addition (50–60% decrease at 8 and 24 hours for miR-206 and miR-322) (Figure R-1 B). Down-regulation of miRNA expression to a similar extent was also observed in cells cultured in the absence of serum (Figure R-1 C).

A

miRNA	Value
mmu-miR-503*	0.1648
mmu-miR-206	0.2219
mmu-miR-99b*	0.2249
mmu-miR-28*	0.3063
mmu-miR-135a*	0.3138
mmu-miR-720	0.3147
mmu-miR-378	0.3336
mmu-let-7a*	0.3387
mmu-miR-805	0.3467
mmu-miR-149	0.3494
mmu-miR-130b*	0.4011
mmu-miR-29a*	0.4060
mmu-miR-709	0.4311
mmu-miR-27b*	0.4373
mmu-miR-33*	0.4397
mmu-miR-744*	0.4461
mmu-miR-22	0.4471
mmu-miR-322*	0.4482
mmu-miR-30a*	0.4680
mmu-miR-193*	0.4981
mmu-miR-18a*	1.2170
mmu-miR-24-2*	1.8075

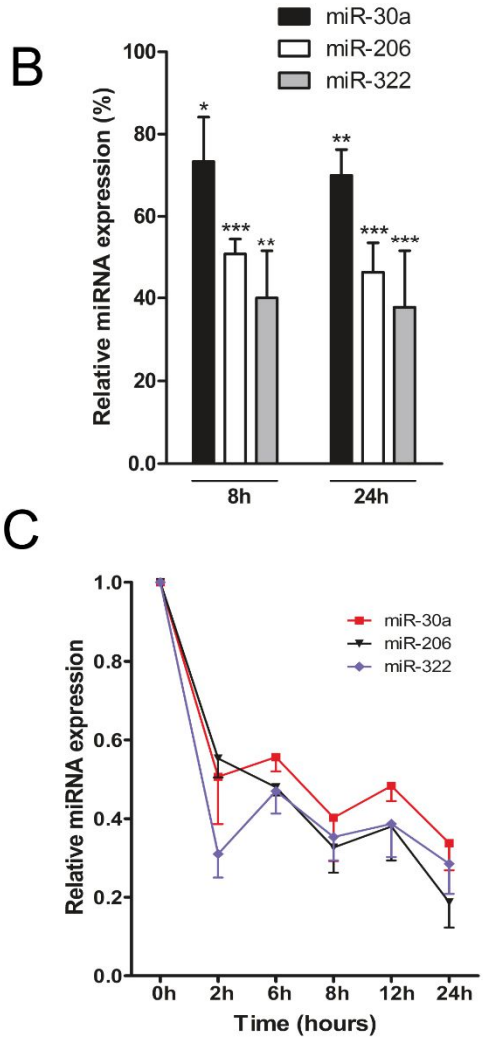

Figure R-1. Expression profile of miRNAs during osteoblast differentiation. (A) miRNA array expression data from C2C12 cells treated with BMP-2 for 8 hours. Red denotes higher expression and green denotes lower expression relative to expression in control cells. Only miRNAs with a 2-fold reduction in expression are shown. **(B&C)** Expression of miR-30a, miR-206 and miR-322 was analyzed during osteoblast differentiation. Time course experiments were performed with 2 nM BMP-2 treatment with **(B)** or without **(C)** 10% fetal bovine serum. The indicated miRNAs were isolated from C2C12 cell cultures, measured by RT-qPCR, normalized to U6 RNA and plotted as relative expression to time 0. Data represent the mean ± SEM (n=5).

miRNA EXPRESSION		
miRNA	**Δ Ct mean *vs* U6**	**S.E.M**
miR-30a	3.65	0.489
miR-206	2.38	0.258
miR-322	3.84	0.243

Table R-1. Relative expression of miR-30a, miR-206 and miR-322. The indicated miRNAs from C2C12 cells were measured by RT-qPCR and expressed as ΔCt relative to U6 expression. Data represent the mean ± SEM (n=6).

We extended our observations to primary cultures of murine BM-MSCs and MC3T3-E1 cells. BMP-2 treatment of BM-MSCs or MC3T3-E1 cells for 24 hours caused similar miR-322 expression down-regulation, whereas miR-30a expression remained not significantly altered with respect to the miR control (Figure R-2 A&B). We also analyzed differentiation of MC3T3-E1 cells in medium containing ascorbic acid and β-glycerophosphate. In this case, although differentiation led to similar effects as BMP-2 addition on miR-30a and miR- 206 expression levels, it induced a significant increase in miR- 322 levels instead (Figure R-2 C).

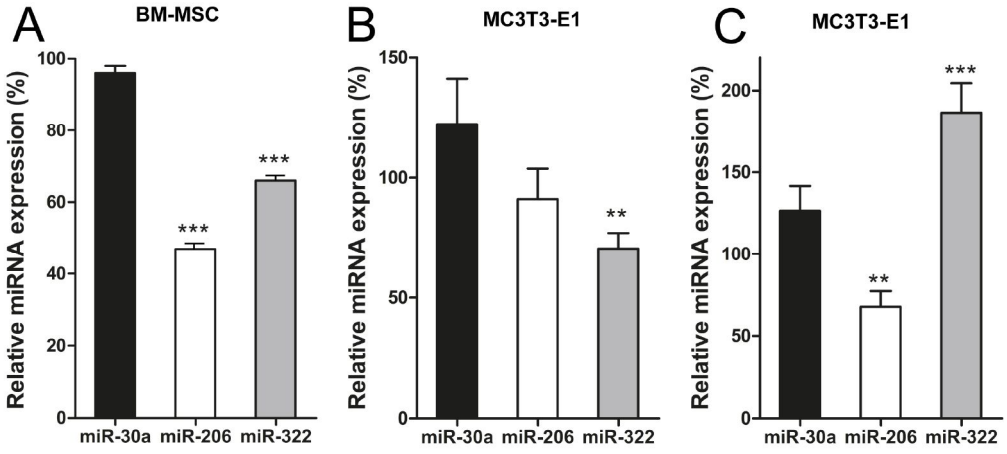

Figure R-2. miR-322 is also BMP-modulated in other osteoblast models. BM-MSCs **(A)** and MC3T3-E1 **(B)** were treated with BMP-2 in the absence of serum for 24 hours, and the indicated miRNAs were measured by RT-qPCR. **(C)** MC3T3-E1 cells were treated or not with differentiation medium for 10 days and the indicated miRNAs were measured by RT-qPCR. Data represent the mean ± SEM (n=5).

1.1.2 Study of miR-30a, miR-206a and miR-322 in osteoblast differentiation

To further test whether the selected miRNAs affect osteoblast differentiation, C2C12 cells were transfected with miRNA mimics or anti-miRs of miR-30a, miR-206, and miR-322. First, we checked how transfection of these Pre-miRs and Anti-miRs was working using BLOCK-iT™ Alexa Fluor® Red Fluorescent Control (Figure R-3 A). Furthermore, we determined if we were achieving a physiological level of miRNA overexpression or repression. Consistently, transfection of Pre-miR-322 led to increased levels of miR-322, whereas transfection of Anti-miR-322 led to a 40% decrease in expression of endogenous miR-322 (Figure R-3 B).

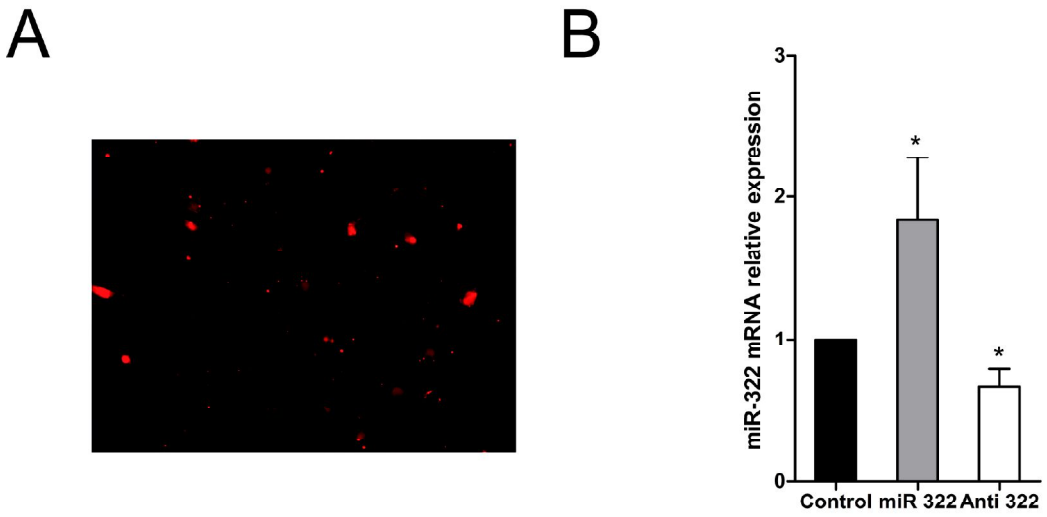

Figure R-3. Overexpression of miRNA mimics and inhibitors. (A) Alexa Fluor Red Fluorescent Control used for verification of C2C12 transfection. Magnification 20x. **(B)** C2C12 cells were transfected with miR-322 mimic, anti-miR-322 or miR-control for 24 hours and miR-322 was analyzed by RT-qPCR. Data represent the mean ± SEM (n=3).

Thus, C2C12 cells were transfected with Pre-miRs of miR-30a, miR-206a and miR-322 and treated with BMP-2 for 16 hours. Their effects were first assessed by characterizing the mRNA expression levels of the main osteoblast-determining transcription factors. It is well known that BMP addition to C2C12 cells stimulates expression of known osteogenic markers (Karsenty, 2008; Nakashima and de Crombrugghe, 2003; Nakashima et al., 2002; Ulsamer et al., 2008). Overexpression of miRNA mimics produced a significant increase in *Osx*, *Runx2*, *Msx2*, osteocalcin, and *Ibsp* mRNA levels by miR-322 and increases in *Runx2* and *Ibsp* by miR-206 (Figure R-4 A). Upon BMP-2 stimulation, ectopic expression of a miR-322 mimic resulted in a significant accumulation of *Osx*, *Runx2*, *Msx2*, and *Ibsp* mRNA levels compared with

expression of a control miRNA mimic. miR-30a transfection reduced both basal and BMP-stimulated *Dlx5* mRNA expression.

We also analyzed the effects of miRNAs at protein level (Figure R-4 B). Although OSX protein expression increased significantly after miR-322 transfection, miR-206 and miR-30a overexpression led to an OSX decrease, possibly indicating negative osteoblast regulation (Figure R-4 B).

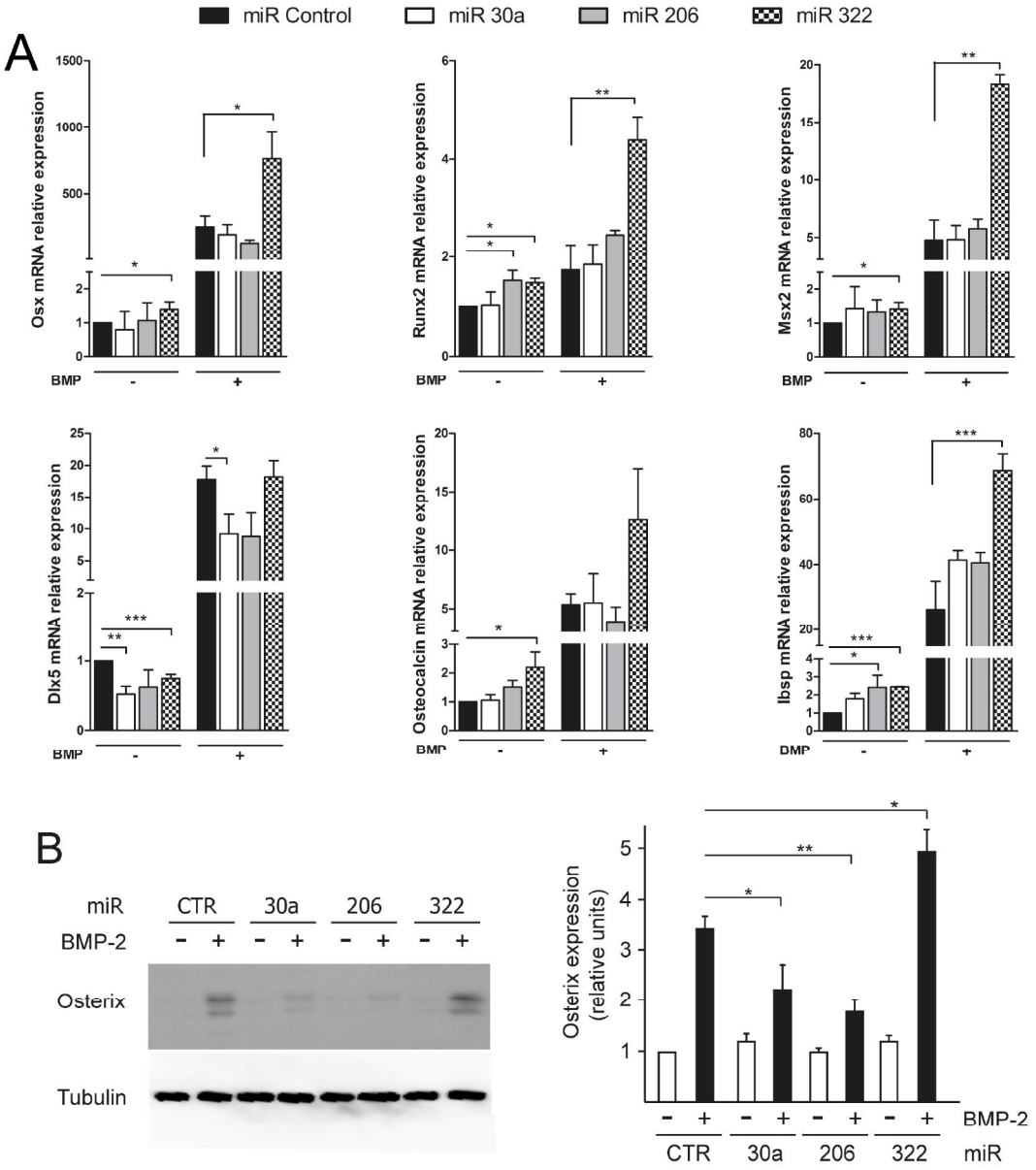

Figure R-4. miR-322 enhances *Osx*, *Msx2* and *Runx2* expression. (A) C2C12 cells were transfected with the indicated miRNA mimics without serum for 8 hours and treated with BMP-2 overnight. RT-qPCR for the indicated genes was performed and *Gapdh* was used as an internal control. Results are plotted as expression relative to untreated Pre-miR control-transfected cells (n=4-9). **(B)** C2C12 cells were transfected with the indicated miRNA mimics and treated with BMP-2 for 24 hours and OSX and tubulin were detected by immunoblotting (left panel). Quantification of the results is shown (right panel) (n=3). Data represent the mean ± SEM

We also analyzed overexpression of miRNA mimics in MC3T3-E1 cells, an osteoblast cellular model independent of BMP activation. MC3T3-E1 cells were seeded, transfected with miRNA mimics for 8 hours and treated with differentiation medium overnight (without BMP). Similar to C2C12 cells, *Osx*, *Runx2*, and *Msx2* mRNA levels were significantly increased by miR-322 (Figure R-5). Altogether, these results suggested that miR-322 might be important for osteogenic differentiation and led us to investigate its molecular mechanisms of action.

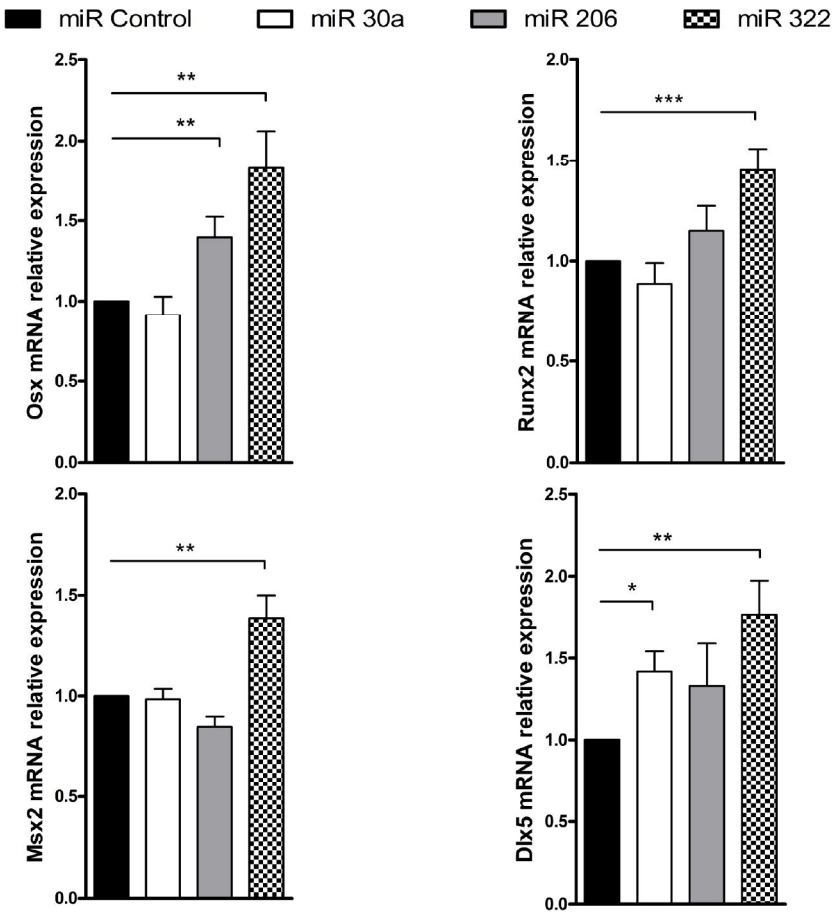

Figure R-5. Effects of miR-322 in MC3T3-E1 cells. MC3T3-E1 cells were transfected with the indicated miRNA mimics for 8 hours and treated with differentiation medium overnight. RT-qPCR for the indicated genes was performed and *Gapdh* was used as an internal control. Results are plotted as expression relative to untreated Pre-miR control-transfected cells (n=4-6). Data represent the mean ± SEM.

C2C12 cells differentiate into myoblasts and generate multinuclear myotubes in the presence of low levels of serum. However, BMP-2 is able to trans-differentiate them from the myoblast to the osteoblast lineage (Katagiri et al., 1994). To investigate whether miR-322 can also influence their myogenic differentiation, C2C12 cells were transfected with miR-322 or miR control and followed up for myotube formation.

Experiments revealed a complete lack of myotube formation up to 4 days in miR-322-overexpressing cells while anti-miR transfected ones remained as control (Figure R-6).

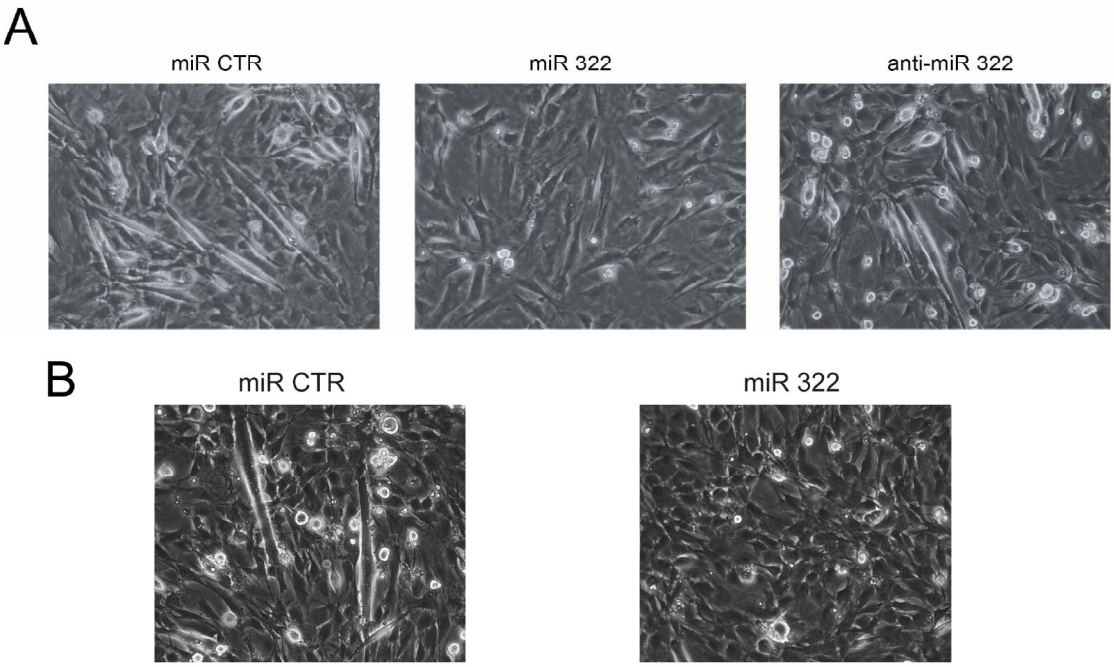

Figure R-6. miR-322 effect on myotube formation. miR-322 mimic-transfected C2C12 cells were maintained in medium without serum for 4 days and myotube progression. **(A)** miR-322 transfected cells are compared with Pre-miR control and anti-miR-322 transfected cells. Magnification 20x. **(B)** miR-322 transfected cells are compared with Pre-miR control. Magnification 40x.

Given the results obtained with the miR-322 overexpression experiments, we then performed miR-322 loss-of-function experiments. Therefore, Anti-miR-322 was transfected in cells in the presence or absence of BMP-2 to assess again the effect on osteogenic genes. The decrease in miR-322 levels led to a significantly lower induction of *Osx* and *Runx2* mRNAs by BMP-2 while Dlx5 and Msx2 levels remained unchanged (Figure R-7).

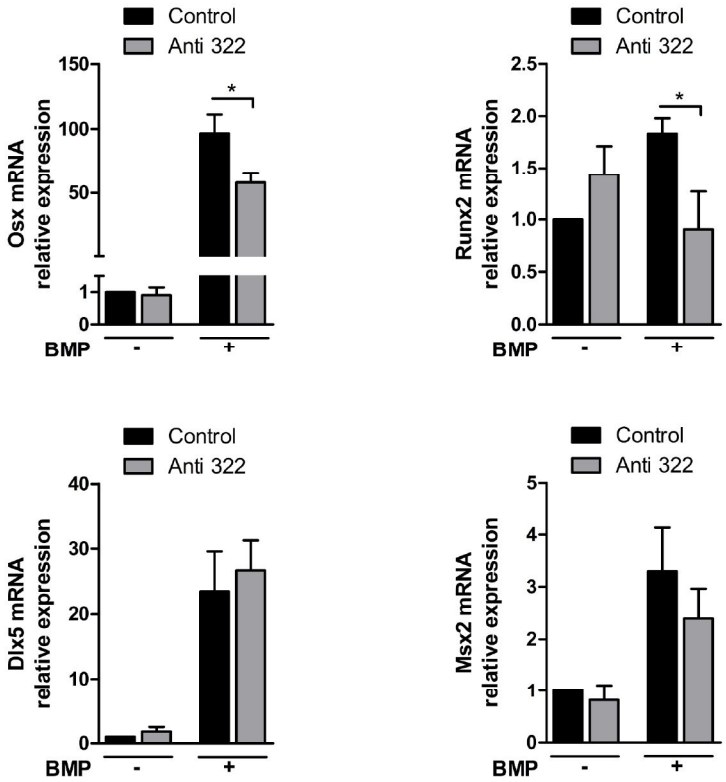

Figure R-7. Effects of anti-miR-322 in C2C12 cells. C2C12 cells were transfected for 8 hours with Anti-miR-322 and treated with BMP-2 overnight. The indicated mRNAs were measured by RT-qPCR, normalized to *Gapdh* and expressed as relative expression (n=4-5). Data represent the mean ± SEM.

1.1.3 Lack of direct interaction between miR-322 and the Smad pathway

As presented in the Introduction chapter, Smad proteins have been found to play critical roles in BMP-induced osteoblast differentiation (Massague et al., 2005). The above results suggested that miR-322 was able to increase expression of osteogenic genes in response to BMP-2. Thus, we decided to determine whether miR-322 directly modulates SMAD phosphorylation and signaling by performing time course experiments of BMP-2 activation. C2C12 cells were transfected with Pre-miR-322 and treated with BMP-2 at different time points. Ectopic expression of miR-322 led to a slight decrease in SMAD1 expression that became significant after 8 hours of BMP-2 addition (Figure R-8 A). However, immunoblotting showed no significant changes in the ratio between phosphorylated and total SMAD1 levels (Figure R-8 A). These results suggest that the effect of miR-322 in osteoblast differentiation is not likely related to a direct change in SMAD or phospho-SMAD1 levels. In parallel, SMAD1 and phospho-SMAD1 levels were also evaluated by immunoblotting after transfection with Anti-miR-322 and BMP-2 addition. Again, no significant changes were observed in phospho-Smad activation (Figure R-8 B).

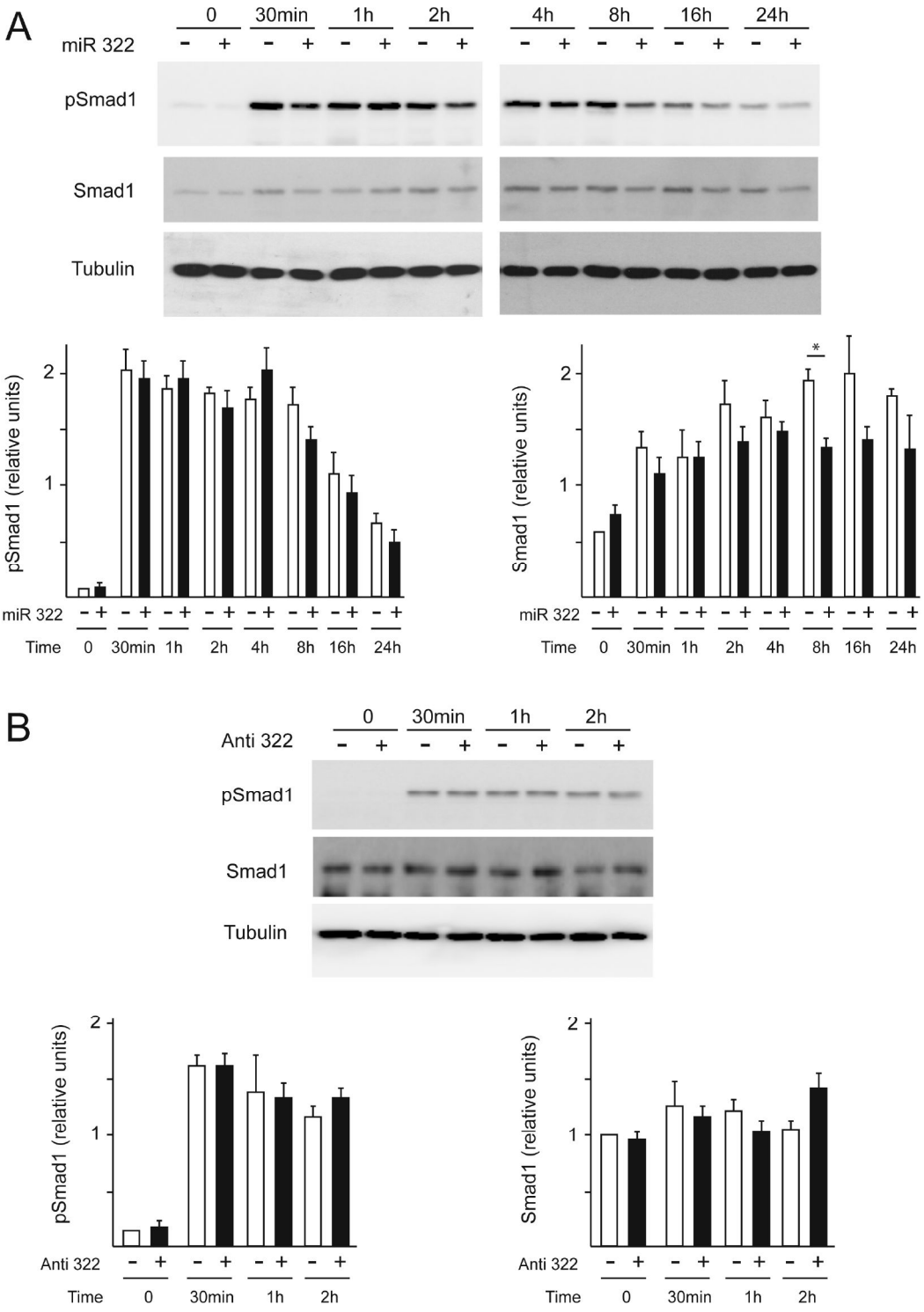

Figure R-8. miR-322 effects on BMP-Smad signaling. (A) C2C12 cells were transfected with miR-322 mimic and treated with 2 nM BMP-2 at indicated times. Levels of SMAD1 and phospho-SMAD1 were detected by Western Blot and normalized to tubulin expression. Quantification of the results is shown in the lower panels (n=3). **(B)** C2C12 cells were transfected with miR-322 inhibitor and treated with BMP-2 at the indicated times. Levels of SMAD1 and phoshpo-SMAD1 were detected and normalized with tubulin expression. Results were quantified and shown as relative expression (n=3). Data represent the mean ± SEM.

1.2 miR-322 Exerts Effects in Osteoblast Differentiation by Inhibition of Tob2 Expression

1.2.1 Tob2 is a target of miR-322

The essential role of *Runx2* and *Osx* in bone development led us to analyze the mechanisms regulated by miR-322 in osteoblast differentiation. We performed bioinformatic target prediction using DIANA, miRanda, and TargetScan prediction software. Putative targeted genes included *HoxA10* and *Dlx5* (osteogenic transcription factors); activin receptors IIA and IIB, *Smurf1*, *Smad7*, and *Smad1* (BMP signaling); and *Cdc25A* and *Tob2* (cell proliferation and differentiation) (Table R-2). Some of these targets were experimentally validated after miRNA mimic transfection. Thus, C2C12 cells were transfected with Pre-mir-206, Pre-miR-30a and Pre-miR-322 and the mRNA of some selected putative targets (*Tob2*, *Smad7* and *Smurf1*) were analyzed. The results showed that the expression of *Tob2* mRNA and the induction of *Tob2* and *Smad7* mRNAs by BMP-2 (6-fold increase for *Smad7*) were significantly decreased in miR-322-transfected cells, whereas no significant differences were found for miR-30a and miR-206 assays (Figure R-9 A). *Smurf1* mRNA levels were not altered in any case. We also checked *Tob2* mRNA levels after Anti-miR-322 transfection and it was significantly increased, both at basal state and after BMP-2 addition (Figure R-9 B).

TARGET PREDICTION	
miRNA	**Putative target**
miR-30a	*Runx2*, *Msx2*, *Acvr1*
miR-206	*Ets1*, *Dlx5*, *Satb2*, *Pax3*, *Cdk6*, *HDAC4*
miR-322	*Smad7*, *Cdc25A/B*, *ActRIIA/B*, *Smad5*, *Tob2*, *Smad1*, *HoxA10*, *Dlx5*, *Smurf1*

Table R-2. List of putative target genes related to osteoblast differentiation for the miRNAs analyzed.

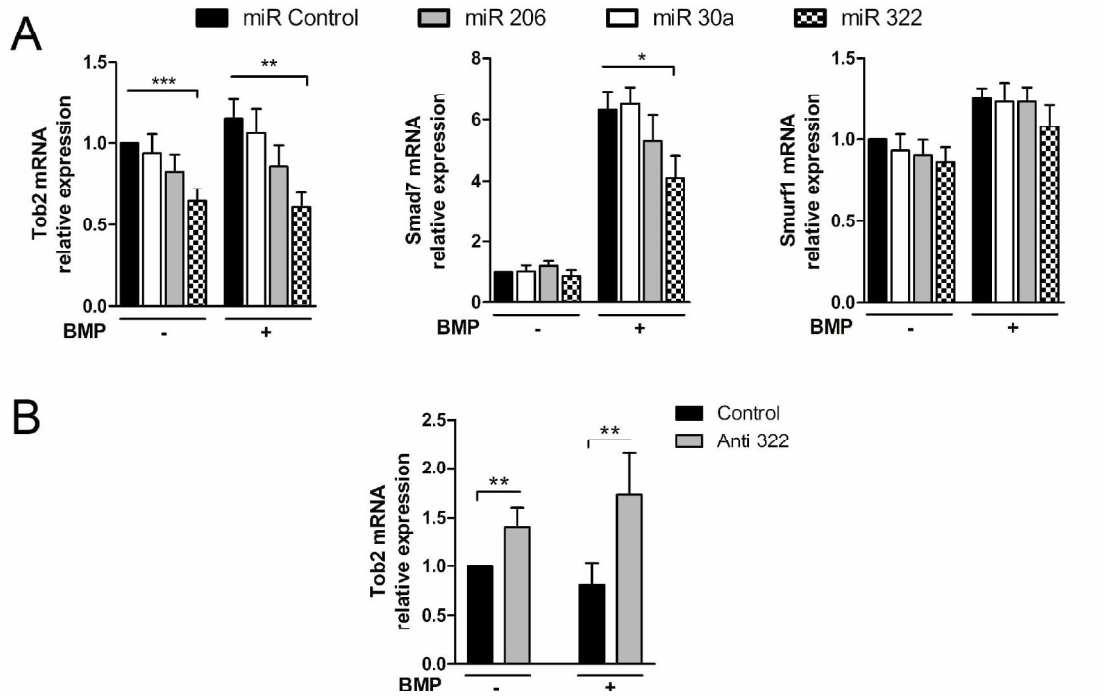

Figure R-9. miR-322 inhibits *Tob2* mRNA. C2C12 cells were transfected with selected miRNAs mimics **(A)** or miR-322 inhibitor **(B)** without serum for 8 hours and treated with BMP-2 overnight. *Tob2* *Smurf1* and *Smad7* expression was detected by RT-qPCR, normalized to *Gapdh* and expressed relative to the miR control transfection (n=4-7). Data represent the mean ± SEM.

The results led us to focus on *Tob2* regulation by miR-322. To further confirm the relation between miR-322 and our putative target *Tob2*, time course experiments in C2C12 cells were assessed. As shown previously, miR-322 progressively decreased after BMP-2 treatment in C2C12 cells (Figure R-1 B&C). In correlation with miR-322 down-regulation, BMP-2 addition also promoted increasing levels of *Tob2* mRNA expression during time (Figure R-10). These results supported the relation between miR-322 and *Tob2* expression.

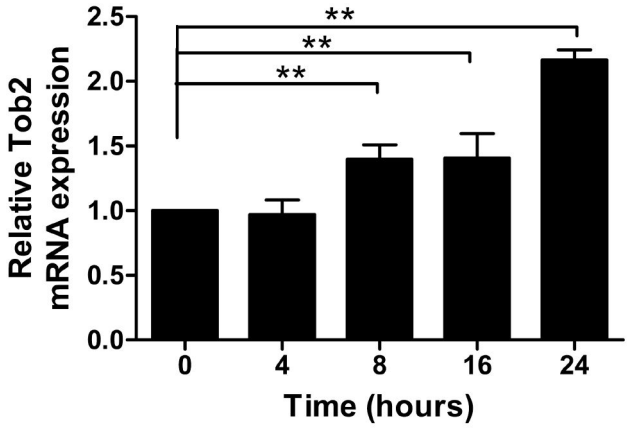

Figure R-10. *Tob2* mRNA expression in C2C12 cells after BMP-2 addition. C2C12 cells were treated with BMP-2 for different periods of time. RT-qPCR for *Tob2* mRNA was performed and *Gapdh* was used as internal control (n=4). Data represent the mean ± SEM.

We then analyzed whether changes in *Tob2* mRNA in response to miR-322 reduction or increase correlated with changes in TOB2 protein levels. Accordingly, quantification of western blot analysis revealed a significant decrease in TOB2 levels after transfection of a miR-322 mimic and a significant increase after Anti-miR-322 transfection (Figure R-11).

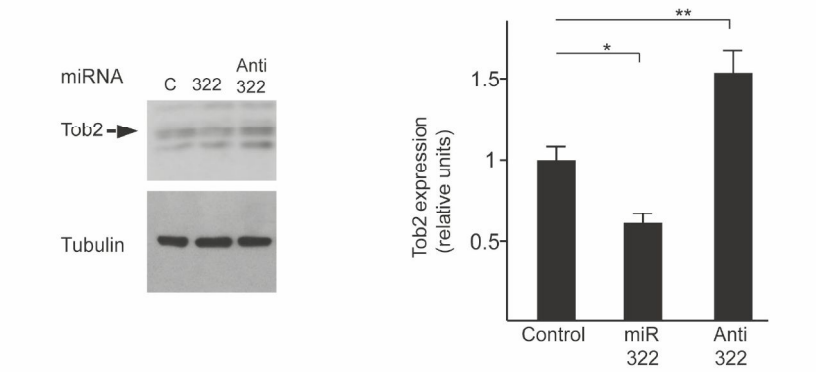

Figure R-11. miRNA-322 affects TOB2 protein expression. C2C12 cells were transfected with 20 nM miRNA mimic or inhibitor and TOB2 and tubulin were detected by western blotting (left panel). Right panel shows the relative TOB2 levels normalized to tubulin expression (n=3) Data represent the mean ± SEM.

To confirm our previous results in other osteoblast models, we performed lentivirus-mediated overexpression experiments in BM-MSCs. BM-MSCs were obtained from mice and were transduced with either a lentiviral construct expressing miR-322 or a control. mRNA was extracted after 10 days of culture in osteogenic medium. Consistent with the data from C2C12 cell cultures, miR-322 accumulation in BM-MSCs

also repressed *Tob2* and *Smad7* expression and induced significantly higher *Osx* mRNA levels compared with cells transduced with lentiviral control (Figure R-12). Taken together, these results provide evidence that miR-322 negatively regulates *Tob2* expression in mesenchymal cells.

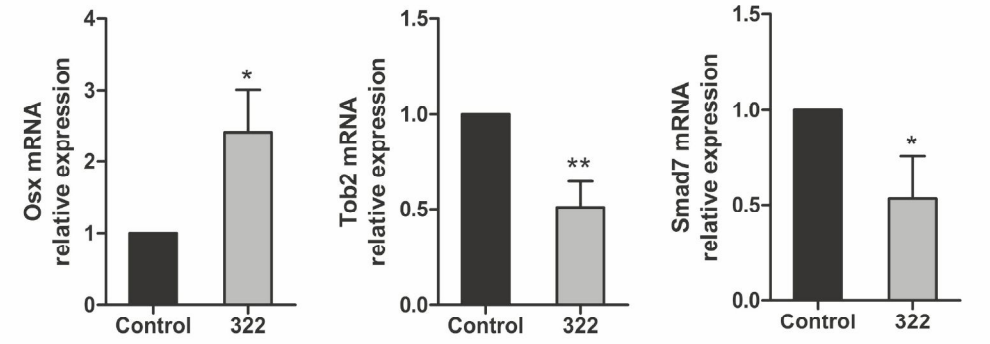

Figure R-12. *Tob2* and *Osx* are also regulated by miR-322 in BM-MSCs. BM-MSCs were infected with viral particles containing mmu-miR-322 or miR control overnight. Transduced cells were selected with puromycin for 4 days and cultured with osteogenic medium for 10 days. mRNAs were analyzed by RT-qPCR and results were normalized to *Gapdh* and plotted as relative expression (n=4). Data represent the mean ± SEM.

miRNAs are able to repress gene expression by binding to seed site sequences located within the 3'-UTR of mRNAs. To further confirm our previous results, we proceed to study the *Tob2* 3'-UTR in order to examine whether miR-322 can directly regulate *Tob2* expression. We first determined the presence of a putative target region of miR-322 at position +1769 by using miRNA target prediction tools. Then, the characterization of the specific *Tob2* 3'-UTR sequence bound by miR-322 was possible due to the generation of *Renilla* luciferase reporter plasmids. We generated *Renilla* constructs carrying the wild-type *Tob2* 3'-UTR or a construct with the miR-322-binding sequence mutated (Figure R-13 A).

To examine whether miR-322 can directly regulate *Tob2* expression by its binding to the specific 3'-UTR sequence of *Tob2*, C2C12 and MC3T3-E1 cells were co-transfected with miR-322 and the wild-type construct or with miR-322 and the mutant. The same co-transfections were also performed using miR-control. Luciferase activity of these experiments revealed that wild-type *Tob2* 3'-UTR construct was significantly inhibited after co-transfection with miR-322 in C2C12 or MC3T3-E1 (Figure R-13 B&C). Moreover, the mutant *Tob2* construct lacking the possible binding region of miR-322 was refractory to the decrease in luciferase activity after miR-322 ectopic expression. Altogether, these results provide evidence that miR-322 acts as an inhibitor of *Tob2* mRNA expression through binding to the characterized region located in its 3'-UTR.

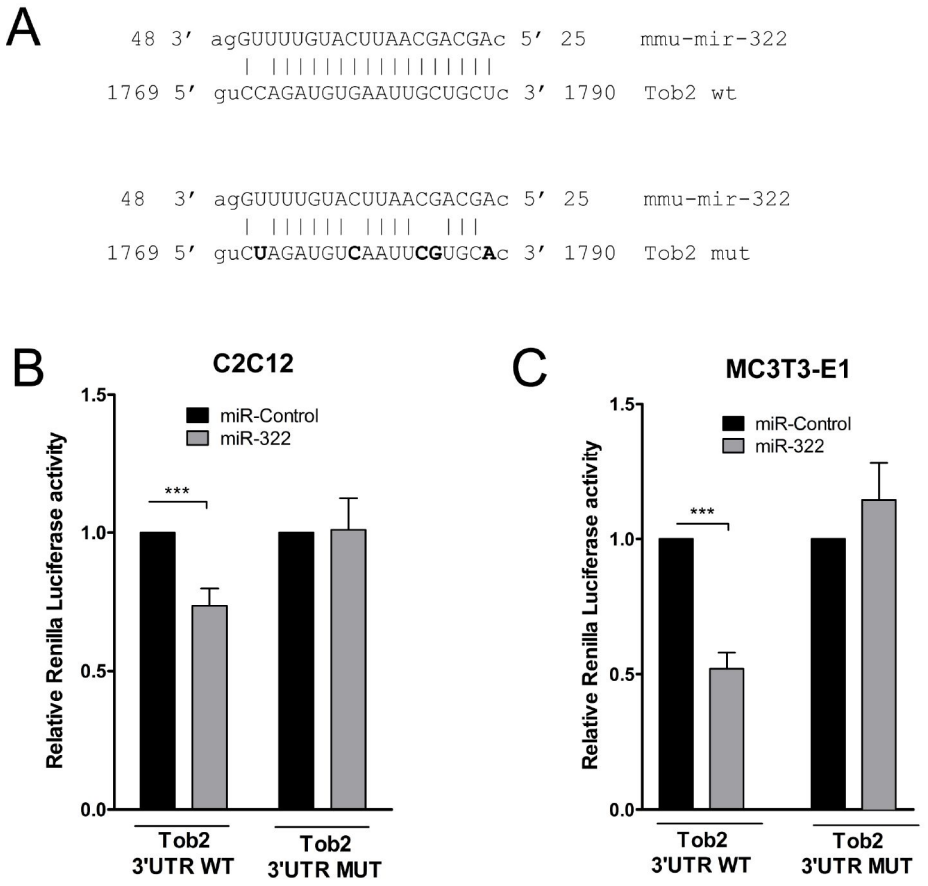

Figure R-13. *Tob2* is a direct target of miR-322. (A) Schematic representation of the alignment of the mouse *Tob2* mRNA 3'-UTR predicted to be targeted by miR-322. Mutations generated within the region corresponding to the seed sequence were included in the mutant *Tob2* 3'-UTR construct. C2C12 **(B)** or MC3T3 **(C)** were co-transfected with the Renilla luciferase reporter plasmid carrying the wild-type (WT) or mutant (MUT) *Tob2* 3'-UTR and miR-322 or miR-Control respectively. After 8 hours, cells were cultured until confluence for 16 hours and luciferase activity was analyzed and normalized to β-galactosidase expression. Relative luciferase activities are expressed (n=4-6). Data represent the mean ± SEM.

1.2.2 TOB2 accelerates decay of *Osterix* mRNA levels

Although Smad signaling was already tested, we further analyzed the possible effects of miR-322/Tob2 on the BMP-Smad target genes. We performed reporter assays using *Id1* and *Cox2* luciferase constructs previously generated in our lab and with a strong responsiveness to BMP signaling (Lopez-Rovira et al., 2002; Susperregui et al., 2011). Luciferase plasmids were co-transfected with constructs overexpressing *Tob2*, miR-322 or Anti-miR-322 in C2C12 cells. No major differences were observed in *Id1* neither in *Cox2* luciferase activities even after BMP-2 treatment (Figure R-14).

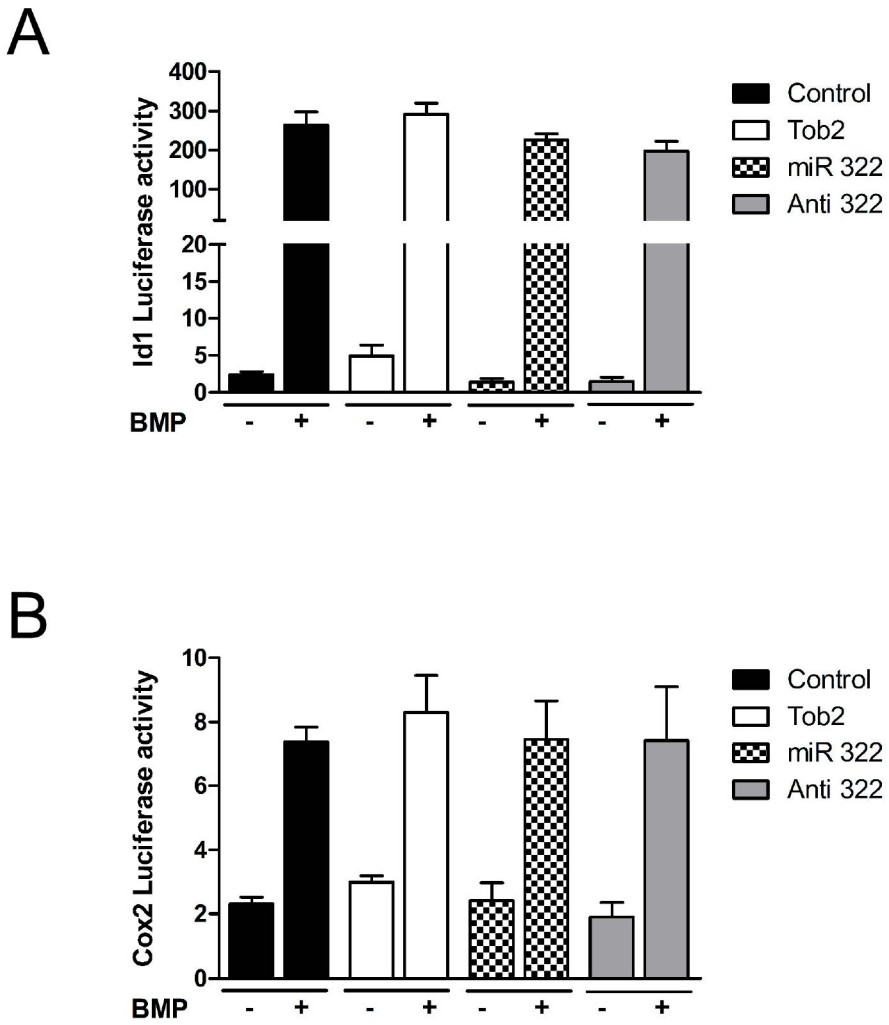

Figure R-14. *Tob2* or miR-322 do not alter transcriptional responses of *Id1* and *Cox2* reporter constructs. **(A-B)** C2C12 cells were co-transfected with *Id1* **(A)** or *Cox2* **(B)** reporter constructs and miR-control, miR-322, anti-322 or *Tob2* for 8 hours. Luciferase activity was detected after 16 hours of BMP-2 treatment and values were normalized with β-galactosidase activity. Data represent the mean ± SEM for triplicates from 4-8 independent experiments.

Tob-deficient mice present higher bone mass due to an increased number of osteoblasts and accelerated bone formation rate (Yoshida et al., 2000). Thus, Tob proteins have been studied as negative regulators of bone formation, although the mechanisms of this regulatory role are mostly unknown. Previous studies identified TOB not only as a general regulator of mRNA decay (Ezzeddine et al., 2007; Funakoshi et al., 2007) but also as a specific regulator by binding to CPEB2-4 (cytoplasmic polyadenylation element-binding protein) and recruiting CNOT7 deadenylase to the target mRNAs (Hosoda et al., 2011). Taking into account these previous studies, we hypothesized whether TOB2 could also regulate the mRNA degradation of specific osteogenic genes and we carried out mRNA decay assays by inducing ectopic expression of *Tob2*, miR-322 or miR-control in C2C12 cells. Once cells were transfected,

actinomycin D (a known inhibitor of mRNA synthesis) was added to the media and mRNA expression of specific genes was quantified by qPCR at different time points and compared with the mRNA expression before actinomycin D treatment. mRNA expression of some genes was already modified by the transfections before actinomycin D treatment. As shown above, *Osx* and *Runx2* were already up-regulated by miR-322 transfection and repressed by *Tob2* accumulation. Overexpression of *Tob2* also reduced the basal levels of expression *Smad7* and *Dlx5* (Figure R-15 A).

After actinomycin D addition, overexpression of *Tob2* construct reduced the half-life of *Osx* transcripts (significant reduction after 1 hour) and the increase of miR-322 led to significant stabilization of *Osx* mRNA and *Runx2* to a lesser extent (Figure R-15 B). *Smad7*, *Dlx5* and *Msx2* mRNA degradation was not significantly changed in any case.

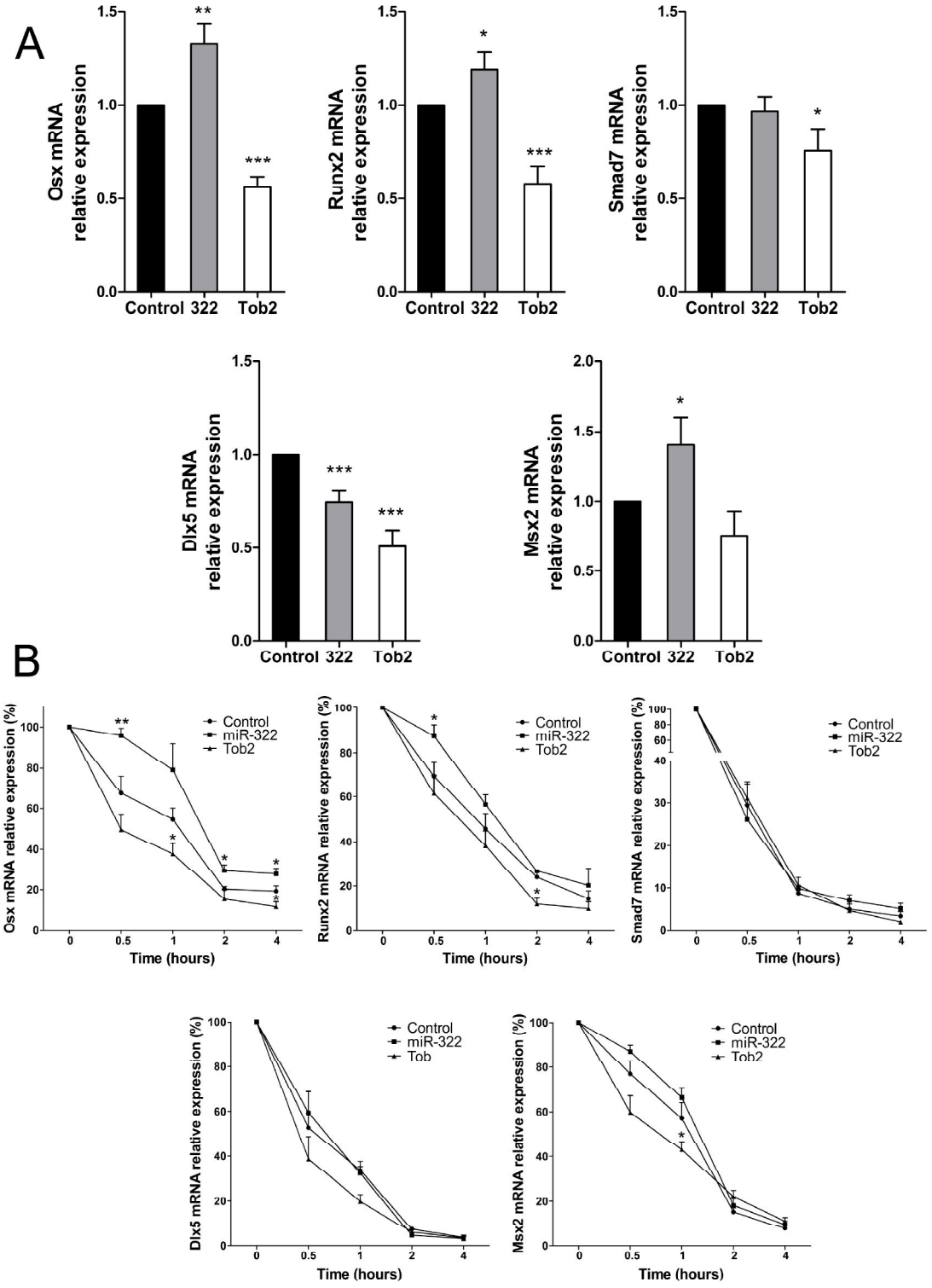

Figure R-15. miR-322 stabilizes *Osx* mRNA via *Tob2* repression in C2C2 cells. (A-B) C2C12 cells were transfected with *Tob2*, mir-322 or miR-control during 8 hours, cultured overnight and treated with BMP-2 for two hours before actinomycin D addition. (**A**) Expression of the indicated mRNAs at time zero. Mean expression of selected genes is plotted as relative to miR-control transfection ± S.E.M (n=6) (**B**) Actinomycin D was added and mRNAs were collected at the indicated times. RT-qPCR was performed using *Gapdh* as endogenous control. Data are expressed as relative to control transfection mRNA levels at time 0 ± S.E.M (n=7-8).

To confirm these observations, mRNA decay assays were repeated in MC3T3-E1 cell line. Overexpression of miR-322 also increased the expression of *Osx*, *Runx2*, *Dlx5* and *Msx2* mRNA (Figure R-16 A) and after actinomycin D treatment, accumulation of miR-322 significantly decreased the rate of *Osx* mRNA degradation (Figure R-16 B). Altogether, these data suggest that TOB2 modifies the mRNA decay of specific target genes as osterix.

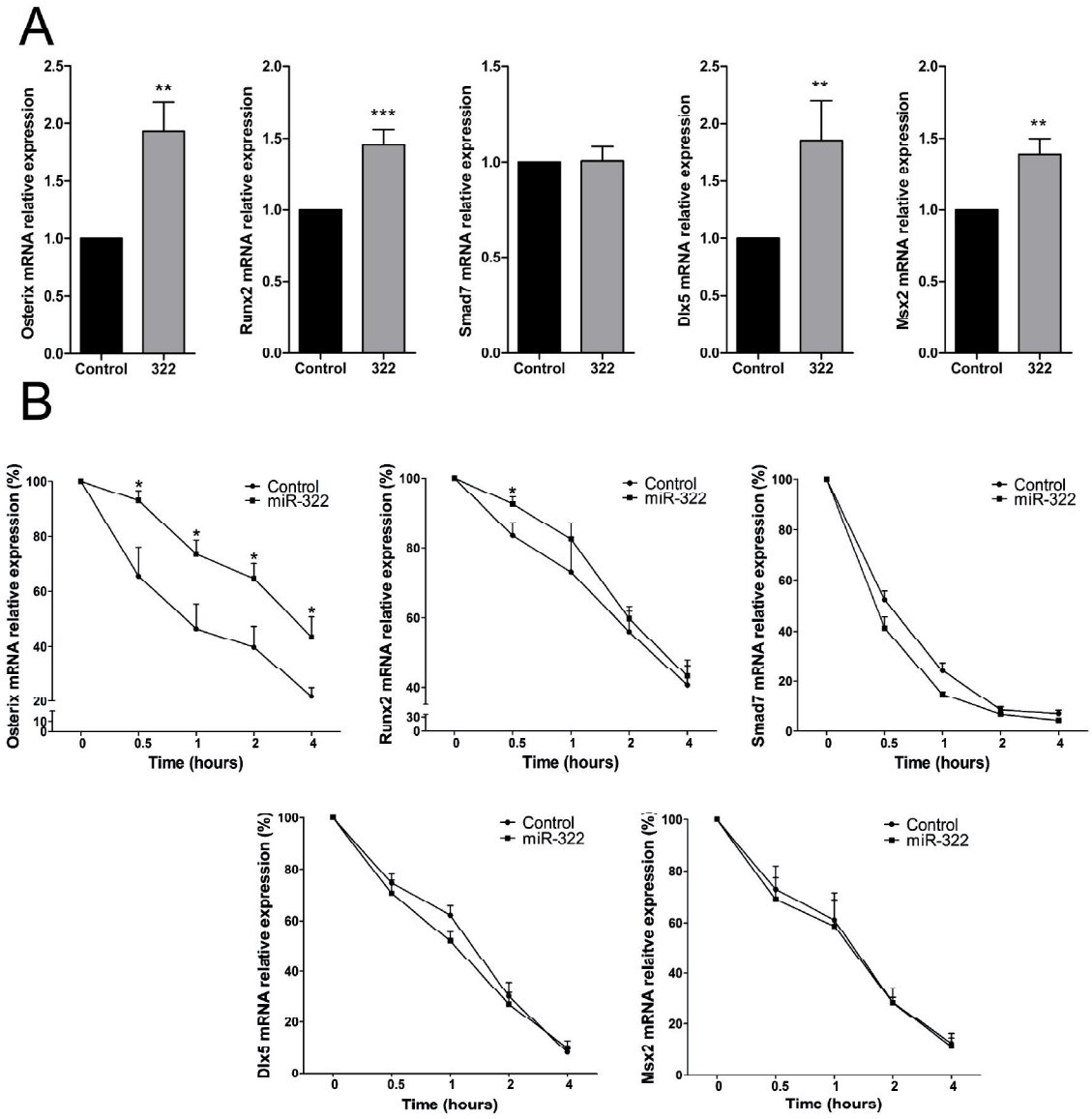

Figure R-16. miR-322 stabilizes *Osx* mRNA in MC3T3-E1 cells. (A-B) MC3T3-E1 cells were transfected with mir-322 or miR-control during 8 hours and cultured overnight. (**A**) Expression of the indicated mRNAs at time zero. Mean expression of selected genes is plotted as relative to miR-control transfection ± S.E.M (n=4). (**B**) Actinomycin D was added and mRNAs were collected at the indicated times. RT-qPCR was performed using *Gapdh* as endogenous control. Data are expressed as relative to control transfection mRNA levels at time o ± S.E.M (n=4).

Since some studies had shown that TOB and CPEB2-4 can interact and specifically intensify the rapid decay of particular transcripts (Ezzeddine et al., 2012) we continued our research by studying the possibility that *Osx* mRNA could be a direct target bound by TOB2 and CPEB2-4 and, as a consequence, specifically decayed. We analyzed osterix 3'-UTR sequences and interestingly, *Osx* mRNA presents secondary structures containing a similar stem-loop structure bound by CPEB2-4 (Figure R-17 A). To prove direct binding of TOB2 and CPEB2-4 to *Osx* prior to specific decay, we developed RNA pull-down assays using two different biotinylated oligonucleotides (Osx#1 and Osx#2) corresponding to distinct stem-loop sequences found in the 3'-UTR of *Osx* mRNA and a control oligonucleotide (Figure R-17 A). Each oligonucleotide was incubated with cell lysates from transfected HeLa cells (Tob2, CPEB4 or both) and precipitated by streptavidin-sepharose beads. Either expressed alone or in combination, CPEB4 and TOB2 were able to bind specifically to the Osx#1 sequence and to the Osx#2 to a lesser extent (Figure R-17 B). Taken together, these results strongly indicate that miR-322 increases *Osx* mRNA expression via inhibition of *Tob2* mRNA.

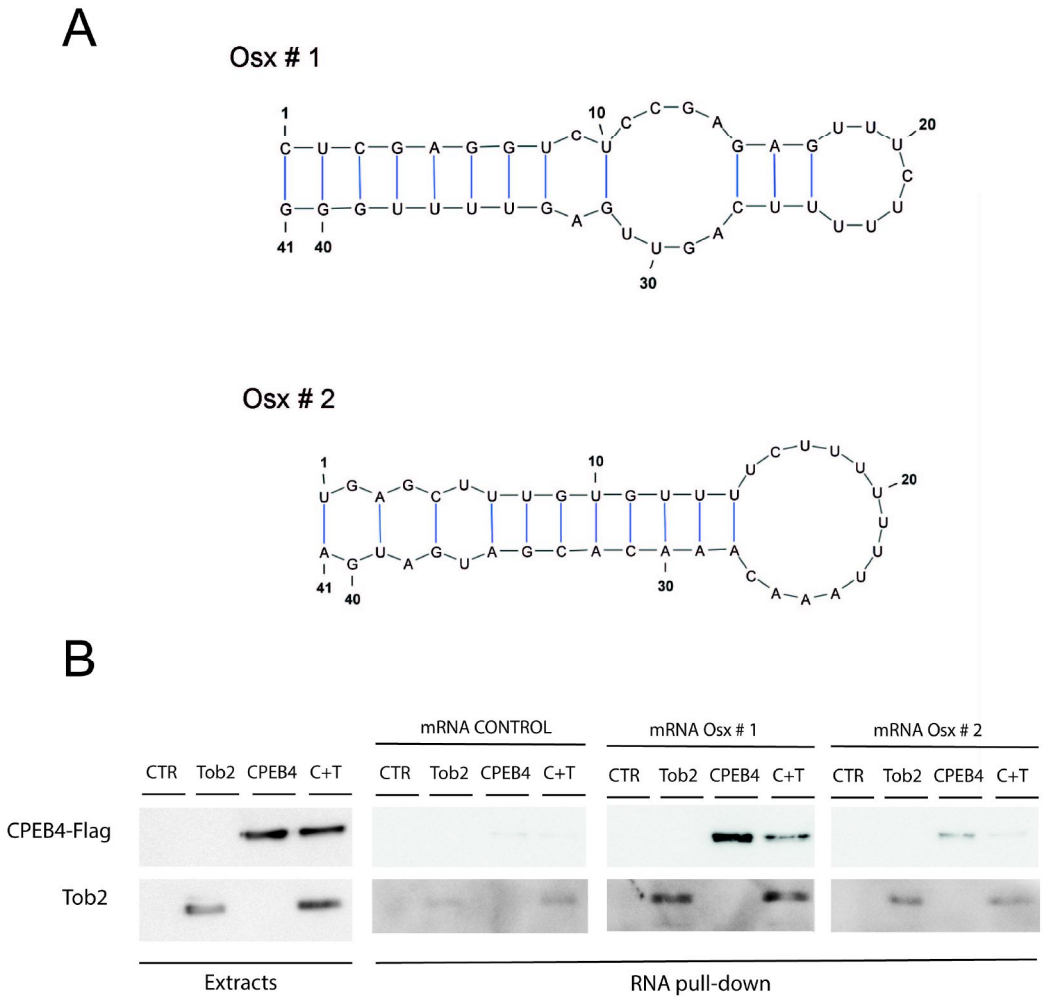

Figure R-17. TOB2 binds to the *Osx* 3'-UTR. (A) *Osx* 3'-UTR sequences found to form stem-loop structures compatible to those shown to bind CPEB2-4. **(B)** HeLa cells were transfected with GFP, Tob2, CPEB4 or CPEB4 and Tob2 (indicated as C+T). RNA pull-down assay was performed using cell lysates from these cells, biotinylated RNAs from (A) and streptavidin sepharose beads. TOB2 and CPEB4 presence was confirmed by Western Blot.

2 ROLE OF PI3K IN BONE DEVELOPMENT AND HOMEOSTASIS

2.1 *p110α* Deletion Leads to a Osteoporotic Phenotype

2.1.1 Specific deletion of *p110α* in mutant mice

To first determine the relative contributions of class IA PI3K subunits in bone, we analyzed the expression of the distinct isoforms in calvariae from adult mice and from primary osteoblasts. In both cases, *p110α* was the most highly expressed subunit, followed by *p110β* (Figure R-18).

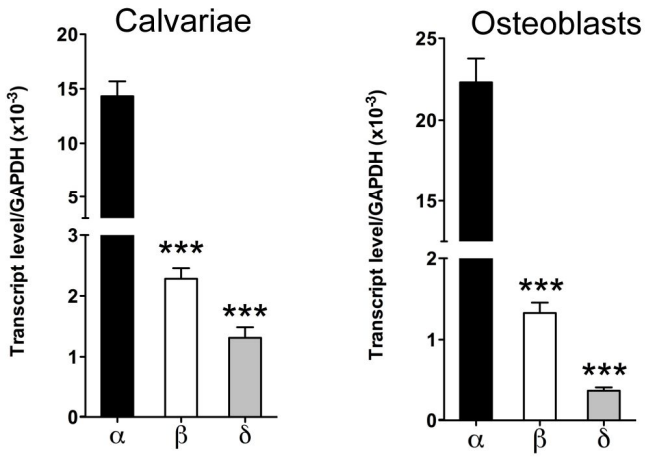

Figure R-18. Relative expression of *p110* isoforms in bone. mRNA expression of *p110α* isoforms in calvariae from 12-week-old male mice and primary osteoblast culture (α: *p110α*, β: *p110β*, δ: *p110δ*) (n=4-5). Bars represent the mean ± SEM.

Aiming to establish the impact of PI3K in regulating bone formation, osteoblast-specific *p110α* mutant mice were generated by means of a Cre recombinase adjacent to the 2.3-*Col1a1* promoter (hereafter *p110α*$^{f/f}$*;Col1a1-Cre*). Osteoblast-specific *p110α*-deficient mice (*p110α*$^{f/f}$*;Col1a1-Cre*) were generated by crossing heterozygous *Col1a1-Cre* mice (Tg(*Col1a1-cre*)1Kry from Jackson Lab) (Dacquin et al., 2002) with homozygous mutants carrying loxP sites flanking exons 18 and 19 of the *p110α* alleles (Graupera et al., 2008).

Conventional PCR was used to determine the genotype of the offspring. DNA was extracted from a 2-3 mm piece of tail and a specific set of primers for *Col1a1-Cre* and for *p110α* led us to identify mutant animals versus control (Figure R-19) (primers detailed in Table M-17). Only males were included in experiments for further phenotype analysis. When using pups for osteoblast isolation and culture, both males and females were used.

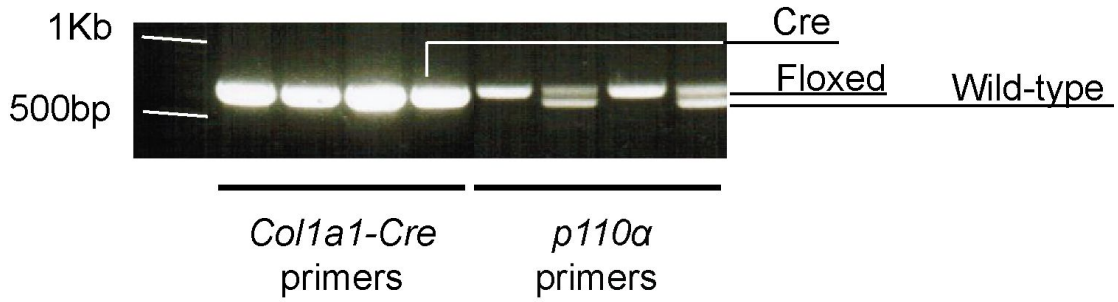

Figure R-19. Conventional PCR for the detection of *p110α*$^{f/f}$*;Col1a1-Cre* animals. Genotyping was performed using two different sets of primers, thus allowing the identification of the *Col1a1-Cre* allele and the *p110α* floxed and/or wild-type allele. Expected bands: 650 bp (wild-type allele), 570 bp (floxed allele) and 650 pb (Cre allele).

First, we confirmed that *p110α* deletion does not affect body mass, as demonstrated by the growth curve of the mutant and control mice (Figure R-20 A). Both phenotypes had comparable body mass and, moreover, the weight of several analyzed organs were also similar (Figure R-20 B).

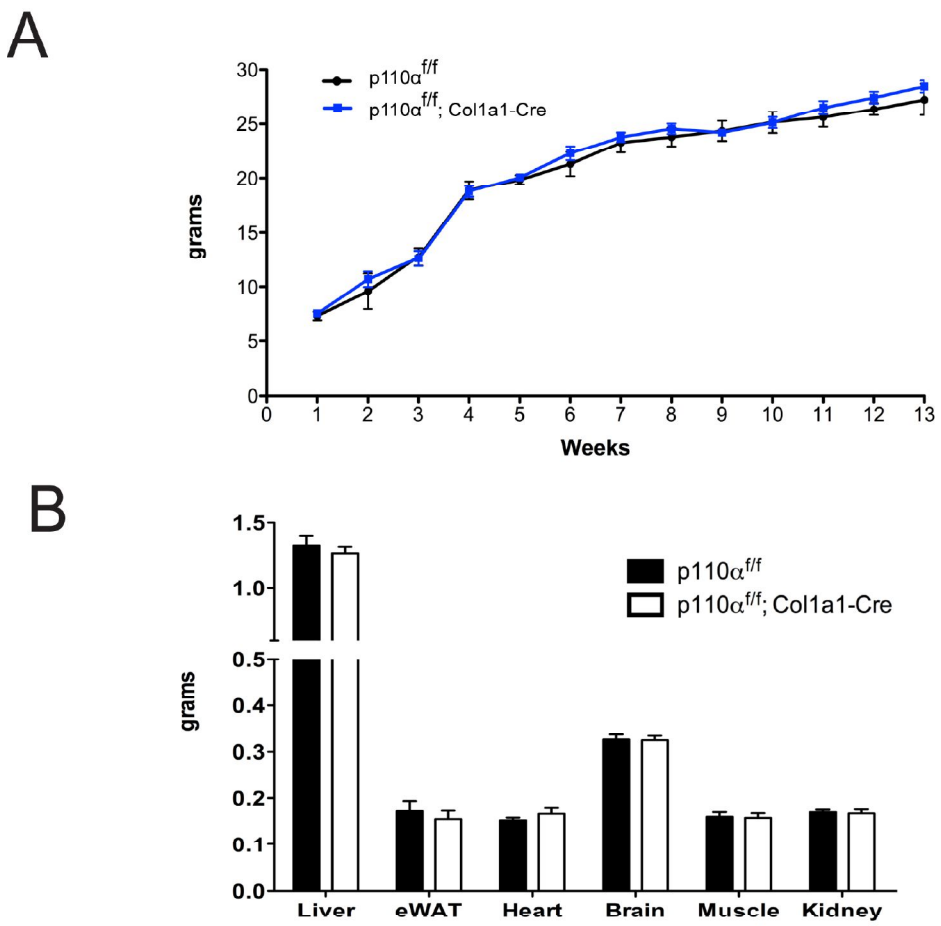

Figure R-20. Growth curve and tissue weight of *p110α*$^{f/f}$*;Col1a1-Cre* mice. (A) Growth curve of male *p110α*$^{f/f}$*;Col1a1-Cre* and control (*p110α*$^{f/f}$) mice until the 13th week of age (n=10-18 mice/group). **(B)** Tissue weight of animals described in A. (n=5 mice/group). Bars represent the mean ± SEM.

Then, we isolated calvariae from *p110α*-deficient and control mice in order to verify the deletion of *p110α* and to check other PI3K isoforms at mRNA and protein level. As expected, *p110α* mRNA and protein expression from *p110α*$^{f/f}$*;Col1a1-Cre* mice calvariae was significantly reduced, whereas the levels of other isoforms or p85 were not affected (Figure R-21).

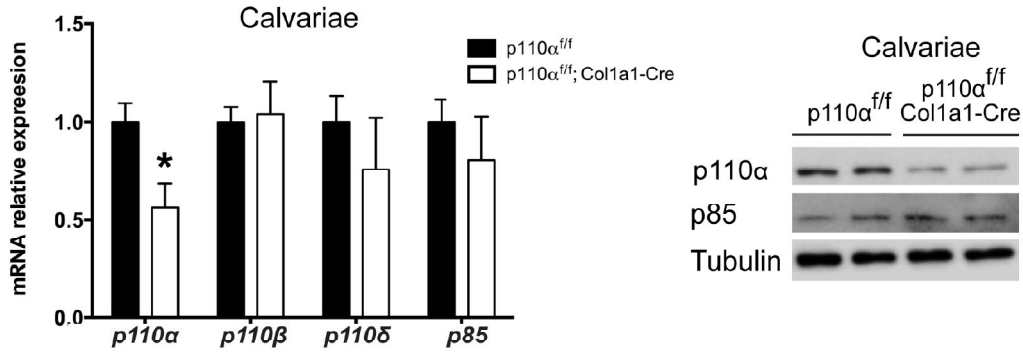

Figure R-21. mRNA and protein levels of *p110α* in knock-out mice. Relative expression of p110 isoforms and p85 in calvariae from 12-week-old male *p110α$^{f/f}$;Col1a1-Cre* and control (*p110α$^{f/f}$*) mice (n=4 mice/group). Right panel shows western blot analysis of p110α and p85 in calvariae from *p110α$^{f/f}$;Col1a1-Cre* and control newborn pups. Bars represent the mean ± SEM.

2.1.2 Histomorphometric analysis of *p110α$^{f/f}$;Col1a1-Cre* mice

To further analyze the effects of *p110α* deletion in osteoblasts, hindlimbs from 12-week old *p110α$^{f/f}$;Col1a1-Cre* and control mice were isolated. Soft tissue was removed from femur and tibia and distal femurs were studied using micro-computed tomography scanning (µCT). µCT technique allows the measurement and quantification of bone structures by using x-rays to generate serial section images of the specimen and, later on, to create a virtual 3-D model.

Thus, bone formation in *p110α$^{f/f}$;Col1a1-Cre* mice was studied in distal femurs at trabecular and cortical level. Representative images of cortical midshaft are shown in Figure R-22 A. *p110α$^{f/f}$;Col1a1-Cre* animals presented lower (13% decrease) cortical bone volume (BV) associated with reduced cortical thickness (Ct.Th) and perimeter (B.Pm) around the midshaft (Figure R-22 B).

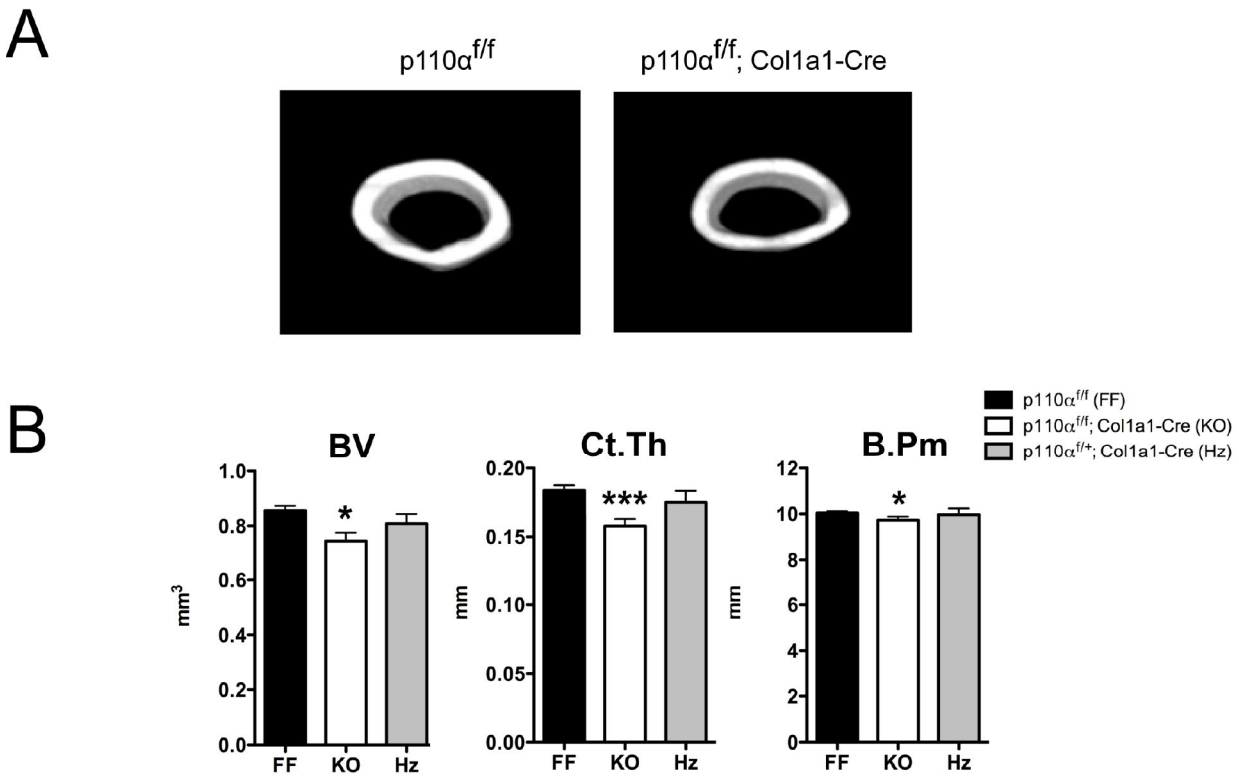

Figure R-22. µCT study of cortical bone of *p110α$^{f/f}$;Col1a1-Cre* mice reveals a osteopenic phenotype. µCT analysis was performed in 12-week-old mutant (*p110α$^{f/f}$;Col1a1-Cre*), heterozygote (*p110α$^{f/+}$;Col1a1-Cre*) and control (*p110α$^{f/f}$*) male mice. **(A)** Representative µCT images of cortical bone at the femoral midshaft. **(B)** Cortical µCT analysis: BV (bone volume), Ct.Th (cortical thickness) and B.Pm (bone perimeter) (n=7-8 mice/group). Bars represent the mean ± SEM.

Additionally, trabecular analysis was performed and representative images of trabecular area of distal femurs are shown (Figure R-23 A). Femurs from mutant mice also presented 30% less trabecular bone volume (BV/TV) due to a significantly lower trabecular number (Tb.N) and thickness (Tb.Th) (Figure R-23 B). Bone mineral density from the selected area was also affected by the loss of *p110α* (Figure R-23 B).

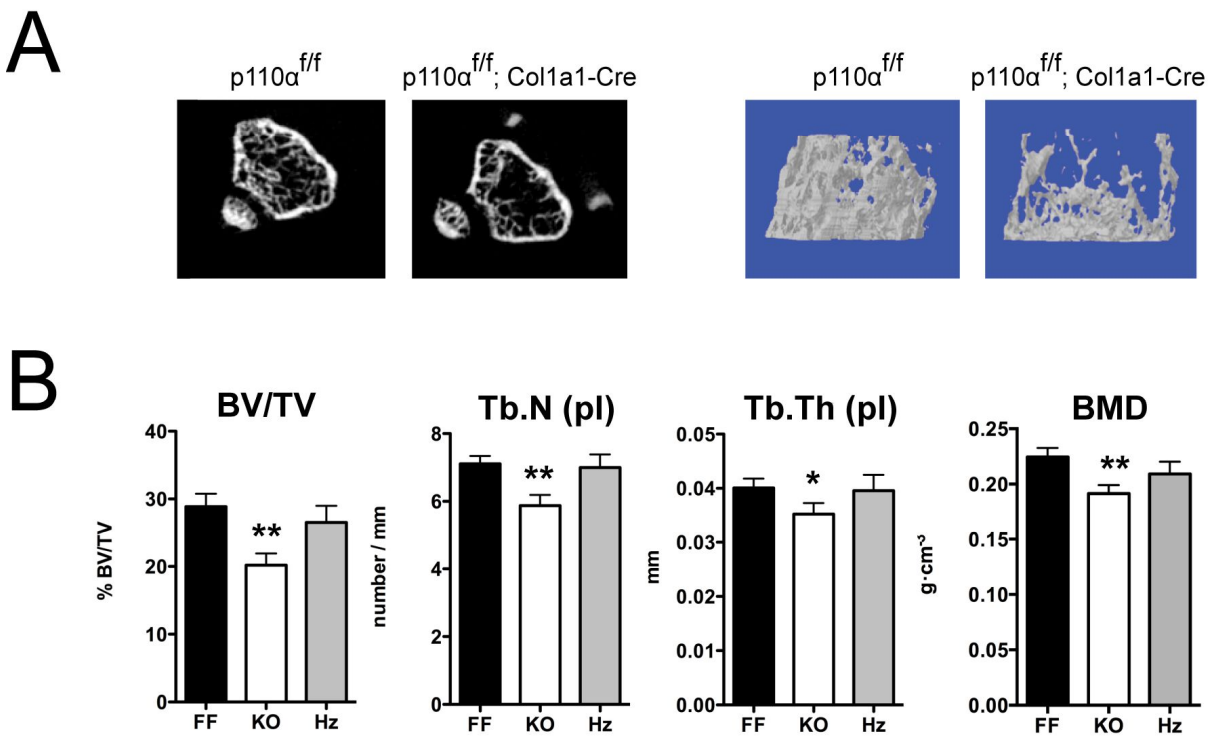

Figure R-23. µCT study of trabecular bone of *p110α$^{f/f}$;Col1a1-Cre* mice. (A) Representative 2D and 3D µCT images of cancellous bone of distal femoral epiphyses**. (B)** Trabecular analysis: BV/TV (bone volume/tissue volume), Tb.N (trabecular number), Tb.Th (trabecular thickness). BMD (bone mineral density) (n=7-8 mice/group). Bars represent the mean ± SEM.

The same procedure of hindlimb isolation was performed for histological analysis and posterior tissue preparation for paraffin-embedding included EDTA decalcification. Also glycol-methacrylate embedding was used for some stains (see chapter 9).

Goldner Trichrome staining is an important histological technique in the bone field as it allows differentiation among mature and immature (osteoid) bone tissue. Goldner Trichrome staining of tibiae sections evidenced a reduction of osteoid thickness and perimeter in cancellous bone, although the number of osteoblasts per bone area was not affected (Figure R-24).

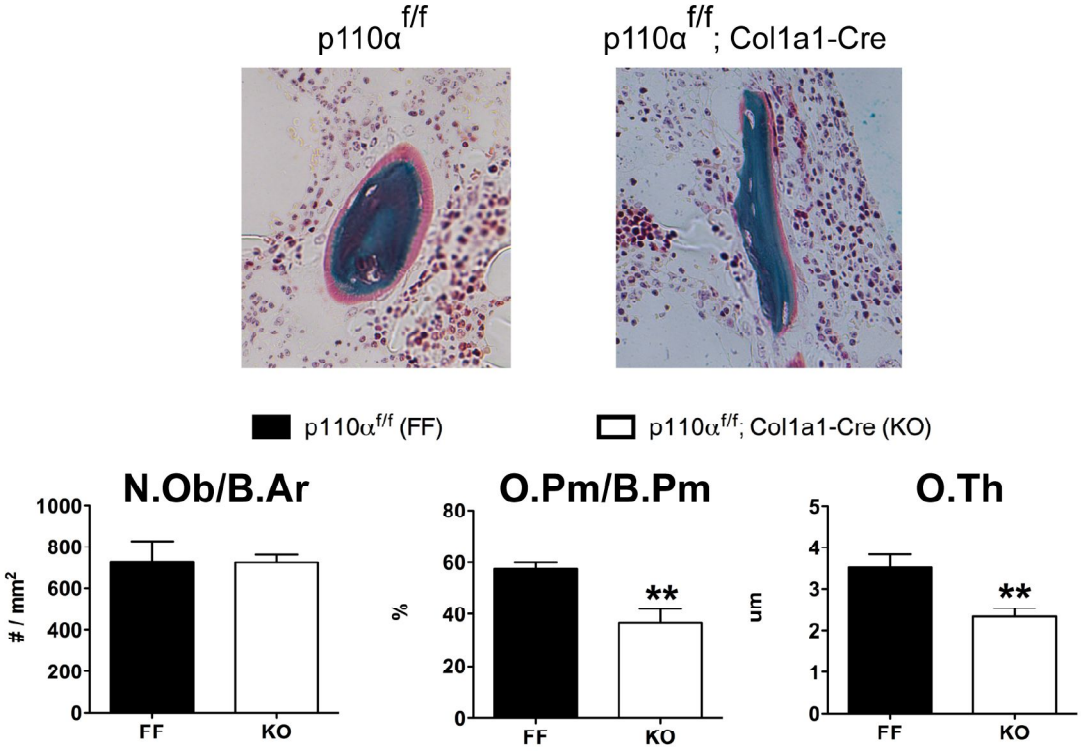

Figure R-24. Osteoid quantification of cancellous bone from tibiae sections. Upper panel shows representative Goldner Trichrome-stained trabecular bone sections (40x). Bar graphs show the number of osteoblasts per bone area (N.Ob/B.Ar), osteoid perimeter per bone perimeter (O.Pm/B.Pm) and osteoid thickness (O.Th). (n=6-7 mice). Bars represent the mean ± SEM.

Also osteoid thickness was reduced when assessing cortical bone of the same samples (Figure R-25 A). Goldner Trichorme staining was also performed in calvariae samples of *p110α*$^{f/f}$*;Col1a1-Cre* and control mice evidencing a reduced calvarial thickness in *p110α* deficient mice (Figure R-25 B).

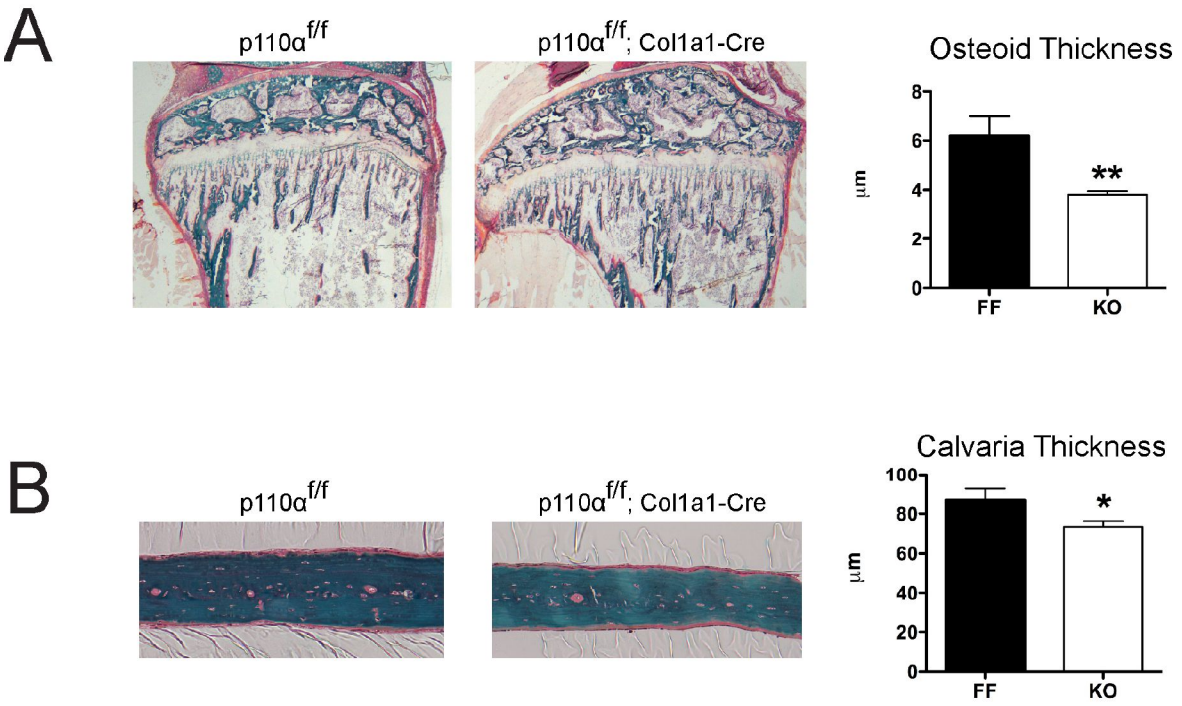

Figure R-25. Goldner Trichrome staining in tibia and calvaria from adult mice. (A) Representative images of tibiae from *p110α$^{f/f}$;Col1a1-Cre* and control (*p110α$^{f/f}$*) mice (4x). Right panel shows quantification of cortical osteoid thickness (n=5-6 mice/group). **(B)** Representative images of Goldner Trichrome-stained calvariae from *p110α$^{f/f}$;Col1a1-Cre* and control (*p110α$^{f/f}$*) mice (20x) (n=4-5 mice/group). Bar graph shows quantification of calvaria thickness. Bars represent the mean ± SEM.

Thus, both µCT and histological results from femurs and tibiae from *p110α$^{f/f}$;Col1a1-Cre* mice revealed an important impairment on bone structure at adulthood.

Bone formation rate can be determined by dynamic histomorphometric measurements in young animals. The use of calcein, which incorporate into newly calcifying bone, allows the calculation of bone kinetics indices. 6-week-old animals were injected with two sequential subcutaneous doses of calcein (10mg/Kg) delivered 7 and 2 days prior to sacrifice. Again, hindlimbs were isolated and processed for glycol-methacrylate embedding, as fluorochrome observation requires no decalcification. This technique revealed a significantly reduced mineral apposition and bone formation rates (MAR and BFR, respectively) in cortical (Figure R-26 A&B) and trabecular femoral bone of *p110α$^{f/f}$;Col1a1-Cre* mice (Figure R-26 C).

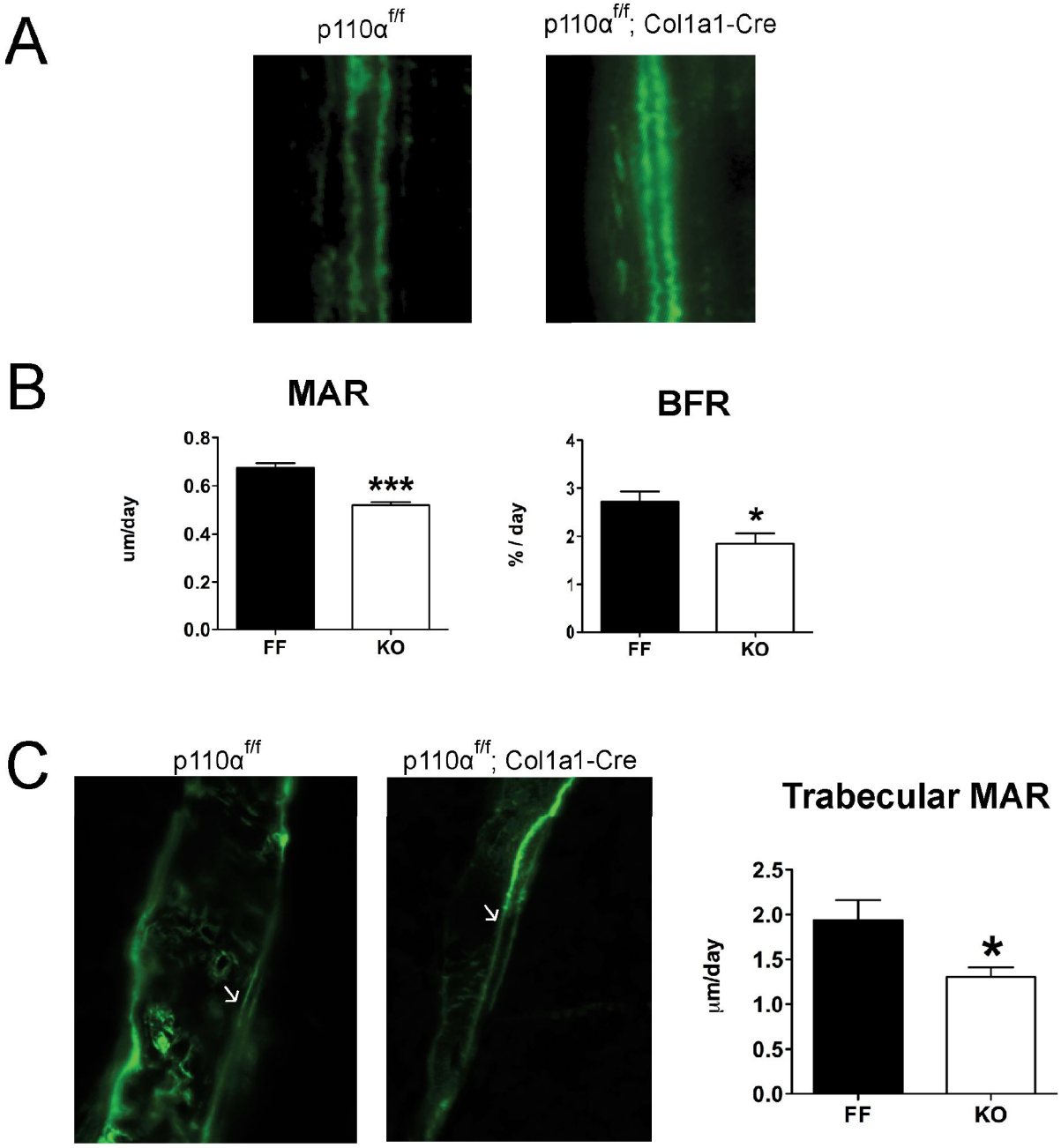

Figure R-26. Study of dynamic *in vivo* calcein labeling shows impairment in bone deposition. (A) Representative images of double calcein labeling of calvariae from 6-week-old *p110α$^{f/f}$;Col1a1-Cre* (40x). **(B)** Bar graphs show mineral apposition rate (MAR) and bone formation rate (BFR) (n=4-5 mice/group). **(C)** Representative images of double calcein labeling of cancellous bone from tibiae from animals described in A (40x). Right panel shows trabecular MAR (n=4-5 mice/group). Bars represent the mean ± SEM.

2.1.3 Disruption of *p110α* impairs osteoblast function but not osteoclastogenesis

To identify the underlying reason for the osteopenic phenotype of the *p110α* mutant mice, we proceeded to study the osteoblast function by a molecular approach. First, calvariae from 12-week-old *p110α*$^{f/f}$*;Col1a1-Cre* and control mice were isolated and we used a customized TLDA to perform a screening of osteogenic markers. Calvariae from *p110α*$^{f/f}$*;Col1a1-Cre* mice presented reduced expression of several osteogenic genes, including alkaline phosphatase (*Alpl*), *Bglap* (osteocalcin (*OC*)), *Col1a1*, *Msx2* or *Osx* (Figure R-27 A).

Concordant with the down-regulation of *Osx* mRNA, OSX protein levels were almost abolished in *p110α* mutant mice. Effectors of PI3K signaling (pAKT, pS6) were also consistently reduced by the loss-of-function of *p110α* (Figure R-27 B).

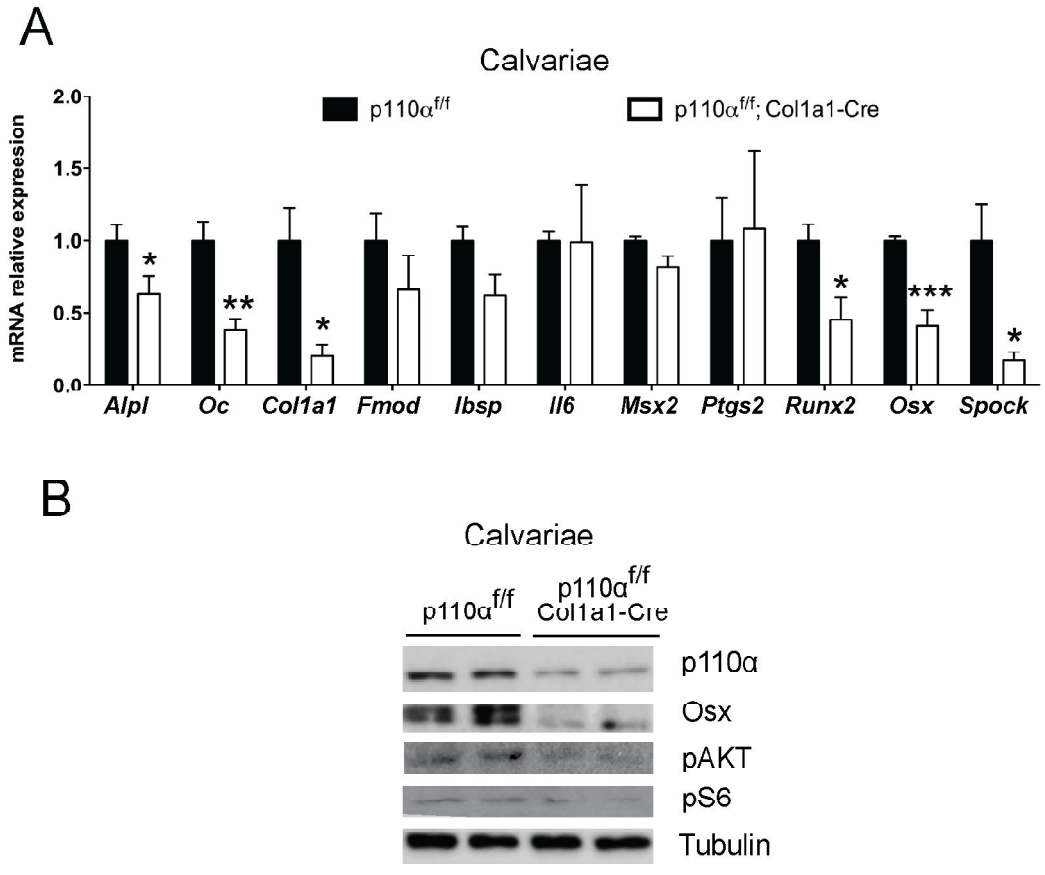

Figure R-27. Disruption of *p110α* impairs osteoblast function. (A) mRNA expression of bone markers in calvariae from 12-week-old *p110α*$^{f/f}$*;Col1a1-Cre* and control mice (n=4-5 mice/group). **(B)** Western blot of calvariae from newborn pups. Bars represent the mean ± SEM.

Since the *p110α*$^{f/f}$*;Col1a1-Cre* phenotype described above could also arise partially from an alteration in osteoclasts, we next examined whether an increase in osteoclastogenesis contributed to the osteopenic phenotype. Osteoblasts activate osteoclasts by the RANK-RANKL signaling system, linking osteoblast lineage and hematopoiesis-derived cells for osteoclast differentiation and activation. Together with M-CSF, RANK signaling is the main signaling pathway involved in osteoclast maturation. RANK stimulation by osteoblast RANK ligand leads to the activation of several osteoclast-specific genes as tartrate-resistant acid phosphatase (*Trap*). OPG (osteoprotegerin) is produced by osteoblasts and can block RANK, therefore inhibiting osteoclast differentiation. Thus, the RANKL/OPG ratio must be accurately balanced to control osteoclastogenesis.

Given these facts, tibiae sections were stained for specific TRAP detection and although *p110α*$^{f/f}$*;Col1a1-Cre* mice presented a reduction in osteoclast number, no significant differences were found in the ratio between osteoclast number and bone surface (Figure R-28 A&B). Moreover, *Trap* mRNA expression and the relative *Rankl/Opg* ratio were not altered in calvariae of *p110α* mutants (Figure R-28 C).

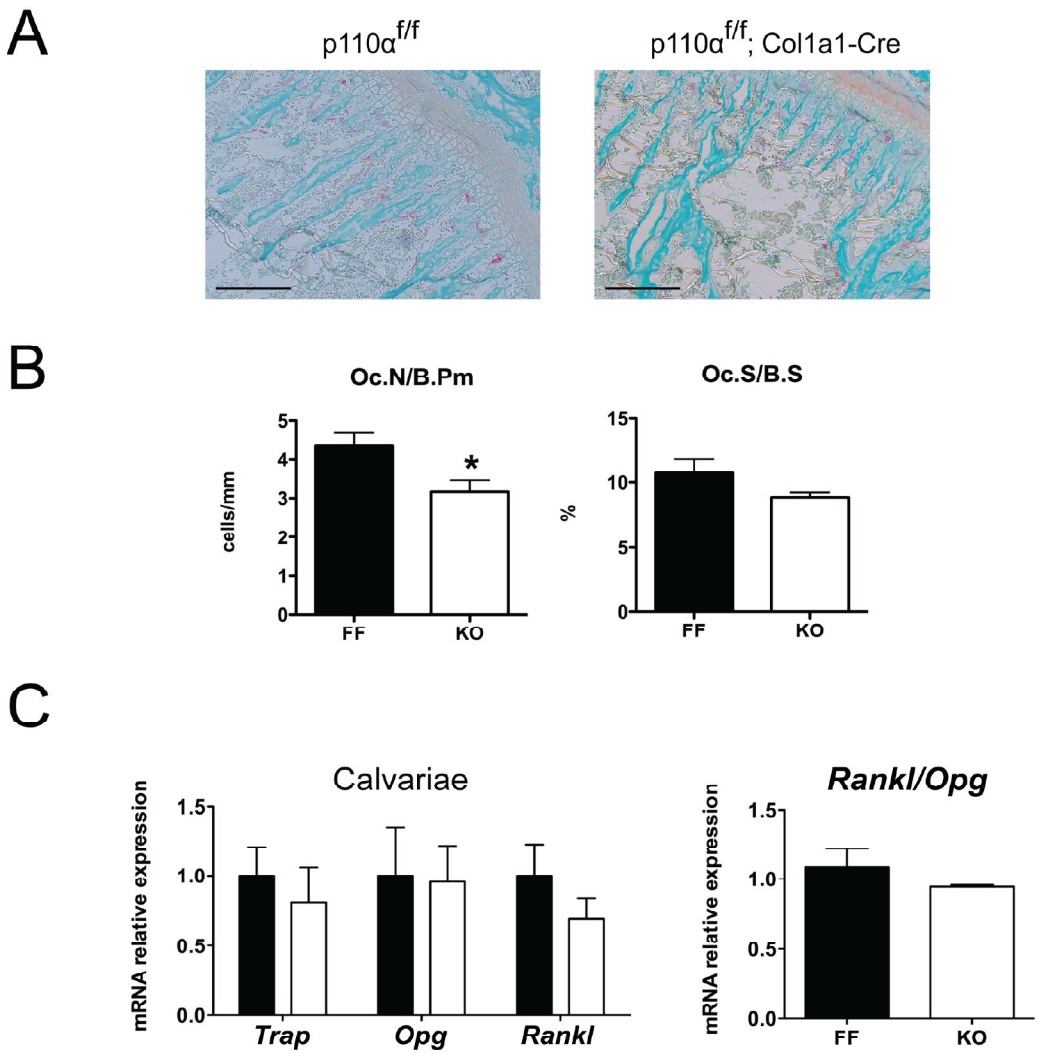

Figure R-28. Osteoclast function is not altered in *p110α*$^{f/f}$*;Col1a1-Cre* mice. 12-week-old *p110α*$^{f/f}$*;Col1a1-Cre* and control mice were studied. **(A)** Representative images of TRAP-stained tibiae sections (20x). **(B)** Bar graphs show osteoclast number/bone perimeter (Oc.N/B.Pm) and osteoclast surface/bone surface (Oc.S/B.S) from TRAP-stained tibiae (n=4-6 mice/group). **(C)** Left panel shows *Trap*, *Opg* and *Rankl* mRNA expression in calvariae (n=3-5 mice/group). Right panel shows *Rankl/Opg* ratio (n=3-5 mice/group). Bars represent the mean ± SEM.

NTX (N-terminal telopeptide of type I collagen) is a marker of osteoclast activity and is used to measure the rate of bone turnover. Blood samples were obtained from mutant and control mice by collection from the posterior vena cava (terminal procedure, see 7.2). Serum NTX levels from mutant and control mice showed no differences, confirming that there were no significant changes in bone resorption (Figure R-29).

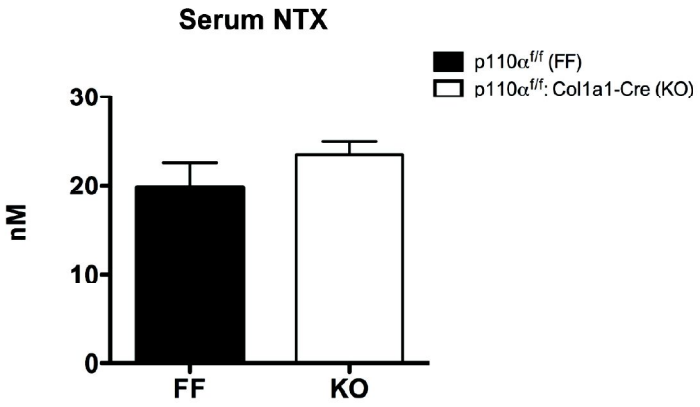

Figure R-29. Serum NTX levels are not changed in mutant mice. Quantification of NTX present in serum from 12-week-old *p110α*$^{f/f}$;*Col1a1-Cre* and control mice (n=7-9). Bars represent the mean ± SEM.

Taken together, these findings underpin a deficiency in osteoblast activity, rather than increased osteoclast function, on the onset of the reduced bone mass phenotype.

2.1.4 Analysis of changes in proliferation and apoptosis in *p110α* mutant mice

We further analyzed how *p110α* loss affects proliferation and apoptosis in osteoblasts. For this aim, sections of tibiae from *p110α*$^{f/f}$;*Col1a1-Cre* newborn mice were used for Ki-67 immunohistochemistry and for TUNEL assay.

Ki-67 is a protein associated with cell proliferation and is used as a cellular marker to determine the level of proliferation. Ki-67 immunochemistry was performed in tibiae from mutant and control mice and Ki-67 positive osteoblasts were recognized by counting cuboidal-shaped cells present in the uppermost part of the inner face of the bone slices. The number of Ki-67 positive osteoblasts was not altered in mutant versus control mice (Figure R-30 A).

DNA fragmentation represents a characteristic hallmark of apoptosis. Widely used methods to determine apoptosis include DNA fragmentation assays. TUNEL (terminal deoxynucleotidyl transferase dUTP nick end labeling) is a common method for detecting DNA fragments resulting from apoptotic signaling cascades. TUNEL assay is based on the identification of double-stranded and single-stranded DNA breaks (nicks) that can be identified by the use of terminal deoxynucleotidyl transferase (TdT), an enzyme that will add labeled dUTPS. A significant increase in TUNEL positive cells was detected in tibiae from *p110α*-deficient mice (Figure R-30 B). Moreover, higher levels of cleaved caspase 3 were detected in bone tissues of mutant mice, whereas the amount of LC3-II (an autophagy marker) remained unchanged (Figure R-30 C).

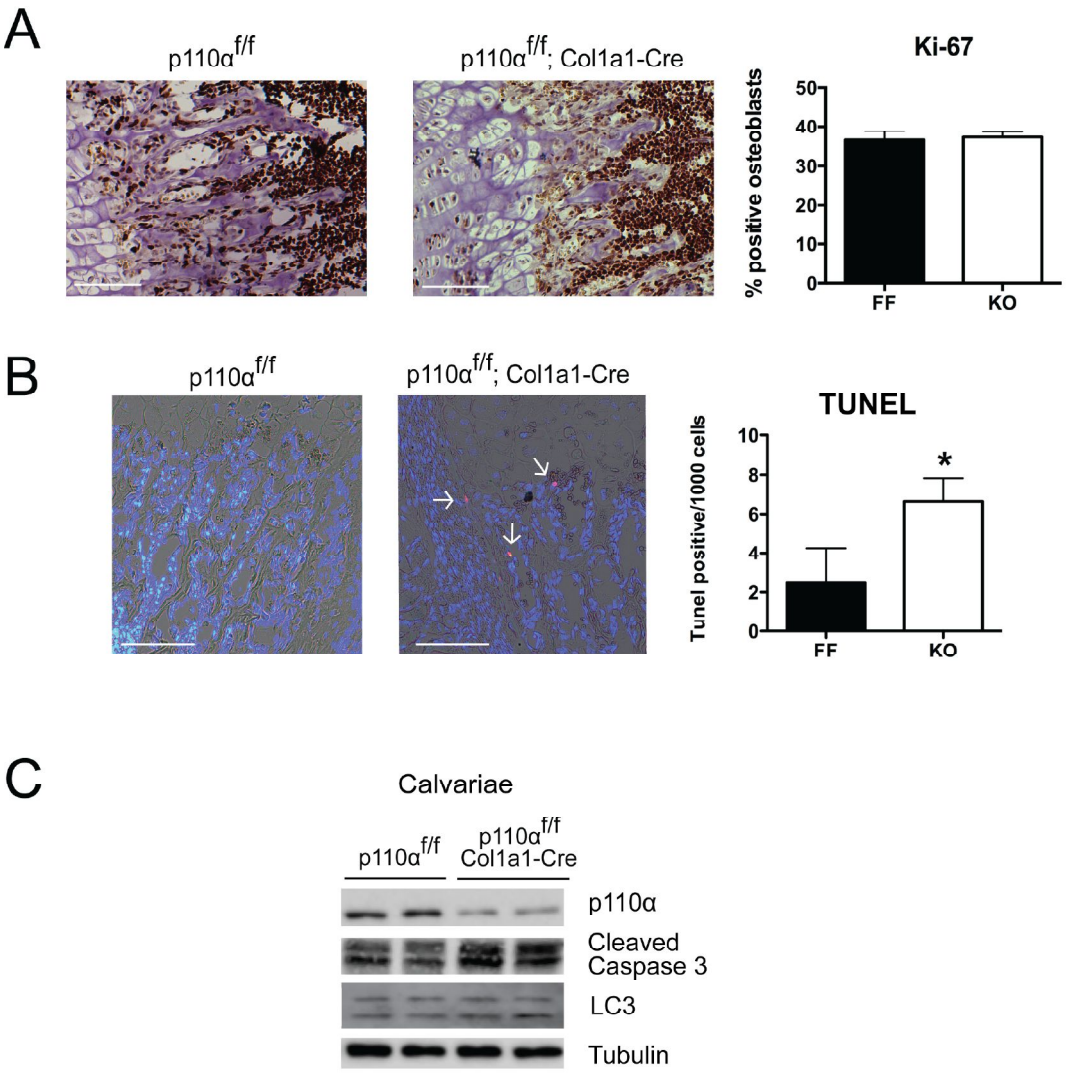

Figure R-30. Quantification of proliferation and apoptosis *in vivo*. (A) Tibiae from *p110α$^{f/f}$;Col1a1-Cre* and control newborn pups were analyzed for Ki-67 immunohistochemistry. Left panels show representative images (20x). (n=4-6 mice/group). **(B)** Bone sections were also used for TUNEL analysis (n=4 mice/group). Representative images are shown in left panels (20x) **(C)** Western blot of calvariae previously used in Figure R-27 A. Immunoblot shows changes in cleaved caspase 3 levels and no important changes in LC3. Bars represent the mean ± SEM.

2.1.5 Study of serum biomarkers alterations in *p110α$^{f/f}$;Col1a1-Cre*

After blood collection from the posterior vena cava, serum from *p110α$^{f/f}$;Col1a1-Cre* and *p110α$^{f/f}$* mice were sent to "Servei de Bioquímica Clínica Veterinària" from Universitat Autònoma de Barcelona. Alkaline phosphatase is an enzyme that is crucial for an accurate ossification (Hessle et al., 2002) and is produced by different tissues. However, it is well established that bone is the main contributor to the concentration of alkaline phosphatase in serum (Epstein, 1988).

Thus, among all the screened parameters and in agreement with the decreased osteogenic markers, serum levels of alkaline phosphatase were also significantly reduced in *p110α*-defective mice (Table R-3). Also serum levels of calcium were affected by *p110α* deletion to a lesser extent (Table R-3).

SERUM BIOMARKERS				
Parameter	**p110α$^{f/f}$**	**p110α$^{f/f}$; Col1a1-Cre**	**p value**	
Calcium (mg/dl)	9.310 ± 0.069	9.046 ± 0.069	**0.0147**	*
Iron (μg/ml)	143.881 ± 6.068	138.069 ± 5.593	0.4887	ns
Alkaline phosphatase (UI/l)	92.875 ± 1.917	78.439 ± 2.767	**0.0014**	**
Phosphorous (mg/dl)	5.400 ± 0.069	5.515 ± 0.409	0.8545	ns

Table R-3. The analysis of serum biomarkers confirms alkaline phosphatase reduction. Serum from 12-week-old male *p110α$^{f/f}$;Col1a1-Cre* and control (*p110α$^{f/f}$*) mice was obtained and calcium, iron, alkaline phosphatase and phosphorous was determined (n=9-13). Data represent the mean ± SEM.

2.2 Post-natal Deletion of *p110α* also Affects Osteoblast Differentiation

2.2.1 *p110α* deletion in mice under *Osx1-Cre* promoter

Osteoblast-specific gene loss driven by a Cre-recombinase fused to the *Col1a1* promoter allows embryonic deletion as soon as day E14.5 (Dacquin et al., 2002). To investigate whether *p110α* was also essential for postnatal bone acquisition and homeostasis, we generated mice with deletion of *p110α* in osteo-chondroprogenitors using an *Osx1-Cre* doxycycline-responsive promoter (thereafter *p110α$^{f/f}$;Osx1-Cre*). Pregnant females were kept under a doxycycline regime in drinking water, which was removed after the litter was born between postnatal days 0 and 2 (P0-P2).

p110α deletion was validated by mRNA and western blots of mutant (*p110α$^{f/f}$;Osx1-Cre*) and control mice (Figure R-31 A&B). Neither the other p110 subunits nor p85 was affected by postnatal deletion of *p110α* (Figure R-31 A&B).

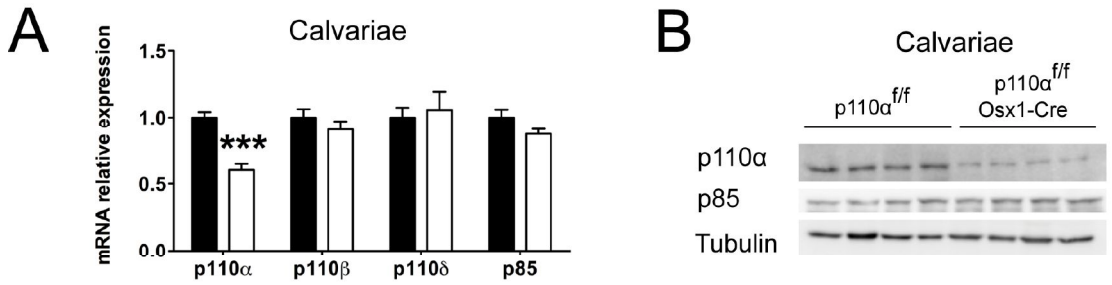

Figure R-31. *p110α* deletion efficiency in calvariae from 12-week-old male *p110α$^{f/f}$;Osx1-Cre* and control mice. (A) Relative mRNA expression of *p110* isoforms and *p85* in calvariae from 12-week-old male *p110α$^{f/f}$;Osx1-Cre* and control mice. (n=5-7 mice/group) **(B)** Western blot analysis of calvariae from *p110α$^{f/f}$;Osx1-Cre* and control newborn pups. Bars represent the mean ± SEM.

Previous studies have shown that animals carrying the *Osx1-Cre* promoter allele presented a cortical bone phenotype (Davey et al., 2012). Although this phenotype seems to be overcome in adulthood, we included both floxed (*p110α$^{f/f}$*) and Cre (*p110α$^{+/+}$;Osx1-Cre*) controls in our first approaches to assure precise interpretation of the phenotype.

Again, PCR was used to determine the genotype of the *Osx1-Cre* strain. Specific primers for *Osx1-Cre* and for *p110α* (the same as for *p110α$^{f/f}$;Col1a1-Cre*) led us to identify knock-out animals versus control (Figure R-32).

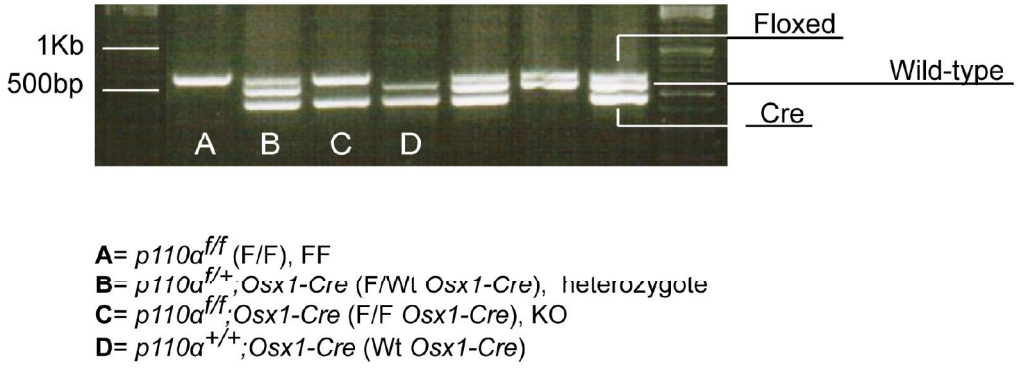

Figure R-32. Conventional PCR for *p110α$^{f/f}$;Osx1-Cre* detection. A new set of primers was used for the identification of the *Osx1-Cre* allele. *p110α$^{f/f}$* was detected with the same primers as for *p110α$^{f/f}$;Col1a1-Cre*. Expected bands: 650 bp (wild-type allele), 570 bp (floxed allele) and 510 pb (*Osx1-Cre* allele).

First, we confirmed that *p110α* deletion driven by *Osx1-Cre* promoter do not affect body mass, as demonstrated by the growth curve of the animals. Neither mutant mice nor mice carrying just *Osx1-Cre* had any alterations in body weight, thereby suggesting no gross phenotype derived by the presence of *Osx1-Cre* allele (Figure R-33 A). Moreover, the weight of the main tissues was also similar when comparing mutant and control mice (Figure R-33 B).

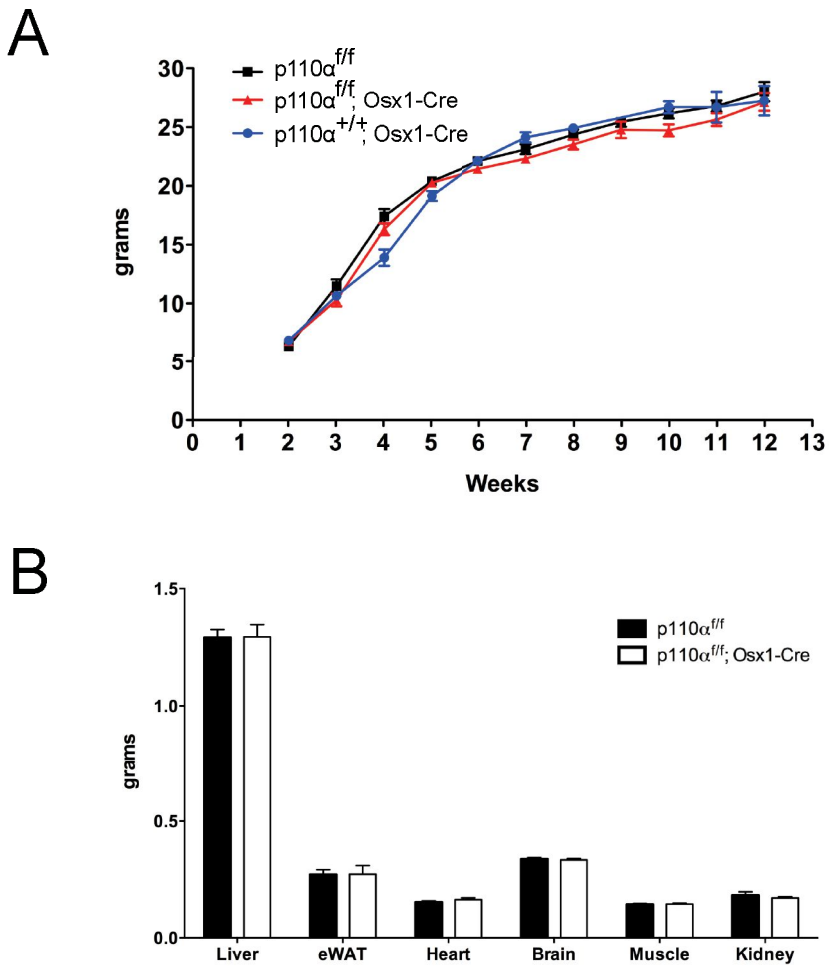

Figure R-33. No differences in growth curve and tissue weight of *p110α*$^{f/f}$*;Osx1-Cre* mice. (A) Growth curve of male *p110α*$^{f/f}$*;Osx1-Cre*, *p110α*$^{+/+}$*;Osx1-Cre* and control (*p110α*$^{f/f}$) mice until the 13th week of age (n=8-22 mice/group). **(B)** Tissue weight of animals described in A. (n=8-22 mice/group). Bars represent the mean ± SEM.

2.2.2 *p110α* deletion is also essential for normal postnatal bone homeostasis

Consistent with the results from *p110α*$^{f/f}$*;Col1a1-Cre* mice, µCT analyses from *p110α*$^{f/f}$*;Osx1-Cre* femurs revealed decreased cortical and trabecular bone volume as well as trabecular number and thickness (Figure R-34 A&B). Mutant mice were significantly affected by *p110α*$^{f/f}$ deletion even when compared to *p110α*$^{+/+}$*;Osx1-Cre*, which did not present phenotype at all.

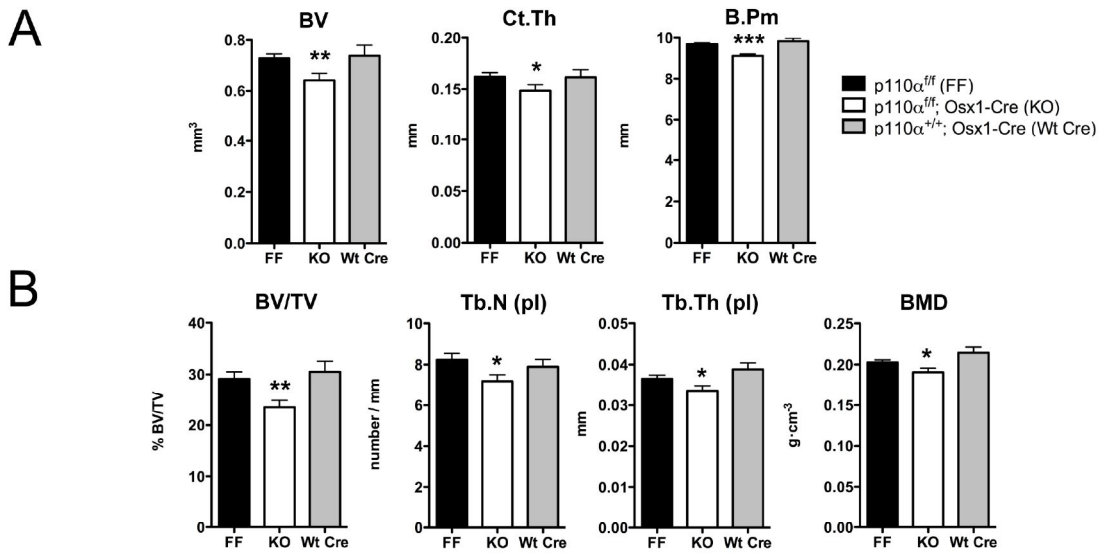

Figure R-34. Trabecular and cortical bone are also reduced in *p110α$^{f/f}$;Osx1-Cre* mice. µCT analysis was performed in 12-week-old mutant (*p110α$^{f/f}$;Osx1-Cre*), control (*p110α$^{f/f}$*) and Wt-Cre (*p110α$^{+/+}$Osx1-Cre*) male mice. **(A)** Cortical µCT parameters (n=8-10 mice/group). **(B)** Trabecular analysis and BMD (n=10-17 mice/group). Bars represent the mean ± SEM.

µCT representative images evidence the differences in cortical and trabecular bone between *p110α$^{f/f}$;Osx1-Cre* and control mice (Figure R-35).

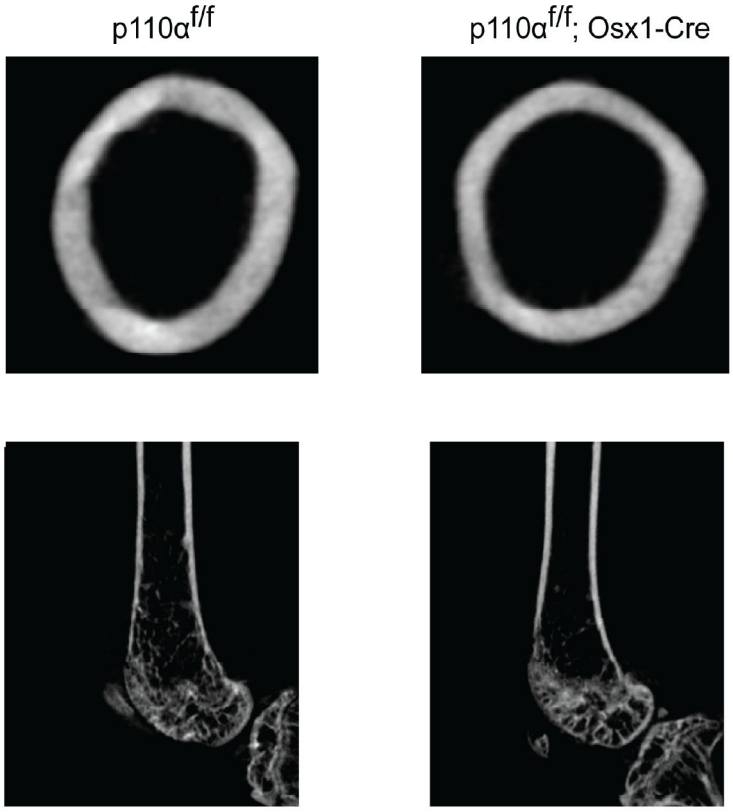

Figure R-35. µCT images of distal femurs from *p110α$^{f/f}$;Osx1-Cre* and control mice.

We further checked the mineral apposition and bone formation rates in *p110α*$^{f/f}$*;Osx1-Cre* mice and they were also lower in mutant mice compared to control, denoting a lack of appropriate bone formation and turnover (Figure R-36).

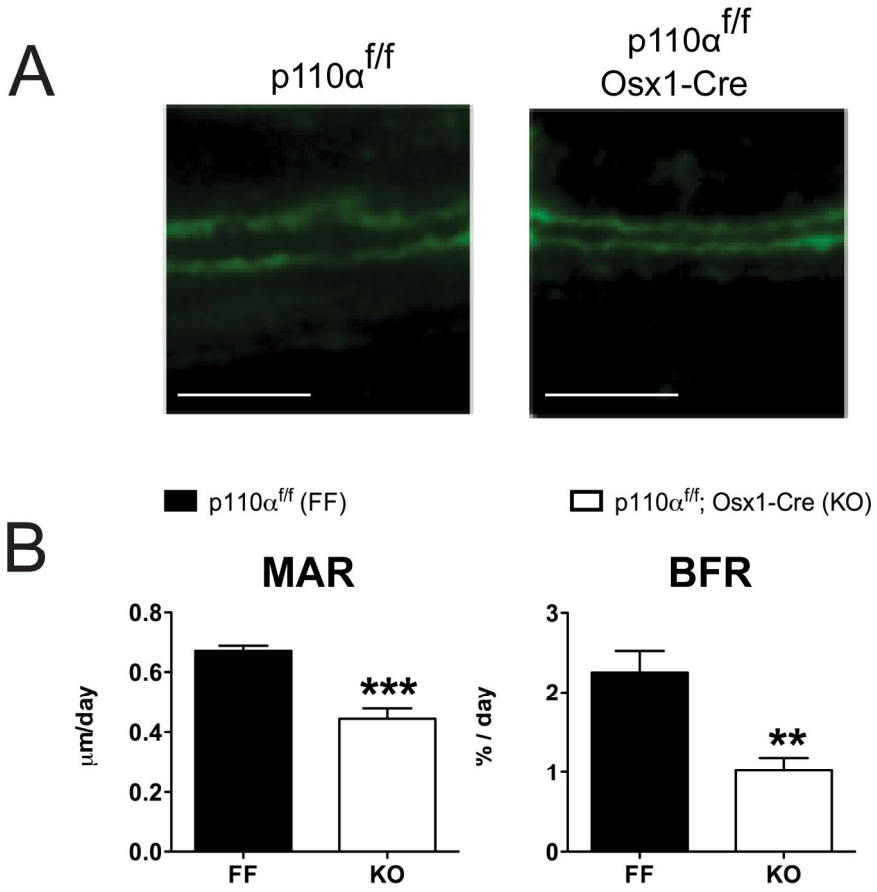

Figure R-36. Bone deposition is altered in *p110α*$^{f/f}$*;Osx1-Cre* mice. (A) Representative images and analysis of dynamic histomorphometry by double calcein labeling of calvariae from 6-week-old *p110α*$^{f/f}$*;Osx1-Cre* and control mice (40x) (n=4-6 mice/group). **(B)** Quantification of MAR (mineral apposition rate) and BFR (bone formation rate) from animals described in A. Bars represent the mean ± SEM.

We examined whether *p110α*$^{f/f}$*;Osx1-Cre* mice had defects in osteoblasts similar to the *p110α*$^{f/f}$*;Col1a1-Cre* mice. Calvariae from *p110α*$^{f/f}$*;Osx1-Cre* adult mice also had lower expression of *Alpl*, *Bglap (OC)*, *Col1a1* or *Osx* mRNA (Figure R-37 A). OSX protein levels were also diminished in mutant mice, and as expected, AKT signaling was down-regulated after *p110α* deletion (Figure R-37 B).

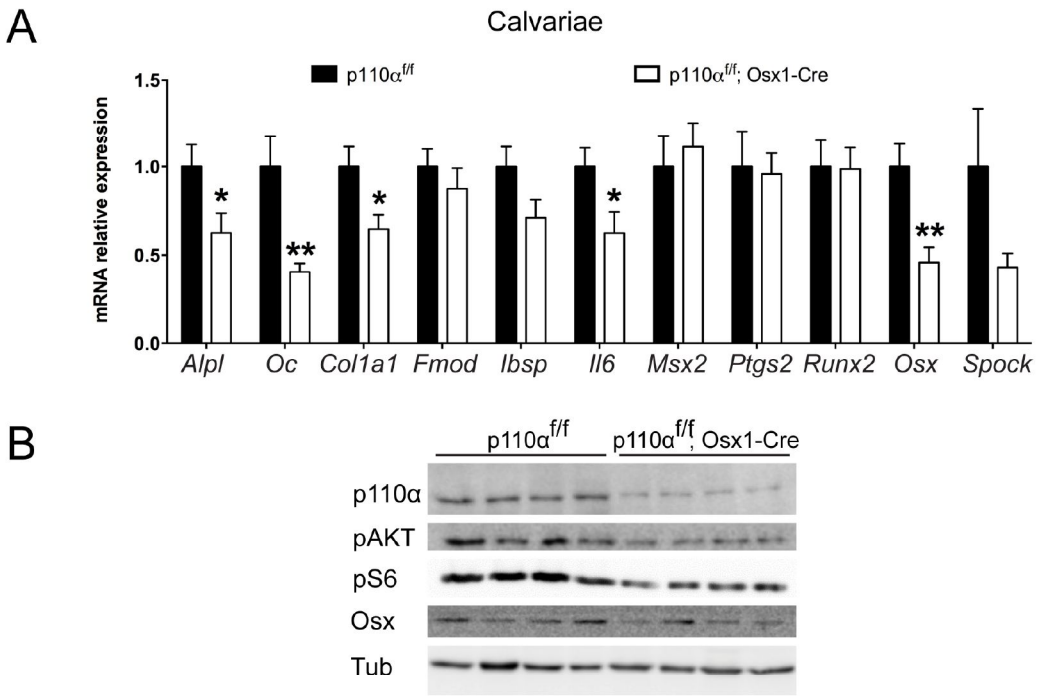

Figure R-37. Osteoblast markers are also affected when *p110α* is deleted post-natally in *p110α$^{f/f}$;Osx1-Cre* mice. (A) mRNA expression of calvariae from 12-week-old *p110α$^{f/f}$;Osx1-Cre* and control mice. (n=6-9 mice/group). **(B)** Western blot of p110α and downstream effectors (pAKT, pS6) and OSX from extracts of the same calvariae as Figure R-31 B. Bars represent the mean ± SEM.

Additionally, serum levels of some bone markers were also analyzed and ALPL was also decreased in these mice (Table R-4), whereas serum NTX was not significantly modified (Figure R-38). These results imply that *p110α* is not only crucial for bone development but also for postnatal bone deposition and homeostasis.

SERUM BIOMARKERS

Parameter	p110α$^{f/f}$	p110α$^{f/f}$; Osx1-Cre	p value	
Calcium (mg/dl)	9.792 ± 0.073	9.687 ± 0.055	0.2572	ns
Iron (μg/ml)	147.592 ± 4.541	146.337 ± 3.366	0.82321	ns
Alkaline phosphatase (UI/l)	94.026 ± 1.799	72.615 ± 1.579	**<0.0001**	***
Phosphorous (mg/dl)	6.855 ± 0.298	6.253 ± 0.300	0.1690	ns

Table R-4. Alkaline phosphatase is also reduced in serum from *p110α$^{f/f}$;Osx1-Cre* mice. Serum from 12-week-old male *p110α$^{f/f}$;Osx1-Cre* and control (*p110α$^{f/f}$*) mice was obtained and calcium, iron, alkaline phosphatase and phosphorous was analyzed (n=14-16 mice/group). Data represent the mean ± SEM.

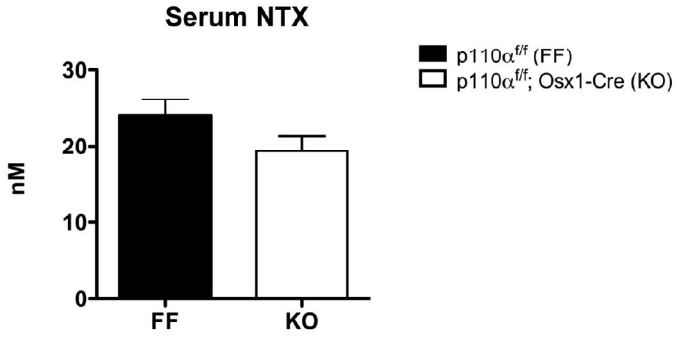

Figure R-38. NTX quantification. Serum from 12-week-old male *p110α*$^{f/f}$*;Osx1-Cre* and control (*p110α*$^{f/f}$) mice was obtained (n=8 mice/group). Bars represent the mean ± SEM.

2.3 Apoptosis and Proliferation Analysis in Osteoblasts Lacking *p110α*

Two different models were used in order to assess the *in vitro* approach of the molecular mechanism involved in the *p110α* mutant phenotype. Briefly, one of the models was based on direct isolation of *p110α*$^{f/f}$*;Osx1-Cre* osteoblasts. Since *Osx1-Cre* allows the prevention of *p110α* deletion through doxycycline treatment, primary cultures were maintained under doxycycline until the experiment was performed. The second model involved *in vitro* retroviral infection of osteoblasts from *p110α*$^{f/f}$ mice. Both systems are extensively described in sections 1.2.2 & 3.2 from Materials & Methods.

Thus, prior to the experiments, osteoblasts from *p110α*$^{f/f}$*;Osx1-Cre* pups were cultured in the absence of doxycycline for 96 hours to induce Cre expression (KO condition). Deletion of *p110α* was confirmed by qPCR and western blot (Figure R-39 A&B). Osteoblasts lacking *p110α* exhibited the expected down-regulation of PI3K signaling as shown by reduced pAKT and pS6 (Figure R-39 B).

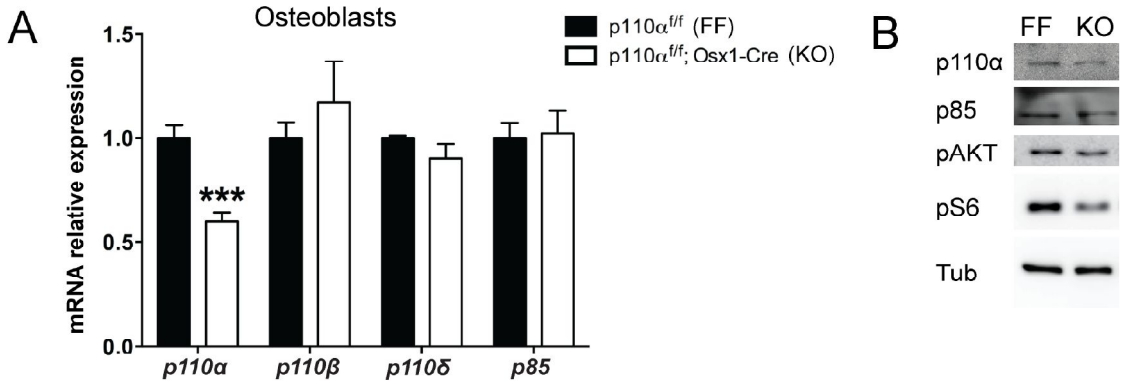

Figure R-39. Deletion of *p110α* in vitro. *p110α*$^{f/f}$;*Osx1-Cre* and *p110α*$^{f/f}$ pups were genotyped and calvariae were used for the isolation of primary osteoblasts. Osteoblasts were maintained with doxycycline in the media until the experiments were performed. For osteoblasts to be considered KO, doxycycline was removed from the media for 4 days. **(A)** mRNA expression of osteoblasts from *p110α*$^{f/f}$ (FF) and *p110α*$^{f/f}$;*Osx1-Cre* cultured without doxycycline for 96 hours (KO). **(B)** Western blot analysis of the osteoblasts described in A. Bars represent the mean ± SEM.

We then measured osteoblast proliferation *in vitro* by BrdU incorporation assay. BrdU is an analog of thymidine and is incorporated into newly synthesized DNA of replicating cells thus further permitting the detection of proliferating cells by using specific antibodies. After *p110α* deletion *in vitro*, osteoblasts displayed a lower proliferation rate (Figure R-40 A).

Annexin labeling allows the determination of apoptosis. Primary osteoblasts were serum-starved prior to flow cytometry analysis in order to sensitize them to apoptosis. Osteoblasts deficient in *p110α* increased their sensitivity to apoptosis (Figure R-40 B).

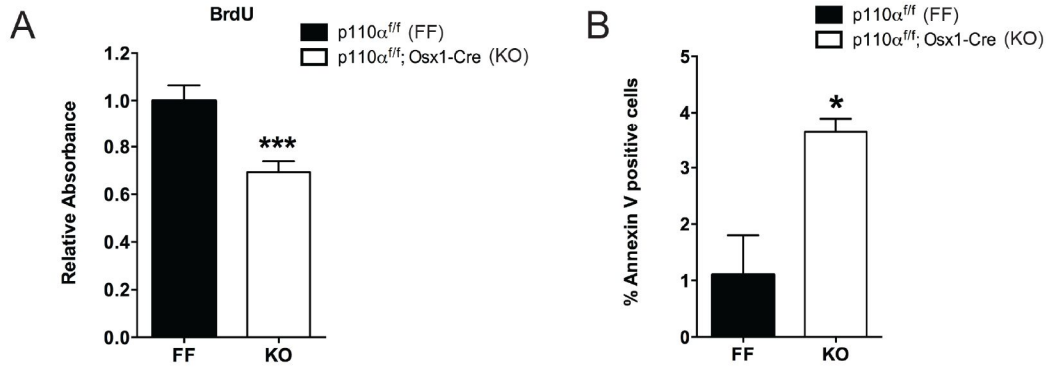

Figure R-40. *p110α* deficiency in primary osteoblast cultures increases apoptosis. (A) BrdU incorporation of osteoblasts treated as in Figure R-39 (n=4-6). **(B)** Percentage of annexin positive cells from osteoblasts treated as in (A) and subjected to 1% FBS for 24 hours and to serum depletion for an additional incubation overnight (n=3). Bars represent the mean ± SEM.

Due to the difficulty of precise *p110α* deletion using the doxycycline system in osteoblasts isolated from *p110α$^{f/f}$;Osx1-Cre* mice, we also generated retroviruses expressing a tamoxifen-inducible Cre vector. Osteoblasts from control newborn pups (*p110α$^{f/f}$*) were infected with mock virus (retrovirus expressing puromycin resistance only) or with the inducible Cre vector (*p110α$^{f/f}$;CreER^{T2}*). Accordingly with osteoblasts from *p110α$^{f/f}$;Osx1-Cre* mice after doxycycline removal, mRNA and protein levels of osteoblasts with retroviral deletion of *p110α* were decreased in *p110α$^{f/f}$;CreER^{T2}* cells only after tamoxifen treatment (Figure R-41 A&B).

We further confirmed the decrease in the expression of osteoblast markers following *p110α* deletion (*Alpl*, *Col1a1*, *Bglap* (*OC*), *Osx*). In agreement with the *in vivo* data, the mRNA levels of osteogenic genes were significantly down-regulated after 96 hours of tamoxifen treatment (Figure R-41 C). Altogether, *p110α* loss in osteoblasts *in vitro* leads to impaired differentiation, a lower proliferation rate and increased sensitivity to apoptosis.

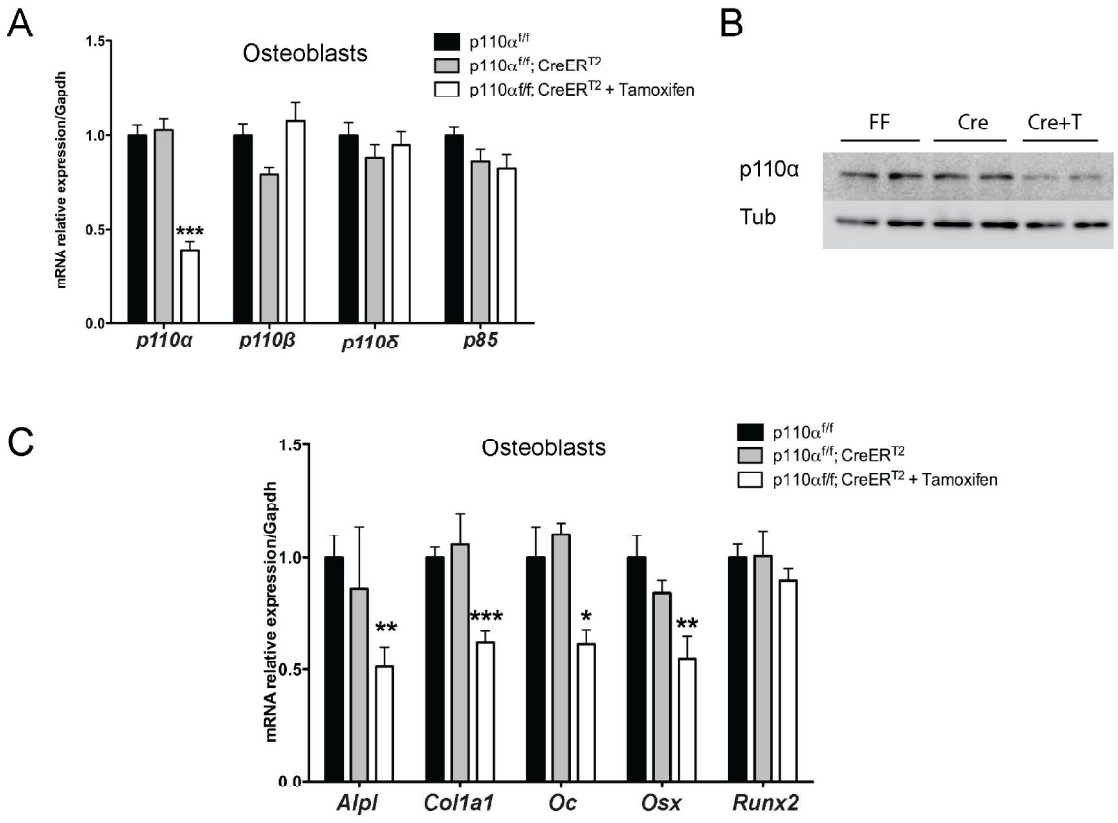

Figure R-41. Deletion of *p110α* by retroviral infection impairs osteoblast differentiation. Control osteoblasts from *p110α$^{f/f}$* mice were infected with mock retrovirus (FF/p110α$^{f/f}$) or CreER^{T2} retrovirus (Cre/p110α$^{f/f}$;CreER^{T2}) and then treated or not with tamoxifen for 96 hours to induce Cre expression. **(A&B)** mRNA expression levels and western blot of infected osteoblasts (n=4-9). **(C)** mRNA expression of osteoblast differentiation markers from osteoblasts treated as above (n=5-9). Bars represent the mean ± SEM.

2.4 Description of the Phenotype of Mice Lacking *p110β*

We next hypothesized whether *p110β* could also be relevant for bone development. Since *p110β* is expressed in osteoblasts to a lesser extent, our first hypothesis was that likely *p110β* was not so deeply involved. Thus, we generated and analyzed the *p110β*$^{f/f}$;*Col1a1-Cre* mice.

2.4.1 *p110β* mutant mice also presents an osteopenic phenotype

Osteoblast-specific deletion of *p110β* was achieved by the same strategy used for *p110α*$^{f/f}$;*Col1a1-Cre* mice. *p110β*$^{f/f}$;*Col1a1-Cre* animals were generated by crossing *p110α*$^{+/+}$;*Col1a1-Cre* animals with *p110β*$^{f/f}$ (loxP sites flanking exons 21 and 22 of the *p110β* alleles). A representative image of the PCR used for the identification of floxed alleles is shown in Figure R-42.

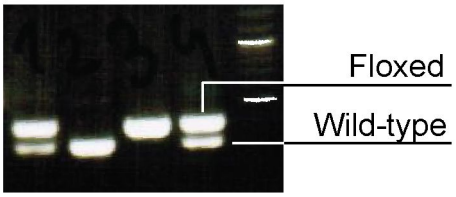

Figure R-42. Identification of floxed and wild-type *p110β* allele. Conventional PCR using a new set of primers allowed us to identify *p110β*$^{f/f}$;*Col1a1-Cre* mice. For *Col1a1-Cre* allele the same set of primers as for *p110α* was used. Both alleles (floxed and wild-type) were observed in agarose gels under the 500 bp gene marker. Expected bands: 372 bp (floxed allele), 304 bp (wild-type allele).

Mice with p110β loss-of-function in bones (*p110β*$^{f/f}$;*Col1a1-Cre*) also had an osteopenic phenotype although adult weight (at 12-weeks of age) was similar in both *p110β*$^{f/f}$;*Col1a1-Cre* and control mice (Figure R-43).

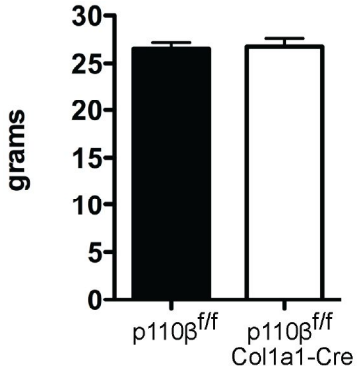

Figure R-43. Adult weight is similar in *p110β*$^{f/f}$;*Col1a1-Cre* and control mice. 12-14-week-old mice were weighted before sacrifice (n=5-13 mice/group). Bars represent the mean ± SEM.

µCT images and analysis showed that *p110β* mutant mice also exhibited lower cortical and trabecular values when compared to control littermates (Figure R-44 & Table R-5).

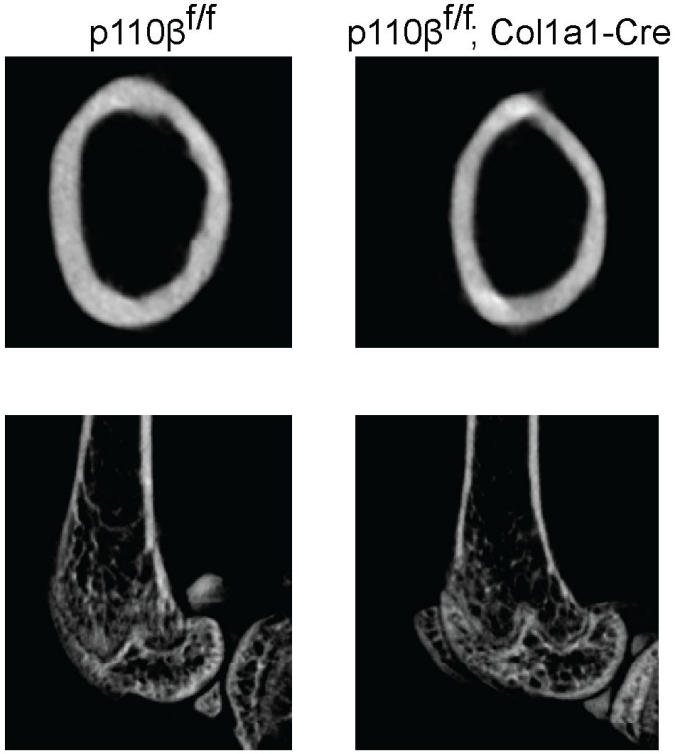

Figure R-44. µCT representative images of distal femurs from *p110β*$^{f/f}$;*Col1a1-Cre* and control mice.

μCT analysis				
Cortical	**p110β$^{f/f}$**	**p110β$^{f/f}$; Col1a1-Cre**	**p value**	
BV (mm^3)	0.836 ± 0.020	0.721 ± 0.024	0.0017	**
B.Pm (mm)	10.050 ± 0.149	9.509 ± 0.169	0.0165	*
Ct.Th (mm)	0.179 ± 0.003	0.163 ± 0.003	0.0023	***
Trabecular				
BV/TV (%)	37.27 ± 1.793	29.21 ± 2.029	0.0058	**
Tb.Th (mm)	0.046 ± 0.002	0.036 ± 0.001	0.0014	**
Tb.N (#/mm)	8.235 ± 0.185	7.961 ± 0.313	0.2264	ns
BMD (g·cm^3)	0.252 ± 0.009	0.209 ± 0.006	0.0019	**

Table R-5. Deletion of *p110β in vivo* exposes a defective bone phenotype. μCT analysis of *p110β$^{f/f}$;Col1a1-Cre* and control male mice at 12 weeks of age. Cortical and trabecular data shows a significant reduction in mutant mice (n=6-8 mice/group). Data represent the mean ± SEM.

Specific *p110β* subunit deletion was also borne out by checking mRNA and protein levels of p110α and p110β in addition to p85. pS6 was also measured as evidence of PI3K signal down-regulation (Figure R-45 A&B). Again, mRNA analysis from calvariae confirmed osteoblast differentiation impairment based on the decline in the expression of *Alpl*, *Col1a1* and *Bglap (OC)* (Figure R-45 B).

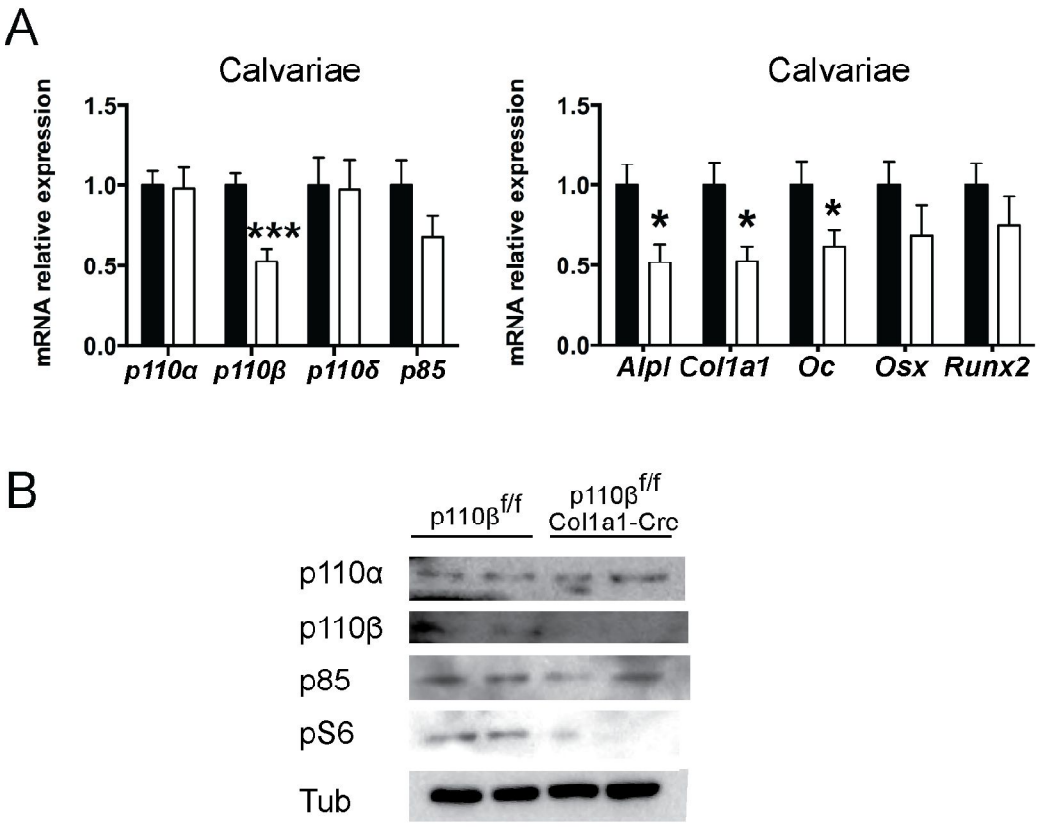

Figure R-45. *p110β* is also relevant for osteoblast differentiation. (A) mRNA expression analysis of *p110β*$^{f/f}$;*Col1a1-Cre* and control male mice at 12 weeks of age (n=9-16 mice/group). **(B)** Western blot analysis of calvariae from *p110β*$^{f/f}$;*Col1a1-Cre* and control newborn mice. Bars represent the mean ± SEM.

2.4.2 Effects of *p110β* deletion *in vitro*

Acute loss of *p110β* in primary osteoblast cultures was achieved by retroviral infection of CreER^{T2} as previously described. After transduction, osteoblasts strongly reduced *p110β* mRNA and protein levels and led to a reduction in AKT signaling (Figure R-46 A&B).

Osteoblast markers as *Osx* and *Runx2* among others were also reduced by the lack of *p110β* (Figure R-46 A). However, when compared to the effects of *p110α* loss, *p110β* deletion led to milder effects on expression of osteoblastic genes.

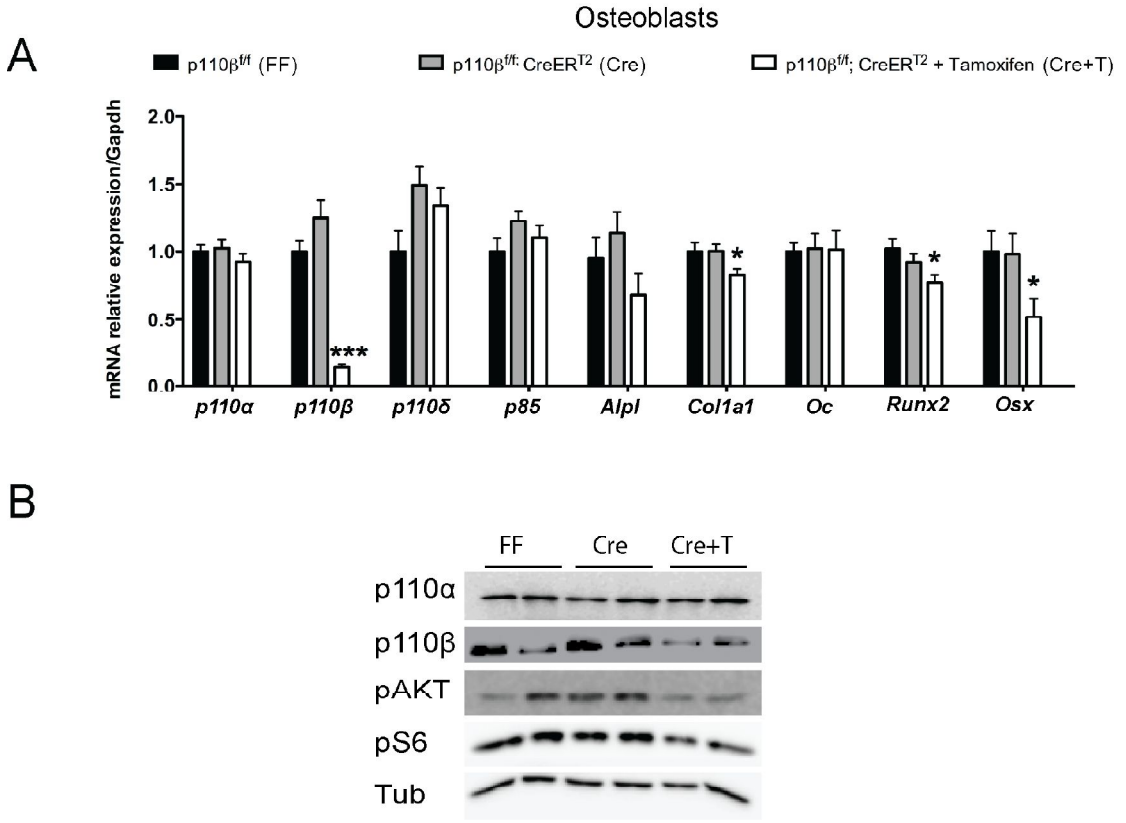

Figure R-46. Retroviral deletion of *p110δ* reduces osteoblast markers. Osteoblasts were transduced with mock or *CreER*^{T2} virus, obtaining *p110δ*$^{f/f}$, *p110δ*$^{f/f}$;*CreER*^{T2}, and *p110δ*$^{f/f}$;*CreER*^{T2} + tamoxifen (KO cells). **(A)** mRNA expression of PI3K subunits and osteoblast markers from infected osteoblasts (n=6-10). **(B)** Western blot analysis of the levels of p110α, p110β, pAKT and pS6 from transduced osteoblasts. Bars represent the mean ± SEM.

In vivo and *in vitro* approaches of p110β deletion allow us to confirm no compensatory p110α increment in the mRNA or protein (Figure R-45 & Figure R-46). Unexpectedly, the results obtained from *p110δ* mutant mice indicated an important role for the p110β isoform in skeletal development. The phenotype caused by the loss of this subunit suggests that even though the loss of either one of the two isoforms is sufficient for a measureable phenotype, the deletion of *p110δ* leads to a less dramatic impairment in the osteoblast differentiation.

2.5 Study of Pharmacological Inhibitors of Specific p110 Isoforms and Other Downstream PI3K Effectors

Overactivation of the PI3K signaling by inactivation of PTEN or gain of function of p110 isoforms is frequent in human tumors (Thorpe et al., 2015; Vanhaesebroeck et al.,

2010b). For these reasons, several isoform-specific inhibitors are currently being tested in clinical trials with promising success. *In vitro* experiments using pan-specific and isoform-specific PI3K inhibitors have suggested that PI3K signaling is absolutely required for osteoblast function and bone development (Guntur and Rosen, 2011; McGonnell et al., 2012; Smith et al., 2013).

To further study the possible differential role of distinct PI3K subunits and their downstream effectors, we tested the effect of pharmacological inhibitors for p110α (A66) and p110β (TGX-221) on wild type osteoblasts. We also tested rapamycin (TORC1 inhibitor) and CHIR 99021 (GSK3 inhibitor). Osteoblasts were treated with 10μM of each inhibitor (unless rapamycin which was used at 1μM) for 30 minutes and then IGF1 was added for 4 additional hours. Western blot analysis shows pAKT, pFOXO, pGSK3, pS6K and tubulin (Figure R-47).

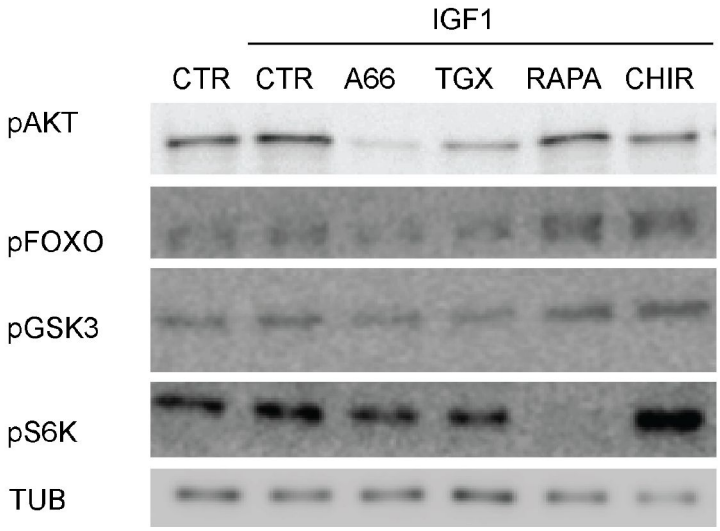

Figure R-47. Western blot from wild-type osteoblasts treated with specific inhibitors. CTR (treated with DMSO), A66 (p110α inhibitor), TGX (p110β inhibitor), RAPA (rapamycin, TORC1 inhibitor), CHIR (GSK3 inhibitor).

Among all the inhibitors, A66 was the one to strongly inhibit pAKT (Thr308) *in vitro*, followed by TGX. p110α inhibitor also diminished pFOXO and pGSK3 levels and there was a slight effect on pS6K protein expression.

Rapamycin clearly inhibited mTORC1, which was evidenced by the completely lack of a downstream effector pS6K but there were no alterations in pAKT levels. GSK3 inhibitor did not change osteoblast pGSK3 levels as expected by its mechanism of action. We also tested the effects of the selected inhibitors on proliferation and apoptosis. BrdU assay was done after 16 hours of pharmacological inhibition and 5 hours of BrdU

incorporation. p110α- and rapamycin-inhibited cells presented a reduced BrdU incorporation when compared to DMSO treated osteoblasts (Figure R-48 A).

For annexin staining, wild-type cells were seeded in 10% FBS media and next day media was replaced for one containing 1% FBS (24 hours). Ultimately, cells were treated with the inhibitors for an additional over-night in depleted media and annexin assay was performed by flow cytometry. Among all the PI3K downstream effectors tested, just osteoblasts treated with p110α inhibitor presented a higher level of apoptosis (A66 inhibitor) (Figure R-48 B).

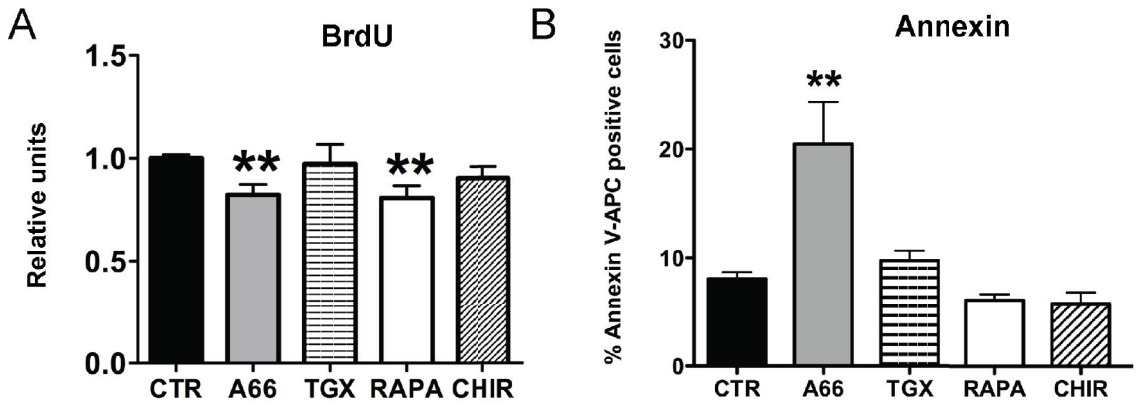

Figure R-48. Proliferation and apoptosis assay in pharmacological-inhibited osteoblasts. (A) Wild type osteoblasts were treated with the indicated inhibitors for 16 hours and BrdU was added for 5 additional hours. BrdU incorporation was related to control (n= 3). **(B)** Wild type osteoblasts were cultured with 1% FBS for 24 hours and then depleted of serum for 16 hours during treatment with the indicated inhibitors. Annexin-stained cells were quantified by flow cytometry (n=3-6). Bars represent mean ± SEM.

2.6 Study of the Lack of *p110α* and *p110β* Isoforms

The finding that both isoforms contributed to bone development made us investigate whether the deficiency of both isoforms would have additive effects in bone formation.

2.6.1 Osteopenic phenotype in mice lacking *p110α* and *p110β* in osteoblasts

Animals from the *p110α*$^{f/f}$*;Col1a1-Cre* colony were crossed with floxed *p110β* mice to generate *p110αβ*$^{f/f}$*;Col1a1-Cre* mice and their control (*p110αβ*$^{f/f}$) littermates. The above-mentioned PCRs where used to identify the double mutant mice (*p110αβ*$^{f/f}$*;Col1a1-Cre*) and their control littermates (*p110αβ*$^{f/f}$).

First we checked the mRNA and protein levels of both isoforms in calvariae from *p110αβ$^{f/f}$;Col1a1-Cre* mice and again, there was not compensatory effect from p110δ isoform or p85 (Figure R-49 A&B). pAKT and pS6 were decreased in double mutant mice as shown by western blot. Moreover, and concordantly with the above described mutant phenotypes, the mRNA levels of important osteogenic genes (*Alpl, Col1a1, Bglap (OC), Osx, and Runx2*) were down-regulated (Figure R-49 A). OSX decrease was further confirmed by immunoblot of calvariae samples (Figure R-49 B).

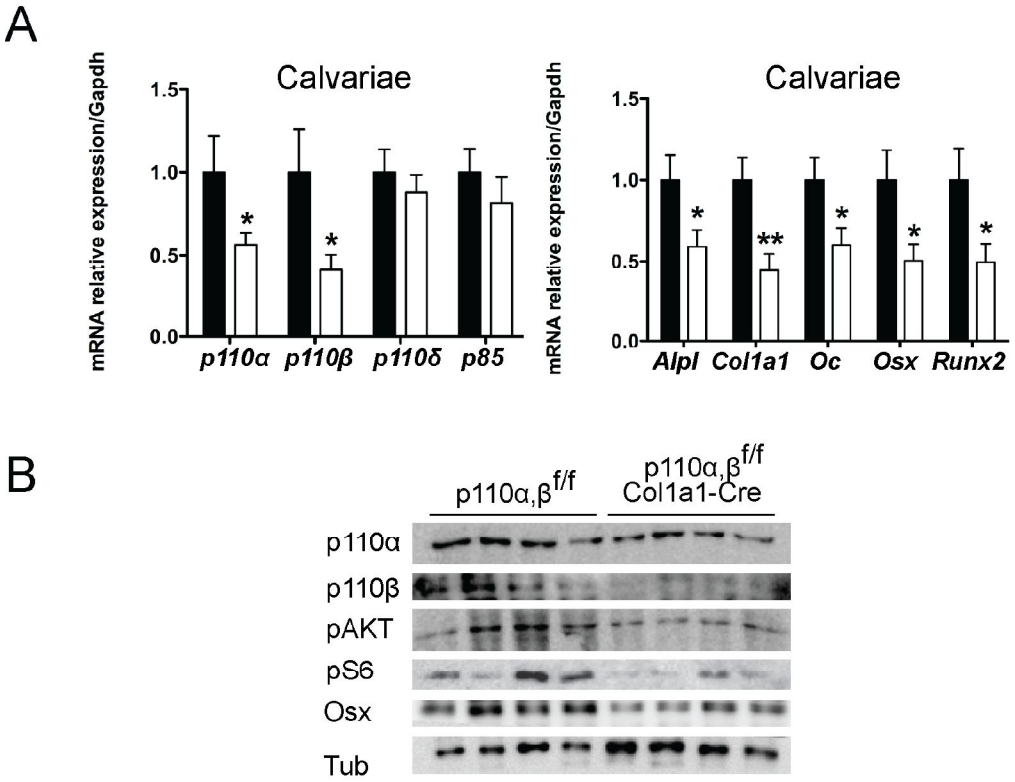

Figure R-49. Deletion of *p110α* and *p110β* led to a deficient osteoblast differentiation. (A) mRNA expression of the *p110* subunits, *p85* and the osteoblast markers of *p110αβ$^{f/f}$;Col1a1-Cre* and control mice at 12 weeks of age (n=5-8 mice/group). **(B)** Western blot analysis of calvariae from *p110αβ$^{f/f}$;Col1a1-Cre* and control newborn mice. Bars represent mean ± SEM.

To further study the phenotype of the *p110αβ$^{f/f}$;Col1a1-Cre* mice, femurs from double mutant animals were processed for μCT analysis. Reconstructed images of the cortical and trabecular area of *p110αβ$^{f/f}$;Col1a1-Cre* mice showed similar defects to those of *p110α* mutant mice (Figure R-50). Data from μCT analysis revealed an osteopenia comparable to the osteopenic phenotype of *p110α;Col1a1-Cre* animals (Table R-6).

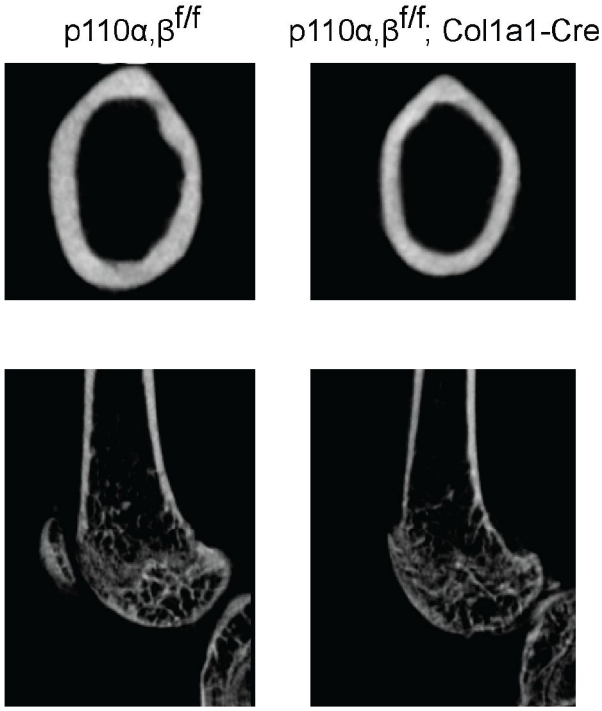

Figure R-50. Representative images of µCT analysis. *p110αβ$^{f/f}$;Col1a1-Cre* mice present a clearly osteopenic phenotype. Both cortical and trabecular bone volume is reduced in those animals.

µCT analysis				
Cortical	**p110α,β$^{f/f}$**	**p110α,β$^{f/f}$; Col1a1-Cre**	**p value**	
BV (mm^3)	0.820 ± 0.018	0.726 ± 0.027	0.0047	**
B.Pm (mm)	9.937 ± 0.101	9.544 ± 0.104	0.0198	*
Ct.Th (mm)	0.179 ± 0.002	0.163 ± 0.003	0.0027	**
Trabecular				
BV/TV (%)	32.43 ± 1.906	22.55 ± 1.893	0.0011	**
Tb.Th (mm)	0.038± 0.001	0.032 ± 0.001	0.0019	**
Tb.N (#/mm)	8.816 ± 0.395	7.257 ± 0.214	0.0006	***
BMD (g·cm^3)	0.230 ± 0.001	0.188 ± 0.062	0.0148	*

Table R-6. Osteopenia in mice lacking *p110α* and *p110β*. Data from µCT analyses of *p110αβ$^{f/f}$;Col1a1-Cre* and control mice at 12 weeks of age (n=10-14 mice/group). Data represent mean ± SEM.

To analyze osteoclastogenesis in *p110αβ* mutants, *Trap* RNA expression and the relative *Rankl/Opg* ratio were measured in animals at 12 weeks of age showing no significant alterations in calvariae of *p110αβ* mutants (Figure R-51).

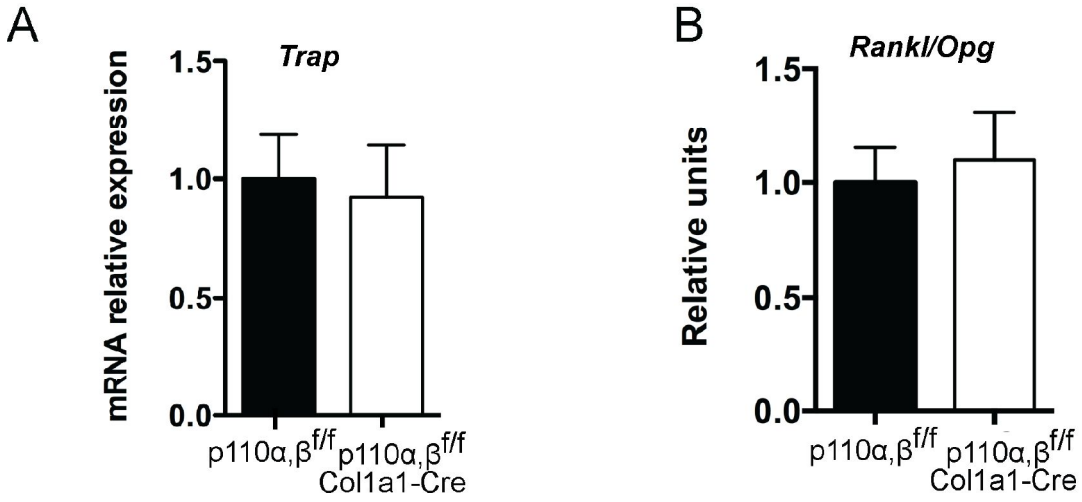

Figure R-51. Osteoclasts are not affected in *p110αβ* mutant mice. *Trap* expression and the relative *Rankl/Opg* ratio were not affected by the lack of *p110α* and *p110β* (n=6-7 mice/group). Bars represent mean ± SEM.

2.6.2 Osteoblastogenesis is affected in *p110αβ;CreER^{T2}* cells

Retroviral-driven deletion of *p110α* and *p110β* decreased the levels of both isoforms at the RNA and protein levels and resulted in impaired osteoblast differentiation as indicated by *Alpl, Bglap (OC), Col1a1, Runx2* and *Osx* gene expression. Western blot also showed reduced PI3K downstream effectors as phospho-AKT or phospho-S6 (Figure R-52 A&B).

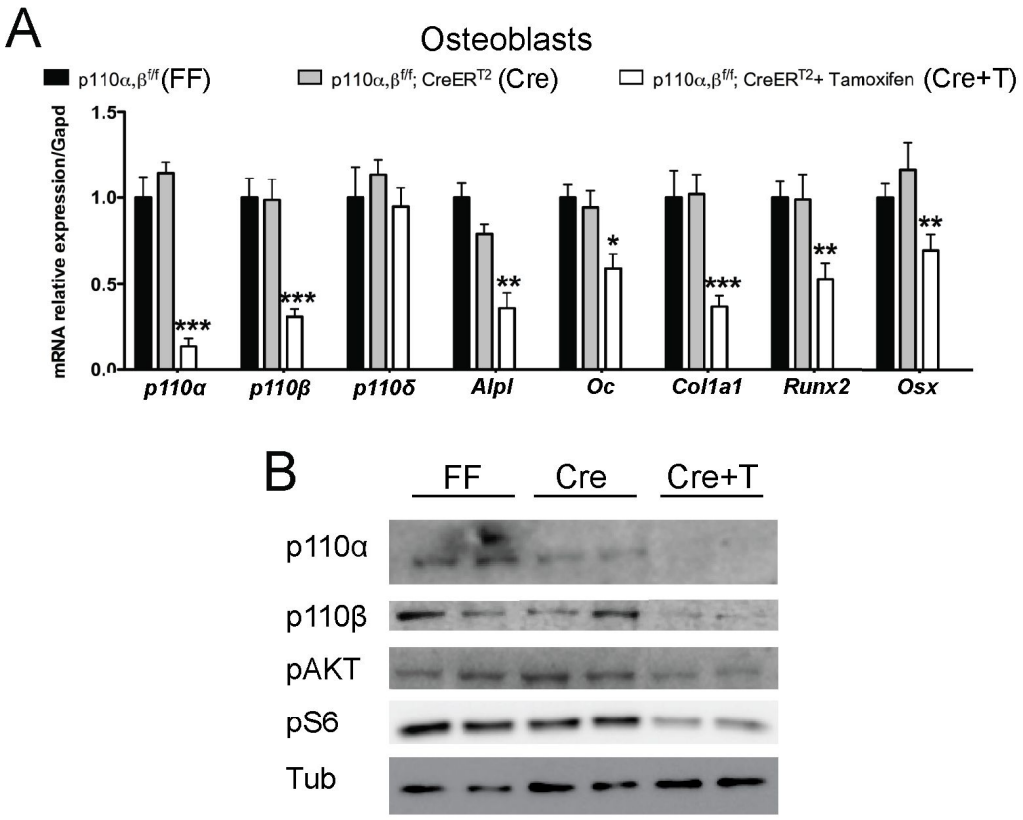

Figure R-52. *In vitro* deletion of *p110α* and *p110β* shows a deficient osteoblast differentiation. (A) mRNA expression of PI3K subunits and osteoblast markers in osteoblasts transduced as above (n=7-16) **(B)** Western blot analysis of transduced osteoblasts. Bars represent mean ± SEM.

We confirmed increased osteoblast sensitivity to apoptosis by performing TUNEL assays of *p110αβ*-deficient cells. The apoptotic ratio was higher in cells lacking both PI3K isoforms (Figure R-53 A&B). Moreover, in order to know whether the role of *p110α* in apoptosis was a characteristic of this specific subunit or it also occurred in *p110β*-lacking cells, evaluation of annexin staining in different osteoblast cultures was performed. Results from osteoblasts with loss of *p110α*, *p110β* or both isoforms suggested (as the results obtained using the specific-isoform pharmacological inhibitors) that *p110α* is the main isoform involved in the sensitization of the cells to apoptotic stimuli (Figure R-53 C). In both assays (TUNEL and annexin staining) osteoblasts were again maintained under serum-restricted media prior to the experiments.

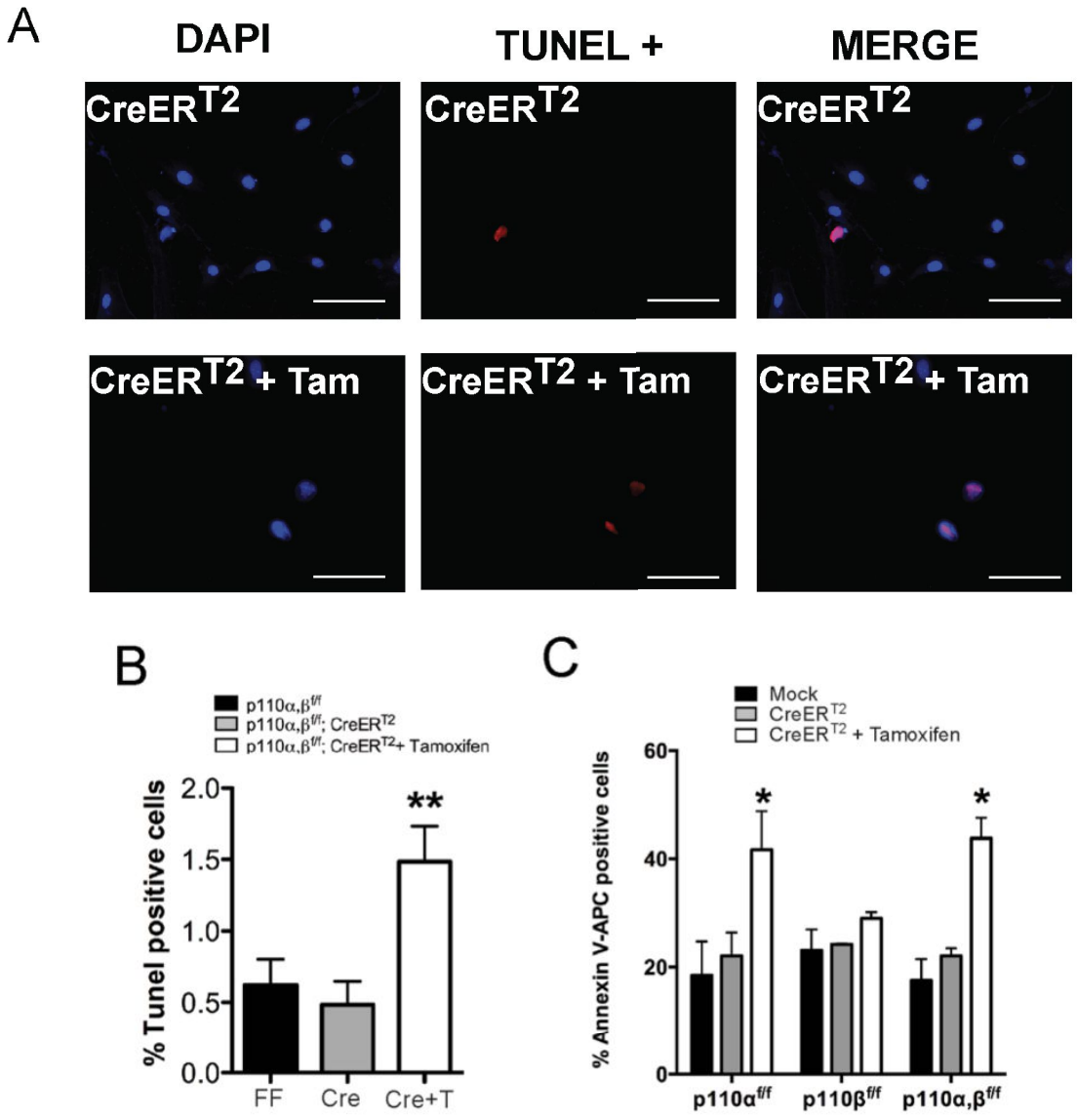

Figure R-53. *p110α* subunit is the one involved in the sensitization to apoptosis. (A) Representative TUNEL images of transduced *p110αβ*$^{f/f}$ osteoblasts (scale bar, 100 μm). **(B)** Panel shows quantification of TUNEL positive cells (n=6). **(C)** Primary cultures of osteoblasts isolated from *p110α*$^{f/f}$, *p110β*$^{f/f}$ and *p110αβ*$^{f/f}$ newborn mice were transduced with CreER^{T2}. Cells were cultured with 1% serum for 24 hours and without serum for an additional 16 hours to sensitize them to apoptosis. Bar graph represents the percentage of annexin positive cells (n=3-4). Bars represent mean ± SEM.

2.7 Class I PI3K Deletion Results in Higher GSK3 Activity Leading to Lower SMAD1 Protein Levels

2.7.1 *p110αβ*-deficient osteoblasts are unable to respond appropriately to BMP signaling

To clarify the mechanisms underlying osteopenia in PI3K-deficient models, we determined the response to the osteogenic cytokines IGF1, BMP-2 and Wnt3a (Chen et al., 2004; Regard et al., 2012; Wan and Cao, 2005) (Figure R-54 A).

Treatment of *p110αβ*-deleted osteoblasts with IGF1 or BMP-2 revealed a reduced ability of these cells to activate the BMP and Wnt target genes *Axin2, Smad7, Id1* or *JunB*. Basal levels of *Axin2, Smad7* and *Id1* were already decreased in tamoxifen-treated $p110\alpha\beta^{f/f};CreER^{T2}$ cells. Moreover, BMP-2 induction of *Smad7, Id1* or *JunB* was partially abolished in mutant cells (Figure R-54 A). Similarly, expression of osteoblast-specific genes was refractory to induction by IGF1 and BMP-2 in *p110αβ*-depleted osteoblasts, suggesting that cells lacking PI3K signaling have defective responses to BMP and Wnt (Figure R-54 B).

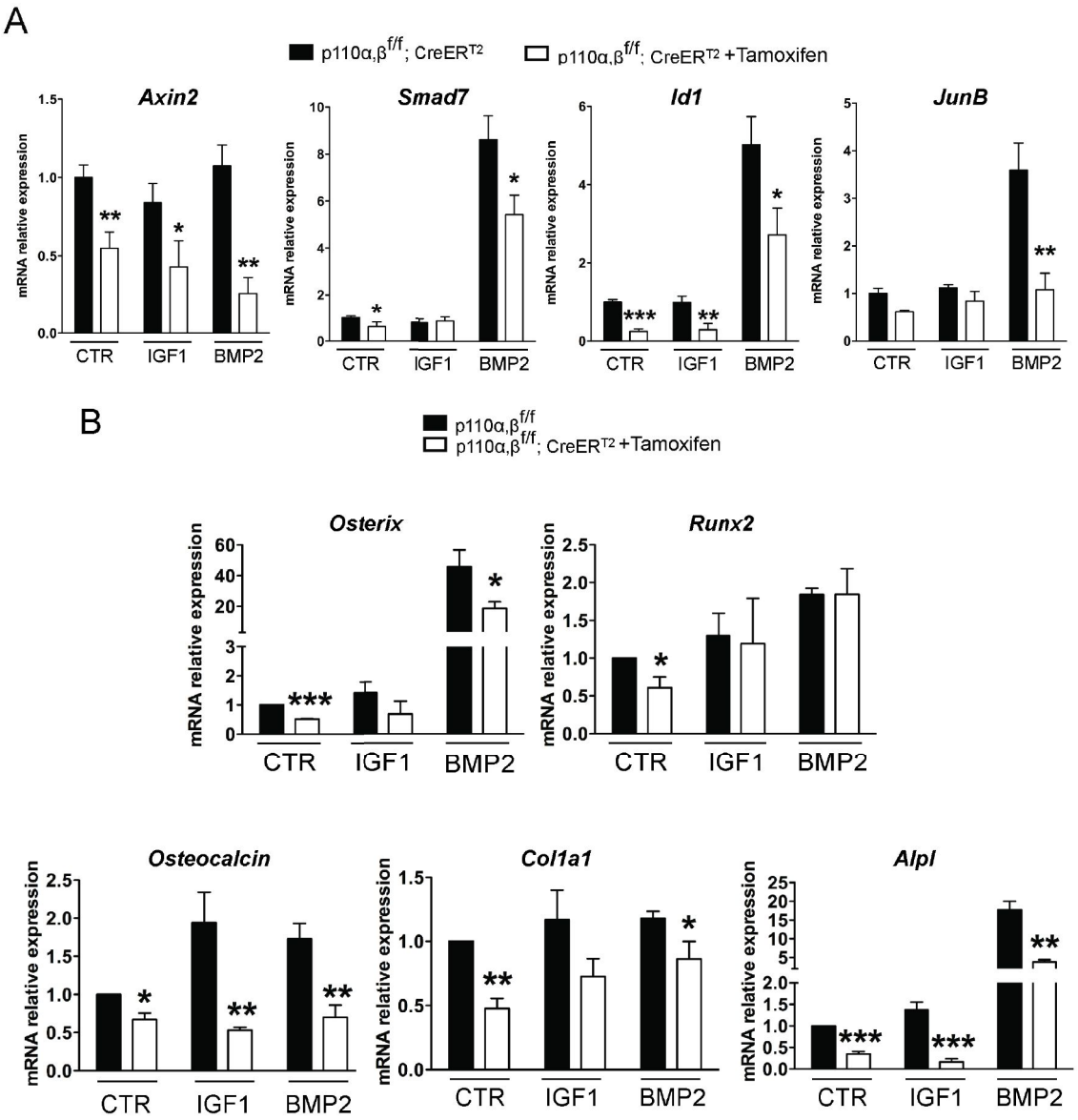

Figure R-54. Osteoblasts lacking *p110αβ* have defective responses to IGF1 and BMP stimulation. Osteoblasts from *p110αβ*$^{f/f}$ mice were infected with CreER^{T2} retrovirus and treated or not with tamoxifen. *Axin2*, *Smad7*, *Id1* and *JunB* mRNA levels were analyzed after IGF1 (10 nM) or BMP-2 treatment (2 nM) (n=6-10). *Osterix*, *Runx2*, *Osteocalcin*, *Col1a1* and *Alpl* mRNA levels were analyzed after 16 hours of IGF1 (10 nM) or BMP-2 (2 nM) treatment and are relative to control (n=6-10). Bars represent the mean ± SEM.

As mentioned in the introduction chapter, SMAD1 and β-catenin transcription factors transduce canonical BMP and Wnt signaling, respectively, and regulate the expression of key osteogenic genes (Karsenty et al., 2009; Massague et al., 2005; Ortuno et al., 2010; Rodriguez-Carballo et al., 2011).

After the results showed above, we hypothesized that probably PI3K deletion was disrupting both SMAD1 and Wnt signaling. To test this assumption, we analyzed the

expression of genes targeted by the aforementioned pathways in calvariae from *p110αβ*$^{f/f}$*;Col1a1*-Cre mice and as speculated, the expression of BMP and Wnt target genes was strongly down-regulated in those mice (Figure R-55).

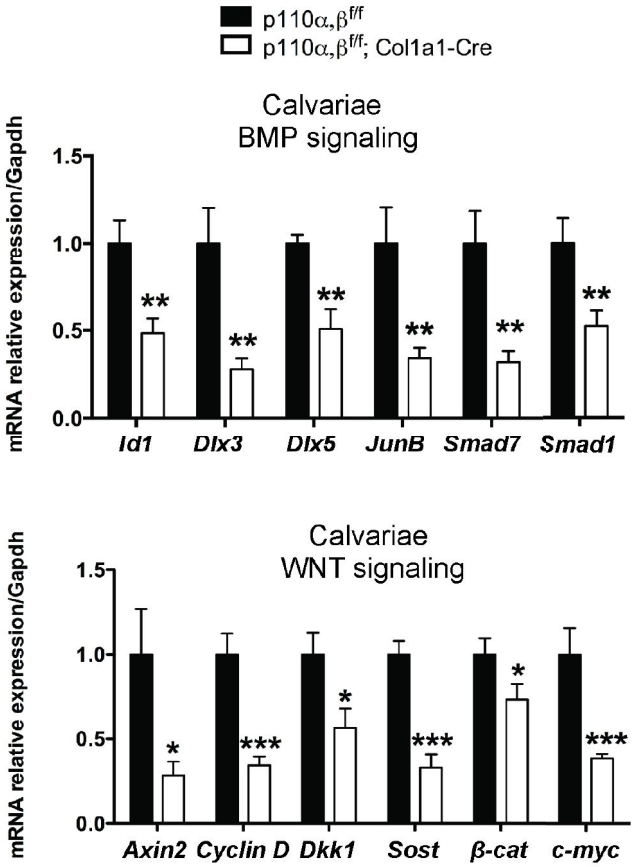

Figure R-55. BMP and Wnt signaling in mice lacking *p110α* and *p110β*. Calvariae from 12-week-old *p110αβ*$^{f/f}$*;Col1a1-Cre* and control mice were used to analyze the expression of BMP and Wnt target genes (n=5-8 mice/group). Bars represent the mean ± SEM.

Western blot analysis from calvarial extracts also demonstrated significantly lower cellular levels of SMAD1 and β-catenin and also lower levels of C-terminal phosphorylated SMAD1 (Figure R-56 A). BMP-2 response in osteoblasts after *p110αβ* deletion by retroviral transduction of CreER^{T2} was also studied (Figure R-56 B). Basal levels of SMAD1 were reduced by *p110αβ* depletion, and BMP-dependent phosphorylation of SMAD1 was almost completely abrogated. Interestingly, we observed an increase in total protein levels of SMAD1 after addition of BMP-2 (Figure R-56 B).

Previous studies have shown that phosphorylation of the linker region of SMAD1 by MAPK primes SMAD1 for direct phosphorylation by GSK3 and leads to SMAD1 degradation (Fuentealba et al., 2007; Sapkota et al., 2007). After analysis of AKT-

mediated inhibitory phosphorylation of GSK3, we observed reduced levels in *p110αβ*-deleted osteoblasts.

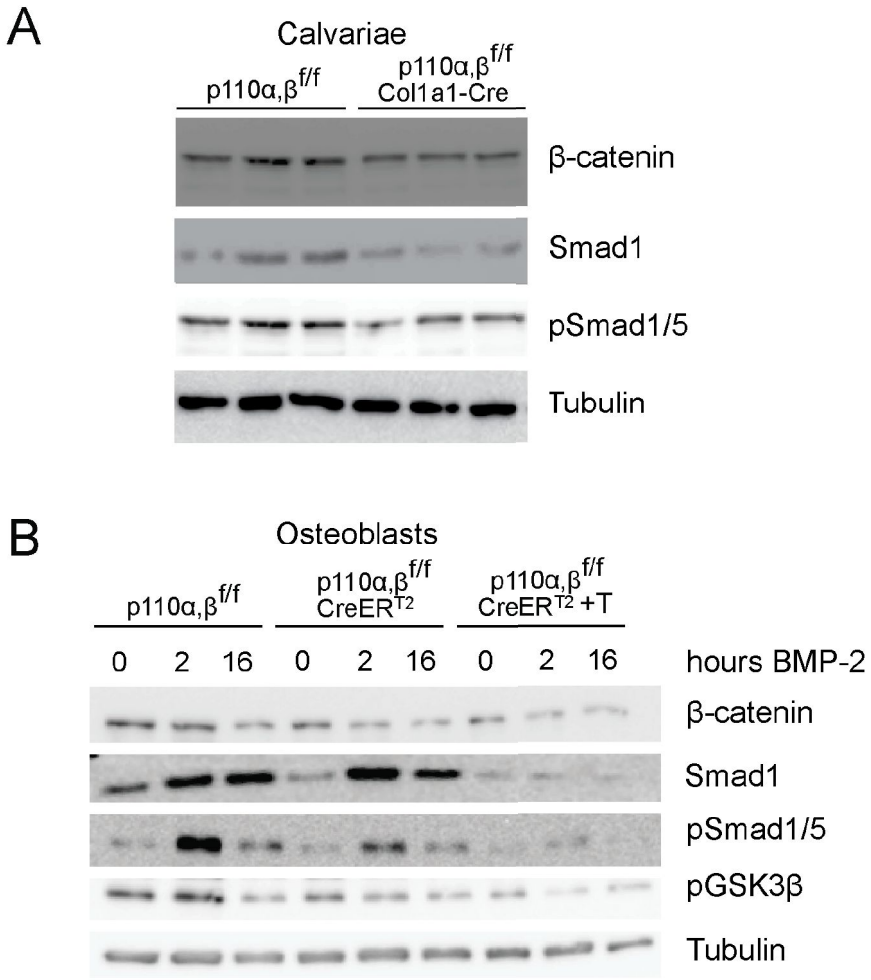

Figure R-56. Impaired BMP and Wnt signaling in *p110αβ*-mutant mice and *p110αβ*-deficient osteoblasts. **(A)** Calvariae from Figure R-55 were used for western blot analysis of β-catenin, SMAD and pSMAD1 levels. **(B)** Western blot of osteoblasts transduced with CreER^{T2} as described above were stimulated with BMP-2 for 2 or 16 hours.

Furthermore, we checked *Smad1* mRNA levels in cultured osteoblasts after *p110αβ* loss and as seen in calvariae form mutant mice (Figure R-55), *Smad1* mRNA levels were also reduced (Figure R-57). Thus, changes in SMAD1 protein levels likely result from a combination of transcriptional and posttranslational events.

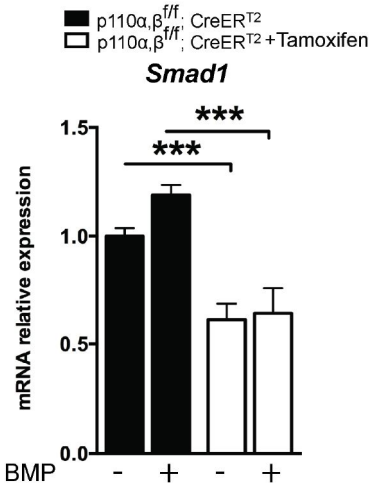

Figure R-57. *Smad1* mRNA levels in *p110αβ*-deficient osteoblasts. Osteoblasts from *p110αβ*$^{f/f}$ mice were infected with CreER^{T2} retrovirus and treated or not with tamoxifen. Then, 0.2 nM BMP-2 was added for 2 hours and *Smad1* mRNA expression was evaluated (n=4-6). Bars represent the mean ± SEM.

To additionally confirm these observations we tested the effects of an acute pharmacological inhibition of p110α in wild type osteoblasts. The A66 inhibitor (specific for p110α isoform) led to lower levels of SMAD1 and β-catenin and a lack of responsiveness of SMAD1 phosphorylation to BMP-2. These effects correlated with lower levels of phosphorylated GSK3 (Figure R-58).

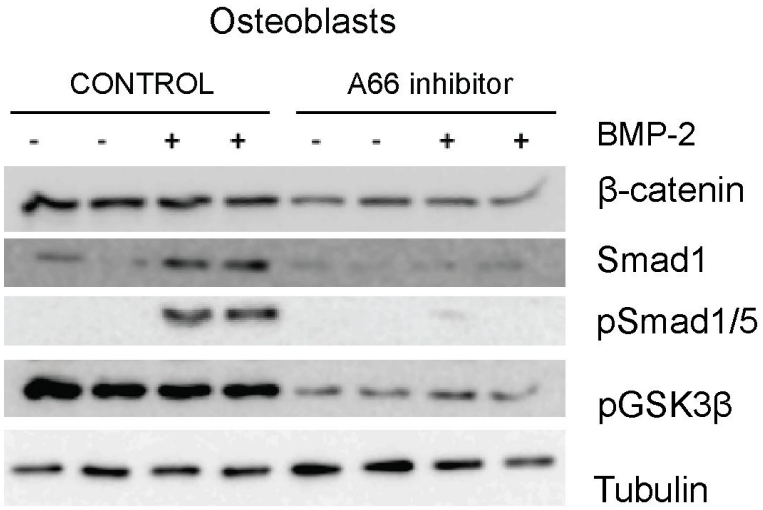

Figure R-58. Pharmacological inhibition of *p110α* reduced the protein levels of pGSK3*β*, SMAD1 and pSMAD1/5. Western blot analysis of wild type osteoblasts treated with 10 μM A66 (p110α inhibitor) for 16 hours and then treated with 0.2 nM BMP-2 for 30 minutes.

Inhibition of GSK3 activity leads to a partial recovery of SMAD1 phosphorylation

In order to corroborate our hypothesis, we tested whether pharmacological inhibition of GSK3 activity was able to normalize SMAD1 and phospho-SMAD1 levels and

therefore BMP signaling. For this aim, we took advantage of two known GSK3 inhibitors, CHIR99021 and LiCl. Treatment of *p110αβ*-depleted cells with CHIR990121 increased the levels of SMAD1 and partially recovered SMAD1 phosphorylation (Figure R-59 A). Similarly, addition of LiCl to A66-pretreated osteoblasts (p110α inhibitor) partially recovered SMAD1 expression and its carboxy-terminal phosphorylation levels (Figure R-59 B).

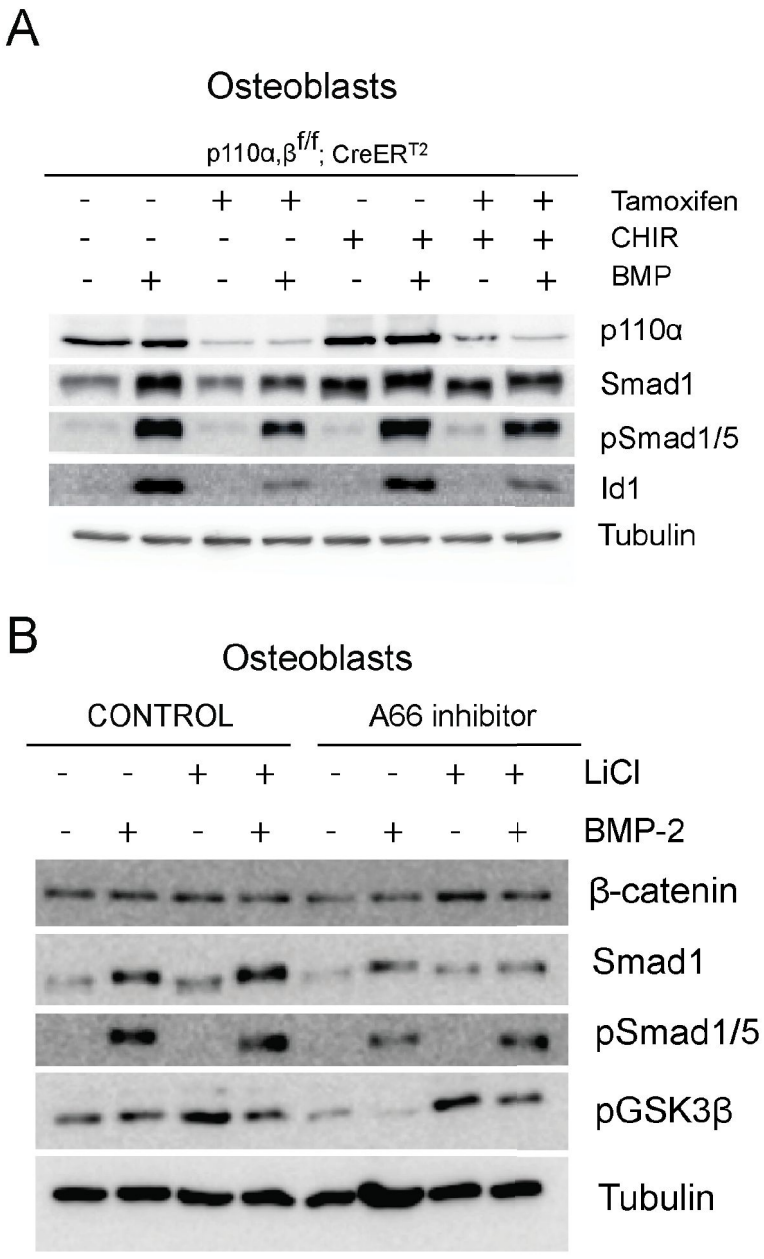

Figure R-59. GSK3 inhibitor partially recovers the phenotype of osteoblasts lacking *p110α* and *p110β*. (A) Western blot analysis of *p110αβ*$^{f/f}$ cells transduced with CreER^{T2} as previously described and treated with 10 μM CHIR 99021 for 6 hours and then with 0.2 nM BMP for 2 additional hours. **(B)** Control osteoblasts from *p110αβ*$^{f/f}$ mice were treated with 10 μM A66 for 16 hours and then LiCl (20 mM) was added for 2 hours. BMP-2 was used at 0.2 nM for 30 minutes.

In addition, we analyzed the expression of BMP and Wnt target genes in *p110-αβ*-depleted osteoblasts after treatment with CHIR99021. If GSK3 inhibition was partially reverting the described phenotype, then the expression of previously reported affected target genes should also normalize. Accordingly, BMP/Wnt target genes as *Smad7* or *Axin2* were rescued by CHIR99021 (Figure R-60).

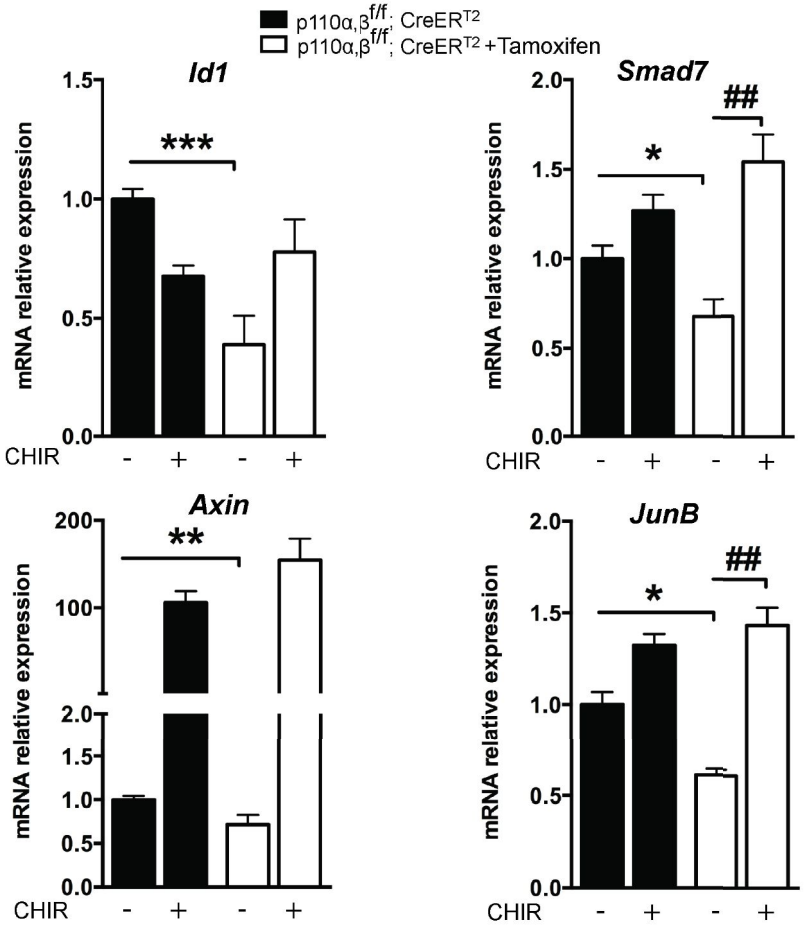

Figure R-60. mRNA expression of *p110αβ*-deficient osteoblasts treated with GSK3 inhibitor. Osteoblasts infected as above were treated with CHIR99021 for 8 hours, and mRNA expression of *Id1*, *Smad7*, *Axin* and *JunB* was evaluated (n=5-11). Asterisks refer to significance between osteoblasts infected with CreER^{T2} retrovirus and treated with tamoxifen compared to mock-infected osteoblasts. Similarly, # refers to significance between osteoblasts infected with CreER^{T2} retrovirus and treated with tamoxifen treated or not with CHIR99021. Bars represent the mean ± SEM.

2.7.2 SMAD1 overexpression restores BMP responsiveness and osteoblast-specific gene expression

Since double null cells presented a clear lack of Smad signaling we then proceeded to overexpress SMAD1 hoping to succeed in the reversion of the effects of *p110αβ*

deletion. Ectopic expression of SMAD1 in *p110-αβ*-depleted osteoblasts was performed by retroviral infection. SMAD1 accumulation was able to reestablish the basal and the C-terminal phosphorylation levels of SMAD1 of osteoblasts lacking *p110α* and *p110β* (Figure R-61 A). More importantly, SMAD1 recovery completely normalized the levels of osteoblast-specific genes (Figure R-61 B). Altogether these data suggest that depletion of SMAD1 levels is a major factor responsible for the osteopenic phenotype observed in class I PI3K-deficient mice.

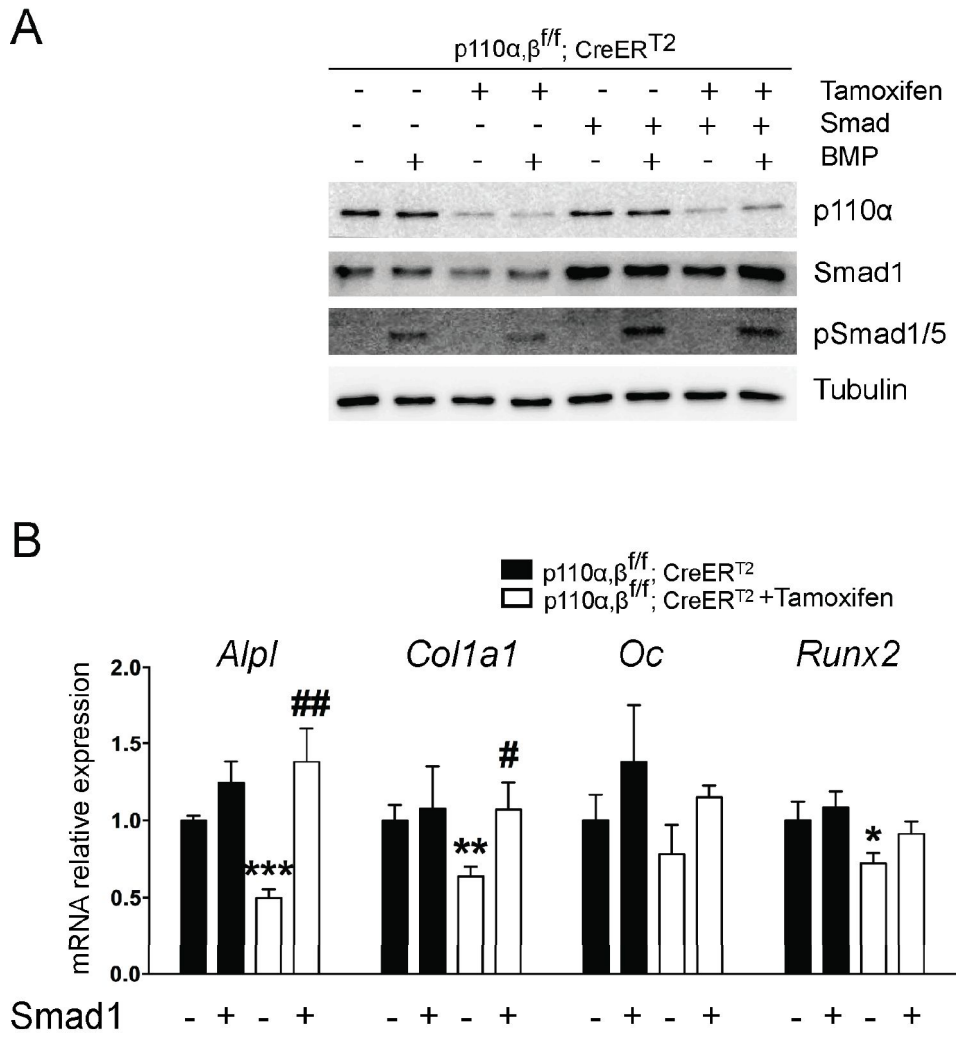

Figure R-61. Effects of Smad overexpression in osteoblasts lacking *p110α* and *p110β*. (A) Western blot of *p110αβ*$^{f/f}$ osteoblasts that were co-transduced with CreER^{T2} and GFP or Smad1 retrovirus and treated with or without tamoxifen. **(B)** *Alpl*, *Col1a1*, *Bglap* (*OC*), *Runx2* and *Osx* mRNA levels of osteoblasts transduced as (A). Asterisks refer to significance between osteoblasts infected with CreER^{T2} retrovirus and treated with tamoxifen compared to mock-infected osteoblasts. Similarly, # refers to significance between osteoblasts infected with CreER^{T2} retrovirus and treated with tamoxifen transduced or not with SMAD1 (n=4-6). Bars represent the mean ± SEM.

Pequeña alegría de laboratorio#4

Recuperar un experimento del año pasado y que tenga la fecha exacta del día actual

DISCUSSION

1 miR-322 in Osteoblast Differentiation

MicroRNAs are important post-transcriptional regulators in all cell types and osteoblast differentiation-related miRNAs have been widely studied looking for specific networks fine-tuning bone development. Adult bone maintenance and remodeling are very dynamic processes that rely on several signaling pathways but also on the tight control of their response. Given the importance of this meticulous regulation, miRNAs are ideal major players of the osteoblastic differentiation path and have become an important topic of research during last years.

This thesis has identified miR-322 as an miRNA down-regulated by BMP-2 and has demonstrated for the first time that miR-322 is involved in osteoblast differentiation. miR-322 is clustered with miR-503, miR-351 and miR-450 and its orthologous miRNA in human is hsa-424. It is located in chromosome X and two different mature miRNAs have been described arising from the miR-322 locus. One is originated from the 5' arm of the precursor sequence, was named miR-322-5p and validated experimentally as homologous to miR-424 from human. The other mature miRNA arises from the 3' arm and is the miR-322. Landgraf et al. confirmed that the 5' arm product is the predominant one and that its mature sequence is CAGCAGCAAUUCAUGUUUUGGA (microRNA.org). Expression of miR-322 is highly enriched in fibroblasts and cells of mesenchymal lineage (microRNA.org).

1.1 miR-322 and BMP Signaling Crosstalk

Our findings add a new role and a novel target for miR-322 during osteoblast differentiation. After BMP-2 addition, miR-322 level progressively decreases in C2C12 and MC3T3-E1 cells and primary cultures of BM-MSCs suggesting that miR-322/miR-351/miR-450/miR-503 cluster is repressed by the addition of the cytokine. Concordantly, miR-503 was also highly down-regulated in our first miRNA screen together with miR-322.

Smad proteins are the signal transducers of the BMP pathway and have been found to regulate miRNA expression both by transcriptional and post-transcriptional mechanisms (Blahna and Hata, 2012). *In vitro* and *in vivo* miRNA expression-profiling studies confirm that R-Smads modulate a set of microRNAs transcriptionally through the presence of Smad binding elements (SBEs) in their promoters. In addition, Smads can also modulate miRNA levels indirectly through activation of transcription factors that associate with their promoters (Blahna and Hata, 2012).

Moreover, Smad proteins have been shown to regulate specific miRNAs by means of their processing and maturation process, through interaction with the Drosha complex (Davis et al., 2008). Smad proteins translocate to the nucleus in respond to ligand stimulation and associate with the large Drosha/DGCR8/p68 microprocessor complex, facilitating the cleavage of pri-miRNA to pre-miRNA by Drosha (Davis et al., 2008). Moreover, Davis et al. later described the so-called R-SBE (RNA Smad binding elements) motifs, consensus sequences (5' CAGAC 3') similar to the Smad binding elements (SBEs) found in the promoter region of Smad target genes. When Smad proteins bind (through MH1 domain) to these R-SBE motifs present in pri-miRNAs, they provide an optimal landing site for DGCR8 and/or Drosha, thereby promoting a more efficient cleavage of specific pri-miRNAs upon TGFβ-BMP stimulation (Davis et al., 2010).

None of the miRNAs corresponding to the miR-322 cluster contain this CAGAC sequence, probably indicating that the regulation concerning miR-322 depends on direct transcriptional repression as has been demonstrated in other miRNAs. For instance, transcriptional repression of miR-29 by Smad-binding to the promoter promotes renal fibrosis (Qin et al., 2011) and TGFβ induces Smad3/4 complex binding to the miR-24 promoter inhibiting its expression in myoblasts (Sun et al., 2009). None of the miR-322 clustered miRNAs have a SBE that could suggest direct binding of Smad proteins to their promoter. However, as it has been exposed previously, Smad proteins can also activate indirectly the transcription of specific genes through their binding to additional transcription factors.

As stated in the introductory chapter, BMP-2 treatment induces the up-regulation of important osteogenic transcription factors. C2C12 cells are murine pre-myoblasts that undergo osteoblasts under BMP-2 treatment (Katagiri et al., 1994). MC3T3-E1 cells are in a more advanced stage in the osteoblastic differentiated process since they were originated from a clone of a primary osteoblast culture. Both cell lines are widely used as osteoblast-like cells in the study of the osteoblast differentiation process and several miRNA studies have been performed using these models (Inose et al., 2009; Li et al., 2008). For instance, Li et al. conducted an miRNA screening during BMP2-induced osteogenesis in C2C12 cells and found that the expression of almost all miRNAs was down-regulated during osteoblast differentiation (Li et al., 2008). These data are consistent with the work of this thesis, where BMP addition progressively down-regulated most of the miRNAs analyzed.

Regarding the C2C12 model, it has been recently reported that under BMP stimuli, C2C12 inhibits the processing of myomiRs (muscle-specific miRNAS and myogenic miRNAs) due to the association of phosphorylated R-SMADs and Co-SMAD with phosphorylated KH-type splicing regulatory protein (KSRP) in the nucleus (Pasero et al., 2012). KSRP is a single-strand RNA-binding protein that is essential for the maturation of myomiRs and for the establishment of the myogenic lineage in C2C12 cells (Briata et al., 2012); thus, KSRP sequestering by SMADs blocks myogenic differentiation in favor of the osteoblast lineage. In our work, miR-322 overexpression was able to block the myogenic capacity of the C2C12 cell line since miR-322 transfection led to a lack of myotube formation. Moreover overexpression of miR-322 increased the levels of important genes as *Osx*, *Runx2* or *Msx2* in C2C12 and MC3T3-E1. Concordantly, osterix and *Runx2* mRNA levels were reduced when miR-322 was inhibited using an anti-sense miRNA. In addition, osterix protein levels were also increased after miR-322 accumulation.

As well as miR-322, many others miRNAs are regulated by BMP treatment. A well-studied miRNA regulated by BMPs is miR-206 (Inose et al., 2009; Sato et al., 2009). The expression of miR-206 is down-regulated by BMPs in C2C12 cells and its overexpression blocks osteoblast differentiation due to its effect on *connexin43* mRNA, required for osteoblastic gene expression and function (Lecanda et al., 1998; Plotkin and Bellido, 2013). These results are in concordance with our work since miR-206 was clearly repressed during BMP treatment in C2C12. Sato *et al.* have also suggested that BMP control of miR-206 occurs post-transcriptionally in C2C12 cells by the repression of pri-miR processing, and other studies have indicated that miR-206 is also required for myogenic differentiation in the same model (Kim et al., 2006; Sato et al., 2009). Moreover, miR-206 transgenic mice expressing miR-206 in osteoblasts (2.3kb *Col1a1* promoter) suffer from reduced bone mass because of a decrease in bone formation

(Inose et al., 2009). TGFβ inhibits both miR-206 expression and myogenic differentiation *in vitro* through an increase in HDAC4 protein expression (Winbanks et al., 2011).

miR-125b inhibits the proliferation of ST2 cells (murine MSCs) and BMP-4 stimulation also attenuates its expression in these cells. Thus, miR-125b inhibits osteoblast differentiation, possibly regulating the early stages of osteoblastogenesis (Mizuno et al., 2008). miR-141/-200a act as *Dlx5* and *Osx* repressors and are also regulated by BMP-2 in the MC3T3-E1 cell line. Under BMP treatment, the expression of both miRNAs is down-regulated, thus avoiding *Dlx5* and *Osx* miRNA-related repression (Itoh et al., 2009).

Thus, BMPs coordinate a wide range of changes in miRNA expression and in turn, miRNAs can negatively or positively regulate BMP signaling (Figure D-1) (Inose et al., 2009). It has been introduced the involvement of the BMP-Smad pathway in the induction of osteoblast related genes. miRNAs can regulate R-Smad expression as is the case of *Smad1*, that has emerged as a target of miR-26a in osteogenic differentiation of human adipose-tissue-derived stem cells (Luzi et al., 2008). These studies indicate that miR-26a restrains osteoblast commitment when reaching terminal differentiation (Luzi et al., 2008). Several miRNAs have been described to target Smad proteins. For instance, miR-133 and miR-135 are negative regulators of osteogenesis that act by directly targeting *Runx2* and *Smad5* respectively, thereby inhibiting osteogenic differentiation (Li et al., 2008). Additionally, miR-30 family members have been widely studied as regulators of osteoblast differentiation, mainly through the suppression of the expression of *Smad1* and *Runx2* transcription factors (Eguchi et al., 2013; Huang et al., 2014; Wu et al., 2012; Zhang et al., 2011c). Actually, our results also provided evidence that miR-30a is involved in BMP-mediated differentiation, as miR-30a was also down-regulated in C2C12 after BMP treatment. miR-199a* also represses the 3'-UTR *Smad1* transcript (Lin et al., 2009).

In order to clarify whether miR-322 expression was affecting directly Smad signaling, the cellular levels of total and phosphorylated SMAD1 were analyzed. No major changes were found, suggesting a lack of interaction between miR-322 and Smad proteins. Additionally, the luciferase activity of *Id1* and *Cox2* reporter constructs did not change after miR-322 or anti-miR-322 overexpression. *Id1* and *Cox2* genes are highly responsive to BMP-2 treatment and therefore the lack of variations in the luciferase activity after miR-322 and anti-miR-322 transfection implies that miR-322 has no major effects over BMP signaling (Lopez-Rovira et al., 2002; Susperregui et al., 2011).

miRNAs regulate mRNA expression by direct interaction with the 3'-UTR of specific mRNAs, therefore constituting an important post-transcriptional regulation

mechanism. As seen above, miRNAs can affect BMP signaling by targeting R-Smad proteins but they can also target I-Smads. miR-21 inhibits translation of SMAD7 therefore decreasing protein levels without changes in mRNA expression (Li et al., 2015). SMAD7 belongs to the inhibitory Smads (I-Smads) family which is the main inhibitory mechanism of the cooperative signaling of R-Smad and Co-Smad proteins (Ross and Hill, 2008).

BMP receptors are also targeted by miRNAs. For instance, the expression of miR-210 is up-regulated during BMP-4-induced osteoblast differentiation of mouse mesenchymal ST2 cells. miR-210 positively regulates osteoblast commitment by targeting the *Acvr1b* receptor (type 1 receptor) (Mizuno et al., 2009) and the BMPR2 is also suggested to be targeted by miR-31 (Gao et al., 2011). The 3′-UTR of the *acvr1/alk2* gene has recently been studied *in vitro* to elucidate miRNAs that when expressed induce BMP signaling alterations in fibrodysplasia ossificans progressiva (FOP) (Mura et al., 2012). FOP patients present higher sensitivity to BMP signaling and their life expectancy is not very high. Thus the discovery of miRNAs involved in the post-transcriptional control of this receptor could give hope to new therapies.

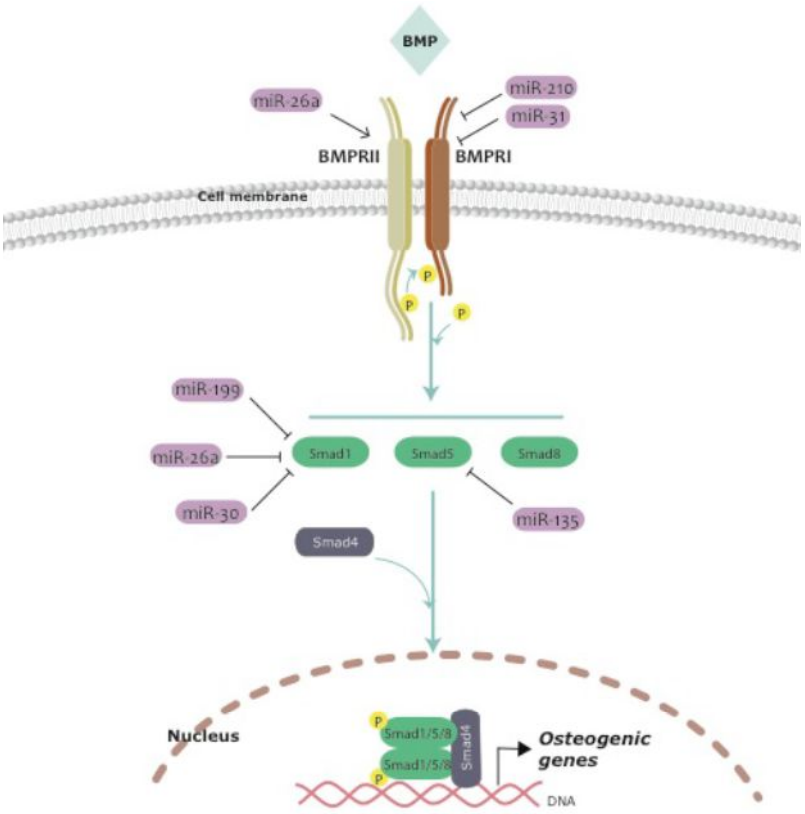

Figure D-1. Interplay between the BMP pathway and miRNAs. miRNAs act at different steps of BMP signaling: from those involving BMP receptors to those involving SMADs. miR-30, miR-26a and miR-199 suppress *Smad1* levels and miR-135 affects *Smad5* expression. Other miRNAs affect the BMP receptor, as is the case of miR-26a, miR-210 and miR-31. All these miRNAs are somehow affecting BMP signaling and therefore they are exerting regulatory functions over osteogenic genes.

Several other pathways besides BMP are involved in osteoblast differentiation (Wnt, Notch, IGFs, hedgehogs, etc.), and these are also post-transcriptionally regulated by miRNAs. It is clear nowadays that not only can the expression of a single miRNA fluctuate during cell fate commitment but also a specific miRNA can target different mRNAs depending on the cellular stage. Moreover, a single miRNA can affect several signaling pathways simultaneously, allowing a cooperative effect or the fine-tuned expression of specific mRNAs. Determining how miRNAs regulate and are regulated by different pathways and how they interact to orchestrate a singular scenario for each differentiation step remains a tremendous challenge. In addition, bone-specific *in vivo* approaches have occasionally yielded controversial results compared with *in vitro* information, probably due to the influence of the cell environment and alterations in osteoblast–osteoclast communication.

1.2 Tob2 is a Target of miR-322

miR-322 has been previously studied together with miR-503 in myogenesis as promoters of cell cycle quiescence and differentiation by down-regulation of Cdc25A (Sarkar et al., 2010). Recently, miR-322 has been also described to repress TRAF3 (TNF receptor-associated factor 3) promoting cell survival in neural stem cells (Gu et al., 2015).

In silico prediction of possible targets for miR-322 included *Tob2*, *Smad7* and *Smurf1*. They were selected for their importance in osteoblast differentiation and therefore further studies with miRNA mimics were performed.

Additional experiments revealed that *Smurf1* mRNA was not affected by miR-322 overexpression. However this data is not sufficient for dismiss *Smurf1* as a miR-322 target since protein levels should be checked in order to completely discard it. Actually, miR-322 and mir-503 have been described recently as regulators of Smurf2 expression using an intestinal cell line. Their binding to *Smurf2* 3'-UTR repress its translation although there are no changes in *Smurf2* mRNA levels (Cao et al., 2014). Thus, it is probable that miR-322 effect on *Smurf1* expression in our model also arise from translational repression and not from mRNA degradation.

We found *Smad7* also as a putative target of miR-322 in C2C12 cells and BM-MSCs. SMAD7 belongs to the inhibitory Smads (I-Smads) family, which is the main inhibitory mechanism of the cooperative signaling of R-Smad and Co-Smad proteins (Ross and Hill, 2008). However, as stated in the previous section, no major changes were found in the quantification of SMAD and phosphorylated SMAD levels and therefore this target was not chosen for further studies.

When assessing *Tob2* mRNA, it was significantly reduced in basal state but also after BMP treatment when miR-322 was ectopically overexpressed. Loss-of-function experiments also demonstrated higher *Tob2* when miR-322 levels were reduced. These results placed *Tob2* as a target of miR-322 and this work further confirmed it by using Renilla luciferase assays. Wild type and a mutant form of *Tob2* 3'-UTR were used to confirm *Tob2* as a target of miR-322. Wild type *Tob2* construct was significantly repressed after miR-322 co-transfection while mutant construct was refractory to the repression by miR-322. Thus, we have demonstrated direct evidence of the binding site of miR-322 in the *Tob2* 3'-UTR.

TOB1 and TOB2 proteins constitute a Tob subfamily and belong to the BTG/Tob antiproliferative factor protein family (Mauxion et al., 2009; Winkler, 2010). Tob proteins have a highly conserved N-terminal region that in vertebrates is 117 amino acid-long and includes box A and box B domains, the most conserved domains in all

BTG/Tob family proteins. The N-terminal region and specially the box B domain, plays an important role in forming protein complexes with target proteins and for exerting biological effects (Figure D-2) (Jia and Meng, 2007). In addition to their roles in cell proliferation, BTG/Tob proteins have been also implicated in embryonic development, cellular differentiation, cancer suppression and apoptosis.

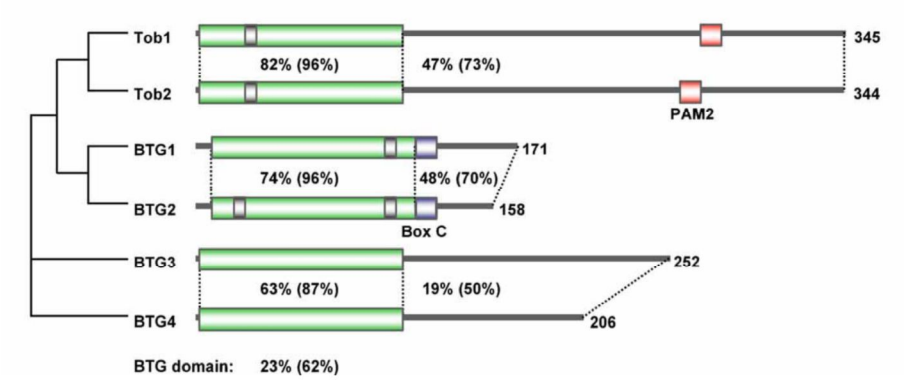

Figure D-2. Overview of the human BTG/Tob protein family. The schematic representations of the BTG/Tob members highlights the conserved BTG domain (green) and the conserved PAM2 (red) and Box C (purple) motifs in Tob1/Tob2 and BTG1/BTG2, respectively. Also indicated are the sizes of the proteins (amino acids) and the percentage identical (similar) amino acids in the BTG domain and the C-terminal regions, respectively. Adapted from (Winkler, 2010).

Tob genes have emerged as key players in mediating post-transcriptional gene expression by regulating mRNA deadenylation and therefore cytoplasmic mRNA levels (Ezzeddine et al., 2012). It is suggested that Tob proteins act through two different mechanisms: while TOBs are able to promote non-specific size reduction of the poly(A) tails in the general mRNA population, they can also specifically accelerate both deadenylation and decay of particular transcripts. For this specific effect of TOB proteins, interactions with sequence-specific RNA-binding proteins are needed (Ezzeddine et al., 2007; Ezzeddine et al., 2012).

Deadenylation is mediated by two major cytoplasmic deadenylase complexes, PAN2-PAN3 (poly (A) nucleases) and CCR4-CAF1. It has been proposed that after translational termination, the termination complex eRF1-eRF3 is released from a poly(A)-binding protein, PABC1, and in turn the two mRNA deadenylase complexes bind to PABPC1 to degrade the poly(A) tail in order to initiate mRNA decay (Funakoshi et al., 2007).

Tob proteins interact with PABP by the two PAM2 motifs present in the TOB long C-terminal region and therefore, those are needed to promote deadenylation (Ezzeddine et al., 2007). Moreover, Tob proteins promote mRNA deadenylation and decay by recruiting CAF1 poly(A) nuclease to the 3' poly(A) tail-PABP complex which is required

for Tob-mediated deadenylation and decay. Thus, a model in which Tob proteins form a complex with CCR4-CAF1 deadenylases is proposed. In fact, the conserved BTG domain of Tob proteins mediate the interactions with the CAF1a and CAF1b (CNOT7 and CNOT8 in mammals) catalytic subunits of the CCR4-CAF1 (CCR4-NOT) deadenylase complex and does not appear to require other CCR4-CAF1 components (Doidge et al., 2012; Hosoda et al., 2011). Horiuchi et al. described the crystal structure of the TOB-CNOT7 complex, demonstrating the mode of interaction between the two proteins and proposing CNOT (Caf1) as the bridge between TOB and the CCR4-NOT complex (Horiuchi et al., 2009).

In opposition to deadenylation, cytoplasmic polyadenylation is involved in some aspects of translational activation in which cytoplasmic polyadenylation element-binding protein (CPEB) binds to a cis-acting element (CPE, cytoplasmic polyadenylation element) in the 3'-UTR of the target mRNA and constitutes a binding platform for a poly(A) polymerase. However, in vertebrates there is also additional CPEB-like sequence-specific RNA-binding proteins (CPEB2-CPEB4) that do not bind the usual CPEs (UUUUUAU) but recognize a RNA secondary structure with U-rich loops, interacting with single-stranded uredines as well as double-stranded stems present in the 3'-UTR of the target mRNA (Hosoda et al., 2011; Huang et al., 2006). These CPEB-like proteins seem to regulate translation in a polyadenylation-independent manner (Figure D-3). For instance, Hosoda et al. described how Tob proteins binds to the sequence-specific RNA protein CPEB3 and mediates the interaction between CPEB3 and CAF1 deadenylase (Hosoda et al., 2011).

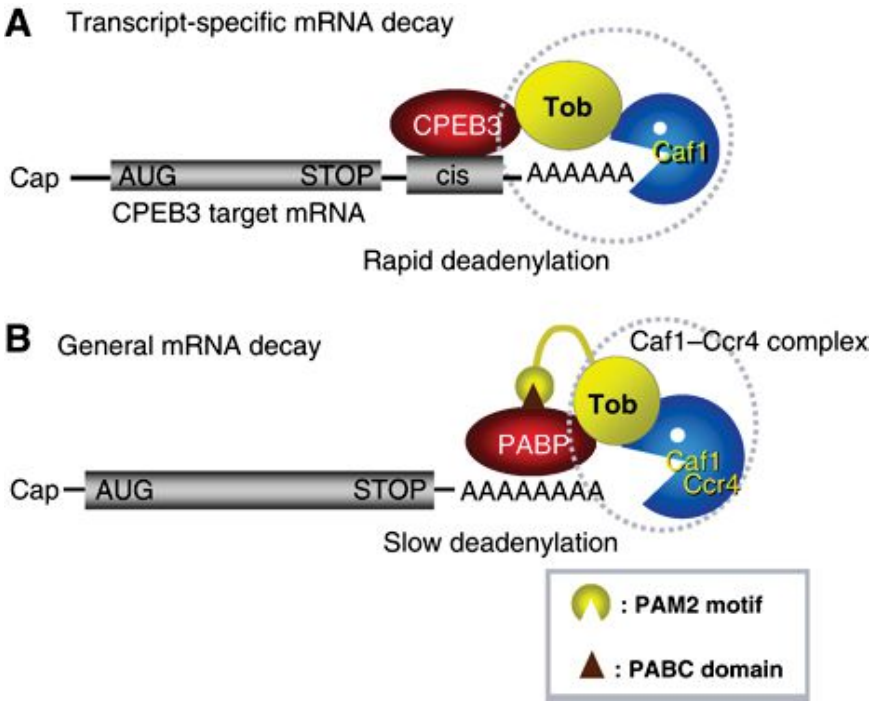

Figure D-3. Schematic representation of mRNA decay mechanisms. (A) Transcript-specific mRNA decay. TOB directly binds CPEB2-4 proteins and CAF1. **(B)** General mRNA decay. TOB is needed for the interaction with PABP (through PAM2 motifs) and CAF1. Adapted from (Hosoda et al., 2011).

Furthermore, a previous study showed that CPEB3 binds to the 3'-UTR of AMPA receptor (*GluR2*) mRNA and negatively regulates its expression, becoming the only known target of CPEB3 at present (Huang et al., 2006). Moreover, in the same study a minimal sequence for CPEB binding was proposed (Figure D-4). Thus, TOB mediates CPEB3-accelerated mRNA deadenylation by recruiting CAF1 to CPEB3's target (Hosoda et al., 2011). Therefore, there is a dual role for Tob proteins in general and specific mRNA decay mechanisms but it has been suggested that the transcript-specific regulation by Tob via interaction with CPEBs is dominant over the general regulation via PABPC (Hosoda et al., 2011).

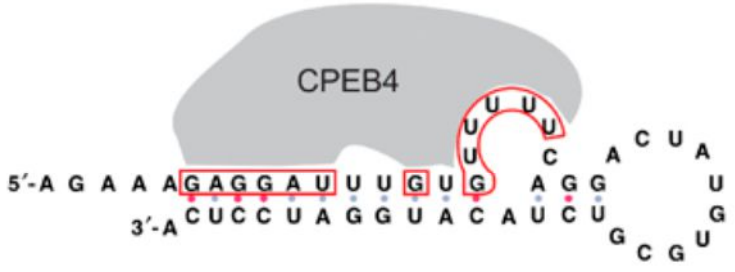

Figure D-4. Predicted RNA secondary structure and nucleotides bound by CPEB4. Minimal RNA sequence required for CPEB4-RBD binding based on RNA footprint assays. Adapted from (Huang et al., 2006).

In our work, we tested the ability of TOB2 to regulate the mRNA degradation of specific genes by mRNA decay assays in C2C12 and MC3T3. The use of Actinomycin D (inhibitor of mRNA synthesis) allows us to prove that overexpression of TOB2 reduced the half-life of osterix transcripts whereas overexpression of miR-322 (and therefore a reduction of *Tob2*) increased levels of *Osx* mRNA. These results suggested that TOB2 is specifically promoting mRNA deadenylation and decay of *Osterix* transcript. Moreover, analysis of the osterix 3'-UTR revealed secondary structures with a stem-loop structure similar to those bound by CPEB2-4 (Huang et al., 2006). RNA pull-down assays showed that these *Osx* sequences are directly bound by CPEB4 and TOB2. Thus, we hypothesize that *Osx* mRNA can be bound by TOB2 and CPEB2-4 and as a consequence, specifically degraded.

Moreover, *in silico* analysis showed that CPEB2-4 are also putative targets of miR-322 and miR-503, whereas they do not target CPEB1 (CPEB protein involved in cytoplasmic polyadenylation). This suggests that in addition to *Tob2*, miR-322 could also target CPEB genes to coordinately regulate *Osx* expression. However, future work is necessary to discern which CPEB-like proteins are involved in the interaction between TOB2 and stem-loop structures in the 3'-UTR of *Osx* and other osteogenic genes.

CPEB3 and 4 are more than 95% identical in their RNA binding domain (RBD) and TOB binds to this highly conserved RBD. Thus, Tob proteins could regulate the targets of CEPB3 and CPEB4 (Hosoda et al., 2011). All CPEB-like proteins have similar structure in which most of the carboxy-terminal region is composed of two RNA recognition motifs (RRMs) and two zinc fingers. Those domains are needed for CPEB-like proteins to bind to RNA.

Our data are in agreement with previous studies showing that, although *Tob1* knock-out mice are born without apparent phenotypic abnormalities, *Tob1*-deficient adult mice have higher bone mass compared with wild-type mice (Yoshida et al., 2000). Our data also can explain why *Tob* deficiency enhances osteoblast activity blocking osteoporosis induced by ovariectomy (Usui et al., 2004). Furthermore, mice deficient in *Cnot7* (*Caf1*), the Tob-interacting deadenylase, also exhibit a high bone mass phenotype and increased responses to BMPs (Washio-Oikawa et al., 2007).

mRNA decay has been shown to be highly relevant in a number of physiological processes (Schoenberg and Maquat, 2012). However, there are few examples of this post-transcriptional regulatory mechanism in bone development. For instance, polymorphisms in the 3'-UTR of vitamin D receptor (*VDR*) lead to differential mRNA decay and increased risk of osteoporosis (Fang et al., 2005). In addition, it has been shown that AU-rich elements mediate stabilization of *collagenase-3* mRNA in osteoblasts (Rydziel et al., 2004). Thus, our results propose that new target genes

displaying compatible TOB-interacting secondary structures at their 3'-UTR could be subjected to specific mRNA repression by Tob family members as we suggest in our work for osterix. More importantly, our findings strongly suggest that control of specific mRNA decay is relevant in bone development and homeostasis.

In summary, we have demonstrated that down-regulation of miR-322 in response to BMP-2 acts as a negative regulator of osterix expression. We also identified Tob2 accumulation as an important step in fine-tuning the expression of osterix and other osteogenic transcription factors during osteoblast differentiation. Then, miR-322, by means of *Tob2* down-regulation, adjusts the expression levels of some of osteoblast-specific genes, particularly *Osx* (Figure D-5).

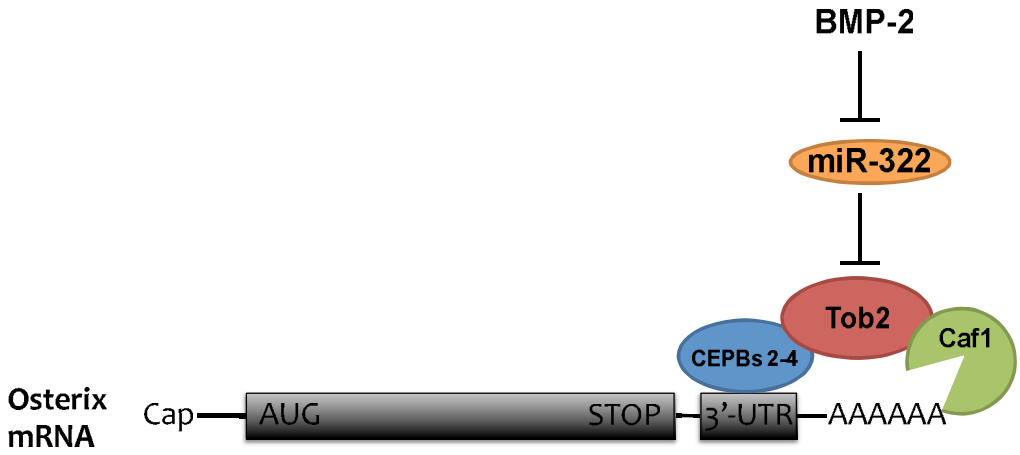

Figure D-5. Schematic representation of miR-322/Tob2 network. BMP-2 down-regulates miR-322 expression. miR-322 binds to the 3'-UTR of *Tob2* mRNA and drives its degradation. TOB2 is forming a complex with CEPB-like proteins and CAF1 (CNOT7) deadenylase, targeting specific mRNAs for further deadenylation and decay. Adapted from (Hosoda et al., 2011).

TOB2 can also be regulated post-transcriptionally by other mechanisms such as phosphorylation. ERK and JNK MAPK can phosphorylate TOB2 negatively regulating its antiproliferative activity (Jia and Meng, 2007). However, the ability of Tob proteins to promote mRNA deadenylation and decay is independent of the phosphorylation status of these residues.

Moreover, Tob proteins have been shown to associate with the MH2 domains of Smad proteins and to repress Smad transcriptional complexes (Yoshida et al., 2000). These two mechanisms may contribute, in an additive way, to a lower BMP response although we did not find any alteration in SMAD protein levels or in *Id1/Cox2* promoter activity after miR-322 overexpression. Nevertheless, analysis of the quantitative role of

miR-322-mediated *Smad7* and *Tob2* repression in the induction of *Osx* transcripts by miR-322 also awaits further study.

Functional redundancy has been stated for TOB1 and TOB2. Both genes are paralogs of one another and studies have made several observations indicating functional similarity for TOB1 and TOB2 proteins. Actually, both proteins bind simultaneously to PABP and CAF1 (Ezzeddine et al., 2007), promote mRNA deadenylation and decay via a PABP-dependent mechanism (Ezzeddine et al., 2007) and suppress cell growth via a pathway connected with their deadenylation-enhancing function (Ezzeddine et al., 2012). All these data support redundant functions for both proteins. However there are also reports of specific functions for both proteins and therefore probably distinctive roles remain to be discovered.

1.3 miRNAs and Osteoblast Differentiation

miRNAs are important regulators of osteoblast differentiation and they can exert their function in each step of the differentiation process (Figure D-6). As in the case of miR-322, other miRNAs are post-transcriptionally regulating *Osx* mRNA. Shi et al. described miR-214 as a down-regulated miRNA during BMP2-induced osteoblast differentiation in C2C12 cells. miR-214 antagomir leads to overexpression of *Osx* and other related osteoblast markers such as *Alpl, Col1a1* and *Bglap* (Shi et al., 2013). In addition, it has also been reported that miR-214 inhibits *Twist* (which in turns inhibits the activity of Runx2 as transcription factor) in intra-hepatic cholangiocarcinoma and moreover, is over-expressed in elderly patients with fractures, where it directly targets *ATF4* (Li et al., 2012; Wang et al., 2013).

In vivo studies comparing differentially expressed miRNAs between calvaria from E18.5 *Osx*-deficient or wild type embryos revealed that *Osx*-deficient osteoblasts displayed miR-204/211 overexpression. As it is known that Osx-deficient calvariae present increased Runx2 expression (Zhou et al., 2010), Chen et al. have suggested that miR-204/211 accumulation would dampen Runx2 overexpression and that Osx coordinately regulates the levels of this miRNA to maintain correct *Runx2* expression (Chen et al., 2013).

A regulatory loop for *Osx* expression involves miR-93 in primary osteoblasts. During osteoblast mineralization, osterix can bind to the miR-93 promoter to repress its transcription and, since miR-93 also targets *Osx* mRNA, this facilitates maintenance of osterix levels (Yang et al., 2012). Shi et al. also reported down-regulation of miR-93 during differentiation of C2C12 under BMP stimulation (Shi et al., 2013). These mechanisms are as in the case of miR-322, fine-tuning *Osx* expression.

Changes in miR-637 levels have the capacity to maintain the balance between osteoblast and adipocyte differentiation in hMSCs (human MSCs) by inhibition of *Osx* and activation of adipogenic markers such as *PPARγ* (peroxisome proliferator-activated receptor-γ) and *c/EBPα* (CCAAT/enhancer-binding protein-α) (Zhang et al., 2011b). Other miRNAs have also been shown to determine osteoblast-adipocyte balance in vitro (Li et al., 2013; Liao et al., 2013; Wang et al., 2013). For instance, miR-3077-5p and miR-705, which work together as negative regulators of osteoblast differentiation through *Runx2* and *Hoxa10* suppression, eventually lead to a positive regulation of adipogenic differentiation (Liao et al., 2013).

It has been reported that miR-31 can directly regulate *Osx* 3'UTR. An increase in *Osx* mRNA expression due to low expression of miR-31 can play a role in osteosarcoma, as seen in the MG-63 osteosarcoma cell line (Baglio et al., 2013).

Dlx5 is a BMP-responsive gene that is activated through a responsive element in its proximal promoter. Moreover, DLX5 interacts with the *Osx* promoter and mediates BMP2-induced *Osx* expression independently of Runx2 (Lee et al., 2003; Ulsamer et al., 2008). Thus, miRNAS affecting osterix modulators will also affect OSX levels. For instance, miR-141 and 200a have been found to act as *Dlx5* and *Osx* repressors, and it has been demonstrated that both bind to *Dlx5* mRNA *in vitro* (Itoh et al., 2009). Moreover, miR-141 and 200a target *p38α* in mouse models of ovarian cancer, in agreement with previous screenings in human ovarian adenocarcinomas (Mateescu et al., 2011). Positive effects of p38 phosphorylation have been observed in DLX5 transcriptional activity and in *Osx* stability (Ortuno et al., 2010; Ulsamer et al., 2008); consequently, miR-141 and 200a activity in osteoblast lineages is also probably mediated by changes in p38 phosphorylation of DLX5 and OSX.

Since *Osx* and *Runx2* expressions are tightly related, miRNAs targeting proteins involved in their upstream regulatory pathways will affect the expression of both genes. This is the case of miR-138, inhibited during human MSC osteoblast differentiation, which targets FAK (focal adhesion kinase) and ERK1/ERK2 (extracellular signal-related kinase) pathways, leading to decreased phosphorylation of RUNX2 and a lower expression of OSX (Eskildsen et al., 2011). Other studies have elucidated additional mechanisms connecting miRNAs to osteoblast differentiation by means of targeting different osteoblast differentiation pathways (Inose et al., 2009; Kapinas et al., 2010; Li et al., 2009b; Mizuno et al., 2008; Wang and Xu, 2010; Zhang et al., 2012).

Obviously, specific miRNAs are also regulating *Runx2* mRNA expression. *Runx2* mRNA has a very long 3'-UTR, which probably contains multiple regulatory elements (Huang et al., 2010). It is therefore not surprising that several examples of post-transcriptional *Runx2* mRNA regulation through miRNAs have been described.

miR-204/-211 specifically binds to the 3'-UTR of *Runx2* and inhibits osteoblast differentiation by promoting adipocyte commitment from mesenchymal progenitors (C3H10T1/2, ST2, and hMSCs) (Huang et al., 2010). Furthermore, as RUNX2 has the capacity to regulate the expression of *Bglap* from day E15.5 onwards (Ducy and Karsenty, 1995), miR-204 accumulation leads to the repression of *Bglap* expression (Huang et al., 2010)

miR-133 also inhibits *Runx2* translation, and its expression is down-regulated by BMPs in C2C12 cells (Li et al., 2008). Studies carried out by independent groups have reported controversial results on the function of miR-31 during osteoblast commitment of human MSCs. As explained previously, it has been reported that miR-31 can directly regulate *Osx* mRNA but it is also involved in *Runx2* post-transcriptional regulation. Gao et al. have described miR-31 to be a down-regulated miRNA during osteoblast differentiation *in vitro*, indicating that Runx2 is one of its physiological targets (Gao et al., 2011). However, miR-31 was later identified as an up-regulated miRNA in a similar study of hMSC differentiation and osterix was confirmed to be one of its targets, indicating a regulatory network (Baglio et al., 2013). Other *in vitro* studies have elucidated a regulatory loop involving miR-31, *Runx2*, and *Satb2*: down-regulation of miR-31 expression by RUNX2 in differentiating BM-MSCs facilitates osteogenic commitment due to an increase in SATB2 protein expression (Deng et al., 2013).

As presented in the introduction chapter, SATB2 can bind to AT-rich sequences, activating the transcription of particular genes (Britanova et al., 2005). SATB2 physically interacts with and enhances the activity of RUNX2 and ATF4 and moreover increases OC transcription by binding to its promoter (Conner and Hornick, 2013; Dobreva et al., 2006). In addition it has been reported that SATB2 acts in cooperation with RUNX2 to up-regulate *Osx* expression (Zhang et al., 2011a). Therefore any miRNA regulating SATB2 expression will indirectly control RUNX2 activity and in turn osteoblast differentiation. For instance, the miR-23a~27a~24-2 cluster inhibits osteogenesis *in vitro* by down-regulation of *Satb2* through direct binding of the three miRNAs to its 3'UTR region. Moreover, RUNX2 directly suppresses expression of the cluster whereas complementarily miR-23a targets *Runx2* (Hassan et al., 2010).

Interestingly, other clusters have also been studied, such as the auto-regulatory feedback loops controlling *Runx2* expression. miR-3960/miR-2861 is transactivated by RUNX2 *in vitro*, thereby maintaining its own levels of expression by blocking *Hoxa* and *Hdac5*, negative regulators of osteoblast differentiation (Dobreva et al., 2006; Hu et al., 2011; Kanzler et al., 1998; Li et al., 2009a). Furthermore, an *in vivo* approach has demonstrated that *Satb2* is also targeted by miR-34s, affecting osteoblast proliferation (Wei et al., 2012).

Several miRNAs are being described periodically, targeting mRNAs of other genes besides *Runx2* and *Osx* that are involved in osteoblast differentiation. For example, recent studies on *Bglap2*-miR-214 transgenic mice overexpressing miR-214 have revealed its inhibitory role in regulating bone formation. *In vitro* manipulation of miR-214 revealed that direct targeting of *Atf4* was required in order to inhibit osteoblast activity (Wang et al., 2013).

As seen above, it should be noted that one particular miRNA may act as a switch for selection of different cell commitment processes. miR-96, miR-124 and miR-199a have been studied in human BM-MSCs and have been found to be differentially expressed during osteogenic, adipogenic or chondrogenic induction: whereas miR-124 is expressed exclusively in adipocytes, miR-199a is up-regulated in osteoblasts and chondrocytes (Laine et al., 2012).

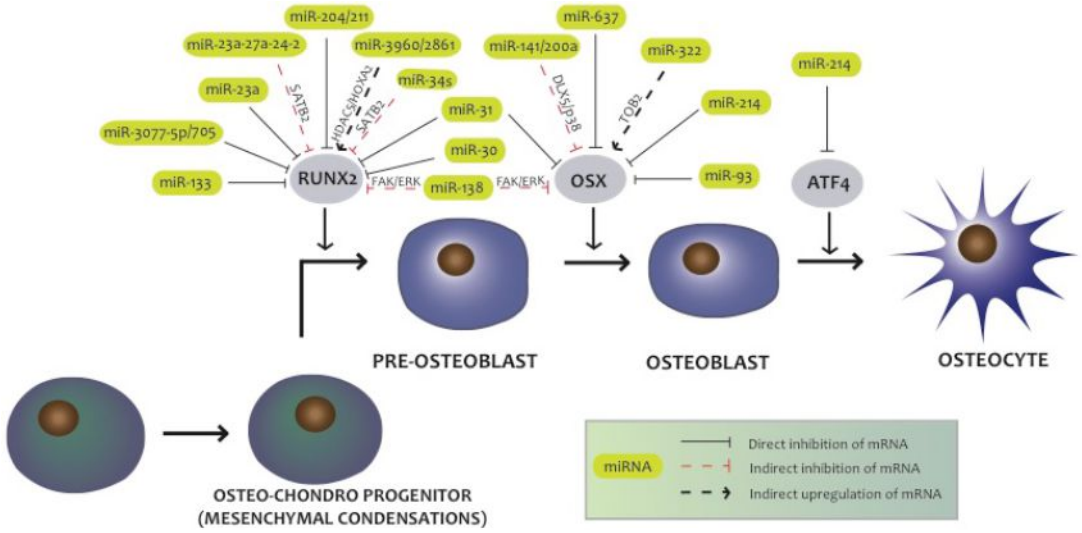

Figure D-6. Schematic summary of miRNA roles in osteoblast differentiation. A cohort of transcription factors tightly regulates osteoblast commitment from osteo-chondroprogenitors during skeletal development. miRNAs are important players during this commitment regulating the expression of these transcription factors, therefore allowing or blocking the differentiation process.

As concluding remarks, the current identification of a vast number of skeletal-cell-specific miRNAs, each of them with a list of putative targets, has yielded the present challenge of understanding their biological functions. From the data obtained to date, we know that most miRNAs exert their functional effects via multiple target mRNAs, usually by cooperatively targeting genes in the same pathway. Similarly, there is also redundancy, as the same mRNA is targeted by different miRNAs. The very sensitive nature of developmental programs and signaling pathways renders them the perfect candidates for techniques utilizing the dose-dependent effects of miRNAs. In bone physiology, miRNAs are extremely useful nodes, acting as feedback or feed-forward

devices that allow buffering effects that confer robustness to skeletal development programs. miRNAs serve as finely tuned precision regulators of the expression of those genes that confer cellular identity and promote differentiation. Moreover, individual miRNAs may even operate as switches to induce differential cell fates. These properties clearly support the notion that the mutation or dysregulation of miRNAs would profoundly affect expression patterns and contribute to skeletal pathologies. Fortunately, these properties also open up opportunities for designing smart therapies based on miRNAs and small RNAs. miRNAs, which are easy to deliver into cells, are intrinsically highly specific and could regulate several targets at the same time. Thus, it is highly feasible that miRNAs, as well as antago-miRNAs, may be used in the future as drugs to treat skeletal pathologies.

2 ROLE OF PI3K IN BONE BIOLOGY

Our results provide a description of the osteoblast-specific *p110α* and *p110β* mutant mice phenotypes as well as the double knock out where impaired osteogenesis arises from the result of a crosstalk between IGF1, BMP and Wnt signaling pathways.

2.1 Previous Genetic Models for the Study of PI3K Signaling

Genetic and pharmacological studies have documented the relevance of PI3K/AKT signaling in skeletal development. *Pten* deletion and therefore overstimulation of PI3K pathway has been a useful approach for the elucidation of PTEN and PI3K function in bone biology. Liu et al. used a Cre recombinase system under the control of the OC promoter to study the lack of *Pten* in mice. Specific osteoblast deletion of the negative regulator of the PI3K pathway revealed increased bone mass due to higher osteoblast number and higher levels of key osteoblastic genes as *Runx2*, *Alpl*, *Col1a1* or *Osteocalcin* (Liu et al., 2007b). Later, Guntur et al. described the phenotype related to the lack of *Pten* in osteoprogenitors using *Dermo1-Cre* to specifically delete *Pten* already in mesenchymal condensations (Guntur et al., 2011). Again, mineralization and therefore bone mineral density was increased. The main feature of these mice is the increase of *Fgf18* expression together with enhanced FGF signaling. Moreover the expression of *Spry2* (sprouty homolog 2), a gene involved in the uncoupling between FGF receptor and Ras-Raf signaling was decreased thus contributing to enhance FGF signaling. Noticeably, markers as *Osterix* or *Osteocalcin* were up-regulated. Osteo-chondroprogenitors lacking *Pten* were also assessed using the type II collagen gene

promoter (*Col2a1-Cre*) showing increased skeletal size and higher trabecular and cortical bone (Ford-Hutchinson et al., 2007).

Class I PI3K signaling exerts its effects mainly by means of the key effector AKT. Effects of PI3K in cell growth and proliferation have been also exposed thanks to *Akt* mutant mice and actually, global *Akt* deletions have been also a key for the understanding of PI3K function in bone formation and osteoblast differentiation. In 2003, the double mutant mice lacking AKT1 and AKT2 were generated. These mice presented no tissue specificity in AKT deficiency and actually, they died shortly after birth. The phenotype was characterized as dwarfism since total body weight was dramatically reduced and was accompanied with muscular atrophy and impaired skin development (Peng et al., 2003). Some years later, specific-*Akt1* mutant mice were described. *Akt1*-null mice presented reduced cortical and trabecular bone as well as reduced mineral apposition rate and bone formation rate. *In vitro* studies on isolated osteoblasts revealed that AKT1-FOXO3a-BIM axis was the responsible for BIM up-regulation and enhanced apoptosis in osteoblasts lacking *Akt1* (Kawamura et al., 2007). Controversially, higher osteoblast differentiation (by means of Runx2 overexpression) was described through *in vitro* approaches using murine mesenchymal cell lines (C3H10T1/2) lacking *Akt1* (Mukherjee and Rotwein, 2012). Probably this disagreement arises from the differentiation stage of the *in vitro* model used. AKT1 and AKT2 are ubiquitously expressed and are the main protein isoforms in bone. However, as stated above, *Akt1* deficiency has been related to dwarfism while *Akt2* null mice present mostly a diabetic phenotype (Garofalo et al., 2003). AKT3 is found in lower rates in several cell types but is highly expressed in testis and brain. Actually, *Akt3* deletion in mice produces impaired brain development (McGonnell et al., 2012).

It is important to emphasize that deficiency of PI3K leads to distinct biological outputs among different tissues. PTEN and AKT signaling have been studied in numerous cell types since the biological response to the activation of PI3K/AKT pathway appears to manifest in a tissue-specific fashion. For example, *Pten* loss in the liver resulted in increased organ size while disruption of *Pten* in adipocytes and muscle increases sensibility to insulin, but did not alter the number of cells or the overall size of these organs (Liu et al., 2007b).

AKT and PTEN pathways have been used as a tool for the study of the extracellular signaling involved in osteoblast differentiation. Among these important cascades there is the fibroblast growth factor (FGF), the insulin-like growth factor (IGF1) and the insulin signaling. In fact, global *Akt1/2* mutant mice were considered to have a comparable phenotype to that acquired by the lack IGF1 receptor (IGF1R) (Liu et al., 1993; Peng et al., 2003). Insulin, IGF1 and FGF signaling work basically by

tyrosine/kinase receptors and therefore they all induce mainly the activation of PI3K and MAPK.

The liver produces the majority of the IGF1, although osteoblasts are also able to produce it. It is the most abundant growth factor found in bone matrix and has paracrine and autocrine effects that ultimately regulate osteoblast differentiation. Recent genetic studies through IGF1 receptor deletions were performed using *Osteocalcin* and *Osterix* promoters as inducers of *Cre* expression. *Osteocalcin*-driven deletion of IGF1R led to decreased trabecular and cortical bone parameters due to mineralization impairment (Zhang et al., 2002) while the genetic model using *Osterix-Cre* system described a decreased bone mass phenotype mainly because the decrease in mTOR activity lead to reduced IGF1 and IGFBP3 (IGF binding protein 3) present in the bone matrix (Xian et al., 2012).

Insulin, like IGF1, has been shown to be anabolic in bone. Insulin effects in osteoblasts have been extensively studied and again, osteoblast-specific mutant models have been used. Insulin receptor is abundant in osteoblast cells but not in osteocytes. Fulzele et al. described that insulin inhibits TWIST2 (a RUNX2 inhibitor) allowing higher RUNX2 activity. In this model, OC overexpression (by means of RUNX2 increased transcriptional activity) increases its endocrine effects inducing the expression of adiponectin in fat cells (and therefore enhancing the sensibility to insulin) and the stimulation of β cells in the pancreas. This network provides a positive insulin feedback where osteoblast function is crucial (Fulzele et al., 2010).

In addition to genetic models, experiments using pan-specific and isoform-specific PI3K inhibitors in skeletal tissues have suggested that PI3K signaling is essential for osteoblast function and bone development (Gamell et al., 2008; Grey et al., 2010; Guntur and Rosen, 2011; McGonnell et al., 2012; Vanhaesebroeck et al., 2010b).

2.2 Class I PI3K is Crucial for Bone Development and Homeostasis

As seen in the introduction chapter, global *p110α* and *p110β* deletion in mice has been carried out with the resulting embryonic lethality (Bi et al., 2002; Bi et al., 1999a). However, despite all these previous data, there was no information on the specific role of distinct class IA PI3K isoforms in bone biology before this thesis. In our project, we generated mice with isoform-specific conditional deletions of *p110α* and/or *p110β* in osteoblasts and we have revealed that PI3Kα and β isoforms are major regulators of osteoblast differentiation and survival. Deletion of either *p110α* and/or *p110β* impairs

osteoblast differentiation by decreasing the expression of key osteoblast-determining transcription factors and their transcriptional targets.

p110α and *p110β in vivo* deletion has been carried out by the use of the Cre recombinase system. Collagen type I promoter drove the expression of the recombinase and therefore the deletion was produced specifically in osteoblasts. *Col1a1-Cre* mice allowed the deletion of *p110α* during early bone development (from E14.5 (Dacquin et al., 2002)) and caused an osteopenic phenotype in bones of both endochondral and intramembranous origin. Mice lacking *p110α* in osteoblasts presented reduced bone mineral density as seen for µCT analysis and histological sections. However, total body weight was not altered at any time during animal growth.

Some functional redundancy among p110 isoforms exists in numerous cellular processes. However, this redundancy is not universally observed and appears to be dependent on the cell type and stimulus (Vanhaesebroeck et al., 2010a). Prior to this report, the relative contributions of p110α and p110β in bone development were completely unknown. We show that deletion of either *p110α* or *p110β* promotes an osteopenic phenotype and decrease downstream AKT targets, suggesting that both isoforms are required for bone formation and that functional redundancy exists. However, some differential contributions in osteoblasts were also observed.

Unexpectedly, bone-specific *p110β* mutant mice also presented an important osteopenic phenotype. Although levels of *p110β* mRNA are reduced when compared to those of *p110α*, the lack of *p110β* in osteoblasts also impairs bone formation. Since that moment, literature was suggesting that *p110α* could be the important isoform involved in bone biology (Grey et al., 2010; Smith et al., 2013), but this work underpins the crucial role of p110β in the achievement of an appropriate bone development and homeostasis.

p110α is critical for early bone formation and development. Moreover, our results further demonstrate that this requirement is also maintained for postnatal bone homeostasis. In order to confirm this statement we took advantage of an inducible *Cre* system (*Osx1a1-Cre*), which allows the deletion of *p110α* at 1-2 days of age. Thus, the *Osx1a1-Cre* system permitted us to specifically delete p110α isoform just after birth. In this model where the deletion occurs when bone architecture is already established, BMD and cortical thickness in adult mice were approximately 40-50% of those observed in control siblings. Postnatal *p110α* deletion led to significant loss of either calvarial, cortical or trabecular bone at 12 weeks of age therefore indicating alteration of endochondral and intramembranous ossification. It was previously described that expression of *Osx1a1-Cre* allele is sufficient for the manifestation of a skeletal phenotype and body weight reduction that arise from the recombinase expression

itself (Davey et al., 2012). For this reason we included both floxed (*p110α*$^{f/f}$) and Cre (*p110α*$^{+/+}$*;Osx1-Cre*) controls in our first approaches. However, the use of doxycycline for achieving delayed deletion and the results in body weight measurements stated no significant changes due to the recombinase allele itself.

Dynamic changes in bone formation rate and assays with osteoblast cultures suggest that osteopenia in *p110α* mutant mice mainly stems from a cell-autonomous effect in osteoblast differentiation and function. Loss of *p110α* in bone leads to decreases in mineral apposition rate and bone formation rate in concordance with the reduction of the same parameters seen in AKT or IGF1 mutant mice (Kawamura et al., 2007; Zhang et al., 2002). But osteopenia phenotype can result from deficiency in osteoblast differentiation and/or function or for an increased osteoclast activity. For example, deletion of *Akt1* in a mesenchymal cell line leads to decreased osteoclast differentiation *in vitro* presumably because of a reduction in the liberation of RANKL and M-CSF in the medium (Mukherjee and Rotwein, 2012).

Specific TRAP activity staining was not altered in *p110α* mutant mice although a non-significant mild decrease in osteoclast number was seen. *Rankl/Opg* ratio and NTX levels (a marker of osteoclast activity) were not altered and therefore we concluded that the osteopenic phenotype was due to osteoblast deficiency rather than osteoclast impairment.

Osteoclast activity is also crucial for an appropriate bone development and PI3K has been also involved in the control of bone resorption through the regulation of osteoclast differentiation. *p110β* increases its expression during regular osteoclast differentiation and its pharmacological inhibition blocks the development of TRAP positive cells (Nakamura et al., 1995). Mutant mice lacking *p110β* in osteoclasts presented higher bone volume and although osteoclast number was not altered, they were unable to form actin rings, to cell fusion for the achievement of multinucleated osteoclasts and to release cathepsin K by means of acid vesicles (Gyori et al., 2014). A similar phenotype was observed after p85 deletion in osteoclasts. Bone resorption activity was decreased due to a defective ruffled border that led to intracellular accumulation of vesicles and decreased cathepsin K levels in the culture supernatant. Thus, the lack of p85 regulatory subunit leads to an osteopetrotic phenotype, highlighting the importance of the class IA PI3k also in osteoclasts (Shinohara et al., 2012).

2.3 Different Contributions of p110 Isoforms to Osteoblast Proliferation and Apoptosis

When *p110α* was deleted *in vitro*, slow proliferation rate and higher sensitivity to apoptosis was seen in cultured osteoblasts. However, there were no significant changes in the total number and proliferation rate of osteoblasts in bones of *p110α*-deficient mice. These data mirror those previously obtained in *Pten*-deficient mice, where the number of osteoblast was increased (Guntur et al., 2011; Liu et al., 2007b). Moreover, *in vivo* deletion of *p110β* did not increase apoptosis in osteoblasts, but it also produced a strong bone phenotype. These results agree with those showing that hematopoietic and mesenchymal cells are able to survive and proliferate normally with extremely reduced PI3K activity (Foukas et al., 2006).

As mentioned, acute deletion of *p110β in vitro* did not increase sensitivity to apoptosis but impaired expression of osteogenic markers in a milder way than *p110α*-deficient osteoblasts. Pharmacological inhibition of specific p110α and p110β subunits also corroborates the fact that p110α is the subunit involved in proliferative/apoptotic changes *in vitro*, since the use of A66 (p110α inhibitor) but not the p110β-specific inhibitor TGX-221 decreases proliferation and increases apoptosis upon serum deprivation. These differential effects between isoforms likely arise from their relative expression levels in osteoblasts and not from distinct intrinsic signaling abilities. Moreover, the differential implication of each subunit also suggests that the effects of PI3K-deletion in osteoblast proliferation and apoptosis are not the main cause of bone loss, since *p110α* and p110β present a similar phenotype. Concordantly, divergent roles for *p110α* and p110β have been already described in other models (Matheny and Adamo, 2010; Utermark et al., 2012).

TUNEL assays and cytometry of annexin positive osteoblasts revealed obvious increased sensibility to apoptosis in *p110α*-deficient osteoblasts after serum starvation. TUNEL assay and higher cleaved caspase 3 was also observed in *p110α* mutant mice, therefore corroborating the effect of *p110α* loss in apoptosis. However, the mechanism involving PI3K to caspase activation and increased programmed cell death in this model is still unclear. In some experiments lacking *p110α* we detected some BIM overexpression at protein level, which has been widely related to apoptosis in osteoblasts (Akiyama and Tanaka, 2011; Liang et al., 2008). PI3K/AKT axis has been linked to BIM mainly by FOXO proteins since the nuclear entry of FOXO3a transcriptionally increases BIM expression. AKT-mediated phosphorylation of FOXO3a is disrupted in *Akt1* null mice, enhancing its nuclear localization and therefore increasing the transactivation of BIM. (Kawamura et al., 2007). However our results

showing BIM overexpression were not always observed and further studies need to be performed in order to understand the implications of p110α in apoptosis.

FOXOs transcriptional activity have been related to pro-apoptotic but also to antiproliferative signals and additionally, FOXOs are also considered critical players in limiting ROS production since they transcribe genes with anti-oxidant properties (Ambrogini et al., 2010; Rached et al., 2010a). Further discussion concerning FOXOs activities will be mentioned later in this chapter.

2.4 PI3K is Necessary for a Complete Osteoblast Differentiation

Lack of class IA PI3K isoforms leads to similar changes in the expression of osteoblast-specific transcription factors in calvaria, long bone and osteoblast cultures. Whereas *Runx2* expression was significantly reduced only after double deletion of *p110α and* p110β, *Osx* expression was suppressed in all cases involving p110α loss-of-function. Osterix has been shown to transcriptionally regulate the expression of *Col1a1, Ibsp, Osteocalcin* and *Fmod* (Ortuno et al., 2010). Thus, lower levels of *Osterix* could account for impaired osteoblast maturation and function, through decreased transcription of these genes. Moreover, although OSX and RUNX2 transcription factors lack direct AKT phosphorylation sites, active AKT signaling has been shown to inhibit the binding and transcriptional activity of RUNX2 through FOXO1 (Yang et al., 2011). Thus, FOXO1 inhibits RUNX2 binding to its specific binding elements (OSE2) in the *Osteocalcin* promoter, suggesting that IGF1/insulin signaling favors OC expression by preventing FOXO1 from inhibiting RUNX2 in osteoblasts (Yang et al., 2011). Accordingly to these data, Runx2 mRNA levels were not changed in our p110α and p110β mutants. However, a likely decrease in RUNX2 activity has to be taken into account. In connection to possible PI3K effects over Runx2 activity, it has been described that AKT interacts with and phosphorylates SMURF2, increasing its degradation and therefore enhancing RUNX2 stability (Choi et al., 2014).

Regarding to bone mass, FOXO proteins seems to have a negative role in bone development although there is some controversy. Combined deletion of *Foxo1, -3* and *-4* in osteoprogenitors revealed a high bone mass phenotype that is mainly due to higher Wnt signaling and subsequently, higher proliferation (Iyer et al., 2013). This is due to a β-catenin shift between the pool linked to TCF/Lef transcription factors and the β-catenin that binds to FOXOs after ROS-mediated activation (Iyer et al., 2013). However, FOXOs also interact with ATF4 potentiating both FOXO and ATF4 transcriptional activity and therefore positively affecting bone formation by promoting protein synthesis and stress resistance (Rached et al., 2010b). Thus, FOXO activity and

transcriptional partners seems to be divergent depending on the differentiation status of the mesenchymal cell. While in mature osteoblasts FOXO is needed for a correct protein synthesis and ROS resistance, in osteoblast progenitors FOXO can associate with β-catenin limiting the pool of β-catenin available for an appropriate Wnt signaling.

Given the information obtained from FOXO mutants, the phenotype derived by the loss of *p110α* and *p110β* subunits seems not to relay in FOXO activity since a disruption of AKT signaling in mature osteoblasts would derive in a more active FOXO activity and therefore the expected phenotype will not correlate with the data from this work.

FOXO is also clearly involved in glucose homeostasis. As stated above, RUNX2 activity and therefore osteocalcin levels can be regulated by FOXOs (Yang et al., 2011). Furthermore, osteoblast-specific FoxO1 deficiency in mice suggests that FOXO1 in osteoblasts regulates both the expression and carboxylation of osteocalcin. FoxO1 directly binds to the promoter and inhibits osteocalcin while additionally stimulates *Esp* (osteotesticular phosphatase) gene expression (responsible for osteocalcin carboxylation) (Rached et al., 2010a).

Despite all the studies above-mentioned where changes in FOXO activity led to different phenotypes, no major changes were found in our models when assessing the phosphorylated status of FOXO proteins. Thus, the overall phenotype does not result from alterations in FOXO activity.

Acute loss of *p110α* and *p110β* in osteoblasts also revealed slight differences among the contribution of each isoform in the expression of osteoblast-related genes. Whereas *p110α* deletion led to decreases in *Alpl*, *Col1a1*, *Osteocalcin* and *Osterix*, disruption of *p110β* only impaired the expression of *Col1a1*, *Runx2* and *Osterix* mRNAs in a lesser extent. Again, these differences might fall on the relative ratio of expression between *p110α* and *p110β*.

2.5 BMP-PI3K Crosstalk During Bone Formation and Homeostasis

In bone development, the PI3K/AKT signaling has been mechanistically less comprehensively studied and the precise mediators are unknown. In previous work, activation of TORC1 by deletion of *Tsc1* or *Tsc2* led to increased bone mass through expansion of the osteoprogenitor pool but hampered osteoblast differentiation (Fang et al., 2015; Riddle et al., 2014). As previously discussed, deletion of FOXOs had some divergent results (Iyer et al., 2013; Rached et al., 2010b).

GSK3 is a multifunctional kinase that is constitutively active and negatively regulated by numerous signaling pathways such as PI3K/AKT and canonical Wnt. Evidence

suggests a negative role for GSK3 activity in osteogenesis. Kugimiya et al. described the phenotype of the *Gsk3β* heterozygous mice, which presented increased bone mass due to an enhanced RUNX2 transcriptional activity. These findings were a consequence of the suppression of the GSK3β-mediated inhibitory phosphorylation of RUNX2 (Kugimiya et al., 2007). Later the osteoblast-specific *Gsk3β* mutant was generated and confirmed osteopetrotic changes with higher trabecular bone mass (Gillespie et al., 2013).

Our data identified GSK3 activity as a novel node of integration for multiple osteogenic signals. Not only calvaria from mutant mice but also osteoblasts lacking class I PI3K presented a reduction in phosphorylated GSK3β levels. Total β-catenin was also reduced, suggesting an increase in the amount of activated GSK3β versus the inactive phosphorylated GSK3β.

Wnt canonical signaling is characterized by the accumulation of cytoplasmic β-catenin. The activation starts with Wnt ligand binding to the G-protein coupled Frizzled (Fzd) receptor and LRP5/6 (LDL-receptor related protein 5/6) co-receptor. When receptors are inactivated, β-catenin is constitutively phosphorylated by a destructive complex form by axin, APC (adenomatous Polyposis Coli) and GSK3β which work as signal for the β-TrCP (β-transducin repeat-containing protein) E3 ligase for further ubiquitination and proteosomal degradation. In this manner, levels of β-catenin remain low. However, when Wnt ligand binds to Frizzled and LRP5/6 receptors, the subsequent activation of Dishevelled (Dvl) inhibits GSK3β, which stops phosphorylating β-catenin. Therefore, β-catenin accumulation leads to nuclear translocation where along with TCF/Lef1 transcription factors activate the expression of specific Wnt target genes. Several molecules negatively affect the Wnt pathway at different points and have been shown to be highly important for bone biology. Dickkopf (Dkk) family members or SOST (gene encoding sclerostin) antagonize Wnt signaling by binding to LRP5 and 6, whereas SFRPs (secreted frizzled-related proteins) sequester Wnts away from binding to the receptors (Bafico et al., 2001; Wu and Nusse, 2002).

Wnt signaling has been widely positively related to osteoblast differentiation and osteogenesis although it depends on the state of specification of the target cell. Thus, *in vitro* studies have generated controversial results and theories exist about either a positive or a negative influence. Most data indicate that β-catenin acts positively to maintain stem cell pluripotency and self-renewal; however, once MSCs reach commitment to osteo-chondroprogenitors, β-catenin promotes osteoblast progression. Moreover, Wnt signaling leads to *Runx2* expression due to a Tcf regulatory element in its promoter (Gaur et al., 2005) and has been proved to work cooperatively with BMP signaling to induce other osteogenic genes such as *Osx*, *Dlx5*, and *Msx2* (Rodriguez-Carballo et al., 2011).

Canonical BMP and Wnt early target genes were strongly decreased in calvariae from *p110* double mutant mice. Important BMP-induced genes as *Id1*, *JunB* or *Smad7* among others where clearly down-regulated. Moreover, the expression of Wnt target genes as cyclin D, *Dkk1* or *Sost* was also decreased, suggesting that both pathways are affected when PI3K signaling is disrupted. Thus, osteoblasts not only fail to express direct downstream effectors of AKT but also genes from other key signaling pathways. Furthermore, stimulation of PI3K deleted-osteoblasts with BMP or IGF1 revealed a deficiency in the ability to activate BMP and Wnt target genes as *Axin2*, *Id1* or *JunB* suggesting that cells lacking PI3K have defective IGF1, BMP and Wnt responses.

Previous studies have shown that MAPK and GSK3 pathways can interfere with BMP signaling (Sapkota et al., 2007). Fuentealba et al. described a link between Wnt/GSK3 pathway and the duration of the BMP/SMAD signal. They showed that MAPK and GSK3 phosphorylations of the linker region of SMAD1 regulates the duration of BMP signal (Figure D-7) (Fuentealba et al., 2007). GSK3-mediated phosphorylation of SMAD requires the priming phosphorylation of MAPK sites and lead to the polyubiquitination of SMAD1 by the SMURF1 and -2 E3 ubiquitin ligase (Chong et al., 2010; Murakami et al., 2003). Consequently, Wnt signaling enhances the BMP/SMAD1 signal by decreasing the level of GSK3-phosphorylated sites (Fuentealba et al., 2007). Moreover, further cooperation comes from the fact that GSK3 activity also governs nuclear levels of β-catenin and transcriptional cooperativity between SMAD1 and β-catenin exists in the promoters of key osteogenic genes (Rodriguez-Carballo et al., 2011).

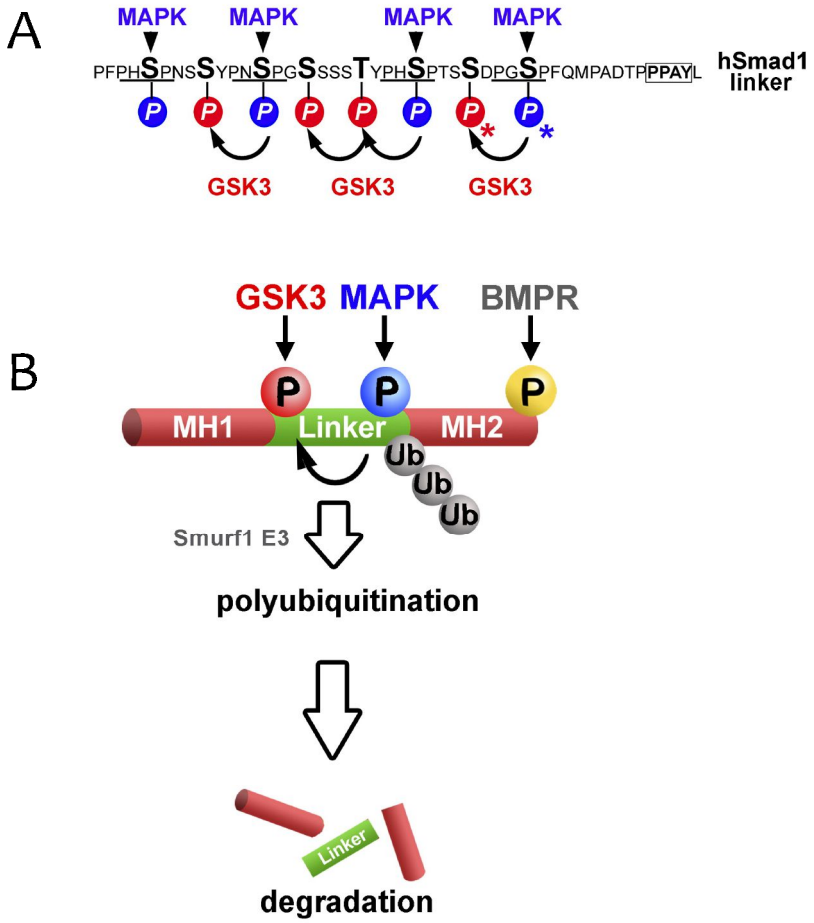

Figure D-7. Phosphorylation sites of the linker region of SMAD proteins. MAPK phosphorylations prime for GSK3 phosphorylations in the linker region of SMAD proteins. This will promote SMAD ubiquitination and further degradation. Adapted from (Fuentealba et al., 2007).

Thus, GSK3-regulated cellular levels of SMAD1 integrate signals from PI3K activators and Wnts with those of the BMPs to give a coordinated osteogenic readout. Our results conclude that genetic but also pharmacological inhibition of PI3K blocks the inhibitory phosphorylation of GSK3 and regulates SMAD1 protein stability. PI3K mutant mice and osteoblasts present higher GSK3 activity, thus interfering and regulating SMAD signaling by increasing phosphorylation of its linker region and therefore enhancing its degradation. This crosstalk between Wnt/GSK3 and BMP signaling pathway has been also described in other models (Saijilafu et al., 2013; Song et al., 2014). The mechanism proposed for the PI3K-mutant phenotype is in concordance with the results obtained in the osteoblast-specific *Gsk3β* mutant mice, where the lack of *Gsk3β* leads to an increase in bone mass. Furthermore, our results also demonstrate that effects on SMAD1 levels present in the PI3K mutant mice were partially reversed *in vitro* by pharmacological inhibition of GSK3. Direct targets of BMP and Wnt signaling such as *Id1*, *Smad7* or *Axin* were also restored after GSK3 inhibition.

We found that *Smad1* transcription was also dependent on PI3K signaling, suggesting that both the reduced transcription and the higher degradation of SMAD1 protein can account for the low cellular levels of SMAD1 after blockade of PI3K function. As stated above, *in vitro* and *in vivo* experiments showed a reduction in phosphorylated GSK3 and SMAD1 levels, which led to impaired osteoblast-specific gene expression. Additionally to GSK3 inhibition, ectopic expression of exogenous SMAD1 also partially reversed the decrease in important osteoblast genes such as *Alpl*, *Col1a1* or *Osterix*. This fact suggests the impact of phosphorylated SMAD1 in the contribution of the PI3K phenotype. Further studies are needed to assess whether other SMAD isoforms besides SMAD1 would also restore the expression of osteoblast-genes.

Surprisingly, a deeper study of SMAD proteins during the characterization of the class I PI3K phenotype lead us to suggest that the integrative role of SMAD1 relies on its limited amount in osteoblasts, contrary to the observations of other groups which suggested that only a small fraction of SMAD is phosphorylated after BMP physiological levels and that there is a pool of inactive SMAD remaining most of the time (Kuroda et al., 2005). In our *in vitro* protein expression approaches, even sub-maximal activation by BMP-2 (0.2 nM) shifted electrophoretically 100% of cellular SMAD1, which suggest that all the SMAD present in the osteoblast is being phosphorylated. Interestingly, BMP receptor-mediated carboxy-terminal phosphorylation of SMAD1 also enhances its stability, further suggesting an exquisite post-translational regulation of its cellular amounts.

In summary, we propose that the effects observed in PI3K mutant mice arise from increased GSK3 activity and lower SMAD1 levels in *p110α/β*-deficient osteoblasts (Figure D-8). Thus, we postulate that the PI3K/AKT/GSK3/SMAD pathway is a central nexus in networks that govern osteoblast differentiation and homeostasis and that these findings represent a molecular framework to understand numerous evidences showing cooperative activation of osteoblast differentiation and function by IGFs, Wnts and BMPs (Lian et al., 2006; Regard et al., 2012; Xian et al., 2012; Zhang et al., 2013).

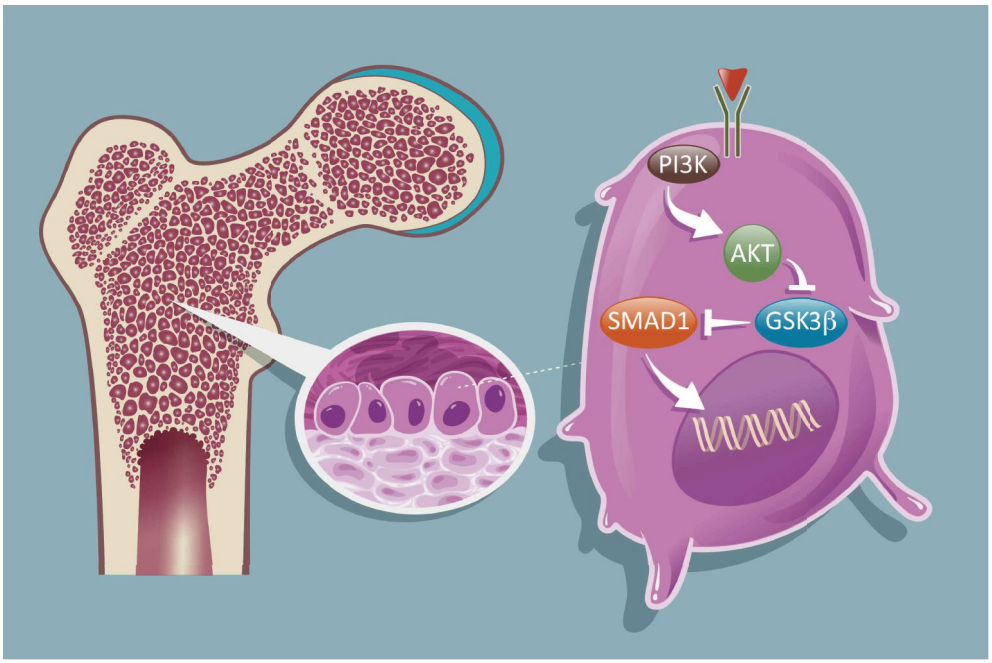

Figure D-8. Proposed mechanism for PI3K/AKT/GSK3/SMAD network. In normal conditions, PI3K stimulates AKT, which in turns phosphorylates and inhibits GSK3. GSK3 inhibition leads to a lower phosphorylation in SMAD linker region and, therefore, SMAD is no longer GSK3-marked for ubiquitination and degradation. This stability allows the transcription factor to be able to form SMAD complexes and to translocate into the nucleus in order to initiate the transcription of important osteoblast-related genes.

2.6 Contribution of This Work to the Field of p110 Inhibitors Therapies

The PI3K/AKT pathway is one of the most frequently dysregulated signaling pathways in cancer and an important target for drug development. PI3K signaling plays an important role in tumorigenesis, cell proliferation, survival, motility and angiogenesis. The activation of this pathway is frequently observed in a variety of tumor types and can occur through several mechanisms including amplification or gain-of-function mutations in the PIK3CA gene encoding p110α or the AKT1 gene. Inactivation of PTEN also occurs through mutation, deletion or epigenetic silencing (Rodon et al., 2013).

Our data show that efficient bone remodeling throughout life requires PI3K function and that even specific p110α and/or p110β inhibitors would result in significant on-target skeletal adverse effects. Thus, given the growing interest in p110α and β inhibitors as pharmaceutical agents in oncology and hematology, the evaluation of these inhibitors should include assessment of their skeletal actions. Bone homeostasis depends on the coupled activity of osteoblasts and osteoclasts. Then, the specific effects of PI3K signaling on the activity of osteoclasts should also be analyzed.

However, some *in vivo* evidence suggest a most prominent role on osteoblasts in terms of global bone structure maintenance since treatment of mice with pan- or p110α-specific inhibitors led to decreased bone mass and strength (Grey et al., 2010; Smith et al., 2013).

Our results also offer a bright side for treatment of osteosclerotic pathologies. For instance, patients suffering from fibrodysplasia ossificans progressive (FOP) develop heterotopic ossification induced by episodes of trauma and inflammation. All sporadic and inherited clinical cases are shown to carry an activating mutation of the BMP type I receptor ACVR1 that results in much higher sensitivity to BMP signaling (Shore et al., 2006). Current treatment options are only palliative and symptom-modifying. These patients could benefit from p110α and p110β inhibitors, which ultimately would increase GSK3β activity and in turn would decrease BMP signaling through the reduction of phosphorylated SMAD proteins.

Pequeña alegría de laboratorio#5

Encajar la varilla del tanque de nitrógeno a la primera

CONCLUSIONS

1 MIR-322 IN OSTEOBLAST DIFFERENTIATION

1 BMP treatment in C2C12 down-regulates expression of most miRNAs, as seen for miR-322, miR- 206 and miR-30a.

2 Overexpression of miR-322 increases *Osx*, *Runx2*, *Msx2* and *Ibsp* mRNA basal levels and also after BMP treatment in C2C12. Basal levels of *Osx*, *Runx2* and *Dlx5* genes are also increased in MC3T3.

3 miR-322 directly targets 3'-UTR *Tob2* and mediates its degradation.

4 Tob2 and CPEB2-4 alone or in combination can bind specifically to stem-loop sequences found in the *Osx* 3'-UTR sequence.

5 *Osx* mRNA can be bound by TOB2 and CPEB2-4 and, as a consequence, be specifically degraded.

2 ROLE OF PI3K IN BONE BIOLOGY

1 Osteoblast-specific *p110α* deletion in mice (*p110α$^{f/f}$;Col1a1-Cre*) impairs bone development and homeostasis leading to an osteoporotic phenotype. *p110α$^{f/f}$;Col1a1-Cre* mice display decreased bone mass, affecting both trabecular and cortical bone. Deletion of *p110α* hampers osteoblast differentiation. Bone resorption is also compromised.

2 Post-natal deletion of *p110α* also affects osteoblast differentiation. The phenotype driven by *p110α$^{f/f}$;Osx1-Cre* mice is similar to that of *p110α$^{f/f}$;Col1a1-Cre.* Thus, bone remodeling also requires PI3K function.

3 *p110β* is also crucial for bone development and osteoblast function as seen by the osteoblast-specific loss of *p110β in vivo* (*p110β$^{f/f}$;Col1a1-Cre*). This finding suggests that both isoforms are required for bone formation and that functional redundancy exists.

4 Osteoblasts lacking *p110α* present higher sensibility to apoptosis. *p110β* loss-of-function is not involved in the apoptotic changes observed in the double PI3K mutant mice since the deletion of this specific isoform *in vitro* do not affect apoptosis rate. Moreover, osteoblasts lacking both isoforms present an apoptotic rate comparable to osteoblasts lacking only *p110α.* This data is corroborated when using specific pharmacological inhibitors of p110 subunits.

5 Acute deletion of *p110β in vitro* leads to milder reduction of the osteogenic markers. These differential effects between isoforms likely arise from their

relative expression levels in osteoblasts and not from distinct intrinsic signaling abilities.

6 Class I PI3K deletion results in higher GSK3 activity as seen by the decrease in phosphorylated GSK3 levels. Increased GSK3 activity leads to lower SMAD1 and C-terminal-phosphorylated SMAD1 levels.

7 The phenotype resulting from the lack of class I PI3K is partially restored by GSK3 inhibitors and by ectopic overexpression of SMAD1 *in vitro*.

Pequeña alegría de laboratorio#6

Olvidarte de una electroforesis y que al recordarla, corras y esté justo dónde la necesitas

MATERIALS & METHODS

1 CELL CULTURE

During the present thesis, different cell lines and primary cultures have been used as a model for the different experiments. Each line must be cultured in a specific culture medium depending on its requirements.

Nowadays, different cell culture media are available, all coming from an original recipe firstly reported by Harry Eagle. Typically, fetal bovine serum (FBS) is added to this media, as well as pyruvate, glutamine or antibiotics. The two main media used during the experimental work have been:

- DMEM (Dulbeccoos Modified Eagle's Medium) (01-055-1A, Biological Industries).
- α-MEM (Minimum Essential Medium Eagle Alpha Modification): this medium has a different concentration of vitamins and amino acids in comparison with DMEM. Above all, the main difference is the higher concentration of ascorbic acid, important for the maintenance of the osteoblastic features of different cell lines (M8042, Sigma).

If not otherwise specified, normally the "complete media" was supplemented as follows:

- 10% FBS
- 50 U/ml penicillin
- 50 µg/ml streptomycin
- 2 mM sodium pyruvate
- 2 mM L-glutamine

When "differentiation media" is mentioned, 10 mM beta-glycerophosphate and 50 µg/ml ascorbic acid was added to regular supplemented α-MEM (to complete α-MEM). In some specified experiments, 1 nM dexamethasone was also added.

All cells used were cultured and maintained during experiments at 37°C with 5% CO_2 in a humidified chamber.

1.1 Cell Lines

Each cell line represents a different stage among the osteoblast differentiation process and should be maintained in concrete conditions in order not to alter its characteristics.

1.1.1 C2C12

C2C12 is a murine cell line considered as pre-myoblast because of its determination to differentiate into myoblasts. This cell line remains undifferentiated when cultured with 10% FBS supplemented DMEM and moreover, is able to change its lineage from myoblastic to osteoblastic under BMP-2 treatment. This is the reason why it is so used as a model for the study of osteoblastic differentiation.

1.1.2 MC3T3-E1

This cell line is in a more advanced stage in the osteoblastic differentiation process. They originated from a cell clone of a primary osteoblast culture from murine calvariae. MC3T3-E1 cells are cultured using α-MEM. Once in confluence, this cell line is able to induce mineralization and calcification by producing hydroxyapatite crystals and represents, probably, the most used cell line for the study of the osteoblasts.

1.1.3 HEK-293

HEK (human embryonic kidney) cells were originally generated by transformation of human embryonic kidney cells. During this thesis, HEK cells were promptly used as a transfection host due to its efficacy in transfection protocols. Regular DMEM is used to maintain this cell line.

1.1.4 Platinum-E

The Platinum-E cell line (Plat-E) is a retrovirus packaging cell line based on a 293T cell line (HEK cells constitutively expressing the simian virus 40-SV40- large T antigen) and was originated using constructs with EF1α promoter to ensure the expression of retroviral proteins (gag, pol and env). The expression of these genes allows retroviral packaging with a single plasmid transfection. Platinum-E cells present puromycin and blasticidine resistance due to the constructs used to insert retroviral genes. Thus, for the maintenance of the cell line, blasticidine (5 μg/ml) and puromycin (1 μg/ml) is added to regular supplemented DMEM.

1.1.5 NIH/3T3

3T3 cell line is a commonly used fibroblast cell line originally obtained from Swiss albino mouse embryo tissue. They are good transfection hosts and they are widely accepted as the standard target cells for titrating retrovirus due to their high efficiency to be transduced. This cell line is cultured using complete DMEM.

1.1.6 HeLa

Human epithelial cells originated from adenocarcinoma and used mainly during this thesis as transfection host. Complete DMEM was used for their maintenance.

1.2 Primary Cultures

Primary cultures are originated from a specific processed tissue and they must be used for experiments among the first passages before they become senescent and/or die. The primary cultures used during this thesis are always of animal origin (mice).

1.2.1 Bone Marrow Mesenchymal Stem Cells (BM-MSCs)

The protocol used is based in the one published by Soleimani and Nadri (Soleimani and Nadri, 2009). The aim is to specifically collect the BM-MSCs from the bone marrow content.

1. Use 6 to 8 week old mice. Sacrifice and dissect hind limbs. Introduce them into a 50ml *falcon* full of complete DMEM media.
2. Working under the hood from now on, remove muscle and connective tissue from both the tibia and the femur by scrapping the diaphysis of the bone. After cleaning, go through clean media to wash possible existing animal's fur. Store the bones in complete DMEM.
3. Harvest the bone marrow by using a sterile syringe. Cut both ends of the tibia and femur just below the joints and insert a 25-gauge needle attached to a syringe containing complete media. Flush the bone marrow and collect it in a 50ml tube.
4. Once all the bones have been flushed, use the pipette to disaggregate possible blood clots and then filter the cell suspension through a 70-mm filter mesh to remove bone spicules or muscle and cell clumps.
5. Culture the filtered cell containing media in a culture dish. 1.5-2 ml of the cell suspension must be used for each well of a 6-well plate. Incubate cells at normal conditions.

6 Change media every 8 hours-12 hours for up to 72 hours of initial culture. The medium must be changed slowly not to induce MSC's detachment. After 72 hours, wash with PBS and add fresh medium every 3 days.
7 Once 70% confluence is achieved, selective trypsinization must be performed. Wash the cells with PBS and add 0.5 ml of 0.25% trypsin/1 mM ethylenediaminetetraacetic acid (for a well of a 6-well plate, 1 ml for a 100 mm dish) for 2-3 minutes at room temperature.
8 Neutralize the trypsin by adding complete medium and culture the mix in a new plate/dish. Discard the non-lifted cells.

> The time and temperature of trypsinization is very important! If is higher than 2 minutes and/or 25°C, non-MSCs together with MSCs would be lifted from plastic culture dishes!

9 Change media every 3 days as normal cell culture using complete DMEM.

This primary culture can be frozen and used later with a regular cell freezing protocol.

1.2.2 Osteoblasts

Primary osteoblasts cultures are established from mice pups. Calvariae from P0 to P5 pups are used. A minimum of 5 individuals is required and the culture is maintained with complete α-MEM.

The procedure used for osteoblast extraction is as follows:

Calvaria isolation

1 Euthanize pups by decapitation.
2 Collect tail if necessary (for genotyping).
3 Clean pup head with 70% ethanol.
4 Cut the skin away and scratch softly the calvaria surface in order to remove the periostium.
5 Hold the head with forceps placed through the orbits and cut the calvaria.
6 Prepare a 12- or 24-well dish with sterile PBS + 1% P/S (penicillin/streptomycin)
7 Transfer calvaria to a well containing PBS + 1% P/S.
8 Repeat steps 1 to 7 for all remaining pups.

> If genotyping is needed, transfer calvariae from PBS dish to a dish containing complete medium and incubate at 37°C/5%CO2 for 1-2 days until PCR is performed. Then proceed to next step.

Calvaria digestion (8-10 pups)

1 Prepare the digestion mix solution:
- 2 mg/ml collagenase II (620 µl) (LS004176, Worthington)

- 6.4 ml Trypsin
- 24.8 ml PBS
- 1% P/S

  Doxycycline was added in osteoblasts extracted from mice with Tet-Off (1 µg/ml, 4690 Sigma).

2 Sterilize mix solution using a 0.22 µm filter and keep on ice.
3 Remove sagittal suture with scissors and cut up calvaria.
4 Pool all calvaria slices (divided per genotype if needed) into 50 ml canonical tube containing 10mL PBS. Rinse 3 times with PBS.
5 Add 8-10 ml of digest mix solution to the tube. Tighten cap and incubate at 37°C for 5 minutes in a warm shaking bath.
6 Discard supernatant. The aim of this pre-digestion is to remove cells and/or tissue surrounding the bone.
7 Add fresh 10 ml digest mix to calvariae.
8 With loose cap, incubate at 37°C for 15 minutes in a warm shaking bath.
9 Shake by hand for a few seconds.
10 Incubate for an additional 15 minutes.
11 Take out digest mix solution and pour it in a new 50 ml canonical tube. Add 10 ml of fresh complete medium. Incubate at 37°C while next digestion is performed.
12 Add fresh 10 ml digest mix to calvariae (repeat the procedure).
13 Once finished, add 10 ml of fresh complete medium and save the new supernatant combining it with that from step 6.
14 Spin down cells at 3000 rpm for 5 minutes.
15 Aspirate supernatant.
16 Resuspend in complete α-MEM and place onto a 60 mm dish (depending on the size of the cell pellet or on the number of pups used).

  The remaining calvaria pieces can be also plated with fresh media in a separate plate. Remaining osteoblast cells will arise from the slices in the following days.

17 Change media the following day. Replace media every 3 days.

Ideally, experiments should be performed between passage numbers 3 to 6. Normally, 3 weeks after the culture of osteoblast digestion the cells begin to go under senescence and are not desirable for experimental work.

1.3 Treatments and Reagents

During the experimental work of this thesis several treatments have been used in order to trigger different cell processes as for example, induction of osteoblast

differentiation or inhibition of specific signaling pathways. Table M-1 summarizes some of the reagents used for this aim.

REAGENTS				
Name	**Description**	**Dose**	**Stock, diluted in**	**Reference**
BMP-2 protein	Induction of osteoblast differentiation	2/0.2 nM	2 µM, PBS 0.1%BSA	R&D Systems
IGF1 protein	Stimulation of PI3K signaling	10 nM	10 µM, PBS 0.1%BSA	ab9861, abcam
Wnt3a protein	Stimulation of Wnt signaling	100 ng/ml	50 mM, PBS 0.1%BSA	R&D systems
A66	p110α inhibitor	10 µM	10 mM, DMSO	S2636, Selleckchem
TGX-221	p110β inhibitor	10 µM	10 mM, DMSO	S1169, Selleckchem
CHIR 99021	GSK3α/β inhibitor	10 µM	10mM, DMSO	361559, Calbiochem

Table M-1. Cell culture reagents.

2 WORKING WITH BACTERIA

Bacteria culture was used mainly as a tool for the cloning of DNA sequences. The creation of new vectors expressing mutated proteins was crucial for validating miRNA targets and for the generation of retroviral plasmids, which were essential for the incorporation of ectopic proteins into osteoblasts.

2.1 Transformation of Competent Cells

Transformation is the procedure by which we introduce foreign DNA into bacteria. As stated above, transformation of bacteria with plasmids is essential for storing and replicating plasmids.

Transformations were performed by thermal shock using DH5α cells that have been previously treated with $CaCl_2$ and therefore they were DH5α competent cells. Once transformed, bacteria were seeded in agar plates containing the specific antibiotic needed for the selection of the plasmid-containing cells. After an overnight incubation, some of the colonies were selected and grown in order to obtain a bigger amount of plasmid and/or be able to check the properties of the new plasmid.

DNA is further obtained using Wizard Plus Miniprep DNA purification system (A7510, Promega) or the QIAfilter Plasmid maxi kit (12263, Qiagen), depending on the needs.

3 WORKING WITH VIRUSES

Due to the difficulty of transfecting primary cultures with normal transfection methods, the use of viruses have been crucial for the *in vitro* approaches during this thesis.

3.1 Lentiviral Infection

Lentiviruses were directly purchased to infect primary cultures (BM-MSCs and osteoblasts). The transduction of target cells was performed as specified below:

1 Seed cells to achieve 10-20% confluence the next day using the appropriate complete medium.

   - For a 12-well plate, count cells and seed approximately $4x10^4$ cells in each well.
   - It's important to seed extra wells to use them as controls for the further antibiotic selection.

2 Next day, for each well of a 12-well plate proceed as follows:

   - Pour 500 µl of complete medium.
   - Add 2 µg/ml of Polybrene
     - Polybrene is a polycation that reduces charge repulsion between the virus and the cellular membrane. The optimum concentration of Polybrene may be determined for every type of cell because excessive exposure can be toxic.

3 Add 4 µl of lentivirus stock (10^7 IU/ml) → MOI=1

4 Next day, remove medium and add fresh complete medium with puromycin to start antibiotic selection. If possible, check the expression of the fluorescent tag.

> 👍 Using miRNA lentiviruses we set 2 µg/ml as the optimal concentration for puromycin selection (48 hours).
>
> 👍 Use a non-transduced well as control to know when puromycin has already killed all the non-infected cells.

5 After 48 hours of selection, remove and discard medium and add new fresh complete medium. Let the cells recover for 48 hours.
6 Perform the analysis as usual.

3.2 Retroviruses

3.2.1 Retrovirus generation

Platinum-E cell line is used to generate retrovirus. Although this cell line is normally cultured with puromycin and blasticidine (in order to maintain only the transformed cells), a media without antibiotics (just with P/S, complete DMEM) must be used during thawing. From then on, antibiotics should be added to the media.

During retrovirus production, incubate cells at 37°C, 5% CO_2. The protocol for Plat-E transfection is as follows:

1 Approximately 24 hours before transfection, seed Plat-E cells without blasticidine and puromycin. The cells should be 50-70% confluent at the time of transfection. Use complete medium with FBS up to 8 ml for each 100 mm plate.
2 After 16 to 24 hours, start transfection protocol. We use Lipofectamine LTX & Plus Reagent and the indicated amount of DNA below (indications for 2 100mm plates):
   - Dilution 1:
     - 1750 µl Opti-MEM
     - 70 µl Lipofectamine LTX
   - Dilution 2:
     - 1750 µl Opti-MEM
     - 16 µg of retroviral plasmid
     - 4 µg DNA envelope plasmid (pMD2.G)

       > 👍 Plat-E cells are already expressing the proteins needed to package the retroviral plasmid. However, co-transfecting some µg of the plasmid encoding the envelope proteins increases retroviral production.

     - 20 µl Plus Reagent
3 Add dilution 2 to dilution 1 and incubate for 15 minutes.
4 Distribute half the volume among each 100 mm plate (already containing 8 ml of medium).

👍 Be careful when pouring the transfection mix! Cells are very sensitive to detachment! Try to do it drop by drop with a 1 ml pipette.

5 Leave the cells with transfection cocktail for 48 hours.

👍 72 hours is ok if there the week-end is coming ☺

☠ **CAUTION!** Cells begin to express retroviral particles from 5 hours post-transfection! Dishes must be placed in an appropriate virus culture room.

6 After 24 hours, GFP can be evaluated (if the transfected retroviral plasmid is expressing it).

7 After 48 hours, use a 20 ml syringe to harvest the retroviral supernatants and use a cellulose acetate filter of 0.45 microns to remove cellular debris.

👍 Nitrocellulose filters bind proteins present in the membrane of retrovirus and destroys them. Don't use them!

☠ **CAUTION!** Medium contains infectious retrovirus!

☠ **CAUTION!** Don't use 0.22-micron filter since it will retain viral particles and the supernatant will not present infectious capacity.

Retroviral supernatant can be stored both at 4°C or at -20°C. Freshly harvested virus can be stored at 4°C during 10 days (maximum) before perceptibly loosing its efficiency. Note that each freeze-thaw cycle can reduce the functional activity by up to 2-4 fold. All experiments were done with fresh supernatant.

3.3 Transducing Target Cells with Retroviruses

The following protocol is a general method for transducing adherent primary cultures such as osteoblasts with retroviruses. It is important to consider that, in order to be transduced by a retrovirus, the target cell must be dividing.

To produce consistent transduction results it is necessary to titrate the retrovirus stock in order to determine the amount of volume necessary for an optimal infection.

NIH/3T3 cells were used to determine viral titer. After using different volumes of supernatant together with increasing concentrations of Polybrene, we established the best conditions for primary culture transduction:

- 500 µl of viral supernatant
- 5 µg/ml of Polybrene

We also performed different infections and we conclude that culture centrifugation during infection increases transduction efficiency.

The final protocol for primary culture infection proceeds as follows:

1 Seed cells to achieve 20-40% confluence the next day.

> 👍 When working with osteoblasts, count cells with a Neubauer chamber and seed between 8-10x10^5 cells in a 6-well plate (in each well).
>
> 👍 It's important to seed extra wells to use them as controls for further antibiotic selection.

2 Next day, for each well of a 6-well plate proceed as follows:
- Pour 500 µl of retroviral supernatant.
- Add 500 µl of complete medium (target cells regular medium).
- Add 5 µg/ml of Polybrene.

> 👍 When performing co-infections, 250 µl of each supernatant was used. In the case of co-transfection using pMSCV-GFP-FlagSMAD1, the efficiency of SMAD1 plasmid was much lower and we used both supernatants with a ratio of 1:8.
>
> ☠ During this step and from then on an appropriate virus culture room should be used.

3 Centrifuge plates at 400 x g for 30 minutes.

> 👍 Literature recommends centrifuging at 32°C to increase infection efficiency. A room temperature centrifuge is acceptable if a 32°C unit is not available.

4 After 24 hours, remove and discard the virus-containing medium and replace it with fresh complete medium.

5 Incubate cells for 24 hours more to allow your gene product to accumulate in the target cells.

6 Start antibiotic selection using the concentration of antibiotic optimal for the specific cell line

> 👍 For osteoblasts, a concentration of 5 µg/ml of puromycin during 24-36 hours is enough for a good antibiotic selection (using plasmids listed below).
>
> 👍 Use a non-transduced well as control to know when puromycin has already killed all the non-infected cells.

7 After 24-36 hours, remove selection medium and add fresh medium for additional 24 hours.

8 When using an inducible system, add the appropriate drug or any other treatment.

> 👍 1 µM of tamoxifen was used for the pMSCV-Cre-ERT2 plasmid.

9 After that, harvest cells for analysis as usual.

Viral plasmids and reagents needed are described in Table M-2 & Table M-3.

VIRAL PLASMIDS		
Name	**Expressing**	**Reference**
LentimiRa-GFP-mmu-mir-322	miR-322 Puromycin resistance	mm15354, abm
Lenti-III-mir-GFP-Blank	Scramble Puromycin resistance	M002, abm
pMSCV-GFP	GFP	Gift from Dr. Maribel Parra
pMSCV-GFP-Cre	Cre + GFP	24064, Addgene
pMSCV-Puro-Cre-ERT2	Cre Puromycin resistance Tamoxifen inducible	22776, Addgene
pMSCV-Puro	Puromycin resistance	Gift from Dr. Maribel Parra
pMD2.G	Envelope proteins	Gift from Dr. Maribel Parra
pMSCV-Flag-hSmad1	Smad1	Made in lab. See 4.4.2

Table M-2. Viral plasmids.

REAGENTS		
Name	**Reference**	**Final Concentration**
Puromycin dihydrochloride	P8833, Sigma-Aldrich	2-5 µg/ml
4-Hydroxytamoxifen	H7904, Sigma-Aldrich	1 µM
Hexadimethrine bromide (Polybrene)	107689, Sigma-Aldrich	5 µg/ml
Lipofectamine LTX & Plus Reagent	15338100, Life Technologies	7 µl/ml (approx.)

Table M-3. Reagents for retrovirus generation and infection.

4 MOLECULAR BIOLOGY TECHNIQUES

4.1 Working with microRNAs

4.1.1 microRNA isolation

We used mirVana miRNA Isolation kit (Life Technologies) for the extraction of microRNAs from cells. This procedure combines an organic extraction with a glass-fiber filter purification to finally obtain either total RNA or a fraction of RNA enriched for small RNA (containing mostly RNAs under 200 bases). The isolation procedure was carried out as follows:

Cell lysis

1. Aspirate and discard culture medium and rinse with PBS twice. Place the culture plate on ice.
2. Remove de PBS and add 300 µl of lysis/binding solution.
3. Vortex vigorously and pipet lysate to homogenate.

   At this point, the procedure can be stopped and samples stored at -80°C.

Organic extraction

1. Add 30 µl of miRNA homogenate additive (1/10 volume of lysate volume) to the cell lysate and mix well by vortexing.
2. Leave the mixture on ice for 10 minutes.
3. Add 300 µl of acid-phenol:chloroform (1:1 volume to the original lysate volume).

> 👍 Be sure to withdraw the volume from the bottom phase in the bottle of acid-phenol:chloroform because the upper phase it's just an aqueous buffer!

4 Vortex for 30-60 seconds to mix
5 Centrifuge for 5 minutes at maximum speed (10,000 g) at room temperature to separate the aqueous and organic phases. After centrifugation, the interphase should be compact; if not, repeat centrifugation.
6 Carefully remove the aqueous (upper!) phase without disturbing the lower phase and transfer it to a fresh tube. Note the volume removed.

Enrichment procedure for small RNAs

1 Add 1/3 volume of 100% ethanol to the aqueous phase recovered from the organic extraction. Mix thoroughly by vortexing or inverting the tube several times.
2 For each sample, place a filter cartridge into one of the collection tubes supplied with the kit.
3 Pipet the lysate/ethanol mixture (from the previous step) onto the filter cartridge. Up to 700 µl can be applied to a filter cartridge at a time.

> 👍 For volumes greater than 700 µl, apply the mixture in successive applications to the same filter.

4 Centrifuge at 10,000 x g for 15 seconds to pass the mixture through the filter.

> ☠ **CAUTION!** Spinning harder than this may damage the filters.

5 Collect the filtrate. If successive centrifugations are required, transfer the flow-through to a fresh tube and repeat until all the mixture is through the filter. Measure the total volume of the filtrate.

> 👍 At this point, the filter contains an RNA fraction that is depleted of small RNAs. This fraction can be recovered if desired by treating the filter as further described.

6 Add 2/3 volume room temperature 100% ethanol to the filtrate (flow-through). For example, if 300 µl of filtrate is recovered, add 200 µl of 100% ethanol.
7 For each sample, place a second filter cartridge into one of the tubes supplied.
8 Pipet the filtrate/ethanol mixture onto the filter.
9 Centrifuge at 10,000 x g for 15 seconds.
10 Discard the flow-through. At this point the fraction of small RNAs is attached to the filter. We don't need the filtrate anymore.
11 Apply 700 µl of miRNA washing solution 1 to the filter and centrifuge for 5-10 seconds. Discard the flow-through.
12 Apply 500 µl of washing solution 2/3 to the filter and centrifuge for 5-10 seconds. Discard the flow-through.

13 Repeat step 12.
14 Transfer the filter cartridge into a clean sterile *eppendorf* and apply 100 µl of pre-heated (95°C) elution solution and close the cap.
15 Spin at maximum speed for 20-30 seconds to recover small RNAs.
16 Collect the filtrate (which contains the RNA) and store it at -20°C or colder.

If considering recovering the RNA fraction depleted of small RNAs from the first filter cartridge, steps 11 to 16 must be performed in this filter.

microRNA concentration and purity was quantified using a nanodrop spectrophotometer (Thermo Scientific).

4.1.2 microRNA single assays: retrotranscription & PCR

microRNA retrotranscription

We used Taqman Small RNA Assays products to perform specific microRNA retrotranscription (RT). Samples were retrotranscribed using a TaqMan MicroRNA Reverse Transcription Kit. To prepare a single RT reaction mix, pipet the components described in Table M-4 into each tube (7 µl final volume):

microRNA RT REACTION MIX	
Component	**Volume (µl)**
100 mM dNTPs	0.15
MultiScribe Reverse Transcriptase, 50 U/µl	1.00
10x Reverse Transcription Buffer	1.50
RNase inhibitor, 20 U/µl	0.19
Nuclease-free water	4.16

Table M-4. microRNA RT reaction mix recipe.

1 Prepare a RT master mix by scaling volumes listed in Table M-4 to the desired number of RT reactions. Add 1 or 2 to the final number of reactions to account for pipetting losses.
2 Mix gently and centrifuge to bring solution to the bottom of the tube. Place the RT master mix on ice until the microRNA reaction is prepared.
3 For each 15-µl RT reaction, combine 7 µl of master mix (reaction mix), 3 µl of primer and 5 µl of RNA sample (RNA + water). The kit recommends to use 1 to

10 ng of total RNA per reaction so must prepare the samples before mixing it with the RT reaction mix. Place in a tube 10 ng of RNA and add water up to 5 µl.

> If more than 10 ng of retrotranscribed RNA is needed for further studies, double all the microRNA RT reaction volumes.

4 For each tube of RNA sample prepared, dispense 15 µl of the RT master mix.
5 Add 3 µl of RT primer into the corresponding RT reaction tube.
6 Cap each tube, invert several times to mix and centrifuge briefly to bring solution to the bottom of the tube. Keep on ice until you are ready to load the thermal cycler.
7 Set the reaction volume in the thermal cycler to 15 µl and load the reaction tube.
8 Perform the reverse transcription by using the thermal cycler program summarized in Table M-5. Store samples at 4°C if not continuing immediately to qPCR (quantitative PCR).

PCR CONDITIONS		
Step	**Time (min)**	**Temperature (°C)**
HOLD	30	16
HOLD	30	42
HOLD	5	85
HOLD	∞	4

Table M-5. microRNA retrotranscription conditions.

qPCR amplification

Before this step, TaqMan MicroRNA reverse transcription Kit was used to synthesize single-stranded cDNA from RNA samples before qPCR. qPCR amplification of cDNA from microRNAs is performed similar as general cDNA amplifications using TaqMan reagents. To prepare qPCR reaction:

1 Calculate the number of reactions that you need for each assay (performing three replicates of each reaction), being sure to include on each plate an endogenous control and a no template control (NTC) for each assay on the plate.

2 Prepare a microcentrifuge tube for each sample (to be run in triplicates) and scale volumes to the desired number of reactions (depending on the number of probes to test in each sample).
3 Pipet the following components into each tube (final volume=20 µl). Replicate volumes should include 20% excess to compensate for volume loss during pipetting.

qPCR REACTION MIX	
Component	**Volume (µl) for a single reaction**
TaqMan Small RNA Assay (20x) - probe	1.00
Product from RT reaction	1.33
TaqMan Universal PCR Master Mix II (2x)	10
Nuclease-free water	7.67

Table M-6. Reaction mix for microRNA amplification.

4 Cap the tube and invert several times to mix. Centrifuge the tube briefly.
5 Transfer 20 µl of the complete qPCR reaction mix into each of 3 wells on a 384-well plate.
6 Seal the plate with the appropriate cover.
7 Centrifuge the plate briefly (1200 rpm for two minutes) and load the plate into the instrument using the standard run mode with the following parameters (Table M-7) and start the run.

qPCR SOFTWARE PARAMETERS				
Step	**Optional AmpErase UNG activity**	**Enzyme activation**	**PCR**	
	HOLD	**HOLD**	**CYCLE (40 cyles)**	
			Denature	**Anneal/extend**
Temperature	50 °C	95 °C	95 °C	60 °C
Time	2 minutes	10 minutes	15 seconds	60 seconds

Table M-7. PCR parameters for microRNA amplification.

4.1.3 microRNA TaqMan Low Density Array (TLDA)

TLDAs are 384-well plates that are pre-loaded with TaqMan gene expression probes. Each TLDA we used was evaluating up to eight cDNA samples generated in reverse transcription. Like regular microRNA TaqMan assays, the samples that will be loaded in the TLDA must be retrotranscribed using random primers from a High Capacity cDNA kit (TaqMan MicroRNA Reverse Transcription Kit) but instead of using specific miRNA primers, using a pool of them named as Megaplex RT primers.

The Megaplex RT primers are highly multiplexed pools designed to significantly streamline the workflow when profiling many miRNA targets in a single experiment. The RT master mix should be prepared as specified in Table M-8 (for each sample).

microRNA MEGAPLEX RT REACTION	
Component	**Volume (µl)**
Megaplex RT Primers	0.8
dNTPS (100mM)	0.2
MultiScribe Reverse Transcriptase, 50U/ µl	1.5
$MgCl_2$ (25mM)	0.9
10x Reverse Trasncription Buffer	0.8
RNase inhibitor, 20U/ µl	0.2
Nuclease-free water	0.2
Total	**4.5**

Table M-8. microRNA RT reaction.

Once the above reagents are combined to generate a RT master mix (take into account the number of samples to use), invert the tubes to mix and centrifuge briefly. When the RT reaction is done (following the same thermal cycler conditions as for regular microRNA assays, Table M-5), perform the reaction for the array as described in Table M-9.

microRNA ARRAY qPCR	
Component	**Volume (µl) for one array**
TaqMan Universal PCR Master Mix, No AmpErase, 2x	450
Megaplex RT product	20
Nuclease-free water	430
Total	**900**

Table M-9. microRNA array PCR preparation.

After the microRNA array PCR mix is prepared:

1. Dispense 100 µl of the PCR reaction mix into each port of the TaqMan microRNA array.
2. Centrifuge and seal the array.

   CAUTION! It's really important to follow the supplier's instructions about how to seal and centrifuge the TLDA. The way you do it can substantially change the results of the array.

3. Import the SDS setup file (SDS.txt) located on the Information CD supplied with the TLDA.
4. Load the TLDA and run the array.

For our miRNA screening, we used a TaqMan Rodent miRNA Array B card v3.

4.1.4 Transfecting miRNAs

miRNAs were transfected using Lipofectamine RNAiMAX and always using cells previously seeded in a 6-well plate.

miRNA mimics (pre-miRs) and inhibitors (anti-miRs) were purchased from Ambion (Applied Biosystems) in order to analyze the effects that miRNAs have on biological processes or on an endogenous target. Pre-miRs are small, partially double-stranded RNAs that mimic endogenous precursor miRNAs. They include one strand that is identical to and effectively mimics a known mature miRNA and they are designed and modified to optimize selection of the correct strand of each pre-miR.

On the other hand, anti-miRs are designed to bind to and inhibit the activity of endogenous miRNAs when introduced into cells.

The protocol to transfect exogenous miRNAs was established as follows:

1 Seed cells the previous day in order to have them at 50% confluence at the moment of transfection.
2 For each well to transfect (6-well):
   - Dilute 50 pmol of RNA in 250 µl of opti-mem medium and mix.
   - Dilute 4 µl of RNAiMAX in 250 µl of opti-mem and mix.
   - Combine both dilutions, mix and incubate for 10-20 minutes at room temperature.
3 Add the transfection mix to the well containing 2.5 ml of regular medium or depleted medium

> Use one of the wells to transfect a control. We used BLOCK-iT Alexa Fluor Red Fluorescent Control with the same transfection conditions. BLOCK-iT is an ideal indicator of lipid-mediated transfection efficiency for RNAi experiments, particularly those using the Lipofectamine RNAiMAX.

Transfecting reagents are summarized in Table M-10.

REAGENTS FOR miRNA TRANSFECTION

Name	Reference
Pre-miR-322 (mmu-miR-322)	PM11080, Ambion (Applied Biosystems)
Pre-miR-206 (hsa-miR-206)	PM10409, Ambion (Applied Biosystems)
Pre-miR-30a (hsa-miR-30a)	PM11062, Ambion (Applied Biosystems)
Pre-miR-control	PM17010, Ambion (Applied Biosystems)
Anti-miR-322	AM11080, Ambion (Applied Biosystems)
Anti-miR-206	AM10409, Ambion (Applied Biosystems)
Anti-miR-30a	AM11062, Ambion (Applied Biosystems)
Anti-miR-control	AM17010, Ambion (Applied Biosystems)
BLOCK-iT Alexa Fluor Red Fluorescent Control	14750-100, Life Technologies
Lipofectamine RNAiMAX	13778-075, Invitrogen (Life Technologies)
Lipofectamine LTX & Plus Reagent	15338100, Invitrogen (Life Technologies)
Opti-MEM	11058-021, Gibco (Life Technologies)

Table M-10. Reagents for miRNA transfections.

4.2 RNA Isolation and Retrotranscription

RNA isolation has been performed using Ultraspec 10500 (BL10200, Biotecx) and TRIsure (BIO-38033, Bioline) for cell culture and tissue samples. Both products are based on the isolation of RNA by means of phenol and chloroform and we followed the protocol given by the manufacturers. The reason of using two different products was just based on commercial issues and we first tested that results were comparable using both products.

The retrotranscription (RT) is the process of transforming RNA into cDNA, mandatory in order to proceed to RNA relative quantification using the qPCR technique. We used the kit *High Capacity cDNA Reverse Transcription Kit* (Applied Biosystems) and we followed the manufacturer's protocol. Before RT preparation, total RNA was quantified using Nanodrop spectrophotometer (Thermo Scientific).

4.3 Quantitative PCR (qPCR)

Quantitative PCR (qPCR) was always performed after retrotranscription of RNA, therefore also abbreviated RT-qPCR. This technique allows quantifying the expression of the selected genes related to one or several endogenous controls (or housekeeping).

When using TLDA, 500 ng of sample were diluted in a final volume of 50 µl of water. 50 µl of MasterMix was then added to achieve 100 µl of total volume. This volume was charged in each fill reservoir of the TLDA. Then the card (TLDA) has to be centrifuged (1200 rpm x 1 minute, twice) and sealed before performing the run.

When working with regular 384-well plates, 11 µl of total volume was used per well and the mix was performed as follows:

- 0.5 µl cDNA (generally at 100 ng/µl)
- 4.5 µl sterile water
- 0.5 µl TaqMan probe
- 5.5 µl MasterMix or SensiFAST (2x)

In order to minimize errors, the total amount of volume needed for every reagent was calculated for all the wells using the same probe. Moreover, duplicates or triplicates for every sample were performed.

In both cases (384-well plate and TLDA) the qPCR was accomplished in a HT-7900 FAST thermocycler, from Applied Biosystems (from the scientific and technological center, Campus de Bellvitge).

The material used for the preparation of the samples is indicated in Table M-11.

qPCR MATERIAL		
Product	**Manufacturer**	**Reference**
Probes	Applied Biosystems	Different for every single probe
MasterMix	Applied Biosystems	58003365-01
SensiFAST™ Probe Hi-ROX Kitk	Bioline	BIO-82002
MicroAMP®Optical 384-Well Reaction Plate with barcode	Applied Biosystems	4309849
Costumed TLDA	Applied Biosystems	Costumed

Table M-11. Materials for qPCR assays.

4.4 DNA constructions

Plasmids are essential for our research in the lab and the transfection of eukaryotic cells is an indispensable technique. Several constructs have been used during this thesis. Commercial viral plasmids are described in Table M-2. The rest of the constructs used are all summarized in Table M-12.

PLASMIDS		
Product	**Origin**	**Reference**
pFLAG-CMV-hCPEB4	Dr. R.Méndez	Gift from Dr. Raúl Méndez
Cox2-luciferase reporter	Lab	Lab, (Susperregui et al., 2011)
Id1-luciferase reporter	Lab	Lab, (Lopez-Rovira et al., 2002)

Table M-12. Plasmids for protein overexpression and luciferase assays.

Moreover, next section provides the information about the generation of new plasmids specifically focused in the work of this thesis.

4.4.1 Renilla luciferase reporter constructs: Tob2-3'UTR wt and Tob2-3'UTR mutant

To determine the target region of miR-322, the 3'-UTR of the mouse *Tob2* cDNA was amplified from genomic DNA using primers: 5'-TGCTGAAGTCTAGAGACCATCAGGCTT-3' and 5'-CTCCATCTAGAAAAAGGATTCGCCCAGG-3' for the wild type and 5'-TGCTGAAGTCTAGAGACCATCAGGCTT-3' and 5'-AGAGTGGTCTAGATGTCAATTCGTGCACC-3' for the mutant construct. The product of both amplifications was cloned between de XbaI sites of the pRL-SV40 vector (Promega).

4.4.2 pMSCV-GFP-Flag-SMAD1

Flag-Smad1 was obtained by digestion of pCMV5-Flag-Smad1 plasmid (14044, Addgene) with BglII/BamHI. pMSCV-eGFP-Cre (24064, Addgene) was digested with BglII/BamHI and further treated with phosphatase alkaline. Flag-Smad1 was then cloned into the pMSCV backbone.

4.5 DNA Transfection

Transfection of eukaryotic cells is an indispensible molecular biology technique used to introduce ectopic DNA to a living cell. We performed transfections using Lipofectamine LTX + Plus reagent in C2C12, MC3T3-E1, HeLa and 293-Platinum E cells. The general protocol used for a single well of a 6-well-plate is as follows:

1. Seed cells the day prior to transfection. Cells should be 60 to 80% confluent next day.
2. In an *eppendorf* containing 250 µl of OptiMEM (Gibco), add 2 µg of the selected DNA (plasmid). If co-transfecting, the total amount of DNA should not exceed 2 µg. Then add the number of µl of Plus Reagent that equals the total number of µg added in the mix.

   > GFP plasmids are used to control the transfection efficiency. After 24 hours it is possible to check the expression of GFP (green protein) under fluorescence microscopy.

3. In another *eppendorf*, pour 250 µl of OptiMEM and add 9 µl of Lipfectamine LTX (Invitrogen).
4. Then mix the reagents contained in both *eppendorfs* and let it rest for 15 minutes at room temperature in order to allow the formation of liposomes.
5. Pour the total amount of OptiMEM (500 µl) in the well containing 1.5 ml of complete regular media.

6 Next day cells are ready to treat. Media can be replaced for an FBS-depleted one before treatment. In some cell lines, Lipofectamine is strongly toxic and media should be replaced 4 to 6 hours after addition of liposomes.

4.6 Luciferase Assays

We used luciferase systems in order to test the ability of some treatments or conditions to stimulate specific promoters. Luciferase reporter constructs can be co-transfected with other plasmids for the evaluation of the capacity of some proteins to work as transcription factors or as effectors of specific signaling pathways.

The general protocol for a luciferase assay is as follows (reference: 6 wells of a 24-multi well):

1 Seed cells the day prior to transfection. Cells should be 60-80% the next day.

> You should calculate the number of wells needed for all your conditions. It is important to assume at least three times the same condition (triplicates) in order to counteract the variability in the luminometer values.

2 In an *eppendorf* containing 330 µl of OptiMEM (Gibco), add 2 µg of Luciferase or Renilla reporter plasmid or the corresponding µg if co-transfecting two or more plasmids (the total amount of DNA should not exceed 4 µg per well). Then add 0.5 µg of the β-galactosidase plasmid (used later as a control of transfection efficiency).

3 In another *eppendorf*, pour 330 µl of OptiMEM and add 4 µl of Lipfectamine 2000 (Invitrogen).

4 Then mix the reagents contained in both *eppendorfs* and let it rest for 15 minutes at room temperature in order to allow the formation of liposomes.

5 Pour the total amount of transfection mix distributed in the 6 wells (150 µl each) and fill up until µl 500 with complete regular media.

6 Next day cells are ready to treat. Media can be replaced for an FBS-depleted one before treatment. In some cell lines, Lipofectamine is strongly toxic and media should be replaced 4 to 6 hours after addition of liposomes. Some treatments need 24 to 48 hours before luciferase analysis.

7 Once ready for luciferase reading, clean the well with cold PBS (twice) and pour 50 µl of Luciferase Lysis Buffer (E153A, Promega). Leave it 10 minutes in the shaker at room temperature.

> **CAUTION!** Lysis Buffer is originally 5x. You should dilute in sterile water until 1x the total amount needed.

8 For the luciferase reading use the luminometer establishing 15 seconds of integration time and 3 seconds of delay. Use a new *eppendorf* each time

containing 15 µl of the lysed sample plus 50 µl of the luciferase assay reagent (E1501, Promega). Firefly luciferase, a protein that catalyzes luciferin oxidation, generates light together with oxyluciferin production.

☠ **CAUTION!** Write down your values! Each time you perform a new lecture the value will disappear from the screen!

9 Finally, incubate 30 µl of lysed sample with 100 µl of the reaction buffer for β-galactosidase activity determination (631712, Clontech) and incubate for 40 minutes to 1 hour at room temperature. Use the luminometer again for the determination.

👍 If there are a lot of samples, determine β-galactosidase activity twice (inverting the order the second time) and calculate the mean.

👍 It is important to have a negative control without β-galactosidase plasmid transfection in order to calculate the background of the luminometer reading.

4.7 Western Blot

Western Blot analysis allows the evaluation and quantification of protein levels within a cell culture or tissue.

We used SDS-PAGE gels, normally around 10 to 15% of 40% acrylamide/BIS (161-0148, Bio-Rad) and generally, samples were lysated by using Sample Buffer and later quantified using a BCA protein assay kit (23225, Thermo Scientific). Samples were then mixed with LSB (laemmli sample buffer) prior to charging them into the running gel. The buffers and material used for Western Blot technique are listed in Table M-13.

WESTERN BLOT: BUFFERS AND MATERIALS		
Solution	**Concentration**	**Recipe (1 Liter) / Reference**
Running Buffer	10X	250 mM Tris-HCl 192 mM Glycin 1% SDS pH: 8.3
Wet Transfer Buffer	10x. At time of dilution (1x) 20% Methanol must be added.	250 mM Tris-HCl 192 mM Glycin pH: 8.3
Semi-dry Transfer Buffer (anode)	1X	0.3 M Tris-base 20% Methanol
Semi-dry Transfer Buffer (cathode)	1X	40 mM 6-aminocaproic acid 20% Methanol
Laemmli Sample Buffer	4X	12.5 ml 1M Tris pH: 6.8 + 4 g SDS + 4ml H_2O_2→ heat until dissolved and adjust to pH: 6.8. Add 10 mg bromofenol blue + 20 ml glycerol + 6 ml β-mercaptoetanol Final volume 50 ml.
Immobilion ® Transfer Membrane (PVDF)		iPVH00010, Merck
TBS-T (Tris-buffered saline-tween 20)	20X	200 mM Tris-Hcl 3 M NaCl 10 ml Tween-20 pH: 7.5
Sample Buffer (Lysis)	1X	500 mM Tris pH: 6.8 10% Glycerol 2% SDS

Table M-13. Buffers and materials for Western Blot.

During this thesis two different systems of protein transference have been used. When performing wet transfer system, gel-membrane sandwiches were maintained at 400 mA during 1.5 hours. When using semi-dry system, the transfer was achieved after 30 minutes at 1 A as maximum and 25 V constantly. These conditions are the "standard protocol" from Trans-Blot Turbo Transfer System.

In both cases, membranes were later blocked for an hour using 5% of non-fat dried milk in TBS-T (tris-buffered saline-tween-20) at room temperature. Then, membranes were washed with TBS-T 3 times (5 minutes - 10 minutes - 5 minutes) and the selected pieces

of membranes were incubated with the specific primary antibodies at 4°C overnight (or for 1 hour at room temperature occasionally).

Primary antibodies were generally diluted in TBS-T with 5% BSA (bovine serum albumin). The list of primary antibodies and the dilution used during this thesis is detailed in Table M-14.

WESTERN BLOT: PRIMARY ANTIBODIES

Antibody	Manufacturer	Reference	Dilution
Osterix	Abcam	22552	1:1000
Tob2	Sigma	T2948	1:1000
Flag-M2	Sigma	F3165	1:1000
Smad1	CST	69446	1:1000
pSMAD1/5/8 Ser465/467	CST	9511S	1:1000
pGSK3 α/β Ser21/Ser9	CST	9331S	1:1000
β-catenin	BD Bioscience	610154	1:1000
Id1	Santa Cruz	sc-488	1:500
p110α	CST	4249S	1:1000
p110β	Santa Cruz	sc-602	1:250
p85α	Merk-Millipore	04-403	1:1000
Caspase-3	CST	9662S	1:1000
pAKT Thr308	CST	9275	1:1000
pS6 Ser235/236	CST	2211	1:1000
LC3	MBL	PM036	1:1000
Bim	CST	2933S	1:1000
pFOXO Thr24/32	CST	9464S	1:1000
α-Tubulin	Calbiochem	CP06	1:5000

Table M-14. Primary antibodies.

Finally, once the incubation with the primary antibody was finished, membranes were washed again with TBS-T (3x) and were incubated with a horseradish peroxidase-

conjugated anti-rabbit or anti-mouse IgG antibody (secondary antibody). We used two different secondary antibodies: from Amersham and from Sigma. We used them as follows:

- Amersham: anti-rabbit (NA931V, 1:2500), anti-mouse (NA934V, 1:5000).
- Sigma: for the anti-rabbit (A0545) we first made a pre-dilution of 1 µl in 38 µl of TBS-T. From that stock we used 1:2500. For the anti-mouse (A9917), the pre-dilution was done with 1 µl of antibody and 19 µl of TBS-T. Final dilution was 1:5000.

In all cases, secondary antibodies were used diluted in 1% of non-fat dried milk in TBS-T at room temperature for one hour.

Then, TBS-T was used for washes followed by incubation with EZ-ECL Western Blot reagent (20-500-500, Biological Industries / RPN2106, GE Healthcare). Chemiluminescent image capture of immunoblots was performed with the Fujifilm LAS 3000 device and quantification of protein expression was carried out using Fujifilm MultiGauge software.

> If after developing the membrane you want to incubate a different primary antibody, just wash a little bit the membrane, block again with 5% of non-fat dried milk in TBS-T (for at least 30 minutes) and incubate again with the new antibody.

4.8 RNA pull-down assay

RNA pull-down assay was performed using HeLa cells. Cells were transfected for 4 hours using Lipofectamine LTX (Invitrogen). GFP was used as a transfection control. Summarizing, the protocol is as follows:

1. Harvest cells by adding lysis buffer (1.5 ml for a 100 mm dish, 250 µl for a well of 6-well plate). Leave it for 15 minutes at 4°C in the shaker. Then, collect lysate into new sterile *eppendorfs*.
2. Centrifuge lysates for 5 minutes at 16,000 g.
3. Keep supernatant and separate part of it as a control of the lysate (add Sample Buffer and boil 10 minutes at 95°C).
4. Use the remaining supernatant to continue the protocol. Add yeast RNA (0.5 mg/mg of protein, Sigma) to block non-specific binding. Add some µls of streptavidin-sepharose beads to also avoid unspecific binding. Let the mix shake 20 minutes at 4°C. Then centrifuge again 5 minutes at 16,000xg at 4°C.
5. Take supernatant, add 200 units/ml RNAsin (Promega) and split extract into the number of conditions you want to test. In our case 3 RNAs were used (two biotinylated sequences of 3' UTR *Osterix* RNAs and one RNA control).

6 Dilute biotinylated RNAs in RNA structure buffer, denature at 65°C for 5 minutes and cool them slowly for 20 minutes.

7 Incubate 1 µg of each RNA with cell lysates for 60 minutes at 4°C. Then add 25-30 µl of Streptavidin-Sepharose (17-5113-01, GE Healthcare) and incubate at 4°C for an extra 60 min.

> Streptavidin-sepharose beads are maintained in ethanol. Before using them, wash the total amount needed with lysis buffer and briefly centrifuge (1 minute at 1,000 x g). Then, wash a second time and resuspend the beads so that proportion of beads:lysis buffer will be 50:50.

8 Wash beads (5 times at 1,000 x g) with lysis buffer and mix final extract with 100 µl of Sample Buffer (1x). Bound proteins can be detected by Western blotting.

RNA PULL-DOWN ASSAY BUFFERS

Buffer	Recipe	Notes
Lysis buffer	50 mM Tris, pH: 7 100 mM KCl 5 mM $MgCl_2$ 10%Glycerol 1 mM DTT 0.2% Nonidet P40	Mix all reagents in DEPC water except DTT and autoclave. In the last moment add DTT and protease and phosphatase inhibitors from Table M-16.
RNA structure buffer	10 mM Tris, pH: 7 100 mM KCl 10 mM $MgCl_2$	

Table M-15. RNA pull-down assay buffers.

INHIBITORS			
Inhibitor	**Reference**	**Stock, diluted in**	**Dilution**
Protease inhibitors			
Leupeptin	L2023-5MG, Sigma	5 mg/ml, sterile water	1:1000
Aprotinin	A4529-5MG, Sigma	2 mg/ml, Hepes 10 mM pH: 8	1:1000
Pepstatin	P-5318, Sigma	1 mg/ml, acetic acid: ethanol (1:9)	1:1000
Benzamidine	12072-10G, Sigma	10 mg/ml, sterile water	1:100
PMSF	P7626, Sigma	100 mM, isopropanol	1:100
Phosphatase inhibitors			
NaF	A3904, AppliChem	1 M, sterile water	1:100
β-glycerophosphate	50020, Fluka	1 M, sterile water	1:100

Table M-16. Protease and phosphatase inhibitors.

5 PROLIFERATION AND APOPTOSIS DETERMINATION *IN VITRO*

5.1 Cell Proliferation ELISA BrdU

For the quantification of cell proliferation we used a colorimetric immunoassay based on the measurement of BrdU incorporation during DNA synthesis. A non-radiactive alternative to [^{3}H]-thymidine was used to label de DNA of mitotically active cells: 5-bromo-2'-deoxyuridine (BrdU). The incorporation of the pyrimidine analogue BrdU instead of thymidine into the DNA proliferating cells allows the posterior detection by immunoassay. We used the Cell Proliferation ELISA BrdU Colorimetric (11 647 229 001, Roche) and we followed the manufacturer's instructions. Summarizing, the protocol was as follows:

1 Seed 1,000 or 5,000 cells in a 96-well plate (depending on the proliferation rate).

2 Label the cells with BrdU (2 to 24 hours). Add the BrdU labeling solution in the cells with normal media.

> 👍 Some blanks are needed: It's important to leave some wells without cells (with medium) and some wells with cells but without adding BrdU labeling.

3 After labeling, remove medium, fix cells and add anti-BrdU-POD working solution for 90 minutes at room temperature (monoclonal antibody from mouse-mouse hybrid cells conjugated with peroxidase).

4 Wash wells and add substrate solution at room temperature and develop until color is sufficient for photometric detection (30 minutes approximately). Absorbance of 96-well-plates was measured in an ELISA reader at 450 nm after the addition of 25 µl of 1M H_2SO_4.

5.2 Annexin V Apoptosis Detection

The apoptosis rate of osteoblasts was quantified by flux cytometry using Annexin V Apoptosis Detection Kit (88-8007, eBioscience). We followed manufacturer's protocol. Since flux cytometry of adherent cells is complicated, tight control of some variables is determinant. Moreover, osteoblast primary culture has limited passages and even more after retroviral infection, cells start quiescence. It is difficult to obtain a large number of cells for each condition and to reach all the controls needed for the technique. For this, every condition used for osteoblast annexin staining ranged between 1,5 and $3x10^5$ cells.

A general overview of the technique is as follows:

1 Seed cells in 100 mm dishes. Perform the treatment needed and be aware that you will need a positive control.

   - Positive control is obtained by treating your cells with 1 µM Staurosporine overnight. Reserve a dish for that!
   - You will need several other controls! Reserve extra dishes for:
     - Living cells with no staining.
     - Living cells with annexin but without propidium iodide (IP).
     - Living cells without annexin but with IP.
     - Living cells with both stains.
     - Dead cells with the same conditions as above.

2 Collect media from plates in a 50 ml *falcon*. Then wash cells twice with PBS and collect everything in the same *falcon*.

3 Add 1 ml of trypsine until cells detach from the plate (3 minutes approximately). Add some ml of media to be able to resuspend cells and mix carefully.

   CAUTION! It is really important to control and exactly reproduce the time of trypsinization and the number of pipettings during the cell detachment.

4 Add the mix of trypsin plus media into the same container as PBS and centrifuge it at 800 x g for 5 minutes. Then discard supernatant and resuspend the pellet in 1 ml of PBS.

5 Count the cells in each condition and transfer the same number of cells to clean *eppendorfs*. Centrifuge all the *eppendorfs* (800 x g, 5 minutes) then discard supernatant and add 200-500 µl of binding buffer (provided with the kit).

☠ **CAUTION!** It's crucial to avoid creating foam in the *eppendorf* during binding buffer washes.

6 Centrifuge again (800 x g, 5 minutes) to not leave any traces of trypsin, PBS, or media. Then add the annexin diluted into binding buffer as follows:
   - For each sample, add 5 µl of annexin and 100 µl of binding buffer
   - Prepare a mix with all the volumes needed for all the samples and distribute.

7 Leave the samples with the annexin in the dark for 10-15 minutes at room temperature, then centrifuge again (800 x g, 5 minutes) and wash with binding buffer again.

8 After last centrifuge, add propidium iodide (IP) mix:
   - 5 µl of IP + 200 µl of binding buffer.
   - Again, first prepare a mix with all the IP solution needed and distribute.

9 After the addition of propidium iodide the samples are ready to perform FACS (fluorescence-activated cell sorting) analysis.

5.3 TUNEL Assay *in vitro*

TUNEL assay was achieved using In Situ Cell Death Detection Kit TMR Red (12 156 792 910, Roche) in osteoblast primary cultures. TUNEL assay is based on the detection of single- and double-stranded DNA breaks that occur at the early stages of apoptosis. TUNEL reaction mixture contains TdT and fluorescein-dUTP that during incubation, TdT catalyzes the addition of fluorescein-dUTP at free 3'-OH groups in single- and double-stranded DNA.

Infected osteoblasts were seeded in coverslips and later treated with or without Tamoxifen during 4 days in order to induce Cre expression. Last day medium was replaced for FBS-free medium for an over-night and next day TUNEL assay was performed. A general view of the protocol is as follows:

1 Fix cells with 4% PFA (in PBS, pH: 7.4) for 1 hour at room temperature.
2 Rinse coverslips with PBS.
3 Incubate with permeabilisation solution (0.1% Triton X-100 in 0.1 sodium citrate buffer) for two minutes on ice (2-8°C).

   👍 Permeabilisation buffer must be fresh!

4 Rinse the coverslips twice with PBS at room temperature.
5 For a positive control, treat one of the coverslips with DNAse 1 hour at room temperature (3,000 U DNAse in 50 mM Tris-HCl, pH: 7.5 plus 1 mg/ml BSA).
6 Add TUNEL reaction mixture and incubate 60 minutes at 37°C in a humidified atmosphere in the dark.

- The total amount of TUNEL reaction mixture will be 50 µl per sample. Count the total number of samples and mix reagents as follows:
  - Half the volume will be TUNEL Dilution Buffer
  - The other half will be 90% labeling solution + 10% enzyme

7 Rinse coverslips 3 times in PBS for 5 minutes each.
8 Add DAPI (1 µg/ml, D9542, Sigma) diluted in PBS and incubate for 20 minutes.
9 Rinse coverslips 3 times in PBS for 5 minutes each.
10 Mount coverslips with ProLong Gold antifade reagent (P36939, Life Technologies).

After mounting, leave the slides rest horizontally in the dark at room temperature and store it at 4°C from then on. The ratio of cells presenting label incorporated in the damaged sites of the DNA can be visualized by fluorescence microscopy (microscope Nikon E800, Scientific and Technological center, Bellvitge).

6 MICE COLONY AND MAINTENANCE

6.1 Mice Generation

Osteoblast-specific *p110α*-deficient mice (*p110α$^{f/f}$;Col1a1-Cre*) were generated by crossing heterozygous *Col1a1-Cre* mice (Tg(*Col1a1-cre*)1Kry from Jackson Lab) (Dacquin et al., 2002) with homozygous mutants carrying loxP sites flanking exons 18 and 19 of the *p110α* alleles (Graupera et al., 2008). *Col1a1-Cre* mice were backcrossed on to C57BL/6 background for 8 generations prior to use. *p110α$^{f/f}$;Col1a1-Cre* mice were fertile and born in the Mendelian ratio, and they were crossed with *p110α$^{f/f}$* to obtain experimental (*p110α$^{f/f}$;Col1a1-Cre*) and control (*p110α$^{f/f}$*) littermates.

The same strategy was used for *p110β$^{f/f}$;Col1a1-Cre* animals (loxP sites flanking exons 21 and 22 of the *p110β* alleles) (Guillermet-Guibert et al., 2008). *p110αβ$^{f/f}$;Col1a1-Cre* mice were generated by crossing *p110α$^{f/f}$; Col1a1-Cre* animals with *p110β$^{f/f}$*.

For the *p110α$^{f/f}$;Osx1-Cre* strain, heterozygous *Osx1-Cre* mice (Tg(*Sp7-tTA,tetO-EGFP/cre*)) from Jackson Lab) (Rodda and McMahon, 2006) were crossed with *p110α$^{f/f}$* animals. The *Osx1-Cre* mouse line contains a tTA and a tetracycline-responsive element that suppresses the expression of Cre recombinase under doxycycline administration. *Osx1-Cre* mouse progenitors were exposed to a doxycycline regime during pregnancy (0.2 mg/ml in drinking water), and once the litter was born, doxycycline was removed maximum 2 days post-delivery.

6.2 Genotyping

Mouse DNA was isolated from a 3-mm piece of mouse tail using NucleoSpin Tissue (740952.250, Macherey-Nagel). A PCR-based genotyping assay was performed to identify every transgenic mouse. Specific primers from Roche were used for each colony (Table M-17).

PCR PRIMERS FOR MICE GENOTYPING		
Name	**Detects**	**Sequence (5'-3')**
ColCrePr1*	*Col1a1-Cre*	CAGTCGTCGGAGCAGACGGGAGT
ColCrePr2*	*Col1a1-Cre*	AATCGCGAACATCTTCAGGTTCTGCG
ColCreDSh*	*Col1a1-Cre*	TCCGTCTCTGGTGTAGCTGATGATCC
ColCreUp*	*Col1a1-Cre*	GATCTCCGGTATTGAAACTCCAGC
OsxCre1	*Osx1a1-Cre*	CTCTTCATGAGGAGGACCCT
OsxTGCK	*Osx1a1-Cre*	GCCAGGCAGGTGCCTGGACAT
Ma36-PI3K1	p110α	CCTAAGCCCTTAAAGCCTTAC
ma47-PI3K2	p110α	ACTGCCATGCAGTGGAGAAGCC
B1B3	p110β	AGTGAACGCTATGCATCACACCAGC
B2B98	p110β	AAGTACAAACATCCAAGCAA

Table M-17. PCR primers for mice genotyping.
*Col1a1-Cre allele was detected by using two possible different set of primers.

The recipe used for the genotyping of the animals is detailed in Table M-18.

GENOTYPING PCR MIX	
Reagent	**Volume**
Genomic DNA from mouse tail	2 µl
My Taq Mix (2x) (BIO-25042, Bioline)	10 µl
Primers	25 pmol for each of the beta primers (B1B3 and B2B98) 12.5 pmol for the rest
Sterile water	Until 20 µl of final volume

Table M-18. Genotyping PCR mix preparation.

GENOTYPING PCR CONDITIONS		
Step	**Time (min)**	**Temperature (°C)**
HOLD	3	94
40 cycles	0:30	94
	0:30	65
	72	0:30
	72	7
HOLD	∞	4

Table M-19. Genotyping PCR conditions.

6.3 Colony Maintenance

Mice were housed under controlled conditions and fed *ad libitum* with water and a 14% protein diet (Teklad 2014, Harlan). Unless otherwise stated, animal experiments were performed in 12 to 14-week-old male mice. When referring to newborn pups, male animals from P2-P7 were used. All procedures were approved by the Ethics Committee for Animal Experimentation of the Generalitat de Catalunya.

7 WORKING WITH MICE

7.1 Tissue Dissection

Generally, tissue dissection was performed with living animals under anesthesia. We used Isoflorane (57132.9, Esteve) as inhalational anesthesia and mice were sacrificed by cervical dislocation after tissue removal.

Mainly, the tissues obtained during the experiments accomplished in this thesis were: calvaria, brain, liver, kidneys, epididymal fat pad, heart, hindlimb, gastrocnemius muscle and brain.

When tissue was obtained for further RNA or protein extraction, samples were immediately submerged in liquid nitrogen and subsequently stored at -80°C. For other purposes, samples were kept in 4% paraformaldehyde (PFA).

7.2 Serum Analysis

7.2.1 Blood collection

Blood collection was achieved from the posterior vena cava. It was the first procedure performed once the animal was anesthetized and the abdomen was cleaned with ethanol. The protocol followed for vena cava exposure was:

1. Open the abdominal cavity making a V–cut through the skin and the abdominal wall (Figure M-1-1).
2. Move the intestines to the right side and pull the liver forward a little bit (Figure M-1-2).
3. Between two of the liver lobes you can locate the thickest part of the posterior vena cava (Figure M-1-3).
4. Using a 25-gauge needle and 1 ml syringe, insert the needle slowly and draw blood slowly. Pause from time to time if the vessel wall collapses until no more blood is available (Figure M-1-4).

> Pull and tight the plunger a few times before inserting the needle into the vein otherwise the plunger is normally excessively stacked and you will need extra force to start drawing blood.

5 Pour the blood into a sterile *eppendorf* and let it coagulate at room temperature (1-3 hours).

6 Then centrifuge *eppendorfs* (1,500 x g, 5 minutes, 4°C). Transfer supernatant to a new tube and centrifuge again (1,500 x g, 5 minutes, 4°C).

Serum was stored in 55 µl aliquots (PCR *eppendorfs*) at -80°C until needed.

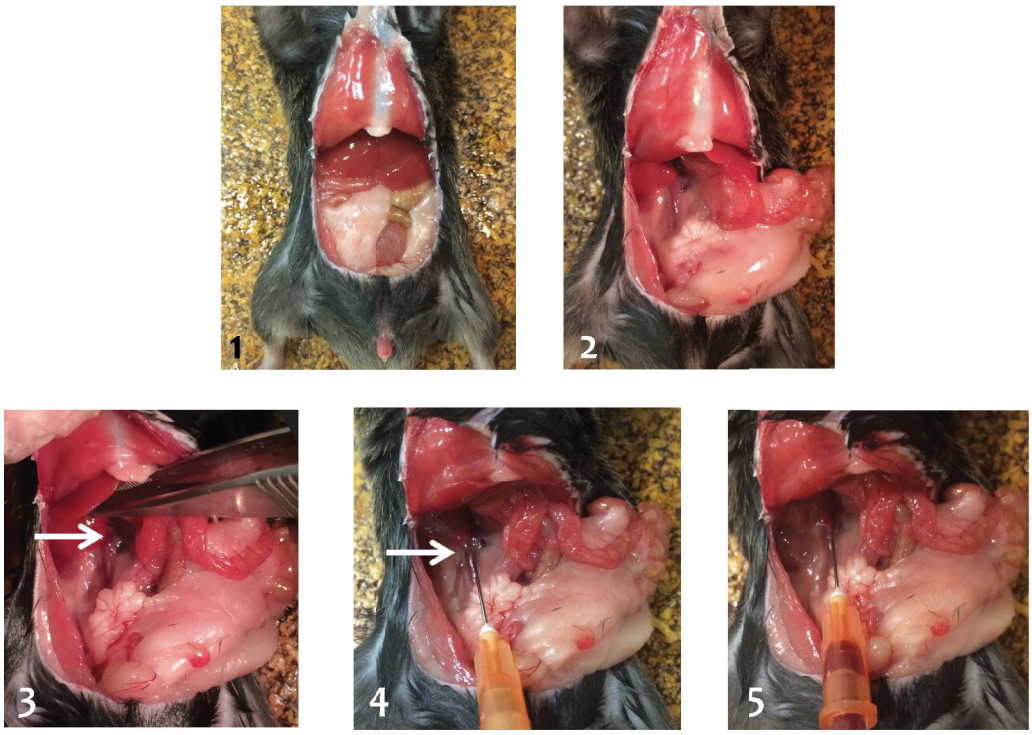

Figure M-1. Blood extraction procedure. Blood was obtained from the posterior vena cava. **(1)** The abdominal cavity is opened performing a V-cut through the skin and the abdominal wall. **(2)** The intestines are displaced to the right side in order to approach puncture site. **(3)** Posterior vena cava is recognized between the liver lobes. **(4&5)** Insert a 25-gauge needle and slowly draw blood.

7.2.2 Biochemical determinations

The analysis of serum values (alkaline phosphatase, calcium, iron and phosphorous) was performed by the staff of the Servei de Bioquímica Clínica, Facultat de Veterinària (Universitat Autònoma de Barcelona).

7.2.3 NTX determination

NTX (N- terminal telopeptide of type I collagen) was quantified using the mouse crosslinked N-telopeptide of type I collagen Elisa Kit (CSB-E09242) from Cusabio following the manufacturer`s instructions.

8 X-RAY MICRO COMPUTED TOMOGRAPHY (MICRO-CT)

8.1 Imaging

Long bones from mice were dissected, cleaned of soft tissue and fixed in 4% PFA for 24 hours.

High-resolution images from the femur and tibia were acquired using a micro tomographic imaging system (Skyscan 1076; Sky-scan) in accordance with the recommendations of the American Society for Bone and Mineral Research (ASBMR).

Samples were scanned in air at 50 kV and 200 µA with an exposure time of 800 ms, using a 1-mm aluminum filter and an isotropic voxel size of 9 µm. Two-dimensional images were obtained every 0.6° for 180° rotation.

8.2 Reconstruction and General Measurements

Two-dimensional captures were subsequently reconstructed in order to later obtain 3D images using *NRecon* reconstruction software. µCT analyses were carried out with the *CT-Analyser* (SkyScan).

For trabecular measurements, manual VOI was employed, starting at 100 slices from the distal growth plate of the femur and extending to the diaphysis for 150 slices. Thus,

ROI was manually drawn every 25 stacks. Cortical measurements were performed by delineating the femur medial cortex for 100 slices around the femoral midshaft.

A Gaussian noise filter was applied for the reconstruction and a global binary minimum threshold was manually established at 15 for trabecular analysis and 100 for cortical analysis. Moreover, reconstruction was performed under the following parameters:

- Automatic misalignment
- Beam hardening: 31%
- Ring artifacts correction: 8
- Threshold defect pixel masking: 5%

8.3 Bone Mineral Density Measurement

In order to determine the bone mineral density of the samples, we scanned two different phantoms fitting with the size of the mice long bones (2 mm diameter approximately). Once two-dimensional images were obtained under the same settings as samples, the reconstruction was achieved with the same software conditions as for trabecular measurements.

The phantoms used are made of hydroxyapatite and they have a known density of 0.75g/cm^3 and 0.25g/cm^3. This allowed us to compare our samples with known densities achieving a real bone mineral density value for our samples.

9 HISTOMORPHOMETRIC ANALYSIS

9.1 Tissue Preparation

Bone tissues for histomorphometric analysis must be fixed and processed prior to paraffin or methacrylate embedding. First, soft tissue has to be removed in both cases.

9.1.1 Paraffin processing of tissue

1 Bone tissue must be fixed by infusion using fresh 4% PFA. Fix the tissue just after isolation and for 24 hours at 4°C. Normally 10 ml of PFA are enough to fix hindlimbs, vertebrae and/or calvariae.

2 Wash briefly with PBS for 1 hour (use shaker). If tissue is not going to be processed immediately, place in PBS + azida (50 µg/ml) for long storage.

3 Bone must be decalcified or else it will not be cut by the microtome. Different techniques can be used to achieve decalcification:

- Decalcifier II (00460, Surgipath): commercial solution made of EDTA and HCl. After PBS washing, samples are placed in 10 ml of Decalcifier solution for 3 days. Useful for a prompt decalcification.

  If bones are not properly decalcified after 3 days, change for fresh solution and leave samples for some more days.

  CAUTION! This solution is not useful for some stains (i.e. TRAP) because HCl can impede further reactions.

- 16% EDTA: bones can alternatively be decalcified using EDTA for 10-15 days (replacing new EDTA every 3-5 days). This method is slower but it allows all kinds of histological stains.

  If you are not sure of the stains you will perform, better use this decalcification system.

4 Dehydrate samples in increasing concentrations of ethanol. The aim of this protocol is to displace the water from the tissue to further infiltrate it with the wax.
   - 30% ethanol, 1 hour
   - 60% ethanol, 1 hour
   - 70% ethanol, overnight
   - 90% ethanol, 1 hour
   - 100% ethanol, 1 hour
   - 100% ethanol, 1 hour
   - 100% ethanol, 1 hour
   - Butyl alcohol overnight
   - Xylene clearing:
   - Xylene I, 1 hour
   - Xylene II, 1 hour
   - Xylene III, 1 hour
5 Paraffin embedding:
   - Paraffin I, 4 hours
   - Paraffin II, overnight

    Steps 4 to 5 can be all carried out automatically in a tissue-processing machine. Bones should be placed in histological cassettes to facilitate the process.

6 Preparation of the tissue cassettes.
   - Paraffin III. Cassettes are immersed in a paraffin bath (65 °C). Individually, each cassette is prepared over a cold plate. A little bit of liquid paraffin is poured in a metal mold. Once it is starting to cold, the sample is correctly placed and part of the cassette is then used to fix the sample. Some more paraffin is added to fill up the cassette. Once the piece is totally cold (30 minutes, 4°C) the paraffin cassette can be unmolded.
   - Leave the paraffin cassette in the fridge (4°C) until microtome sectioning.
7 Microtome sectioning:
   - The microtome has a mechanism for advancing the block across the knife. The distance (and therefore the thickness of the section) is usually set at 4-5 microns for paraffin embedded tissues.
   - Remove the excess of paraffin surrounding the sample with a knife.
   - Let the tissue blocks to cool in the freezer for half an hour prior to sectioning. That will help to obtain nicer sections.

- Place the paraffin block in the microtome and cut the sections. Serial sections are obtained at once (4-5). Leave the chain of sections floating on a warm water bath, which will help to remove wrinkles.
- Pick up sections from the water bath using a glass microscopic slide. If the floating paraffin is too long, break it in two pieces before picking them up.

  Glass slides must be treated three times with poly-L-Lysine (P8920, Sigma) in order to allow a stronger interaction with the paraffin sections. That will avoid loss of sections during routine histologic staining procedures. For the poly-L-Lysine treatment proceed as follows:

  - Pour a drop of diluted poly-L-lysine solution in a clean slide and place a second slide above.
  - Let the poly-L-lysine for 5 minutes
  - Dry slides at 60°C for one hour or at room temperature overnight.
  - Repeat the procedure thrice.
  - Store the poly-L-lysinated slides at 4°C.

8 Place the glass slides in a warm oven (37°C) overnight. If proceeding directly to staining/immuno protocols, put them in a 60°C oven for 30 minutes and start directly with the hydration protocol.

9.1.2 Methacrylate processing of tissue for routine examination of undecalcified bone

1 Tissue must be fixed by infusion using fresh 4% PFA. Fix the tissue just after isolation and for 24 hours at 4°C. Normally 10 ml of PFA are enough to fix hindlimbs, vertebrae or calvariae.

2 Dehydrate samples in increasing concentrations of ethanol:
- 30% ethanol, 24 hours
- 60% ethanol, 24 hours
- 80% ethanol, 24 hours
- 96% ethanol, 24 hours
- 100% ethanol, 24 hours
- 100% ethanol, 24 hours
- 100% Xylene, 24 hours
- Technovit 7200, 24 hours
- Technovit 7200, 14 days (protected from light)

We used glycolmethacrylate (Technovit 7200 VLC, 8038347, Leica) but different resins can be used to produce hard blocks. Initially, resins are fluid and infiltrate the tissue after dehydration, solidifying later during polymerization.

CAUTION! Technovit is eye and skin irritating!

3 Preparation of the tissue blocks and polymerization:
   - The tissue must be placed in an appropriate embedding mold that will not react with the resin.
   - After placing the sample, new clean Technovit 7200 is used to cover and fill the mold.

     👍 Identify each sample by inserting a little piece of paper with the name just prior to polymerization. Pencil writing is ok!

4 Subsequently, Technovit polymerization is performed by light exposure using the photopolymerization unit Histolux (Exact, Kulzer) in two stages. During the first stage the embedding medium is polymerized almost completely at a low light intensity so that the polymerization temperature does not exceed 40° C and no cracks will form (white light, 2 hours). The final polymerization is done at high light intensity (UV light, 4 hours) during the second stage. Total polymerization time is 6 hours.

5 Microtome sectioning: due to the hardness of the undecalcified tissue and the plastic block, methacrylate-embedded samples are sectioned with glass or diamond knives.

     👍 We used a diamond microtome from the microscopy services of CCiT-UB (Servei de crio-microscòpia electrònica, centres científics i tecnològics, UB), located at Parc Científic de Barcelona (PCB).

6 In order to place the plastic block into the microtome (from CCiT-UB) it should fit the holder. That is, the piece must measure at maximum 0.6 x 0.7 x 1 cm.

7 Use a Dremel with a PVC specific cutting accessory (SC476) to achieve the measures and to polish the piece. The tissue must be exposed during this process.

     ☠ **CAUTION!** Protect yourself from methacrylate residues using globes, glasses and coat during Dremel manipulation. Hot shavings will pop-out!

8 Methacrylate sectioning:
   - Diamond knife allows slides from 1.2 to 1.7 microns.
   - Use special glass slides for methacrylate slices. Menzel-Gläser superfrost plus microscope slides (J1800AMNZ, Thermo Scientific) were used to increased plastic adhesion and to avoid excessive background in later staining procedures.

9.2 Histological Stains

For almost all histological stains using paraffin-embedding sections, slides should be free of wax and rehydrated prior to protocol procedure. This standard protocol is as follows:

1 Dewax:
   - Place all the slides in a bucket and leave it in the oven (60°C) for 30 minutes.
   - Xylene I, 2 minutes
   - Xylene II, 2 minutes
2 Hydrate:
   - 100% ethanol, 2 minutes
   - 96% ethanol, 2 minutes
   - 80% ethanol, 2 minutes
   - 70% ethanol, 2 minutes
   - Distilled water, 2 minutes

     👍 If waiting for starting the staining protocol, leave the bucket of slices in PBS better than in distilled water.

After the majority of the stains, a dehydration procedure is also needed before mounting:

1 Dehydrate:
   - 96% ethanol, seconds
   - 96% ethanol, seconds
   - 100% ethanol, seconds
   - 100% ethanol, 3 minutes
   - Ethanol-Xylene 50:50, 2 minutes
   - Xylene I, 3 minutes
   - Xylene II, 3 minutes
   - Xylene III, 3 minutes
2 Mount immediately with DPX mounting media.

9.2.1 Hematoxylin-Eosin (paraffin & methacrylate)

After dewaxing and rehydrating samples to distilled water:

1 Place in Harris' hematoxylin for 3.5 minutes.
2 Wash with tap water.
3 Wash in acidic alcohol.
4 Clean with tap water.
5 Place in ammoniacal water (0.03% ammonium) for a few seconds.
6 Wash with tap water for 5 minutes.
7 Rinse in 70% ethanol (a few seconds).
8 80% ethanol (a few seconds).
9 Place in eosin bucket for 1.5 minutes.
10 Wash in dH20 (a few seconds).

Dehydrate slides and mount coverglasses.

Working solutions

Eosin

- Stock: 1 g eosin Y (yellowish) in 20 ml dH20.
- Working solution:
  - 200 ml stock solution + 600 ml 80% ethanol.
  - Add 0.5% glacial acetic acid just before use.

Harris hematoxylin

- Solution A: 5 g hematoxylin (mw: 302,3g/mol) + 50 ml 95% ethanol.
- Solution B: 183.6 g potassium alum (potassium aluminum sulfate) + 950 ml H20 + 2.5 g mercuric oxide.

Mix both solutions, add 1 g of potassium iodide and let it rest for 24 hours in order to allow artificial maturation. Next day add 20 ml of glacial acetic acid. For a natural maturation you should wait 3 months before use it.

9.2.2 Toluidin blue (paraffin & methacrilate)

Deparaffinize and hydrate samples to distilled water, then:

1. Place in toluidine blue for 30 seconds.
2. Dehydrate slides and mount coverglass.

Working solutions

Toluidine blue

Mix solution A and solution B as follows:

- Solution A:
  - 8 g sodium tetraborate (Borax)
  - 8 g toluidine blue
  - 800 ml dH20
- Solution B:
  - 8 g Pyronin G
  - 200 ml dH20

9.2.3 Goldner's Masson trichrome (paraffin)

After dewaxing, hydrate samples to distilled water, then:

1 Place in Weigert's Hematoxylin for 10 minutes.
2 Wash in running tap water for 10 minutes.
3 Rinse in distilled water.
4 Stain in Masson solution for 5 minutes.
5 Wash in 1% acetic acid.
6 Place in phosphomolybdic acid-orange G solution until collagen is decolorized.
7 Wash in 1% acetic acid (30 seconds).
8 Place in light green for 5 minutes.
9 Rinse in 1% acetic acid, 5 minutes.
10 Dehydrate slides and mount coverglasses.

Stain results

- Nuclear chromatin: brownish black
- Cytoplasm: bright red
- Erythrocytes: orange
- Muscle: red
- Collagen: green

9.2.4 Goldner`s Masson trichrome (methacrylate)

Hydrate samples to distilled water, then:

1 Place in Harris' hematoxylin for 15 minutes at 60°C. Original Weigert's hematoxylin staining produce a dark background difficult to eliminate in plastic embedded samples.
2 Wash in running tap water until clean.
3 Rinse in distilled water.
4 Stain in Masson solution for 7 minutes.
5 Wash in 2% acetic acid.
6 Place in phosphomolybdic acid-orange G solution until collagen is decolorized (5 minutes).
7 Wash in 2% acetic acid.
8 Place in light green for 15 minutes at 60°C.
9 Wash in 2% acetic acid.
10 Wash in distilled water for 5 minutes.
11 Dehydrate slides and mount coverglass.

Stain results

- Nuclear chromatin: dark blue

- Cytoplasm: bright red
- Muscle: red
- Collagen: green

Working solutions (both paraffin & methacrylate sections)

Weigert's hematoxylin

- Weigert's iron hematoxylin A:
  - 5 g hematoxylin
  - 1 g potassium iodate
  - 500 ml absolute ethanol
- Weigert's iron hematoxylin B:
  - 20 ml ferric chloride, 30% aqueous
  - 5 ml hydrochloric acid, 35%
  - 475 ml dH20

Both solutions are stable for one year. Mix equal parts of A and B prior to use. Mixed solution will remain stable for 3-4 days, do not keep pre-made working solution.

Masson solution

- Stock solutions
  - Acid fuchsin: 1 g acid fuchsin, 100ml $_dH_2O$, 1 ml acetic acid
  - Ponceau Xylidine: 1 g ponceau xylidine, 100 ml $_dH_2O$, 1 ml acetic acid
  - Azophloxine: 0.5 g azophloxine, 100ml $_dH_2O$, 0.2 ml acetic acid
- Final working solution:
  - 33 ml acid fuchsin + 66 ml ponceau xylidine + 20 ml azophloxine
  - 880 ml glacial acetic acid

    👍 Working solution is re-usable.

Phosphomolybdic acid/Orange-G solution

- Add 10 g of Orange G to 500 ml $_dH_2O$ and dissolve
- 15 g phosphomolybdic acid

    👍 Solution is stable for 6 months.

Light green solution

- 0.5 g light green
- 1 ml acetic acid
- 500 ml $_dH_2O$

    👍 Working solution is re-usable.

9.3 TRAP (tartrate-resistant acid phosphatase)

This stain can be used in paraffin and methacrylate sections. After dewaxing and hydrating samples to distilled water:

1 Warm 500 ml basic incubation solution (BI solution) to 37°C (oven).
2 Use this pre-warmed solution to fill 2 staining buckets, each with 200 ml of BI solution. Leave BI solution at 37°C while slides are going through dewaxing/ rehydration process.
3 Take 1 bucket and add 2 ml of napthol-ether substrate to the BI solution. Place slides into the bucket and incubate at 37°C for 1 hour (oven).
4 A few minutes before incubation time is up, mix 4 ml sodium nitrite solution and 4 ml pararosaniline dye. Mix gently by hand for 30 seconds and then let sit for 2 minutes.
5 Add this solution to the second pre-heated bucket of BI solution, mix well and transfer the incubated slides from the first bucket to the second one without rinsing. Develop at 37°C for 5-12 minutes. Check periodically under microscope during development for desired intensity of red in osteoclasts and proceed immediately to next step if tissue shows any non-specific red stain.

   For paraffin embedded tissues the estimated time will be 4 minutes, for methacrylate, 7.

6 Rinse 3 times with distilled water.
7 Counterstain with a 0.02% fast green solution for 45 seconds.
8 Rinse with distilled water.
9 Dehydrate as follows:
   - 95% ethanol, 45 seconds.
   - 2 x 100% ethanol, 45 seconds each.
10 Clear in 3 changes of Xylene and coverslip.

Stain results

- Osteoclasts: bright red.
- Background: green.

Working solutions

Basic stock incubation medium

- 9.2 g sodium acetate, anhydrous
- 11.4 g sodium tartrate, dibasic dehydrate
- 1000 ml $_dH_2O$
- 2.8 ml glacial acetic acid

Dissolve and adjust PH to 4.7 – 5.0 with 5 M sodium hydroxide. Stable for 6 months at room temperature.

Naphtol AS-BI phosphate substrate

- 0.1 g Naphtol AS-BI Phosphate (N2125, Sigma)
- 5 ml 2-Ethoxiethanol (128082, Sigma)

Dissolve and store at 4°C for 5 weeks. For one bucket of slides (200 ml), half of the Naphtol AS-BI phosphate is enough (50 mg Naphtol + 2.5 ml 2-Ethoxiethanol).

Sodium nitrite

Dissolve 1 g sodium nitrite ($NaNO_2$) in 25ml distilled water. Store at 4°C.

Pararosaniline Dye

Dissolve 1 g Pararosaniline Dye in 20 ml 2M HCl (83 ml HCl [36.5-38.0%] in 417 ml distilled water). Mix well and filter before use.

9.4 Calcein

In bone tissue study, fluorochromes are used for the assessment of cancellous or endocortical bone turnover and the measurement of the bone rate formation and resorption (van Gaalen et al., 2010).

Fluorochrome labels, when bound to calcium ions, can be incorporated at sites of mineralization in the form of hydroxyapatite crystals. This means that the label indicates all sites of mineralization in the body. In the first 24-36 hours after administration the label is stabilized and the kidneys rapidly excrete the unincorporated label. As a result, the fluorescent label demarcates the mineralization front at the time of administration and can be detected in histological sections without any further staining or decalcification. If labels are administrated at different times, bone formation rate can be also measured.

We used calcein green as fluorochorme (C0875, Sigma) diluted in 2% $NaHCO_3$. We injected the animals subcutaneously with a dosage of 10mg/Kg of fresh made and filtered calcein. The injection was done the day 7 and 2 before sacrifice. At the moment of sacrifice, bones were dissected as usual and left for 24 hours in 4% PFA before starting the protocol for plastic embedding (methacrylate) seen in section 9.1.2.

After methacrylate sectioning, fluorescence microscopy is used to take representative images and to assess different bone dynamic values. Some parameters are defined below:

- **MS (Mineralizing Surface).** The extent of bone surface actively mineralizing.

$$MS = \left(dLs + \frac{sLS}{2}\right)/BS$$

Where dLS means double labeled surfaces and sLS single labeled surfaces (µm). BS corresponds to the total extent of bone surface.

- **MAR (Mineral Apposition Rate).** Rate at which osteoblasts are making matrix, which calcifies at a constant rate and incorporates the labels.

$$MAR = {}^{Ir.L.Th}/_{Ir.L.t}$$

Where Ir.L.Th is the distance between labels (µm) and Ir.L.t the time between injections of labels (days).

- **BFR (Bone Formation Rate).** It takes into account how much of the bone surface is actively mineralizing, which depends on the number of OBs that are active.

$$BFR = MAR \times (MS/BS)$$

9.5 Ki-67 Immunochemistry (paraffin)

After dewaxing and rehydrating samples to distilled water:

1. Antigen retrieval: heat 500 ml of citrate buffer 0.01 M in a beaker until boiling, then introduce the samples for 10 minutes. Remove the beaker from the heater and let the samples to cool slowly (inside the buffer) for 20 minutes.
2. Wash with phosphate buffer pH: 7.4 0.1 M, 5 minutes.
3. Permeabilize sections for 5 minutes with PBS + 0.2% Triton X-100.
4. Wash again with phosphate buffer, 5 minutes.
5. Block endogenous peroxidase activity. All cells have some (especially erythrocytes). Perform the blocking mix using 160 ml PBS + 20 ml methanol + 20 ml 30% hydrogen peroxidase.

   ☠ **CAUTION!** Be careful with 30% H_2O_2, it is highly concentrated and it burns your skin!

6. Wash with PBS, 3 times x 5 minutes.

   👍 If using PAP pen to delimitate the samples, now is the moment.

7. Avoid unspecific signal by blocking with serum from the same species used to produce the secondary antibody (normally NGS – normal goat serum) 1 hour at room temperature. Dilution 1:30 should be done using PBS. Calculate 80-120 µl per slide.

8 Apply primary antibody. Calculate a total volume of 80-120 µl per slide. Normally, primary antibodies are prepared using PBS + 0.1% NGS.

- Anti-Ki67 antibody was a gift from Dr. Francesc Viñals and it was already diluted in a ready-to-use solution. Suggested solution for the same anti-Ki67 antibody is 1:100-1:200 (Ki67-clone SP6- from Thermo Scientific).

  👍 A little piece of parafilm can be used in the top of the antibody in order to cover the entire sample with a single drop. Slides should be placed in a humid chamber overnight at 4°C.

9 Next day, allow the slides to warm at room temperature for 1 hour.

10 Wash with PBS, 3 x 5 minutes

11 Prepare secondary antibody. Anti-Ki67 is a rabbit monoclonal antibody. Use a 1:100 dilution in PBS 0.1% NGS. Let the samples 1 hour at room temperature in the humid chamber.

  👍 Our secondary antibodies are biotinylated and do not carry peroxidase.

12 Wash with PBS 3 x 5 minutes

13 Add streptavidin (which carries peroxidase) 1:400 in PBS 0.1% NGS, 1 hour at room temperature.

14 Wash again with PBS 3 x 5 minutes.

15 Develop reaction with DAB (diaminobenzidine). Peroxidase enzyme will use DAB as a substrate and will oxidize it, producing an easily observable brown color. The peroxidase breaks the hydrogen peroxide into water and oxygen is used to oxidize the DAB, which will pass from soluble to insoluble (precipitating). For one bucket (200 ml):

- PBS, 200ml
- 1% DAB → introduce the bottom of a crystal Pasteur pipette into DAB until the indent, then pour it in the PBS.

  👍 If DAB is in good conditions it should not change the color of PBS.

  ☠ **CAUTION!** DAB is very toxic. Be careful when manipulating it and with all the material used in contact with it.

- Dissolve DAB and filter.

  👍 This step is very important!! Otherwise DAB will appear as big solutes in the tissue and will dirt the preparation.

- Incubate the slides with the filtered solution for 5 minutes. Then, add 200 µl 30% H_2O_2 directly into the bucket and incubate at room temperature in the dark.
- The total incubation time is relative, but 10-20 minutes is normally enough for most of the antibodies. The intensity of the color will not further increase after 45 minutes.

16 Wash with PBS for 5 minutes.
17 Rinse with distilled water.
18 Place the slides in a hematoxylin bucket for seconds. It is important not to dye excessively with hematoxylin in order to not hide the DAB signal. Hematoxylin is used just to help in the identification of anatomical structures.
19 Rinse with tap water. Place the bucket down the tap and allow water to slowly run into it until water runs clear.
20 Dehydrate slides and mount coverglass.

Working solutions

Citrate Buffer (1X)

- 2.1 g citrate acid
- 900 ml distilled water
- Adjust to pH: 6 and complete to 1 liter.

Phosphate Buffer (0.4M)

- 10.6 g NaH_2PO_4 (9.2g $NaH_2PO_4 \cdot 2H_2O$)
- 56 g K_2HPO_4
- 1 liter distilled water. It is not necessary to adjust pH, it should be directly 7.3-7.4

9.6 TUNEL assay *in vivo*

TUNEL assays were performed in paraffin-embedded samples from newborn mice. The bases of the technique are summarized in section ·5.3. We followed the manufacturer's protocol as described in "labeling protocol for difficult tissue" section having special considerations:

1 Dewax tissue sections by standard procedure.
2 Wash slides with PBS.
3 Proteinase K treatment: use 15 µg/ml of proteinase K diluted in 10 mM Tris. Incubate for 30 minutes at 37°C.
4 Rinse the slides twice with PBS at room temperature.
5 Perform a positive control: treat with DNAse 10 minutes at room temperature (3,000 U DNAse in 50mM Tris-HCl, pH: 7.5 plus 1mg/ml BSA).
6 Add TUNEL reaction mixture and incubate 60 minutes at 37°C in a humidified atmosphere in the dark.

👍 The total amount of TUNEL reaction mixture will be 50 µl per sample. Count the total number of samples and mix reagents as follows:

- Half the volume will be TUNEL Dilution Buffer

- The other half will be 90% labeling solution + 10% enzyme

7 Rinse slides three times in PBS for 5 minutes each.
8 Add DAPI (1 µg/ml) diluted in PBS and incubate for 20 minutes.
9 Rinse slides three times in PBS for 5 minutes each.
10 Mount coverslip with ProLong Gold antifade reagent (Life Technologies).

Samples were analyzed using Nikon microscope E800.

10 STATISTICAL ANALYSIS

The results are always expressed as the mean ± SEM. Unpaired, two-tailed Student's *t* test was employed for statistical analysis. Differences were considered significant at p values lower than 0.05: *p<0.05, **p<0.01, and ***p<0.001. When # symbols were used to distinguish different statistic analysis within the same figure, significance is detailed in the figure legend.

GraphPad Prism 5.0a and 6.0c software was used for graph representations and statistical analysis.

Pequeña alegría de laboratorio#7

Tirar el medio de un 12-well volcando la placa y que los cubres para las inmunos no se caigan.

REFERENCES

A

Acampora, D., Merlo, G.R., Paleari, L., Zerega, B., Postiglione, M.P., Mantero, S., Bober, E., Barbieri, O., Simeone, A., and Levi, G. (1999). Craniofacial, vestibular and bone defects in mice lacking the Distal-less-related gene Dlx5. Development *126*, 3795-3809.

Akiyama, H., Chaboissier, M.C., Martin, J.F., Schedl, A., and de Crombrugghe, B. (2002). The transcription factor Sox9 has essential roles in successive steps of the chondrocyte differentiation pathway and is required for expression of Sox5 and Sox6. Genes & development *16*, 2813-2828.

Akiyama, H., Kim, J.E., Nakashima, K., Balmes, G., Iwai, N., Deng, J.M., Zhang, Z., Martin, J.F., Behringer, R.R., Nakamura, T., *et al.* (2005). Osteo-chondroprogenitor cells are derived from Sox9 expressing precursors. Proceedings of the National Academy of Sciences of the United States of America *102*, 14665-14670.

Akiyama, T., and Tanaka, S. (2011). Bim: guardian of tissue homeostasis and critical regulator of the immune system, tumorigenesis and bone biology. Archivum immunologiae et therapiae experimentalis *59*, 277-287.

Alessi, D.R., Caudwell, F.B., Andjelkovic, M., Hemmings, B.A., and Cohen, P. (1996). Molecular basis for the substrate specificity of protein kinase B; comparison with MAPKAP kinase-1 and p70 S6 kinase. FEBS letters *399*, 333-338.

Ambrogini, E., Almeida, M., Martin-Millan, M., Paik, J.H., Depinho, R.A., Han, L., Goellner, J., Weinstein, R.S., Jilka, R.L., O'Brien, C.A., *et al.* (2010). FoxO-mediated defense against oxidative stress in osteoblasts is indispensable for skeletal homeostasis in mice. Cell metabolism *11*, 136-146.

Anderson, H.C., Sipe, J.B., Hessle, L., Dhanyamraju, R., Atti, E., Camacho, N.P., and Millan, J.L. (2004). Impaired calcification around matrix vesicles of growth plate and bone in alkaline phosphatase-deficient mice. The American journal of pathology *164*, 841-847.

Arcaro, A., and Wymann, M.P. (1993). Wortmannin is a potent phosphatidylinositol 3-kinase inhibitor: the role of phosphatidylinositol 3,4,5-trisphosphate in neutrophil responses. The Biochemical journal *296 (Pt 2)*, 297-301.

Artigas, N., Urena, C., Rodriguez-Carballo, E., Rosa, J.L., and Ventura, F. (2014). Mitogen-activated protein kinase (MAPK)-regulated interactions between Osterix and Runx2 are critical for the transcriptional osteogenic program. The Journal of biological chemistry *289*, 27105-27117.

B

Backer, J.M. (2010). The regulation of class IA PI 3-kinases by inter-subunit interactions. Current topics in microbiology and immunology *346*, 87-114.

Bafico, A., Liu, G., Yaniv, A., Gazit, A., and Aaronson, S.A. (2001). Novel mechanism of Wnt signalling inhibition mediated by Dickkopf-1 interaction with LRP6/Arrow. Nature cell biology *3*, 683-686.

Baglio, S.R., Devescovi, V., Granchi, D., and Baldini, N. (2013). MicroRNA expression profiling of human bone marrow mesenchymal stem cells during osteogenic differentiation reveals Osterix regulation by miR-31. Gene *527*, 321-331.

Bartel, D.P. (2004). MicroRNAs: genomics, biogenesis, mechanism, and function. Cell *116*, 281-297.

Bi, L., Okabe, I., Bernard, D.J., and Nussbaum, R.L. (2002). Early embryonic lethality in mice deficient in the p110beta catalytic subunit of PI 3-kinase. Mammalian genome : official journal of the International Mammalian Genome Society *13*, 169-172.

Bi, L., Okabe, I., Bernard, D.J., Wynshaw-Boris, A., and Nussbaum, R.L. (1999a). Proliferative defect and embryonic lethality in mice homozygous for a deletion in the p110alpha subunit of phosphoinositide 3-kinase. The Journal of biological chemistry *274*, 10963-10968.

Bi, W., Deng, J.M., Zhang, Z., Behringer, R.R., and de Crombrugghe, B. (1999b). Sox9 is required for cartilage formation. Nature genetics *22*, 85-89.

Bi, W., Huang, W., Whitworth, D.J., Deng, J.M., Zhang, Z., Behringer, R.R., and de Crombrugghe, B. (2001). Haploinsufficiency of Sox9 results in defective cartilage primordia and premature skeletal mineralization. Proceedings of the National Academy of Sciences of the United States of America *98*, 6698-6703.

Blahna, M.T., and Hata, A. (2012). Smad-mediated regulation of microRNA biosynthesis. FEBS letters *586*, 1906-1912.

Borchert, G.M., Lanier, W., and Davidson, B.L. (2006). RNA polymerase III transcribes human microRNAs. Nature structural & molecular biology *13*, 1097-1101.

Boskey, A.L., Moore, D.J., Amling, M., Canalis, E., and Delany, A.M. (2003). Infrared analysis of the mineral and matrix in bones of osteonectin-null mice and their wildtype controls. Journal of bone and mineral research : the official journal of the American Society for Bone and Mineral Research *18*, 1005-1011.

Briata, P., Lin, W.J., Giovarelli, M., Pasero, M., Chou, C.F., Trabucchi, M., Rosenfeld, M.G., Chen, C.Y., and Gherzi, R. (2012). PI3K/AKT signaling determines a dynamic switch between distinct KSRP functions favoring skeletal myogenesis. Cell death and differentiation *19*, 478-487.

Britanova, O., Akopov, S., Lukyanov, S., Gruss, P., and Tarabykin, V. (2005). Novel transcription factor Satb2 interacts with matrix attachment region DNA elements in a tissue-specific manner and demonstrates cell-type-dependent expression in the developing mouse CNS. The European journal of neuroscience *21*, 658-668.

Bruce, D.L., and Sapkota, G.P. (2012). Phosphatases in SMAD regulation. FEBS letters *586*, 1897-1905.

Burke, J.E., and Williams, R.L. (2015). Synergy in activating class I PI3Ks. Trends in biochemical sciences *40*, 88-100.

C

Cantley, L.C. (2002). The phosphoinositide 3-kinase pathway. Science *296*, 1655-1657.

Cantley, L.C., and Neel, B.G. (1999). New insights into tumor suppression: PTEN suppresses tumor formation by restraining the phosphoinositide 3-kinase/AKT pathway. Proceedings of the National Academy of Sciences of the United States of America *96*, 4240-4245.

Cao, S., Xiao, L., Rao, J.N., Zou, T., Liu, L., Zhang, D., Turner, D.J., Gorospe, M., and Wang, J.Y. (2014). Inhibition of Smurf2 translation by miR-322/503 modulates TGF-beta/Smad2 signaling and intestinal epithelial homeostasis. Molecular biology of the cell *25*, 1234-1243.

Cardone, M.H., Roy, N., Stennicke, H.R., Salvesen, G.S., Franke, T.F., Stanbridge, E., Frisch, S., and Reed, J.C. (1998). Regulation of cell death protease caspase-9 by phosphorylation. Science *282*, 1318-1321.

Carthew, R.W., and Sontheimer, E.J. (2009). Origins and Mechanisms of miRNAs and siRNAs. Cell *136*, 642-655.

Celil, A.B., and Campbell, P.G. (2005). BMP-2 and insulin-like growth factor-I mediate Osterix (Osx) expression in human mesenchymal stem cells via the MAPK and protein kinase D signaling pathways. The Journal of biological chemistry *280*, 31353-31359.

Celil, A.B., Hollinger, J.O., and Campbell, P.G. (2005). Osx transcriptional regulation is mediated by additional pathways to BMP2/Smad signaling. Journal of cellular biochemistry *95*, 518-528.

Chen, D., Zhao, M., and Mundy, G.R. (2004). Bone morphogenetic proteins. Growth factors *22*, 233-241.

Chen, Q., Liu, W., Sinha, K.M., Yasuda, H., and de Crombrugghe, B. (2013). Identification and characterization of microRNAs controlled by the osteoblast-specific transcription factor Osterix. PloS one *8*, e58104.

Choi, Y.H., Gu, Y.M., Oh, J.W., and Lee, K.Y. (2011). Osterix is regulated by Erk1/2 during osteoblast differentiation. Biochemical and biophysical research communications *415*, 472-478.

Choi, Y.H., Kim, Y.J., Jeong, H.M., Jin, Y.H., Yeo, C.Y., and Lee, K.Y. (2014). Akt enhances Runx2 protein stability by regulating Smurf2 function during osteoblast differentiation. The FEBS journal *281*, 3656-3666.

Chong, P.A., Lin, H., Wrana, J.L., and Forman-Kay, J.D. (2010). Coupling of tandem Smad ubiquitination regulatory factor (Smurf) WW domains modulates target specificity. Proceedings of the National Academy of Sciences of the United States of America *107*, 18404-18409.

Conner, J.R., and Hornick, J.L. (2013). SATB2 is a novel marker of osteoblastic differentiation in bone and soft tissue tumours. Histopathology *63*, 36-49.

Corral, D.A., Amling, M., Priemel, M., Loyer, E., Fuchs, S., Ducy, P., Baron, R., and Karsenty, G. (1998). Dissociation between bone resorption and bone formation in osteopenic transgenic mice. Proceedings of the National Academy of Sciences of the United States of America *95*, 13835-13840.

Crotti, T.N., Sharma, S.M., Fleming, J.D., Flannery, M.R., Ostrowski, M.C., Goldring, S.R., and McHugh, K.P. (2008). PU.1 and NFATc1 mediate osteoclastic induction of the mouse beta3 integrin promoter. Journal of cellular physiology *215*, 636-644.

Cui, Y., Jean, F., Thomas, G., and Christian, J.L. (1998). BMP-4 is proteolytically activated by furin and/or PC6 during vertebrate embryonic development. The EMBO journal *17*, 4735-4743.

Dacquin, R., Starbuck, M., Schinke, T., and Karsenty, G. (2002). Mouse alpha1(I)-collagen promoter is the best known promoter to drive efficient Cre recombinase expression in osteoblast. Developmental dynamics : an official publication of the American Association of Anatomists *224*, 245-251.

D

Datta, S.R., Dudek, H., Tao, X., Masters, S., Fu, H., Gotoh, Y., and Greenberg, M.E. (1997). Akt phosphorylation of BAD couples survival signals to the cell-intrinsic death machinery. Cell *91*, 231-241.

Davey, R.A., Clarke, M.V., Sastra, S., Skinner, J.P., Chiang, C., Anderson, P.H., and Zajac, J.D. (2012). Decreased body weight in young Osterix-Cre transgenic mice results in delayed cortical bone expansion and accrual. Transgenic research *21*, 885-893.

Davis, B.N., Hilyard, A.C., Lagna, G., and Hata, A. (2008). SMAD proteins control DROSHA-mediated microRNA maturation. Nature *454*, 56-61.

Davis, B.N., Hilyard, A.C., Nguyen, P.H., Lagna, G., and Hata, A. (2010). Smad proteins bind a conserved RNA sequence to promote microRNA maturation by Drosha. Molecular cell *39*, 373-384.

Davis-Dusenbery, B.N., and Hata, A. (2010). Mechanisms of control of microRNA biogenesis. Journal of biochemistry *148*, 381-392.

Deng, Y., Wu, S., Zhou, H., Bi, X., Wang, Y., Hu, Y., Gu, P., and Fan, X. (2013). Effects of a miR-31, Runx2, and Satb2 regulatory loop on the osteogenic differentiation of bone mesenchymal stem cells. Stem cells and development *22*, 2278-2286.

Derynck, R., and Zhang, Y.E. (2003). Smad-dependent and Smad-independent pathways in TGF-beta family signalling. Nature *425*, 577-584.

Dobreva, G., Chahrour, M., Dautzenberg, M., Chirivella, L., Kanzler, B., Farinas, I., Karsenty, G., and Grosschedl, R. (2006). SATB2 is a multifunctional determinant of craniofacial patterning and osteoblast differentiation. Cell *125*, 971-986.

Dodig, M., Kronenberg, M.S., Bedalov, A., Kream, B.E., Gronowicz, G., Clark, S.H., Mack, K., Liu, Y.H., Maxon, R., Pan, Z.Z., *et al.* (1996). Identification of a TAAT-containing motif required for high level expression of the COL1A1 promoter in differentiated osteoblasts of transgenic mice. The Journal of biological chemistry *271*, 16422-16429.

Doidge, R., Mittal, S., Aslam, A., and Winkler, G.S. (2012). The anti-proliferative activity of BTG/TOB proteins is mediated via the Caf1a (CNOT7) and Caf1b (CNOT8) deadenylase subunits of the Ccr4-not complex. PloS one *7*, e51331.

Domin, J., Harper, L., Aubyn, D., Wheeler, M., Florey, O., Haskard, D., Yuan, M., and Zicha, D. (2005). The class II phosphoinositide 3-kinase PI3K-C2beta regulates cell migration by a PtdIns3P dependent mechanism. Journal of cellular physiology *205*, 452-462.

Drissi, H., Luc, Q., Shakoori, R., Chuva De Sousa Lopes, S., Choi, J.Y., Terry, A., Hu, M., Jones, S., Neil, J.C., Lian, J.B., *et al.* (2000). Transcriptional autoregulation of the bone related CBFA1/RUNX2 gene. Journal of cellular physiology *184*, 341-350.

Du, K., Herzig, S., Kulkarni, R.N., and Montminy, M. (2003). TRB3: a tribbles homolog that inhibits Akt/PKB activation by insulin in liver. Science *300*, 1574-1577.

Ducy, P. (2000). Cbfa1: a molecular switch in osteoblast biology. Developmental dynamics : an official publication of the American Association of Anatomists *219*, 461-471.

Ducy, P., Desbois, C., Boyce, B., Pinero, G., Story, B., Dunstan, C., Smith, E., Bonadio, J., Goldstein, S., Gundberg, C., *et al.* (1996). Increased bone formation in osteocalcin-deficient mice. Nature *382*, 448-452.

Ducy, P., and Karsenty, G. (1995). Two distinct osteoblast-specific cis-acting elements control expression of a mouse osteocalcin gene. Molecular and cellular biology *15*, 1858-1869.

Ducy, P., Starbuck, M., Priemel, M., Shen, J., Pinero, G., Geoffroy, V., Amling, M., and Karsenty, G. (1999). A Cbfa1-dependent genetic pathway controls bone formation beyond embryonic development. Genes & development *13*, 1025-1036.

Ducy, P., Zhang, R., Geoffroy, V., Ridall, A.L., and Karsenty, G. (1997). Osf2/Cbfa1: a transcriptional activator of osteoblast differentiation. Cell *89*, 747-754.

E

Eguchi, T., Watanabe, K., Hara, E.S., Ono, M., Kuboki, T., and Calderwood, S.K. (2013). OstemiR: a novel panel of microRNA biomarkers in osteoblastic and osteocytic differentiation from mesencymal stem cells. PloS one *8*, e58796.

Ehrlich, M., Gutman, O., Knaus, P., and Henis, Y.I. (2012). Oligomeric interactions of TGF-beta and BMP receptors. FEBS letters *586*, 1885-1896.

Engelman, J.A., Luo, J., and Cantley, L.C. (2006). The evolution of phosphatidylinositol 3-kinases as regulators of growth and metabolism. Nature reviews Genetics *7*, 606-619.

Epstein, S. (1988). Serum and urinary markers of bone remodeling: assessment of bone turnover. Endocrine reviews 9, 437-449.

Eskildsen, T., Taipaleenmaki, H., Stenvang, J., Abdallah, B.M., Ditzel, N., Nossent, A.Y., Bak, M., Kauppinen, S., and Kassem, M. (2011). MicroRNA-138 regulates osteogenic differentiation of human stromal (mesenchymal) stem cells in vivo. Proceedings of the National Academy of Sciences of the United States of America *108*, 6139-6144.

Everts, V., Delaisse, J.M., Korper, W., Jansen, D.C., Tigchelaar-Gutter, W., Saftig, P., and Beertsen, W. (2002). The bone lining cell: its role in cleaning Howship's lacunae and initiating bone formation. Journal of bone and mineral research : the official journal of the American Society for Bone and Mineral Research *17*, 77-90.

Ezzeddine, N., Chang, T.C., Zhu, W., Yamashita, A., Chen, C.Y., Zhong, Z., Yamashita, Y., Zheng, D., and Shyu, A.B. (2007). Human TOB, an antiproliferative transcription factor, is a poly(A)-binding protein-dependent positive regulator of cytoplasmic mRNA deadenylation. Molecular and cellular biology *27*, 7791-7801.

Ezzeddine, N., Chen, C.Y., and Shyu, A.B. (2012). Evidence providing new insights into TOB-promoted deadenylation and supporting a link between TOB's deadenylation-enhancing and antiproliferative activities. Molecular and cellular biology *32*, 1089-1098.

F

Fabian, M.R., Sonenberg, N., and Filipowicz, W. (2010). Regulation of mRNA translation and stability by microRNAs. Annual review of biochemistry *79*, 351-379.

Fang, C., Yu, J., Luo, Y., Chen, S., Wang, W., Zhao, C., Sun, Z., Wu, W., Guo, W., Han, Z., *et al.* (2015). Tsc1 is a Critical Regulator of Macrophage Survival and Function. Cellular physiology and biochemistry : international journal of experimental cellular physiology, biochemistry, and pharmacology *36*, 1406-1418.

Fang, Y., van Meurs, J.B., d'Alesio, A., Jhamai, M., Zhao, H., Rivadeneira, F., Hofman, A., van Leeuwen, J.P., Jehan, F., Pols, H.A., *et al.* (2005). Promoter and 3'-untranslated-region haplotypes in the vitamin d receptor gene predispose to osteoporotic fracture: the rotterdam study. American journal of human genetics *77*, 807-823.

Fantl, W.J., Escobedo, J.A., Martin, G.A., Turck, C.W., del Rosario, M., McCormick, F., and Williams, L.T. (1992). Distinct phosphotyrosines on a growth factor receptor bind to specific molecules that mediate different signaling pathways. Cell *69*, 413-423.

Feng, X.H., and Derynck, R. (1997). A kinase subdomain of transforming growth factor-beta (TGF-beta) type I receptor determines the TGF-beta intracellular signaling specificity. The EMBO journal *16*, 3912-3923.

Feng, X.H., and Derynck, R. (2005). Specificity and versatility in tgf-beta signaling through Smads. Annual review of cell and developmental biology *21*, 659-693.

Ferron, M., McKee, M.D., Levine, R.L., Ducy, P., and Karsenty, G. (2012). Intermittent injections of osteocalcin improve glucose metabolism and prevent type 2 diabetes in mice. Bone *50*, 568-575.

Foletta, V.C., Lim, M.A., Soosairajah, J., Kelly, A.P., Stanley, E.G., Shannon, M., He, W., Das, S., Massague, J., and Bernard, O. (2003). Direct signaling by the BMP type II receptor via the cytoskeletal regulator LIMK1. The Journal of cell biology *162*, 1089-1098.

Ford-Hutchinson, A.F., Ali, Z., Lines, S.E., Hallgrimsson, B., Boyd, S.K., and Jirik, F.R. (2007). Inactivation of Pten in osteo-chondroprogenitor cells leads to epiphyseal growth plate abnormalities and skeletal overgrowth. Journal of bone and mineral research : the official journal of the American Society for Bone and Mineral Research *22*, 1245-1259.

Foukas, L.C., Claret, M., Pearce, W., Okkenhaug, K., Meek, S., Peskett, E., Sancho, S., Smith, A.J., Withers, D.J., and Vanhaesebroeck, B. (2006). Critical role for the p110alpha phosphoinositide-3-OH kinase in growth and metabolic regulation. Nature *441*, 366-370.

Fritsch, R., de Krijger, I., Fritsch, K., George, R., Reason, B., Kumar, M.S., Diefenbacher, M., Stamp, G., and Downward, J. (2013). RAS and RHO families of GTPases directly regulate distinct phosphoinositide 3-kinase isoforms. Cell *153*, 1050-1063.

Fuentealba, L.C., Eivers, E., Ikeda, A., Hurtado, C., Kuroda, H., Pera, E.M., and De Robertis, E.M. (2007). Integrating patterning signals: Wnt/GSK3 regulates the duration of the BMP/Smad1 signal. Cell *131*, 980-993.

Fulzele, K., Riddle, R.C., DiGirolamo, D.J., Cao, X., Wan, C., Chen, D., Faugere, M.C., Aja, S., Hussain, M.A., Bruning, J.C., *et al.* (2010). Insulin receptor signaling in osteoblasts regulates postnatal bone acquisition and body composition. Cell *142*, 309-319.

Funakoshi, Y., Doi, Y., Hosoda, N., Uchida, N., Osawa, M., Shimada, I., Tsujimoto, M., Suzuki, T., Katada, T., and Hoshino, S. (2007). Mechanism of mRNA deadenylation: evidence for a molecular interplay between translation termination factor eRF3 and mRNA deadenylases. Genes & development *21*, 3135-3148.

G

Galli, C., Fu, Q., Wang, W., Olsen, B.R., Manolagas, S.C., Jilka, R.L., and O'Brien, C.A. (2009). Commitment to the osteoblast lineage is not required for RANKL gene expression. The Journal of biological chemistry *284*, 12654-12662.

Gamell, C., Osses, N., Bartrons, R., Ruckle, T., Camps, M., Rosa, J.L., and Ventura, F. (2008). BMP2 induction of actin cytoskeleton reorganization and cell migration requires PI3-kinase and Cdc42 activity. Journal of cell science *121*, 3960-3970.

Gamell, C., Susperregui, A.G., Bernard, O., Rosa, J.L., and Ventura, F. (2011). The p38/MK2/Hsp25 pathway is required for BMP-2-induced cell migration. PloS one *6*, e16477.

Gamez, B., Rodriguez-Carballo, E., and Ventura, F. (2013). BMP signaling in telencephalic neural cell specification and maturation. Frontiers in cellular neuroscience *7*, 87.

Gao, J., Yang, T., Han, J., Yan, K., Qiu, X., Zhou, Y., Fan, Q., and Ma, B. (2011). MicroRNA expression during osteogenic differentiation of human multipotent mesenchymal stromal cells from bone marrow. Journal of cellular biochemistry *112*, 1844-1856.

Gao, T., Furnari, F., and Newton, A.C. (2005). PHLPP: a phosphatase that directly dephosphorylates Akt, promotes apoptosis, and suppresses tumor growth. Molecular cell *18*, 13-24.

Gao, Y., Jheon, A., Nourkeyhani, H., Kobayashi, H., and Ganss, B. (2004). Molecular cloning, structure, expression, and chromosomal localization of the human Osterix (SP7) gene. Gene *341*, 101-110.

Garofalo, R.S., Orena, S.J., Rafidi, K., Torchia, A.J., Stock, J.L., Hildebrandt, A.L., Coskran, T., Black, S.C., Brees, D.J., Wicks, J.R., *et al.* (2003). Severe diabetes, age-dependent loss of adipose tissue, and mild growth deficiency in mice lacking Akt2/PKB beta. The Journal of clinical investigation *112*, 197-208.

Gaur, T., Hussain, S., Mudhasani, R., Parulkar, I., Colby, J.L., Frederick, D., Kream, B.E., van Wijnen, A.J., Stein, J.L., Stein, G.S., *et al.* (2010). Dicer inactivation in osteoprogenitor cells compromises fetal survival and bone formation, while excision in differentiated osteoblasts increases bone mass in the adult mouse. Developmental biology *340*, 10-21.

Gaur, T., Lengner, C.J., Hovhannisyan, H., Bhat, R.A., Bodine, P.V., Komm, B.S., Javed, A., van Wijnen, A.J., Stein, J.L., Stein, G.S., *et al.* (2005). Canonical WNT signaling promotes osteogenesis by directly stimulating Runx2 gene expression. The Journal of biological chemistry *280*, 33132-33140.

Gazzerro, E., and Canalis, E. (2006). Bone morphogenetic proteins and their antagonists. Reviews in endocrine & metabolic disorders *7*, 51-65.

Gillespie, J.R., Bush, J.R., Bell, G.I., Aubrey, L.A., Dupuis, H., Ferron, M., Kream, B., DiMattia, G., Patel, S., Woodgett, J.R., *et al.* (2013). GSK-3beta function in bone regulates skeletal development, whole-body metabolism, and male life span. Endocrinology *154*, 3702-3718.

Gohda, J., Akiyama, T., Koga, T., Takayanagi, H., Tanaka, S., and Inoue, J. (2005). RANK-mediated amplification of TRAF6 signaling leads to NFATc1 induction during osteoclastogenesis. The EMBO journal *24*, 790-799.

Graupera, M., Guillermet-Guibert, J., Foukas, L.C., Phng, L.K., Cain, R.J., Salpekar, A., Pearce, W., Meek, S., Millan, J., Cutillas, P.R., *et al.* (2008). Angiogenesis selectively requires the p110alpha isoform of PI3K to control endothelial cell migration. Nature *453*, 662-666.

Greenblatt, M.B., Shim, J.H., and Glimcher, L.H. (2013). Mitogen-activated protein kinase pathways in osteoblasts. Annual review of cell and developmental biology *29*, 63-79.

Greenblatt, M.B., Shim, J.H., Zou, W., Sitara, D., Schweitzer, M., Hu, D., Lotinun, S., Sano, Y., Baron, R., Park, J.M., *et al.* (2010). The p38 MAPK pathway is essential for skeletogenesis and bone homeostasis in mice. The Journal of clinical investigation *120*, 2457-2473.

Grey, A., Chaussade, C., Empson, V., Lin, J.M., Watson, M., O'Sullivan, S., Rewcastle, G., Naot, D., Cornish, J., and Shepherd, P. (2010). Evidence for a role for the p110-alpha isoform of PI3K in skeletal function. Biochemical and biophysical research communications *391*, 564-569.

Gu, H., Yu, J., Dong, D., Zhou, Q., Wang, J.Y., and Yang, P. (2015). The miR-322-TRAF3 circuit mediates the pro-apoptotic effect of high glucose on neural stem cells. Toxicological sciences : an official journal of the Society of Toxicology *144*, 186-196.

Guillermet-Guibert, J., Bjorklof, K., Salpekar, A., Gonella, C., Ramadani, F., Bilancio, A., Meek, S., Smith, A.J., Okkenhaug, K., and Vanhaesebroeck, B. (2008). The p110beta isoform of phosphoinositide 3-kinase signals downstream of G protein-coupled receptors and is functionally redundant with p110gamma. Proceedings of the National Academy of Sciences of the United States of America *105*, 8292-8297.

Guntur, A.R., Reinhold, M.I., Cuellar, J., Jr., and Naski, M.C. (2011). Conditional ablation of Pten in osteoprogenitors stimulates FGF signaling. Development *138*, 1433-1444.

Guntur, A.R., and Rosen, C.J. (2011). The skeleton: a multi-functional complex organ: new insights into osteoblasts and their role in bone formation: the central role of PI3Kinase. The Journal of endocrinology *211*, 123-130.

Guo, H., Ingolia, N.T., Weissman, J.S., and Bartel, D.P. (2010). Mammalian microRNAs predominantly act to decrease target mRNA levels. Nature *466*, 835-840.

Gurdon, J.B., and Bourillot, P.Y. (2001). Morphogen gradient interpretation. Nature *413*, 797-803.

Gyori, D., Csete, D., Benko, S., Kulkarni, S., Mandl, P., Dobo-Nagy, C., Vanhaesebroeck, B., Stephens, L., Hawkins, P.T., and Mocsai, A. (2014). The phosphoinositide 3-kinase isoform PI3Kbeta regulates osteoclast-mediated bone resorption in humans and mice. Arthritis & rheumatology *66*, 2210-2221.

H

Ha, M., and Kim, V.N. (2014). Regulation of microRNA biogenesis. Nature reviews Molecular cell biology *15*, 509-524.

Hadjidakis, D.J., and Androulakis, II (2006). Bone remodeling. Annals of the New York Academy of Sciences *1092*, 385-396.

Han, J., Lee, Y., Yeom, K.H., Nam, J.W., Heo, I., Rhee, J.K., Sohn, S.Y., Cho, Y., Zhang, B.T., and Kim, V.N. (2006). Molecular basis for the recognition of primary microRNAs by the Drosha-DGCR8 complex. Cell *125*, 887-901.

Hassan, M.Q., Gordon, J.A., Beloti, M.M., Croce, C.M., van Wijnen, A.J., Stein, J.L., Stein, G.S., and Lian, J.B. (2010). A network connecting Runx2, SATB2, and the miR-23a~27a~24-2 cluster regulates the osteoblast differentiation program. Proceedings of the National Academy of Sciences of the United States of America *107*, 19879-19884.

Hassan, M.Q., Tare, R.S., Lee, S.H., Mandeville, M., Morasso, M.I., Javed, A., van Wijnen, A.J., Stein, J.L., Stein, G.S., and Lian, J.B. (2006). BMP2 commitment to the osteogenic lineage involves activation of Runx2 by DLX3 and a homeodomain transcriptional network. The Journal of biological chemistry *281*, 40515-40526.

Hata, Y., Miura, M., Asato, R., Kita, T., Oba, K., Kawahara, S., Arita, R., Kohno, R., Nakao, S., and Ishibashi, T. (2010). Antiangiogenic mechanisms of simvastatin in retinal endothelial cells. Graefe's archive for clinical and experimental ophthalmology = Albrecht von Graefes Archiv fur klinische und experimentelle Ophthalmologie *248*, 667-673.

Hatta, M., Yoshimura, Y., Deyama, Y., Fukamizu, A., and Suzuki, K. (2006). Molecular characterization of the zinc finger transcription factor, Osterix. International journal of molecular medicine *17*, 425-430.

Hawkins, P.T., Anderson, K.E., Davidson, K., and Stephens, L.R. (2006). Signalling through Class I PI3Ks in mammalian cells. Biochemical Society transactions *34*, 647-662.

He, J., Zhang, J.F., Yi, C., Lv, Q., Xie, W.D., Li, J.N., Wan, G., Cui, K., Kung, H.F., Yang, J., *et al.* (2010). miRNA-mediated functional changes through co-regulating function related genes. PloS one *5*, e13558.

Hessle, L., Johnson, K.A., Anderson, H.C., Narisawa, S., Sali, A., Goding, J.W., Terkeltaub, R., and Millan, J.L. (2002). Tissue-nonspecific alkaline phosphatase and plasma cell membrane glycoprotein-1 are central antagonistic regulators of bone mineralization. Proceedings of the National Academy of Sciences of the United States of America *99*, 9445-9449.

Hill, C.S. (2009). Nucleocytoplasmic shuttling of Smad proteins. Cell research *19*, 36-46.

Hinck, A.P. (2012). Structural studies of the TGF-betas and their receptors - insights into evolution of the TGF-beta superfamily. FEBS letters *586*, 1860-1870.

Hobert, O. (2008). Gene regulation by transcription factors and microRNAs. Science *319*, 1785-1786.

Holt, K.H., Olson, L., Moye-Rowley, W.S., and Pessin, J.E. (1994). Phosphatidylinositol 3-kinase activation is mediated by high-affinity interactions between distinct domains within the p110 and p85 subunits. Molecular and cellular biology *14*, 42-49.

Horiuchi, M., Takeuchi, K., Noda, N., Muroya, N., Suzuki, T., Nakamura, T., Kawamura-Tsuzuku, J., Takahasi, K., Yamamoto, T., and Inagaki, F. (2009). Structural basis for the antiproliferative activity of the Tob-hCaf1 complex. The Journal of biological chemistry *284*, 13244-13255.

Hosoda, N., Funakoshi, Y., Hirasawa, M., Yamagishi, R., Asano, Y., Miyagawa, R., Ogami, K., Tsujimoto, M., and Hoshino, S. (2011). Anti-proliferative protein Tob negatively regulates CPEB3 target by recruiting Caf1 deadenylase. The EMBO journal *30*, 1311-1323.

Hu, P., and Schlessinger, J. (1994). Direct association of p110 beta phosphatidylinositol 3-kinase with p85 is mediated by an N-terminal fragment of p110 beta. Molecular and cellular biology *14*, 2577-2583.

Hu, R., Liu, W., Li, H., Yang, L., Chen, C., Xia, Z.Y., Guo, L.J., Xie, H., Zhou, H.D., Wu, X.P., *et al.* (2011). A Runx2/miR-3960/miR-2861 regulatory feedback loop during mouse osteoblast differentiation. The Journal of biological chemistry *286*, 12328-12339.

Huang, G., Shigesada, K., Ito, K., Wee, H.J., Yokomizo, T., and Ito, Y. (2001). Dimerization with PEBP2beta protects RUNX1/AML1 from ubiquitin-proteasome-mediated degradation. The EMBO journal *20*, 723-733.

Huang, J., Zhao, L., Xing, L., and Chen, D. (2010). MicroRNA-204 regulates Runx2 protein expression and mesenchymal progenitor cell differentiation. Stem cells *28*, 357-364.

Huang, Q., Jiang, Z., Meng, T., Yin, H., Wang, J., Wan, W., Cheng, M., Yan, W., Liu, T., Song, D., *et al.* (2014). MiR-30a inhibits osteolysis by targeting RunX2 in giant cell tumor of bone. Biochemical and biophysical research communications *453*, 160-165.

Huang, Y.S., Kan, M.C., Lin, C.L., and Richter, J.D. (2006). CPEB3 and CPEB4 in neurons: analysis of RNA-binding specificity and translational control of AMPA receptor GluR2 mRNA. The EMBO journal *25*, 4865-4876.

I

Inose, H., Ochi, H., Kimura, A., Fujita, K., Xu, R., Sato, S., Iwasaki, M., Sunamura, S., Takeuchi, Y., Fukumoto, S., *et al.* (2009). A microRNA regulatory mechanism of osteoblast differentiation. Proceedings of the National Academy of Sciences of the United States of America *106*, 20794-20799.

Itoh, T., Nozawa, Y., and Akao, Y. (2009). MicroRNA-141 and -200a are involved in bone morphogenetic protein-2-induced mouse pre-osteoblast differentiation by targeting distal-less homeobox 5. The Journal of biological chemistry *284*, 19272-19279.

Iyer, S., Ambrogini, E., Bartell, S.M., Han, L., Roberson, P.K., de Cabo, R., Jilka, R.L., Weinstein, R.S., O'Brien, C.A., Manolagas, S.C., *et al.* (2013). FOXOs attenuate bone formation by suppressing Wnt signaling. The Journal of clinical investigation *123*, 3409-3419.

J

Jackson, S.P., Schoenwaelder, S.M., Goncalves, I., Nesbitt, W.S., Yap, C.L., Wright, C.E., Kenche, V., Anderson, K.E., Dopheide, S.M., Yuan, Y., *et al.* (2005). PI 3-kinase p110beta: a new target for antithrombotic therapy. Nature medicine *11*, 507-514.

Jamieson, S., Flanagan, J.U., Kolekar, S., Buchanan, C., Kendall, J.D., Lee, W.J., Rewcastle, G.W., Denny, W.A., Singh, R., Dickson, J., *et al.* (2011). A drug targeting only p110alpha can block phosphoinositide 3-kinase signalling and tumour growth in certain cell types. The Biochemical journal *438*, 53-62.

Jia, S., Liu, Z., Zhang, S., Liu, P., Zhang, L., Lee, S.H., Zhang, J., Signoretti, S., Loda, M., Roberts, T.M., *et al.* (2008). Essential roles of PI(3)K-p110beta in cell growth, metabolism and tumorigenesis. Nature *454*, 776-779.

Jia, S., and Meng, A. (2007). Tob genes in development and homeostasis. Developmental dynamics : an official publication of the American Association of Anatomists *236*, 913-921.

K

Kang, S., Denley, A., Vanhaesebroeck, B., and Vogt, P.K. (2006). Oncogenic transformation induced by the p110beta, -gamma, and -delta isoforms of class I phosphoinositide 3-kinase. Proceedings of the National Academy of Sciences of the United States of America *103*, 1289-1294.

Kang, S.S., Kwon, T., Kwon, D.Y., and Do, S.I. (1999). Akt protein kinase enhances human telomerase activity through phosphorylation of telomerase reverse transcriptase subunit. The Journal of biological chemistry *274*, 13085-13090.

Kanzler, B., Kuschert, S.J., Liu, Y.H., and Mallo, M. (1998). Hoxa-2 restricts the chondrogenic domain and inhibits bone formation during development of the branchial area. Development *125*, 2587-2597.

Kapinas, K., and Delany, A.M. (2011). MicroRNA biogenesis and regulation of bone remodeling. Arthritis research & therapy *13*, 220.

Kapinas, K., Kessler, C., Ricks, T., Gronowicz, G., and Delany, A.M. (2010). miR-29 modulates Wnt signaling in human osteoblasts through a positive feedback loop. The Journal of biological chemistry *285*, 25221-25231.

Karaplis, A.C. (2008). Embryonic Development of Bone and Regulation of Intramembranous and Endochondral Bone Formation In Principles of Bone Biology (San Diego, California: Academic Press).

Karsenty, G. (2008). Transcriptional control of skeletogenesis. Annual review of genomics and human genetics *9*, 183-196.

Karsenty, G., Ducy, P., Starbuck, M., Priemel, M., Shen, J., Geoffroy, V., and Amling, M. (1999). Cbfa1 as a regulator of osteoblast differentiation and function. Bone *25*, 107-108.

Karsenty, G., Kronenberg, H.M., and Settembre, C. (2009). Genetic control of bone formation. Annual review of cell and developmental biology *25*, 629-648.

Karsenty, G., and Oury, F. (2012). Biology without walls: the novel endocrinology of bone. Annual review of physiology *74*, 87-105.

Karsenty, G., and Oury, F. (2014). Regulation of male fertility by the bone-derived hormone osteocalcin. Molecular and cellular endocrinology *382*, 521-526.

Katagiri, T., Yamaguchi, A., Komaki, M., Abe, E., Takahashi, N., Ikeda, T., Rosen, V., Wozney, J.M., Fujisawa-Sehara, A., and Suda, T. (1994). Bone morphogenetic protein-2 converts the differentiation pathway of C2C12 myoblasts into the osteoblast lineage. The Journal of cell biology *127*, 1755-1766.

Katso, R.M., Pardo, O.E., Palamidessi, A., Franz, C.M., Marinov, M., De Laurentiis, A., Downward, J., Scita, G., Ridley, A.J., Waterfield, M.D., *et al.* (2006). Phosphoinositide 3-Kinase C2beta regulates cytoskeletal organization and cell migration via Rac-dependent mechanisms. Molecular biology of the cell *17*, 3729-3744.

Kawamura, N., Kugimiya, F., Oshima, Y., Ohba, S., Ikeda, T., Saito, T., Shinoda, Y., Kawasaki, Y., Ogata, N., Hoshi, K., *et al.* (2007). Akt1 in osteoblasts and osteoclasts controls bone remodeling. PloS one 2, e1058.

Kenner, L., Hoebertz, A., Beil, F.T., Keon, N., Karreth, F., Eferl, R., Scheuch, H., Szremska, A., Amling, M., Schorpp-Kistner, M., *et al.* (2004). Mice lacking JunB are osteopenic due to cell-autonomous osteoblast and osteoclast defects. The Journal of cell biology *164*, 613-623.

Kim, H.K., Lee, Y.S., Sivaprasad, U., Malhotra, A., and Dutta, A. (2006). Muscle-specific microRNA miR-206 promotes muscle differentiation. The Journal of cell biology *174*, 677-687.

Kim, Y.J., Lee, M.H., Wozney, J.M., Cho, J.Y., and Ryoo, H.M. (2004). Bone morphogenetic protein-2-induced alkaline phosphatase expression is stimulated by Dlx5 and repressed by Msx2. The Journal of biological chemistry *279*, 50773-50780.

Kimura, N., Matsuo, R., Shibuya, H., Nakashima, K., and Taga, T. (2000). BMP2-induced apoptosis is mediated by activation of the TAK1-p38 kinase pathway that is negatively regulated by Smad6. The Journal of biological chemistry *275*, 17647-17652.

Klippel, A., Escobedo, J.A., Hu, Q., and Williams, L.T. (1993). A region of the 85-kilodalton (kDa) subunit of phosphatidylinositol 3-kinase binds the 110-kDa catalytic subunit in vivo. Molecular and cellular biology *13*, 5560-5566.

Kobayashi, N., Kadono, Y., Naito, A., Matsumoto, K., Yamamoto, T., Tanaka, S., and Inoue, J. (2001). Segregation of TRAF6-mediated signaling pathways clarifies its role in osteoclastogenesis. The EMBO journal *20*, 1271-1280.

Kobayashi, T., Lu, J., Cobb, B.S., Rodda, S.J., McMahon, A.P., Schipani, E., Merkenschlager, M., and Kronenberg, H.M. (2008). Dicer-dependent pathways regulate chondrocyte proliferation and differentiation. Proceedings of the National Academy of Sciences of the United States of America *105*, 1949-1954.

Komori, T. (2006). Regulation of osteoblast differentiation by transcription factors. Journal of cellular biochemistry *99*, 1233-1239.

Komori, T., Yagi, H., Nomura, S., Yamaguchi, A., Sasaki, K., Deguchi, K., Shimizu, Y., Bronson, R.T., Gao, Y.H., Inada, M., *et al.* (1997). Targeted disruption of Cbfa1 results in a complete lack of bone formation owing to maturational arrest of osteoblasts. Cell *89*, 755-764.

Korchynskyi, O., and ten Dijke, P. (2002). Identification and functional characterization of distinct critically important bone morphogenetic protein-specific response elements in the Id1 promoter. The Journal of biological chemistry 277, 4883-4891.

Kugimiya, F., Kawaguchi, H., Ohba, S., Kawamura, N., Hirata, M., Chikuda, H., Azuma, Y., Woodgett, J.R., Nakamura, K., and Chung, U.I. (2007). GSK-3beta controls osteogenesis through regulating Runx2 activity. PloS one 2, e837.

Kukita, T., Wada, N., Kukita, A., Kakimoto, T., Sandra, F., Toh, K., Nagata, K., Iijima, T., Horiuchi, M., Matsusaki, H., *et al.* (2004). RANKL-induced DC-STAMP is essential for osteoclastogenesis. The Journal of experimental medicine 200, 941-946.

Kundu, M., Javed, A., Jeon, J.P., Horner, A., Shum, L., Eckhaus, M., Muenke, M., Lian, J.B., Yang, Y., Nuckolls, G.H., *et al.* (2002). Cbfbeta interacts with Runx2 and has a critical role in bone development. Nature genetics 32, 639-644.

Kuroda, H., Fuentealba, L., Ikeda, A., Reversade, B., and De Robertis, E.M. (2005). Default neural induction: neuralization of dissociated Xenopus cells is mediated by Ras/MAPK activation. Genes & development 19, 1022-1027.

Kurosu, H., Maehama, T., Okada, T., Yamamoto, T., Hoshino, S., Fukui, Y., Ui, M., Hazeki, O., and Katada, T. (1997). Heterodimeric phosphoinositide 3-kinase consisting of p85 and p110beta is synergistically activated by the betagamma subunits of G proteins and phosphotyrosyl peptide. The Journal of biological chemistry 272, 24252-24256.

L

Laine, S.K., Alm, J.J., Virtanen, S.P., Aro, H.T., and Laitala-Leinonen, T.K. (2012). MicroRNAs miR-96, miR-124, and miR-199a regulate gene expression in human bone marrow-derived mesenchymal stem cells. Journal of cellular biochemistry 113, 2687-2695.

Lecanda, F., Towler, D.A., Ziambaras, K., Cheng, S.L., Koval, M., Steinberg, T.H., and Civitelli, R. (1998). Gap junctional communication modulates gene expression in osteoblastic cells. Molecular biology of the cell 9, 2249-2258.

Lee, B., Thirunavukkarasu, K., Zhou, L., Pastore, L., Baldini, A., Hecht, J., Geoffroy, V., Ducy, P., and Karsenty, G. (1997). Missense mutations abolishing DNA binding of the osteoblast-specific transcription factor OSF2/CBFA1 in cleidocranial dysplasia. Nature genetics *16*, 307-310.

Lee, I., Ajay, S.S., Yook, J.I., Kim, H.S., Hong, S.H., Kim, N.H., Dhanasekaran, S.M., Chinnaiyan, A.M., and Athey, B.D. (2009). New class of microRNA targets containing simultaneous 5'-UTR and 3'-UTR interaction sites. Genome research *19*, 1175-1183.

Lee, M.H., Kim, Y.J., Yoon, W.J., Kim, J.I., Kim, B.G., Hwang, Y.S., Wozney, J.M., Chi, X.Z., Bae, S.C., Choi, K.Y., *et al.* (2005). Dlx5 specifically regulates Runx2 type II expression by binding to homeodomain-response elements in the Runx2 distal promoter. The Journal of biological chemistry *280*, 35579-35587.

Lee, M.H., Kwon, T.G., Park, H.S., Wozney, J.M., and Ryoo, H.M. (2003). BMP-2-induced Osterix expression is mediated by Dlx5 but is independent of Runx2. Biochemical and biophysical research communications *309*, 689-694.

Lee, N.K., Sowa, H., Hinoi, E., Ferron, M., Ahn, J.D., Confavreux, C., Dacquin, R., Mee, P.J., McKee, M.D., Jung, D.Y., *et al.* (2007). Endocrine regulation of energy metabolism by the skeleton. Cell *130*, 456-469.

Lee, R.C., Feinbaum, R.L., and Ambros, V. (1993). The C. elegans heterochronic gene lin-4 encodes small RNAs with antisense complementarity to lin-14. Cell *75*, 843-854.

Lee-Hoeflich, S.T., Causing, C.G., Podkowa, M., Zhao, X., Wrana, J.L., and Attisano, L. (2004). Activation of LIMK1 by binding to the BMP receptor, BMPRII, regulates BMP-dependent dendritogenesis. The EMBO journal *23*, 4792-4801.

Lefebvre, V., Behringer, R.R., and de Crombrugghe, B. (2001). L-Sox5, Sox6 and Sox9 control essential steps of the chondrocyte differentiation pathway. Osteoarthritis and cartilage / OARS, Osteoarthritis Research Society *9 Suppl A*, S69-75.

Li, B., Han, Q., Zhu, Y., Yu, Y., Wang, J., and Jiang, X. (2012). Down-regulation of miR-214 contributes to intrahepatic cholangiocarcinoma metastasis by targeting Twist. The FEBS journal *279*, 2393-2398.

Li, H., Li, T., Wang, S., Wei, J., Fan, J., Li, J., Han, Q., Liao, L., Shao, C., and Zhao, R.C. (2013). miR-17-5p and miR-106a are involved in the balance between osteogenic and adipogenic differentiation of adipose-derived mesenchymal stem cells. Stem cell research *10*, 313-324.

Li, H., Xie, H., Liu, W., Hu, R., Huang, B., Tan, Y.F., Xu, K., Sheng, Z.F., Zhou, H.D., Wu, X.P., *et al.* (2009a). A novel microRNA targeting HDAC5 regulates osteoblast differentiation in mice and contributes to primary osteoporosis in humans. The Journal of clinical investigation *119*, 3666-3677.

Li, H., Yang, F., Wang, Z., Fu, Q., and Liang, A. (2015). MicroRNA-21 promotes osteogenic differentiation by targeting small mothers against decapentaplegic 7. Molecular medicine reports *12*, 1561-1567.

Li, Z., Hassan, M.Q., Jafferji, M., Aqeilan, R.I., Garzon, R., Croce, C.M., van Wijnen, A.J., Stein, J.L., Stein, G.S., and Lian, J.B. (2009b). Biological functions of miR-29b contribute to positive regulation of osteoblast differentiation. The Journal of biological chemistry *284*, 15676-15684.

Li, Z., Hassan, M.Q., Volinia, S., van Wijnen, A.J., Stein, J.L., Croce, C.M., Lian, J.B., and Stein, G.S. (2008). A microRNA signature for a BMP2-induced osteoblast lineage commitment program. Proceedings of the National Academy of Sciences of the United States of America *105*, 13906-13911.

Lian, J.B., Stein, G.S., Javed, A., van Wijnen, A.J., Stein, J.L., Montecino, M., Hassan, M.Q., Gaur, T., Lengner, C.J., and Young, D.W. (2006). Networks and hubs for the transcriptional control of osteoblastogenesis. Reviews in endocrine & metabolic disorders *7*, 1-16.

Liang, M., Russell, G., and Hulley, P.A. (2008). Bim, Bak, and Bax regulate osteoblast survival. Journal of bone and mineral research : the official journal of the American Society for Bone and Mineral Research *23*, 610-620.

Liao, L., Yang, X., Su, X., Hu, C., Zhu, X., Yang, N., Chen, X., Shi, S., Shi, S., and Jin, Y. (2013). Redundant miR-3077-5p and miR-705 mediate the shift of mesenchymal stem cell lineage commitment to adipocyte in osteoporosis bone marrow. Cell death & disease *4*, e600.

Lin, E.A., Kong, L., Bai, X.H., Luan, Y., and Liu, C.J. (2009). miR-199a, a bone morphogenic protein 2-responsive MicroRNA, regulates chondrogenesis via direct targeting to Smad1. The Journal of biological chemistry *284*, 11326-11335.

Lindmo, K., and Stenmark, H. (2006). Regulation of membrane traffic by phosphoinositide 3-kinases. Journal of cell science *119*, 605-614.

Liu, F., Ventura, F., Doody, J., and Massague, J. (1995). Human type II receptor for bone morphogenic proteins (BMPs): extension of the two-kinase receptor model to the BMPs. Molecular and cellular biology *15*, 3479-3486.

Liu, J., Huang, Q., Higdon, J., Liu, W., Xie, T., Yamashita, T., Cheon, K., Cheng, C., and Zuo, J. (2005). Distinct gene expression profiles and reduced JNK signaling in retinitis pigmentosa caused by RP1 mutations. Human molecular genetics *14*, 2945-2958.

Liu, J.P., Baker, J., Perkins, A.S., Robertson, E.J., and Efstratiadis, A. (1993). Mice carrying null mutations of the genes encoding insulin-like growth factor I (Igf-1) and type 1 IGF receptor (Igf1r). Cell *75*, 59-72.

Liu, P., Cheng, H., Roberts, T.M., and Zhao, J.J. (2009). Targeting the phosphoinositide 3-kinase pathway in cancer. Nature reviews Drug discovery *8*, 627-644.

Liu, T., Gao, Y., Sakamoto, K., Minamizato, T., Furukawa, K., Tsukazaki, T., Shibata, Y., Bessho, K., Komori, T., and Yamaguchi, A. (2007a). BMP-2 promotes differentiation of osteoblasts and chondroblasts in Runx2-deficient cell lines. Journal of cellular physiology *211*, 728-735.

Liu, W., Toyosawa, S., Furuichi, T., Kanatani, N., Yoshida, C., Liu, Y., Himeno, M., Narai, S., Yamaguchi, A., and Komori, T. (2001). Overexpression of Cbfa1 in osteoblasts inhibits osteoblast maturation and causes osteopenia with multiple fractures. The Journal of cell biology *155*, 157-166.

Liu, X., Bruxvoort, K.J., Zylstra, C.R., Liu, J., Cichowski, R., Faugere, M.C., Bouxsein, M.L., Wan, C., Williams, B.O., and Clemens, T.L. (2007b). Lifelong accumulation of bone in mice lacking Pten in osteoblasts. Proceedings of the National Academy of Sciences of the United States of America *104*, 2259-2264.

Lopez-Rovira, T., Chalaux, E., Massague, J., Rosa, J.L., and Ventura, F. (2002). Direct binding of Smad1 and Smad4 to two distinct motifs mediates bone morphogenetic protein-specific transcriptional activation of Id1 gene. The Journal of biological chemistry *277*, 3176-3185.

Lund, E., Guttinger, S., Calado, A., Dahlberg, J.E., and Kutay, U. (2004). Nuclear export of microRNA precursors. Science *303*, 95-98.

Luzi, E., Marini, F., Sala, S.C., Tognarini, I., Galli, G., and Brandi, M.L. (2008). Osteogenic differentiation of human adipose tissue-derived stem cells is modulated by the miR-26a targeting of the SMAD1 transcription factor. Journal of bone and mineral research : the official journal of the American Society for Bone and Mineral Research *23*, 287-295.

Lytle, J.R., Yario, T.A., and Steitz, J.A. (2007). Target mRNAs are repressed as efficiently by microRNA-binding sites in the 5' UTR as in the 3' UTR. Proceedings of the National Academy of Sciences of the United States of America *104*, 9667-9672.

M

Maddika, S., Panigrahi, S., Wiechec, E., Wesselborg, S., Fischer, U., Schulze-Osthoff, K., and Los, M. (2009). Unscheduled Akt-triggered activation of cyclin-dependent kinase 2 as a key effector mechanism of apoptin's anticancer toxicity. Molecular and cellular biology *29*, 1235-1248.

Maehama, T., and Dixon, J.E. (1998). The tumor suppressor, PTEN/MMAC1, dephosphorylates the lipid second messenger, phosphatidylinositol 3,4,5-trisphosphate. The Journal of biological chemistry *273*, 13375-13378.

Maffucci, T., Cooke, F.T., Foster, F.M., Traer, C.J., Fry, M.J., and Falasca, M. (2005). Class II phosphoinositide 3-kinase defines a novel signaling pathway in cell migration. The Journal of cell biology *169*, 789-799.

Maier, U., Babich, A., and Nurnberg, B. (1999). Roles of non-catalytic subunits in gbetagamma-induced activation of class I phosphoinositide 3-kinase isoforms beta and gamma. The Journal of biological chemistry *274*, 29311-29317.

Manning, B.D., and Cantley, L.C. (2007). AKT/PKB signaling: navigating downstream. Cell *129*, 1261-1274.

Manolagas, S.C. (2000). Birth and death of bone cells: basic regulatory mechanisms and implications for the pathogenesis and treatment of osteoporosis. Endocrine reviews *21*, 115-137.

Massague, J. (1990). The transforming growth factor-beta family. Annual review of cell biology *6*, 597-641.

Massague, J. (1998). TGF-beta signal transduction. Annual review of biochemistry *67*, 753-791.

Massague, J., Attisano, L., and Wrana, J.L. (1994). The TGF-beta family and its composite receptors. Trends in cell biology *4*, 172-178.

Massague, J., Seoane, J., and Wotton, D. (2005). Smad transcription factors. Genes & development *19*, 2783-2810.

Mateescu, B., Batista, L., Cardon, M., Gruosso, T., de Feraudy, Y., Mariani, O., Nicolas, A., Meyniel, J.P., Cottu, P., Sastre-Garau, X., *et al.* (2011). miR-141 and miR-200a act on ovarian tumorigenesis by controlling oxidative stress response. Nature medicine *17*, 1627-1635.

Matheny, R.W., Jr., and Adamo, M.L. (2010). PI3K p110 alpha and p110 beta have differential effects on Akt activation and protection against oxidative stress-induced apoptosis in myoblasts. Cell death and differentiation *17*, 677-688.

Matsushita, T., Chan, Y.Y., Kawanami, A., Balmes, G., Landreth, G.E., and Murakami, S. (2009). Extracellular signal-regulated kinase 1 (ERK1) and ERK2 play essential roles in osteoblast differentiation and in supporting osteoclastogenesis. Molecular and cellular biology *29*, 5843-5857.

Mattick, J.S., and Makunin, I.V. (2006). Non-coding RNA. Human molecular genetics *15 Spec No 1*, R17-29.

Mauxion, F., Chen, C.Y., Seraphin, B., and Shyu, A.B. (2009). BTG/TOB factors impact deadenylases. Trends in biochemical sciences *34*, 640-647.

Mayo, L.D., and Donner, D.B. (2001). A phosphatidylinositol 3-kinase/Akt pathway promotes translocation of Mdm2 from the cytoplasm to the nucleus. Proceedings of the National Academy of Sciences of the United States of America *98*, 11598-11603.

McGonnell, I.M., Grigoriadis, A.E., Lam, E.W., Price, J.S., and Sunters, A. (2012). A specific role for phosphoinositide 3-kinase and AKT in osteoblasts? Frontiers in endocrinology *3*, 88.

Milona, M.A., Gough, J.E., and Edgar, A.J. (2003). Expression of alternatively spliced isoforms of human Sp7 in osteoblast-like cells. BMC genomics *4*, 43.

Miyama, K., Yamada, G., Yamamoto, T.S., Takagi, C., Miyado, K., Sakai, M., Ueno, N., and Shibuya, H. (1999). A BMP-inducible gene, dlx5, regulates osteoblast differentiation and mesoderm induction. Developmental biology *208*, 123-133.

Miyazono, K., Kamiya, Y., and Morikawa, M. (2010). Bone morphogenetic protein receptors and signal transduction. Journal of biochemistry *147*, 35-51.

Miyazono, K., and Miyazawa, K. (2002). Id: a target of BMP signaling. Science's STKE : signal transduction knowledge environment *2002*, pe40.

Mizoguchi, F., Izu, Y., Hayata, T., Hemmi, H., Nakashima, K., Nakamura, T., Kato, S., Miyasaka, N., Ezura, Y., and Noda, M. (2010). Osteoclast-specific Dicer gene deficiency suppresses osteoclastic bone resorption. Journal of cellular biochemistry *109*, 866-875.

Mizuno, Y., Tokuzawa, Y., Ninomiya, Y., Yagi, K., Yatsuka-Kanesaki, Y., Suda, T., Fukuda, T., Katagiri, T., Kondoh, Y., Amemiya, T., *et al.* (2009). miR-210 promotes osteoblastic differentiation through inhibition of AcvR1b. FEBS letters *583*, 2263-2268.

Mizuno, Y., Yagi, K., Tokuzawa, Y., Kanesaki-Yatsuka, Y., Suda, T., Katagiri, T., Fukuda, T., Maruyama, M., Okuda, A., Amemiya, T., *et al.* (2008). miR-125b inhibits osteoblastic differentiation by down-regulation of cell proliferation. Biochemical and biophysical research communications *368*, 267-272.

Moreno-Moya, J.M., Vilella, F., and Simon, C. (2014). MicroRNA: key gene expression regulators. Fertility and sterility *101*, 1516-1523.

Mori-Akiyama, Y., Akiyama, H., Rowitch, D.H., and de Crombrugghe, B. (2003). Sox9 is required for determination of the chondrogenic cell lineage in the cranial neural crest. Proceedings of the National Academy of Sciences of the United States of America *100*, 9360-9365.

Mueller, T.D., and Nickel, J. (2012). Promiscuity and specificity in BMP receptor activation. FEBS letters *586*, 1846-1859.

Muise-Helmericks, R.C., Grimes, H.L., Bellacosa, A., Malstrom, S.E., Tsichlis, P.N., and Rosen, N. (1998). Cyclin D expression is controlled post-transcriptionally via a phosphatidylinositol 3-kinase/Akt-dependent pathway. The Journal of biological chemistry *273*, 29864-29872.

Mukherjee, A., and Rotwein, P. (2012). Selective signaling by Akt1 controls osteoblast differentiation and osteoblast-mediated osteoclast development. Molecular and cellular biology *32*, 490-500.

Mundlos, S., Otto, F., Mundlos, C., Mulliken, J.B., Aylsworth, A.S., Albright, S., Lindhout, D., Cole, W.G., Henn, W., Knoll, J.H., *et al.* (1997). Mutations involving the transcription factor CBFA1 cause cleidocranial dysplasia. Cell *89*, 773-779.

Mura, M., Cappato, S., Giacopelli, F., Ravazzolo, R., and Bocciardi, R. (2012). The role of the 3'UTR region in the regulation of the ACVR1/Alk-2 gene expression. PloS one *7*, e50958.

Murakami, G., Watabe, T., Takaoka, K., Miyazono, K., and Imamura, T. (2003). Cooperative inhibition of bone morphogenetic protein signaling by Smurf1 and inhibitory Smads. Molecular biology of the cell *14*, 2809-2817.

Myers, M.G., Jr., Sun, X.J., Cheatham, B., Jachna, B.R., Glasheen, E.M., Backer, J.M., and White, M.F. (1993). IRS-1 is a common element in insulin and insulin-like growth factor-I signaling to the phosphatidylinositol 3'-kinase. Endocrinology *132*, 1421-1430.

N

Nakamura, I., Takahashi, N., Sasaki, T., Tanaka, S., Udagawa, N., Murakami, H., Kimura, K., Kabuyama, Y., Kurokawa, T., Suda, T., *et al.* (1995). Wortmannin, a specific inhibitor of phosphatidylinositol-3 kinase, blocks osteoclastic bone resorption. FEBS letters *361*, 79-84.

Nakashima, K., and de Crombrugghe, B. (2003). Transcriptional mechanisms in osteoblast differentiation and bone formation. Trends in genetics : TIG *19*, 458-466.

Nakashima, K., Zhou, X., Kunkel, G., Zhang, Z., Deng, J.M., Behringer, R.R., and de Crombrugghe, B. (2002). The novel zinc finger-containing transcription factor osterix is required for osteoblast differentiation and bone formation. Cell *108*, 17-29.

Nakashima, T., Hayashi, M., Fukunaga, T., Kurata, K., Oh-Hora, M., Feng, J.Q., Bonewald, L.F., Kodama, T., Wutz, A., Wagner, E.F., *et al.* (2011). Evidence for osteocyte regulation of bone homeostasis through RANKL expression. Nature medicine *17*, 1231-1234.

Nishimura, R., Wakabayashi, M., Hata, K., Matsubara, T., Honma, S., Wakisaka, S., Kiyonari, H., Shioi, G., Yamaguchi, A., Tsumaki, N., *et al.* (2012). Osterix regulates calcification and degradation of chondrogenic matrices through matrix metalloproteinase 13 (MMP13) expression in association with transcription factor Runx2 during endochondral ossification. The Journal of biological chemistry *287*, 33179-33190.

Nishio, Y., Dong, Y., Paris, M., O'Keefe, R.J., Schwarz, E.M., and Drissi, H. (2006). Runx2-mediated regulation of the zinc finger Osterix/Sp7 gene. Gene *372*, 62-70.

Nogueira, V., Park, Y., Chen, C.C., Xu, P.Z., Chen, M.L., Tonic, I., Unterman, T., and Hay, N. (2008). Akt determines replicative senescence and oxidative or oncogenic premature senescence and sensitizes cells to oxidative apoptosis. Cancer cell *14*, 458-470.

Nohe, A., Hassel, S., Ehrlich, M., Neubauer, F., Sebald, W., Henis, Y.I., and Knaus, P. (2002). The mode of bone morphogenetic protein (BMP) receptor oligomerization determines different BMP-2 signaling pathways. The Journal of biological chemistry *277*, 5330-5338.

O

O'Brien, C.A., Nakashima, T., and Takayanagi, H. (2013). Osteocyte control of osteoclastogenesis. Bone *54*, 258-263.

Onichtchouk, D., Chen, Y.G., Dosch, R., Gawantka, V., Delius, H., Massague, J., and Niehrs, C. (1999). Silencing of TGF-beta signalling by the pseudoreceptor BAMBI. Nature *401*, 480-485.

Orimo, H. (2010). The mechanism of mineralization and the role of alkaline phosphatase in health and disease. Journal of Nippon Medical School = Nippon Ika Daigaku zasshi *77*, 4-12.

Ortuno, M.J., Ruiz-Gaspa, S., Rodriguez-Carballo, E., Susperregui, A.R., Bartrons, R., Rosa, J.L., and Ventura, F. (2010). p38 regulates expression of osteoblast-specific genes by phosphorylation of osterix. The Journal of biological chemistry *285*, 31985-31994.

Ortuno, M.J., Susperregui, A.R., Artigas, N., Rosa, J.L., and Ventura, F. (2013). Osterix induces Col1a1 gene expression through binding to Sp1 sites in the bone enhancer and proximal promoter regions. Bone *52*, 548-556.

Otto, F., Thornell, A.P., Crompton, T., Denzel, A., Gilmour, K.C., Rosewell, I.R., Stamp, G.W., Beddington, R.S., Mundlos, S., Olsen, B.R., *et al.* (1997). Cbfa1, a candidate gene for cleidocranial dysplasia syndrome, is essential for osteoblast differentiation and bone development. Cell *89*, 765-771.

Oury, F., Ferron, M., Huizhen, W., Confavreux, C., Xu, L., Lacombe, J., Srinivas, P., Chamouni, A., Lugani, F., Lejeune, H., *et al.* (2013). Osteocalcin regulates murine and human fertility through a pancreas-bone-testis axis. The Journal of clinical investigation *123*, 2421-2433.

Oury, F., Sumara, G., Sumara, O., Ferron, M., Chang, H., Smith, C.E., Hermo, L., Suarez, S., Roth, B.L., Ducy, P., *et al.* (2011). Endocrine regulation of male fertility by the skeleton. Cell *144*, 796-809.

Pasero, M., Giovarelli, M., Bucci, G., Gherzi, R., and Briata, P. (2012). Bone morphogenetic protein/SMAD signaling orients cell fate decision by impairing KSRP-dependent microRNA maturation. Cell reports 2, 1159-1168.

Peng, X.D., Xu, P.Z., Chen, M.L., Hahn-Windgassen, A., Skeen, J., Jacobs, J., Sundararajan, D., Chen, W.S., Crawford, S.E., Coleman, K.G., *et al.* (2003). Dwarfism, impaired skin development, skeletal muscle atrophy, delayed bone development, and impeded adipogenesis in mice lacking Akt1 and Akt2. Genes & development *17*, 1352-1365.

Plotkin, L.I., and Bellido, T. (2013). Beyond gap junctions: Connexin43 and bone cell signaling. Bone 52, 157-166.

Powis, G., Bonjouklian, R., Berggren, M.M., Gallegos, A., Abraham, R., Ashendel, C., Zalkow, L., Matter, W.F., Dodge, J., Grindey, G., *et al.* (1994). Wortmannin, a potent and selective inhibitor of phosphatidylinositol-3-kinase. Cancer research 54, 2419-2423.

Q

Qin, W., Chung, A.C., Huang, X.R., Meng, X.M., Hui, D.S., Yu, C.M., Sung, J.J., and Lan, H.Y. (2011). TGF-beta/Smad3 signaling promotes renal fibrosis by inhibiting miR-29. Journal of the American Society of Nephrology : JASN 22, 1462-1474.

R

Rached, M.T., Kode, A., Silva, B.C., Jung, D.Y., Gray, S., Ong, H., Paik, J.H., DePinho, R.A., Kim, J.K., Karsenty, G., *et al.* (2010a). FoxO1 expression in osteoblasts regulates glucose homeostasis through regulation of osteocalcin in mice. The Journal of clinical investigation *120*, 357-368.

Rached, M.T., Kode, A., Xu, L., Yoshikawa, Y., Paik, J.H., Depinho, R.A., and Kousteni, S. (2010b). FoxO1 is a positive regulator of bone formation by favoring protein synthesis and resistance to oxidative stress in osteoblasts. Cell metabolism *11*, 147-160.

Regard, J.B., Zhong, Z., Williams, B.O., and Yang, Y. (2012). Wnt signaling in bone development and disease: making stronger bone with Wnts. Cold Spring Harbor perspectives in biology *4*.

Riddle, R.C., Frey, J.L., Tomlinson, R.E., Ferron, M., Li, Y., DiGirolamo, D.J., Faugere, M.C., Hussain, M.A., Karsenty, G., and Clemens, T.L. (2014). Tsc2 is a molecular checkpoint controlling osteoblast development and glucose homeostasis. Molecular and cellular biology *34*, 1850-1862.

Robledo, R.F., Rajan, L., Li, X., and Lufkin, T. (2002). The Dlx5 and Dlx6 homeobox genes are essential for craniofacial, axial, and appendicular skeletal development. Genes & development *16*, 1089-1101.

Rodda, S.J., and McMahon, A.P. (2006). Distinct roles for Hedgehog and canonical Wnt signaling in specification, differentiation and maintenance of osteoblast progenitors. Development *133*, 3231-3244.

Rodon, J., Dienstmann, R., Serra, V., and Tabernero, J. (2013). Development of PI3K inhibitors: lessons learned from early clinical trials. Nature reviews Clinical oncology *10*, 143-153.

Rodriguez-Carballo, E., Gamez, B., Mendez-Lucas, A., Sanchez-Freutrie, M., Zorzano, A., Bartrons, R., Alcantara, S., Perales, J.C., and Ventura, F. (2015). p38alpha function in osteoblasts influences adipose tissue homeostasis. FASEB journal : official publication of the Federation of American Societies for Experimental Biology *29*, 1414-1425.

Rodriguez-Carballo, E., Gamez, B., Sedo-Cabezon, L., Sanchez-Feutrie, M., Zorzano, A., Manzanares-Cespedes, C., Rosa, J.L., and Ventura, F. (2014). The p38alpha MAPK function in osteoprecursors is required for bone formation and bone homeostasis in adult mice. PloS one 9, e102032.

Rodriguez-Carballo, E., Ulsamer, A., Susperregui, A.R., Manzanares-Cespedes, C., Sanchez-Garcia, E., Bartrons, R., Rosa, J.L., and Ventura, F. (2011). Conserved regulatory motifs in osteogenic gene promoters integrate cooperative effects of canonical Wnt and BMP pathways. Journal of bone and mineral research : the official journal of the American Society for Bone and Mineral Research 26, 718-729.

Rodriguez-Viciana, P., Sabatier, C., and McCormick, F. (2004). Signaling specificity by Ras family GTPases is determined by the full spectrum of effectors they regulate. Molecular and cellular biology 24, 4943-4954.

Ross, S., and Hill, C.S. (2008). How the Smads regulate transcription. The international journal of biochemistry & cell biology 40, 383-408.

Ruby, J.G., Jan, C.H., and Bartel, D.P. (2007). Intronic microRNA precursors that bypass Drosha processing. Nature 448, 83-86.

Rydziel, S., Delany, A.M., and Canalis, E. (2004). AU-rich elements in the collagenase 3 mRNA mediate stabilization of the transcript by cortisol in osteoblasts. The Journal of biological chemistry 279, 5397-5404.

S

Sadhu, C., Dick, K., Tino, W.T., and Staunton, D.E. (2003). Selective role of PI3K delta in neutrophil inflammatory responses. Biochemical and biophysical research communications 308, 764-769.

Saijilafu, Hur, E.M., Liu, C.M., Jiao, Z., Xu, W.L., and Zhou, F.Q. (2013). PI3K-GSK3 signalling regulates mammalian axon regeneration by inducing the expression of Smad1. Nature communications 4, 2690.

Sapkota, G., Alarcon, C., Spagnoli, F.M., Brivanlou, A.H., and Massague, J. (2007). Balancing BMP signaling through integrated inputs into the Smad1 linker. Molecular cell 25, 441-454.

Sarkar, S., Dey, B.K., and Dutta, A. (2010). MiR-322/424 and -503 are induced during muscle differentiation and promote cell cycle quiescence and differentiation by down-regulation of Cdc25A. Molecular biology of the cell *21*, 2138-2149.

Sato, M.M., Nashimoto, M., Katagiri, T., Yawaka, Y., and Tamura, M. (2009). Bone morphogenetic protein-2 down-regulates miR-206 expression by blocking its maturation process. Biochemical and biophysical research communications *383*, 125-129.

Satokata, I., Ma, L., Ohshima, H., Bei, M., Woo, I., Nishizawa, K., Maeda, T., Takano, Y., Uchiyama, M., Heaney, S., *et al.* (2000). Msx2 deficiency in mice causes pleiotropic defects in bone growth and ectodermal organ formation. Nature genetics *24*, 391-395.

Scheufler, C., Sebald, W., and Hulsmeyer, M. (1999). Crystal structure of human bone morphogenetic protein-2 at 2.7 A resolution. Journal of molecular biology *287*, 103-115.

Schoenberg, D.R., and Maquat, L.E. (2012). Regulation of cytoplasmic mRNA decay. Nature reviews Genetics *13*, 246-259.

Seitz, H., and Zamore, P.D. (2006). Rethinking the microprocessor. Cell *125*, 827-829.

Shao, Z., Bhattacharya, K., Hsich, E., Park, L., Walters, B., Germann, U., Wang, Y.M., Kyriakis, J., Mohanlal, R., Kuida, K., *et al.* (2006). c-Jun N-terminal kinases mediate reactivation of Akt and cardiomyocyte survival after hypoxic injury in vitro and in vivo. Circulation research *98*, 111-118.

Shekar, S.C., Wu, H., Fu, Z., Yip, S.C., Nagajyothi, Cahill, S.M., Girvin, M.E., and Backer, J.M. (2005). Mechanism of constitutive phosphoinositide 3-kinase activation by oncogenic mutants of the p85 regulatory subunit. The Journal of biological chemistry *280*, 27850-27855.

Shi, K., Lu, J., Zhao, Y., Wang, L., Li, J., Qi, B., Li, H., and Ma, C. (2013). MicroRNA-214 suppresses osteogenic differentiation of C2C12 myoblast cells by targeting Osterix. Bone *55*, 487-494.

Shi, Y., Hata, A., Lo, R.S., Massague, J., and Pavletich, N.P. (1997). A structural basis for mutational inactivation of the tumour suppressor Smad4. Nature *388*, 87-93.

Shi, Y., and Massague, J. (2003). Mechanisms of TGF-beta signaling from cell membrane to the nucleus. Cell *113*, 685-700.

Shinohara, M., Nakamura, M., Masuda, H., Hirose, J., Kadono, Y., Iwasawa, M., Nagase, Y., Ueki, K., Kadowaki, T., Sasaki, T., *et al.* (2012). Class IA phosphatidylinositol 3-kinase regulates osteoclastic bone resorption through protein kinase B-mediated vesicle transport. Journal of bone and mineral research : the official journal of the American Society for Bone and Mineral Research *27*, 2464-2475.

Shioi, T., Kang, P.M., Douglas, P.S., Hampe, J., Yballe, C.M., Lawitts, J., Cantley, L.C., and Izumo, S. (2000). The conserved phosphoinositide 3-kinase pathway determines heart size in mice. The EMBO journal *19*, 2537-2548.

Shirakabe, K., Yamaguchi, K., Shibuya, H., Irie, K., Matsuda, S., Moriguchi, T., Gotoh, Y., Matsumoto, K., and Nishida, E. (1997). TAK1 mediates the ceramide signaling to stress-activated protein kinase/c-Jun N-terminal kinase. The Journal of biological chemistry *272*, 8141-8144.

Shore, E.M., Xu, M., Feldman, G.J., Fenstermacher, D.A., Cho, T.J., Choi, I.H., Connor, J.M., Delai, P., Glaser, D.L., LeMerrer, M., *et al.* (2006). A recurrent mutation in the BMP type I receptor ACVR1 causes inherited and sporadic fibrodysplasia ossificans progressiva. Nature genetics *38*, 525-527.

Sims, N.A., and Gooi, J.H. (2008). Bone remodeling: Multiple cellular interactions required for coupling of bone formation and resorption. Seminars in cell & developmental biology *19*, 444-451.

Smith, G.C., Ong, W.K., Costa, J.L., Watson, M., Cornish, J., Grey, A., Gamble, G.D., Dickinson, M., Leung, S., Rewcastle, G.W., *et al.* (2013). Extended treatment with selective phosphatidylinositol 3-kinase and mTOR inhibitors has effects on metabolism, growth, behaviour and bone strength. The FEBS journal *280*, 5337-5349.

Soleimani, M., and Nadri, S. (2009). A protocol for isolation and culture of mesenchymal stem cells from mouse bone marrow. Nature protocols *4*, 102-106.

Song, J., McColl, J., Camp, E., Kennerley, N., Mok, G.F., McCormick, D., Grocott, T., Wheeler, G.N., and Munsterberg, A.E. (2014). Smad1 transcription factor integrates BMP2 and Wnt3a signals in migrating cardiac progenitor cells. Proceedings of the National Academy of Sciences of the United States of America *111*, 7337-7342.

Song, M.S., Salmena, L., and Pandolfi, P.P. (2012). The functions and regulation of the PTEN tumour suppressor. Nature reviews Molecular cell biology *13*, 283-296.

Songyang, Z., Shoelson, S.E., Chaudhuri, M., Gish, G., Pawson, T., Haser, W.G., King, F., Roberts, T., Ratnofsky, S., Lechleider, R.J., *et al.* (1993). SH2 domains recognize specific phosphopeptide sequences. Cell *72*, 767-778.

Stambolic, V., Suzuki, A., de la Pompa, J.L., Brothers, G.M., Mirtsos, C., Sasaki, T., Ruland, J., Penninger, J.M., Siderovski, D.P., and Mak, T.W. (1998). Negative regulation of PKB/Akt-dependent cell survival by the tumor suppressor PTEN. Cell *95*, 29-39.

Starega-Roslan, J., Koscianska, E., Kozlowski, P., and Krzyzosiak, W.J. (2011). The role of the precursor structure in the biogenesis of microRNA. Cellular and molecular life sciences : CMLS *68*, 2859-2871.

Stephens, L., Anderson, K., Stokoe, D., Erdjument-Bromage, H., Painter, G.F., Holmes, A.B., Gaffney, P.R., Reese, C.B., McCormick, F., Tempst, P., *et al.* (1998). Protein kinase B kinases that mediate phosphatidylinositol 3,4,5-trisphosphate-dependent activation of protein kinase B. Science *279*, 710-714.

Stock, M., and Otto, F. (2005). Control of RUNX2 isoform expression: the role of promoters and enhancers. Journal of cellular biochemistry *95*, 506-517.

Stokoe, D., Stephens, L.R., Copeland, T., Gaffney, P.R., Reese, C.B., Painter, G.F., Holmes, A.B., McCormick, F., and Hawkins, P.T. (1997). Dual role of phosphatidylinositol-3,4,5-trisphosphate in the activation of protein kinase B. Science *277*, 567-570.

Suire, S., Condliffe, A.M., Ferguson, G.J., Ellson, C.D., Guillou, H., Davidson, K., Welch, H., Coadwell, J., Turner, M., Chilvers, E.R., *et al.* (2006). Gbetagammas and the Ras binding domain of p110gamma are both important regulators of PI(3)Kgamma signalling in neutrophils. Nature cell biology *8*, 1303-1309.

Sun, D., Martinez, C.O., Ochoa, O., Ruiz-Willhite, L., Bonilla, J.R., Centonze, V.E., Waite, L.L., Michalek, J.E., McManus, L.M., and Shireman, P.K. (2009). Bone marrow-derived cell regulation of skeletal muscle regeneration. FASEB journal : official publication of the Federation of American Societies for Experimental Biology *23*, 382-395.

Susperregui, A.R., Gamell, C., Rodriguez-Carballo, E., Ortuno, M.J., Bartrons, R., Rosa, J.L., and Ventura, F. (2011). Noncanonical BMP signaling regulates cyclooxygenase-2 transcription. Molecular endocrinology *25*, 1006-1017.

T

Takayanagi, H., Kim, S., Koga, T., Nishina, H., Isshiki, M., Yoshida, H., Saiura, A., Isobe, M., Yokochi, T., Inoue, J., *et al.* (2002). Induction and activation of the transcription factor NFATc1 (NFAT2) integrate RANKL signaling in terminal differentiation of osteoclasts. Developmental cell *3*, 889-901.

Tanaka, S., Nakamura, K., Takahasi, N., and Suda, T. (2005). Role of RANKL in physiological and pathological bone resorption and therapeutics targeting the RANKL-RANK signaling system. Immunological reviews *208*, 30-49.

Tang, Y.Y., Shi, J., Zhang, L., Davis, A., Bravo, J., Warren, A.J., Speck, N.A., and Bushweller, J.H. (2000). Energetic and functional contribution of residues in the core binding factor beta (CBFbeta) subunit to heterodimerization with CBFalpha. The Journal of biological chemistry *275*, 39579-39588.

Thorpe, L.M., Yuzugullu, H., and Zhao, J.J. (2015). PI3K in cancer: divergent roles of isoforms, modes of activation and therapeutic targeting. Nature reviews Cancer *15*, 7-24.

Tondravi, M.M., McKercher, S.R., Anderson, K., Erdmann, J.M., Quiroz, M., Maki, R., and Teitelbaum, S.L. (1997). Osteopetrosis in mice lacking haematopoietic transcription factor PU.1. Nature *386*, 81-84.

U

Ulsamer, A., Ortuno, M.J., Ruiz, S., Susperregui, A.R., Osses, N., Rosa, J.L., and Ventura, F. (2008). BMP-2 induces Osterix expression through up-regulation of Dlx5 and its phosphorylation by p38. The Journal of biological chemistry *283*, 3816-3826.

Urist, M.R. (1965). Bone: formation by autoinduction. Science *150*, 893-899.

Usui, M., Yoshida, Y., Tsuji, K., Oikawa, K., Miyazono, K., Ishikawa, I., Yamamoto, T., Nifuji, A., and Noda, M. (2004). Tob deficiency superenhances osteoblastic activity after ovariectomy to block estrogen deficiency-induced osteoporosis. Proceedings of the National Academy of Sciences of the United States of America *101*, 6653-6658.

Utermark, T., Rao, T., Cheng, H., Wang, Q., Lee, S.H., Wang, Z.C., Iglehart, J.D., Roberts, T.M., Muller, W.J., and Zhao, J.J. (2012). The p110alpha and p110beta isoforms of PI3K play divergent roles in mammary gland development and tumorigenesis. Genes & development *26*, 1573-1586.

V

van Gaalen, S.M., Kruyt, M.C., Geuze, R.E., de Bruijn, J.D., Alblas, J., and Dhert, W.J. (2010). Use of fluorochrome labels in in vivo bone tissue engineering research. Tissue engineering Part B, Reviews *16*, 209-217.

Vanhaesebroeck, B., Guillermet-Guibert, J., Graupera, M., and Bilanges, B. (2010a). The emerging mechanisms of isoform-specific PI3K signalling. Nature reviews Molecular cell biology *11*, 329-341.

Vanhaesebroeck, B., Leevers, S.J., Ahmadi, K., Timms, J., Katso, R., Driscoll, P.C., Woscholski, R., Parker, P.J., and Waterfield, M.D. (2001). Synthesis and function of 3-phosphorylated inositol lipids. Annual review of biochemistry *70*, 535-602.

Vanhaesebroeck, B., Leevers, S.J., Panayotou, G., and Waterfield, M.D. (1997a). Phosphoinositide 3-kinases: a conserved family of signal transducers. Trends in biochemical sciences 22, 267-272.

Vanhaesebroeck, B., Stephens, L., and Hawkins, P. (2012). PI3K signalling: the path to discovery and understanding. Nature reviews Molecular cell biology *13*, 195-203.

Vanhaesebroeck, B., Vogt, P.K., and Rommel, C. (2010b). PI3K: from the bench to the clinic and back. Current topics in microbiology and immunology *347*, 1-19.

Vanhaesebroeck, B., Welham, M.J., Kotani, K., Stein, R., Warne, P.H., Zvelebil, M.J., Higashi, K., Volinia, S., Downward, J., and Waterfield, M.D. (1997b). P110delta, a novel phosphoinositide 3-kinase in leukocytes. Proceedings of the National Academy of Sciences of the United States of America 94, 4330-4335.

Vasudevan, K.M., and Garraway, L.A. (2010). AKT signaling in physiology and disease. Current topics in microbiology and immunology *347*, 105-133.

Vasudevan, S., Tong, Y., and Steitz, J.A. (2007). Switching from repression to activation: microRNAs can up-regulate translation. Science *318*, 1931-1934.

Ventura, F., Doody, J., Liu, F., Wrana, J.L., and Massague, J. (1994). Reconstitution and transphosphorylation of TGF-beta receptor complexes. The EMBO journal *13*, 5581-5589.

Vimalraj, S., and Selvamurugan, N. (2012). MicroRNAs: Synthesis, Gene Regulation and Osteoblast Differentiation. Current issues in molecular biology *15*, 7-18.

Vlahos, C.J., Matter, W.F., Hui, K.Y., and Brown, R.F. (1994). A specific inhibitor of phosphatidylinositol 3-kinase, 2-(4-morpholinyl)-8-phenyl-4H-1-benzopyran-4-one (LY294002). The Journal of biological chemistry *269*, 5241-5248.

W

Wagner, D.O., Sieber, C., Bhushan, R., Borgermann, J.H., Graf, D., and Knaus, P. (2010). BMPs: from bone to body morphogenetic proteins. Science signaling *3*, mr1.

Wan, M., and Cao, X. (2005). BMP signaling in skeletal development. Biochemical and biophysical research communications *328*, 651-657.

Wang, T., and Xu, Z. (2010). miR-27 promotes osteoblast differentiation by modulating Wnt signaling. Biochemical and biophysical research communications *402*, 186-189.

Wang, X., Guo, B., Li, Q., Peng, J., Yang, Z., Wang, A., Li, D., Hou, Z., Lv, K., Kan, G., *et al.* (2013). miR-214 targets ATF4 to inhibit bone formation. Nature medicine *19*, 93-100.

Washio-Oikawa, K., Nakamura, T., Usui, M., Yoneda, M., Ezura, Y., Ishikawa, I., Nakashima, K., Noda, T., Yamamoto, T., and Noda, M. (2007). Cnot7-null mice exhibit high bone mass phenotype and modulation of BMP actions. Journal of bone and mineral research : the official journal of the American Society for Bone and Mineral Research *22*, 1217-1223.

Wei, J., Shi, Y., Zheng, L., Zhou, B., Inose, H., Wang, J., Guo, X.E., Grosschedl, R., and Karsenty, G. (2012). miR-34s inhibit osteoblast proliferation and differentiation in the mouse by targeting SATB2. The Journal of cell biology *197*, 509-521.

Welch, H.C., Coadwell, W.J., Ellson, C.D., Ferguson, G.J., Andrews, S.R., Erdjument-Bromage, H., Tempst, P., Hawkins, P.T., and Stephens, L.R. (2002). P-Rex1, a PtdIns(3,4,5)P3- and Gbetagamma-regulated guanine-nucleotide exchange factor for Rac. Cell *108*, 809-821.

Wheeler, M., and Domin, J. (2006). The N-terminus of phosphoinositide 3-kinase-C2beta regulates lipid kinase activity and binding to clathrin. Journal of cellular physiology *206*, 586-593.

Wicks, S.J., Grocott, T., Haros, K., Maillard, M., ten Dijke, P., and Chantry, A. (2006). Reversible ubiquitination regulates the Smad/TGF-beta signalling pathway. Biochemical Society transactions *34*, 761-763.

Winbanks, C.E., Wang, B., Beyer, C., Koh, P., White, L., Kantharidis, P., and Gregorevic, P. (2011). TGF-beta regulates miR-206 and miR-29 to control myogenic differentiation through regulation of HDAC4. The Journal of biological chemistry *286*, 13805-13814.

Winkler, G.S. (2010). The mammalian anti-proliferative BTG/Tob protein family. Journal of cellular physiology *222*, 66-72.

Worby, C.A., and Dixon, J.E. (2014). Pten. Annual review of biochemistry *83*, 641-669.

Wu, C.H., and Nusse, R. (2002). Ligand receptor interactions in the Wnt signaling pathway in Drosophila. The Journal of biological chemistry *277*, 41762-41769.

Wu, T., Zhou, H., Hong, Y., Li, J., Jiang, X., and Huang, H. (2012). miR-30 family members negatively regulate osteoblast differentiation. The Journal of biological chemistry *287*, 7503-7511.

Wymann, M.P., Bulgarelli-Leva, G., Zvelebil, M.J., Pirola, L., Vanhaesebroeck, B., Waterfield, M.D., and Panayotou, G. (1996). Wortmannin inactivates phosphoinositide 3-kinase by covalent modification of Lys-802, a residue involved in the phosphate transfer reaction. Molecular and cellular biology *16*, 1722-1733.

X

Xian, L., Wu, X., Pang, L., Lou, M., Rosen, C.J., Qiu, T., Crane, J., Frassica, F., Zhang, L., Rodriguez, J.P., *et al.* (2012). Matrix IGF-1 maintains bone mass by activation of mTOR in mesenchymal stem cells. Nature medicine *18*, 1095-1101.

Xiao, G., Gopalakrishnan, R., Jiang, D., Reith, E., Benson, M.D., and Franceschi, R.T. (2002a). Bone morphogenetic proteins, extracellular matrix, and mitogen-activated protein kinase signaling pathways are required for osteoblast-specific gene expression and differentiation in MC3T3-E1 cells. Journal of bone and mineral research : the official journal of the American Society for Bone and Mineral Research *17*, 101-110.

Xiao, G., Jiang, D., Gopalakrishnan, R., and Franceschi, R.T. (2002b). Fibroblast growth factor 2 induction of the osteocalcin gene requires MAPK activity and phosphorylation of the osteoblast transcription factor, Cbfa1/Runx2. The Journal of biological chemistry *277*, 36181-36187.

Xiao, G., Jiang, D., Thomas, P., Benson, M.D., Guan, K., Karsenty, G., and Franceschi, R.T. (2000). MAPK pathways activate and phosphorylate the osteoblast-specific transcription factor, Cbfa1. The Journal of biological chemistry *275*, 4453-4459.

Xiong, J., Onal, M., Jilka, R.L., Weinstein, R.S., Manolagas, S.C., and O'Brien, C.A. (2011). Matrix-embedded cells control osteoclast formation. Nature medicine *17*, 1235-1241.

Xu, M.Q., Feldman, G., Le Merrer, M., Shugart, Y.Y., Glaser, D.L., Urtizberea, J.A., Fardeau, M., Connor, J.M., Triffitt, J., Smith, R., *et al.* (2000). Linkage exclusion and mutational analysis of the noggin gene in patients with fibrodysplasia ossificans progressiva (FOP). Clinical genetics *58*, 291-298.

Y

Yamashita, M., Fatyol, K., Jin, C., Wang, X., Liu, Z., and Zhang, Y.E. (2008). TRAF6 mediates Smad-independent activation of JNK and p38 by TGF-beta. Molecular cell *31*, 918-924.

Yang, L., Cheng, P., Chen, C., He, H.B., Xie, G.Q., Zhou, H.D., Xie, H., Wu, X.P., and Luo, X.H. (2012). miR-93/Sp7 function loop mediates osteoblast mineralization. Journal of bone and mineral research : the official journal of the American Society for Bone and Mineral Research *27*, 1598-1606.

Yang, S., Xu, H., Yu, S., Cao, H., Fan, J., Ge, C., Fransceschi, R.T., Dong, H.H., and Xiao, G. (2011). Foxo1 mediates insulin-like growth factor 1 (IGF1)/insulin regulation of osteocalcin expression by antagonizing Runx2 in osteoblasts. The Journal of biological chemistry *286*, 19149-19158.

Yang, X., Matsuda, K., Bialek, P., Jacquot, S., Masuoka, H.C., Schinke, T., Li, L., Brancorsini, S., Sassone-Corsi, P., Townes, T.M., *et al.* (2004). ATF4 is a substrate of RSK2 and an essential regulator of osteoblast biology; implication for Coffin-Lowry Syndrome. Cell *117*, 387-398.

Yingzi Yang, D., J.J. de Gorter, Peter ten Dijke, F.Patrick Ross, Lynda F. Bonewald, Gerhard Sengle, Lynn Y. Sakai, Adele L.Boskey and Pamela Gehron Robey. (2013). Section I: Molecular, Cellular, and Genetic Determinants of Bone structure and Formation. Chapters 1 to 6. In Primer on the Metabolic Bone Diseases and Disorders of Mineral Metabolism, T.A.S.f.B.a.M.R. (ASBMR), ed. (Wiley-Blackwell).

Yoshida, C.A., Komori, H., Maruyama, Z., Miyazaki, T., Kawasaki, K., Furuichi, T., Fukuyama, R., Mori, M., Yamana, K., Nakamura, K., *et al.* (2012). SP7 inhibits osteoblast differentiation at a late stage in mice. PloS one *7*, e32364.

Yoshida, C.A., Yamamoto, H., Fujita, T., Furuichi, T., Ito, K., Inoue, K., Yamana, K., Zanma, A., Takada, K., Ito, Y., *et al.* (2004). Runx2 and Runx3 are essential for chondrocyte maturation, and Runx2 regulates limb growth through induction of Indian hedgehog. Genes & development *18*, 952-963.

Yoshida, Y., Tanaka, S., Umemori, H., Minowa, O., Usui, M., Ikematsu, N., Hosoda, E., Imamura, T., Kuno, J., Yamashita, T., *et al.* (2000). Negative regulation of BMP/Smad signaling by Tob in osteoblasts. Cell *103*, 1085-1097.

Yu, J., Zhang, Y., McIlroy, J., Rordorf-Nikolic, T., Orr, G.A., and Backer, J.M. (1998). Regulation of the p85/p110 phosphatidylinositol 3'-kinase: stabilization and inhibition of the p110alpha catalytic subunit by the p85 regulatory subunit. Molecular and cellular biology *18*, 1379-1387.

Z

Zhang, J., Li, A.M., Liu, B.X., Han, F., Liu, F., Sun, S.P., Li, X., Cui, S.J., Xian, S.Z., Kong, G.Q., *et al.* (2013). Effect of icarisid II on diabetic rats with erectile dysfunction and its potential mechanism via assessment of AGEs, autophagy, mTOR and the NO-cGMP pathway. Asian journal of andrology *15*, 143-148.

Zhang, J., Tu, Q., Grosschedl, R., Kim, M.S., Griffin, T., Drissi, H., Yang, P., and Chen, J. (2011a). Roles of SATB2 in osteogenic differentiation and bone regeneration. Tissue engineering Part A *17*, 1767-1776.

Zhang, J.F., Fu, W.M., He, M.L., Wang, H., Wang, W.M., Yu, S.C., Bian, X.W., Zhou, J., Lin, M.C., Lu, G., *et al.* (2011b). MiR-637 maintains the balance between adipocytes and osteoblasts by directly targeting Osterix. Molecular biology of the cell *22*, 3955-3961.

Zhang, M., Xuan, S., Bouxsein, M.L., von Stechow, D., Akeno, N., Faugere, M.C., Malluche, H., Zhao, G., Rosen, C.J., Efstratiadis, A., *et al.* (2002). Osteoblast-specific knockout of the insulin-like growth factor (IGF) receptor gene reveals an essential role of IGF signaling in bone matrix mineralization. The Journal of biological chemistry *277*, 44005-44012.

Zhang, Y., Xie, R.L., Croce, C.M., Stein, J.L., Lian, J.B., van Wijnen, A.J., and Stein, G.S. (2011c). A program of microRNAs controls osteogenic lineage progression by targeting transcription factor Runx2. Proceedings of the National Academy of Sciences of the United States of America *108*, 9863-9868.

Zhang, Y., Xie, R.L., Gordon, J., LeBlanc, K., Stein, J.L., Lian, J.B., van Wijnen, A.J., and Stein, G.S. (2012). Control of mesenchymal lineage progression by microRNAs targeting skeletal gene regulators Trps1 and Runx2. The Journal of biological chemistry *287*, 21926-21935.

Zhang, Y.W., Yasui, N., Ito, K., Huang, G., Fujii, M., Hanai, J., Nogami, H., Ochi, T., Miyazono, K., and Ito, Y. (2000). A RUNX2/PEBP2alpha A/CBFA1 mutation displaying impaired transactivation and Smad interaction in cleidocranial dysplasia. Proceedings of the National Academy of Sciences of the United States of America *97*, 10549-10554.

Zhao, J.J., Cheng, H., Jia, S., Wang, L., Gjoerup, O.V., Mikami, A., and Roberts, T.M. (2006). The p110alpha isoform of PI3K is essential for proper growth factor signaling and oncogenic transformation. Proceedings of the National Academy of Sciences of the United States of America *103*, 16296-16300.

Zheng, Z., Amran, S.I., Thompson, P.E., and Jennings, I.G. (2011). Isoform-selective inhibition of phosphoinositide 3-kinase: identification of a new region of nonconserved amino acids critical for p110alpha inhibition. Molecular pharmacology *80*, 657-664.

Zhou, X., Zhang, Z., Feng, J.Q., Dusevich, V.M., Sinha, K., Zhang, H., Darnay, B.G., and de Crombrugghe, B. (2010). Multiple functions of Osterix are required for bone growth and homeostasis in postnatal mice. Proceedings of the National Academy of Sciences of the United States of America *107*, 12919-12924.

Ziros, P.G., Basdra, E.K., and Papavassiliou, A.G. (2008). Runx2: of bone and stretch. The international journal of biochemistry & cell biology *40*, 1659-1663.

PUBLICATIONS

THE JOURNAL OF BIOLOGICAL CHEMISTRY VOL. 288, NO. 20, pp. 14264–14275, May 17, 2013

MicroRNA-322 (miR-322) and Its Target Protein Tob2 Modulate Osterix (*Osx*) mRNA Stability*[S]

Received for publication, October 31, 2012, and in revised form, March 7, 2013 Published, JBC Papers in Press, April 5, 2013, DOI 10.1074/jbc.M112.432104

Beatriz Gámez, Edgardo Rodríguez-Carballo[1], Ramon Bartrons, José Luis Rosa, and Francesc Ventura[2]

From the Departament de Ciències Fisiològiques II, Universitat de Barcelona, and L'Institut d'Investigació Biomèdica de Bellvitge (IDIBELL), E-08907 L'Hospitalet de Llobregat, Barcelona, Spain

Background: miRNAs exert important roles during osteoblast proliferation and differentiation.
Results: miR-322 induces expression of osteogenic genes by down-regulation of expression of *Tob2*, which binds to the 3′-UTR of *Osx* and modulates its degradation.
Conclusion: miR-322 and its target Tob2 are regulators of osteogenesis through control of *Osx* mRNA degradation.
Significance: We have identified a miRNA-transcription factor network that allows fine-tuning of the osteoblast differentiation program.

Osteogenesis depends on a coordinated network of signals and transcription factors such as Runx2 and Osterix. Recent evidence indicates that microRNAs (miRNAs) act as important post-transcriptional regulators in a large number of processes, including osteoblast differentiation. In this study, we performed miRNA expression profiling and identified miR-322, a BMP-2-down-regulated miRNA, as a regulator of osteoblast differentiation. We report miR-322 gain- and loss-of-function experiments in C2C12 and MC3T3-E1 cells and primary cultures of murine bone marrow-derived mesenchymal stem cells. We demonstrate that overexpression of miR-322 enhances BMP-2 response, increasing the expression of *Osx* and other osteogenic genes. Furthermore, we identify Tob2 as a target of miR-322, and we characterize the specific *Tob2* 3′-UTR sequence bound by miR-322 by reporter assays. We demonstrate that Tob2 is a negative regulator of osteogenesis that binds and mediates degradation of *Osx* mRNA. Our results demonstrate a new molecular mechanism controlling osteogenesis through the specific miR-322/Tob2 regulation of specific target mRNAs. This regulatory circuit provides a clear example of a complex miRNA-transcription factor network for fine-tuning the osteoblast differentiation program.

Skeletal development depends on the activity of osteoblasts that derive from condensations of mesenchymal cells. In addition, bone is constantly remodeled throughout life, and it requires stringent control of a program of gene activation and suppression in response to physiological signals. Understanding this regulatory mechanism is important for developing new strategies to treat pathological states such as osteoporosis and osteosclerosis. For the specification of mesenchymal cells to distinct terminal phenotypes, cohorts of tissue-specific transcription factors and coregulators mediate the expression of genes required for the functions of a particular differentiated tissue. Molecular and genetic research has identified Osterix (Osx), Runx2, Dlx5, Msx2, and ATF4, among others, as important transcription factors essential for osteoblast differentiation (1, 2). Osx and Runx2 have been widely accepted as master osteogenic factors because neither Runx2- nor Osx-null mice form mature osteoblasts (3, 4).

Osteoblast lineage specification and maturation of osteoprogenitors are also controlled by multiple extracellular ligands. Bone morphogenetic proteins (BMPs)[3] belong to the TGF-β superfamily and, together with Wnt proteins, are the main extracellular cues involved in the activation of skeleton-related genes for formation of cartilage and bone. BMP signals are transduced by Smad proteins and have been shown to stimulate Runx2 and Osx *in vitro* and *in vivo* (5–10).

Recently, microRNAs (miRNAs) have emerged as important regulators in various developmental, physiological, and pathological conditions, including cell differentiation and function (11). miRNAs are small noncoding RNAs that mediate translational inhibition or degradation of the transcript by binding to complementary sites in the 3′-UTRs or coding regions of target mRNAs (12). Recent studies indicate that miRNAs are important players during osteogenic differentiation, and the identification of new miRNAs characterizing genetic and metabolic abnormalities provides new approaches for treatment of diseases (13–19). It has been shown that depletion of miRNAs in the osteoblast lineage through conditional ablation of the *Dicer* gene causes evident skeletal phenotypes (20). Interestingly, previous studies have shown differential requirements of miRNA control at early and late steps of osteogenesis, suggesting that miRNAs are required for embryonic bone development as well as for bone homeostasis in the adult skeleton.

BMP and TGF-β are known to regulate miRNA biogenesis through ribonuclease 3, also known as Drosha (21). BMP-2 has

* This work was supported in part by Ministerio de Educación y Ciencia Grant BFU2011-24254, the Fundació La Marató de TV3, and Instituto de Salud Carlos III Grant RETIC RD06/0020.
[S] This article contains supplemental Figs. S1–S5 and Tables 1 and 2.
[1] Recipient of a fellowship from L'Institut d'Investigació Biomèdica de Bellvitge (IDIBELL).
[2] To whom correspondence should be addressed: Dept. de Ciències Fisiològiques II, Universitat de Barcelona, IDIBELL, C/Feixa Llarga s/n, E-08907 L'Hospitalet de Llobregat, Spain. Tel.: 34-9340-24281; Fax: 34-9340-24268; E-mail: fventura@ub.edu.

[3] The abbreviations used are: BMP, bone morphogenetic protein; miRNA, microRNA; BM-MSC, bone marrow-derived mesenchymal stem cell; qPCR, quantitative PCR.

been shown to down-regulate a cohort of miRNAs that target inhibitors of multiple osteogenic pathways in premyogenic cells, including BMP and Wnt receptors and their ligands as well as transcriptional regulators and MAPK signaling components (15, 22–26). Interestingly, the few miRNAs that are strongly up-regulated by BMP-2 in premyogenic cells target essential factors for muscle cell differentiation, thereby repressing their differentiation to myocytes.

In this study, we characterized miR-322, a novel BMP-2-down-regulated miRNA, and investigated its effects on osteoblast differentiation. We identified Tob2 as its target and showed that Tob2 regulated *Osx* mRNA degradation. We propose a regulatory mechanism in which miR-322/Tob2 controls *Osx* degradation and allows an integrated post-transcriptional control of multiple osteogenic genes.

EXPERIMENTAL PROCEDURES

Plasmids, Reagents, and Antibodies—pME18S-hTob2 was provided by Dr. T. Yamamoto. pFLAG-CMV-hCPEB4 was provided by Dr. R. Méndez. To determine the target region of miR-322, the 3′-UTR of the mouse *Tob2* cDNA was amplified from genomic DNA using primers 5′-TGCTGAAGTCTAGAGACCATCAGGCTT-3′ and 5′CTCCCATCTAGAAAAAGGATTCGCCCAGG-3′ for the wild type and primers 5′-TGCTGAAGTCTAGAGACCATCAGGCTT-3′ and 5′AGAGTGGTCTAGATGTCAATTCGTGCACC for the mutant construct and cloned between the XbaI sites of the pRL-SV40 vector (Promega, Madison, WI). Biotinylated RNA oligonucleotides were from Sigma: Osx1, 5′-AUCCUCGAGGUCUCCGAGAGUUUCUUUUUCAGUUGAGUUUUGGG-3′; Osx2, 5′-CCUGAGCUUUGUGUUUUCUUUUUUUAAACAAACACGAUGAUGAU-3′; control, 5′-CUCUCUCCGAGGGGCAGGGUUCCUCCC-3′. *Cox2-* and *Id1*-luciferase reporter constructs were described previously (27, 28). BMP-2 was from R&D Systems (Minneapolis, MN) and used at a final concentration of 2 nM. Actinomycin D (Sigma) was used at final concentration of 10 μg/ml. The following antibodies were used at 1:1000 for immunoblotting: anti-Osx (Abcam, Cambridge, UK); anti-Smad1 and anti-phospho-Smad (Cell Signaling, Beverly, MA); anti-Tob2 and anti-FLAG (Sigma); and anti-α-tubulin (Sigma). Immunocomplexes were visualized with a horseradish peroxidase-conjugated anti-rabbit or anti-mouse IgG antibody (1:10,000), followed by incubation with ECL Western blot reagent (GE Healthcare). Chemiluminescent image capture of immunoblots was performed with the Fujifilm LAS 3000 device. Quantification of protein expression was performed using Fujifilm MultiGauge software and is expressed as relative values using α-tubulin as a control.

Cell Culture, Differentiation, and Transfections—Bone marrow-derived mesenchymal stem cells (BM-MSCs) were isolated and cultured as described previously (8) and treated for 24 h with BMP-2 (2 nM) before miRNA isolation. C2C12 and HeLa cell lines were maintained as described previously (9). The MC3T3-E1 cell line was maintained in α-modified Eagle's medium supplemented with 10% FBS. To induce C2C12 cell differentiation, the medium was replaced with DMEM without serum, and BMP-2 (2 nM) was added. To induce MC3T3-E1 cell differentiation, the medium was replaced with α-modified Eagle's medium with 10% FBS, 50 μM ascorbic acid, and 5 mM β-glycerophosphate. Cells were transiently transfected using Lipofectamine RNAiMAX (Invitrogen) for miRNAs and Lipofectamine LTX (Invitrogen) for cotransfection with plasmids. Transfection efficiency was assessed by GFP or BLOCK-iT Alexa Fluor Red fluorescent control (Ambion, Paisley, United Kingdom). Pre-miR™ and Anti-miR™ (Ambion) were used at final concentration of 20 nM.

Microarray and RT-qPCR Analysis—Total RNA was isolated from C2C12 cells, MC3T3-E1 cells, or BM-MSCs using the Ultraspec RNA isolation system (Biotecx, Houston, TX). 3 μg of total RNA was reverse-transcribed using a High Capacity cDNA reverse transcription kit (Applied Biosystems). miRNAs were isolated using a mirVana miRNA isolation kit (Applied Biosystems), and reverse transcription was performed using a TaqMan microRNA reverse transcription kit (Applied Biosystems). Initial miRNA screening was performed using TaqMan Array Rodent MicroRNA B Card v3 (Applied Biosystems). miRNA qPCRs were performed using specific probes (TaqMan microRNA assays). All quantitative PCRs were carried out using the ABI Prism 7900HT fast real-time PCR system and the TaqMan 5′-nuclease probe method (Applied Biosystems). mRNA transcripts were normalized to GAPDH expression, and miRNA transcripts were normalized to U6 expression.

Luciferase Reporter Assays—Cells were transfected for 8 h without serum and treated with BMP-2 for 16–24 h. Luciferase activities were quantified using the luciferase assay system or the *Renilla* luciferase assay system (Promega). Luciferase values were normalized using β-galactosidase detection kit II (Clontech, Palo Alto, CA).

Lentiviral Transduction—LentimiRa-GFP-mmu-mir-322 and Lenti-IIII-mir-GFP control virus (ABM Inc., Richmond, British Columbia, Canada) were used for BM-MSC transduction at a multiplicity of infection of 1, and efficiency was controlled by the GFP coexpressed in the same construct. Polybrene (Sigma) was used at final concentration of 2 μg/ml to enhance viral infection. Puromycin was used to select infected cells at 2 μg/ml. Selected MSCs were cultured for 5 days in osteogenic differentiating medium (DMEM supplemented with pyruvate, glutamine, penicillin/streptomycin, 50 μg/ml ascorbic acid, and 5 mM β-glycerophosphate).

RNA Pulldown Assay—HeLa cells were transfected for 4 h using Lipofectamine LTX. GFP was used as a transfection control. Cells were harvested by adding lysis buffer (50 mM Tris (pH 7), 100 mM KCl, 5 mM $MgCl_2$, 10% glycerol, 1 mM DTT, 0.2% Nonidet P-40, and protease and phosphatase inhibitors). Lysates were centrifuged for 5 min at 16,000 × *g*. Yeast RNA (0.5 mg/mg of protein; Sigma) was added to the supernatant to block nonspecific binding. Biotinylated RNAs were denatured at 65 °C for 5 min and cooled for 20 min in 10 mM Tris (pH 7), 100 mM KCl, and 10 mM $MgCl_2$. 0.5 μg of each RNA was incubated with cell lysates for 60 min at 4 °C, including 200 units/ml RNasin (Promega). 25 μl of streptavidin-Sepharose (GE Healthcare) was added and further incubated at 4 °C for 60 min. Beads were washed five times with lysis buffer. Bound proteins were detected by Western blotting.

Analysis of miRNA Target Data Set—In silico putative targets were screened for each of the differentially expressed miRNAs

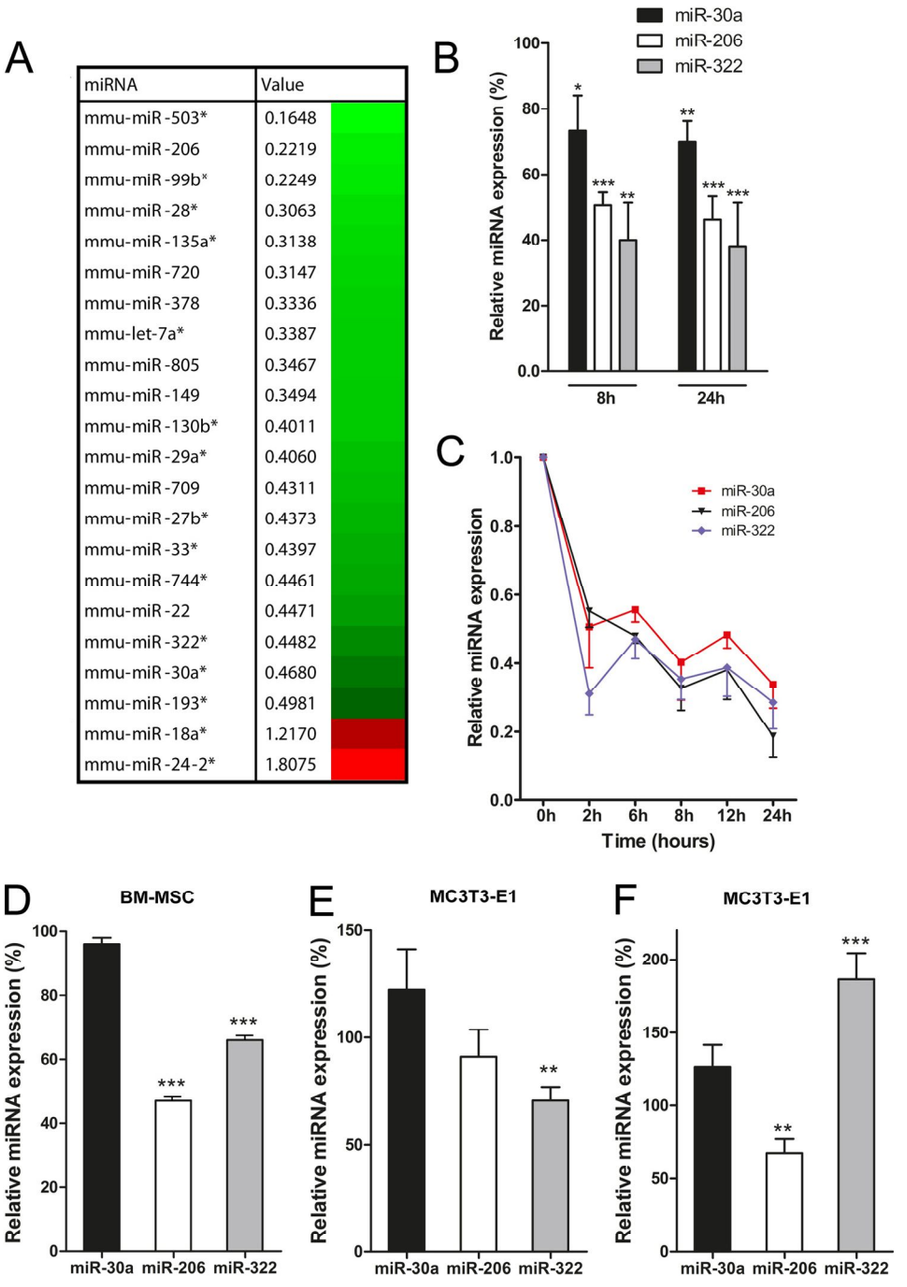

FIGURE 1. **Expression profile of miRNAs during osteoblast differentiation.** *A*, miRNA array expression data from C2C12 cells treated with BMP-2 for 8 h. *Red* denotes higher expression, and *green* denotes lower expression relative to expression in control cells. Only miRNAs with a 2-fold reduction in expression are shown. *B* and *C*, expression of miR-30a, miR-206, and miR-322 was analyzed during osteoblast differentiation. Time course experiments were performed with 2 nM BMP-2 treatment with (*B*) or without (*C*) 10% fetal bovine serum. The indicated miRNAs were isolated from C2C12 cells cultures as described under "Experimental Procedures," measured by RT-qPCR, normalized to U6 RNA, and plotted as relative expression to time 0 (means ± S.E. of five independent experiments). BM-MSCs (*D*) and MC3T3-E1 cells (*E*) were treated with BMP-2 in the absence of serum for 24 h, and the indicated miRNAs were measured by RT-qPCR. *F*, MC3T3-E1 cells were treated or not with differentiation medium for 10 days, and the indicated miRNAs were measured by RT-qPCR in five independent experiments. *, $p < 0.05$; **, $p < 0.01$; ***, $p < 0.001$.

by three different algorithms: DIANA-microT v5.0 (29), miRanda (30), and TargetScan 6.2 (31).

Statistical Analysis—Statistical analysis was performed using Student's *t* test or two-way analysis of variance, followed by Bonferroni multiple-comparison tests. Quantitative data are presented as means ± S.E. Differences were considered significant at *p* values of <0.05.

RESULTS

miRNA Expression Profile during BMP-2-induced Osteoblast Differentiation—To identify miRNAs whose expression is altered during osteoblast differentiation, C2C12 cells were treated with BMP-2 (2 nM) in medium without serum for 8 h. Independent experiments were performed under the same conditions, and a miRNA expression profile was obtained (Fig. 1*A*).

In agreement with previous results, global analysis indicated that most of the significantly changed miRNAs were down-regulated in response to BMP-2 (13, 14). For instance, miR-206 was shown to decrease during C2C12 cell differentiation (25), and miR-30 family members are also down-regulated by BMP-2 (32).

To verify these results, miR-30a, miR-206, and miR-322 were chosen for further study. These miRNAs were expressed at relatively high levels in C2C12 cells (supplemental Table 1). To confirm the array data, kinetic assays of BMP induction in the presence and absence of serum were performed, and the expression of selected miRNAs was detected by qPCR. Time course results were consistent with array data: miR-30a, miR-206, and miR-322 all steadily decreased after BMP-2 addition (~50–60% decrease at 8 and 24 h for miR-206 and miR-322) (Fig. 1*B*). Down-regulation of miRNA expression to a similar extent was also observed in cells cultured in the absence of serum (Fig. 1*C*). We extended our observations to primary cultures of murine BM-MSCs and MC3T3-E1 cells. BMP-2 treatment of BM-MSCs or MC3T3-E1 cells for 24 h caused similar miR-322 expression down-regulation, whereas miR-30a expression remained not significantly altered with respect to the miR control (Fig. 1, *D* and *E*). We also analyzed differentiation of MC3T3-E1 cells in medium containing ascorbic acid and β-glycerophosphate. In this case, although differentiation led to similar effects as BMP-2 addition on miR-30a and miR-206 expression levels, it induced a significant increase in miR-322 levels instead (Fig. 1*F*).

Effects of miR-30a, miR-206a, and miR-322 on Osteoblast Differentiation—To determine whether the selected miRNAs affect osteoblast differentiation, C2C12 cells were transfected with mimics of miR-30a, miR-206, and miR-322 and treated with BMP-2 for 16 h. Their effects were first assessed by characterizing the mRNA expression levels of the main osteoblast-determining transcription factors. It is well known that BMP addition to C2C12 cells stimulates expression of known osteogenic markers (1, 2, 4, 9, 33). Overexpression of miRNA mimics produced a significant increase in *Osx*, *Runx2*, *Msx2*, osteocalcin, and *Ibsp* mRNA levels by miR-322 and increases in *Runx2* and *Ibsp* by miR-206 (Fig. 2*A*). Upon BMP-2 stimulation, ectopic expression of a miR-322 mimic resulted in a significant accumulation of *Osx*, *Runx2*, *Msx2*, and *Ibsp* mRNA levels compared with expression of a control miRNA mimic. miR-30a transfection reduced both basal and BMP-stimulated *Dlx5* mRNA expression. We also analyzed the effects of miRNAs at the protein level (Fig. 2*B*). Although Osx protein expression increased significantly after miR-322 transfection, miR-206 and miR-30a overexpression led to an Osx decrease, possibly indicating negative osteoblast regulation, in accordance with previous work (13, 32). C2C12 cells differentiate into myoblasts and generate multinuclear myotubes in the presence of low levels of serum. However, BMP-2 is able to transdifferentiate them from the myoblast to the osteoblast lineage (34). To investigate whether miR-322 can also influence their myogenic differentiation, C2C12 cells were transfected with miR-322 or miR control and followed up for myotube formation (Fig. 2*C*). Experiments revealed a complete lack of myotube formation up to 4 days in miR-322-overexpressing cells.

We also analyzed overexpression of miRNA mimics in MC3T3-E1 cells, an osteoblast cellular model independent of BMP activation. Similar to C2C12 cells, *Osx*, *Runx2*, and *Msx2* mRNA levels were significantly increased by miR-322 (Fig. 3*A*). Altogether, these results suggested that miR-322 might be important for osteogenic differentiation and led us to investigate its molecular mechanisms of action.

We then performed miR-322 loss-of-function experiments. Consistently, transfection of Pre-miR-322 led to increased levels of miR-322, whereas transfection of Anti-miR-322 led to a 40% decrease in expression of endogenous miR-322 (supplemental Fig. S1). Therefore, Anti-miR-322 was transfected in cells in the presence or absence of BMP-2 to assess the effect on osteogenic genes. The decrease in miR-322 levels led to a significantly lower induction of *Osx* and *Runx2* mRNAs by BMP-2 (Fig. 3*B*).

Lack of Direct Interaction between miR-322 and the Smad Pathway—Smad proteins have been found to play critical roles in osteoblast differentiation induced by BMPs (7). The above results suggested that miR-322 was able to increase expression of osteogenic genes in response to BMP-2. Thus, we decided to determine whether miR-322 directly modulates Smad phosphorylation and signaling by performing time course experiments of BMP-2 activation. Ectopic expression of miR-322 led to a slight decrease in Smad1 expression that became significant after 8 h of BMP-2 addition (supplemental Fig. S2*A*). However, immunoblotting showed no significant changes in the ratio between phosphorylated and total Smad1 levels (supplemental Fig. S2*A*, *left* panel). These results suggest that the effect of miR-322 in osteoblast differentiation is not likely related to a direct change in phospho-Smad1 levels. In parallel, Smad1 and phospho-Smad1 levels were evaluated by immunoblotting after transfection with Anti-miR-322 and BMP-2 addition. No significant changes were observed in phospho-Smad activation (supplemental Fig. S2*B*).

Tob2 Is a Target of miR-322—The essential role of Runx2 and Osx in bone development led us to analyze the mechanisms regulated by miR-322 in osteoblast differentiation. Bioinformatic target prediction was carried out using DIANA, miRanda, and TargetScan prediction software. Putative targeted genes included *HoxA10* and *Dlx5* (osteogenic transcription factors); activin receptors IIA and IIB, *Smurf1*, *Smad7*, and *Smad1* (BMP signaling); and *Cdc25A* and *Tob2* (cell proliferation and differentiation) (supplemental Table 2). These targets were experimentally validated after miRNA mimic transfection. The results showed that the expression of *Tob2* mRNA and the induction of *Tob2* and *Smad7* mRNAs by BMP-2 (6-fold increase for *Smad7*) were significantly decreased in miR-322-transfected cells, whereas no significant differences were found for miR-30a and miR-206 assays (Fig. 4*A*). *Smurf1* mRNA levels were not altered in any case. Moreover, Anti-miR-322 transfection increased *Tob2* mRNA levels, both basal levels and after BMP-2 addition (Fig. 4*B*). The results led us to focus on Tob2 regulation by miR-322. Time course experiments in C2C12 cells showed that, in correlation with the miR-322 expression decrease, BMP-2 addition promoted higher levels of *Tob2* mRNA expression (supplemental Fig. S3).We also analyzed whether changes in *Tob2* mRNA in response to miR-322 correlated with changes in Tob2 protein levels. Quantification of Western blot analysis

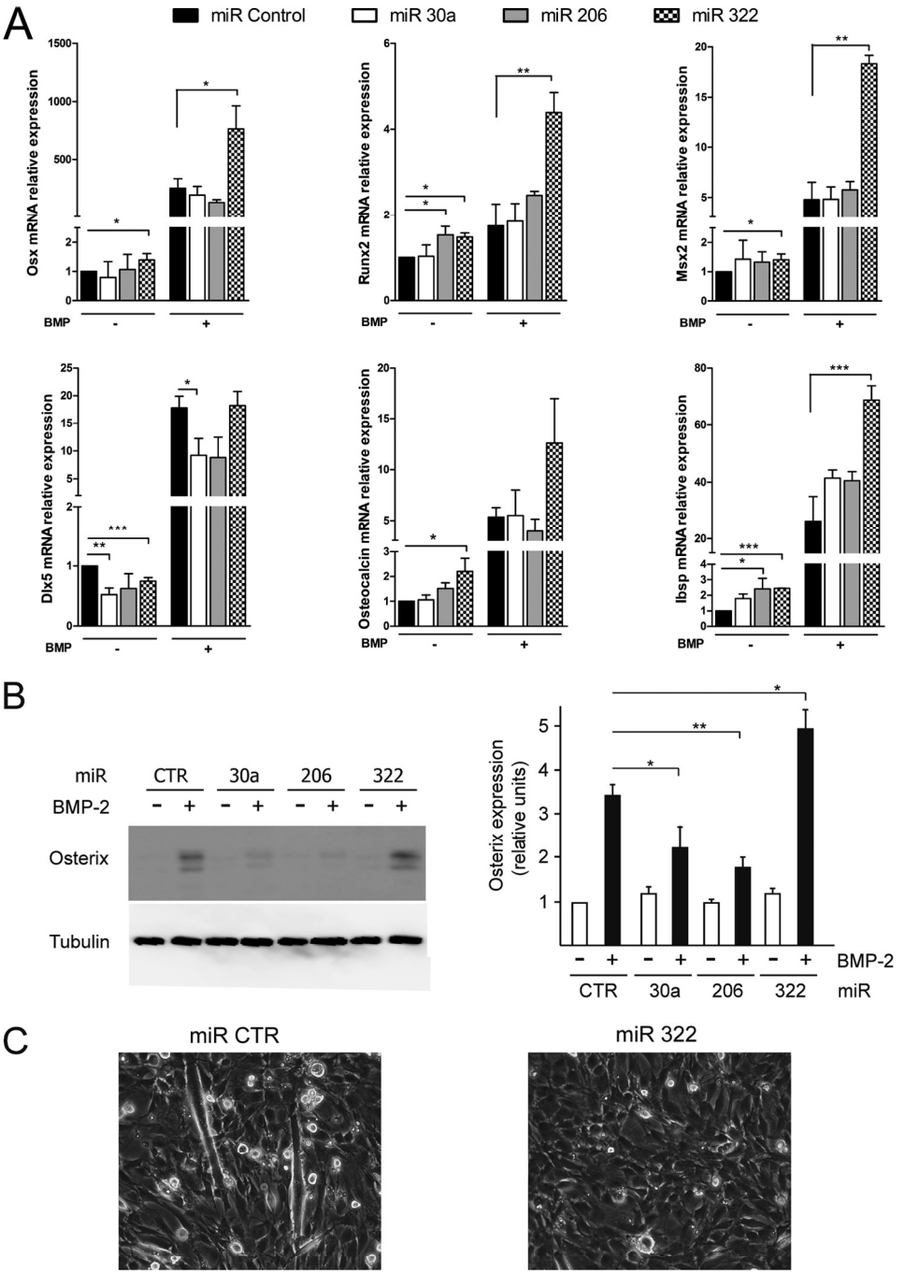

FIGURE 2. **miR-322 enhances *Osx*, *Msx2*, and *Runx2* expression.** *A*, C2C12 cells were transfected with the indicated miRNA mimics without serum for 8 h and treated with BMP-2 overnight. RT-qPCR for the indicated genes was performed, and GAPDH was used as an internal control. Results are plotted as expression relative to untreated Pre-miR control-transfected cells (means ± S.E. of four to nine independent experiments). *B*, C2C12 cells were transfected with the indicated miRNA mimics and treated with 2 nM BMP-2 for 24 h, and Osx and tubulin were detected by immunoblotting (*left panel*). Quantification of the results of three independent experiments is shown (*right panel*). *C*, miR-322 mimic-transfected C2C12 cells were maintained in medium without serum for 4 days, and myotube progression was compared with Pre-miR control-transfected cells. *, $p < 0.05$; **, $p < 0.01$; ***, $p < 0.001$.

revealed a significant decrease in Tob2 levels after transfection of a miR-322 mimic and a significant increase after Anti-miR-322 transfection (Fig. 4*C*). To confirm our previous results, we performed lentivirus-mediated overexpression experiments in BM-MSCs. Cells were transduced with either a lentiviral construct expressing miR-322 or a control, and mRNA was extracted after 10 days of culture in osteogenic medium (Fig. 4*D*). Consistent with the data from C2C12 cell cultures, miR-322 accumulation repressed *Tob2* and *Smad7* expression and induced significantly higher *Osx* mRNA levels compared with cells transduced with a lentiviral control. Taken together, these results provide evidence that miR-322 negatively regulates *Tob2* expression in mesenchymal cells.

We attempted to confirm these observations using luciferase reporter constructs to examine whether miR-322 can directly regulate *Tob2* expression. miRNAs are able to repress gene expression by binding to seed site sequences located within the 3′-UTR of mRNA (12). We determined the presence of a puta-

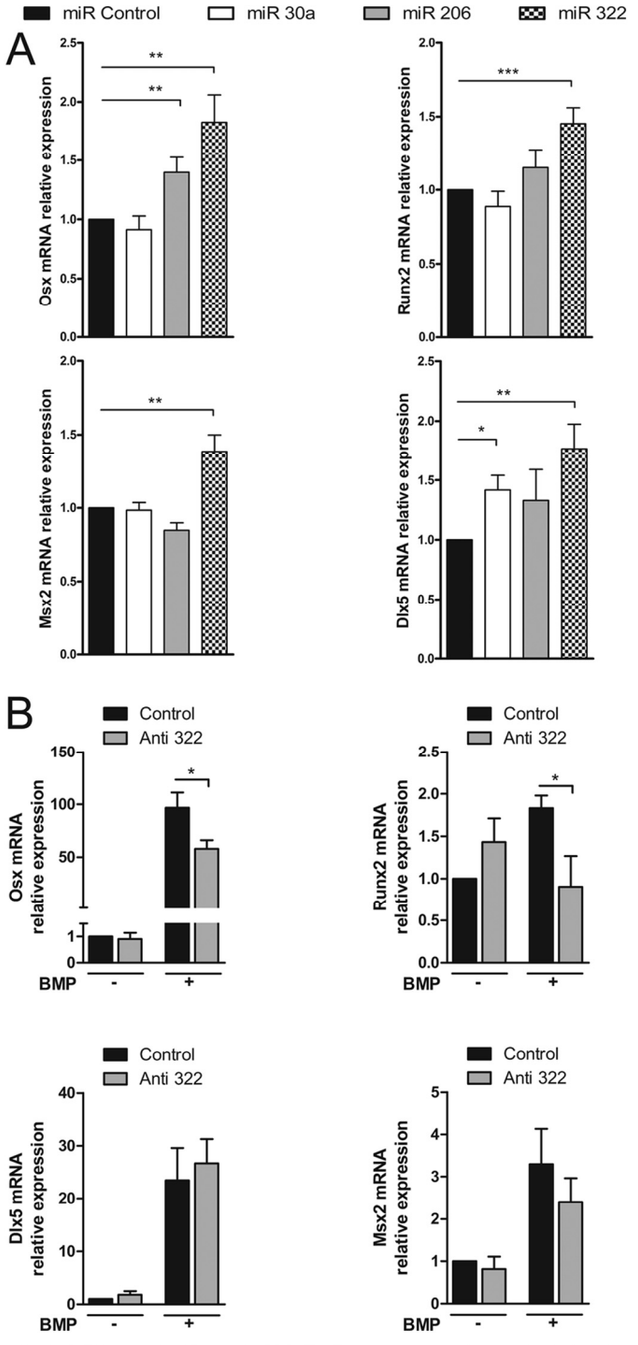

FIGURE 3. **Effects of miR-322 in MC3T3-E1 cells and antisense inhibitor for miR-322 in C2C12 cells.** *A*, MC3T3-E1 cells were transfected with the indicated miRNA mimics for 8 h and treated with differentiation medium overnight. RT-qPCR for the indicated genes was performed, and GAPDH was used as an internal control. Results are plotted as expression relative to untreated Pre-miR control-transfected cells (means ± S.E. of four to six independent experiments). *B*, C2C12 cells were transfected for 8 h with Anti-miR-322 and treated with BMP-2 overnight. The indicated mRNAs were measured by RT-qPCR, normalized to GAPDH, and expressed as relative expression (means ± S.E. of four to five independent experiments). *, $p < 0.05$; **, $p < 0.01$; ***, $p < 0.001$.

tive target region of miR-322 at position +1769 of *Tob2* mRNA using miRNA target prediction tools. We generated *Renilla* luciferase reporter constructs containing the wild-type *Tob2* 3′-UTR or a construct with the miR-322-binding sequence mutated (Fig. 5*A*). The luciferase activity of the wild-type *Tob2* 3′-UTR construct was significantly inhibited after cotransfection with miR-322 in C2C12 or MC3T3-E1 cells (Fig. 5, *B* and *C*). Furthermore, the mutant *Tob2* 3′-UTR construct lacking the possible binding region of miR-322 was refractory to the decrease in luciferase activity after miR-322 mimic cotransfection. These results provide evidence that miR-322 acts as an inhibitor of *Tob2* mRNA expression through binding to a region located in its 3′-UTR.

Tob2 Accelerates Decay of Osx mRNA Levels—Tob1-deficient mice have a higher bone mass due to an increased number of osteoblasts and an accelerated bone formation rate (35). Thus, Tob proteins act as negative regulators of bone formation, although the mechanisms of this regulatory role are mostly unknown. We then further examined how miR-322/Tob2 increases osteoblast-related genes and their interaction with the BMP-Smad pathway. First, we analyzed luciferase activity using *Id1* and *Cox2* promoter constructs with strong responsiveness to BMP signaling, previously generated in our group (27, 28). Luciferase reporter constructs were cotransfected with constructs overexpressing Tob2, miR-322, or Anti-miR-322. No major differences in luciferase activities were observed (supplemental Fig. S4).

Previous studies identified Tob not only as a general regulator of mRNA decay (36, 37) but also as a specific regulator by binding to CPEB2–4 (cytoplasmic polyadenylation element-binding protein) and recruiting Cnot7 deadenylase to the target mRNAs (38). To analyze the ability of Tob2 to regulate the mRNA degradation of specific genes, we performed mRNA decay assays. The mRNA levels of C2C12 cells overexpressing Tob2, miR-322, or miR control were quantified by qPCR at different time points after treatment with actinomycin D (a known inhibitor of mRNA synthesis). mRNA expression of the genes analyzed was already modified by the transfections before actinomycin D treatment (Fig. 6*A*). Overexpression of Tob2 reduced the basal levels of expression of *Osx*, *Runx2*, *Smad7*, and *Dlx5*. Moreover, overexpression of miR-322 also led to increased levels of *Osx* and *Runx2* mRNAs. In the mRNA decay assays after actinomycin D addition, overexpression of Tob2 reduced the half-live of *Osx* transcripts (significant reduction after 1 h). Moreover, accumulation of miR-322 led to significant stabilization of *Osx* mRNA and *Runx2* to a lesser extent (Fig. 6*B*). *Smad7*, *Dlx5*, and *Msx2* mRNA degradation was not significantly altered in any case. These data indicate that Tob2 modifies the mRNA decay of specific target genes. To further our observations, we performed the same experiments in MC3T3-E1 cells. Expression of the genes analyzed was also already modified by transfection of the miR-322 mimic. *Osx*, *Runx2*, *Dlx5*, and *Msx2* mRNA expression was significantly increased (Fig. 7*A*). mRNA decay assays after actinomycin D addition further demonstrated that overexpression of miR-322 led to a significantly slower rate of *Osx* mRNA decay (Fig. 7*B*). In view of our results, we hypothesized that *Osx* mRNA could be a direct target bound by Tob2 and CPEB2–4 and, as a consequence, specifically decayed. We analyzed 3′-UTR sequences, and interestingly, *Osx* has compatible secondary structures containing a similar stem-loop structure bound by CPEB2–4 (supplemental Fig. S5) (39). We performed RNA

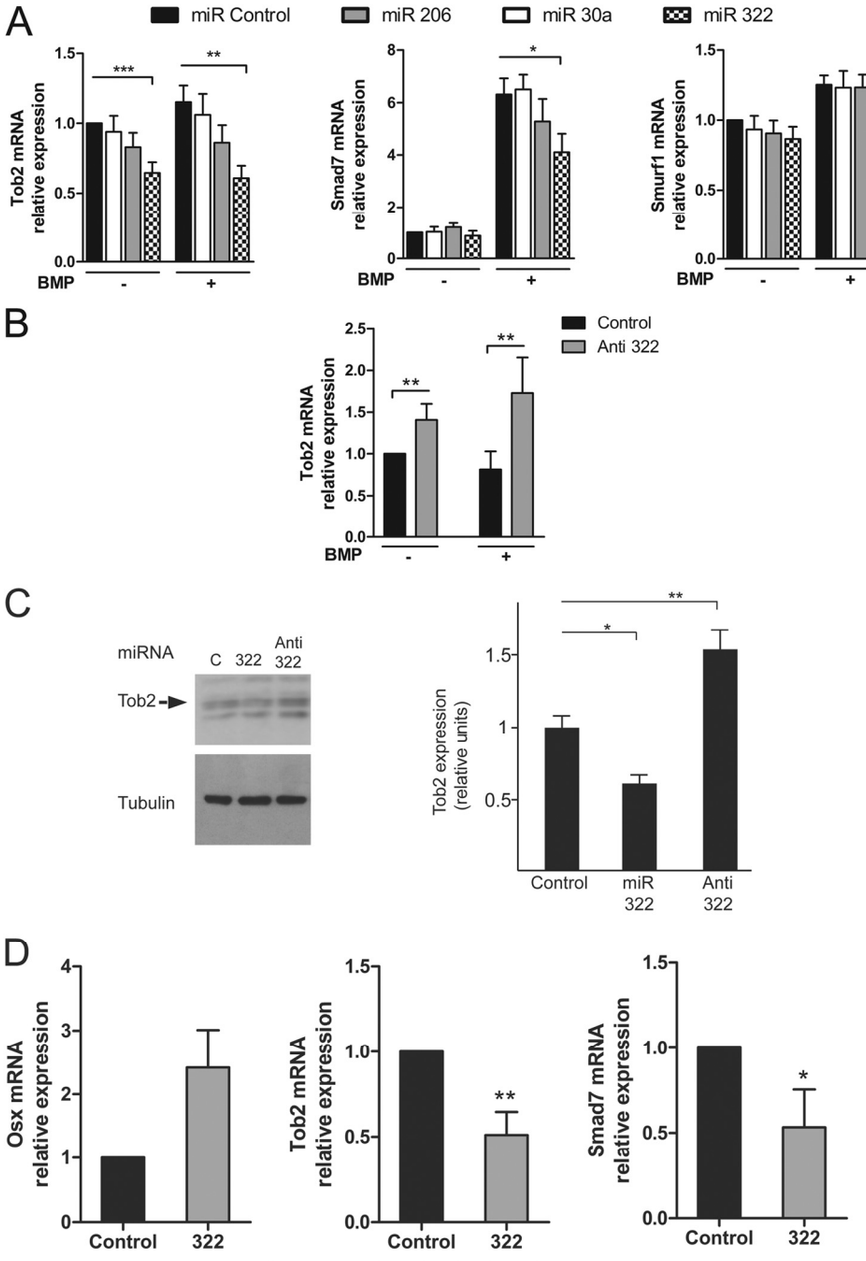

FIGURE 4. **miR-322 inhibits *Tob2* expression.** C2C12 cells were transfected with selected miRNA mimics (*A*) or miR-322 inhibitor (*B*) without serum for 8 h and treated with BMP-2 overnight. *Tob2*, *Smurf1*, and *Smad7* expression was detected by RT-qPCR, normalized to GAPDH, and expressed relative to the miR control transfection. All values represent the means ± S.E. of four to seven independent experiments. *C*, C2C12 cells were transfected with 20 nM miRNA mimic or inhibitor, and Tob2 and tubulin were detected by Western blotting (*left panel*). The *right panel* shows the relative Tob2 levels normalized to tubulin expression. *D*, BM-MSCs were infected with viral particles containing mmu-miR-322 or miR control overnight. Transduced cells were selected with puromycin for 4 days as described under "Experimental Procedures." Cells were cultured until confluence with osteogenic medium and collected to analyze the indicated mRNAs by RT-qPCR. Results were normalized to GAPDH and plotted as relative expression (means ± S.E. of three to four independent experiments). *, $p < 0.05$; **, $p < 0.01$; ***, $p < 0.001$.

pulldown assays using two oligonucleotides corresponding to distinct stem-loop sequences found in the 3′-UTR of *Osx* mRNA and a control RNA. Either expressed alone or in combination, CPEB4 and Tob2 were able to bind specifically the *Osx* 3′-UTR sequences (Fig. 7*C*).

Taken together, these results strongly suggest that miR-322 increases *Osx* mRNA expression via inhibition of *Tob2* mRNA. Furthermore, our data suggest that the well known effects of Tob proteins on bone development and homeostasis could derive, at least partly, from the role of Tob in the specific degradation and decay of *Osx* mRNA.

DISCUSSION

In our study, we identified miR-322 as a miRNA down-regulated by BMP-2. We have demonstrated for the first time that miR-322 is involved in osteoblast differentiation by targeting

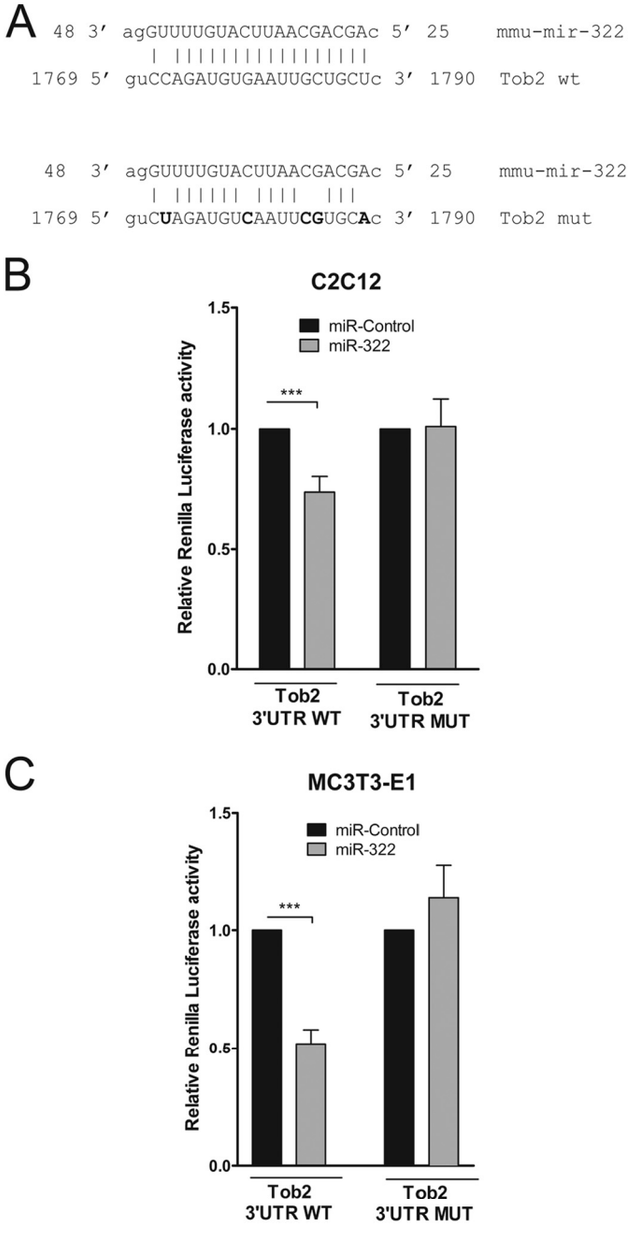

FIGURE 5. ***Tob2* is a direct target of miR-322.** *A*, schematic representation of the alignment of the mouse *Tob2* mRNA 3′-UTR predicted to be targeted by miR-322. Mutations generated within the region corresponding to the seed sequence were included in the mutant *Tob2* 3′-UTR construct. C2C12 (*B*) or MC3T3-E1 (*C*) cells were cotransfected with the *Renilla* luciferase reporter plasmid carrying the wild-type or mutant (*MUT*) *Tob2* 3′-UTR and miR-322 or miR control, respectively. After 8 h, cells were cultured until confluence for 16 h, and luciferase activity was analyzed and normalized to β-galactosidase expression. Relative luciferase activities are expressed as means ± S.E. for triplicates from four to six independent experiments. ***, $p < 0.001$.

Tob2. We reported that overexpression of miR-322 decreases *Tob2* mRNA and protein expression and leads to increased levels of the transcription factor Osx. Furthermore, we have demonstrated direct evidence of the binding site of miR-322 in the *Tob2* 3′-UTR. We propose a molecular description of the mechanism whereby the osteogenic master gene *Osx* is controlled post-transcriptionally through a mechanism driven by miR-322/Tob2. More importantly, our findings strongly suggest that control of specific mRNA decay is relevant in bone development and homeostasis.

miR-322 has been previously studied together with miR-503 in myogenesis as promoters of cell cycle quiescence and differentiation by down-regulation of Cdc25A (40). Expression of miR-322 (which is clustered with miR-503, miR-351, and miR-450) is highly enriched in fibroblasts and cells of the mesenchymal lineage (microRNA.org). Our findings add a new role and a novel target of miR-322 during osteoblast differentiation. Our results also show that, after differentiation by BMP-2, the miR-322 level progressively decreases in C2C12 and MC3T3-E1 cells and primary cultures of BM-MSCs. We have mentioned the up-regulated expression of osteogenic transcription factors during BMP-2 treatment. Then, miR-322, by means of *Tob2* down-regulation, adjusts the expression levels of some of these factors, particularly *Osx*. This profile seems to allow the transcriptional up-regulation of the osteogenic transcription factors, whereas miR-322 may later exert a regulatory mechanism that allows fine-tuning of bone homeostasis.

Our results suggest that the miR-322/miR-351/miR-450/miR-503 cluster is repressed by the addition of BMP-2 (miR-503 was also highly down-regulated in our screen). Smad proteins, the signal transducers of the BMP pathway, have been found to regulate miRNA expression through both transcriptional and post-transcriptional mechanisms (41). Like mRNAs, miRNAs are transcribed by RNA polymerase II and have been shown to be subjected to either positive or negative transcriptional regulation through Smad-containing transcriptional enhancers located in the specific miRNA promoter (41). In addition, Smad proteins have been shown to regulate specific miRNA processing and maturation through interaction with the Drosha complex (21). These miRNAs require a CAGAC sequence at the 3′-end of their mature miRNA sequence to bind and be regulated by the Smad-Drosha complex (42). Because none of the mature miRNAs corresponding to the miR-322 cluster contain this CAGAC sequence, it is likely that regulation of the miR-322 cluster depends on direct transcriptional repression by Smad proteins, as has been demonstrated in other miRNAs (43, 44).

The cellular levels of phosphorylated Smad1 were not significantly modified by the addition of either miR-322 or Anti-miR-322. Notably, we found that Smad7 is also a target of miR-322 in C2C12 cells and BM-MSCs, and it is well known that *Smad7* is induced by BMP-2 as a negative feedback loop. *Smad7* belongs to the inhibitory Smad (I-Smad) family, the main inhibitory mechanism of the cooperative signaling of R-Smad and Co-Smad proteins (45). Moreover, Tob proteins have been shown to associate with the MH2 domains of Smad proteins and to repress Smad transcriptional complexes (35). These two mechanisms may contribute, in an additive way, to a lower BMP response. Nevertheless, analysis of the quantitative role of Smad7 and Tob2 repression in the induction of *Osx* and *Runx2* transcripts by miR-322 also awaits further study.

Although mRNA decay has been shown to be highly relevant in a number of physiological processes (46), there are few examples of this post-transcriptional regulatory mechanism in bone development. For instance, polymorphisms in the 3′-UTR of

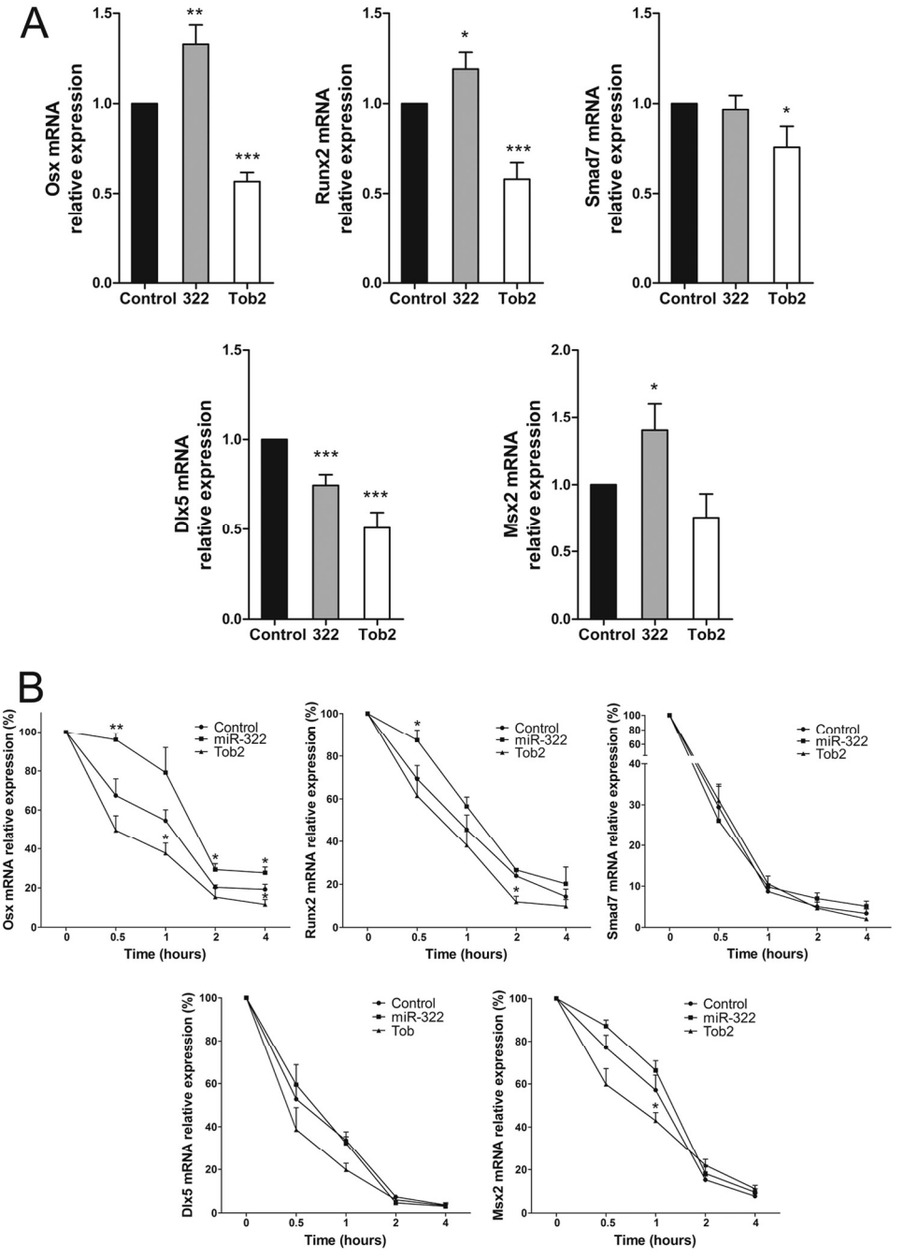

FIGURE 6. **miR-322 stabilizes *Osx* mRNA via Tob2 repression in C2C12 cells.** *A* and *B*, C2C12 cells were transfected with Tob2, miR-322, or miR control for 8 h, cultured overnight, and treated with BMP-2 for 2 h before actinomycin D addition. *A*, expression of the indicated mRNAs at time 0. Expression of selected genes is plotted relative to miR control transfection (means ± S.E. of six independent experiments). *B*, actinomycin D was added, and mRNAs were collected at the indicated times. RT-qPCR was performed using GAPDH as the endogenous control. Data are expressed relative to control transfection mRNA levels at time 0 (means ± S.E. of seven to eight independent experiments). *, $p < 0.05$; **, $p < 0.01$; ***, $p < 0.001$.

VDR lead to differential mRNA decay and increased risk of osteoporosis (47). In addition, it has also been shown that AU-rich elements mediate stabilization of collagenase-3 mRNA in osteoblasts (48). Tob1 and Tob2 proteins constitute a Tob subfamily and belong to the BTG/Tob antiproliferative factor protein family (49, 50). *Tob* genes have emerged as key players in mediating post-transcriptional gene expression by regulating mRNA deadenylation and therefore cytoplasmic mRNA levels (51). Our results suggest that new target genes displaying compatible Tob-interacting secondary structures at their 3′-UTR could be subjected to specific mRNA repression by Tob family members, as we suggest here for *Osx*. These data are in agreement with previous research showing that, although Tob1 knock-out mice are born without apparent phenotypic abnormalities, Tob1-deficient adult mice were shown to have higher bone mass compared with wild-type mice (35). These data also explain why Tob deficiency enhances osteoblast activity blocking osteoporosis induced by ovariectomy (52). Furthermore, mice deficient in Cnot7, the Tob-interacting deadenylase, also exhibit a high bone mass phenotype and increased responses to BMPs (53).

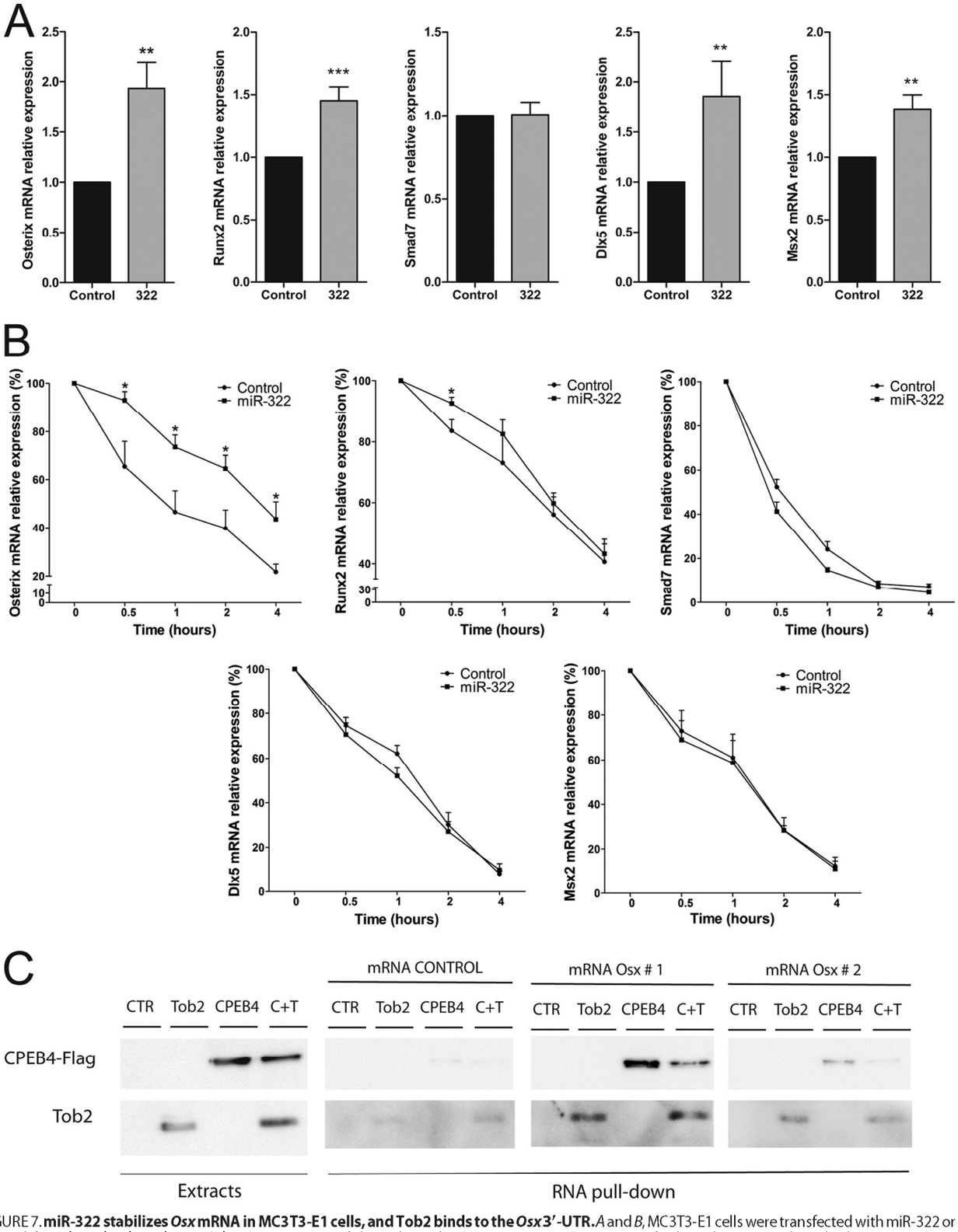

FIGURE 7. **miR-322 stabilizes *Osx* mRNA in MC3T3-E1 cells, and Tob2 binds to the *Osx* 3′-UTR.** *A* and *B*, MC3T3-E1 cells were transfected with miR-322 or miR control for 8 h and cultured overnight. *A*, expression of the indicated mRNAs at time 0. Expression of selected genes is plotted relative to miR control transfection (means ± S.E. of four independent experiments). *B*, actinomycin D was added, and mRNAs were collected at the indicated times. RT-qPCR was performed using GAPDH as the endogenous control. Data are expressed relative to control transfection mRNA levels at time 0 (means ± S.E. of four independent experiments). *C*, HeLa cells were transfected with GFP (control (*CTR*)), Tob2, CPEB4, or CPEB4 and Tob2 (*C+T*). RNA pulldown assay was performed as described under "Experimental Procedures," and the presence of Tob2 and CPEB4 was confirmed by Western blotting. *, $p < 0.05$; **, $p < 0.01$; ***, $p < 0.001$.

Long C-terminal regions of both Tob1 and Tob2 include short conserved PAM2 motifs, which are not found in the other BTG/Tob family members. These motifs mediate direct interactions with the poly(A)-binding protein PABPC1 and Cnot7 simultaneously, contributing to the role of Tob1 and Tob2 in general mRNA deadenylation and mRNA turnover (37). Moreover, it has been shown that Tob proteins can interact with CPEB2–4 and specifically intensify the rapid decay of particular transcripts (51). Whereas CPEB1 binds to the cytoplasmic polyadenylation elements (UUUUUAU) in the 3′-UTR of mRNAs, promoting polyadenylation, CPEB2–4 also bind a sequence other than the cytoplasmic polyadenylation element. Their RNA-binding domains recognize mRNAs with specific secondary structures containing U-rich loops and interact with single-stranded uridines as well as double-stranded stems present in the 3′-UTR of the target mRNA (38, 39). Recent studies showed Tob1 interaction with cytoplasmic CPEB2–4, which negatively regulate the expression of a target by tethering to specific mRNA and mediating recruitment of the deadenylase Cnot7, leading to specific mRNA decay (38). Furthermore, a previous study showed that CPEB3 binds to the 3′-UTR of AMPA receptor (*GluR2*) mRNA and negatively regulates its expression, becoming the only known target of CPEB3 at present (39). The *Osx* 3′-UTR contains secondary structures with a stem-loop structure similar to those bound by CPEB2–4 (supplemental Fig. S4) (39). Our RNA pulldown analysis showed that these sequences are directly bound by CPEB proteins and Tob2. Thus, in view of our results, we hypothesize that *Osx* mRNA could be bound by Tob2 and CPEB2–4 and, as a consequence, specifically degraded. Moreover, *in silico* analysis showed that *CPEB2–4* are also putative targets of miR-322 and miR-503, whereas they do not target *CPEB1*. This suggests that, in addition to Tob2, miR-322 could also target *CPEB* genes to coordinately regulate *Osx* expression. Future work is necessary to discern which CPEB-like proteins are involved in the interaction between Tob2 and stem-loop structures in the 3′-UTR of *Osx* and other osteogenic genes.

In summary, we have demonstrated that down-regulation of miR-322 in response to BMP-2 acts as a negative regulator of Osterix expression. We also identified Tob2 accumulation as an important step in fine-tuning the expression of *Osx* and other osteogenic transcription factors during osteoblast differentiation. This novel mechanism highlights the possibility of exploring new therapeutic approaches targeting Tob proteins to treat bone diseases.

Acknowledgments—We thank Drs. R. Méndez, Q. Yu, and T. Yamamoto for reagents and E. Adanero, E. Castaño, and Benjamin Torrejon for technical assistance.

REFERENCES

1. Nakashima, K., and de Crombrugghe, B. (2003) Transcriptional mechanisms in osteoblast differentiation and bone formation. *Trends Genet.* **19,** 458–466
2. Karsenty, G. (2008) Transcriptional control of skeletogenesis. *Annu. Rev. Genomics Hum. Genet.* **9,** 183–196
3. Ducy, P., Zhang, R., Geoffroy, V., Ridall, A. L., and Karsenty, G. (1997) Osf2/Cbfa1: a transcriptional activator of osteoblast differentiation. *Cell* **89,** 747–754
4. Nakashima, K., Zhou, X., Kunkel, G., Zhang, Z., Deng, J. M., Behringer, R. R., and de Crombrugghe, B. (2002) The novel zinc finger-containing transcription factor Osterix is required for osteoblast differentiation and bone formation. *Cell* **108,** 17–29
5. Chen, D., Zhao, M., and Mundy, G. R. (2004) Bone morphogenetic proteins. *Growth Factors* **22,** 233–241
6. Lee, M. H., Javed, A., Kim, H. J., Shin, H. I., Gutierrez, S., Choi, J. Y., Rosen, V., Stein, J. L., van Wijnen, A. J., Stein, G. S., Lian, J. B., and Ryoo, H. M. (1999) Transient upregulation of CBFA1 in response to bone morphogenetic protein-2 and transforming growth factor β1 in C2C12 myogenic cells coincides with suppression of the myogenic phenotype but is not sufficient for osteoblast differentiation. *J. Cell. Biochem.* **73,** 114–125
7. Massagué, J., Seoane, J., and Wotton, D. (2005) Smad transcription factors. *Genes Dev.* **19,** 2783–2810
8. Rodríguez-Carballo, E., Ulsamer, A., Susperregui, A. R., Manzanares-Céspedes, C., Sánchez-García, E., Bartrons, R., Rosa, J. L., and Ventura, F. (2011) Conserved regulatory motifs in osteogenic gene promoters integrate cooperative effects of canonical Wnt and BMP pathways. *J. Bone Miner. Res.* **26,** 718–729
9. Ulsamer, A., Ortuño, M. J., Ruiz, S., Susperregui, A. R., Osses, N., Rosa, J. L., and Ventura, F. (2008) BMP-2 induces Osterix expression through up-regulation of Dlx5 and its phosphorylation by p38. *J. Biol. Chem.* **283,** 3816–3826
10. Wan, M., and Cao, X. (2005) BMP signaling in skeletal development. *Biochem. Biophys. Res. Commun.* **328,** 651–657
11. Hobert, O. (2008) Gene regulation by transcription factors and microRNAs. *Science* **319,** 1785–1786
12. Bartel, D. P. (2004) MicroRNAs: genomics, biogenesis, mechanism, and function. *Cell* **116,** 281–297
13. Inose, H., Ochi, H., Kimura, A., Fujita, K., Xu, R., Sato, S., Iwasaki, M., Sunamura, S., Takeuchi, Y., Fukumoto, S., Saito, K., Nakamura, T., Siomi, H., Ito, H., Arai, Y., Shinomiya, K., and Takeda, S. (2009) A microRNA regulatory mechanism of osteoblast differentiation. *Proc. Natl. Acad. Sci. U.S.A.* **106,** 20794–20799
14. Li, H., Xie, H., Liu, W., Hu, R., Huang, B., Tan, Y. F., Xu, K., Sheng, Z. F., Zhou, H. D., Wu, X. P., and Luo, X. H. (2009) A novel microRNA targeting HDAC5 regulates osteoblast differentiation in mice and contributes to primary osteoporosis in humans. *J. Clin. Invest.* **119,** 3666–3677
15. Li, Z., Hassan, M. Q., Volinia, S., van Wijnen, A. J., Stein, J. L., Croce, C. M., Lian, J. B., and Stein, G. S. (2008) A microRNA signature for a BMP2-induced osteoblast lineage commitment program. *Proc. Natl. Acad. Sci. U.S.A.* **105,** 13906–13911
16. Lian, J. B., Stein, G. S., van Wijnen, A. J., Stein, J. L., Hassan, M. Q., Gaur, T., and Zhang, Y. (2012) MicroRNA control of bone formation and homeostasis. *Nat. Rev. Endocrinol.* **8,** 212–227
17. Luzi, E., Marini, F., Sala, S. C., Tognarini, I., Galli, G., and Brandi, M. L. (2008) Osteogenic differentiation of human adipose tissue-derived stem cells is modulated by the miR-26a targeting of the SMAD1 transcription factor. *J. Bone Miner. Res.* **23,** 287–295
18. Taipaleenmäki, H., Bjerre Hokland, L., Chen, L., Kauppinen, S., and Kassem, M. (2012) Mechanisms in endocrinology: microRNAs: targets for enhancing osteoblast differentiation and bone formation. *Eur. J. Endocrinol.* **166,** 359–371
19. Williams, A. H., Liu, N., van Rooij, E., and Olson, E. N. (2009) MicroRNA control of muscle development and disease. *Curr. Opin. Cell Biol.* **21,** 461–469
20. Gaur, T., Hussain, S., Mudhasani, R., Parulkar, I., Colby, J. L., Frederick, D., Kream, B. E., van Wijnen, A. J., Stein, J. L., Stein, G. S., Jones, S. N., and Lian, J. B. (2010) Dicer inactivation in osteoprogenitor cells compromises fetal survival and bone formation, while excision in differentiated osteoblasts increases bone mass in the adult mouse. *Dev. Biol.* **340,** 10–21
21. Davis, B. N., Hilyard, A. C., Lagna, G., and Hata, A. (2008) SMAD proteins control DROSHA-mediated microRNA maturation. *Nature* **454,** 56–61
22. Inose, T., Kato, H., Kimura, H., Faried, A., Tanaka, N., Sakai, M., Sano, A., Sohda, M., Nakajima, M., Fukai, Y., Miyazaki, T., Masuda, N., Fukuchi, M., and Kuwano, H. (2009) Correlation between connexin 26 expression and poor prognosis of esophageal squamous cell carcinoma. *Ann. Surg. Oncol.*

16, 1704–1710
23. Kapinas, K., Kessler, C., Ricks, T., Gronowicz, G., and Delany, A. M. (2010) miR-29 modulates Wnt signaling in human osteoblasts through a positive feedback loop. *J. Biol. Chem.* **285,** 25221–25231
24. Lipchina, I., Elkabetz, Y., Hafner, M., Sheridan, R., Mihailovic, A., Tuschl, T., Sander, C., Studer, L., and Betel, D. (2011) Genome-wide identification of microRNA targets in human ES cells reveals a role for miR-302 in modulating BMP response. *Genes Dev.* **25,** 2173–2186
25. Sato, M. M., Nashimoto, M., Katagiri, T., Yawaka, Y., and Tamura, M. (2009) Bone morphogenetic protein-2 down-regulates miR-206 expression by blocking its maturation process. *Biochem. Biophys. Res. Commun.* **383,** 125–129
26. Zhang, Y., Xie, R. L., Croce, C. M., Stein, J. L., Lian, J. B., van Wijnen, A. J., and Stein, G. S. (2011) A program of microRNAs controls osteogenic lineage progression by targeting transcription factor Runx2. *Proc. Natl. Acad. Sci. U.S.A.* **108,** 9863–9868
27. Susperregui, A. R., Gamell, C., Rodríguez-Carballo, E., Ortuño, M. J., Bartrons, R., Rosa, J. L., and Ventura, F. (2011) Noncanonical BMP signaling regulates cyclooxygenase-2 transcription. *Mol. Endocrinol.* **25,** 1006–1017
28. López-Rovira, T., Chalaux, E., Massagué, J., Rosa, J. L., and Ventura, F. (2002) Direct binding of Smad1 and Smad4 to two distinct motifs mediates bone morphogenetic protein-specific transcriptional activation of *Id1* gene. *J. Biol. Chem.* **277,** 3176–3185
29. Vlachos, I. S., Kostoulas, N., Vergoulis, T., Georgakilas, G., Reczko, M., Maragkakis, M., Paraskevopoulou, M. D., Prionidis, K., Dalamagas, T., and Hatzigeorgiou, A. G. (2012) DIANA miRPath v.2.0: investigating the combinatorial effect of microRNAs in pathways. *Nucleic Acids Res.* **40,** W498–W504
30. John, B., Enright, A. J., Aravin, A., Tuschl, T., Sander, C., and Marks, D. S. (2004) Human MicroRNA targets. *PLoS Biol.* **2,** e363
31. Grimson, A., Farh, K. K., Johnston, W. K., Garrett-Engele, P., Lim, L. P., and Bartel, D. P. (2007) MicroRNA targeting specificity in mammals: determinants beyond seed pairing. *Mol. Cell* **27,** 91–105
32. Wu, T., Zhou, H., Hong, Y., Li, J., Jiang, X., and Huang, H. (2012) miR-30 family members negatively regulate osteoblast differentiation. *J. Biol. Chem.* **287,** 7503–7511
33. Ortuño, M. J., Ruiz-Gaspà, S., Rodríguez-Carballo, E., Susperregui, A. R., Bartrons, R., Rosa, J. L., and Ventura, F. (2010) p38 regulates expression of osteoblast-specific genes by phosphorylation of osterix. *J. Biol. Chem.* **285,** 31985–31994
34. Katagiri, T., Yamaguchi, A., Komaki, M., Abe, E., Takahashi, N., Ikeda, T., Rosen, V., Wozney, J. M., Fujisawa-Sehara, A., and Suda, T. (1994) Bone morphogenetic protein-2 converts the differentiation pathway of C2C12 myoblasts into the osteoblast lineage. *J. Cell Biol.* **127,** 1755–1766
35. Yoshida, Y., Tanaka, S., Umemori, H., Minowa, O., Usui, M., Ikematsu, N., Hosoda, E., Imamura, T., Kuno, J., Yamashita, T., Miyazono, K., Noda, M., Noda, T., and Yamamoto, T. (2000) Negative regulation of BMP/Smad signaling by Tob in osteoblasts. *Cell* **103,** 1085–1097
36. Ezzeddine, N., Chang, T. C., Zhu, W., Yamashita, A., Chen, C. Y., Zhong, Z., Yamashita, Y., Zheng, D., and Shyu, A. B. (2007) Human TOB, an antiproliferative transcription factor, is a poly(A)-binding protein-dependent positive regulator of cytoplasmic mRNA deadenylation. *Mol. Cell. Biol.* **27,** 7791–7801
37. Funakoshi, Y., Doi, Y., Hosoda, N., Uchida, N., Osawa, M., Shimada, I., Tsujimoto, M., Suzuki, T., Katada, T., and Hoshino, S. (2007) Mechanism of mRNA deadenylation: evidence for a molecular interplay between translation termination factor eRF3 and mRNA deadenylases. *Genes Dev.* **21,** 3135–3148
38. Hosoda, N., Funakoshi, Y., Hirasawa, M., Yamagishi, R., Asano, Y., Miyagawa, R., Ogami, K., Tsujimoto, M., and Hoshino, S. (2011) Anti-proliferative protein Tob negatively regulates CPEB3 target by recruiting Caf1 deadenylase. *EMBO J.* **30,** 1311–1323
39. Huang, Y. S., Kan, M. C., Lin, C. L., and Richter, J. D. (2006) CPEB3 and CPEB4 in neurons: analysis of RNA-binding specificity and translational control of AMPA receptor GluR2 mRNA. *EMBO J.* **25,** 4865–4876
40. Sarkar, S., Dey, B. K., and Dutta, A. (2010) miR-322/424 and -503 are induced during muscle differentiation and promote cell cycle quiescence and differentiation by down-regulation of Cdc25A. *Mol. Biol. Cell* **21,** 2138–2149
41. Blahna, M. T., and Hata, A. (2012) Smad-mediated regulation of microRNA biosynthesis. *FEBS Lett.* **586,** 1906–1912
42. Davis, B. N., Hilyard, A. C., Nguyen, P. H., Lagna, G., and Hata, A. (2010) Smad proteins bind a conserved RNA sequence to promote microRNA maturation by Drosha. *Mol. Cell* **39,** 373–384
43. Qin, W., Chung, A. C., Huang, X. R., Meng, X. M., Hui, D. S., Yu, C. M., Sung, J. J., and Lan, H. Y. (2011) TGF-β/Smad3 signaling promotes renal fibrosis by inhibiting miR-29. *J. Am. Soc. Nephrol.* **22,** 1462–1474
44. Sun, Q., Zhang, Y., Yang, G., Chen, X., Zhang, Y., Cao, G., Wang, J., Sun, Y., Zhang, P., Fan, M., Shao, N., and Yang, X. (2008) Transforming growth factor-β-regulated miR-24 promotes skeletal muscle differentiation. *Nucleic Acids Res.* **36,** 2690–2699
45. Ross, S., and Hill, C. S. (2008) How the Smads regulate transcription. *Int. J. Biochem. Cell Biol.* **40,** 383–408
46. Schoenberg, D. R., and Maquat, L. E. (2012) Regulation of cytoplasmic mRNA decay. *Nat. Rev. Genet.* **13,** 246–259
47. Fang, Y., van Meurs, J. B., d'Alesio, A., Jhamai, M., Zhao, H., Rivadeneira, F., Hofman, A., van Leeuwen, J. P., Jehan, F., Pols, H. A., and Uitterlinden, A. G. (2005) Promoter and 3′-untranslated-region haplotypes in the vitamin D receptor gene predispose to osteoporotic fracture: the Rotterdam study. *Am. J. Hum. Genet.* **77,** 807–823
48. Rydziel, S., Delany, A. M., and Canalis, E. (2004) AU-rich elements in the collagenase 3 mRNA mediate stabilization of the transcript by cortisol in osteoblasts. *J. Biol. Chem.* **279,** 5397–5404
49. Winkler, G. S. (2010) The mammalian anti-proliferative BTG/Tob protein family. *J. Cell. Physiol.* **222,** 66–72
50. Mauxion, F., Chen, C. Y., Séraphin, B., and Shyu, A. B. (2009) BTG/TOB factors impact deadenylases. *Trends Biochem. Sci.* **34,** 640–647
51. Ezzeddine, N., Chen, C. Y., and Shyu, A. B. (2012) Evidence providing new insights into TOB-promoted deadenylation and supporting a link between TOB's deadenylation-enhancing and antiproliferative activities. *Mol. Cell. Biol.* **32,** 1089–1098
52. Usui, M., Yoshida, Y., Tsuji, K., Oikawa, K., Miyazono, K., Ishikawa, I., Yamamoto, T., Nifuji, A., and Noda, M. (2004) Tob deficiency superenhances osteoblastic activity after ovariectomy to block estrogen deficiency-induced osteoporosis. *Proc. Natl. Acad. Sci. U.S.A.* **101,** 6653–6658
53. Washio-Oikawa, K., Nakamura, T., Usui, M., Yoneda, M., Ezura, Y., Ishikawa, I., Nakashima, K., Noda, T., Yamamoto, T., and Noda, M. (2007) Cnot7-null mice exhibit high bone mass phenotype and modulation of BMP actions. *J. Bone Miner. Res.* **22,** 1217–1223

frontiers in
CELLULAR NEUROSCIENCE

REVIEW ARTICLE
published: 04 June 2013
doi: 10.3389/fncel.2013.00087

BMP signaling in telencephalic neural cell specification and maturation

Beatriz Gámez, Edgardo Rodriguez-Carballo and Francesc Ventura*

Departament de Ciències Fisiològiques II, Institut d'Investigació Biomèdica de Bellvitge, Universitat de Barcelona, L'Hospitalet de Llobregat, Spain

Edited by:
Nelson Osses, Pontificia Universidad Católica de Valparaíso, Chile

Reviewed by:
Marcel Leist, University of Konstanz, Germany
Takumi Takizawa, Gunma University, Japan

***Correspondence:**
Francesc Ventura, Departament de Ciències Fisiològiques II, Institut d'Investigació Biomèdica de Bellvitge, Universitat de Barcelona, C/ Feixa Llarga s/n, E-08907 L'Hospitalet de Llobregat, Spain
e-mail: fventura@ub.edu

Bone morphogenetic proteins (BMPs) make up a family of morphogens that are critical for patterning, development, and function of the central and peripheral nervous system. Their effects on neural cells are pleiotropic and highly dynamic depending on the stage of development and the local niche. Neural cells display a broad expression profile of BMP ligands, receptors, and transducer molecules. Moreover, interactions of BMP signaling with other incoming morphogens and signaling pathways are crucial for most of these processes. The key role of BMP signaling suggests that it includes many regulatory mechanisms that restrict BMP activity both temporally and spatially. BMPs affect neural cell fate specification in a dynamic fashion. Initially they inhibit proliferation of neural precursors and promote the first steps in neuronal differentiation. Later on, BMP signaling effects switch from neuronal induction to promotion of astroglial identity and inhibition of neuronal or oligodendroglial lineage commitment. Furthermore, in postmitotic cells, BMPs regulate cell survival and death, to modulate neuronal subtype specification, promote dendritic and axonal growth and induce synapse formation and stabilization. In this review, we examine the canonical and non-canonical mechanisms of BMP signal transduction. Moreover, we focus on the specific role of BMPs in the nervous system including their ability to regulate neural stem cell proliferation, self-renewal, lineage specification, and neuronal function.

Keywords: BMP, neural differentiation, morphogen, synaptogenesis, neural development, signal transduction

INTRODUCTION

Bone morphogenetic proteins (BMPs) are members of the transforming growth factor β (TGF-β) superfamily (Derynck and Zhang, 2003; Shi and Massague, 2003; Miyazono et al., 2010). BMPs were originally identified as factors that induce bone formation when implanted at ectopic sites (Urist, 1965). Later, it was shown that BMP functions exist in vertebrates as well as in invertebrates and that they perform a wide range of biological action in various cell types and tissues (Chen et al., 2004). BMPs control many indispensable steps in embryogenesis, including the formation and differentiation of the vertebrate nervous system (Mehler et al., 1997; Kishigami and Mishina, 2005; Liu and Niswander, 2005). At initial steps of development, BMP inhibition is required to establish neuroectoderm from ectoderm, although certain levels of BMP signaling are later required for neural crest induction, neural crest cell migration, and spinal cord patterning. At later development stages, BMP signaling promotes astrogliogenesis and inhibition of neuronal or oligodendroglial lineage commitment. Given the functions of BMPs in nervous system development and maintenance, BMP signaling dysfunction and modulation could have a strong impact on various nervous system pathologies as well as their repair processes (Matsuura et al., 2008; Sabo et al., 2009; Ma et al., 2011). In this review, we highlight the main aspects of BMP signaling and BMP's involvement in neural induction and patterning, embryonic and postnatal neuronal differentiation, and the establishment of neuronal connections.

SIGNALING BY BMPs

Bone morphogenetic proteins are the largest subfamily of the TGF-β superfamily, which includes 33 members in mammals. BMPs can be further classified into at least four subgroups: BMP-2/4 group, BMP-5/6/7/8 group, growth and differentiation factor-5,-6,-7 (GDF-5/6/7) group, and BMP-9/10 group (Little and Mullins, 2009; Miyazono et al., 2010; Wagner et al., 2010). BMPs are known to be involved in many developmental and homeostatic processes throughout life. However, the exact function of individual BMPs in a particular tissue and at a specific time during development is far from clear. Due to their pleiotropic roles, genetic manipulation often leads to embryonic lethality, thus precluding analysis of their later embryonic or postnatal functions in multiple tissues and organs (Bragdon et al., 2011). In addition, compensatory functional overlaps between BMPs make interpretation complicated. Furthermore, although we may have a rough estimate of the place and the timing of expression of a particular BMP, many factors present in the extracellular environment are able to modify its exact diffusion rate, morphogen range, and its bioavailability for a target cell (Eldar et al., 2002; Peluso et al., 2011).

BMP SECRETION AND EXTRACELLULAR REGULATION

Bone morphogenetic proteins are synthesized as large precursor proteins comprising an N-terminal signal peptide, which directs the protein to the secretory pathway, a prodomain for proper folding and a C-terminal mature peptide (Sieber et al., 2009). BMPs

are first secreted and then proteolitically cleaved upon dimerization by serine proteases such as furin or PC6, releasing the mature peptide (Cui et al., 1998). Active BMPs consist of two monomers stabilized by three intramolecular disulfide bonds, known as cysteine knots, and an inter-dimer disulfide bond (Scheufler et al., 1999). Mature forms may be either homo- or hetero-dimers consisting of different BMP gene products. It has been shown *in vivo* and *in vitro* that some hetero-dimerization could lead to increased functional activity (Valera et al., 2010). In some cases, the cleaved prodomain remains attached to the mature form, as in the case of TGF-β, leading to reduced bioavailability and retention in the extracellular matrix (Ramel and Hill, 2012).

This restricted availability to their membrane receptors is mostly emphasized by the existence of highly regulated diffusible and cell surface-bound antagonists. There are more than a dozen diffusible antagonists that include chordin, noggin, follistatin, and chordin-like proteins (Rider and Mulloy, 2010; Walsh et al., 2010; Zakin and De Robertis, 2010). Binding of antagonists physically prevents BMPs from binding to their cognate receptors by masking the epitopes involved in ligand–receptor interactions (Groppe et al., 2002; **Figure 1**). Subsequent cleavage of chordin by tolloid zinc metalloproteinases triggers the release of active BMPs from the chordin/BMP complex (Peluso et al., 2011). Twisted gastrulation (Tsg) has a dual role in distinct model systems, acting as either a BMP antagonist or as an agonist. In the case of chordin, the stability of the chordin/BMP complex is greatly increased by *Tsg* (Chang et al., 2001; Ross et al., 2001).

Finally, regulation of BMP transport is crucial for its role as a morphogen. It has been shown that BMP-2 has the ability to link directly to heparan sulfate proteoglycans (HSPGs).

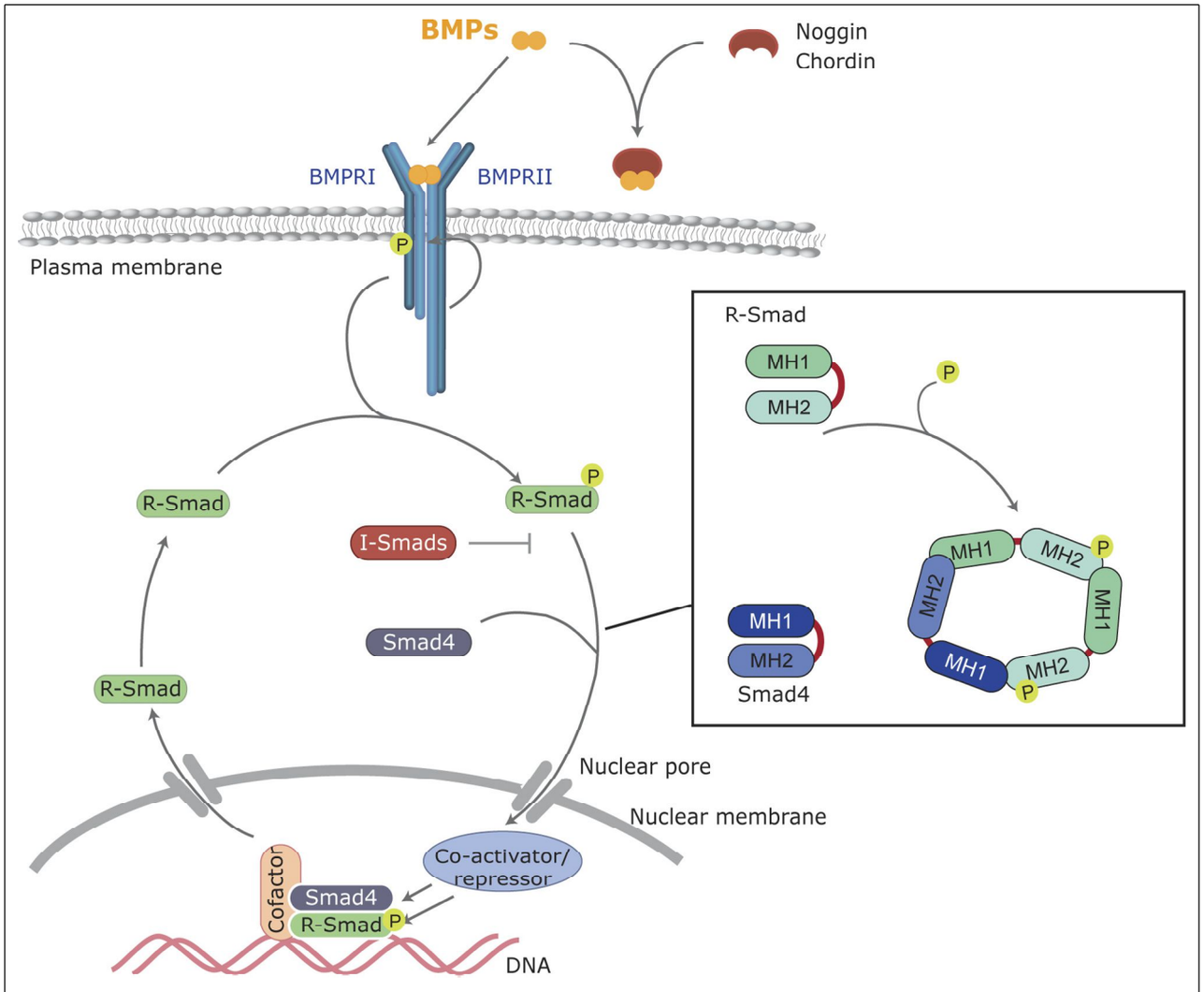

FIGURE 1 | Canonical BMP signaling. BMPs bind to the BMP receptors type I and II, and then type II receptor phosphorylates and activates the type I BMP receptor. Activated type I receptor phosphorylates R-Smads, which associate with the common Smad (Smad4) and enter the nucleus, where they regulate transcriptional processes. BMP signaling can be inhibited by extracellular antagonists, such as Noggin and Chordin, or intracellularly by I-Smads.

In several experimental models, extracellular HSPGs and collagen IV have been involved in the regulation of BMP transport (Ruppert et al., 1996; Osses et al., 2006). Collagen IV binds to BMP-4 and chordin homologs, sequestering them in the extracellular matrix. As mentioned above, Tsg, acting as a BMP agonist, releases chordin/BMP complexes from the collagen IV matrix, allowing their diffusion (Sawala et al., 2012). Thus, all these events of binding of BMPs to the extracellular matrix and/or to antagonists allow the formation of specific gradients through regulated solubility and bioavailability and constitute the first level of signal modulation.

BMP RECEPTORS AND RECEPTOR ACTIVATION

Bone morphogenetic proteins bind to a heterotetrameric complex of transmembrane receptors known as type I and II serine/threonine kinase receptors (Mueller and Nickel, 2012). Both types of receptors contain an N-terminal extracellular binding domain, a single transmembrane region, and an intracellular serine/threonine kinase domain (Shi and Massague, 2003; Feng and Derynck, 2005; Miyazono et al., 2010). Strong evidence confirms that both type I and II receptors, acting in coordination, are required for complete signal transduction. BMPs can bind to type I in the absence of type II receptors but when both types are present in the membrane of target cells their binding affinity is highly increased (Hinck, 2012; **Figure 2**). Based on their structures and functions, type I BMP receptors can be divided into the Bmpr1A and Bmpr1B group (also known as Alk3 and Alk6) and the Acvrl1 and Acvr1 group (also known as Alk1 and Alk2; Hinck, 2012). These groups show slight preferences for binding to specific BMPs. For instance, BMP-2 and -4 bind preferentially Bmpr1A and Bmpr1B whereas BMP-5, -6, and -7 additionally bind to Acvr1 (Liu et al., 1995). It is also well established that BMPs bind to three distinct type II receptors, namely Bmpr2, Acvr2A, and Acvr2B (**Figure 2**). Bmpr2 shows a unique, long C-terminal extension that allows specific recruitment of intracellular transducers. A question arises as to how such a limited number of signaling receptors allows binding of a large number of ligand members. One simple answer would rely on promiscuous interactions between shared ligands and several receptors (Hinck, 2012; Mueller and Nickel, 2012). However, combinatorial interactions of different type I and II receptors should allow selectivity and specificity of ligand binding as well as intracellular signaling in target cells. Numerous *in vivo* examples confirm the unique functions for an individual BMPs that are not shared even for closely related ligands with similar receptor binding affinities *in vitro* (Saremba et al., 2008; Meynard et al., 2009; Perron and Dodd, 2011, 2012). Further study into the molecular mechanisms that drive such functional specificity in living organisms is needed.

Moreover, co-receptors have been shown to modulate ligand binding and downstream signaling events. Members of the repulsive guidance molecule (RGM) family are

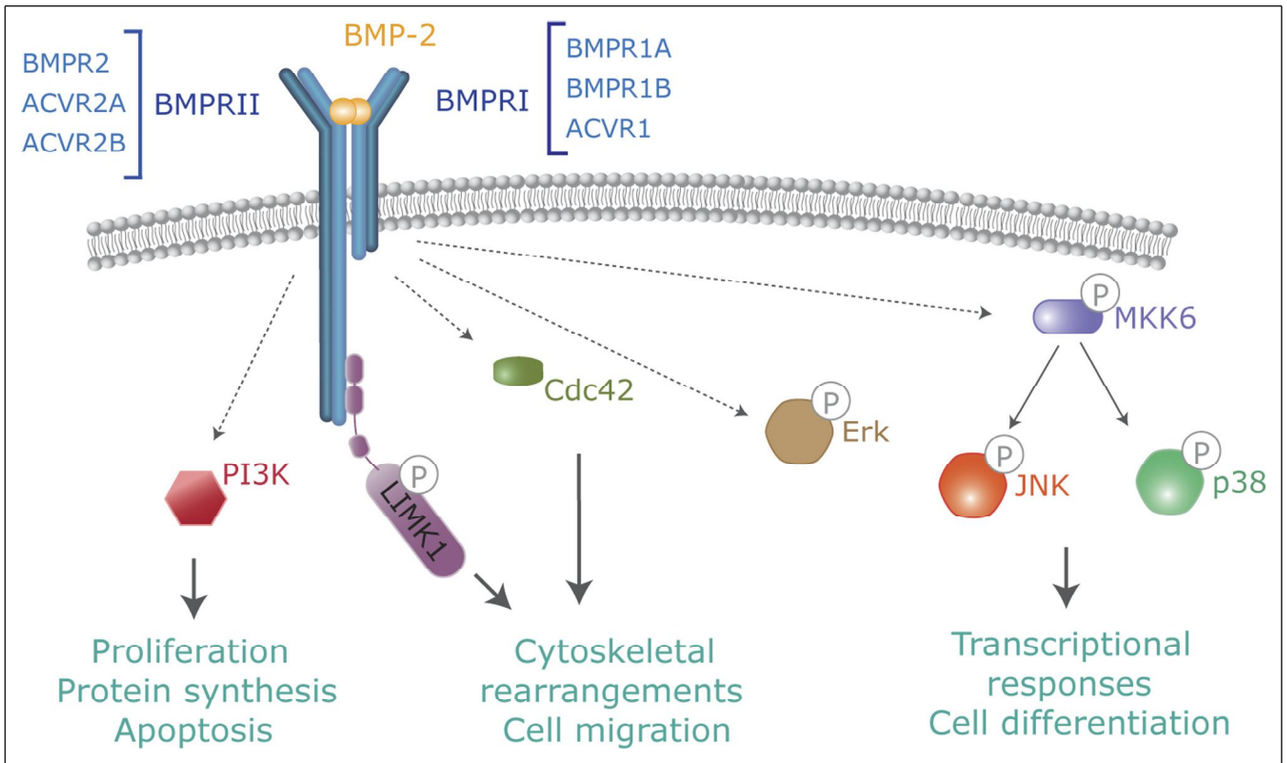

FIGURE 2 | Non-canonical BMP signaling. In addition to Smads, activated BMP receptors activate several intracellular pathways which modulate BMP-dependent cellular responses. Pathways include TAK-p38, PI3-kinase, Cdc42 or activation of LIMK by binding to the BMPR-II cytoplasmic tail.

glycophosphatidylinositol (GPI)-anchored co-receptors for BMP-2 and -4 and enhance responses at low BMP concentrations (Xia et al., 2007). Dragon and hemojuvelin (RGMb and c, respectively) also interact with BMP receptors and ligands and enhance responses for BMP-2 and -6. It has been shown that hemojuvelin plays a major role in regulation of iron metabolism in hepatocytes by increasing the binding affinity of BMP receptors for BMP-6 (Babitt et al., 2006). In addition to facilitating co-receptors, other membrane proteins function as suppressors of BMP signaling. For instance, Bambi is a transmembrane protein, structurally related to type I receptors that act as pseudoreceptor. Bambi forms a stable receptor complex but, since it lacks the intracellular kinase domain, inhibits transduction by titrating available type II receptors (Onichtchouk et al., 1999).

Type I and II BMP receptors show some ligand-independent affinity for each other. In the absence of a ligand, small amounts of pre-existing homo- and hetero-dimer receptor complexes are present at the cell surface (Ehrlich et al., 2012). However, ligand binding dramatically increases oligomerization involving type I and II complexes. Ligand-induced oligomerization promotes type II-dependent phosphorylation of a specific domain of type I receptors (known as the GS domain; **Figure 1**). Upon phosphorylation of the GS domain the type I receptor kinase is converted to its active conformation (Wrana et al., 1994). Thus, the kinase activity of type I receptors is the major intracellular transducer: whereas mutated or kinase-deficient type I receptors block most of the cellular responses to the ligand, constitutively active type I receptors (induced by pathological mutations or artificially designed) are able to signal most of the responses in the absence of type II receptors or ligands (Wieser et al., 1995).

INTRACELLULAR Smad SIGNALING FROM BMP RECEPTORS

Smads are the main and best-known intracellular signal transducers for BMP receptors. According to their structural and functional properties, three different types of Smads have been defined: the receptor-regulated Smads (R-Smad) Smad1, -2,-3,-5, and -8; a common mediator Smad, Smad4; and the inhibitory Smads Smad6 and -7 (Shi and Massague, 2003; Sieber et al., 2009; Miyazono et al., 2010). Active type I kinases phosphorylate R-Smads at serine residues located in their C-terminus. Specific phosphorylation of different R-Smads depends on the L45 loop of the type I receptor (Feng and Derynck, 1997). All the BMP type I receptors mentioned above (BMPR1A, BMPR1B, Acvr1, and Acvrl1) phosphorylate Smad1, Smad5, and Smad8, which are thus defined as BMP-activated Smads. Phosphorylation and activation of R-Smads disrupts the autoinhibitory interaction between the N-terminal (MAD homology 1, MH1) and C-terminal (MH2) domains of Smad monomers (Shi et al., 1997). This favors the formation of a multimeric complex composed of two molecules of R-Smad and one molecule of Smad4 interacting through their MH2 domain (**Figure 1**). On the new conformation, the nuclear import signal is exposed and the complexes translocate into the nucleus where they execute distinct transcriptional regulatory functions (Feng and Derynck, 2005; Hill, 2009).

Intracellular BMP signaling, as shown for transduction of all other morphogens described so far, is subjected to a growing number of cross-talk mechanisms with other extracellular ones, as well as regulation by internal cues, in order to integrate a final cell response. For instance, the inhibitory Smads, Smad6, and Smad7, block BMP signaling by preventing phosphorylation of R-Smads by type I receptors in a dominant negative fashion by binding to active receptor complexes (Derynck and Zhang, 2003). Another known mechanism is the degradation of Smads through the ubiquitin–proteasome pathway. Several homologous to E6-associated protein C-terminus (HECT)-type E3 ligases, such as Smurf-1,-2, or Nedd4-2, interact and ubiquitinate Smads and, when complexed with I-Smads, BMP receptors (Wicks et al., 2006). Degradation of Smads is also regulated by mitogen-activated protein (MAP) kinase and Gsk-3 phosphorylation allowing specific interaction with MAP kinase and Wnt signaling cascades (Fuentealba et al., 2007).

NON-CANONICAL SIGNALING FROM BMP RECEPTORS

In addition to Smads, BMPs activate other intracellular signaling pathways relevant to their cell functions. Non-canonical BMP signaling includes Rho-like small GTPases, phosphatidylinositol 3-kinase/Akt (PI3K/Akt) or various types of MAP kinases (Derynck and Zhang, 2003; Zhang, 2009; **Figure 2**). Mechanistically, it is well established that BMPs regulate the Tak1/p38 pathway through recruitment and ubiquitylation of Traf6 by activated receptor complexes (Sorrentino et al., 2008; Yamashita et al., 2008). BMPs trigger canonical and non-canonical pathways simultaneously, driving to a specific cellular output (Ulsamer et al., 2008; Xu et al., 2008; Susperregui et al., 2011). Several studies indicate that BMP-mediated cell migration or axon and dendrite growth requires activation of the small GTPase Cdc42 and Limk activities. Most of these effects are Smad-independent, but depend on Limk binding to the long cytoplasmatic tail of Bmpr2 complexes (Foletta et al., 2003; Lee-Hoeflich et al., 2004). Furthermore, additional reports indicate that activation of Limk also requires the activation of Paks through Cdc42 and PI3K, as well as p38 MAP kinase activities (Gamell et al., 2008, 2011). The specific abilities of distinct receptors or receptor combinations to activate these non-canonical pathways and promote specific signaling outcomes need to be studied.

BMPs IN NERVOUS SYSTEM DEVELOPMENT AND MAINTENANCE

In recent years, there has been exponential progress in the clarification of the role of BMPs at different stages of nervous system development. BMP ligands and receptors are expressed in very complex patterns throughout neural development in all regions of the central and peripheral nervous system (Ebendal et al., 1998; Miyagi et al., 2011). Evidence clearly demonstrates that these pleiotropic cytokines have a very dynamic role: from the early steps of neuralization and patterning to an instructive role in neural precursor fate commitment and neuronal wiring (Liu and Niswander, 2005). Evidence also extends their role in postnatal brain as well as peripheral nervous system development and maintenance (Bond et al., 2012; **Figure 3**).

EXPRESSION AND ROLE OF BMPs AND RECEPTORS IN TELENCEPHALIC TISSUES

Bone morphogenetic proteins and their antagonists are expressed throughout neural development with a complex chronological and

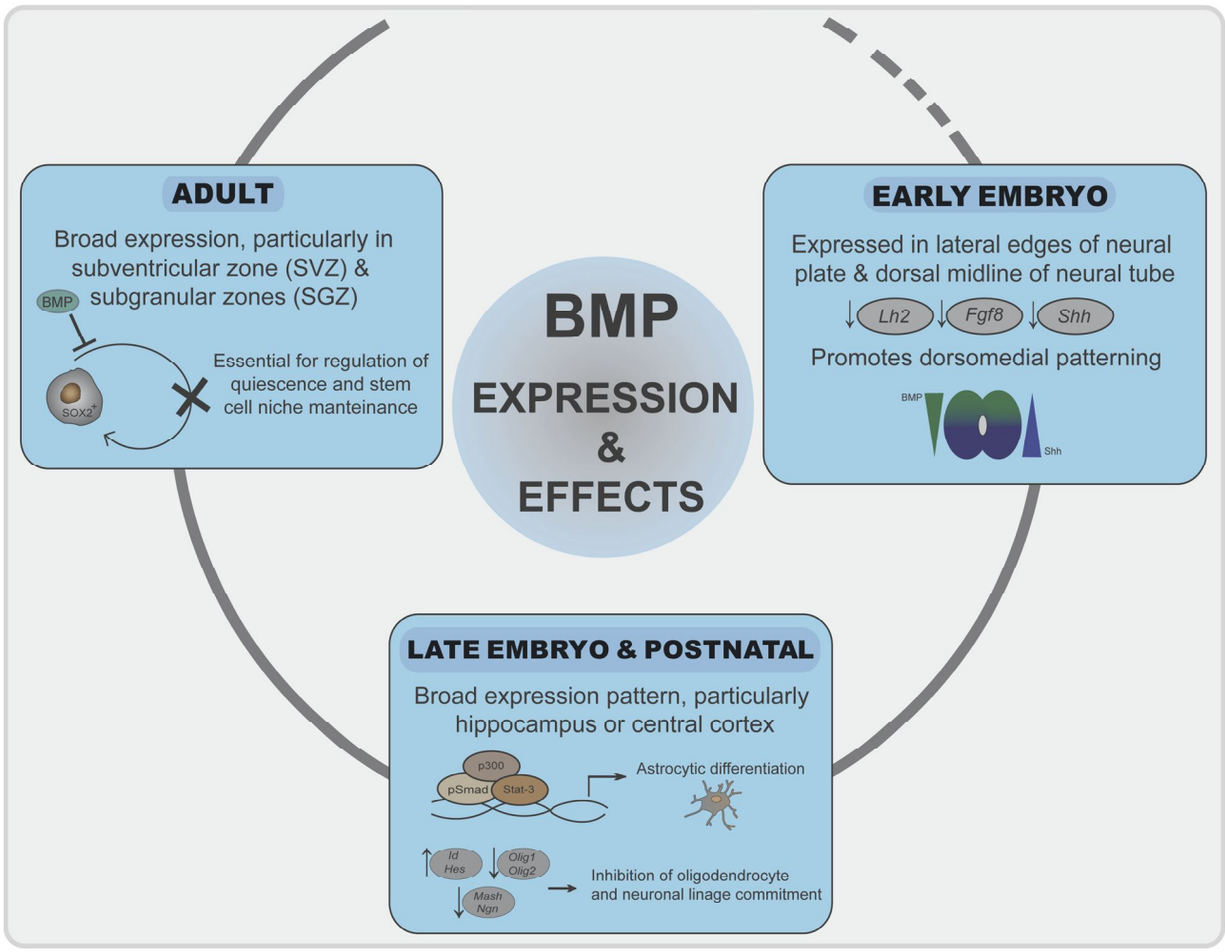

FIGURE 3 | Roles of BMP signaling in neural development. Initially, inhibition of BMP signaling is required for neuroectoderm induction. BMPs generate a signaling gradient and promote dorsomedial identity. BMP signaling is prominent at the dorsal telencephalic midline and in the marginal zone neurons, where it correlates negatively with expression of the cortical selector *Lhx2*, *Fgf8*, or *Shh*. In late embryogenesis and postnatally, BMP signaling promotes astroglial commitment by activation astrocyte-specific promoters through a Stat3-p300/CBP-Smad1 complex. At the same time represses commitment to the other two neural lineages by inducing Ids and Hes proteins. In adulthood, a balanced BMP signaling is required for regulation of quiescence and differentiation of neural stem cell populations in the SVZ and SGZ.

overlapping location that is only known to a limited extent. In early-developing neural tissue, BMPs are expressed particularly at the lateral edges of the neural plate and later on in the dorsal midline of the neural tube (Mehler et al., 1997; Chen and Panchision, 2007). During vertebrate development, the rostral–dorsal part of the neural plate gives rise to the telencephalon, the most complex region of the nervous system. The two signaling centers in the dorsal midline of the telencephalon, the roof plate and the cortical hem, secrete several BMPs (Furuta et al., 1997). These BMPs generate a signaling gradient and promote dorsomedial identity. Mice that are transgenic for specific BMP-dependent reporters indicate that, at embryonic stages, high BMP signaling is prominent at the dorsal telencephalic midline and in the marginal zone neurons, where it correlates negatively with expression of the cortical selector *Lhx2* (Doan et al., 2012). BMPs also reduce the expression of the anterior forebrain markers *Fgf8* or *Shh* (Anderson et al., 2002; **Figure 3**). *Chordin* and *noggin* double mutant embryos further emphasize the importance of the appeasement of BMP signaling for proper ventral forebrain development (Anderson et al., 2002). During further embryo development, brain expression of BMP-2, -4, -5, -6, and -7 peaks around postnatal day 4 with a broad expression pattern (Mehler et al., 1997; Sabo et al., 2009). Particular areas of the telencephalon, such as the hippocampus or cerebral cortex, show strong postnatal BMP activation (Doan et al., 2012). In adult telencephalon, there is also broad expression of BMPs at most locations and cell types, suggesting also a pivotal role in the adult brain. Interestingly, expression of BMPs and their antagonists specifically remain in the two areas where neurogenesis continues in the adult [the subventricular zone (SVZ) and subgranular zones (SGZ); Bond et al., 2012]. Expression of BMPs, from stem cells and neural progenitors, and noggin, secreted from ependymal cells, is essential for stem cell niche maintenance and

neuroblast survival (Lim et al., 2000; Mira et al., 2010; **Figure 3**). Moreover, increased expression of BMPs occurs after distinct brain and spinal cord injuries and suggest a role of BMP signaling in neural cell survival and repair (Sabo et al., 2009).

Bone morphogenetic protein receptors are expressed at high levels throughout all stages of embryonic development but show different expression patterns. *Bmpr1A* is expressed earlier than *Bmpr1B*. *Bmpr2* is mostly restricted to proliferative regions of the nervous system, whereas *Acvr2* and *Acvr1* have also been detected in early neural development and are expressed at high levels in adult brain. Bmpr1A and Bmpr1B are required separately in some development processes although in several studies of neural development, each receptor could, at least partially, compensate for the loss of the other. For instance, deletion of *Bmpr1B* causes no obvious forebrain phenotype (Yi et al., 2000). However, the requirement of BMP signaling for dorsal telencephalic development is shown after forebrain-specific ablation of *Bmpr1A* or the double knock-out of *Bmpr1A* and *Bmpr1B*, which leads to holoprosencephaly (Fernandes et al., 2007). However, later ablation only affects formation of the dentate gyrus of the hippocampus (Caronia et al., 2010). In adult telencephalon, expression of all these receptors remains, with *Bmpr1A* the most abundant and broadly expressed one (Miyagi et al., 2011). All cell types (neurons, astroglia, oligodendroglia, or ependymal cells) express combinations of these receptors (Chalazonitis et al., 2011; Bond et al., 2012). Interestingly, some reports suggest that their expression pattern is differentially distributed within a single neuron, with Bmpr1A mainly expressed in cell bodies and Bmpr1B in dendrites (Miyagi et al., 2011).

BMPs IN EMBRYONIC AND ADULT NEURAL CELL SPECIFICATION

The central and peripheral nervous systems originate from neural progenitor cells, which proliferate and give rise to the three main neural cell types: neurons, astrocytes, and oligodendrocytes. The specification and differentiation of the distinct cell types require interactions between cell-autonomous molecular mechanisms and external signaling cues (Mehler et al., 1997; Mehler, 2002; Liu and Niswander, 2005). Remarkably, BMPs are critical for progenitor cell specification and maintenance of a particular phenotype through dynamic transcriptional regulation (Bond et al., 2012). BMPs decrease proliferation of neural progenitors in cell culture models as well as *in vivo* in combination with other signaling molecules and internal cues (Chmielnicki et al., 2004; Sun et al., 2011; Benraiss et al., 2012).

BMP role in neurogenesis

Neurogenesis is promoted by proneuronal basic helix-loop-helix (bHLH) transcription factors including Mash1, Neurogenin, or NeuroD, which form hetero-dimers with ubiquitously expressed bHLH E proteins, such as the E2A gene products, E12 and E47, through their HLH domain (Ross et al., 2003; Hsieh, 2012). Hetero-dimers bind to DNA through their basic domain and activate the transcription of genes that have E boxes in their promoter region (**Figure 4A**). One subfamily of HLH factors, known as Id proteins, lacks this basic region. Hetero-dimerization of Id with bHLH is sufficient to block their DNA binding and function (Norton, 2000; Ruzinova and Benezra, 2003). Moreover, Ids not only inhibit transcriptional function but also promote the degradation of neurogenic bHLH by sequestering ubiquitous E proteins (Vinals et al., 2004; **Figure 4B**). Similarly, the Hes family of bHLH transcriptional repressors blocks neuronal differentiation through a dominant negative function on E protein availability as well as through direct binding on specific promoters and recruitment of members of the Grouch family of transcriptional repressors (**Figure 4B**). BMPs have been shown to be strong inducers of both *Id* and *Hes* family members (Ross et al., 2003). Thus, Id and Hes family members are thought to be major molecular players in the negative effects of BMPs on commitment and differentiation of neuronal precursors (Takizawa et al., 2003; Imayoshi et al., 2008). Furthermore, BMPs have been proved to increase the expression of the transcriptional repressor *Rest/Nsrf*. Expression of *Rest/Nsrf* allows continuous repression of the neuronal markers in cells committed to other lineages (Kohyama et al., 2010). In addition to their effects on embryonic neurogenesis, BMPs are widely accepted as relevant molecules in adult neurogenesis. In adult telencephalon, neural stem cell populations are maintained in two niches: the SVZ and the SGZ of the dentate gyrus. Colak et al. (2008) showed, through conditional deletion of *Smad4* or noggin infusion, that BMP signaling was required for adult neurogenesis. Noggin can also expand hippocampal progenitors in the SGZ (Bonaguidi et al., 2008). Infusion of Noggin and genetic deletion of either *Bmpr1A* or *Smad4* further demonstrate the role of BMP signaling in regulation of quiescence of neural stem cells from SGZ, restraining their proliferation and allowing these niches to maintain long-term neurogenic ability (Mira et al., 2010). BMP signaling is also required for positional identity and neuronal subtype specification. Endogenously produced BMPs inhibit the expression of a telencephalic gene profile, which was revealed by addition of noggin or other pharmacological signaling inhibitors (Bertacchi et al., 2013). BMPs are also involved in regulation of a transcriptional network to generate forebrain cholinergic neurons (Bissonnette et al., 2011). They also determine a temporally and spatially restricted requirement for generation of glutamatergic neurons in cerebellum (Fernandes et al., 2012).

BMP role in oligodendrogenesis

Oligodendrocyte specification and maturation depend on the function of transcription factors that include Olig1, Olig2, and Sox10. Olig2 directs early oligodendrocyte specification and Olig1 promotes oligodendrocyte maturation and is required for repair of demyelinated lesions (Lu et al., 2002; Ligon et al., 2006; Li and Richardson, 2008). BMPs inhibit the development of several stages of oligodendrocyte differentiation as well as the timing of myelination as shown by expression analysis markers of oligodendrocyte differentiation such as A2B5, galactocerebroside, or myelin protein expression (Hall and Miller, 2004; Samanta and Kessler, 2004; Chen and Panchision, 2007; See and Grinspan, 2009; Weng et al., 2012). Conversely, noggin blocks production of astrocytes from oligodendrocyte precursors in culture (Sim et al., 2006). BMP-4 stimulation increases oligodendrocyte progenitor proliferation in a model of induced demyelination. More importantly, addition of noggin increases the number of mature oligodendrocytes and increased the remyelination of injured axons

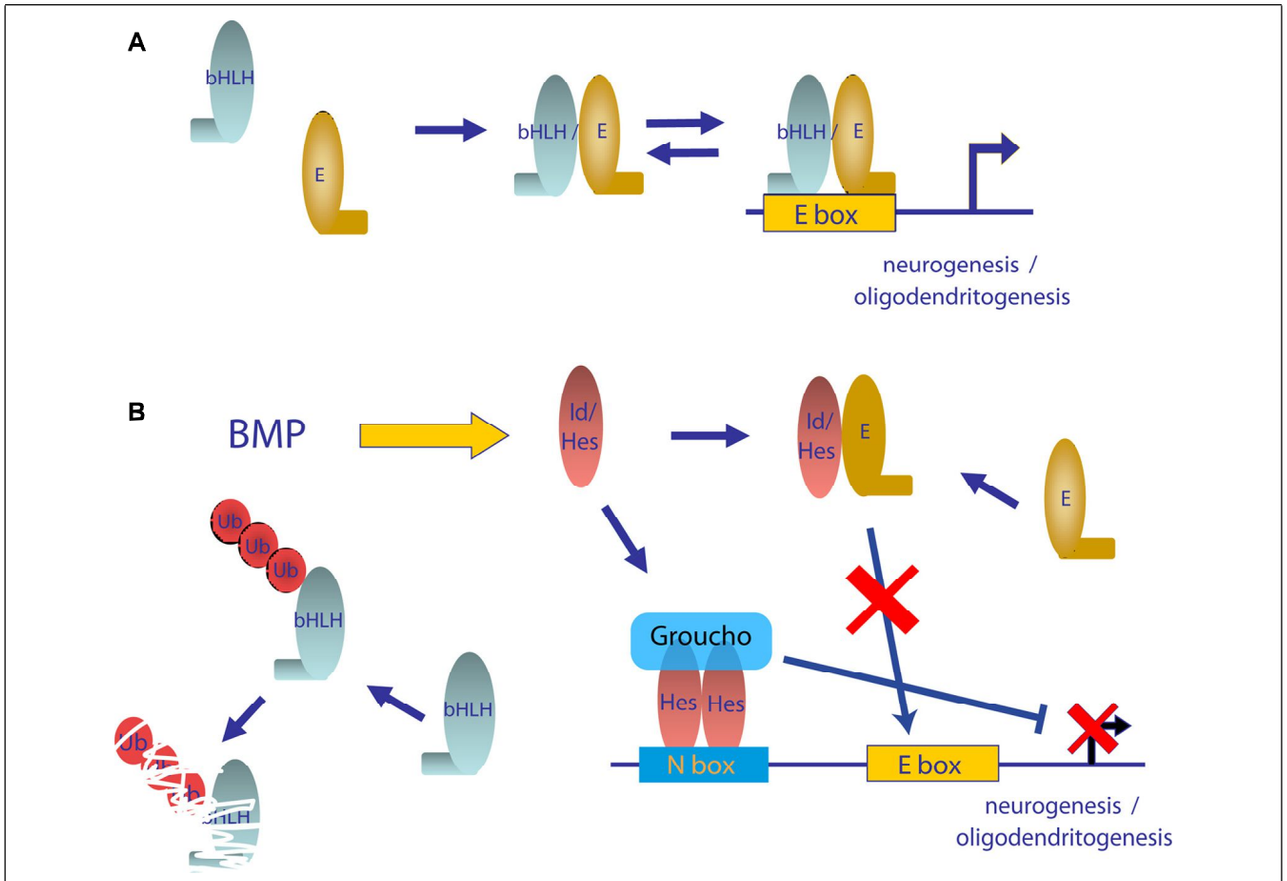

FIGURE 4 | Model of mechanism of repression of neurogenic bHLH transcription factors by BMPs. (A) In differentiating neurogenic precursors, bHLH transcription factors hetero-dimerizes with E proteins, which bind to E boxes and promote expression of neuronal genes. **(B)** Activation of the BMP signaling pathway leads to increased levels of Id and Hes proteins. Id and Hes proteins sequester E proteins away from bHLH transcription factors, which leads to transcriptionally inactive complexes and also enhance degradation of bHLH monomers. Furthermore Hes proteins can bind to N boxes sequences in neural promoters and recruit the Groucho family of transcriptional repressors.

in the corpus callosum (Sabo et al., 2011; Wu et al., 2012; Sabo and Cate, 2013). At the molecular level, BMP-induced expression of Id and Hes proteins seems to be also relevant in such a process by sequestering Olig1 and Olig2 which also belong to the bHLH family of transcription factors (Cheng et al., 2007; Bilican et al., 2008). Additional targets of Notch, such as *Jag1*, *Hey1*, and *Hey2*, are upregulated by BMP in oligodendrocytes through increased epigenetic modification at these loci (Wu et al., 2012). Inhibition of *Olig2* expression by direct binding of Smad4 to the *Olig2* promoter has also been demonstrated (Bilican et al., 2008; **Figure 3**). Recently, it has also been shown that the Smad-interacting protein-1 (Sip1) is an essential *in vivo* modulator of myelination. Sip1 antagonizes BMP signaling acting as a transcriptional repressor of Smad activity, while promoting activation of Olig1/Olig2 transcriptional activity and induction of I-Smads (Weng et al., 2012).

BMP role in astrocytogenesis

In opposition to the repression of neuronal and oligodendrocyte development, during the late embryonic and postnatal periods, BMP signaling strongly induces astrocyte differentiation (Gross et al., 1996; Mehler et al., 1997; Fukuda et al., 2007; See et al., 2007). BMPs promote the generation of astrocytes from precursors in a variety of embryonic neural cells (Gross et al., 1996; Mehler et al., 1997; Mehler, 2002; Bonaguidi et al., 2005). Implantation of noggin-producing cells induced the appearance of increased numbers of oligodendrocyte precursors whereas high BMP signaling inhibits oligodendrocyte precursors and promote astrogliogenesis (Mabie et al., 1999; Mekki-Dauriac et al., 2002; Wu et al., 2012). BMP signaling in the SVZ promotes astroglial lineage commitment and block differentiation of neurons and oligodendrocytes, whereas noggin suppresses astrocyte determination (Chmielnicki et al., 2004; Colak et al., 2008). LIF and BMPs synergize to promote astrocytic differentiation by activating astrocyte-specific promoters through a Stat3-p300/CBP-Smad1 complex (Nakashima et al., 1999; **Figure 3**). The ability of BMPs and Stat3 to promote astrogliogenesis has been shown to be dependent on the histone acetylation/deacetylation machinery (Scholl et al., 2012). Another study indicated that Smad action is not required for gliogenesis but is promoted by BMPs through

mammalian target of rapamycin/FKBP12-rapamycin-associated protein (mTor/Frap) phosphorylation of Stats (Rajan et al., 2003). Interestingly, Bmpr1A or Bmpr1B signaling exerts opposing effects on initial astrocytic hypertrophy after injury, suggesting that distinct BMPs engaging different receptor complexes exert separate activities on gliogenesis. The ability of BMPs to promote maturation of astroglia is further emphasized by the fact that activation of BMP signaling inhibits the tumorigenic potential of human glioblastoma-initiating cells (Piccirillo et al., 2006). Furthermore, Ezh2-dependent epigenetic silencing of *Bmpr1B* desensitizes tumor-initiating glioblastoma cells to differentiation and contributes to their tumorigenicity (Lee et al., 2008).

BMP SIGNALING IN NEURITE AND AXON OUTGROWTH, GUIDANCE AND SYNAPSE FORMATION

After neurogenesis has been completed, several sequential events are needed to establish neuronal circuits: polarized outgrowth of axons and dendrites, axon path finding toward the appropriate synaptic partner cell and establishment and maintenance of the synapse. Growing evidence in several experimental models points to BMP regulation of all these events. For instance, BMP ligands display positive regulation of the number, length, and branching of neurites in neurons from diverse neuronal origins, including cortical and hippocampal neurons (Le Roux et al., 1999; Withers et al., 2000; Lee-Hoeflich et al., 2004; Podkowa et al., 2010). Similarly, BMPs have been included as inductive signals promoting growth cone guidance as well as axonal orientation and path finding. Most of the data arise from studies of the sensory projection neurons of the spinal cord. BMP-7 and GDF-7 supplied by the roof plate orient axons of commissural neurons away from the roof plate and regulate their rate of extension through the spinal cord toward the floor plate (Augsburger et al., 1999; Butler and Dodd, 2003; Yamauchi et al., 2008, 2013; Sanchez-Camacho and Bovolenta, 2009). Guideposts are discrete groups of glial or neuronal cells that provide discontinuous information in intermediate positions along the path of growing axons (Sanchez-Camacho and Bovolenta, 2009). The corpus callosum represents the major forebrain commissure connecting the two cerebral hemispheres. Midline crossing of callosal axons is controlled by several glial and neuronal guideposts specifically located along the callosal path. BMP-7 has been shown to be required at different steps of organization and differentiation of these guidepost cells, which allows formation of the corpus callosum (Sanchez-Camacho et al., 2011). Additional evidence also indicates that BMP-7, secreted from the meninges, is involved in a morphogenic cascade, including Wnt3a and GDF-5, allowing correct corpus callosum development and prevents premature axon projection (Choe et al., 2012). It is not clear which signaling mechanisms are activated by BMP in these processes. In contrast to the slow timing of neural and glial specification, the very rapid time course of BMP-induced axonal orientation suggests transcription-independent pathways, probably depending on cytoskeletal actin remodeling and c-Jun N-terminal kinase (Jnk)-mediated microtubule stabilization (Augsburger et al., 1999; Wen et al., 2007; Podkowa et al., 2010; Perron and Dodd, 2011). Regulation of the cytoskeleton by BMPs has been linked to activation of Limk1 activation. Limk1 and Limk2 are closely related kinases that phosphorylate and inactivate actin-depolymerizing proteins such as cofilin or ADF. Limk1 has been shown to be activated by several BMPs in neural cells through specific binding to the Bmpr2 cytoplasmic tail and a further activation mechanism that involves Rho GTPases and PI3-kinase (Foletta et al., 2003; Lee-Hoeflich et al., 2004; Eaton and Davis, 2005; Gamell et al., 2008). Limk phosphorylation of cofilin/ADF is counteracted by the action of the Slingshot phosphatase, which is activated at later times after BMP addition and enables chemotactic responses to change from attraction to repulsion (Wen et al., 2007).

An intriguing functional and mechanistic question is that, whereas the closely related BMP-6 and -7 both induce the differentiation of commissural neurons, only BMP-7 is able to orients its axons *in vitro* and is required for appropriate axon projection *in vivo* (Perron and Dodd, 2011, 2012). Both ligands have been reported to bind hetero-dimers consisting of Acvr2A or Bmpr2 with Acvr1, Bmpr1A or Bmpr1B in numerous cellular models (Mueller and Nickel, 2012). However, the facts that a single amino acid swapping allows BMP-6 to orient axons and *vice versa* and that binding of BMP-6 to type I receptor depends on N-glycosylation, suggest that distinct receptor recruitment is involved in these functional differences (Saremba et al., 2008; Perron and Dodd, 2012). Changes in expression of BMP receptor subunits at growth cones have been shown after motor neuronal differentiation (Benavente et al., 2012). Moreover, whereas neuronal specification is a redundant function of Bmpr1A and Bmpr1B, axon outgrowth and regulation of cofilin activity only depend on *Bmpr1B* (Yamauchi et al., 2008, 2013).

BMP role in synaptogenesis

Once axons reach their corresponding target, two-way communication between presynaptic and postsynaptic cells is needed for synaptic establishment and homeostasis during development and for proper synaptic plasticity. The *Drosophila* larval neuromuscular junction (NMJ) is a useful model for genetic and biochemical studies of synaptic function (Collins and DiAntonio, 2007). Development of the synapse requires an anterograde as well as retrograde input from the synaptic terminal and target cell. BMP signaling is an indispensable component of retrograde signaling in the NMJ (Henriquez et al., 2011). The muscle-secreted BMP ligand *glass bottom boat* (*Gbb*), signals through presynaptic *wishful thinking* (*Wit*), the Bmpr2 homolog, and the receptor type I homologs *thick veins* and *saxophone* (*Tkv* and *Sax*, respectively; Aberle et al., 2002; Marques et al., 2002, 2003; Rawson et al., 2003). *Wit* mutant larvae show complete presynaptic detachment, which could be rescued by its expression in presynaptic cells (Aberle et al., 2002; Marques et al., 2002). Similarly, *Gbb* expression in muscle, but not in neurons, rescues NMJ defects observed in *Gbb* mutants (Marques et al., 2003). Retrograde *Gbb* activation of synaptic receptors has two parallel effects. One is activation of Limk1 that allows stabilization of the synapse. In the absence of *Limk1*, synaptic footprints are observed in the NMJ. In these footprints the presynaptic components are missing (Eaton and Davis, 2005). Since presynaptic development precedes postsynaptic development, synaptic footprints have been interpreted as being the remnants of mature synaptic contacts that have formed and then retracted. The other effect involves activation of the Smad homologs *Mad* and *Medea*

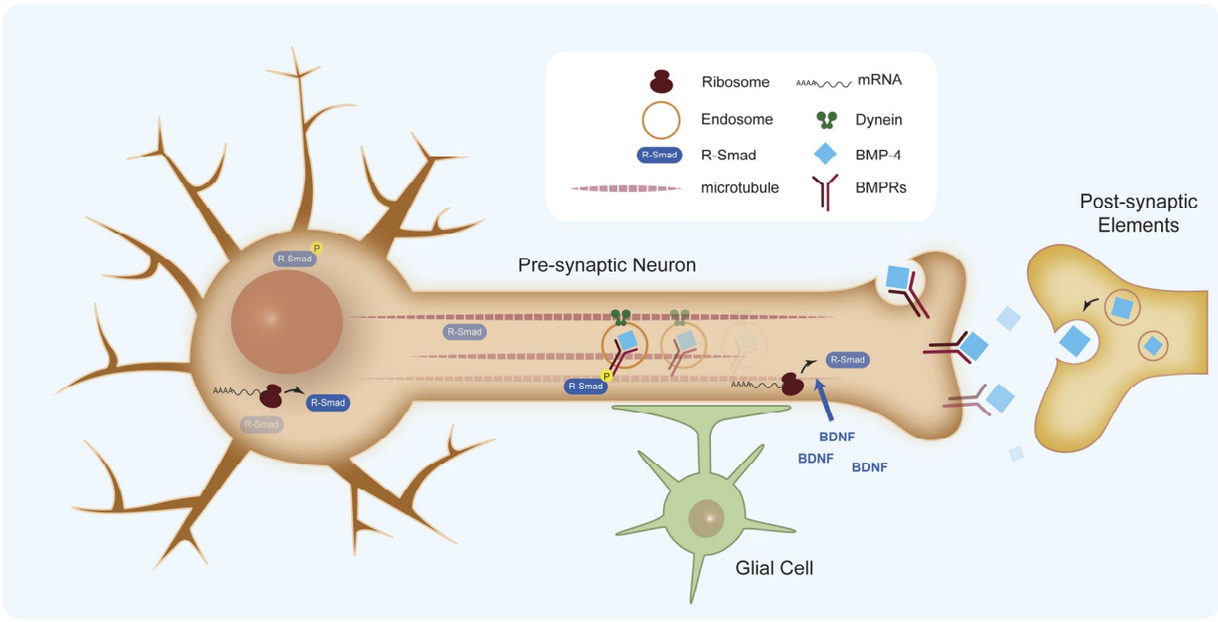

FIGURE 5 | Retrograde signaling of BMPs in synapse formation. BMP retrograde transport of endocytosed BMP receptors by dynein motors. Effective retrograde BMP signal also involves specific translation of Smad protein in the axons.

and their transport to the neuronal soma to regulate transcription at the nucleus (**Figure 5**). There, Mad-dependent transcription of the Rac-guanine nucleotide exchange factor (GEF) *Trio* is relevant for proper NMJ growth and branching since transgenic expression of *Trio* partially rescues BMP signaling mutant larvae (Ball et al., 2010). Therefore, canonical and non-canonical pathways are involved in coordination of the synaptic growth and stability of NMJ. Interestingly, genes related to several motor diseases such as hereditary spastic paraplegia or amyotrophic lateral sclerosis, have been shown to regulate BMP retrograde signaling in model systems (Bayat et al., 2011; Henriquez et al., 2011).

An important aspect in BMP retrograde communication is how signals at the synaptic terminal are conveyed to the nucleus to regulate transcription. It has been shown that BMP retrograde signaling along the axon requires dynein retrograde motors (McCabe et al., 2003). Recently, retrograde transport of endocytosed BMP receptors has been demonstrated, which suggests two populations of phosphorylated Smad transducers, one at the synaptic terminal and one at the cell body (Smith et al., 2012; **Figure 5**). However, studies of the murine trigeminal sensory system indicate that an effective retrograde BMP signal also involves specific translation of Smad protein in the axon, which is transported to the cell body by dynein motors (Ji and Jaffrey, 2012). Axonal translation of Smads is activated by brain-derived neurotrophic factor (BDNF), thus coupling both morphogens in the homeostasis of synapses. Some questions remain about the exact place of Smad activation and the role of the additional Smads translated in the axon when it is commonly accepted that the intracellular pool of unphosphorylated Smads is relatively high. Another relevant aspect is the role of glial cells in the regulation of synaptogenesis. Glia, associate intimately with synaptic terminals and are required for synaptogenesis. Recent work on NMJ points to a new member of the BMP ligand family, *Maverick* (*Mav*), in controlling synthesis and release of *Gbb*. Mav is released in glial cells surrounding the synapse and reinforces BMP retrograde signaling by transcriptional regulation of the synthesis of *Gbb* in postsynaptic cells (Fuentes-Medel et al., 2012). Altogether, evidence points to a very relevant role of BMP ligands in the coordination of several cell types and signaling mechanisms during synaptogenesis.

ACKNOWLEDGMENTS

We thank Drs Soledad Alcántara and Natalia Artigas for valuable discussions and her critical reading of this manuscript. We also thank C. Gamell and C. Saldarriaga for their help in preparing the manuscript and figures. E. Rodríguez-Carballo is a recipient of a fellowship from IDIBELL. Research supported by grants from the MEC (BFU2011-24254), Fundació La Marató de TV3 and ISCIII (RETIC RD06/0020).

REFERENCES

Aberle, H., Haghighi, A. P., Fetter, R. D., McCabe, B. D., Magalhaes, T. R., and Goodman, C. S. (2002). wishful thinking encodes a BMP type II receptor that regulates synaptic growth in *Drosophila*. *Neuron* 33, 545–558. doi: 10.1016/S0896-6273(02)00589-5

Anderson, R. M., Lawrence, A. R., Stottmann, R. W., Bachiller, D., and Klingensmith, J. (2002). Chordin and noggin promote organizing centers of forebrain development in the mouse. *Development* 129, 4975–4987.

Augsburger, A., Schuchardt, A., Hoskins, S., Dodd, J., and Butler, S. (1999). BMPs as mediators of roof plate repulsion of commissural neurons. *Neuron* 24, 127–141. doi: 10.1016/S0896-6273(00)80827-2

Babitt, J. L., Huang, F. W., Wrighting, D. M., Xia, Y., Sidis, Y., Samad, T. A., et al. (2006). Bone morphogenetic protein

signaling by hemojuvelin regulates hepcidin expression. *Nat. Genet.* 38, 531–539. doi: 10.1038/ng1777

Ball, R. W., Warren-Paquin, M., Tsurudome, K., Liao, E. H., Elazzouzi, F., Cavanagh, C., et al. (2010). Retrograde BMP signaling controls synaptic growth at the NMJ by regulating trio expression in motor neurons. *Neuron* 66, 536–549. doi: 10.1016/j.neuron.2010.04.011

Bayat, V., Jaiswal, M., and Bellen, H. J. (2011). The BMP signaling pathway at the *Drosophila* neuromuscular junction and its links to neurodegenerative diseases. *Curr. Opin. Neurobiol.* 21, 182–188. doi: 10.1016/j.conb.2010.08.014

Benavente, F., Pinto, C., Parada, M., Henriquez, J. P., and Osses, N. (2012). Bone morphogenetic protein 2 inhibits neurite outgrowth of motor neuron-like NSC-34 cells and up-regulates its type II receptor. *J. Neurochem.* 122, 594–604. doi: 10.1111/j.1471-4159.2012.07795.x

Benraiss, A., Bruel-Jungerman, E., Lu, G., Economides, A. N., Davidson, B., and Goldman, S. A. (2012). Sustained induction of neuronal addition to the adult rat neostriatum by AAV4-delivered noggin and BDNF. *Gene Ther.* 19, 483–493. doi: 10.1038/gt.2011.114

Bertacchi, M., Pandolfini, L., Murenu, E., Viegi, A., Capsoni, S., Cellerino, A., et al. (2013). The positional identity of mouse ES cell-generated neurons is affected by BMP signaling. *Cell. Mol. Life Sci.* 70, 1095–1111. doi: 10.1007/s00018-012-1182-3

Bilican, B., Fiore-Heriche, C., Compston, A., Allen, N. D., and Chandran, S. (2008). Induction of Olig2 precursors by FGF involves BMP signalling blockade at the Smad level. *PLoS ONE* 3:e2863. doi: 10.1371/journal.pone.0002863

Bissonnette, C. J., Lyass, L., Bhattacharyya, B. J., Belmadani, A., Miller, R. J., and Kessler, J. A. (2011). The controlled generation of functional basal forebrain cholinergic neurons from human embryonic stem cells. *Stem Cells* 29, 802–811. doi: 10.1002/stem.626

Bonaguidi, M. A., McGuire, T., Hu, M., Kan, L., Samanta, J., and Kessler, J. A. (2005). LIF and BMP signaling generate separate and discrete types of GFAP-expressing cells. *Development* 132, 5503–5514. doi: 10.1242/dev.02166

Bonaguidi, M. A., Peng, C. Y., McGuire, T., Falciglia, G., Gobeske, K. T., Czeisler, C., et al. (2008). Noggin expands neural stem cells in the adult hippocampus. *J. Neurosci.* 28, 9194–9204. doi: 10.1523/JNEUROSCI.3314-07.2008

Bond, A. M., Bhalala, O. G., and Kessler, J. A. (2012). The dynamic role of bone morphogenetic proteins in neural stem cell fate and maturation. *Dev. Neurobiol.* 72, 1068–1084. doi: 10.1002/dneu.22022

Bragdon, B., Moseychuk, O., Saldanha, S., King, D., Julian, J., and Nohe, A. (2011). Bone morphogenetic proteins: a critical review. *Cell. Signal.* 23, 609–620. doi: 10.1016/j.cellsig.2010.10.003

Butler, S. J., and Dodd, J. (2003). A role for BMP heterodimers in roof plate-mediated repulsion of commissural axons. *Neuron* 38, 389–401. doi: 10.1016/S0896-6273(03)00254-X

Caronia, G., Wilcoxon, J., Feldman, P., and Grove, E. A. (2010). Bone morphogenetic protein signaling in the developing telencephalon controls formation of the hippocampal dentate gyrus and modifies fear-related behavior. *J. Neurosci.* 30, 6291–6301. doi: 10.1523/JNEUROSCI.0550-10.2010

Chalazonitis, A., D'Autreaux, F., Pham, T. D., Kessler, J. A., and Gershon, M. D. (2011). Bone morphogenetic proteins regulate enteric gliogenesis by modulating ErbB3 signaling. *Dev. Biol.* 350, 64–79. doi: 10.1016/j.ydbio.2010.11.017

Chang, C., Holtzman, D. A., Chau, S., Chickering, T., Woolf, E. A., Holmgren, L. M., et al. (2001). Twisted gastrulation can function as a BMP antagonist. *Nature* 410, 483–487. doi: 10.1038/35068583

Chen, D., Zhao, M., and Mundy, G. R. (2004). Bone morphogenetic proteins. *Growth Factors* 22, 233–241. doi: 10.1080/08977190412331279890

Chen, H. L., and Panchision, D. M. (2007). Concise review: bone morphogenetic protein pleiotropism in neural stem cells and their derivatives – alternative pathways, convergent signals. *Stem Cells* 25, 63–68. doi: 10.1634/stemcells.2006-0339

Cheng, X., Wang, Y., He, Q., Qiu, M., Whittemore, S. R., and Cao, Q. (2007). Bone morphogenetic protein signaling and olig1/2 interact to regulate the differentiation and maturation of adult oligodendrocyte precursor cells. *Stem Cells* 25, 3204–3214. doi: 10.1634/stemcells.2007-0284

Chmielnicki, E., Benraiss, A., Economides, A. N., and Goldman, S. A. (2004). Adenovirally expressed noggin and brain-derived neurotrophic factor cooperate to induce new medium spiny neurons from resident progenitor cells in the adult striatal ventricular zone. *J. Neurosci.* 24, 2133–2142. doi: 10.1523/JNEUROSCI.1554-03.2004

Choe, Y., Siegenthaler, J. A., and Pleasure, S. J. (2012). A cascade of morphogenic signaling initiated by the meninges controls corpus callosum formation. *Neuron* 73, 698–712. doi: 10.1016/j.neuron.2011.11.036

Colak, D., Mori, T., Brill, M. S., Pfeifer, A., Falk, S., Deng, C., et al. (2008). Adult neurogenesis requires Smad4-mediated bone morphogenic protein signaling in stem cells. *J. Neurosci.* 28, 434–446. doi: 10.1523/JNEUROSCI.4374-07.2008

Collins, C. A., and DiAntonio, A. (2007). Synaptic development: insights from *Drosophila*. *Curr. Opin. Neurobiol.* 17, 35–42. doi: 10.1016/j.conb.2007.01.001

Cui, Y., Jean, F., Thomas, G., and Christian, J. L. (1998). BMP-4 is proteolytically activated by furin and/or PC6 during vertebrate embryonic development. *EMBO J.* 17, 4735–4743. doi: 10.1093/emboj/17.16.4735

Derynck, R., and Zhang, Y. E. (2003). Smad-dependent and Smad-independent pathways in TGF-beta family signalling. *Nature* 425, 577–584. doi: 10.1038/nature02006

Doan, L. T., Javier, A. L., Furr, N. M., Nguyen, K. L., Cho, K. W., and Monuki, E. S. (2012). A Bmp reporter with ultrasensitive characteristics reveals that high Bmp signaling is not required for cortical hem fate. *PLoS ONE* 7:e44009. doi: 10.1371/journal.pone.0044009

Eaton, B. A., and Davis, G. W. (2005). LIM Kinase1 controls synaptic stability downstream of the type II BMP receptor. *Neuron* 47, 695–708. doi: 10.1016/j.neuron.2005.08.010

Ebendal, T., Bengtsson, H., and Soderstrom, S. (1998). Bone morphogenetic proteins and their receptors: potential functions in the brain. *J. Neurosci. Res.* 51, 139–146. doi: 10.1002/(SICI)1097-4547(19980115)51:2

Ehrlich, M., Gutman, O., Knaus, P., and Henis, Y. I. (2012). Oligomeric interactions of TGF-beta and BMP receptors. *FEBS Lett.* 586, 1885–1896. doi: 10.1016/j.febslet.2012.01.040

Eldar, A., Dorfman, R., Weiss, D., Ashe, H., Shilo, B. Z., and Barkai, N. (2002). Robustness of the BMP morphogen gradient in *Drosophila* embryonic patterning. *Nature* 419, 304–308. doi: 10.1038/nature01061

Feng, X. H., and Derynck, R. (1997). A kinase subdomain of transforming growth factor-beta (TGF-beta) type I receptor determines the TGF-beta intracellular signaling specificity. *EMBO J.* 16, 3912–3923. doi: 10.1093/emboj/16.13.3912

Feng, X. H., and Derynck, R. (2005). Specificity and versatility in TGF-β signaling through Smads. *Annu. Rev. Cell Dev. Biol.* 21, 659–693. doi: 10.1146/annurev.cellbio.21.022404.142018

Fernandes, M., Antoine, M., and Hebert, J. M. (2012). SMAD4 is essential for generating subtypes of neurons during cerebellar development. *Dev. Biol.* 365, 82–90. doi: 10.1016/j.ydbio.2012.02.017

Fernandes, M., Gutin, G., Alcorn, H., McConnell, S. K., and Hebert, J. M. (2007). Mutations in the BMP pathway in mice support the existence of two molecular classes of holoprosencephaly. *Development* 134, 3789–3794. doi: 10.1242/dev.004325

Foletta, V. C., Lim, M. A., Soosairajah, J., Kelly, A. P., Stanley, E. G., Shannon, M., et al. (2003). Direct signaling by the BMP type II receptor via the cytoskeletal regulator LIMK1. *J. Cell Biol.* 162, 1089–1098. doi: 10.1083/jcb.200212060

Fuentealba, L. C., Eivers, E., Ikeda, A., Hurtado, C., Kuroda, H., Pera, E. M., et al. (2007). Integrating patterning signals: Wnt/GSK3 regulates the duration of the BMP/Smad1 signal. *Cell* 131, 980–993. doi: 10.1016/j.cell.2007.09.027

Fuentes-Medel, Y., Ashley, J., Barria, R., Maloney, R., Freeman, M., and Budnik, V. (2012). Integration of a retrograde signal during synapse formation by glia-secreted TGF-beta ligand. *Curr. Biol.* 22, 1831–1838. doi: 10.1016/j.cub.2012.07.063

Fukuda, S., Abematsu, M., Mori, H., Yanagisawa, M., Kagawa, T., Nakashima, K., et al. (2007). Potentiation of astrogliogenesis by STAT3-mediated activation of bone morphogenetic protein-Smad signaling in neural stem cells. *Mol. Cell. Biol.* 27, 4931–4937. doi: 10.1128/MCB.02435-06

Furuta, Y., Piston, D. W., and Hogan, B. L. (1997). Bone morphogenetic proteins (BMPs) as regulators of dorsal forebrain development. *Development* 124, 2203–2212.

Gamell, C., Osses, N., Bartrons, R., Ruckle, T., Camps, M., Rosa, J. L., et al. (2008). BMP2 induction of actin cytoskeleton reorganization and cell migration requires PI3-kinase and Cdc42 activity. *J. Cell Sci.* 121, 3960–3970. doi: 10.1242/jcs.031286

Gamell, C., Susperregui, A. G., Bernard, O., Rosa, J. L., and Ventura, F. (2011). The p38/MK2/Hsp25

pathway is required for BMP-2-induced cell migration. *PLoS ONE* 6:e16477. doi: 10.1371/journal.pone.0016477

Groppe, J., Greenwald, J., Wiater, E., Rodriguez-Leon, J., Economides, A. N., Kwiatkowski, W., et al. (2002). Structural basis of BMP signalling inhibition by the cystine knot protein Noggin. *Nature* 420, 636–642. doi: 10.1038/nature01245

Gross, R. E., Mehler, M. F., Mabie, P. C., Zang, Z., Santschi, L., and Kessler, J. A. (1996). Bone morphogenetic proteins promote astroglial lineage commitment by mammalian subventricular zone progenitor cells. *Neuron* 17, 595–606. doi: 10.1016/S0896-6273(00)80193-2

Hall, A. K., and Miller, R. H. (2004). Emerging roles for bone morphogenetic proteins in central nervous system glial biology. *J. Neurosci. Res.* 76, 1–8. doi: 10.1002/jnr.20019

Henriquez, J. P., Krull, C. E., and Osses, N. (2011). The Wnt and BMP families of signaling morphogens at the vertebrate neuromuscular junction. *Int. J. Mol. Sci.* 12, 8924–8946. doi: 10.3390/ijms12128924

Hill, C. S. (2009). Nucleocytoplasmic shuttling of Smad proteins. *Cell Res.* 19, 36–46. doi: 10.1038/cr.2008.325

Hinck, A. P. (2012). Structural studies of the TGF-betas and their receptors – insights into evolution of the TGF-beta superfamily. *FEBS Lett.* 586, 1860–1870. doi: 10.1016/j.febslet.2012.05.028

Hsieh, J. (2012). Orchestrating transcriptional control of adult neurogenesis. *Genes Dev.* 26, 1010–1021. doi: 10.1101/gad.187336.112

Imayoshi, I., Shimogori, T., Ohtsuka, T., and Kageyama, R. (2008). Hes genes and neurogenin regulate non-neural versus neural fate specification in the dorsal telencephalic midline. *Development* 135, 2531–2541. doi: 10.1242/dev.021535

Ji, S. J., and Jaffrey, S. R. (2012). Intra-axonal translation of SMAD1/5/8 mediates retrograde regulation of trigeminal ganglia subtype specification. *Neuron* 74, 95–107. doi: 10.1016/j.neuron.2012.02.022

Kishigami, S., and Mishina, Y. (2005). BMP signaling and early embryonic patterning. *Cytokine Growth Factor Rev.* 16, 265–278. doi: 10.1016/j.cytogfr.2005.04.002

Kohyama, J., Sanosaka, T., Tokunaga, A., Takatsuka, E., Tsujimura, K., Okano, H., et al. (2010). BMP-induced REST regulates the establishment and maintenance of astrocytic identity. *J. Cell Biol.* 189, 159–170. doi: 10.1083/jcb.200908048

Lee, J., Son, M. J., Woolard, K., Donin, N. M., Li, A., Cheng, C. H., et al. (2008). Epigenetic-mediated dysfunction of the bone morphogenetic protein pathway inhibits differentiation of glioblastoma-initiating cells. *Cancer Cell* 13, 69–80. doi: 10.1016/j.ccr.2007.12.005

Lee-Hoeflich, S. T., Causing, C. G., Podkowa, M., Zhao, X., Wrana, J. L., and Attisano, L. (2004). Activation of LIMK1 by binding to the BMP receptor, BMPRII, regulates BMP-dependent dendritogenesis. *EMBO J.* 23, 4792–4801. doi: 10.1038/sj.emboj.7600418

Le Roux, P., Behar, S., Higgins, D., and Charette, M. (1999). OP-1 enhances dendritic growth from cerebral cortical neurons in vitro. *Exp. Neurol.* 160, 151–163. doi: 10.1006/exnr.1999.7194

Li, H., and Richardson, W. D. (2008). The evolution of Olig genes and their roles in myelination. *Neuron Glia Biol.* 4, 129–135. doi: 10.1017/S1740925X09990251

Ligon, K. L., Kesari, S., Kitada, M., Sun, T., Arnett, H. A., Alberta, J. A., et al. (2006). Development of NG2 neural progenitor cells requires Olig gene function. *Proc. Natl. Acad. Sci. U.S.A.* 103, 7853–7858. doi: 10.1073/pnas.0511001103

Lim, D. A., Tramontin, A. D., Trevejo, J. M., Herrera, D. G., Garcia-Verdugo, J. M., and Alvarez-Buylla, A. (2000). Noggin antagonizes BMP signaling to create a niche for adult neurogenesis. *Neuron* 28, 713–726. doi: 10.1016/S0896-6273(00)00148-3

Little, S. C., and Mullins, M. C. (2009). Bone morphogenetic protein heterodimers assemble heteromeric type I receptor complexes to pattern the dorsoventral axis. *Nat. Cell Biol.* 11, 637–643. doi: 10.1038/ncb1870

Liu, A., and Niswander, L. A. (2005). Bone morphogenetic protein signalling and vertebrate nervous system development. *Nat. Rev. Neurosci.* 6, 945–954.

Liu, F., Ventura, F., Doody, J., and Massague, J. (1995). Human type II receptor for bone morphogenic proteins (BMPs): extension of the two-kinase receptor model to the BMPs. *Mol. Cell. Biol.* 15, 3479–3486. doi: 10.1038/nrn1805

Lu, Q. R., Sun, T., Zhu, Z., Ma, N., Garcia, M., Stiles, C. D., et al. (2002). Common developmental requirement for Olig function indicates a motor neuron/oligodendrocyte connection. *Cell* 109, 75–86. doi: 10.1016/S0092-8674(02)00678-5

Ma, C. H., Brenner, G. J., Omura, T., Samad, O. A., Costigan, M., Inquimbert, P., et al. (2011). The BMP coreceptor RGMb promotes while the endogenous BMP antagonist noggin reduces neurite outgrowth and peripheral nerve regeneration by modulating BMP signaling. *J. Neurosci.* 31, 18391–18400. doi: 10.1523/JNEUROSCI.4550-11.2011

Mabie, P. C., Mehler, M. F., and Kessler, J. A. (1999). Multiple roles of bone morphogenetic protein signaling in the regulation of cortical cell number and phenotype. *J. Neurosci.* 19, 7077–7088.

Marques, G., Bao, H., Haerry, T. E., Shimell, M. J., Duchek, P., Zhang, B., et al. (2002). The *Drosophila* BMP type II receptor wishful thinking regulates neuromuscular synapse morphology and function. *Neuron* 33, 529–543. doi: 10.1016/S0896-6273(02)00595-0

Marques, G., Haerry, T. E., Crotty, M. L., Xue, M., Zhang, B., and O'Connor, M. B. (2003). Retrograde Gbb signaling through the Bmp type 2 receptor wishful thinking regulates systemic FMRFa expression in *Drosophila*. *Development* 130, 5457–5470. doi: 10.1242/dev.00772

Matsuura, I., Taniguchi, J., Hata, K., Saeki, N., and Yamashita, T. (2008). BMP inhibition enhances axonal growth and functional recovery after spinal cord injury. *J. Neurochem.* 105, 1471–1479. doi: 10.1111/j.1471-4159.2008.05251.x

McCabe, B. D., Marques, G., Haghighi, A. P., Fetter, R. D., Crotty, M. L., Haerry, T. E., et al. (2003). The BMP homolog Gbb provides a retrograde signal that regulates synaptic growth at the *Drosophila* neuromuscular junction. *Neuron* 39, 241–254. doi: 10.1016/S0896-6273(03)00426-4

Mehler, M. F. (2002). Mechanisms regulating lineage diversity during mammalian cerebral cortical neurogenesis and gliogenesis. *Results Probl. Cell Differ.* 39, 27–52. doi: 10.1007/978-3-540-46006-0_2

Mehler, M. F., Mabie, P. C., Zhang, D., and Kessler, J. A. (1997). Bone morphogenetic proteins in the nervous system. *Trends Neurosci.* 20, 309–317. doi: 10.1016/S0166-2236(96)01046-6

Mekki-Dauriac, S., Agius, E., Kan, P., and Cochard, P. (2002). Bone morphogenetic proteins negatively control oligodendrocyte precursor specification in the chick spinal cord. *Development* 129, 5117–5130.

Meynard, D., Kautz, L., Darnaud, V., Canonne-Hergaux, F., Coppin, H., and Roth, M. P. (2009). Lack of the bone morphogenetic protein BMP6 induces massive iron overload. *Nat. Genet.* 41, 478–481. doi: 10.1038/ng.320

Mira, H., Andreu, Z., Suh, H., Lie, D. C., Jessberger, S., Consiglio, A., et al. (2010). Signaling through BMPR-IA regulates quiescence and long-term activity of neural stem cells in the adult hippocampus. *Cell Stem Cell* 7, 78–89. doi: 10.1016/j.stem.2010.04.016

Miyagi, M., Mikawa, S., Hasegawa, T., Kobayashi, S., Matsuyama, Y., and Sato, K. (2011). Bone morphogenetic protein receptor expressions in the adult rat brain. *Neuroscience* 176, 93–109. doi: 10.1016/j.neuroscience.2010.12.027

Miyazono, K., Kamiya, Y., and Morikawa, M. (2010). Bone morphogenetic protein receptors and signal transduction. *J. Biochem.* 147, 35–51. doi: 10.1093/jb/mvp148

Mueller, T. D., and Nickel, J. (2012). Promiscuity and specificity in BMP receptor activation. *FEBS Lett.* 586, 1846–1859. doi: 10.1016/j.febslet.2012.02.043

Nakashima, K., Yanagisawa, M., Arakawa, H., Kimura, N., Hisatsune, T., Kawabata, M., et al. (1999). Synergistic signaling in fetal brain by STAT3-Smad1 complex bridged by p300. *Science* 284, 479–482. doi: 10.1126/science.284.5413.479

Norton, J. D. (2000). ID helix-loop-helix proteins in cell growth, differentiation and tumorigenesis. *J. Cell Sci.* 113(Pt 22), 3897–3905.

Onichtchouk, D., Chen, Y. G., Dosch, R., Gawantka, V., Delius, H., Massague, J., et al. (1999). Silencing of TGF-beta signalling by the pseudoreceptor BAMBI. *Nature* 401, 480–485. doi: 10.1038/46794

Osses, N., Gutierrez, J., Lopez-Rovira, T., Ventura, F., and Brandan, E. (2006). Sulfation is required for bone morphogenetic protein 2-dependent Id1 induction. *Biochem. Biophys. Res. Commun.* 344, 1207–1215. doi: 10.1016/j.bbrc.2006.04.029

Peluso, C. E., Umulis, D., Kim, Y. J., O'Connor, M. B., and Serpe, M. (2011). Shaping BMP morphogen gradients through enzyme-substrate interactions. *Dev. Cell* 21, 375–383. doi: 10.1016/j.devcel.2011.06.025

Perron, J. C., and Dodd, J. (2011). Inductive specification and axonal orientation of spinal neurons mediated by divergent bone morphogenetic protein signaling pathways. *Neural Dev.* 6, 36. doi: 10.1186/1749-8104-6-36

Perron, J. C., and Dodd, J. (2012). Structural distinctions in BMPs underlie divergent signaling in spinal neurons.

Neural Dev. 7, 16. doi: 10.1186/1749-8104-7-16

Piccirillo, S. G., Reynolds, B. A., Zanetti, N., Lamorte, G., Binda, E., Broggi, G., et al. (2006). Bone morphogenetic proteins inhibit the tumorigenic potential of human brain tumour-initiating cells. *Nature* 444, 761–765. doi: 10.1038/nature05349

Podkowa, M., Zhao, X., Chow, C. W., Coffey, E. T., Davis, R. J., and Attisano, L. (2010). Microtubule stabilization by bone morphogenetic protein receptor-mediated scaffolding of c-Jun N-terminal kinase promotes dendrite formation. *Mol. Cell. Biol.* 30, 2241–2250. doi: 10.1128/MCB.01166-09

Rajan, P., Panchision, D. M., Newell, L. F., and McKay, R. D. (2003). BMPs signal alternately through a SMAD or FRAP-STAT pathway to regulate fate choice in CNS stem cells. *J. Cell Biol.* 161, 911–921. doi: 10.1083/jcb.200211021

Ramel, M. C., and Hill, C. S. (2012). Spatial regulation of BMP activity. *FEBS Lett.* 586, 1929–1941. doi: 10.1016/j.febslet.2012.02.035

Rawson, J. M., Lee, M., Kennedy, E. L., and Selleck, S. B. (2003). *Drosophila* neuromuscular synapse assembly and function require the TGF-beta type I receptor saxophone and the transcription factor Mad. *J. Neurobiol.* 55, 134–150. doi: 10.1002/neu.10189

Rider, C. C., and Mulloy, B. (2010). Bone morphogenetic protein and growth differentiation factor cytokine families and their protein antagonists. *Biochem. J.* 429, 1–12. doi: 10.1042/BJ20100305

Ross, J. J., Shimmi, O., Vilmos, P., Petryk, A., Kim, H., Gaudenz, K., et al. (2001). Twisted gastrulation is a conserved extracellular BMP antagonist. *Nature* 410, 479–483. doi: 10.1038/35068578

Ross, S. E., Greenberg, M. E., and Stiles, C. D. (2003). Basic helix-loop-helix factors in cortical development. *Neuron* 39, 13–25. doi: 10.1016/S0896-6273(03)00365-9

Ruppert, R., Hoffmann, E., and Sebald, W. (1996). Human bone morphogenetic protein 2 contains a heparin-binding site which modifies its biological activity. *Eur. J. Biochem.* 237, 295–302. doi: 10.1111/j.1432-1033.1996.0295n.x

Ruzinova, M. B., and Benezra, R. (2003). Id proteins in development, cell cycle and cancer. *Trends Cell Biol.* 13, 410–418. doi: 10.1016/S0962-8924(03)00147-8

Sabo, J. K., Aumann, T. D., Merlo, D., Kilpatrick, T. J., and Cate, H. S. (2011). Remyelination is altered by bone morphogenic protein signaling in demyelinated lesions. *J. Neurosci.* 31, 4504–4510. doi: 10.1523/JNEUROSCI.5859-10.2011

Sabo, J. K., and Cate, H. S. (2013). Signalling pathways that inhibit the capacity of precursor cells for myelin repair. *Int. J. Mol. Sci.* 14, 1031–1049. doi: 10.3390/ijms14011031

Sabo, J. K., Kilpatrick, T. J., and Cate, H. S. (2009). Effects of bone morphogenic proteins on neural precursor cells and regulation during central nervous system injury. *Neurosignals* 17, 255–264. doi: 10.1159/000231892

Samanta, J., and Kessler, J. A. (2004). Interactions between ID and OLIG proteins mediate the inhibitory effects of BMP4 on oligodendroglial differentiation. *Development* 131, 4131–4142. doi: 10.1242/dev.01273

Sanchez-Camacho, C., and Bovolenta, P. (2009). Emerging mechanisms in morphogen-mediated axon guidance. *Bioessays* 31, 1013–1025. doi: 10.1002/bies.200900063

Sanchez-Camacho, C., Ortega, J. A., Ocana, I., Alcantara, S., and Bovolenta, P. (2011). Appropriate Bmp7 levels are required for the differentiation of midline guidepost cells involved in corpus callosum formation. *Dev. Neurobiol.* 71, 337–350. doi: 10.1002/dneu.20865

Saremba, S., Nickel, J., Seher, A., Kotzsch, A., Sebald, W., and Mueller, T. D. (2008). Type I receptor binding of bone morphogenetic protein 6 is dependent on N-glycosylation of the ligand. *FEBS J.* 275, 172–183. doi: 10.1111/j.1742-4658.2007.06187.x

Sawala, A., Sutcliffe, C., and Ashe, H. L. (2012). Multistep molecular mechanism for bone morphogenetic protein extracellular transport in the *Drosophila* embryo. *Proc. Natl. Acad. Sci. U.S.A.* 109, 11222–11227. doi: 10.1073/pnas.1202781109

Scheufler, C., Sebald, W., and Hulsmeyer, M. (1999). Crystal structure of human bone morphogenetic protein-2 at 2.7 A resolution. *J. Mol. Biol.* 287, 103–115. doi: 10.1006/jmbi.1999.2590

Scholl, C., Weibetamuller, K., Holenya, P., Shaked-Rabi, M., Tucker, K. L., and Wolfl, S. (2012). Distinct and overlapping gene regulatory networks in BMP- and HDAC-controlled cell fate determination in the embryonic forebrain. *BMC Genomics* 13:298. doi: 10.1186/1471-2164-13-298

See, J., Mamontov, P., Ahn, K., Wine-Lee, L., Crenshaw, E. B. III, and Grinspan, J. B. (2007). BMP signaling mutant mice exhibit glial cell maturation defects. *Mol. Cell. Neurosci.* 35, 171–182. doi: 10.1016/j.mcn.2007.02.012

See, J. M., and Grinspan, J. B. (2009). Sending mixed signals: bone morphogenetic protein in myelination and demyelination. *J. Neuropathol. Exp. Neurol.* 68, 595–604. doi: 10.1097/NEN.0b013e3181a66ad9

Shi, Y., Hata, A., Lo, R. S., Massague, J., and Pavletich, N. P. (1997). A structural basis for mutational inactivation of the tumour suppressor Smad4. *Nature* 388, 87–93. doi: 10.1038/40431

Shi, Y., and Massague, J. (2003). Mechanisms of TGF-beta signaling from cell membrane to the nucleus. *Cell* 113, 685–700. doi: 10.1016/S0092-8674(03)00432-X

Sieber, C., Kopf, J., Hiepen, C., and Knaus, P. (2009). Recent advances in BMP receptor signaling. *Cytokine Growth Factor Rev.* 20, 343–355. doi: 10.1016/j.cytogfr.2009.10.007

Sim, F. J., Lang, J. K., Waldau, B., Roy, N. S., Schwartz, T. E., Pilcher, W. H., et al. (2006). Complementary patterns of gene expression by human oligodendrocyte progenitors and their environment predict determinants of progenitor maintenance and differentiation. *Ann. Neurol.* 59, 763–779. doi: 10.1002/ana.20812

Smith, R. B., Machamer, J. B., Kim, N. C., Hays, T. S., and Marques, G. (2012). Relay of retrograde synaptogenic signals through axonal transport of BMP receptors. *J. Cell Sci.* 125, 3752–3764. doi: 10.1242/jcs.094292

Sorrentino, A., Thakur, N., Grimsby, S., Marcusson, A., von Bulow, V., Schuster, N., et al. (2008). The type I TGF-beta receptor engages TRAF6 to activate TAK1 in a receptor kinase-independent manner. *Nat. Cell Biol.* 10, 1199–1207. doi: 10.1038/ncb1780

Sun, Y., Hu, J., Zhou, L., Pollard, S. M., and Smith, A. (2011). Interplay between FGF2 and BMP controls the self-renewal, dormancy and differentiation of rat neural stem cells. *J. Cell Sci.* 124, 1867–1877. doi: 10.1242/jcs.085506

Susperregui, A. R., Gamell, C., Rodriguez-Carballo, E., Ortuno, M. J., Bartrons, R., Rosa, J. L., et al. (2011). Noncanonical BMP signaling regulates cyclooxygenase-2 transcription. *Mol. Endocrinol.* 25, 1006–1017. doi: 10.1210/me.2010-0515

Takizawa, T., Ochiai, W., Nakashima, K., and Taga, T. (2003). Enhanced gene activation by Notch and BMP signaling cross-talk. *Nucleic Acids Res.* 31, 5723–5731. doi: 10.1093/nar/gkg778

Ulsamer, A., Ortuno, M. J., Ruiz, S., Susperregui, A. R., Osses, N., Rosa, J. L., et al. (2008). BMP-2 induces Osterix expression through up-regulation of Dlx5 and its phosphorylation by p38. *J. Biol. Chem.* 283, 3816–3826. doi: 10.1074/jbc.M704724200

Urist, M. R. (1965). Bone: formation by autoinduction. *Science* 150, 893–899. doi: 10.1126/science.150.3698.893

Valera, E., Isaacs, M. J., Kawakami, Y., Izpisua Belmonte, J. C., and Choe, S. (2010). BMP-2/6 heterodimer is more effective than BMP-2 or BMP-6 homodimers as inductor of differentiation of human embryonic stem cells. *PLoS ONE* 5:e11167. doi: 10.1371/journal.pone.0011167

Vinals, F., Reiriz, J., Ambrosio, S., Bartrons, R., Rosa, J. L., and Ventura, F. (2004). BMP-2 decreases Mash1 stability by increasing Id1 expression. *EMBO J.* 23, 3527–3537. doi: 10.1038/sj.emboj.7600360

Wagner, D. O., Sieber, C., Bhushan, R., Borgermann, J. H., Graf, D., and Knaus, P. (2010). BMPs: from bone to body morphogenetic proteins. *Sci. Signal.* 3, mr1. doi: 10.1126/scisignal.3107mr1

Walsh, D. W., Godson, C., Brazil, D. P., and Martin, F. (2010). Extracellular BMP-antagonist regulation in development and disease: tied up in knots. *Trends Cell Biol.* 20, 244–256. doi: 10.1016/j.tcb.2010.01.008

Wen, Z., Han, L., Bamburg, J. R., Shim, S., Ming, G. L., and Zheng, J. Q. (2007). BMP gradients steer nerve growth cones by a balancing act of LIM kinase and Slingshot phosphatase on ADF/cofilin. *J. Cell Biol.* 178, 107–119. doi: 10.1083/jcb.200703055

Weng, Q., Chen, Y., Wang, H., Xu, X., Yang, B., He, Q., et al. (2012). Dual-mode modulation of Smad signaling by Smad-interacting protein Sip1 is required for myelination in the central nervous system. *Neuron* 73, 713–728. doi: 10.1016/j.neuron.2011.12.021

Wicks, S. J., Grocott, T., Haros, K., Maillard, M., ten Dijke, P., and Chantry, A. (2006). Reversible ubiquitination regulates the Smad/TGF-beta signalling pathway. *Biochem. Soc. Trans.* 34, 761–763. doi: 10.1042/BST0340761

Wieser, R., Wrana, J. L., and Massague, J. (1995). GS domain mutations that constitutively activate T beta R-I, the downstream signaling component in the TGF-beta receptor complex. *EMBO J.* 14, 2199–2208.

Withers, G. S., Higgins, D., Charette, M., and Banker, G. (2000). Bone morphogenetic protein-7 enhances dendritic growth and receptivity to innervation in cultured hippocampal neurons. *Eur. J. Neurosci.*

12, 106–116. doi: 10.1046/j.1460-9568.2000.00889.x

Wrana, J. L., Attisano, L., Wieser, R., Ventura, F., and Massague, J. (1994). Mechanism of activation of the TGF-beta receptor. *Nature* 370, 341–347. doi: 10.1038/370341a0

Wu, M., Hernandez, M., Shen, S., Sabo, J. K., Kelkar, D., Wang, J., et al. (2012). Differential modulation of the oligodendrocyte transcriptome by sonic hedgehog and bone morphogenetic protein 4 via opposing effects on histone acetylation. *J. Neurosci.* 32, 6651–6664. doi: 10.1523/JNEUROSCI.4876-11.2012

Xia, Y., Yu, P. B., Sidis, Y., Beppu, H., Bloch, K. D., Schneyer, A. L., et al. (2007). Repulsive guidance molecule RGMa alters utilization of bone morphogenetic protein (BMP) type II receptors by BMP2 and BMP4. *J. Biol. Chem.* 282, 18129–18140. doi: 10.1074/jbc.M701679200

Xu, X., Han, J., Ito, Y., Bringas, P. Jr., Deng, C., and Chai, Y. (2008). Ectodermal Smad4 and p38 MAPK are functionally redundant in mediating TGF-beta/BMP signaling during tooth and palate development. *Dev. Cell* 15, 322–329. doi: 10.1016/j.devcel.2008.06.004

Yamashita, M., Fatyol, K., Jin, C., Wang, X., Liu, Z., and Zhang, Y. E. (2008). TRAF6 mediates Smad-independent activation of JNK and p38 by TGF-beta. *Mol. Cell* 31, 918–924. doi: 10.1016/j.molcel.2008.09.002

Yamauchi, K., Phan, K. D., and Butler, S. J. (2008). BMP type I receptor complexes have distinct activities mediating cell fate and axon guidance decisions. *Development* 135, 1119–1128. doi: 10.1242/dev.012989

Yamauchi, K., Varadarajan, S. G., Li, J. E., and Butler, S. J. (2013). Type Ib BMP receptors mediate the rate of commissural axon extension through inhibition of cofilin activity. *Development* 140, 333–342. doi: 10.1242/dev.089524

Yi, S. E., Daluiski, A., Pederson, R., Rosen, V., and Lyons, K. M. (2000). The type I BMP receptor BMPRIB is required for chondrogenesis in the mouse limb. *Development* 127, 621–630.

Zakin, L., and De Robertis, E. M. (2010). Extracellular regulation of BMP signaling. *Curr. Biol.* 20, R89–R92. doi: 10.1016/j.cub.2009.11.021

Zhang, Y. E. (2009). Non-Smad pathways in TGF-beta signaling. *Cell Res.* 19, 128–139. doi: 10.1038/cr.2008.328

Conflict of Interest Statement: The authors declare that the research was conducted in the absence of any commercial or financial relationships that could be construed as a potential conflict of interest.

Received: 22 March 2013; accepted: 21 May 2013; published online: 04 June 2013.

Citation: Gámez B, Rodriguez-Carballo E and Ventura F (2013) BMP signaling in telencephalic neural cell specification and maturation. Front. Cell. Neurosci. 7:87. doi: 10.3389/fncel.2013.00087

MicroRNAs and post-transcriptional regulation of skeletal development

Beatriz Gámez, Edgardo Rodriguez-Carballo and Francesc Ventura

Departament de Ciències Fisiològiques II, Universitat de Barcelona, IDIBELL, C/Feixa Llarga s/n, E-08907 L'Hospitalet de Llobregat, Spain

Correspondence should be addressed to F Ventura
Email
fventura@ub.edu

Abstract

MicroRNAs (miRNAs) have become integral nodes of post-transcriptional control of genes that confer cellular identity and regulate differentiation. Cell-specific signaling and transcriptional regulation in skeletal biology are extremely dynamic processes that are highly reliant on dose-dependent responses. As such, skeletal cell-determining genes are ideal targets for quantitative regulation by miRNAs. So far, large amounts of evidence have revealed a characteristic temporal miRNA signature in skeletal cell differentiation and confirmed the essential roles that numerous miRNAs play in bone development and homeostasis. In addition, microarray expression data have provided evidence for their role in several skeletal pathologies. Mouse models in which their expression is altered have provided evidence of causal links between miRNAs and bone abnormalities. Thus, a detailed understanding of the function of miRNAs and their tight relationship with bone diseases would constitute a powerful tool for early diagnosis and future therapeutic approaches.

Key Words
- miRNAs
- osteoblasts
- osteoclasts
- chondroblasts
- cell differentiation
- bone
- BMPs
- Wnt
- signal transduction

Journal of Molecular Endocrinology
(2014) **52**, R179–R197

Journal of Molecular Endocrinology

Introduction

Skeletal development is a process that involves a complex sequence of events, which are regulated by a wide range of signaling pathways (Karsenty 2008). Yet, it mainly involves only three specific types of cells: chondrocytes in cartilage and osteoblasts and osteoclasts in bone. In recent years, considerable efforts have been devoted to understanding the mechanisms that mediate the transition from mesenchymal stem cells (MSCs) to osteoblast and chondroblast lineages. It is well known that osteoprogenitor maturation is controlled by several extracellular signals including bone morphogenetic proteins (BMPs), hedgehogs, WNTs, and fibroblast growth factors, the actions of which lead to the expression of chondroblast- or osteoblast-specific genes (Karsenty 2008). Osteoclasts arise from hematopoietic cells and are essential for bone resorption during skeletal development, homeostasis, and regeneration (Duong & Rodan 2001, Horowitz *et al.* 2001). Furthermore, there is a strong crosstalk between them: osteoblasts are involved in the regulation of osteoclast differentiation through the receptor activator of nuclear factor κB ligand (RANKL)–RANK pathway, essential for a satisfactory balance between bone deposition and bone resorption throughout life (Duong & Rodan 2001, Karsenty & Wagner 2002).

Recently, numerous studies have shown that microRNAs (miRNAs) are important post-transcriptional regulators in virtually all biological processes (Hobert 2008). The miRNA field has advanced so rapidly that it has become an integral component of the way we think gene expression is regulated in cartilage and bone development. Cell-specific signaling and transcriptional regulation in skeletal biology are extremely dynamic processes that are highly reliant on dose-dependent responses. As such, they are ideal targets for quantitative regulation by miRNAs.

http://jme.endocrinology-journals.org
DOI: 10.1530/JME-13-0294

Published by Bioscientifica Ltd.

Moreover, the multigene regulatory capacity of miRNAs enables them to cooperatively balance the final precursor cell fate. Thus, different miRNAs can act as either positive or negative determinants within multiple pathways involved in skeletal development processes. The expression of miRNAs is finely orchestrated, being upregulated and downregulated to control the differentiation stage of each bone cell, leading to a characteristic temporal miRNA signature in bone development and homeostasis. Nevertheless, despite all the information available about miRNAs and skeletogenesis, few *in vivo* studies have been conducted to validate each miRNA and it remains unclear how *in vivo* changes in specific miRNAs compromise normal bone development. The purpose of this review is to summarize the current knowledge of miRNA function in skeletal cell lineages and to discuss the main miRNA-related skeletal disorders and the therapeutic perspectives that they provide.

miRNAs: biogenesis and function

miRNAs are short, single-strand, noncoding RNAs approximately 20–25 nucleotides long that have emerged as novel tools capable of post-transcriptionally modifying the expression of mature mRNAs and proteins (Bartel 2004, Mattick & Makunin 2006, Hobert 2008; Fig. 1).

The transcription of miRNAs is mostly mediated by RNA polymerase II, but it can also be mediated by RNA polymerase III (Borchert *et al.* 2006). Sequences encoding miRNAs are found around the genome as separate transcriptional units, although a minority of these sequences are located within the introns of coding genes (generally as clustered miRNAs; Kapinas & Delany 2011). miRNAs are first transcribed as long primary units called pri-miRNAs, which contain characteristic secondary loop structures (Starega-Roslan *et al.* 2011). Various miRNAs can be co-transcribed in a single pri-miRNA, possibly inducing additional effects on a single pathway or gene or allowing crosstalk between different pathways (He *et al.* 2010). The characteristic hairpin of pri-miRNAs helps the microprocessor complex containing Drosha (RNAse III) and some cofactors, including the double-strand RNA-binding protein DGCR8 (DiGeorge syndrome critical region gene), to recognize them from among similar structures present in the nucleus (Han *et al.* 2006, Seitz & Zamore 2006). As a result, a 60–80-nucleotide double-strand miRNA precursor (pre-miRNA) is generated. Pre-miRNAs maintain their stem–loop configuration and have a two-nucleotide extension at their 3′-end. However, some precursors arising from short introns (mirtrons) are capable of bypassing Drosha cleavage and are exported (as regular pre-miRNAs) by exportin 5 to the cytoplasm, where they continue canonical miRNA processing (Lund *et al.* 2004). miRNA precursors are cleaved by a second endonuclease (Dicer), resulting in a double strand of about 21–24 nucleotides. Thanks to argonaute 2 (AGO2), a protein present in the RNA-induced silencing complex (RISC), one of the strands is recruited and guides the complex to its target, whereas the other strand (miRNA*) is degraded.

The 5′-end of mature miRNAs contains the seed region (nucleotide positions 2–7 or 2–8), which has the capacity to identify the complementary bases of the 3′-UTR of the

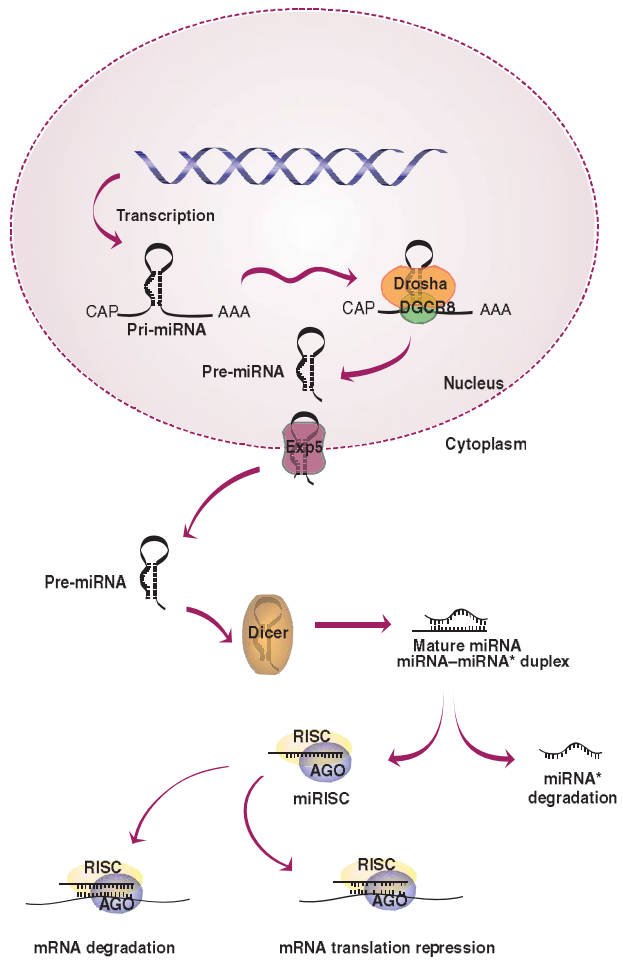

Figure 1
Biogenesis and function of miRNAs. miRNAs are transcribed as long primary transcripts (pri-miRNAs) in the nucleus and are later recognized by Drosha and its cofactor DGCR8 to generate a pre-miRNA. Pre-miRNAs reach the cytoplasm through exportin 5 and are processed by Dicer into a mature miRNA–miRNA* duplex. RNA-induced silencing complex (RISC) recruits the selected miRNA strand and targets the miRNA–RISC complex to the specific 3′-UTR mRNA, while the miRNA* strand is degraded. Depending on the miRNA–mRNA complementarity, miRNA degrades the target mRNA or inhibits its translation. AGO2, argonaute 2.

Journal of Molecular Endocrinology

http://jme.endocrinology-journals.org
DOI: 10.1530/JME-13-0294

Published by Bioscientifica Ltd.

target mRNAs and trigger their cleavage and degradation (Guo *et al.* 2010). Nevertheless, there is usually an imperfect complementarity, and the final effect of miRNA activity is a decrease in protein expression due to translational suppression. Interestingly, miRNAs have also been found to target the 5′-UTRs of mRNAs (Lytle *et al.* 2007, Lee *et al.* 2009) and to induce target translation (Vasudevan *et al.* 2007).

miRNAs and skeletal cell specification

It is well known that miRNAs play an important role in chondrogenic and osteogenic differentiation during cartilage and bone formation (Hobert 2008, Kapinas & Delany 2011). The first *in vivo* approach used to study this was implemented through the conditional ablation of the *Dicer* (*Dicer1*) gene under the control of the *Col2a1* promoter (Kobayashi *et al.* 2008). Mutant mice were found to display severe skeletal growth defects due to a reduction in the number of proliferating chondrocytes, leading to premature death. Evident skeletal phenotypes were similarly observed in mice with *Dicer* deficiency in osteoprogenitor cells (using Cre under the control of the 2.3 kb fragment of the *Col1a1* promoter). The ablation of *Dicer* in progenitors prevents their differentiation and compromises fetal survival (Gaur *et al.* 2010). In addition, Mizoguchi *et al.* (2010) have demonstrated that osteoclast *Dicer* is also crucial for normal osteoclast resorption and osteoblast activity. Osteoclast-specific *Dicer* knockout mice were generated by crossing Cathepsin K-cre mice with Dicer flox mice. These mice were found to exhibit higher bone mass and a decrease in osteoclast surface and number. Additionally, the expression of not only osteoclast-related genes but also osteoblast-related ones (*Col1a1*, *Bglap*, and runt-related transcription factor 2 (*Runx2*)) was found to be downregulated (Mizoguchi *et al.* 2010). These data indicate that miRNAs are important not only during bone development but also for bone homeostasis throughout life.

miRNAs and osteoblast differentiation

Lineage commitment from MSCs to osteoblasts has been well characterized. During embryogenesis, bone development occurs by either endochondral or intramembranous ossification. In both mechanisms, osteoblasts and chondrocytes arise from mesenchymal cell condensations, and the factors that contribute to the transcriptional control of these differentiation processes have been widely studied (Nakashima & de Crombrugghe 2003, Karsenty 2008). Osterix (*Osx*), *Runx2*, distal-less homeodomain-containing family 5 (*Dlx5*), *Msx2*, and *Atf4*, among others, have been identified as essential transcription factors for osteoblast differentiation (Nakashima & de Crombrugghe 2003, Karsenty 2008; Fig. 2).

From a common osteochondroprogenitor, the osteoblast differentiation process encompasses different well-characterized stages. The above-mentioned transcription factors (*Osx*, *Runx2*, and *Atf4*) are indispensable for inducing progression to the osteocyte fate, the most mature form of differentiation. Furthermore, each step of osteoblast progression can be clearly recognized by a cohort of molecules that are differentially expressed. *Runx2* plays an essential role in the first step of differentiation into pre-osteoblasts. Pre-osteoblast-specific markers include alkaline phosphatase and low levels of type 1 collagen. Later, they require *Osx* to reach the mature osteoblast stage and to be able to synthesize extracellular matrix (ECM) proteins. Functional osteoblasts additionally express osteocalcin and bone sialoprotein markers and they are responsible for the future mineralized bone matrix. Although the majority of the cells of the osteoblast population undergo apoptosis, a small fraction will differentiate into osteocytes, the main bone population. Osteocytes are matrix-embedded cells and are important mechanosensors controlling bone formation. Recent studies have also indicated osteocytes to be the main source of RANKL (TNFSF11) and therefore closely related to bone resorption.

Runx2 is the first to be expressed in mesenchymal cell condensations, and from the perspective of molecular biology, it is one of the key transcription factors involved in osteoblast differentiation, together with *Osx* (Karsenty *et al.* 1999, Ducy 2000). *Runx2* is expressed as early as day E10.5 and is necessary and sufficient to identify cells as osteochondroprogenitors, as *Runx2*-null mice are unable to produce mature osteoblasts (Ducy *et al.* 1997, Komori *et al.* 1997, Nakashima & de Crombrugghe 2003). From this stage to chondroblast commitment, Runx2 levels decrease until it almost disappears at day E16.5, whereas during osteoblast differentiation Runx2 levels remain stable and induce osteocalcin (*Bglap*) expression at around day E15.5. Thus, *Runx2*-targeting miRNAs simultaneously modulate osteogenesis and chondrogenesis.

The expression of *Runx2* is regulated by several signaling pathways, including vitamin D3 ($1,25(OH)_2D_3$), transforming growth factor β (TGFβ)/BMP2, and Wnt, among others, and it regulates the expression of numerous osteoblastic genes such as *Osx* (*Sp7*), *Alpl* (alkaline phosphatase), *Col1a1*, *Spp1* (osteopontin), *Ibsp* (bone

Journal of Molecular Endocrinology

http://jme.endocrinology-journals.org
DOI: 10.1530/JME-13-0294

Published by Bioscientifica Ltd.

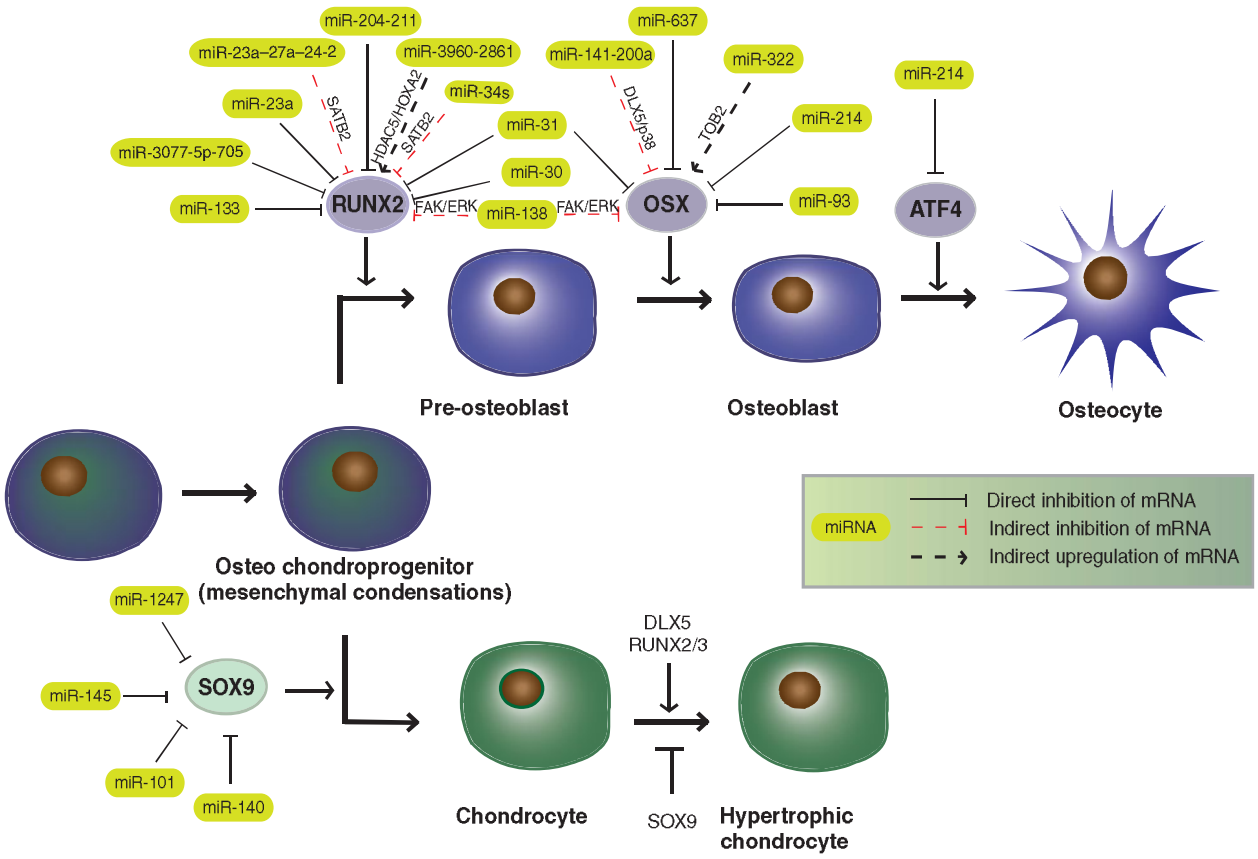

Figure 2

Schematic summary of miRNA role in osteoblast and chondroblast differentiation. A cohort of transcription factors tightly regulates osteoblast and chondroblast commitment from osteochondroprogenitors during skeletal development. miRNAs are important players during this commitment regulating the expression of these transcription factors, therefore allowing or blocking the differentiation process.

sialoprotein), and *Bglap* (osteocalcin). *Runx2* mRNA has a very long 3′-UTR, which probably contains multiple regulatory elements (Huang *et al.* 2010), and it is therefore not surprising that several examples of post-transcriptional *Runx2* mRNA regulation through miRNAs have been described.

miR-204/-211 specifically binds to the 3′-UTR of *Runx2* and inhibits osteoblast differentiation by promoting adipocyte commitment from mesenchymal progenitors (C3H10T1/2, ST2, and hMSCs; Huang *et al.* 2010). Furthermore, as Runx2 has the capacity to regulate the expression of *Bglap* from day E15.5 onwards (Ducy & Karsenty 1995), miR-204 accumulation leads to the repression of *Bglap* expression (Huang *et al.* 2010).

miR-133 also inhibits *Runx2* translation, and its expression is downregulated by BMPs in C2C12 cells (Li *et al.* 2008). Studies carried out by independent groups have reported controversial results on the function of miR-31 during osteoblast commitment of human MSCs. Gao *et al.* (2011) have described miR-31 to be a downregulated miRNA during osteoblast differentiation *in vitro*, indicating that *Runx2* is one of its physiological targets. However, miR-31 was later identified as an upregulated miRNA in a similar study of hMSC differentiation and osterix was confirmed to be one of its targets, indicating a regulatory network (Baglio *et al.* 2013). Other *in vitro* studies have elucidated a regulatory loop involving miR-31, *Runx2*, and *Satb2* (special AT-rich sequence-binding protein 2): downregulation of miR-31 expression by Runx2 in differentiating bone marrow MSCs (BMMSCs) facilitates osteogenic commitment due to an increase in SATB2 protein expression (Deng *et al.* 2013). Additionally, miR-30 family members have been widely studied as regulators of osteoblast differentiation, mainly through the suppression of the expression of *Smad1* and *Runx2* transcription factors (Zhang *et al.* 2011*a*, Wu *et al.* 2012, Eguchi *et al.* 2013).

SATB2 belongs to the family of special AT-rich sequence-binding proteins, members of which are present in the nuclear matrix and can bind to AT-rich sequences,

http://jme.endocrinology-journals.org
DOI: 10.1530/JME-13-0294

Published by Bioscientifica Ltd.

activating the transcription of particular genes (Britanova *et al.* 2005). *In vivo* studies have shown that Satb2 physically interacts with and enhances the activity of Runx2 and Atf4 (Dobreva *et al.* 2006, Conner & Hornick 2013). Coupling these osteoblast-specific transcription factors, Satb2 increases the transcription of *Bglap* by binding to its promoter (Dobreva *et al.* 2006) and can also increase the expression of *Ibsp* by direct attachment to an osteoblast-specific promoter element (Dobreva *et al.* 2006). In addition, although Dobreva *et al.* did not find changes in *Osx* expression, others have reported that Satb2 acts in cooperation with Runx2 to upregulate *Osx* expression (Zhang *et al.* 2011*b*). The miR-23a–27a–24-2 cluster inhibits osteogenesis *in vitro* by downregulating the expression of *Satb2* through the direct binding of the three miRNAs to its 3′-UTR. Moreover, Runx2 directly suppresses the expression of the cluster, whereas complementarily miR-23a targets *Runx2* (Hassan *et al.* 2010). Interestingly, other clusters have also been studied, such as the auto-regulatory feedback loops controlling *Runx2* expression. miR-3960/-2861 is transactivated by Runx2 *in vitro*, thereby maintaining its own levels of expression by blocking the expression of *Hoxa* and *Hdac5*, negative regulators of osteoblast differentiation (Kanzler *et al.* 1998, Dobreva *et al.* 2006, Li *et al.* 2009*a*, Hu *et al.* 2011). Furthermore, an *in vivo* approach has demonstrated that *Satb2* is also targeted by miR-34s, affecting osteoblast proliferation mainly by means of miR-34b and miR-34c. Mice with osteoblast-specific deletion in miR-34bc from day E16.5 (using Cre under the control of the 2.3 kb fragment of *Col1a1* promoter) were found to exhibit increased cortical bone volume, bone mineral density, and cortical thickness of long bones (Wei *et al.* 2012).

Following the expression of *Runx2* in osteoprogenitors, *Osx* further strengthens the establishment of bone cell phenotype. *Osx* belongs to the Sp/Kruppel-like family of transcription factors because of its characteristic DNA-binding domain consisting of three tandem C2H2-type zinc finger motifs at the C-terminus. *Osx* is located downstream of Runx2 and, in fact, Runx2 directly binds to the *Osx* promoter (Nakashima *et al.* 2002, Nishio *et al.* 2006). The expression of *Osx* begins at around day E13.5 and it promotes the expression of osteoblast markers such as *Alpl*, *Ibsp*, and *Bglap*. The expression of *Osx* has been shown to be positively regulated by BMP, insulin-like growth factor 1 (IGF1), and MAPK signaling pathways in undifferentiated MSCs (Celil & Campbell 2005, Celil *et al.* 2005, Ortuno *et al.* 2010), and it can also regulate its own expression by interacting with its own promoter (Yoshida *et al.* 2012).

Obviously, *Osx* can also be post-transcriptionally regulated by miRNAs. Shi *et al.* (2013) described miR-214 as a downregulated miRNA during BMP2-induced osteoblast differentiation in C2C12 cells. miR-214 antagomirs lead to the overexpression of *Osx* and other related osteoblast markers such as *Alpl*, *Col1a1*, and *Bglap*. In addition, it has also been reported that miR-214 inhibits Twist (which inhibits the activity of Runx2 as a transcription factor) in intrahepatic cholangiocarcinomas and is overexpressed in elderly patients with fractures, in whom it directly targets *ATF4* (Li *et al.* 2012, Wang *et al.* 2013*a*). As has been stated above, miR-204/-211 targets *Runx2* mRNA *in vitro*. Furthermore, *in vivo* studies comparing differentially expressed miRNAs in calvaria from day E18.5 *Osx*-deficient and WT embryos have revealed that *Osx*-deficient osteoblasts display miR-204/-211 overexpression. As it is known that *Osx*-deficient calvaria exhibit an increase in *Runx2* expression (Zhou *et al.* 2010), Chen *et al.* (2013*a*) have suggested that miR-204/-211 accumulation would dampen *Runx2* overexpression and that Osx coordinately regulates the levels of this miRNA to maintain correct *Runx2* expression.

A regulatory loop for *Osx* expression involves miR-93 in primary osteoblasts. During osteoblast mineralization, Osx can bind to the miR-93 promoter to repress its transcription and, as miR-93 also targets *Osx* mRNA, this facilitates the maintenance of osterix levels (Yang *et al.* 2012). Shi *et al.* (2013) have also reported the downregulation of miR-93 expression during the differentiation of C2C12 cells under BMP stimulation. Fine-tuning of *Osx* expression by miRNAs is also observed in the miR-322/Tob2 feedback mechanism *in vitro*. The Tob2 protein specifically controls the decay of *Osx* mRNA by regulation of its mRNA deadenylation, while BMP2 represses miR-322 expression and reduces miR-322 binding to the *Tob2* 3′-UTR; thus, higher Tob2 protein levels would control *Osx* levels (Gamez *et al.* 2013).

Changes in miR-637 levels have the capacity to maintain the balance between osteoblast and adipocyte differentiation in hMSCs by the inhibition of *OSX* expression and activation of adipogenic markers such as peroxisome proliferator-activated receptor γ (*PPARγ* (*PPARG*)) and CCAAT/enhancer-binding protein α (*c/EBPα* (*CEBPA*)) (Zhang *et al.* 2011*c*). Other miRNAs have also been shown to determine osteoblast–adipocyte balance *in vitro* (Li *et al.* 2013, Liao *et al.* 2013, Wang *et al.* 2013*b*). For instance, miR-3077-5p and miR-705, which work together as negative regulators of osteoblast differentiation through the suppression of *Runx2* and *Hoxa10* expression, eventually lead to a positive regulation of

http://jme.endocrinology-journals.org
DOI: 10.1530/JME-13-0294

Published by Bioscientifica Ltd.

adipogenic differentiation (Liao *et al.* 2013). As has been mentioned above, it has been reported that miR-31 forms part of a regulatory loop linking *Runx2* and *Satb2*, but it can also directly regulate the 3′-UTR of *Osx*. It has been suggested that an increase in *Osx* expression due to low expression of miR-31 can play a role in osteosarcomas, as observed in the MG-63 osteosarcoma cell line (Baglio *et al.* 2013).

Dlx5 is a BMP-responsive gene activated through a responsive element in its proximal promoter. Moreover, Dlx5 interacts with the *Osx* promoter and mediates BMP2-induced *Osx* expression independently of Runx2 (Lee *et al.* 2003, Ulsamer *et al.* 2008). miR-141 and miR-200a have been found to act as repressors of *Dlx5* and *Osx* expression, and it has been demonstrated that both bind to *Dlx5* mRNA *in vitro* (Itoh *et al.* 2009). Moreover, miR-141 and miR-200a target *p38α* (*Mapk14*) in mouse models of ovarian cancer, in agreement with previous screenings in human ovarian adenocarcinomas (Mateescu *et al.* 2011). Positive effects of p38 phosphorylation have been observed on Dlx5 transcriptional activity and on Osx stability (Ulsamer *et al.* 2008, Ortuno *et al.* 2010); consequently, the activity of miR-141 and miR-200a in osteoblast lineages is also probably mediated by changes in p38 phosphorylation of Dlx5 and Osx.

Recent studies on *Bglap2*–miR-214 transgenic mice overexpressing miR-214 have revealed its inhibitory role in the regulation of bone formation. *In vitro* manipulation of miR-214 revealed that direct targeting of *Atf4* was required to inhibit osteoblast activity (Wang *et al.* 2013*a*). As the expression of *Osx* and *Runx2* is tightly related, miRNAs targeting proteins involved in their upstream regulatory pathways will affect the expression of both. This is the case with miR-138, inhibited during human MSC osteoblast differentiation, which targets the focal adhesion kinase (FAK) and ERK1/2 pathways, leading to decreased phosphorylation of Runx2 and a lower expression of *Osx* (Eskildsen *et al.* 2011). Other studies have elucidated additional mechanisms connecting miRNAs to osteoblast differentiation by means of targeting different osteoblast differentiation pathways (Mizuno *et al.* 2008, Inose *et al.* 2009, Li *et al.* 2009*b*, Kapinas *et al.* 2010, Wang & Xu 2010, Zhang *et al.* 2012*a*).

miRNAs and chondroblast differentiation

In contrast to adipogenic and osteogenic differentiation-related miRNAs, fewer studies have been conducted on chondrogenic differentiation-related miRNAs. The *Runx2* transcription factor also plays an important role in chondrocyte commitment. Runx2 (and Runx3) are transiently necessary for pre-hypertrophic chondrocytes to reach the hypertrophic state (Yoshida *et al.* 2004). *Sox9* (Sry-related HMG box) is one of the main drivers of chondrocyte differentiation and its absence leads to a failure in chondrocyte commitment in $Sox9^{-/-}$ MSCs or knockout mice (Bi *et al.* 1999, 2001, Mori-Akiyama *et al.* 2003). *Sox9* is required for the commitment of osteochondroprogenitors and for *Runx2* expression in mesenchymal cell condensations (Akiyama *et al.* 2002, 2005). Other members of the Sry family, such as *Sox6* and *Sox5*, also play important roles (Lefebvre *et al.* 2001; Fig. 2).

Several miRNAs (miR-1247, miR-145, miR-140, and miR-199a) have been reported to exert an effect on chondrogenesis by eventually affecting *Sox9* expression positively (Karlsen *et al.* 2013) or negatively (Laine *et al.* 2012, Martinez-Sanchez *et al.* 2012, Martinez-Sanchez & Murphy 2013). Of all the miRNAs affecting chondroblast differentiation, miR-140 has received the most research attention to date (He *et al.* 2009, Nakamura *et al.* 2011, Nicolas *et al.* 2011, Yang *et al.* 2011, Gibson & Asahara 2013, Karlsen *et al.* 2013, Papaioannou *et al.* 2013). The results of these studies indicate that miR-140 is one of the main regulators of chondroblast differentiation through its effects on the expression of not only *Sox9* (Karlsen *et al.* 2013), but also several other targets (*Hdac4*, *Sp1*, *Smad3*, and aggrecan) (Pais *et al.* 2010, Nakamura *et al.* 2011, Yang *et al.* 2011, Karlsen *et al.* 2013). Moreover, independent groups have developed miR-140-null mice, which displayed a concordant phenotype with major growth defects of endochondral bones (Miyaki *et al.* 2010, Nakamura *et al.* 2011, Papaioannou *et al.* 2013). Interestingly, Sox9, L-Sox5, and Sox6 have been proved to cooperatively activate the miR-140 promoter *in vivo* and *in vitro* (Miyaki *et al.* 2010, Yang *et al.* 2011, Yamashita *et al.* 2012), as well as other chondrogenic differentiation-related miRNAs (Guerit *et al.* 2013, Martinez-Sanchez & Murphy 2013).

miR-181a is highly expressed in chondrocytes, and it has been suggested that it works as a negative feedback system to preserve the homeostasis of cartilage by targeting *Ccn1* (*Ccna2*; which promotes chondrogenesis) and *Acan* (encoding the protein aggrecan, the major proteoglycan in the cartilage ECM) (Sumiyoshi *et al.* 2013). miR-181b has also been reported to regulate *Col2a1* expression, and its expression is elevated in human osteoarthritic chondrocytes *in vitro* (Song *et al.* 2013*a*). Other miRNAs regulate cell differentiation by targeting chromatin epigenetic modifiers (Tuddenham *et al.* 2006, Guan *et al.* 2011). For instance, miR-365 stimulates chondrocyte differentiation through *Hdac4*

http://jme.endocrinology-journals.org
DOI: 10.1530/JME-13-0294

Published by Bioscientifica Ltd.

repression, thereby increasing the levels of *Ihh* and *Col* X (markers of pre-hypertrophic chondrocytes and hypertrophic chondrocytes respectively; Guan *et al.* 2011).

As has been mentioned above, it should be noted that one particular miRNA may act as a switch for the selection of different cell commitment processes. miR-96, miR-124, and miR-199a have been studied in human BMMSCs and have been found to be differentially expressed during osteogenic, adipogenic, or chondrogenic induction: whereas miR-124 is expressed exclusively in adipocytes, the expression of miR-199a is upregulated in osteoblasts and chondrocytes (Laine *et al.* 2012).

miRNAs and osteoclast differentiation

In contrast to osteoblasts and chondrocytes, osteoclasts arise from hematopoietic cells and are the primary bone-resorbing cells. The transition from mononuclear pre-osteoclasts to mature osteoclasts is dependent on cell–cell fusion and is controlled by sequential exposure to signaling molecules (Fig. 3). Macrophage colony-stimulating factor (M-CSF) and RANKL are the two main cytokines involved in osteoclast differentiation (Manolagas 2000). M-CSF activates the c-Fms receptor, present in early osteoclast precursors, and acts as a survival/proliferation factor by activating Akt, microphthalmia transcription factor (Mitf), or the anti-apoptotic protein B-cell leukemia/lymphoma-associated gene 2 (BCL2). Moreover, M-CSF also stimulates the expression of *Rank* (*Tnfrsf11a*). *Rankl* is a member of the tumor necrosis factor α (TNFα) superfamily present in osteoblasts and stromal cells and can be a membrane-anchored molecule but can also be released as a soluble molecule following proteolytic cleavage. Lately, osteocytes have emerged as an important source of RANKL, indicating a key role for osteocytes in osteoclastogenesis (Nakashima *et al.* 2011, Xiong *et al.* 2011). The RANK–RANKL signaling system links osteoblast lineage and hematopoiesis-derived cells for osteoclast differentiation and activation. Together with M-CSF, RANK signaling is the main signaling pathway involved in osteoclast maturation (Tanaka *et al.* 2005). RANK stimulation leads to the recruitment of TNF receptor-associated

Journal of Molecular Endocrinology

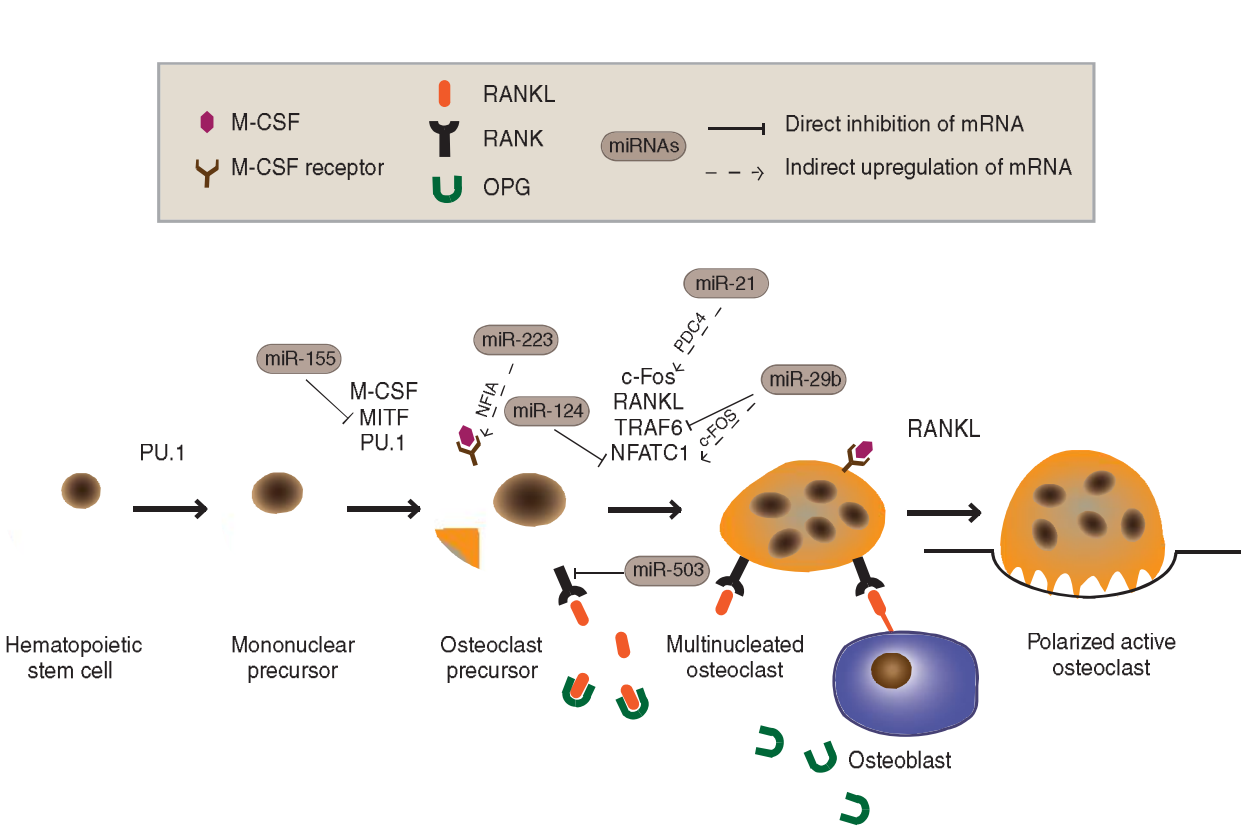

Figure 3
Effects of miRNAs on osteoclast differentiation. miRNAs affect different molecules related to osteoclast commitment such as RANK or M-CSF receptor, among others. miRNA expression leads to changes in osteoclast activity *in vitro* and also to alterations in bone resorption *in vivo*. OPG, osteopontegrin.

http://jme.endocrinology-journals.org
DOI: 10.1530/JME-13-0294

Published by Bioscientifica Ltd.

cytoplasmic factors (TRAFs), mainly TRAF6, leading to the activation of several pathways, including the nuclear factor (NF) and activator of transcription NFATc1. Nfatc1 is widely accepted to be the key transcription factor involved in osteoclast differentiation (Kobayashi *et al.* 2001, Gohda *et al.* 2005). Nfatc1 eventually regulates several osteoclast-specific genes in cooperation with other transcription factors: AP1, PU.1, Mitf, and c-Fos (Tondravi *et al.* 1997, Takayanagi *et al.* 2002, Crotti *et al.* 2008). Their transcriptional targets are osteoclast-specific genes such as tartrate-resistant acid phosphatase (*TRAP* (*ACP5*)), cathepsin K, calcitonin receptor, and dendritic cell-specific transmembrane protein (Kukita *et al.* 2004). RANK can be blocked by osteopontegrin (OPG), therefore inhibiting osteoclast differentiation due to the suppression of RANKL stimuli. OPG is produced by osteoblasts and acts as a decoy receptor, preventing the coupling of RANKL to RANK and therefore reducing osteoclast resorption. Thus, the RANKL:OPG ratio must be accurately balanced to control osteoclastogenesis.

There are relatively few reports on the role of miRNAs in osteoclastogenesis. As in the case of osteoblasts, osteoclast-specific *Dicer* alteration has been shown to profoundly affect osteoclast activity *in vivo* and *in vitro* (Sugatani & Hruska 2009, Mizoguchi *et al.* 2010). In these models, a reduction in the expression of osteoclast markers (the expression of *Trap* and *Nfatc1* mRNA was downregulated) and an increment in the values of bone parameters such as bone volume, trabecular thickness, and trabecular number have been observed, all leading to a mild osteopetrotic phenotype as a consequence of decreased osteoclast number and surface.

Of all the miRNAs involved in osteoclast differentiation, miRNA-223 has been studied the most. It was first identified as being specific to the CD11b-positive myeloid cell line (Chen *et al.* 2004). Sugatani and colleagues further confirmed miR-223 expression in the mouse osteoclast precursor cell line RAW 264.7 and showed that the modulation of pre-miR-223 alters osteoclast differentiation. Moreover, the levels of miR-223 in mouse bone marrow macrophages (BMMs) were found to be higher than those in osteoclasts, indicating that it must be repressed for appropriate osteoclast differentiation to occur (Sugatani & Hruska 2007). In the same study, miR-223 was shown to target *Nfia*, an osteoclastogenesis suppressor that eventually negatively regulates the M-CSF receptor. Later, other groups validated these effects of miR-223 on osteoclastogenesis and revealed PU.1-binding sites in the miR-223 promoter (Fukao *et al.* 2007, Sugatani & Hruska 2009, Shibuya *et al.* 2013). Sugatani *et al.* posited the existence of a feed-forward network whereby M-CSF induces PU.1 in osteoclast precursors, and PU.1 stimulates pri-miR-223 transcription, which, by downregulating the expression of *Nfia*, ultimately increases the levels of M-CSF receptor.

As with several other miRNAs affecting osteoclastogenesis, miRNA-223 has also been studied as a marker gene for rheumatoid arthritis (RA; Shibuya *et al.* 2013). As a result of the *in vitro* miR-223 studies mentioned above, it has been suggested that the increased levels of miR-223 found in RA synovium could be related to the inhibition of osteoclastogenesis. Furthermore, miR-21 has also been identified by Sugatani *et al.* (2011) as a miRNA upregulated during RANKL-induced osteoclastogenesis. Moreover, c-Fos and AP1 were found to be associated with its promoter. miR-21 loss-of-function experiments in a model of RANKL induction of BMMs showed a decrease in c-Fos phosphorylation and lower *Nfatc1* and cathepsin K expression, all due to increased levels of programmed cell death 4 (PDCD4). Taken together, these findings indicate the existence of a new positive loop mechanism involving c-Fos/miR-21/PDCD4 (Sugatani *et al.* 2011). In addition, Mann *et al.* performed a differential miRNA screening using the RAW 264.7 cell line under RANKL and M-CSF treatment to induce osteoclastic differentiation. miR-155 was described in this study as an early inhibitor of *MITF*, a nuclear effector that integrates M-CSF/RANKL signals to initiate the expression of osteoclast-specific genes (Mann *et al.* 2010). The RAW 264.7 cell line can differentiate into either macrophages or osteoclasts, and the results of this study suggest that the upregulation of miR-155 expression facilitates macrophage commitment, therefore inhibiting osteoclast differentiation (by targeting *MITF*). These data indicate that miR-155 is involved in the commitment switch of hematopoietic precursors (Mann *et al.* 2010). Zhang *et al.* (2012*b*) revealed that miR-155 is inhibited by IFNβ during osteoclast differentiation, and they identified the effect of miR-155 on the 3′-UTR of *MITF* and suppressor of cytokine signaling 1 (*SOCS1*). Moreover, miR-155 has been observed to be involved in the pathogenesis of autoimmune arthritis in mice, being proposed as a novel target for the treatment of RA (Bluml *et al.* 2011). Other examples include miR-124, which has been shown to directly target *Nfatc1* expression in BMMs (Lee *et al.* 2013), and miR-503, which targets *Rank* expression (Chen *et al.* 2013*b*).

Some of the miRNAs involved in osteoclast function have been shown to affect osteoclast cytoskeleton or migration. The expression of miR-31 has been found to increase in BMMs under RANKL stimulation. Moreover,

http://jme.endocrinology-journals.org
DOI: 10.1530/JME-13-0294

Published by Bioscientifica Ltd.

it tightly controls cytoskeleton organization in osteoclasts by targeting *Rhoa*, essential for actin ring formation and bone resorption (Mizoguchi *et al.* 2013). Franceschetti *et al.* (2013) reported that all miR-29 family members (miR-29a, miR-b, and miR-c) are induced during osteoclast differentiation of mouse BMMs and RAW 264.7 cell line. However, Rossi *et al.* (2013) reported a decrease in miR-29b expression during human osteoclast differentiation from circulating human precursors. They also demonstrated the inhibition of osteoclastogenesis by miR-29b through the downregulation of *c-FOS* or *NFATC1* expression, while Franceschetti *et al.* (2013) reported new targets such as *Nfia*, *Cdc42*, and *Srgap2*, among others, indicating that miR-29 positively maintains migration and cell commitment to osteoclasts.

Reciprocal interplay between miRNAs and signaling pathways in skeletal biology

Regulation of miRNA expression

Although several osteogenic differentiation-related miRNAs have been identified in the last decade, little is known about their transcriptional regulation. Numerous screenings have been performed to characterize the miRNA expression scenario during different stages of cell differentiation, but fewer studies have attempted to describe the molecular linkage between the stimuli and their regulatory effect on miRNA expression in full detail. miRNA processing and maturation can be regulated through the interaction of additional proteins with the Drosha complex. For instance, SMAD proteins interact with Drosha to specifically regulate the expression of some miRNAs, as in the case of miR-21 (Davis *et al.* 2008). Specific sequences are required in the loop of pri-miRNAs for them to be post-transcriptionally regulated by the SMAD–Drosha complex (Davis *et al.* 2010). Using several different models, it has been shown that miRNA expression can be regulated through several mechanisms, including the regulation of pre-miRNA nuclear export and Dicer cleavage, regulation of promoter activity by methylation and histone modification, or direct regulation of RNA polymerase II recruitment (Davis-Dusenbery & Hata 2010). However, much less is known about the influence of osteogenic signaling inputs on these mechanisms. To summarize the main themes in what is known about the interplay between signaling and miRNAs, we focus on two important pathways in skeletal development: BMP and Wnt.

The interplay between miRNAs and BMP signaling

BMPs form the largest subfamily of the TGFβ superfamily and are profoundly involved in skeletogenesis (Shi & Massague 2003, Miyazono *et al.* 2010). Early events in BMP signaling are initiated through the phosphorylation of specific BMP receptor-regulated SMAD proteins, namely R-SMAD1, R-SMAD5, and R-SMAD8. After phosphorylation, R-SMADs form heteromeric complexes with the common mediator SMAD4, which then migrate to the nucleus and activate the transcription of specific target genes (Shi & Massague 2003). Two additional SMADs are known as inhibitory SMADs, SMAD6 and SMAD7. Furthermore, BMPs can also activate noncanonical, SMAD-independent pathways, mainly MAPK pathways (Erk, p38), the LIMK pathway, or the PI3K pathway, which are also involved in osteoblast differentiation (Shi & Massague 2003, Gamell *et al.* 2008, Ulsamer *et al.* 2008, Ortuno *et al.* 2010).

Several miRNAs negatively or positively regulate BMP signaling (Fig. 4) and, in turn, BMPs coordinate a wide range of changes in miRNA expression (Inose *et al.* 2009). BMP biology has been widely studied in C2C12 cells, switching the differentiation pathway from a myoblastic to an osteoblastic phenotype (Katagiri *et al.* 1994), and several miRNA studies have been performed using this model (Li *et al.* 2008, Inose *et al.* 2009). For instance, Li *et al.* (2008) conducted a miRNA screening during BMP2-induced osteogenesis in C2C12 cells and found that the expression of almost all miRNAs was downregulated during osteoblast differentiation. These data have been confirmed by other groups (Gamez *et al.* 2013). The same authors also described miR-133 and miR-135 as negative regulators of osteogenesis that act by directly targeting *Runx2* and *Smad5* respectively, thereby inhibiting osteogenic differentiation (Li *et al.* 2008). In addition, it has recently been reported that under BMP stimuli, C2C12 inhibits the processing of myomiRs (muscle-specific miRNAS and myogenic miRNAs) due to the association of phosphorylated R-SMADs and Co-SMAD with phosphorylated KH-type splicing regulatory protein (KSRP (KHSRP)) in the nucleus (Pasero *et al.* 2012). KSRP is a single-strand RNA-binding protein that is essential for the maturation of myomiRs and for the establishment of the myogenic lineage in C2C12 cells (Briata *et al.* 2012); thus, KSRP sequestering by SMADs blocks myogenic differentiation in favor of the osteoblast lineage.

Another well-studied miRNA regulated by BMPs is miR-206 (Inose *et al.* 2009, Sato *et al.* 2009). The expression of miR-206 is downregulated by BMPs in C2C12 cells and

http://jme.endocrinology-journals.org
DOI: 10.1530/JME-13-0294

Published by Bioscientifica Ltd.

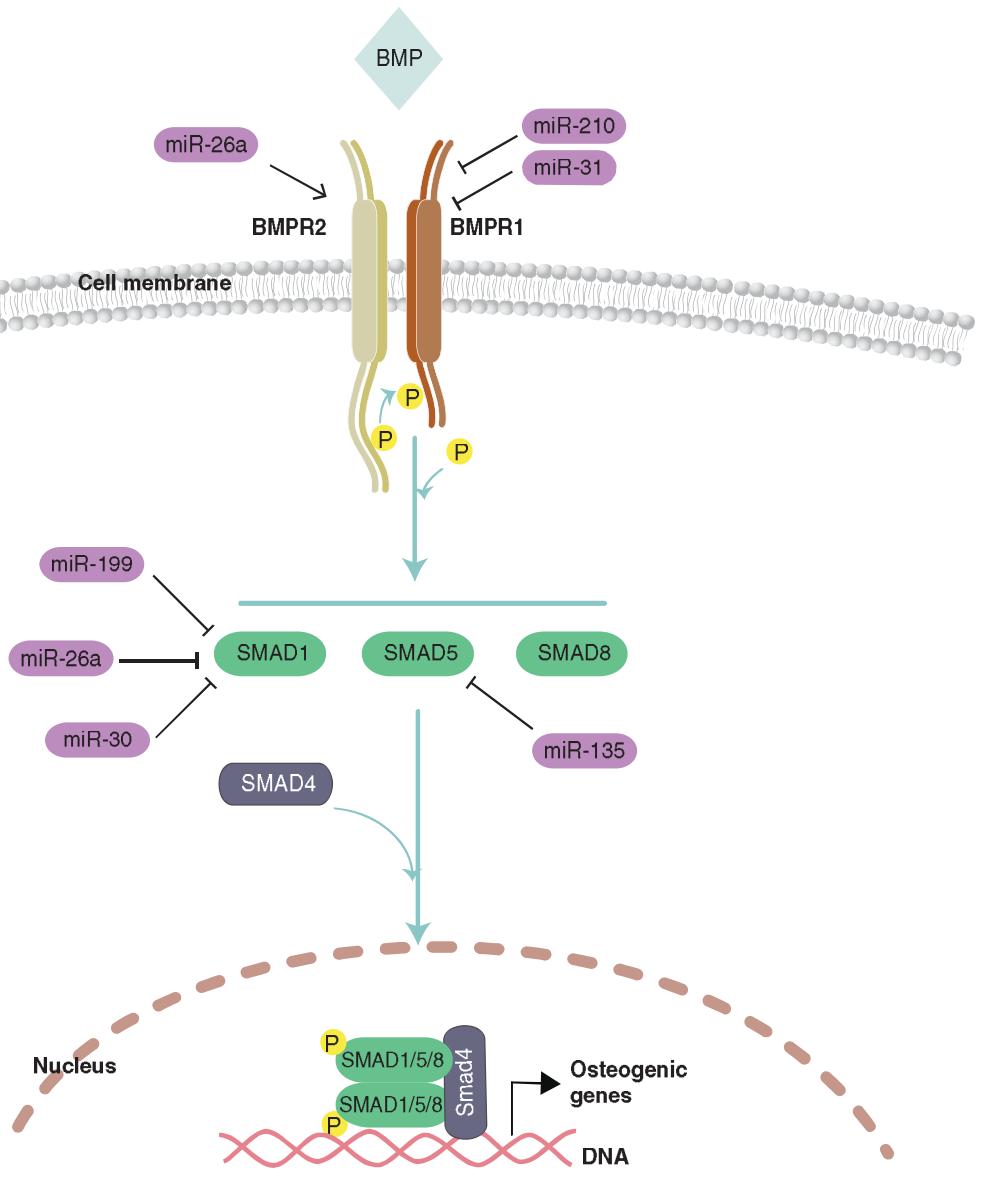

Figure 4
Interplay between the BMP pathway and miRNAs. miRNAs act at different steps of BMP signaling: from those involving BMP receptors to those involving SMADs.

its overexpression blocks osteoblast differentiation due to its effect on connexin43 mRNA, required for osteoblastic gene expression and function (Lecanda *et al.* 1998, Plotkin & Bellido 2013). Sato *et al.* (2009) have also suggested that BMP control of miR-206 occurs post-transcriptionally in C2C12 cells by the repression of pri-miR processing, and other studies have indicated that miR-206 is also required for myogenic differentiation in the same model (Kim *et al.* 2006). Moreover, miR-206 transgenic mice (2.3 kb *Col1a1* promoter) suffer from reduced bone mass because of a decrease in bone formation (Inose *et al.* 2009). TGFβ inhibits both miR-206 expression and myogenic differentiation *in vitro* through an increase in HDAC4 protein expression (Winbanks *et al.* 2011).

miR-125b inhibits the proliferation of ST2 cells (murine MSCs) and BMP4 stimulation attenuates miR-125b expression in these cells. Thus, miR-125b inhibits osteoblast differentiation, possibly regulating the early stages of osteoblastogenesis (Mizuno *et al.* 2008). miR-141/-200a, mentioned above as *Dlx5* and *Osx* repressors, are also regulated by BMP2 in the MC3T3-E1 cell line. Under BMP treatment, the expression of both miRNAs is

http://jme.endocrinology-journals.org
DOI: 10.1530/JME-13-0294

Published by Bioscientifica Ltd.

downregulated, thus avoiding *Dlx5* and *Osx* miRNA-related repression (Itoh *et al.* 2009). The expression of miR-322 is also downregulated by BMP2 and has been shown to indirectly repress *Osx* expression to facilitate further osteogenic differentiation (Gamez *et al.* 2013).

BMP2 also controls miRNAs involved in chondrogenic differentiation: for instance, the expression of miR-199a* is upregulated by BMP2 treatment, and its overexpression in pre-chondrogenic cells (ATDC5) or in the multipotential murine C3H10T1/2 cell line represses the expression of chondroblast markers *Sox9* and *Col2a1*. miR-199a* also represses the 3′-UTR *Smad1* transcript. Taken together, these data indicate that BMP2 reduces the expression of miR-199a*, avoiding *Smad1* post-transcriptional miRNA regulation and repressing chondrogenic differentiation-specific markers (Lin *et al.* 2009).

miRNAs can also regulate R-SMAD expression. In addition to the above-mentioned examples, Smad1 has also emerged as a target of miR-26a in osteogenic differentiation of human adipose-tissue-derived stem cells (Luzi *et al.* 2008). These studies thus indicate that miR-26a restrains osteoblast commitment when reaching terminal differentiation (Luzi *et al.* 2008). Other miRNAs also target BMP receptors. For instance, the expression of miR-210 is upregulated during BMP4-induced osteoblast differentiation of mouse mesenchymal ST2 cells. miR-210 positively regulates osteoblast commitment by targeting the *Acvr1b* receptor (type 1 receptor; Mizuno *et al.* 2009). The 3′-UTR of the *ACVR1/ALK2* gene has recently been studied *in vitro* to elucidate miRNAs that when expressed induce BMP signaling alterations in fibrodysplasia ossificans progressiva (Mura *et al.* 2012). Several additional BMP-modulated miRNAs have been identified (Li *et al.* 2008, 2009*a*, Lin *et al.* 2009, Bae *et al.* 2012, Gamez *et al.* 2013), generally as a result of high-throughput expression analysis but without precise information on their transcriptional control and function.

The interplay between miRNAs and Wnt/β-catenin signaling

Wnt signaling encompasses canonical and noncanonical pathways depending on the implication of β-catenin. Canonical Wnt/β-catenin signaling initiates by binding WNT1 class family members to Frizzled (Fzd) and the co-receptors LDL receptor-related proteins 5 and 6 (Lrp5/6). In the absence of stimuli, β-catenin is normally retained in the cytoplasm by a protein complex involving GSK3β (GSK3B), casein kinase 1a (CK1A (CSNK1A1)), APC, and axin, which is also finally responsible for its ubiquitination and degradation. When the Fzd–LRP receptor complex is stimulated by Wnt binding, recruitment of Disheveled leads to the inhibition of GSK3β activity. Thus, β-catenin accumulates and eventually enters the nucleus, where it binds to Tcf/Lef1 and regulates transcription. Several molecules negatively affect the Wnt pathway at different points and have been shown to be highly important for bone biology. Dickkopf (Dkk) family members or SOST antagonizes Wnt signaling by binding to LRP5 and 6, whereas SFRPs sequester Wnts away from binding to the receptors (Bafico *et al.* 2001, Wu & Nusse 2002; Fig. 5).

In vitro studies have generated controversial results about the effects of Wnt signaling on osteoblast differentiation, and theories exist about either a positive or a negative influence depending on the state of specification of the target cell. Most data indicate that β-catenin acts positively to maintain stem cell pluripotency and self-renewal; however, once MSCs reach commitment to osteochondroprogenitors, β-catenin promotes osteoblast progression. Moreover, Wnt signaling leads to *Runx2* expression due to a Tcf regulatory element in its promoter (Gaur *et al.* 2005) and has been proved to work cooperatively with BMP signaling to induce other osteogenic genes such as *Osx*, *Dlx5*, and *Msx2* (Rodriguez-Carballo *et al.* 2011).

One of the main mechanisms whereby miRNAs affect Wnt signaling is through the inhibition of Wnt/β-catenin pathway repressors (Fig. 5). The expression of miR-218 is upregulated during osteoblast differentiation, leading to an increase in the expression of osteoblast markers such as *Alpl*, *Runx2*, and *Bglap*. These effects correlate with a decreased expression of *Sfrp2*, *Sost*, and *Dkk2*. Moreover, BMP and Wnt stimuli induce higher miR-218 levels, leading to the upregulation of β-catenin and *Tcf1* (*Hnf1a*) expression and therefore linking miR-218 to a positive loop mechanism involving Wnt signaling (Hassan *et al.* 2012). *Dkk1* is also a miRNA target, leading to enhanced Wnt signaling. For instance, miR-29a negatively regulates the expression of not only *Dkk1* but also *Kremen2* (a decoy receptor of Wnt signaling) and *Sfrp2*, thereby potentiating the β-catenin pathway and promoting osteoblast differentiation of hMSCs (Kapinas *et al.* 2010). The expression of miR-29a and miR-29c is induced after osteoblast differentiation of MC3T3-E1, human fetal osteoblastic cells (hFOBs), and human primary osteoblasts. It has been suggested that TCF/LEF-binding sites present in miR-29 promoter are required for Wnt induction of miR-29 expression (Kapinas *et al.* 2009, 2010). *Dkk1* is also targeted by miR-335-5, which binds directly to its 3′-UTR and decreases Dkk1 protein levels

http://jme.endocrinology-journals.org
DOI: 10.1530/JME-13-0294

Published by Bioscientifica Ltd.

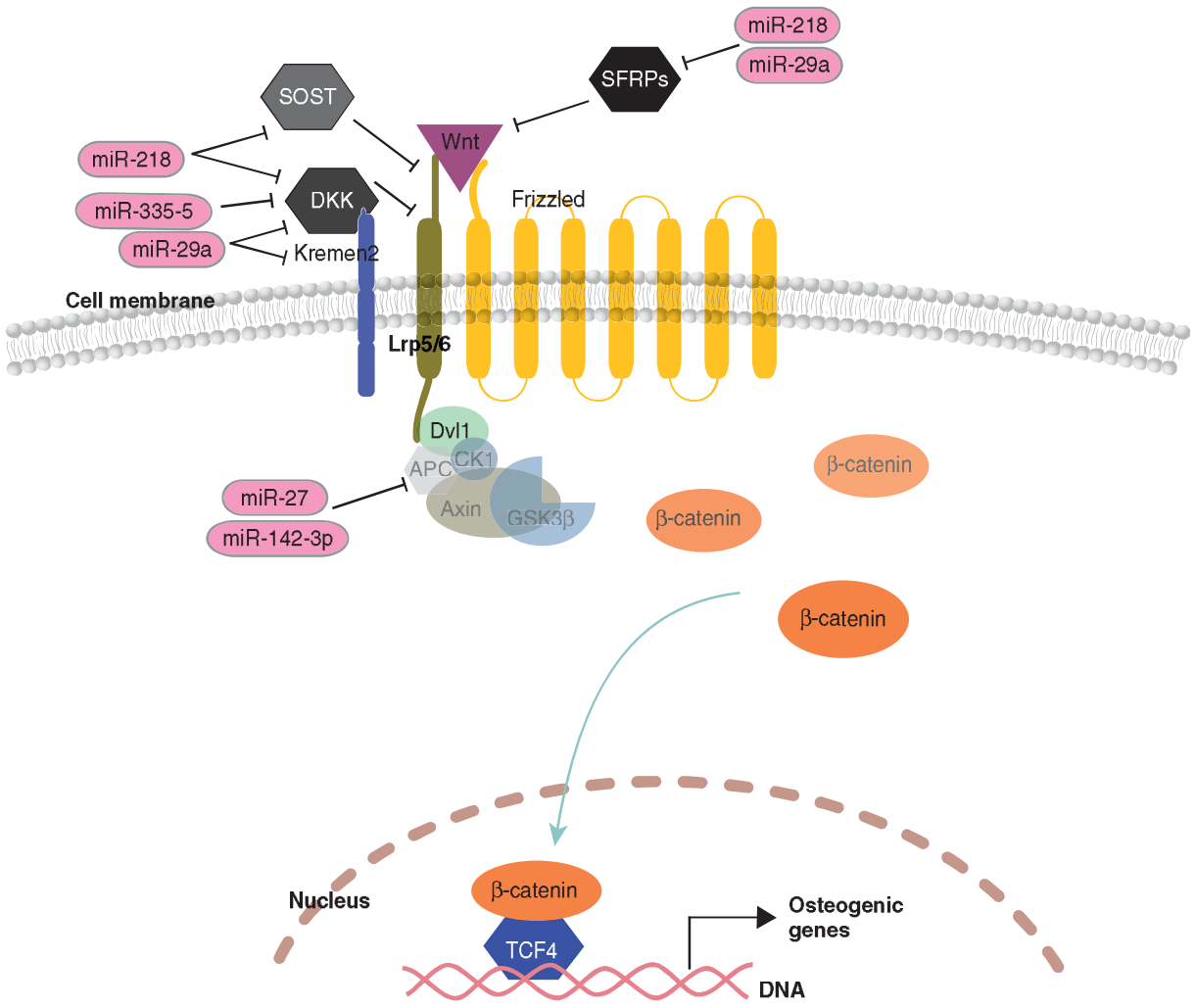

Figure 5
miRNAs involved in the Wnt/β-catenin pathway. miRNAs target several molecules of the Wnt/β-catenin pathway: LRP co-receptors, proteins of the β-catenin degradation complex, or several inhibitory molecules such as DKK or SOST.

during osteoblast differentiation (Zhang *et al.* 2011*d*). It has also been suggested that *Dkk1* levels are post-transcriptionally downregulated by miRNAs, allowing Wnt signaling to support lineage commitment. Ultimately, in the most mature form of osteocytes, the levels of miRNAs affecting *Dkk1* decrease to allow Dkk1 to fine-tune the intensity of Wnt signaling, thereby avoiding disproportionate mineralization (Zhang *et al.* 2011*d*). Another target of miRNA activity is the scaffold protein APC, which is part of the destruction complex of β-catenin. The expression of miR-27 and miR-142-3p is induced in hFOBs and, in turn, these induce osteoblast differentiation. Both promote β-catenin accumulation by targeting APC (Wang & Xu 2010, Hu *et al.* 2013).

Several other pathways are involved in osteoblast differentiation (Notch, IGFs, hedgehogs, etc.), and these are also post-transcriptionally regulated by miRNAs. It is clear nowadays that not only can the expression of a single miRNA fluctuate during cell fate commitment but also a specific miRNA can target different mRNAs depending on the cellular stage. Moreover, a single miRNA can affect several signaling pathways simultaneously, allowing a cooperative effect or the fine-tuned expression of specific mRNAs. One example is miR-34c. Its effect on osteoblasts has been studied *in vitro* and *in vivo*, and it has been shown that it targets not only different factors in the Notch signaling pathway but also *Satb2* and *Runx2* somehow, in a Notch-independent manner (Bae *et al.* 2012). Determining

http://jme.endocrinology-journals.org
DOI: 10.1530/JME-13-0294

Published by Bioscientifica Ltd.

how miRNAs regulate and are regulated by different pathways and how they interact to orchestrate a singular scenario for each differentiation step remains a tremendous challenge. In addition, bone-specific *in vivo* approaches have occasionally yielded controversial results compared with *in vitro* information, probably due to the influence of the cell environment and alterations in osteoblast–osteoclast communication.

miRNAs and skeletal disorders: therapeutic perspectives

miRNAs have emerged as important players in a wide range of pathologies. Multiple screenings have been performed in an attempt to determine miRNA signatures for several skeletal diseases. Osteoarthritis (OA) is the main degenerative articular disease caused by an imbalance between cartilage synthesis and degradation, leading to a progressive loss of movement, functional disability, and joint pain and inflammation. At present, therapy is usually based on symptomatic treatment, mainly using non-steroidal anti-inflammatory drugs (NSAIDs), but these fail to slow articular degeneration and disease progression. Studies on OA have demonstrated that miRNA expression is regulated during this process, indicating the possibility of future miRNA therapies (Iliopoulos *et al.* 2008, Jones *et al.* 2009, Akhtar *et al.* 2010, Diaz-Prado *et al.* 2012). One of the main characteristics of osteoarthritic chondrocytes is the secretion of the pro-inflammatory cytokines interleukin 1β (IL1β) and TNFα. Chondrocyte death occurs in OA and the remaining chondrocytes express *IL1β* (*IL1B*), leading to the upregulation of matrix degradation enzymes such as metalloproteinases (MMPs), particularly MMP13, and the aggrecanases ADAMTS4 and ADAMTS5 (a disintegrin and metalloproteinase with thrombospondin motifs). MMPs and ADAMTS are involved in ECM degradation and OA progression due to their capacity to cleave type 2 collagen or aggrecan respectively.

Several miRNAs are involved in the regulation of IL1β downstream mediators and, in turn, IL1β has been used *in vitro* in human chondrocytes as a model for the study of OA. Numerous miRNAs have been shown to be regulated by IL1β action (Miyaki *et al.* 2009, Dai *et al.* 2012, Matsukawa *et al.* 2013). *MMP13* is regulated directly by miR-27b and miR-127-5p (Akhtar *et al.* 2010, Park *et al.* 2013) or indirectly by miR-27a, miR-9, miR-488, or miR-22 (Iliopoulos *et al.* 2008, Jones *et al.* 2009, Tardif *et al.* 2009, Song *et al.* 2013*b*), among others.

As has been mentioned above, ADAMTS aggrecanases are also important miRNA targets in OA patients and *in vitro* models. Besides its known role in chondrocyte differentiation, miR-140 also plays a central role in OA (Araldi & Schipani 2010). *In vivo*, miR-140 and miR-146a target *ADAMTS5* (Miyaki *et al.* 2009, 2010, Tardif *et al.* 2009, Li *et al.* 2011), while miR-125b targets *ADAMTS4* (Matsukawa *et al.* 2013). Moreover, miR-101 directly inhibits the expression of collagen type II and aggrecan genes through the downregulation of *SOX9* expression (Dai *et al.* 2012). miR-34a is also involved in OA through the regulation of chondrocyte apoptosis and migration (Abouheif *et al.* 2010, Kim *et al.* 2011). Inhibition of miR-34 activity leads to a reduction in IL1β-induced apoptosis in osteoarthritic rat chondrocytes (Abouheif *et al.* 2010). The expression of miR-149 is also downregulated in human primary osteoarthritic chondrocytes and in sw1353 chondrocytes under IL1β/TNFα stimulation and, in turn, miR-149 strongly downregulates the levels of pro-inflammatory cytokines such as IL6, TNFα, and IL1β, thus eventually acting as a feedback loop for cytokine expression (Santini *et al.* 2013). Moreover, it has been shown that *Cox2* (*Ptgs2*) expression requires p38 activity (Susperregui *et al.* 2011) and IL1β stimulation induces p38 activation, leading to a negative regulation of miR-199a* that directly controls the expression of *Cox2* by binding to its 3′-UTR (Akhtar & Haqqi 2012).

Another bone-related disease with an important impact is osteoporosis (OP). In both men and women, loss of bone mass typically starts between 40 and 50 years of age, but there is a major loss in women due to the decrease in estrogen levels after menopause. More importantly, OP leads to a higher risk of fractures among elderly women due to bone fragility, although surprisingly the risk of mortality after a hip fracture is higher in men.

Studies of miR-503 inhibition in mouse models of ovariectomy have shown that miR-503 regulates bone resorption *in vivo*, inhibiting osteoclastogenesis by targeting *Rank* (Chen *et al.* 2013*b*). It has also been suggested that a decrease in miR-2861 expression contributes to OP. miR-2861 has already been shown to be a BMP-induced miRNA, targeting *Hdac5* and therefore involved in Runx2 degradation (Li *et al.* 2009*a*, Hu *et al.* 2011). Li *et al.* (2009*a*) have shown that inhibition of miR-2861, using a specific antisense oligonucleotide introduced by a single tail vein injection, leads to decreased bone mass, reduced osteoblast activity, and osteoblast marker alteration in mice. miR-3077-5p and miR-705 are overexpressed in osteoporotic MSCs. The levels of both miRNAs decrease normally during osteogenic induction to allow the expression of their targets *HOXA10* and *RUNX2*. Liao *et al.* (2013) have shown that knockdown of miR-705 and

Journal of Molecular Endocrinology

http://jme.endocrinology-journals.org
DOI: 10.1530/JME-13-0294

Published by Bioscientifica Ltd.

miR-3077-5p in osteoporotic MSCs is sufficient to restore osteoblast differentiation and mineralization. Moreover, 17β-estradiol injections in ovariectomized mice were found to lead to the recovery of the osteoporotic phenotype and a reduction in miR-705/-3077-5p expression (Liao *et al.* 2013).

miRNAs are also involved in tumor emergence and progression. Nowadays, the use of miRNAs constitutes a novel strategy to improve tumor detection and to predict patient prognosis. One example is miR-132, which was detected as a miRNA expressed at lower levels in osteosarcoma samples. Lower expression of miR-132 is observed in patients with advanced-stage cancer and presenting a poor response to chemotherapy, identifying miR-132 as an indicator of osteosarcoma prognosis (Yang *et al.* 2013). The downregulation of miR-145 expression is also related to poor prognosis in osteosarcoma patients (Tang *et al.* 2013). However, the molecular mechanisms of miR-145 and miR-132 in relation to osteosarcomas are unknown, and further studies are needed to fully understand their involvement in carcinogenesis. miRNA screening has been performed in chondrosarcoma biopsies (Yoshitaka *et al.* 2013), and recently, a study elucidating miRNA changes in osteolytic bone metastasis has been published (Ell *et al.* 2013). During osteolytic bone metastasis, downregulation of the expression of specific miRNAs leads to increased expression of important osteoclastic genes such as *MITF*, *CALCR*, *TRAF6*, and *MMP14*. Furthermore, ectopic overexpression of some miRNAs (pre-miR-141 and pre-miR-219) leads to a reduction in osteolytic bone metastasis (Ell *et al.* 2013).

Thus, a detailed understanding of the function of miRNAs and their tight relationship with bone diseases would constitute a powerful tool for early diagnosis and future therapeutic approaches. Pre-miR or antago-miR therapies have emerged as a novel way to target dysregulated pathways; however, several questions about safety as well as tissue-specific targeting still remain to be answered before clinical applications can be developed.

Concluding remarks

Microarray expression data have provided evidence for the role of miRNAs in several skeletal pathologies. Moreover, mouse models in which their expression is altered have provided evidence of causal links between miRNAs and bone abnormalities. The current identification of a vast number of skeletal-cell-specific miRNAs, each of them with a list of putative targets, has yielded the present challenge of understanding their biological functions. From the data obtained to date, we know that most miRNAs exert their functional effects via multiple target mRNAs, usually by cooperatively targeting genes in the same pathway. Similarly, there is also redundancy, as the same mRNA is targeted by different miRNAs. The very sensitive nature of developmental programs and signaling pathways renders them the perfect candidates for techniques utilizing the dose-dependent effects of miRNAs. In bone physiology, miRNAs are extremely useful nodes, acting as feedback or feed-forward devices that allow buffering effects that confer robustness to skeletal development programs. miRNAs serve as finely tuned precision regulators of the expression of those genes that confer cellular identity and promote differentiation. Moreover, individual miRNAs may even operate as switches to induce differential cell fates. These properties clearly support the notion that the mutation or dysregulation of miRNAs would profoundly affect expression patterns and contribute to skeletal pathologies. Fortunately, these properties also open up opportunities for designing smart therapies based on miRNAs and small RNAs. miRNAs, which are easy to deliver into cells, are intrinsically highly specific and could regulate several targets at the same time. Thus, it is highly feasible that miRNAs, as well as antago-miRNAs, may be used in the future as drugs to treat skeletal pathologies.

Declaration of interest

The authors declare that there is no conflict of interest that could be perceived as prejudicing the impartiality of the review.

Funding

This research was supported by grants from the Ministry of Education of Spain (BFU2011-24254), Fundació La Marató de TV3, and Instituto de Salud Carlos III (ISCIII) (RETIC RD06/0020).

References

Abouheif MM, Nakasa T, Shibuya H, Niimoto T, Kongcharoensombat W & Ochi M 2010 Silencing microRNA-34a inhibits chondrocyte apoptosis in a rat osteoarthritis model *in vitro*. *Rheumatology* **49** 2054–2060. (doi:10.1093/rheumatology/keq247)

Akhtar N & Haqqi TM 2012 MicroRNA-199a* regulates the expression of cyclooxygenase-2 in human chondrocytes. *Annals of the Rheumatic Diseases* **71** 1073–1080. (doi:10.1136/annrheumdis-2011-200519)

Akhtar N, Rasheed Z, Ramamurthy S, Anbazhagan AN, Voss FR & Haqqi TM 2010 MicroRNA-27b regulates the expression of matrix metalloproteinase 13 in human osteoarthritis chondrocytes. *Arthritis and Rheumatism* **62** 1361–1371. (doi:10.1002/art.27329)

Akiyama H, Chaboissier MC, Martin JF, Schedl A & de Crombrugghe B 2002 The transcription factor Sox9 has essential roles in successive steps of the chondrocyte differentiation pathway and is required for expression

Published by Bioscientifica Ltd.

of *Sox5* and *Sox6*. *Genes and Development* **16** 2813–2828. (doi:10.1101/gad.1017802)

Akiyama H, Kim JE, Nakashima K, Balmes G, Iwai N, Deng JM, Zhang Z, Martin JF, Behringer RR, Nakamura T *et al.* 2005 Osteo-chondroprogenitor cells are derived from Sox9 expressing precursors. *PNAS* **102** 14665–14670. (doi:10.1073/pnas.0504750102)

Araldi E & Schipani E 2010 MicroRNA-140 and the silencing of osteoarthritis. *Genes and Development* **24** 1075–1080. (doi:10.1101/gad.1939310)

Bae Y, Yang T, Zeng HC, Campeau PM, Chen Y, Bertin T, Dawson BC, Munivez E, Tao J & Lee BH 2012 miRNA-34c regulates Notch signaling during bone development. *Human Molecular Genetics* **21** 2991–3000. (doi:10.1093/hmg/dds129)

Bafico A, Liu G, Yaniv A, Gazit A & Aaronson SA 2001 Novel mechanism of Wnt signalling inhibition mediated by Dickkopf-1 interaction with LRP6/Arrow. *Nature Cell Biology* **3** 683–686. (doi:10.1038/35083081)

Baglio SR, Devescovi V, Granchi D & Baldini N 2013 MicroRNA expression profiling of human bone marrow mesenchymal stem cells during osteogenic differentiation reveals Osterix regulation by miR-31. *Gene* **527** 321–331. (doi:10.1016/j.gene.2013.06.021)

Bartel DP 2004 MicroRNAs: genomics, biogenesis, mechanism, and function. *Cell* **116** 281–297. (doi:10.1016/S0092-8674(04)00045-5)

Bi W, Deng JM, Zhang Z, Behringer RR & de Crombrugghe B 1999 *Sox9* is required for cartilage formation. *Nature Genetics* **22** 85–89. (doi:10.1038/8792)

Bi W, Huang W, Whitworth DJ, Deng JM, Zhang Z, Behringer RR & de Crombrugghe B 2001 Haploinsufficiency of *Sox9* results in defective cartilage primordia and premature skeletal mineralization. *PNAS* **98** 6698–6703. (doi:10.1073/pnas.111092198)

Bluml S, Bonelli M, Niederreiter B, Puchner A, Mayr G, Hayer S, Koenders MI, van den Berg WB, Smolen J & Redlich K 2011 Essential role of microRNA-155 in the pathogenesis of autoimmune arthritis in mice. *Arthritis and Rheumatism* **63** 1281–1288. (doi:10.1002/art.30281)

Borchert GM, Lanier W & Davidson BL 2006 RNA polymerase III transcribes human microRNAs. *Nature Structural & Molecular Biology* **13** 1097–1101. (doi:10.1038/nsmb1167)

Briata P, Lin WJ, Giovarelli M, Pasero M, Chou CF, Trabucchi M, Rosenfeld MG, Chen CY & Gherzi R 2012 PI3K/AKT signaling determines a dynamic switch between distinct KSRP functions favoring skeletal myogenesis. *Cell Death and Differentiation* **19** 478–487. (doi:10.1038/cdd.2011.117)

Britanova O, Akopov S, Lukyanov S, Gruss P & Tarabykin V 2005 Novel transcription factor Satb2 interacts with matrix attachment region DNA elements in a tissue-specific manner and demonstrates cell-type-dependent expression in the developing mouse CNS. *European Journal of Neuroscience* **21** 658–668. (doi:10.1111/j.1460-9568.2005.03897.x)

Celil AB & Campbell PG 2005 BMP-2 and insulin-like growth factor-I mediate Osterix (Osx) expression in human mesenchymal stem cells via the MAPK and protein kinase D signaling pathways. *Journal of Biological Chemistry* **280** 31353–31359. (doi:10.1074/jbc.M503845200)

Celil AB, Hollinger JO & Campbell PG 2005 Osx transcriptional regulation is mediated by additional pathways to BMP2/Smad signaling. *Journal of Cellular Biochemistry* **95** 518–528. (doi:10.1002/jcb.20429)

Chen CZ, Li L, Lodish HF & Bartel DP 2004 MicroRNAs modulate hematopoietic lineage differentiation. *Science* **303** 83–86. (doi:10.1126/science.1091903)

Chen Q, Liu W, Sinha KM, Yasuda H & de Crombrugghe B 2013*a* Identification and characterization of microRNAs controlled by the osteoblast-specific transcription factor Osterix. *PLoS ONE* **8** e58104. (doi:10.1371/journal.pone.0058104)

Chen C, Cheng P, Xie H, Zhou HD, Wu XP, Liao EY & Luo XH 2013*b* MiR-503 regulates osteoclastogenesis via targeting RANK. *Journal of Bone and Mineral Research* **29** 338–347. (doi:10.1002/jbmr.2032)

Conner JR & Hornick JL 2013 SATB2 is a novel marker of osteoblastic differentiation in bone and soft tissue tumours. *Histopathology* **63** 36–49. (doi:10.1111/his.12138)

Crotti TN, Sharma SM, Fleming JD, Flannery MR, Ostrowski MC, Goldring SR & McHugh KP 2008 PU.1 and NFATc1 mediate osteoclastic induction of the mouse β_3 integrin promoter. *Journal of Cellular Physiology* **215** 636–644. (doi:10.1002/jcp.21344)

Dai L, Zhang X, Hu X, Zhou C & Ao Y 2012 Silencing of microRNA-101 prevents IL-1β-induced extracellular matrix degradation in chondrocytes. *Arthritis Research & Therapy* **14** R268. (doi:10.1186/ar4114)

Davis BN, Hilyard AC, Lagna G & Hata A 2008 SMAD proteins control DROSHA-mediated microRNA maturation. *Nature* **454** 56–61. (doi:10.1038/nature07086)

Davis BN, Hilyard AC, Nguyen PH, Lagna G & Hata A 2010 Smad proteins bind a conserved RNA sequence to promote microRNA maturation by Drosha. *Molecular Cell* **39** 373–384. (doi:10.1016/j.molcel.2010.07.011)

Davis-Dusenbery BN & Hata A 2010 Mechanisms of control of microRNA biogenesis. *Journal of Biochemistry* **148** 381–392. (doi:10.1093/jb/mvq096)

Deng Y, Wu S, Zhou H, Bi X, Wang Y, Hu Y, Gu P & Fan X 2013 Effects of a miR-31, *Runx2*, and *Satb2* regulatory loop on the osteogenic differentiation of bone mesenchymal stem cells. *Stem Cells and Development* **22** 2278–2286. (doi:10.1089/scd.2012.0686)

Diaz-Prado S, Cicione C, Muinos-Lopez E, Hermida-Gomez T, Oreiro N, Fernandez-Lopez C & Blanco FJ 2012 Characterization of microRNA expression profiles in normal and osteoarthritic human chondrocytes. *BMC Musculoskeletal Disorders* **13** 144. (doi:10.1186/1471-2474-13-144)

Dobreva G, Chahrour M, Dautzenberg M, Chirivella L, Kanzler B, Farinas I, Karsenty G & Grosschedl R 2006 SATB2 is a multifunctional determinant of craniofacial patterning and osteoblast differentiation. *Cell* **125** 971–986. (doi:10.1016/j.cell.2006.05.012)

Ducy P 2000 Cbfa1: a molecular switch in osteoblast biology. *Developmental Dynamics* **219** 461–471. (doi:10.1002/1097-0177(2000)9999:9999<::AID-DVDY1074>3.0.CO;2-C)

Ducy P & Karsenty G 1995 Two distinct osteoblast-specific *cis*-acting elements control expression of a mouse osteocalcin gene. *Molecular and Cellular Biology* **15** 1858–1869.

Ducy P, Zhang R, Geoffroy V, Ridall AL & Karsenty G 1997 Osf2/Cbfa1: a transcriptional activator of osteoblast differentiation. *Cell* **89** 747–754. (doi:10.1016/S0092-8674(00)80257-3)

Duong LT & Rodan GA 2001 Regulation of osteoclast formation and function. *Reviews in Endocrine & Metabolic Disorders* **2** 95–104. (doi:10.1023/A:1010063225902)

Eguchi T, Watanabe K, Hara ES, Ono M, Kuboki T & Calderwood SK 2013 OstemiR: a novel panel of microRNA biomarkers in osteoblastic and osteocytic differentiation from mesencymal stem cells. *PLoS ONE* **8** e58796. (doi:10.1371/journal.pone.0058796)

Ell B, Mercatali L, Ibrahim T, Campbell N, Schwarzenbach H, Pantel K, Amadori D & Kang Y 2013 Tumor-induced osteoclast miRNA changes as regulators and biomarkers of osteolytic bone metastasis. *Cancer Cell* **24** 542–556. (doi:10.1016/j.ccr.2013.09.008)

Eskildsen T, Taipaleenmaki H, Stenvang J, Abdallah BM, Ditzel N, Nossent AY, Bak M, Kauppinen S & Kassem M 2011 MicroRNA-138 regulates osteogenic differentiation of human stromal (mesenchymal) stem cells *in vivo*. *PNAS* **108** 6139–6144. (doi:10.1073/pnas.1016758108)

Franceschetti T, Kessler CB, Lee SK & Delany AM 2013 miR-29 promotes murine osteoclastogenesis by regulating osteoclast commitment and migration. *Journal of Biological Chemistry* **288** 33347–33360. (doi:10.1074/jbc.M113.484568)

Fukao T, Fukuda Y, Kiga K, Sharif J, Hino K, Enomoto Y, Kawamura A, Nakamura K, Takeuchi T & Tanabe M 2007 An evolutionarily conserved mechanism for microRNA-223 expression revealed by microRNA gene profiling. *Cell* **129** 617–631. (doi:10.1016/j.cell.2007.02.048)

Gamell C, Osses N, Bartrons R, Ruckle T, Camps M, Rosa JL & Ventura F 2008 BMP2 induction of actin cytoskeleton reorganization and cell migration requires PI3-kinase and Cdc42 activity. *Journal of Cell Science* **121** 3960–3970. (doi:10.1242/jcs.031286)

http://jme.endocrinology-journals.org
DOI: 10.1530/JME-13-0294

Published by Bioscientifica Ltd.

Gamez B, Rodriguez-Carballo E, Bartrons R, Rosa JL & Ventura F 2013 MicroRNA-322 (miR-322) and its target protein Tob2 modulate Osterix (*Osx*) mRNA stability. *Journal of Biological Chemistry* **288** 14264–14275. (doi:10.1074/jbc.M112.432104)

Gao J, Yang T, Han J, Yan K, Qiu X, Zhou Y, Fan Q & Ma B 2011 MicroRNA expression during osteogenic differentiation of human multipotent mesenchymal stromal cells from bone marrow. *Journal of Cellular Biochemistry* **112** 1844–1856. (doi:10.1002/jcb.23106)

Gaur T, Lengner CJ, Hovhannisyan H, Bhat RA, Bodine PV, Komm BS, Javed A, van Wijnen AJ, Stein JL, Stein GS *et al.* 2005 Canonical WNT signaling promotes osteogenesis by directly stimulating *Runx2* gene expression. *Journal of Biological Chemistry* **280** 33132–33140. (doi:10.1074/jbc.M500608200)

Gaur T, Hussain S, Mudhasani R, Parulkar I, Colby JL, Frederick D, Kream BE, van Wijnen AJ, Stein JL, Stein GS *et al.* 2010 Dicer inactivation in osteoprogenitor cells compromises fetal survival and bone formation, while excision in differentiated osteoblasts increases bone mass in the adult mouse. *Developmental Biology* **340** 10–21. (doi:10.1016/j.ydbio.2010.01.008)

Gibson G & Asahara H 2013 MicroRNAs and cartilage. *Journal of Orthopaedic Research* **31** 1333–1344. (doi:10.1002/jor.22397)

Gohda J, Akiyama T, Koga T, Takayanagi H, Tanaka S & Inoue J 2005 RANK-mediated amplification of TRAF6 signaling leads to NFATc1 induction during osteoclastogenesis. *EMBO Journal* **24** 790–799. (doi:10.1038/sj.emboj.7600564)

Guan YJ, Yang X, Wei L & Chen Q 2011 MiR-365: a mechanosensitive microRNA stimulates chondrocyte differentiation through targeting histone deacetylase 4. *FASEB Journal* **25** 4457–4466. (doi:10.1096/fj.11-185132)

Guerit D, Philipot D, Chuchana P, Toupet K, Brondello JM, Mathieu M, Jorgensen C & Noel D 2013 Sox9-regulated miRNA-574-3p inhibits chondrogenic differentiation of mesenchymal stem cells. *PLoS ONE* **8** e62582. (doi:10.1371/journal.pone.0062582)

Guo H, Ingolia NT, Weissman JS & Bartel DP 2010 Mammalian microRNAs predominantly act to decrease target mRNA levels. *Nature* **466** 835–840. (doi:10.1038/nature09267)

Han J, Lee Y, Yeom KH, Nam JW, Heo I, Rhee JK, Sohn SY, Cho Y, Zhang BT & Kim VN 2006 Molecular basis for the recognition of primary microRNAs by the Drosha–DGCR8 complex. *Cell* **125** 887–901. (doi:10.1016/j.cell.2006.03.043)

Hassan MQ, Gordon JA, Beloti MM, Croce CM, van Wijnen AJ, Stein JL, Stein GS & Lian JB 2010 A network connecting Runx2, SATB2, and the miR-23a–27a–24-2 cluster regulates the osteoblast differentiation program. *PNAS* **107** 19879–19884. (doi:10.1073/pnas.1007698107)

Hassan MQ, Maeda Y, Taipaleenmaki H, Zhang W, Jafferji M, Gordon JA, Li Z, Croce CM, van Wijnen AJ, Stein JL *et al.* 2012 miR-218 directs a Wnt signaling circuit to promote differentiation of osteoblasts and osteomimicry of metastatic cancer cells. *Journal of Biological Chemistry* **287** 42084–42092. (doi:10.1074/jbc.M112.377515)

He X, Eberhart JK & Postlethwait JH 2009 MicroRNAs and micromanaging the skeleton in disease, development and evolution. *Journal of Cellular and Molecular Medicine* **13** 606–618. (doi:10.1111/j.1582-4934.2009.00696.x)

He J, Zhang JF, Yi C, Lv Q, Xie WD, Li JN, Wan G, Cui K, Kung HF, Yang J *et al.* 2010 miRNA-mediated functional changes through co-regulating function related genes. *PLoS ONE* **5** e13558. (doi:10.1371/journal.pone.0013558)

Hobert O 2008 Gene regulation by transcription factors and microRNAs. *Science* **319** 1785–1786. (doi:10.1126/science.1151651)

Horowitz MC, Xi Y, Wilson K & Kacena MA 2001 Control of osteoclastogenesis and bone resorption by members of the TNF family of receptors and ligands. *Cytokine & Growth Factor Reviews* **12** 9–18. (doi:10.1016/S1359-6101(00)00030-7)

Hu R, Liu W, Li H, Yang L, Chen C, Xia ZY, Guo LJ, Xie H, Zhou HD, Wu XP *et al.* 2011 A Runx2/miR-3960/miR-2861 regulatory feedback loop during mouse osteoblast differentiation. *Journal of Biological Chemistry* **286** 12328–12339. (doi:10.1074/jbc.M110.176099)

Hu W, Ye Y, Zhang W, Wang J, Chen A & Guo F 2013 miR1423p promotes osteoblast differentiation by modulating Wnt signaling. *Molecular Medicine Reports* **7** 689–693. (doi:10.3892/mmr.2012.1207)

Huang J, Zhao L, Xing L & Chen D 2010 MicroRNA-204 regulates Runx2 protein expression and mesenchymal progenitor cell differentiation. *Stem Cells* **28** 357–364. (doi:10.1002/stem.288)

Iliopoulos D, Malizos KN, Oikonomou P & Tsezou A 2008 Integrative microRNA and proteomic approaches identify novel osteoarthritis genes and their collaborative metabolic and inflammatory networks. *PLoS ONE* **3** e3740. (doi:10.1371/journal.pone.0003740)

Inose H, Ochi H, Kimura A, Fujita K, Xu R, Sato S, Iwasaki M, Sunamura S, Takeuchi Y, Fukumoto S *et al.* 2009 A microRNA regulatory mechanism of osteoblast differentiation. *PNAS* **106** 20794–20799. (doi:10.1073/pnas.0909311106)

Itoh T, Nozawa Y & Akao Y 2009 MicroRNA-141 and -200a are involved in bone morphogenetic protein-2-induced mouse pre-osteoblast differentiation by targeting distal-less homeobox 5. *Journal of Biological Chemistry* **284** 19272–19279. (doi:10.1074/jbc.M109.014001)

Jones SW, Watkins G, Le Good N, Roberts S, Murphy CL, Brockbank SM, Needham MR, Read SJ & Newham P 2009 The identification of differentially expressed microRNA in osteoarthritic tissue that modulate the production of TNF-α and MMP13. *Osteoarthritis and Cartilage* **17** 464–472. (doi:10.1016/j.joca.2008.09.012)

Kanzler B, Kuschert SJ, Liu YH & Mallo M 1998 *Hoxa-2* restricts the chondrogenic domain and inhibits bone formation during development of the branchial area. *Development* **125** 2587–2597.

Kapinas K & Delany AM 2011 MicroRNA biogenesis and regulation of bone remodeling. *Arthritis Research & Therapy* **13** 220. (doi:10.1186/ar3325)

Kapinas K, Kessler CB & Delany AM 2009 miR-29 suppression of osteonectin in osteoblasts: regulation during differentiation and by canonical Wnt signaling. *Journal of Cellular Biochemistry* **108** 216–224. (doi:10.1002/jcb.22243)

Kapinas K, Kessler C, Ricks T, Gronowicz G & Delany AM 2010 miR-29 modulates Wnt signaling in human osteoblasts through a positive feedback loop. *Journal of Biological Chemistry* **285** 25221–25231. (doi:10.1074/jbc.M110.116137)

Karlsen TA, Jakobsen RB, Mikkelsen TS & Brinchmann JE 2013 MicroRNA-140 targets *RALA* and regulates chondrogenic differentiation of human mesenchymal stem cells by translational enhancement of *SOX9* and *ACAN*. *Stem Cells and Development* **23** 290–304. (doi:10.1089/scd.2013.0209)

Karsenty G 2008 Transcriptional control of skeletogenesis. *Annual Review of Genomics and Human Genetics* **9** 183–196. (doi:10.1146/annurev.genom.9.081307.164437)

Karsenty G & Wagner EF 2002 Reaching a genetic and molecular understanding of skeletal development. *Developmental Cell* **2** 389–406. (doi:10.1016/S1534-5807(02)00157-0)

Karsenty G, Ducy P, Starbuck M, Priemel M, Shen J, Geoffroy V & Amling M 1999 Cbfa1 as a regulator of osteoblast differentiation and function. *Bone* **25** 107–108. (doi:10.1016/S8756-3282(99)00111-8)

Katagiri T, Yamaguchi A, Komaki M, Abe E, Takahashi N, Ikeda T, Rosen V, Wozney JM, Fujisawa-Sehara A & Suda T 1994 Bone morphogenetic protein-2 converts the differentiation pathway of C2C12 myoblasts into the osteoblast lineage. *Journal of Cell Biology* **127** 1755–1766. (doi:10.1083/jcb.127.6.1755)

Kim HK, Lee YS, Sivaprasad U, Malhotra A & Dutta A 2006 Muscle-specific microRNA miR-206 promotes muscle differentiation. *Journal of Cell Biology* **174** 677–687. (doi:10.1083/jcb.200603008)

Kim D, Song J, Kim S, Chun CH & Jin EJ 2011 MicroRNA-34a regulates migration of chondroblast and IL-1β-induced degeneration of chondrocytes by targeting EphA5. *Biochemical and Biophysical Research Communications* **415** 551–557. (doi:10.1016/j.bbrc.2011.10.087)

Kobayashi N, Kadono Y, Naito A, Matsumoto K, Yamamoto T, Tanaka S & Inoue J 2001 Segregation of TRAF6-mediated signaling pathways

http://jme.endocrinology-journals.org
DOI: 10.1530/JME-13-0294

Published by Bioscientifica Ltd.

clarifies its role in osteoclastogenesis. *EMBO Journal* **20** 1271–1280. (doi:10.1093/emboj/20.6.1271)

Kobayashi T, Lu J, Cobb BS, Rodda SJ, McMahon AP, Schipani E, Merkenschlager M & Kronenberg HM 2008 Dicer-dependent pathways regulate chondrocyte proliferation and differentiation. *PNAS* **105** 1949–1954. (doi:10.1073/pnas.0707900105)

Komori T, Yagi H, Nomura S, Yamaguchi A, Sasaki K, Deguchi K, Shimizu Y, Bronson RT, Gao YH, Inada M *et al.* 1997 Targeted disruption of *Cbfa1* results in a complete lack of bone formation owing to maturational arrest of osteoblasts. *Cell* **89** 755–764. (doi:10.1016/S0092-8674(00)80258-5)

Kukita T, Wada N, Kukita A, Kakimoto T, Sandra F, Toh K, Nagata K, Iijima T, Horiuchi M, Matsusaki H *et al.* 2004 RANKL-induced DC-STAMP is essential for osteoclastogenesis. *Journal of Experimental Medicine* **200** 941–946. (doi:10.1084/jem.20040518)

Laine SK, Alm JJ, Virtanen SP, Aro HT & Laitala-Leinonen TK 2012 MicroRNAs miR-96, miR-124, and miR-199a regulate gene expression in human bone marrow-derived mesenchymal stem cells. *Journal of Cellular Biochemistry* **113** 2687–2695. (doi:10.1002/jcb.24144)

Lecanda F, Towler DA, Ziambaras K, Cheng SL, Koval M, Steinberg TH & Civitelli R 1998 Gap junctional communication modulates gene expression in osteoblastic cells. *Molecular Biology of the Cell* **9** 2249–2258. (doi:10.1091/mbc.9.8.2249)

Lee MH, Kwon TG, Park HS, Wozney JM & Ryoo HM 2003 BMP-2-induced Osterix expression is mediated by Dlx5 but is independent of Runx2. *Biochemical and Biophysical Research Communications* **309** 689–694. (doi:10.1016/j.bbrc.2003.08.058)

Lee I, Ajay SS, Yook JI, Kim HS, Hong SH, Kim NH, Dhanasekaran SM, Chinnaiyan AM & Athey BD 2009 New class of microRNA targets containing simultaneous 5′-UTR and 3′-UTR interaction sites. *Genome Research* **19** 1175–1183. (doi:10.1101/gr.089367.108)

Lee Y, Kim HJ, Park CK, Kim YG, Lee HJ, Kim JY & Kim HH 2013 MicroRNA-124 regulates osteoclast differentiation. *Bone* **56** 383–389. (doi:10.1016/j.bone.2013.07.007)

Lefebvre V, Behringer RR & de Crombrugghe B 2001 L-Sox5, Sox6 and Sox9 control essential steps of the chondrocyte differentiation pathway. *Osteoarthritis and Cartilage* **9** (Suppl A) S69–S75. (doi:10.1053/joca.2001.0447)

Li Z, Hassan MQ, Volinia S, van Wijnen AJ, Stein JL, Croce CM, Lian JB & Stein GS 2008 A microRNA signature for a BMP2-induced osteoblast lineage commitment program. *PNAS* **105** 13906–13911. (doi:10.1073/pnas.0804438105)

Li H, Xie H, Liu W, Hu R, Huang B, Tan YF, Xu K, Sheng ZF, Zhou HD, Wu XP *et al.* 2009*a* A novel microRNA targeting HDAC5 regulates osteoblast differentiation in mice and contributes to primary osteoporosis in humans. *Journal of Clinical Investigation* **119** 3666–3677. (doi:10.1172/JCI39832)

Li Z, Hassan MQ, Jafferji M, Aqeilan RI, Garzon R, Croce CM, van Wijnen AJ, Stein JL, Stein GS & Lian JB 2009*b* Biological functions of miR-29b contribute to positive regulation of osteoblast differentiation. *Journal of Biological Chemistry* **284** 15676–15684. (doi:10.1074/jbc.M809787200)

Li X, Gibson G, Kim JS, Kroin J, Xu S, van Wijnen AJ & Im HJ 2011 MicroRNA-146a is linked to pain-related pathophysiology of osteoarthritis. *Gene* **480** 34–41. (doi:10.1016/j.gene.2011.03.003)

Li B, Han Q, Zhu Y, Yu Y, Wang J & Jiang X 2012 Down-regulation of miR-214 contributes to intrahepatic cholangiocarcinoma metastasis by targeting Twist. *FEBS Journal* **279** 2393–2398. (doi:10.1111/j.1742-4658.2012.08618.x)

Li H, Li T, Wang S, Wei J, Fan J, Li J, Han Q, Liao L, Shao C & Zhao RC 2013 miR-17-5p and miR-106a are involved in the balance between osteogenic and adipogenic differentiation of adipose-derived mesenchymal stem cells. *Stem Cell Research* **10** 313–324. (doi:10.1016/j.scr.2012.11.007)

Liao L, Yang X, Su X, Hu C, Zhu X, Yang N, Chen X, Shi S, Shi S & Jin Y 2013 Redundant miR-3077-5p and miR-705 mediate the shift of mesenchymal stem cell lineage commitment to adipocyte in osteoporosis bone marrow. *Cell Death & Disease* **4** e600. (doi:10.1038/cddis.2013.130)

Lin EA, Kong L, Bai XH, Luan Y & Liu CJ 2009 miR-199a, a bone morphogenic protein 2-responsive microRNA, regulates chondrogenesis via direct targeting to Smad1. *Journal of Biological Chemistry* **284** 11326–11335. (doi:10.1074/jbc.M807709200)

Lund E, Guttinger S, Calado A, Dahlberg JE & Kutay U 2004 Nuclear export of microRNA precursors. *Science* **303** 95–98. (doi:10.1126/science.1090599)

Luzi E, Marini F, Sala SC, Tognarini I, Galli G & Brandi ML 2008 Osteogenic differentiation of human adipose tissue-derived stem cells is modulated by the miR-26a targeting of the SMAD1 transcription factor. *Journal of Bone and Mineral Research* **23** 287–295. (doi:10.1359/jbmr.071011)

Lytle JR, Yario TA & Steitz JA 2007 Target mRNAs are repressed as efficiently by microRNA-binding sites in the 5′ UTR as in the 3′ UTR. *PNAS* **104** 9667–9672. (doi:10.1073/pnas.0703820104)

Mann M, Barad O, Agami R, Geiger B & Hornstein E 2010 miRNA-based mechanism for the commitment of multipotent progenitors to a single cellular fate. *PNAS* **107** 15804–15809. (doi:10.1073/pnas.0915022107)

Manolagas SC 2000 Birth and death of bone cells: basic regulatory mechanisms and implications for the pathogenesis and treatment of osteoporosis. *Endocrine Reviews* **21** 115–137. (doi:10.1210/edrv.21.2.0395)

Martinez-Sanchez A & Murphy CL 2013 miR-1247 functions by targeting cartilage transcription factor SOX9. *Journal of Biological Chemistry* **288** 30802–30814. (doi:10.1074/jbc.M113.496729)

Martinez-Sanchez A, Dudek KA & Murphy CL 2012 Regulation of human chondrocyte function through direct inhibition of cartilage master regulator SOX9 by microRNA-145 (miRNA-145). *Journal of Biological Chemistry* **287** 916–924. (doi:10.1074/jbc.M111.302430)

Mateescu B, Batista L, Cardon M, Gruosso T, de Feraudy Y, Mariani O, Nicolas A, Meyniel JP, Cottu P, Sastre-Garau X *et al.* 2011 miR-141 and miR-200a act on ovarian tumorigenesis by controlling oxidative stress response. *Nature Medicine* **17** 1627–1635. (doi:10.1038/nm.2512)

Matsukawa T, Sakai T, Yonezawa T, Hiraiwa H, Hamada T, Nakashima M, Ono Y, Ishizuka S, Nakahara H, Lotz MK *et al.* 2013 MicroRNA-125b regulates the expression of aggrecanase-1 (ADAMTS-4) in human osteoarthritic chondrocytes. *Arthritis Research & Therapy* **15** R28. (doi:10.1186/ar4164)

Mattick JS & Makunin IV 2006 Non-coding RNA. *Human Molecular Genetics* **15** R17–R29. (doi:10.1093/hmg/ddl046)

Miyaki S, Nakasa T, Otsuki S, Grogan SP, Higashiyama R, Inoue A, Kato Y, Sato T, Lotz MK & Asahara H 2009 MicroRNA-140 is expressed in differentiated human articular chondrocytes and modulates interleukin-1 responses. *Arthritis and Rheumatism* **60** 2723–2730. (doi:10.1002/art.24745)

Miyaki S, Sato T, Inoue A, Otsuki S, Ito Y, Yokoyama S, Kato Y, Takemoto F, Nakasa T, Yamashita S *et al.* 2010 MicroRNA-140 plays dual roles in both cartilage development and homeostasis. *Genes and Development* **24** 1173–1185. (doi:10.1101/gad.1915510)

Miyazono K, Kamiya Y & Morikawa M 2010 Bone morphogenetic protein receptors and signal transduction. *Journal of Biochemistry* **147** 35–51. (doi:10.1093/jb/mvp148)

Mizoguchi F, Izu Y, Hayata T, Hemmi H, Nakashima K, Nakamura T, Kato S, Miyasaka N, Ezura Y & Noda M 2010 Osteoclast-specific Dicer gene deficiency suppresses osteoclastic bone resorption. *Journal of Cellular Biochemistry* **109** 866–875. (doi:10.1002/jcb.22228)

Mizoguchi F, Murakami Y, Saito T, Miyasaka N & Kohsaka H 2013 miR-31 controls osteoclast formation and bone resorption by targeting RhoA. *Arthritis Research & Therapy* **15** R102. (doi:10.1186/ar4282)

Mizuno Y, Yagi K, Tokuzawa Y, Kanesaki-Yatsuka Y, Suda T, Katagiri T, Fukuda T, Maruyama M, Okuda A, Amemiya T *et al.* 2008 miR-125b inhibits osteoblastic differentiation by down-regulation of cell proliferation. *Biochemical and Biophysical Research Communications* **368** 267–272. (doi:10.1016/j.bbrc.2008.01.073)

http://jme.endocrinology-journals.org
DOI: 10.1530/JME-13-0294

Published by Bioscientifica Ltd.

Mizuno Y, Tokuzawa Y, Ninomiya Y, Yagi K, Yatsuka-Kanesaki Y, Suda T, Fukuda T, Katagiri T, Kondoh Y, Amemiya T *et al.* 2009 miR-210 promotes osteoblastic differentiation through inhibition of *AcvR1b*. *FEBS Letters* **583** 2263–2268. (doi:10.1016/j.febslet.2009.06.006)

Mori-Akiyama Y, Akiyama H, Rowitch DH & de Crombrugghe B 2003 Sox9 is required for determination of the chondrogenic cell lineage in the cranial neural crest. *PNAS* **100** 9360–9365. (doi:10.1073/pnas.1631288100)

Mura M, Cappato S, Giacopelli F, Ravazzolo R & Bocciardi R 2012 The role of the 3′UTR region in the regulation of the *ACVR1/Alk-2* gene expression. *PLoS ONE* **7** e50958. (doi:10.1371/journal.pone.0050958)

Nakamura Y, Inloes JB, Katagiri T & Kobayashi T 2011 Chondrocyte-specific microRNA-140 regulates endochondral bone development and targets *Dnpep* to modulate bone morphogenetic protein signaling. *Molecular and Cellular Biology* **31** 3019–3028. (doi:10.1128/MCB.05178-11)

Nakashima K & de Crombrugghe B 2003 Transcriptional mechanisms in osteoblast differentiation and bone formation. *Trends in Genetics* **19** 458–466. (doi:10.1016/S0168-9525(03)00176-8)

Nakashima K, Zhou X, Kunkel G, Zhang Z, Deng JM, Behringer RR & de Crombrugghe B 2002 The novel zinc finger-containing transcription factor osterix is required for osteoblast differentiation and bone formation. *Cell* **108** 17–29. (doi:10.1016/S0092-8674(01)00622-5)

Nakashima T, Hayashi M, Fukunaga T, Kurata K, Oh-Hora M, Feng JQ, Bonewald LF, Kodama T, Wutz A, Wagner EF *et al.* 2011 Evidence for osteocyte regulation of bone homeostasis through RANKL expression. *Nature Medicine* **17** 1231–1234. (doi:10.1038/nm.2452)

Nicolas FE, Pais H, Schwach F, Lindow M, Kauppinen S, Moulton V & Dalmay T 2011 mRNA expression profiling reveals conserved and non-conserved miR-140 targets. *RNA Biology* **8** 607–615. (doi:10.4161/rna.8.4.15390)

Nishio Y, Dong Y, Paris M, O'Keefe RJ, Schwarz EM & Drissi H 2006 Runx2-mediated regulation of the zinc finger Osterix/Sp7 gene. *Gene* **372** 62–70. (doi:10.1016/j.gene.2005.12.022)

Ortuno MJ, Ruiz-Gaspa S, Rodriguez-Carballo E, Susperregui AR, Bartrons R, Rosa JL & Ventura F 2010 p38 regulates expression of osteoblast-specific genes by phosphorylation of osterix. *Journal of Biological Chemistry* **285** 31985–31994. (doi:10.1074/jbc.M110.123612)

Pais H, Nicolas FE, Soond SM, Swingler TE, Clark IM, Chantry A, Moulton V & Dalmay T 2010 Analyzing mRNA expression identifies Smad3 as a microRNA-140 target regulated only at protein level. *RNA* **16** 489–494. (doi:10.1261/rna.1701210)

Papaioannou G, Inloes JB, Nakamura Y, Paltrinieri E & Kobayashi T 2013 let-7 and miR-140 microRNAs coordinately regulate skeletal development. *PNAS* **110** E3291–E3300. (doi:10.1073/pnas.1302797110)

Park SJ, Cheon EJ, Lee MH & Kim HA 2013 MicroRNA-127-5p regulates matrix metalloproteinase 13 expression and interleukin-1β-induced catabolic effects in human chondrocytes. *Arthritis and Rheumatism* **65** 3141–3152. (doi:10.1002/art.38188)

Pasero M, Giovarelli M, Bucci G, Gherzi R & Briata P 2012 Bone morphogenetic protein/SMAD signaling orients cell fate decision by impairing KSRP-dependent microRNA maturation. *Cell Reports* **2** 1159–1168. (doi:10.1016/j.celrep.2012.10.020)

Plotkin LI & Bellido T 2013 Beyond gap junctions: connexin43 and bone cell signaling. *Bone* **52** 157–166. (doi:10.1016/j.bone.2012.09.030)

Rodriguez-Carballo E, Ulsamer A, Susperregui AR, Manzanares-Cespedes C, Sanchez-Garcia E, Bartrons R, Rosa JL & Ventura F 2011 Conserved regulatory motifs in osteogenic gene promoters integrate cooperative effects of canonical Wnt and BMP pathways. *Journal of Bone and Mineral Research* **26** 718–729. (doi:10.1002/jbmr.260)

Rossi M, Pitari MR, Amodio N, Di Martino MT, Conforti F, Leone E, Botta C, Paolino FM, Del Giudice T, Iuliano E *et al.* 2013 miR-29b negatively regulates human osteoclastic cell differentiation and function: implications for the treatment of multiple myeloma-related bone disease. *Journal of Cellular Physiology* **228** 1506–1515. (doi:10.1002/jcp.24306)

Santini P, Politi L, Vedova PD, Scandurra R & Scotto d'Abusco A 2013 The inflammatory circuitry of miR-149 as a pathological mechanism in osteoarthritis. *Rheumatology International* [in press]. (doi:10.1007/s00296-013-2754-8)

Sato MM, Nashimoto M, Katagiri T, Yawaka Y & Tamura M 2009 Bone morphogenetic protein-2 down-regulates miR-206 expression by blocking its maturation process. *Biochemical and Biophysical Research Communications* **383** 125–129. (doi:10.1016/j.bbrc.2009.03.142)

Seitz H & Zamore PD 2006 Rethinking the microprocessor. *Cell* **125** 827–829. (doi:10.1016/j.cell.2006.05.018)

Shi Y & Massague J 2003 Mechanisms of TGF-β signaling from cell membrane to the nucleus. *Cell* **113** 685–700. (doi:10.1016/S0092-8674(03)00432-X)

Shi K, Lu J, Zhao Y, Wang L, Li J, Qi B, Li H & Ma C 2013 MicroRNA-214 suppresses osteogenic differentiation of C2C12 myoblast cells by targeting Osterix. *Bone* **55** 487–494. (doi:10.1016/j.bone.2013.04.002)

Shibuya H, Nakasa T, Adachi N, Nagata Y, Ishikawa M, Deie M, Suzuki O & Ochi M 2013 Overexpression of microRNA-223 in rheumatoid arthritis synovium controls osteoclast differentiation. *Modern Rheumatology* **23** 674–685. (doi:10.3109/s10165-012-0710-1)

Song J, Lee M, Kim D, Han J, Chun CH & Jin EJ 2013*a* MicroRNA-181b regulates articular chondrocytes differentiation and cartilage integrity. *Biochemical and Biophysical Research Communications* **431** 210–214. (doi:10.1016/j.bbrc.2012.12.133)

Song J, Kim D, Lee CH, Lee MS, Chun CH & Jin EJ 2013*b* MicroRNA-488 regulates zinc transporter SLC39A8/ZIP8 during pathogenesis of osteoarthritis. *Journal of Biomedical Science* **20** 31. (doi:10.1186/1423-0127-20-31)

Starega-Roslan J, Koscianska E, Kozlowski P & Krzyzosiak WJ 2011 The role of the precursor structure in the biogenesis of microRNA. *Cellular and Molecular Life Sciences* **68** 2859–2871. (doi:10.1007/s00018-011-0726-2)

Sugatani T & Hruska KA 2007 MicroRNA-223 is a key factor in osteoclast differentiation. *Journal of Cellular Biochemistry* **101** 996–999. (doi:10.1002/jcb.21335)

Sugatani T & Hruska KA 2009 Impaired micro-RNA pathways diminish osteoclast differentiation and function. *Journal of Biological Chemistry* **284** 4667–4678. (doi:10.1074/jbc.M805777200)

Sugatani T, Vacher J & Hruska KA 2011 A microRNA expression signature of osteoclastogenesis. *Blood* **117** 3648–3657. (doi:10.1182/blood-2010-10-311415)

Sumiyoshi K, Kubota S, Ohgawara T, Kawata K, Abd El Kader T, Nishida T, Ikeda N, Shimo T, Yamashiro T & Takigawa M 2013 Novel role of miR-181a in cartilage metabolism. *Journal of Cellular Biochemistry* **114** 2094–2100. (doi:10.1002/jcb.24556)

Susperregui AR, Gamell C, Rodriguez-Carballo E, Ortuno MJ, Bartrons R, Rosa JL & Ventura F 2011 Noncanonical BMP signaling regulates *cyclooxygenase-2* transcription. *Molecular Endocrinology* **25** 1006–1017. (doi:10.1210/me.2010-0515)

Takayanagi H, Kim S, Koga T, Nishina H, Isshiki M, Yoshida H, Saiura A, Isobe M, Yokochi T, Inoue J *et al.* 2002 Induction and activation of the transcription factor NFATc1 (NFAT2) integrate RANKL signaling in terminal differentiation of osteoclasts. *Developmental Cell* **3** 889–901. (doi:10.1016/S1534-5807(02)00369-6)

Tanaka S, Nakamura K, Takahasi N & Suda T 2005 Role of RANKL in physiological and pathological bone resorption and therapeutics targeting the RANKL–RANK signaling system. *Immunological Reviews* **208** 30–49. (doi:10.1111/j.0105-2896.2005.00327.x)

Tang M, Lin L, Cai H, Tang J & Zhou Z 2013 MicroRNA-145 downregulation associates with advanced tumor progression and poor prognosis in patients suffering osteosarcoma. *OncoTargets and Therapy* **6** 833–838. (doi:10.2147/OTT.S40080)

Tardif G, Hum D, Pelletier JP, Duval N & Martel-Pelletier J 2009 Regulation of the IGFBP-5 and MMP-13 genes by the microRNAs miR-140 and miR-27a in human osteoarthritic chondrocytes. *BMC Musculoskeletal Disorders* **10** 148. (doi:10.1186/1471-2474-10-148)

Tondravi MM, McKercher SR, Anderson K, Erdmann JM, Quiroz M, Maki R & Teitelbaum SL 1997 Osteopetrosis in mice lacking haematopoietic transcription factor PU.1. *Nature* **386** 81–84. (doi:10.1038/386081a0)

http://jme.endocrinology-journals.org
DOI: 10.1530/JME-13-0294

Published by Bioscientifica Ltd.

Tuddenham L, Wheeler G, Ntounia-Fousara S, Waters J, Hajihosseini MK, Clark I & Dalmay T 2006 The cartilage specific microRNA-140 targets histone deacetylase 4 in mouse cells. *FEBS Letters* **580** 4214–4217. (doi:10.1016/j.febslet.2006.06.080)

Ulsamer A, Ortuno MJ, Ruiz S, Susperregui AR, Osses N, Rosa JL & Ventura F 2008 BMP-2 induces Osterix expression through up-regulation of Dlx5 and its phosphorylation by p38. *Journal of Biological Chemistry* **283** 3816–3826. (doi:10.1074/jbc.M704724200)

Vasudevan S, Tong Y & Steitz JA 2007 Switching from repression to activation: microRNAs can up-regulate translation. *Science* **318** 1931–1934. (doi:10.1126/science.1149460)

Wang T & Xu Z 2010 miR-27 promotes osteoblast differentiation by modulating Wnt signaling. *Biochemical and Biophysical Research Communications* **402** 186–189. (doi:10.1016/j.bbrc.2010.08.031)

Wang X, Guo B, Li Q, Peng J, Yang Z, Wang A, Li D, Hou Z, Lv K, Kan G *et al.* 2013*a* miR-214 targets *ATF4* to inhibit bone formation. *Nature Medicine* **19** 93–100. (doi:10.1038/nm.3026)

Wang J, Guan X, Guo F, Zhou J, Chang A, Sun B, Cai Y, Ma Z, Dai C, Li X *et al.* 2013*b* miR-30e reciprocally regulates the differentiation of adipocytes and osteoblasts by directly targeting low-density lipoprotein receptor-related protein 6. *Cell Death & Disease* **4** e845. (doi:10.1038/cddis.2013.356)

Wei J, Shi Y, Zheng L, Zhou B, Inose H, Wang J, Guo XE, Grosschedl R & Karsenty G 2012 miR-34s inhibit osteoblast proliferation and differentiation in the mouse by targeting SATB2. *Journal of Cell Biology* **197** 509–521. (doi:10.1083/jcb.201201057)

Winbanks CE, Wang B, Beyer C, Koh P, White L, Kantharidis P & Gregorevic P 2011 TGF-β regulates miR-206 and miR-29 to control myogenic differentiation through regulation of HDAC4. *Journal of Biological Chemistry* **286** 13805–13814. (doi:10.1074/jbc.M110.192625)

Wu CH & Nusse R 2002 Ligand receptor interactions in the Wnt signaling pathway in *Drosophila*. *Journal of Biological Chemistry* **277** 41762–41769. (doi:10.1074/jbc.M207850200)

Wu T, Zhou H, Hong Y, Li J, Jiang X & Huang H 2012 miR-30 family members negatively regulate osteoblast differentiation. *Journal of Biological Chemistry* **287** 7503–7511. (doi:10.1074/jbc.M111.292722)

Xiong J, Onal M, Jilka RL, Weinstein RS, Manolagas SC & O'Brien CA 2011 Matrix-embedded cells control osteoclast formation. *Nature Medicine* **17** 1235–1241. (doi:10.1038/nm.2448)

Yamashita S, Miyaki S, Kato Y, Yokoyama S, Sato T, Barrionuevo F, Akiyama H, Scherer G, Takada S & Asahara H 2012 L-Sox5 and Sox6 proteins enhance chondrogenic miR-140 microRNA expression by strengthening dimeric Sox9 activity. *Journal of Biological Chemistry* **287** 22206–22215. (doi:10.1074/jbc.M112.343194)

Yang J, Qin S, Yi C, Ma G, Zhu H, Zhou W, Xiong Y, Zhu X, Wang Y, He L *et al.* 2011 MiR-140 is co-expressed with *Wwp2-C* transcript and activated by Sox9 to target *Sp1* in maintaining the chondrocyte proliferation. *FEBS Letters* **585** 2992–2997. (doi:10.1016/j.febslet.2011.08.013)

Yang L, Cheng P, Chen C, He HB, Xie GQ, Zhou HD, Xie H, Wu XP & Luo XH 2012 miR-93/Sp7 function loop mediates osteoblast mineralization. *Journal of Bone and Mineral Research* **27** 1598–1606. (doi:10.1002/jbmr.1621)

Yang J, Gao T, Tang J, Cai H, Lin L & Fu S 2013 Loss of microRNA-132 predicts poor prognosis in patients with primary osteosarcoma. *Molecular and Cellular Biochemistry* **381** 9–15. (doi:10.1007/s11010-013-1677-8)

Yoshida CA, Yamamoto H, Fujita T, Furuichi T, Ito K, Inoue K, Yamana K, Zanma A, Takada K, Ito Y *et al.* 2004 Runx2 and Runx3 are essential for chondrocyte maturation, and Runx2 regulates limb growth through induction of *Indian hedgehog*. *Genes and Development* **18** 952–963. (doi:10.1101/gad.1174704)

Yoshida CA, Komori H, Maruyama Z, Miyazaki T, Kawasaki K, Furuichi T, Fukuyama R, Mori M, Yamana K, Nakamura K *et al.* 2012 SP7 inhibits osteoblast differentiation at a late stage in mice. *PLoS ONE* **7** e32364. (doi:10.1371/journal.pone.0032364)

Yoshitaka T, Kawai A, Miyaki S, Numoto K, Kikuta K, Ozaki T, Lotz M & Asahara H 2013 Analysis of microRNAs expressions in chondrosarcoma. *Journal of Orthopaedic Research* **31** 1992–1998. (doi:10.1002/jor.22457)

Zhang Y, Xie RL, Croce CM, Stein JL, Lian JB, van Wijnen AJ & Stein GS 2011*a* A program of microRNAs controls osteogenic lineage progression by targeting transcription factor Runx2. *PNAS* **108** 9863–9868. (doi:10.1073/pnas.1018493108)

Zhang J, Tu Q, Grosschedl R, Kim MS, Griffin T, Drissi H, Yang P & Chen J 2011*b* Roles of SATB2 in osteogenic differentiation and bone regeneration. *Tissue Engineering. Part A* **17** 1767–1776. (doi:10.1089/ten.tea.2010.0503)

Zhang JF, Fu WM, He ML, Wang H, Wang WM, Yu SC, Bian XW, Zhou J, Lin MC, Lu G *et al.* 2011*c* MiR-637 maintains the balance between adipocytes and osteoblasts by directly targeting Osterix. *Molecular Biology of the Cell* **22** 3955–3961. (doi:10.1091/mbc.E11-04-0356)

Zhang J, Tu Q, Bonewald LF, He X, Stein G, Lian J & Chen J 2011*d* Effects of miR-335-5p in modulating osteogenic differentiation by specifically downregulating Wnt antagonist DKK1. *Journal of Bone and Mineral Research* **26** 1953–1963. (doi:10.1002/jbmr.377)

Zhang Y, Xie RL, Gordon J, LeBlanc K, Stein JL, Lian JB, van Wijnen AJ & Stein GS 2012*a* Control of mesenchymal lineage progression by microRNAs targeting skeletal gene regulators Trps1 and Runx2. *Journal of Biological Chemistry* **287** 21926–21935. (doi:10.1074/jbc.M112.340398)

Zhang J, Zhao H, Chen J, Xia B, Jin Y, Wei W, Shen J & Huang Y 2012*b* Interferon-β-induced miR-155 inhibits osteoclast differentiation by targeting SOCS1 and MITF. *FEBS Letters* **586** 3255–3262. (doi:10.1016/j.febslet.2012.06.047)

Zhou X, Zhang Z, Feng JQ, Dusevich VM, Sinha K, Zhang H, Darnay BG & de Crombrugghe B 2010 Multiple functions of Osterix are required for bone growth and homeostasis in postnatal mice. *PNAS* **107** 12919–12924. (doi:10.1073/pnas.0912855107)

Received in final form 5 February 2014
Accepted 12 February 2014
Accepted Preprint published online 12 February 2014

http://jme.endocrinology-journals.org
DOI: 10.1530/JME-13-0294

Published by Bioscientifica Ltd.

OPEN ACCESS Freely available online

PLOS ONE

The p38α MAPK Function in Osteoprecursors Is Required for Bone Formation and Bone Homeostasis in Adult Mice

Edgardo Rodríguez-Carballo[1], Beatriz Gámez[1], Lara Sedó-Cabezón[1], Manuela Sánchez-Feutrie[3,4,5], Antonio Zorzano[3,4,5], Cristina Manzanares-Céspedes[2], José Luis Rosa[1], Francesc Ventura[1]*

1 Departament de Ciències Fisiològiques II, Universitat de Barcelona, IDIBELL, L'Hospitalet de Llobregat, Spain, **2** Departament de Patologia i Terapèutica Experimental, Universitat de Barcelona, IDIBELL, L'Hospitalet de Llobregat, Spain, **3** Institute for Research in Biomedicine (IRB Barcelona), Barcelona, Spain, **4** Departament de Bioquímica i Biologia Molecular, Facultat de Biologia, Universitat de Barcelona, Barcelona, Spain, **5** CIBER de Diabetes y Enfermedades Metabólicas Asociadas (CIBERDEM), Instituto de Salud Carlos III, Barcelona, Spain

Abstract

Background: p38 MAPK activity plays an important role in several steps of the osteoblast lineage progression through activation of osteoblast-specific transcription factors and it is also essential for the acquisition of the osteoblast phenotype in early development. Although reports indicate p38 signalling plays a role in early skeletal development, its specific contributions to adult bone remodelling are still to be clarified.

Methodology/Principal Findings: We evaluated osteoblast-specific deletion of p38α to determine its significance in early skeletogenesis, as well as for bone homeostasis in adult skeleton. Early p38α deletion resulted in defective intramembranous and endochondral ossification in both calvaria and long bones. Mutant mice showed reduction of trabecular bone volume in distal femurs, associated with low trabecular thickness. In addition, knockout mice also displayed decreased femoral cortical bone volume and thickness. Deletion of p38α did not affect osteoclast function. Yet it impaired osteoblastogenesis and osteoblast maturation and activity through decreased expression of osteoblast-specific transcription factors and their targets. Furthermore, the inducible Cre system allowed us to control the onset of p38α disruption after birth by removal of doxycycline. Deletion of p38α at three or eight weeks postnatally led to significantly lower trabecular and cortical bone volume after 6 or 12 months.

Conclusions: Our data demonstrates that, in addition to early skeletogenesis, p38α is essential for osteoblasts to maintain their function in mineralized adult bone, as bone anabolism should be sustained throughout life. Moreover, our data also emphasizes that clinical development of p38 inhibitors should take into account their potential bone effects.

Citation: Rodríguez-Carballo E, Gámez B, Sedó-Cabezón L, Sánchez-Feutrie M, Zorzano A, et al. (2014) The p38α MAPK Function in Osteoprecursors Is Required for Bone Formation and Bone Homeostasis in Adult Mice. PLoS ONE 9(7): e102032. doi:10.1371/journal.pone.0102032

Editor: Vladimir V. Kalinichenko, Cincinnati Children's Hospital Medical Center, United States of America

Received December 19, 2013; **Accepted** June 13, 2014; **Published** July 9, 2014

Funding: This research was supported by grants from the MEC (Ministry of Education of Spain) (BFU2011-24254) and La Marató de TV3. The funders had no role in study design, data collection and analysis, decision to publish, or preparation of the manuscript.

Competing Interests: The authors have declared that no competing interests exist.

* Email: fventura@ub.edu

Introduction

During development, ossification depends on the activity of osteoblasts that are derived from mesenchymal stem cells. Throughout this process of osteoblastic differentiation, osteochondroprogenitors proliferate and go through a series of steps before becoming mature osteoblasts [1,2,3]. Furthermore, osteocytes are derived from terminally differentiated osteoblasts that remain embedded in the bone-mineralized matrix. Later on in adulthood, bone formation and remodeling remain very dynamic processes that rely on a tight balance between osteoclast resorption and new bone formation by osteoblasts. Any disparity between these two activities causes pathological states such as osteoporosis [4].

Many extracellular stimuli, such as mechanical stress, inflammatory cytokines and growth factors, have been described as regulators of osteoblast differentiation through p38 MAPK signalling [5]. In mammalian cells, four isoforms of p38 Mitogen-Activated Protein Kinases (MAPKs) have been described: p38α (MAPK14), β (MAPK11), γ (MAPK12) and δ (MAPK13) [6]. Some differences in activation have been shown between distinct isoforms, with p38α MAPK being one of the most abundant isoform in osteoblasts and bone [7]. p38 MAPKs are activated by MKK3 and MKK6, which are also downstream of several MAPKKKs, including TAK1, ASK1 and MLKs [6].

p38 MAPK activity, known to play an important role in several steps of the osteoblast lineage progression, is necessary but not sufficient for BMP-induced acquisition of the osteoblast phenotype [8,9,10]. Evaluation of these effects is often based on the commonly used inhibitor, SB203580, which only inhibits p38α and p38β isoforms. Biochemical analysis has identified key osteogenic genes whose expression and/or function are regulated by p38. Evidence shows that p38 activity is required for BMP-induced *Osx* expression in calvaria, as well as bone-marrow-derived mesenchymal stem cells [11,12,13]. Moreover, several reports indicate that p38 phosphorylates critical transcription factors involved in osteoblastogenesis such as DLX5, RUNX2 and OSX [7,13,14,15,16]. Phosphorylation by p38 regulates their

The FASEB Journal • Research Communication

p38α function in osteoblasts influences adipose tissue homeostasis

Edgardo Rodríguez-Carballo,* Beatriz Gámez,* Andrés Méndez-Lucas,* Manuela Sánchez-Freutrie,[†,‡,§] Antonio Zorzano,[†,‡,§] Ramon Bartrons,* Soledad Alcántara,[¶] José Carlos Perales,* and Francesc Ventura*,[1]

*Departamente de Ciències Fisiològiques II and and [¶]Departament de Patologia i Terapèutica Experimental, Universitat de Barcelona, Institut d'Investigació Biomèdica de Bellvitge, L'Hospitalet de Llobregat, Barcelona, Spain; [†]Departament de Bioquímica i Biologia Molecular, Universitat de Barcelona, Barcelona, Spain; [‡]Institute for Research in Biomedicine, Barcelona, Spain; and [§]Centro de Investigación Biomédica en Red (CIBER) de Diabetes y Enfermedades Metabólicas Asociadas, Instituto de Salud Carlos III, Madrid, Spain

ABSTRACT **The skeleton acts as an endocrine organ that regulates energy metabolism and calcium and phosphorous homeostasis through the secretion of osteocalcin (Oc) and fibroblast growth factor 23 (FGF23). However, evidence suggests that osteoblasts secrete additional unknown factors that contribute to the endocrine function of bone. To search for these additional factors, we generated mice with a conditional osteoblast-specific deletion of p38α MAPK known to display profound defects in bone homeostasis. Herein, we show that impaired osteoblast function is associated with a strong decrease in body weight and adiposity ($P < 0.01$). The differences in adiposity were not associated with diminished caloric intake, but rather reflected 20% increased energy expenditure and the up-regulation of uncoupling protein-1 (*Ucp1*) in white adipose tissue (WAT) and brown adipose tissue (BAT) ($P < 0.05$). These alterations in lipid metabolism and energy expenditure were correlated with a decrease in the blood levels of neuropeptide Y (NPY) (40% lower) rather than changes in the serum levels of insulin, Oc, or FGF23. Among all *Npy*-expressing tissues, only bone and primary osteoblasts showed a decline in *Npy* expression ($P < 0.01$). Moreover, the intraperitoneal administration of recombinant NPY partially restored the WAT weight and adipocyte size of p38α-deficient mice ($P < 0.05$). Altogether, these results further suggest that, in addition to Oc, other bone-derived signals affect WAT and energy expenditure contributing to the regulation of energy metabolism.—Rodríguez-Carballo, E., Gámez, B., Méndez-Lucas, A., Sánchez-Freutrie, M., Zorzano, A., Bartrons, R., Alcántara, S., Perales, J. C., Ventura, F. p38α function in osteoblasts influences adipose tissue homeostasis. *FASEB J.* 29, 1414–1425 (2015). www.fasebj.org**

Key Words: bone • NPY • metabolism • adipocyte • energy expenditure • osteocalcin

IN RECENT YEARS, THE SKELETON has been implicated in many physiologic processes beyond locomotion, hematopoiesis, organ protection, or mineral metabolism. In addition to these classic functions, bone has been associated with the development and homeostasis of the entire body. In the 1970s, Garrard *et al.* (1) and Hooper (2) introduced the concept of "bone-governed body proportionality," emphasizing the positive relationship between bone development and body growth. Implicit in this hypothesis is the concept that bone is not only a recipient of hormonal signals but also a transmitter for the integration of inputs and communication of signals to other tissues.

Bone also acts as endocrine organ that regulates mineral metabolism through FGF23 synthesis (3). However, recent evidence highlighting the broad endocrine function of osteoblast-derived Oc was clearly unexpected (4). Osteoblasts have been shown to regulate energy metabolism through the secretion of Oc, which acts on pancreatic islets and adipose tissue (5, 6), and in male fertility (4, 7, 8). Interestingly, only the undercarboxylated forms of Oc (ucOc) are active on target organs (5, 6). A putative receptor for ucOc, *Gprc6a*, has been identified and implicated as the mediator of ucOc actions on pancreatic islets and testicular Leydig cells (9–11). Moreover, as expected for an intertwined endocrine hub, Oc synthesis and post-translational processing are also regulated through factors, such as insulin, serotonin, and adipokines, including leptin or adiponectin (4, 12, 13).

Several genetic studies have suggested that Oc is not the only bone-derived hormone affecting energy metabolism. *Oc* deficiency primarily affected insulin function and

Abbreviations: BAT, brown adipose tissue; eWAT, epidermal white adipose tissue; FF, homozygous floxed p38*α* mice; FGF23, fibroblast growth factor 23; GTT, glucose tolerance test; HFD, high fat diet; ITT, insulin tolerance test; iWAT, inguinal subcutaneaous white adipose tissue; KO, *Osx1-GFP::cre*$^{+/-}$; NEFA, nonesterified fatty acids; NPY, neuropeptide Y;

(*continued on next page*)

[1] Correspondence: Departament de Ciències Fisiològiques II, Universitat de Barcelona, IDIBELL, C/ Feixa Llarga s/n. E-08907, L´Hospitalet de Llobregat, Spain. E-mail: fventura@ub.edu

doi: 10.1096/fj.14-261891

This article includes supplemental data. Please visit *http://www.fasebj.org* to obtain this information.

0892-6638/15/0029-1414 © FASEB

TISSUE ENGINEERING: Part A
Volume 00, Number 00, 2015

DOI: 10.1089/ten.tea.2015.0181

termis
Tissue Engineering
& Regenerative Medicine
International Society

ORIGINAL ARTICLE

Mesenchymal Stem Cells Within Gelatin/$CaSO_4$ Scaffolds Treated *Ex Vivo* with Low Doses of BMP-2 and Wnt3a Increase Bone Regeneration

Rubén Aquino-Martínez, DMD,[1] Edgardo Rodríguez-Carballo, DMD, PhD,[1] Beatriz Gámez,[1] Natalia Artigas,[1] Patricia Carvalho-Lobato, MD,[2] Maria Cristina Manzanares-Céspedes, MD,[2] Jose Luis Rosa, PhD,[1] and Francesc Ventura, PhD[1]

The delivery of osteogenic factors is a proven therapeutic strategy to promote bone regeneration. Bone morphogenetic proteins (BMPs) constitute a family of cytokines with well-known osteogenic and bone regenerative abilities. However, clinical uses of BMPs require high doses that have been associated with complications such as osteolysis, ectopic bone formation, or hematoma formation. In the present work, we sought to improve bone tissue engineering through an approach that combines the use of bone marrow-derived mesenchymal stem cells (BMMSCs), composite scaffolds, and osteoinductive agents. We employed a composite gelatin/$CaSO_4$ scaffold that allows for an early expansion of seeded BMMSCs, which is followed by an increased level of osteogenic differentiation after 10 days in culture. Furthermore, this scaffold enhanced bone formation by BMMSCs in a mouse model of critical-sized calvarial defect. More importantly, our results demonstrate that *ex vivo* pretreatment of BMMSCs with low amounts of BMP-2 (2 nM) and Wnt3a (50 ng/mL) for 24 h cooperatively increases the expression of osteogenic markers *in vitro* and bone regeneration in the critical-sized calvarial defect mouse model. These data provide a strong rationale for the development of an *ex vivo* cooperative use of BMP-2 and Wnt3a. Osteogenic factor cooperation might be applied to reduce the required amount of growth factors while obtaining higher therapeutic effects.

Introduction

UNDERSTANDING THE BASIC principles of the cellular and molecular events regulating osteoblast differentiation is essential for the development of effective approaches to regenerate bones. Autologous bone grafting has been the gold standard for treating bone defects.[1] However, this approach is associated with numerous drawbacks, including the limited availability of grafting material and the morbidity associated with the collection of bone from a second surgery site. Bone tissue engineering has emerged as a potential alternative to overcome the inherent problems of autografts or allografts. The main components involved in tissue-engineered bone regeneration are stem or precursor cells, growth factors and/or cytokines, and appropriate bioactive carriers.[2]

Bioactive scaffolds provide an initial mechanical resistance and allow the attachment, propagation, and differentiation of the transplanted cells. The scaffolds for tissue engineering are classified as inorganic, such as calcium phosphate, or as organic materials, such as collagen or gelatin.[3] Osteoblastic cells show an increased expression of osteogenic markers when they are seeded on three-dimensional (3D) gelatin or collagen sponges compared with the 2D culture conditions.[4] In addition, integrin function has been proven to be essential for early osteoblast differentiation.[5] The calcium ions released from calcium-containing materials enhance osteogenesis because the extracellular calcium plays a critical role in the promotion of the differentiation and function of osteoblasts.[6]

The efficacy of bone morphogenetic proteins (BMPs) for regenerating bone is well known, both in animal models and in several clinical applications, such as bone fracture healing,[7] alveolar cleft defects,[8] spinal fusion,[9] and craniofacial bone defects.[10] As a result, the medical use of BMP-2 and BMP-7 was approved for specific osteoinductive applications. However, most bone regeneration studies using animal models entail supraphysiological doses of BMPs (e.g., 1–45 μg dose of BMP-2 in a femoral segmental defect in rat).[11–13] More importantly, BMP therapy in clinical practice also requires high amounts of BMPs, ranging between 1.5 and 3.3 mg (1.5 mg of BMP-2 or 3.3 mg of BMP-7).

[1]Departament de Ciències Fisiològiques II, Universitat de Barcelona, IDIBELL, L'Hospitalet de Llobregat, Spain.
[2]Unitat d'Anatomia i Embriologia Humana, Departament de Patologia i Terapèutica Experimental, Universitat de Barcelona, IDIBELL, L'Hospitalet de Llobregat, Spain.